



PHD

Theoretical and experimental diesel engine system studies with special reference to temperature and altitude derating

Degong, Dang

Award date:
1989

Awarding institution:
University of Bath

[Link to publication](#)

Alternative formats

If you require this document in an alternative format, please contact:
openaccess@bath.ac.uk

Copyright of this thesis rests with the author. Access is subject to the above licence, if given. If no licence is specified above, original content in this thesis is licensed under the terms of the Creative Commons Attribution-NonCommercial 4.0 International (CC BY-NC-ND 4.0) Licence (<https://creativecommons.org/licenses/by-nc-nd/4.0/>). Any third-party copyright material present remains the property of its respective owner(s) and is licensed under its existing terms.

Take down policy

If you consider content within Bath's Research Portal to be in breach of UK law, please contact: openaccess@bath.ac.uk with the details. Your claim will be investigated and, where appropriate, the item will be removed from public view as soon as possible.

THEORETICAL AND EXPERIMENTAL DIESEL ENGINE SYSTEM STUDIES

**with Special Reference to
Temperature and Altitude Derating**

Submitted by

Dang Degong

For the Degree of Ph.D

of the University of Bath

1989

COPYRIGHT

Attention is drawn to the fact that the copyright of this thesis rests with its author.

This copy of thesis has been supplied on condition that anyone who consults it is understood to recognise that its copyright rests with its author and that no quotation from the thesis and no information derived from it may be published without the prior consent of the author.

This thesis may be made available for consultation within the University Library and may be photocopied or lent to other libraries for the purpose of consultation.

UMI Number: U013842

All rights reserved

INFORMATION TO ALL USERS

The quality of this reproduction is dependent upon the quality of the copy submitted.

In the unlikely event that the author did not send a complete manuscript and there are missing pages, these will be noted. Also, if material had to be removed, a note will indicate the deletion.



UMI U013842

Published by ProQuest LLC 2014. Copyright in the Dissertation held by the Author.
Microform Edition © ProQuest LLC.

All rights reserved. This work is protected against
unauthorized copying under Title 17, United States Code.



ProQuest LLC
789 East Eisenhower Parkway
P.O. Box 1346
Ann Arbor, MI 48106-1346

UNIVERSITY OF BATH		
LIBRARY		
31	15 SEP 1989	
Ph.D.		

5033159

ACKNOWLEDGEMENTS

The author wishes to express his sincere thanks to:

His supervisor, Prof. F. J. Wallace, for his kind guidance, concern and patience during the whole course and writing-up of this thesis, which is most appreciated;

Dr. M. S. Ghadiri-Zare, for his very valuable help and advice in simulation work;

Dr. M. Wilson, for his help in computing and programs;

Mr. J. Hall, Mr. K. Britton and Mr. A. D. Elley, for their help concerning experiments;

The Chinese government and British Council for their support.

SUMMARY

Simulations are carried out on the steady state operations of the turbocharged L10 engine, and of L10 DCE --- both with variable and fixed nozzle turbine respectively. In all these simulations, emphasis is placed on the effects of changing ambient conditions on system performance, and the operations of different systems are compared. In the study of the DCE system, special attention has paid to its performance optimisation for various control variables. An investigation is also carried out into the gearbox losses of the DCE, which is based on the laboratory proto-type Leyland 520 DCE. Further, the Leyland 520 DCE is simulated with emphasis on the effects of gearbox losses and pressure losses in pipes, on system performance, and the results are compared with those obtained from experiments.

The following represents major original input by the author to the programs described in the thesis:

- 1) Systematic optimising feature of the program DCE-VG.
- 2) Complete reprogramming of DCE-FG.
- 3) Gearbox loss analysis.

CONTENTS

ACKNOWLEDGEMENT

SUMMARY

contents	page
CHAPTER 1 INTRODUCTION	1
1.1 General requirements for engine-transmission system for heavy goods vehicles	1
a)High specific power	1
b)Good fuel economy	3
c)Good torque backup	3
d)Good transient response	4
e)Acceptable emission characteristics	5
1.2 Basic turbocharging system	5
1.3 Alternative systems	7
a)Tuned(resonant) intake system	7
b)Variable geometry turbocharging	8
c)Comprex supercharging	9
d)Two-stage turbocharging	10
e)Hyperbar	11
f)Compound and adiabatic engines	11
1.4 The Differential compound engine(DCE)	12
1.4.1 Historical development	12
1.4.2 General characteristics of the DCE	13
1.5 The Effects of changing ambient conditions	16
a)Turbocharged engine system	16

b)The DCE	17
1.6 Scope of this thesis	18
CHAPTER 2 SURVEY OF THE THEORETICAL WORK	19
2.1 Simulation of the turbocharged Cummins L10	
Engine using program EMAT	19
2.1.1 The matching program EMAT	19
2.1.1.1 Main program	19
2.1.1.2 Engine subroutine	21
2.1.1.3 Turbine subroutine	23
2.1.1.4 Compressor subroutine	23
2.1.1.5 Charge cooler subroutine	23
2.1.1.6 Other features	23
2.1.2 VG Turbocharging simulation	23
2.1.3 Derating for altitude and temperature	23
2.2 Simulation of L10 DCE using program DCE	25
2.2.1 The matching program DCE2	
(variable turbine nozzle build)	25
2.2.1.1 The structure of the original program DCE2	25
2.2.1.2 Modified program DCE-VG	28
2.2.2 Simulation of the DCE with fixed nozzle turbine	32
2.2.3 Simulation of the DCE under changing ambient conditions	35
2.3 Optimisation of the DCE system(with VG turbine)	36
CHAPTER 3 DETAILED SIMULATION OF THE TURBOCHARGED	
 CUMMINS L10 ENGINE USING PROGRAM EMAT	38
3.1 Base line results(standard ambient conditions)	39
3.2 Effects of variable geometry turbocharging	40
3.2.1 Effects of turbine match	40
3.2.2 Synthesized VG turbocharged engine operation	43
3.3 System performance under varying ambient conditions	44
3.3.1 Operation at altitude	44
a)Fixed geometry turbocharging	44
b)Variable geometry turbocharging	46
3.3.2 Operation at elevated temperature	47

3.3.3 System operation at elevated altitude and temperature	49
3.4 Summary	49
CHAPTER 4 OPERATION OF THE DCE WITH VARIABLE	
NOZZLE TURBINE	51
4.1 Design consideration	51
4.2 Standard operation	53
4.3 Operation with new compressor map and re-optimisation	56
4.3.1 General approaches	56
a) Compressor re-match	56
b) System re-optimisation for best engine speed	56
4.3.2 Presentation of results	57
4.4 Operation under changing ambient conditions	60
4.4.1 Derating for reduced ambient pressure	61
4.4.1.1 General	61
4.4.1.2 Presentation of results	61
4.4.2 Derating for elevated temperature	64
4.4.2.1 General	64
4.4.2.2 Presentation of results	64
4.4.3 Combined effects of ambient pressure and temperature	66
4.4.4 Discussion	69
CHAPTER 5 OPERATION OF THE DCE WITH FIXED	
GEOMETRY TURBINE	72
5.1 Standard steady state operation	72
5.1.1 Performance calculation	72
5.1.2 Presentation of results	73
5.1.3 Further remarks	76
5.2 Operation with new compressor map	77
5.3 Operation under changing ambient conditions	79
5.3.1 Effects of reduced ambient pressure	80
5.3.2 Effects of elevated temperature	81
5.3.3 Combination of altitude and temperature derating	82
5.4 Discussion	84
5.5 Summary	84

CHAPTER 6 EXPERIMENTS AND EVALUATION OF GEARBOX

LOSSES OF THE LEYLAND 520 DCE	86
6.1 Background	86
6.2 Experimental facilities	87
6.2.1 Mechanical components	87
a)Engine	88
b)Compressor	89
c)Turbine	89
d)Dynamometer	89
e)Geartrains	90
6.2.2 Instrumentation and data acquisition	90
a)Speed	90
b)Torque	91
c)Gas pressures and temperatures	91
d)Gas flows	92
e)Fuel flow	92
f)Injection timing, rack position and nozzle angle	92
6.2.3 Control system	92
a)Engine governor	92
b)Dynamometer control	93
c)Injection timing and turbine nozzle angle	93
d)Bypass flow	93
6.2.4 Data processing	93
6.3 Investigation of gearbox losses	93
a)Compressor operation	95
b)Output shaft operation	97
c)Turbine operation	98
d)Distribution of gearbox losses	100
6.4 Discussion	101
6.5 Computer modelling of gearbox losses	102

CHAPTER 7 SIMULATION OF THE LEYLAND 520 DCE

EXPERIMENTAL PLANT	104
7.1 Brief presentation of the experimental results	104

7.2 Preliminary prediction	105
7.2.1 General	105
7.2.2 Presentation of results	106
7.2.3 Overall performance	107
7.3 Mimicking experimental performance	108
7.3.1 Compressor and turbine performance	110
7.3.2 Effects of pipe losses	110
7.4 Summary	111
REFERENCES	112

**APPENDIX BRIEF COMPARISON OF TRANSIENT RESPONSE OF
VG AND FG VERSIONS OF DCE**

CHAPTER 1

INTRODUCTION

1.1 General Requirements for Engine-Transmission Systems for Heavy Goods Vehicles

Engines for heavy goods vehicles are almost exclusively diesels, at least in Europe. Like all vehicle engines, they are required to work under wide speed and load conditions. Compared with other types, such as stationary power plant and marine propulsion, more stringent requirements have to be met for the duty they perform. The following are the most important aspects which should be considered.

a) High Specific Power Effective transportation can only be achieved with sufficient power. However, for a heavy goods vehicle, like those for any other purpose, high power should be developed with minimum bulk and weight of the system. Obviously smaller weight means more available power for transporting goods, hence greater payload.

Essentially, to this end, the thermodynamic performance of the engine has to be maximized. Besides, it is very important that the various components of the system be carefully designed and hence optimum structure be obtained, reliability being assured with minimum materials.

The power of an engine is determined by its torque and the speed at which it works. An engine with higher torque and speed will produce more power. Conventionally, engine power is expressed by its brake mean effective pressure (BMEP), which is defined as the work done per unit swept volume per cycle, therefore:

$$\text{power} = V_s \cdot \text{BMEP} \cdot n / i$$

V_s swept volume

i rev/cycle

n speed

Clearly, for a specific type of engine (two-stroke or four-stroke) of a specific design (fixed swept volume), its output can be increased by either raising its BMEP or its speed. However, the extent to which the engine speed can be increased is comparatively limited. Usually the friction loss between the moving components increases rapidly with speed. Also, because of high air flow velocity, the volumetric efficiency of the engine will deteriorate and pressure losses along the flow path will increase. Further, at very high speeds a cycle is completed in a very short time. Therefore it will be difficult to achieve effective injection and mixing of fuel with air, which will in turn degrade the effectiveness of the engine cycle. This applies particularly to the small high speed D.I. automotive engine.

Another way to increase the power density of an engine is to increase its BMEP. In fact, much of recent development work has concentrated on this aspect, by the application of supercharging and particularly turbocharging. Fig-1.1 shows the increases in BMEP, accompanied by decreasing specific weight and fuel consumption, for truck engines during the last two decades and a projection for the next few coming years[4].

Since the output of an engine is directly related to the fuel burnt (under normal working condition), and thus to the amount of air charge which can be trapped in the cylinder, it can readily be seen that high specific power can only be obtained by raising the density of the air charge in the cylinder.

Basically, there are two types of supercharging: straight mechanical supercharging and turbocharging. In the first case a blower is driven directly by the engine crankshaft through a gear (Fig-1.2). This means that the compressor power will be provided directly by the engine crankshaft, which will reduce the effective output of the system and hence may not be economical. Further the incorporation of the high ratio gear makes the system potentially less reliable. Nevertheless, mechanical supercharging can take advantages, particularly in terms of good transient response and torque backup. It is being seriously considered for small high speed automotive engines. The alternative is a turbocharger, which consists of a turbine and compressor usually mounted on a single shaft. The exhaust gas from the engine is further expanded through the turbine, hence generating a certain amount of power. The turbine in turn drives the compressor which compresses and delivers the air to the engine. Because much of the otherwise wasted exhaust energy is recovered, the system will work more efficiently than a mechanically supercharged or naturally aspirated engine. Actually, under certain operating

condition the engine inlet pressure exceeds the back pressure, providing additional positive pumping work as well as improved scavenging.

Application of charge cooling can further increase the density of the charge air thereby increasing BMEP. In turbocharging without charge cooling, although the density of the air can be increased, the temperature of the air will increase at the same time. This will offset, to some extent, the increase in air density. Fig-1.3 shows the diagram of a turbocharged intercooled engine system. For highly rated engine, the temperature increase of the air will be higher due to the higher boost ratio. This makes charge cooling more attractive and cost effective.

b) Good Fuel Economy Due to rising oil prices, fuel economy has become an even more important feature of transport costs. Further, it has been realised that the supply of oil is diminishing. This makes the problem more acute. Recently more and more attention has been focused on improving the fuel economy of power plants, no matter of what kind. The engine is the heart of the vehicle, and every effort should be made to make it work efficiently. However, it should be realised that no dramatic breakthrough can be achieved on the basis of the present thermal cycle. Nevertheless, there is still room for refinement. For example, appropriately designed and matched inlet and exhaust systems can reduce the flow losses in these parts; better combustion systems can help the mixing of air and fuel to obtain effective burning; reduction in friction between the moving parts can reach the same goal, etc. Interest has also centred on trying to recover the heat loss to coolant, e.g. adiabatic compounding.

It should be noted that, because of the wide operating range of vehicle engines, their high efficiency area should also be wide.

c) Good Torque Backup[2,5] For a vehicle engine, good torque backup is essential, i.e. its maximum torque should lie at the lowest possible engine speed, preferably at approximately half the rated speed. The vehicle will benefit from high torque at low speeds to provide a margin for acceleration and to allow the vehicle to lug up very steep hills with a limited number of ratios in the gearbox. Fig-1.4 shows the ability of a truck to climb hills if constant power is available over the whole speed range. Superimposed is the vehicle's hill-climbing ability in each gear ratio (five speed ratio) when a typical engine is fitted. The shaded portions represent running conditions falling below the maximum power output of the engine which are not achievable in practice because the engine cannot develop sufficient torque at these speeds. If the torque backup of the system is improved,

these area can be reduced. Fig-1.5 compares three combinations of engine torque backup and gearbox. Line A is an ideal constant power line while B is derived from A after the transmission loss is deducted. With a torque backup of 5% and a five-speed gearbox(Fig-1.5a), the difference between the engine operating line and the ideal constant power line is quite significant and the dynamic performance of the system will be very poor. If a ten-speed gear box is used with the same torque backup(Fig-1.5b), this difference can be reduced, but the gain in performance is at the cost of frequent shift of gearbox setting. However, if the torque backup is raised to a value of 26%, then even with a five-speed gearbox, the loss of power relative to the ideal is substantially reduced, therefore the performance is greatly improved(Fig-1.5c). Ideally if the engine itself can work with its maximum power over a wide speed range, then its torque will rise all the way as its speed is decreased. Consequently, no gearbox at all is necessary for assisting in climbing hills.

d) Good Transient Response[6,7] Vehicle engines are subjected to frequent speed changes, therefore their transient characteristics are very important. Problems arise on sudden increase in fuelling under acceleration or load application. If sufficient air is always available, a proper fuel/air mixture will be obtained and thus power will be developed quickly and the desired operating condition can be reached in a short time. However, if the air is insufficient, the result will be a poor response because the fuelling may have to be restricted to ensure that the air/fuel ratio is always above the critical value. Otherwise, the smoke level will be increased. Usually the response of turbocharged engines will be poorer than that of naturally aspirated engines, since the turbocharger has to be accelerated first to increase the air supply. Particularly, when accelerating the vehicle under load, the lag of the turbocharger will be more severe. In order to reduce smoke, it is usually necessary to supply the fuel in a controlled manner, with a smoke limiter, but at the expense of slower response.

Additional energy can be supplied to help accelerate the turbocharger. One method is to use a store of compressed air. During transient operation, the air may be injected to the compressor impeller. This can assist the acceleration of the turbocharger and provide more air as well. A Pelton wheel turbine may be fitted to the shaft of a turbocharger, operated by high pressure lubricating oil, to accelerate turbocharger under transient operations. Better transient characteristics can be obtained through the Comprex supercharging system and through variable geometry turbocharging.

e)Acceptable Emission Characteristics[3]

With naturally aspirated engines, the smoke limit is in fact a determining factor for the power output that can be developed. These limits rarely arise when certifying turbocharged engines for rated output, but smoke problems can arise with full throttle running at lower engine speeds. This demands that the smoke limiter be adjusted correctly. The same applies to transient operation when the engine is accelerating.

Compared with petrol engines, the diesel engine has a low level of unburnt hydrocarbon(HC) and carbon monoxide(CO). Nitrogen oxides(NOx) are at similar levels and need to be specially treated. Because NOx is produced at high temperature, the measure will be to reduce the maximum cylinder temperature. However, the resultant decrease in temperature may lead to more unburnt HC.

The engine is usually the main source of the noise from the vehicle, at least at lower speeds. The noise can be reduced by control of the rate of heat release of the engine cycle, i.e. reducing the pre-mixed burning, and by proper design of mechanical parts.

Since the 1970s, more attention has been paid to the environmental effects of vehicles, followed by a series of regulations. Fig-1.6 shows legal noise limits, as imposed by the EEC for heavy truck. It can be seen that the requirements have become more and more stringent.

f)Reliability

g)Acceptable First Cost

The importance of these last two items is apparent. However, it should be noted that these requirements are usually interconnected and, very often, measures to improve different aspects of the system may conflict with each other and the final solution can only be a compromise.

1.2 Basic Turbocharging Systems[1,2,8]

The initial purpose of turbocharging is to improve the engine breathing capacity thus increasing power density. A conventionally turbocharged engine system consists of an engine, a compressor and a turbine. The latter two are usually mounted on the same shaft to form a turbocharger. The structure of the system has been shown in Fig-1.3. In vehicle applications the compressor is usually of the centrifugal type while the turbine of the radial inflow type.

The engines in heavy transport application are predominantly four-stroke type. They are positive displacement machines, therefore the mass flow rate is highly dependent on the speed. Fig-1.7 shows the flow characteristics of such an engine. It can be seen that the mass flow capacity varies proportionally with its speed.

Conventionally, the compressor characteristics are presented in terms of pressure ratio against mass flow parameter($\dot{M} \sqrt{T} / P$) for lines of constant speed parameter(N / \sqrt{T}). In addition, contours of constant isentropic efficiency are superimposed, Fig-1.8. It can be seen from this figure that there are essentially three areas on a compressor map. The central area is the stable operating zone. This area is separated from the unstable area on its left by the surge line. Surge is a flow instability which happens when the mass flow rate is reduced while maintaining a constant pressure ratio, a point arising where flow reversal occurs. To the right of this area is the choking region where due to very high air velocities, the mass flow reaches its maximum value.

It can also be seen that due to the surge and choking phenomena, the usable flow range of the compressor at a specific pressure ratio is rather narrow, particularly at higher pressure ratios. The high efficiency area lies near the surge line. It can also be seen that the pressure ratio increases rapidly with speed under stable operating conditions.

The characteristics of a radial inflow turbine can be expressed in a similar way to the compressor map, Fig-1.9. Alternatively it is very often plotted in two separate maps, one in which the mass flow parameter($\dot{M} \sqrt{T} / P$) is plotted on a base of dimensionless speed with turbine pressure ratio as parameter, and the other in which the dimensionless torque is plotted on a base of speed again with pressure ratio as the parameter and with superimposed contours of constant turbine efficiency lines. It can be observed that the turbine pressure ratio(power) increases sharply with increase in mass flow(e.g. at a constant speed).

It can be seen that there is a great difference between the characteristics of the compressor and turbine, and the flow characteristics of the engine; this makes the matching of the system very demanding.

Over the last twenty years or so, turbocharging technology has experienced rapid developments. In addition to higher power density, other benefits are obtained from turbocharging, i.e. a)improved specific fuel consumption, b)improved

emission characteristics and c) better torque backup.

Although the performance of a turbocharged engine is improved, to a great extent, over the naturally aspirated type, limitations still exist. As stated earlier, for vehicle engines, torque backup is very important. Therefore, it will be beneficial to increase the trapped air charge at low engine speeds so that more fuel can be burnt. This implies that the boost ratio at low speed should be higher, demanding more power from the turbine. However, due to its flow characteristics, the turbine power actually diminishes with decreasing engine speed. To obtain the required torque backup, a compromise has to be made, i.e. the fuelling at high speeds is reduced with resultant lower rated power than potentially obtainable. This results from the difficulty in matching the engine and turbocharger.

From a turbine map it can be seen that the turbine pressure ratio(power) increases rapidly with its mass flow rate. The reason for this is that for a specific turbine, when mass flow increases, the relative restriction to it increases thus inducing higher pressure difference across the turbine. However, due to the positive displacement flow characteristics of the engine, mass flow reduces at low speed. This means the relative restriction to the flow is reduced, making it impossible to set up sufficient pressure across the turbine. This is illustrated in Fig-1.10, which shows the available exhaust energy and required compressor power to provide a constant delivery pressure ratio (boost density ratio) of 2:1. It can be seen that this characteristic is just opposite to what is ideally required.

Due to the problem previously discussed, it is usually very difficult to obtain a good match of turbocharger and engine. It is equally difficult to further uprate an engine on the basis of conventional turbocharging system. The narrow flow range of the compressor at high pressure ratio compounds the problem even further.

1.3 Alternative Systems

The demand for higher power and better performance is still increasing. In recent developments, in addition to the effort to improve the performance of the conventional system, researches on alternative systems have also intensified. A variety of proposed schemes with differing initial aims, has emerged and a wide research has been carried out, with varying degrees of success. In the following some representative systems are reviewed.

a) Tuned(Resonant) Intake System[9,10,11] The tuned intake system

is pioneered by Cser, in which the intake manifolds are tuned so that at low engine speeds, the occurrence of a maximum possible pressure in it coincides with inlet valve closing thus assisting the intake process and allowing more air to be trapped. Fig-1.11 shows the schematic layout of the system. Fig-1.12 shows that at an engine speed of 1220rpm, the inlet manifold pressure reaches its maximum value near the inlet valve closing. Because more air is delivered to the cylinder, more fuel can be burnt, thus increasing the torque. This will mitigate the problem of insufficient boost at low engine speed inherently associated with pure turbocharging and a better torque backup can be achieved. However, as also shown in Fig-1.12, the advantage of the system diminishes and the pressure variation in the inlet manifold becomes more and more unfavourable with increasing engine speed. At 2400rpm the instantaneous inlet manifold pressure at the moment of inlet valve closing reaches a low value, the intake process being impaired. This can be seen in Fig-1.13. At lower speeds, the volumetric efficiency is improved over a conventionally turbocharged engine while at higher speeds it deteriorates. This will partially counteract the normal rise in boost pressure with engine speed, with the effect of preventing overboosting and also reducing the width of the operating air flow range on the compressor map. A disadvantage of the system is the increased pumping work during the gas exchange process, at least at low load, leading to increased fuel consumption.

When first introduced, the resonant intake system appeared bulky. However, considerable refinement has been achieved. It has now been used in a number of turbocharged European and Japanese truck engines. For example, Hino uses a control valve to minimise the effect of the system on pumping work at low load. Fig-1.14 shows the improvement in engine performance and the mechanism employed.

b) Variable Geometry Turbocharging[12,13,14] The potential of variable geometry turbocharging has been explored for a long time. The idea arose from the difficulty in matching a turbocharger(especially turbine) to a reciprocating vehicle engine. However, with a VG turbine, the effective flow area of the turbine can be varied so that optimum boost can be maintained over a wide speed and load range. By reducing the flow area with decreasing speeds, low speed boost and torque can be improved. Further, engine overboosting and turbocharger overspeeding can be prevented by increasing the turbine flow area at higher speed. It can also be deduced that, with a variable geometry turbine, fuelling at higher speeds can be increased due to the available ample air supply, increasing the power output. By proper

design considerations(e.g. maximum cylinder pressure), highly rated power units can be achieved through VG turbocharging, which can be considered to be a very effective approach up to a BMEP of 18bar. A very important advantage of VG turbocharging is that improved transient response can be achieved by properly scheduling the device.

However, in practice, the variable units have to work at very high temperatures. It is rather difficult to ensure reliable operation. Also, in order to take full advantage of the system, suitable control systems are required. This will increase complexity. Inevitably, the cost will be higher.

Fig-1.15a shows the optimised flow area schedule, at the turbine inlet, for a variable geometry turbocharged engine. In order to achieve this, a very sophisticated electronic control system becomes a necessity. As can be seen in Fig-1.15b, a control system with microcomputer is implemented for this purpose. Fig-1.16 shows the baseline performance and the fully optimised VG turbocharged performance of the engine system. It can be seen that the entire power envelope has been expanded, with the same limiting conditions(e.g. maximum cylinder pressure). On the limiting torque curve, a substantial gain in peak torque from 1020 to 1160Nm at 1300rpm has been achieved, i.e. 13.72%. Further, fuel economy has been substantially improved(the area encompassed by the contour of 210g/h.kw substantially increased), except for the best fuel consumption due to use of a single entry, as opposed to a twin entry turbine.

A variable geometry turbine only will usually suffice for moderate uprating. However, for very high ratings, a variable geometry compressor may also be required to expand the mass flow range especially at high pressure ratio. This can be achieved with inlet guide vanes or variable diffuser vanes[15,16,17].

c) *Comprex Supercharging*[18,19] The Comprex is a gasdynamic device which uses the energy of the exhaust gas to compress the air in a way fundamentally different from that of a turbocharger. Fig-1.17 shows the basic structure of the device.

The basic operation of this system can be briefly described as follows. As the wheel rotates, there will be repetitions of the following events in sequence when the axial passages on the wheel periphery move past the relevant ports(see the figure) in turn: the pressure waves propagating from the exhaust manifold into the passages compress the existing air which is subsequently delivered into the inlet manifold(at

a pressure similar to that in the exhaust manifold) while the expansion waves propagating out of the passages when the low pressure gas is discharging help the admission of ambient air into the passages.

One advantage of Comprex over turbocharging is the fact that its operation is virtually independent of engine speed because the compression of charge air is by virtue of pressure wave effects. Therefore low speed torque, which is always critical in turbocharged engines, can be achieved with the Comprex system. Further, due to the absence of inertia in the system, transient response can be drastically improved.

Fig-1.18 compares the performance on the limiting torque curve, of a truck engine when turbocharged and supercharged by the Comprex system. Greatly superior performance is shown by the latter over the former, particularly at low speed region. Fig-1.19 shows the comparison of the transient response of the same engine, i.e. on-load acceleration. With Comprex, the boost pressure increases almost instantaneously, which is also reflected in the variation of BMEP and engine speed, etc.

The disadvantage of Comprex is its space requirement and complex installation. It is more expensive to produce. Nevertheless, it has been under continuous development and refinement.

d) Two-stage Turbocharging[20,21] Two-stage turbocharging has been considered as a means of substantially increasing the power density of an engine. Two turbines and compressors are used in series; thus higher pressure ratio can be obtained. Fig-1.20 shows the layout of such a system with intercooling and aftercooling. Usually the match is a combination of a high pressure ratio, narrow flow range and a low pressure ratio, wide flow range compressor. The interaction between the two enables high pressure air to be delivered over the entire engine speed range, particularly at low speed while compressor surge is avoided. Fig-1.21 shows the engine operating lines superimposed on the LP and HP compressor maps. Clearly the HP compressor pressure ratio varies in a very narrow range with engine speed for a particular load. Fig-1.22 shows the performance of the system, very high rating being achieved.

The major advantage of two-stage turbocharging is that two turbochargers of normal pressure ratio and efficiency can be used. Therefore it is a relatively easy and proven method of achieving very high ratings from conventional vehicle engines. However, because it uses an additional turbocharger, the cost will be high.

Also, it will be bulkier and the installation will be more complex. Therefore its application can only be justified for very high ratings with BMEP over about 18bar.

e) Hyperbar[21,22] The Hyperbar system is designed for very high output schemes, and is shown schematically in Fig-1.23. Because of the incorporation of a bypass and an auxiliary combustion chamber between the compressor and the turbine, the turbocharger will be able to work independently of the engine. The operation of the auxiliary combustion chamber provides additional energy to the turbine when necessary, therefore high pressure ratio can be easily obtained as required. Obviously, the problem of insufficient boost at low speeds associated with conventional turbocharging is avoided. Further, the mass flow incompatibility between the engine and the compressor can be reconciled through the bypass. Therefore compressor surge at high pressure, where the flow range is particularly low, is avoided. This can be seen from Fig-1.24, the operating lines of the complete system as well as the engine operating lines being superimposed on the compressor map. Under most operating conditions, in particular at low engine speeds, a large amount of air is bypassed. Very high BMEP is achieved over the entire engine speed range, implying a high rate of fuel input to the auxiliary combustion chamber to achieve the required pressure ratio. As a result, The fuel consumption is high. Indeed, at low speed low load operation the fuel supply to the auxiliary combustion chamber can be several times as high as that to the engine. Further, the operation of the bypass and the auxiliary combustion chamber requires a complex control system. All these factors decide that Hyperbar can only be used in special applications, such as military vehicles, rather than for commercial purposes.

f) Compound and Adiabatic Engines[23,24,25] These schemes are aimed at improving the system efficiency rather than obtaining exceptionally high ratings. Usually only about 40% of the energy of the fuel input can be converted into useful work by the engine, the rest being rejected to the coolant and discharged with the exhaust gas. For turbocharged engines, a certain amount of exhaust energy can be extracted by the turbine for providing high density air. Unfortunately, while at low speed, low load this energy is not sufficient; at high speed, high load it can be excessive. The purpose of compounding is harnessing this excess energy and direct it to the output shaft thus increasing output power. Fig-1.25 shows the Cummins compound scheme, in which the exhaust gas is further expanded through a low pressure turbine which is geared to the output shaft, while Fig-1.26 shows a typical performance map for this scheme in non-adiabatic form.

Generally, the heat to coolant for an engine can be as much as 20-30% of the total energy input. The concept of an adiabatic engine is to reduce or prevent the heat loss to coolant. However, the thermal efficiency of the engine cycle itself can benefit very little from this. The significant effect of insulation is, in fact, that more heat is directed to the exhaust gas. Turbocharged engine can benefit from this because of the resultant high boost ratio, leading to partial energy recovery by more positive pumping work, while excess available energy still exists. Clearly, the potential of adiabatic operation can be further exploited in combination with a compounding system. However, the volumetric efficiency of the engine will decrease due to higher cylinder temperatures. Fig-1.27 shows a prediction of the variation of some parameters of interest in relation to the degree of insulation.

1.4 The Differential Compound Engine(DCE)[26,27,28,29,30]

The differential compound engine is an integrated diesel engine-transmission system, with characteristics particularly favourable for heavy transportation applications. As its name suggests, the DCE has the following features: an fully floating epicyclic geartrain, with the engine connected to the annulus or ring gear, the supercharger compressor to the sun gear and the output shaft to the planet carrier respectively. The exhaust turbine is geared to the output shaft. Due to the incorporation of the epicyclic geartrain, additional freedom is introduced to the system, making systematic optimisation possible.

1.4.1 Historical Development

The concept of the DCE was first proposed more than two decades ago and research work on the DCE has proceeded continuously. The system has been under progressive evolution and refinement. These steps can be briefly summarised as follows:

a)Substitution of a four-stroke engine for the original opposed piston two-stroke engine. The choice of a two-stroke engine in the original DCE scheme was dictated by two considerations:

Firstly, the ability of the two-stroke engine to accommodate large throughflow without incurring the penalty of excessive pressure drops and hence loss of potential turbine power.

Secondly, the expectation that a two-stroke engine would have significantly higher power weight and power bulk ratios than an equivalent four-stroke engine.

However, operating experience with high output, high speed two-stroke engines has shown that thermal loading limitations are severe and that BMEP is limited even with piston cooling. On the other hand, four-stroke engines can operate at higher BMEP's and lower thermal loading, so that better power weight ratio can be achieved.

b) Changes of turbines. Originally, one power turbine and one auxiliary turbine of fixed geometry were used, with the power turbine using the exhaust air while the auxiliary turbine expanded the bypass air. This scheme is shown in Fig-1.28 The auxiliary turbine was only operative at lower output shaft speeds when comparatively large quantity of excessive air was available. With this configuration, the very rapid increase in air flow associated with progressive reduction of output shaft speed, due to the speeding up of the compressor cannot be accommodated by the turbine without exceeding reasonable limits of system pressure, therefore some of the air has to be blown off. Later, both turbines were replaced by those of the variable geometry type, Fig-1.29. This greatly facilitated the matching process of the system. In this scheme, both the power turbine and the auxiliary turbine used the mixture of exhaust gas and excess air, with the former being operative only at higher output shaft speeds but the latter at lower output shaft speeds.

The performance of this scheme at the engine speed of 2400 is shown in Fig-1.30. Very high torque rise was obtained. Particularly, at the low output shaft speed region, the output torque increases sharply as the output shaft speed decreases. It should be noted that for these two early schemes, a higher ratio gear is adopted between the auxiliary turbine and the output shaft than that between the power turbine and the output shaft, in order to increase the torque contribution from the auxiliary turbine to the output shaft.

With the adoption of a four-stroke engine, the auxiliary turbine was dispensed with at a later stage, while a bypass duct was introduced to connect the inlet and exhaust system, Fig-1.31. As a result, the boost can be controlled at will through the settings of turbine nozzle angle and bypass valve. In fact, the prototype to date for research work takes this form.

1.4.2 General Characteristics of the DCE

The ultimate scheme of the DCE is shown in Fig-1.32. A further feature is added to the system, viz. a continuously variable transmission between the turbine and output shaft. In the following, various features of the system will be discussed.

a) The epicyclic gear train is the key factor of the DCE and its characteristics, i.e. the speed relationship between annulus, sun gear and planet carrier, or rather, between engine, compressor and output shaft, are shown in Fig-1.33. It can be seen that there can be a wide combination of engine, output shaft and compressor speeds. Therefore the flexibility of the system is enhanced. This means that the engine and the output shaft speeds can be scheduled in such a manner that, for any desired overall system output, optimum efficiency can be achieved.

More importantly, due to the possibility of relatively independent operation of the engine and the output shaft, the output speed and torque can be varied at will while the engine can still be working in a steady manner. Obviously, as the output shaft speed decreases, its torque will increase if the output shaft power is approximately unchanged. Therefore, much higher torque backup can be obtained than that achievable by the engine itself. It can be seen from the speed relationship, that for a constant engine speed, the compressor speed will increase with decrease of output shaft speed. Therefore the mass flow rate of the system can be increased, so that more fuel can be burnt to increase BMEP and power. This will increase the dynamic performance of the system further. This characteristic is highly desirable but is unobtainable with a conventionally turbocharged engine. Actually, with the DCE, due to the ample air supply available at low output shaft speeds, a constant engine power can be achieved over the full output shaft speed range, therefore a continuous torque rise is available with decrease of output shaft speed. For instance, with the Cummins L10 engine having a rated power of 240kW, a torque ratio of about 4:1 is predicted over an output shaft speed range from 2200rpm to 440rpm. With the DCE, the driveability is thus greatly improved. If a suitable torque converter is incorporated, then the use of any form of multi-ratio change speed gearbox can be eliminated, thus substantially simplifying the transmission system.

Apart from the epicyclic geartrain, there are other aspects which are distinct features of the DCE.

b) The compressor in the DCE is of the rotary positive displacement type; a typical characteristic of such a machine is shown in Fig-1.34. This choice is made to overcome the twin problems associated with the widely used centrifugal compressor, viz. surge and choking. Due to the wide mass flow range required by the system, the centrifugal type with its narrow flow capacity is unsuitable. For example, at full load higher pressure ratios are required over the entire output shaft speed range, particularly at low output shaft speed, therefore surge would be

unavoidable for a centrifugal type. Additionally, use of positive displacement compressor makes the match between the engine and the compressor much easier, because the engine has the similar flow characteristics.

c) Instead of direct linkage between turbine and compressor, the latter is geared to the sun gear while the exhaust turbine is geared to the output shaft. This arrangement has the following implications: (1) The compressor is driven by the sun gear, sufficient power is always available. This overcomes the problem associated with the conventional turbocharging system in which the power supply to the compressor from the turbine is insufficient at low speed and low load while excessive power is available at high speed and load. (2) The connection between turbine and output shaft gives the possibility of better utilisation of the exhaust energy. Because the constraint of direct coupling to the compressor is eliminated, the turbine can be scheduled to run under optimum working conditions. This is realised by the application of a variable nozzle turbine and a continuously variable transmission system interposed between the turbine and the output shaft. By controlling the turbine nozzle angle the optimum turbine power can be obtained without impairing the engine operation by excessive back pressure, while the operation of the CVT can further improve the turbine efficiency by adjusting its blade speed ratio.

d) The bypass duct provides an alternative air path at low output shaft speed when compressor speed is high and excessive air flow is provided relative to engine demand. Basically bypass flow is undesirable, because excessive power is consumed by the compressor, while at the same time turbine inlet temperature coupled with low turbine efficiency, and hence specific power output are reduced. However, the excess air present in the system can be regarded as a torque conversion medium, leading to high output torque. Controlling this excess air by the bypass valve contributes to the excellent transient response of the DCE.

It can be seen that DCE system has a high degree of flexibility. By carefully specifying the value of every individual variable, the state of the system can be determined at which best performance is achieved. However, this also means increased complexity. Therefore a fairly sophisticated control system is required.

In the theoretical part of this thesis the concept of the DCE is applied to the Cummins L10 engine. The work is mainly concentrated on steady state performance prediction and optimisation. Emphasis is placed on the effects of changing ambient conditions on the system performance. In addition, the characteristics of the DCE

are compared with those of the equivalent conventionally turbocharged engine, both system being analysed with fixed nozzle and variable nozzle turbines.

1.5 The Effects of Changing Ambient Conditions[31,32,33]

Vehicle engines are required to work under varying ambient conditions. Naturally this will affect the operation of the compressor, and the trapped conditions will vary. In turn, the performance of the engine cycle will be affected, as will the exhaust conditions, which determine the operation of the turbine. Because of the connection between the turbine and the compressor, there will be some feedback from the former to the latter. As can be seen from Fig-1.35, this is rather complex in nature. For example, higher ambient temperature will result in higher intake temperature, which will lead to higher compression temperature, and hence to better fuel/air mixing, shorter ignition delay and probably smoother combustion. On the other hand, higher ambient temperature means lower intake density, therefore lower air/fuel ratio, this will affect the engine operation adversely. Changes in ambient pressure will also impose drastic changes on the system. Therefore, the outcome will be the result of complex interactions among numerous factors and processes.

The direct result of changes in ambient conditions is the variation in mass flow rate through the system, which will affect engine and therefore overall performance. Firstly, the engine must operate above the minimum permissible air/fuel ratio. Further, there are various limitations on the operation of the system, e.g. mechanical and thermal stresses. For the engine, the maximum cylinder pressure, the exhaust temperature and smoke level are important parameters, the former two being concerned with mechanical and thermal loading. For the turbocharger, both maximum speed and turbine inlet temperature can be limiting factors.

Because of their different structure and characteristics, changes in ambient condition will affect the operation of the turbocharged engine and the DCE in different ways.

a) Turbocharged Engine System When the ambient pressure is reduced, the mass flow through the system will be reduced, although the turbocharger can adjust itself, to some extent, to compensate for this effect, as a result of the engine operating with lower air/fuel ratio hence with increased exhaust temperature. By this process, the turbocharger speed is increased. Obviously, if either turbocharger

speed or exhaust temperature exceed their permissible limits, measures have to be taken to correct this. One approach is to adjust the injection timing. However, if this is not effective enough, then fuelling may have to be reduced. Due to the special match between the engine and the turbocharger, boost ratio increases with engine speed. Therefore, air/fuel ratio will be higher at higher speeds but lower at lower speeds. If further decrease in mass flow occurs, the air/fuel ratio at lower speed will be even worse. Lower air/fuel ratio will lead to lower thermal efficiency. Furthermore, lower air/fuel ratio tends to increase smoke emission. Again, it may be necessary to reduce the fuelling to keep the smoke within its permitted level.

Elevation of ambient temperature will produce similar effects: reduced mass flow rate but without any compensating action whatsoever. Therefore, it seems that this will affect the system operating conditions more severely compared reduction in ambient pressure. It is more likely that some of the system parameters will exceed their limiting values and fuelling will have to be reduced.

b) The DCE The operation of the DCE is likewise subject to the influence of changes in ambient conditions. Interestingly, the DCE can also compensate, to some extent, for the mass flow reduction caused by reduction in ambient pressure, by increasing the compressor pressure ratio. This is due to the power distribution between the ring gear, planet carrier and the sun gear. Further, by altering the engine operating conditions, e.g. varying its speed for constant power, the mass flow rate through the system can be varied, thus satisfying the engine demand. For example, due to decrease in ambient air density resulting from reduction in ambient pressure or elevation in ambient temperature, there can be a mass flow shortage relative to engine mass flow demand. This situation can be adjusted by increasing the engine speed, therefore compressor mass flow is increased.

Automatically, reduction in ambient air density will result in decrease in mass flow rate. Therefore lower air/fuel ratio and higher exhaust temperature. However, due to the inherent flexibility mentioned above, this can be remedied by increasing engine speed, if allowed. In this process, air flow is increased while fuel flow remains unchanged, therefore air/fuel ratio will increase. Because of the relative independent operation of the engine and output shaft, comparatively stable output can be maintained.

A consequence of the application of the epicyclic geartrain in the DCE is that at lower output shaft speed, the compressor speed is higher. When the system works at altitude, the boost ratio tends to increase further. Therefore, a compressor

of high pressure ratio capacity is required. It is also important that under extreme pressure ratios, reasonable compressor efficiency can be achieved.

It should be noted that although the operation of the systems over their entire operating range will be affected by the changes in ambient condition, the operation at full load is of the most importance, which denotes the maximum capacity of the system. Further, it is under this operating condition, there is the danger for the various parameters to exceed their respective limits, therefore the performance should be particularly observed. Nevertheless, again because the wide operating range of the systems, it is worthwhile to have an idea of what happens at part load operation.

1.6 Scope of this Thesis

The bulk of the work described in this thesis is concerned with a detailed performance assessment, based on the Cummins L10 6 cylinder DI Diesel engine, of turbocharged and differentially compounded systems operating both under sea level and high temperature, high altitude conditions. The objective of this work is to show the considerable operational advantages of the DCE system over the conventional turbocharged engine in terms of

**a) Superior torque back up making possible a stepless transmission system,
and**

b) Reduced sensitivity to changing ambient conditions.

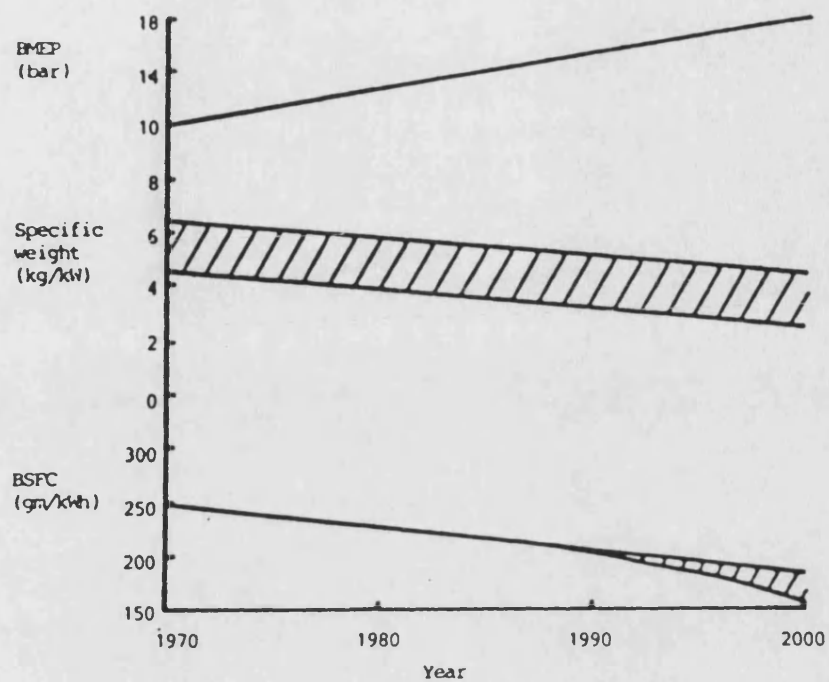


Fig-1.1 Diesel engine development predictions by Muller

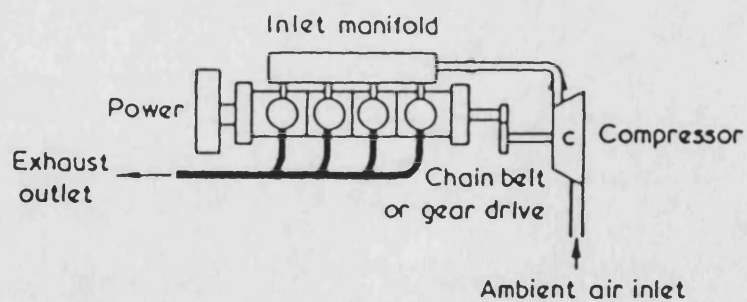


Fig-1.2 Typical arrangement of an engine fitted with a mechanically driven supercharger

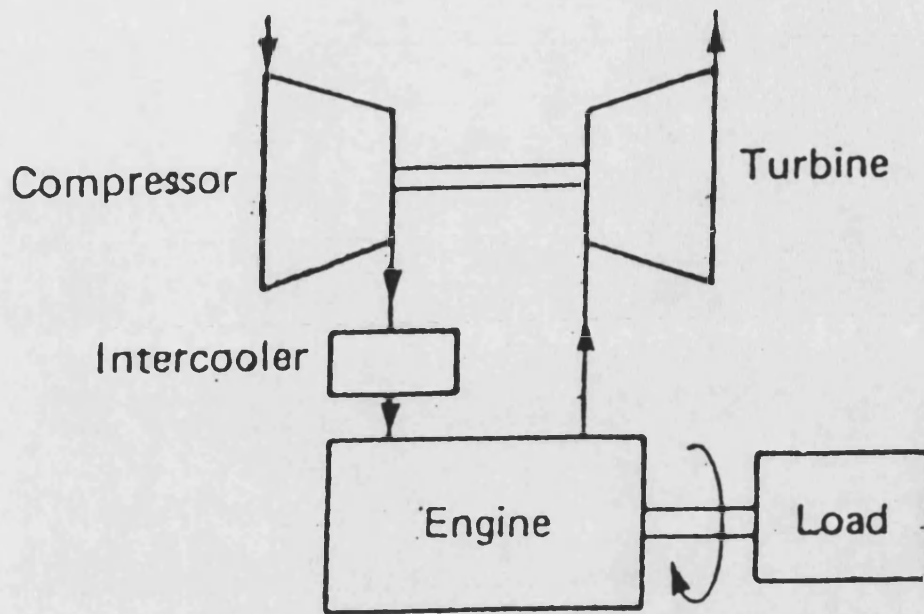


Fig-1.3 A schematic of turbocharged intercooled engine system

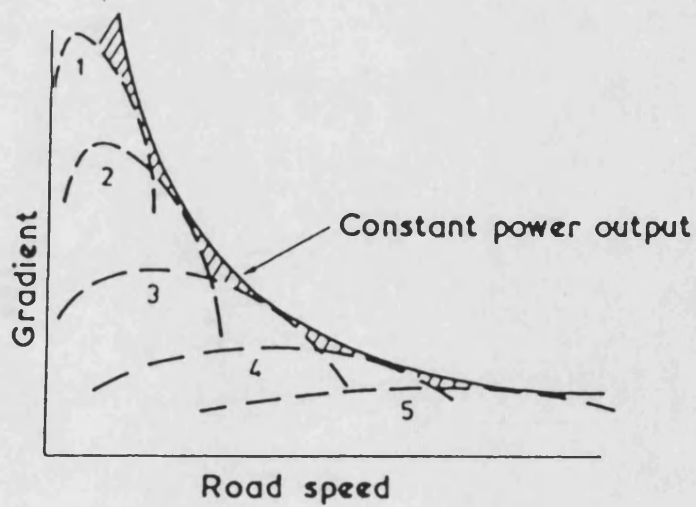


Fig-1.4 Gradient against speed ability of a track with a five-speed gearbox

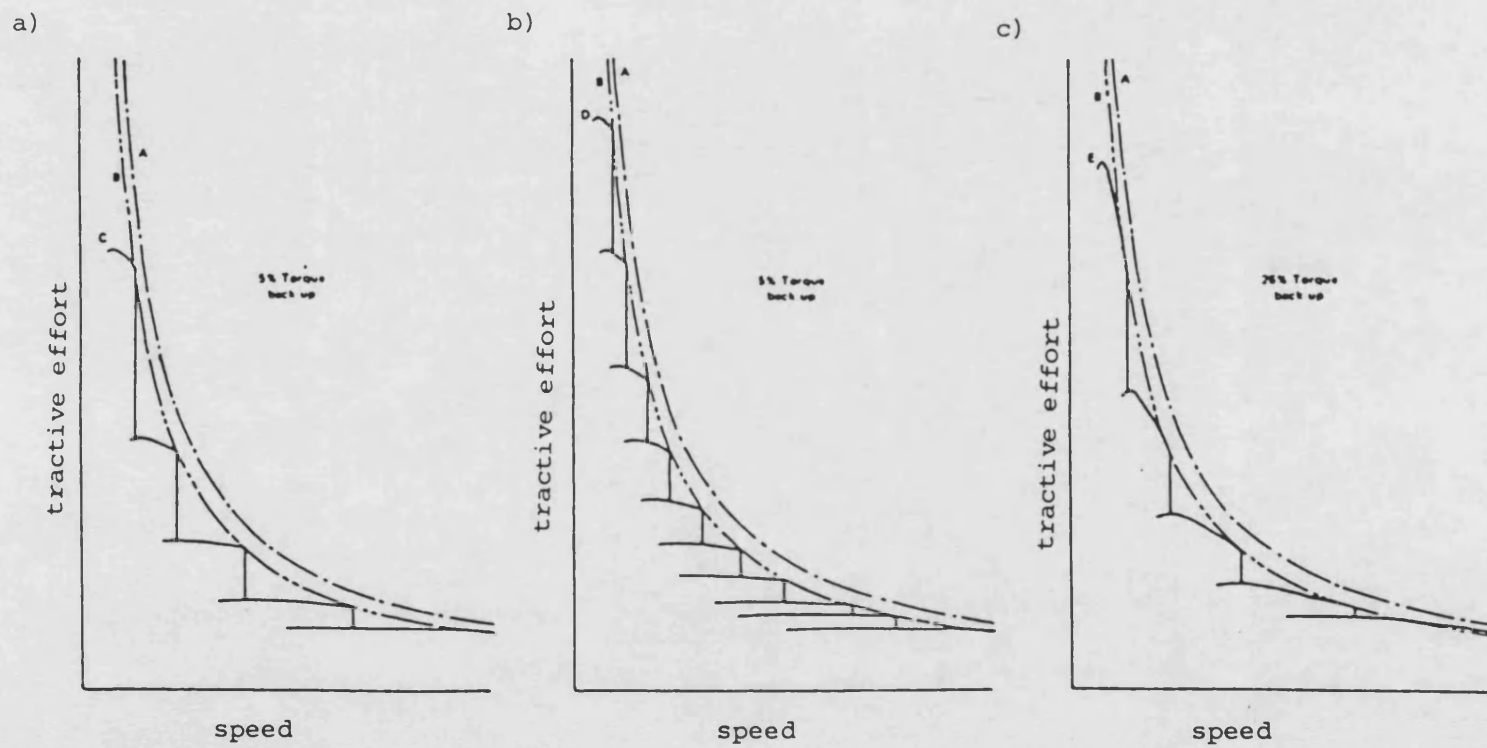


Fig-1.5 The effects of torque backup and gearbox on tractive effort

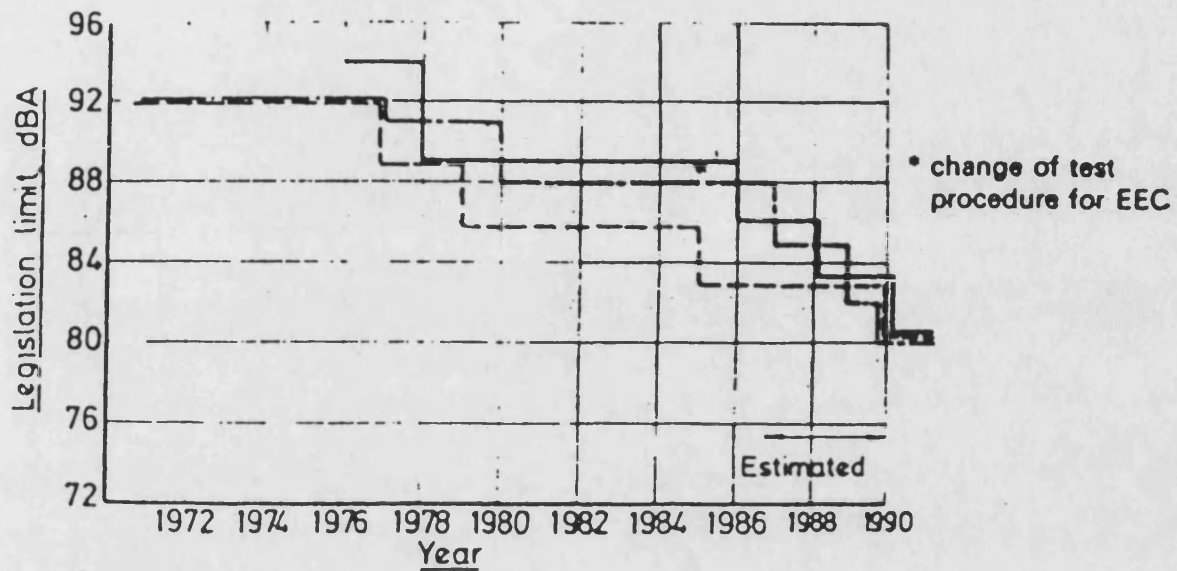


Fig-1.6 Noise limits-past, present and future for heavy trucks

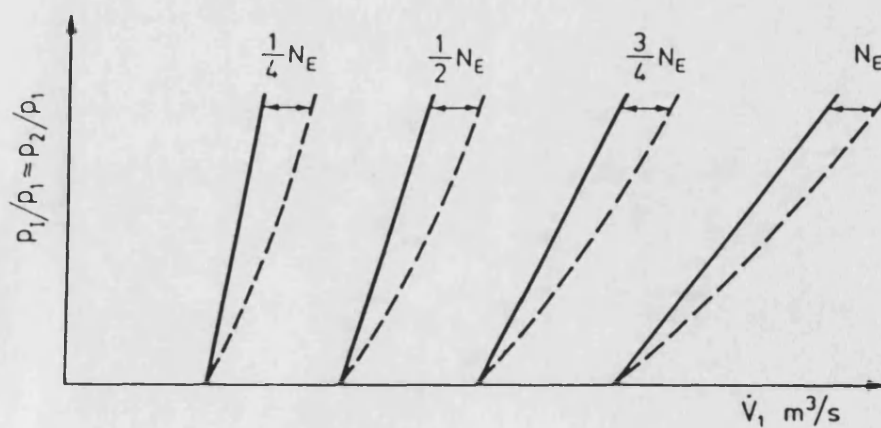


Fig-1.7 Speed characteristics in the pressure/flow rate map of a four-stroke engine

————— without valve overlap
 - - - - - with valve overlap

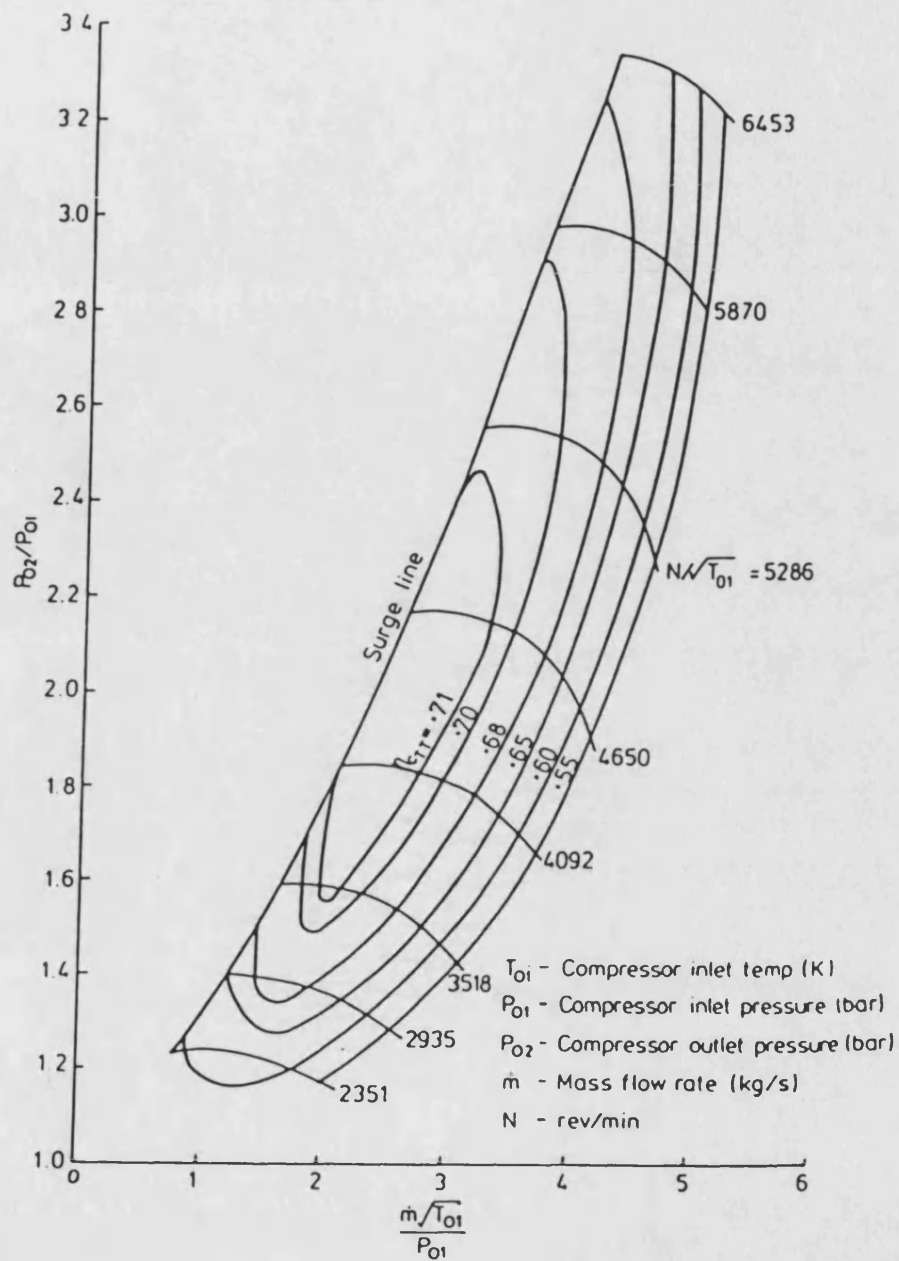


Fig-1.8 Compresor characteristics

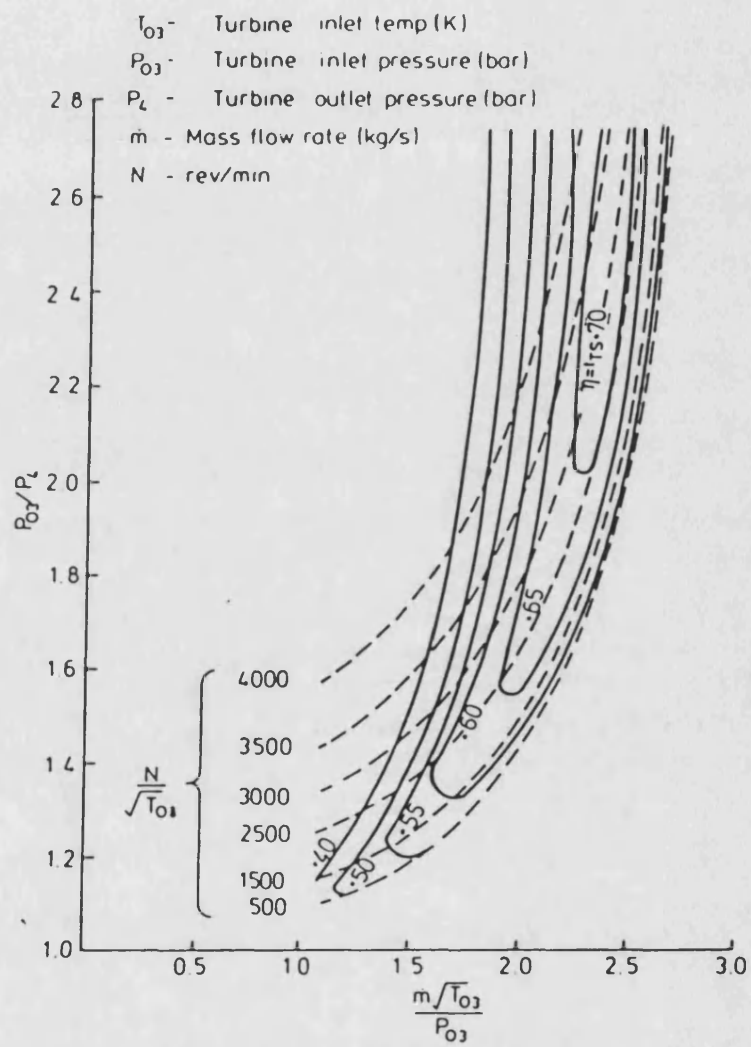
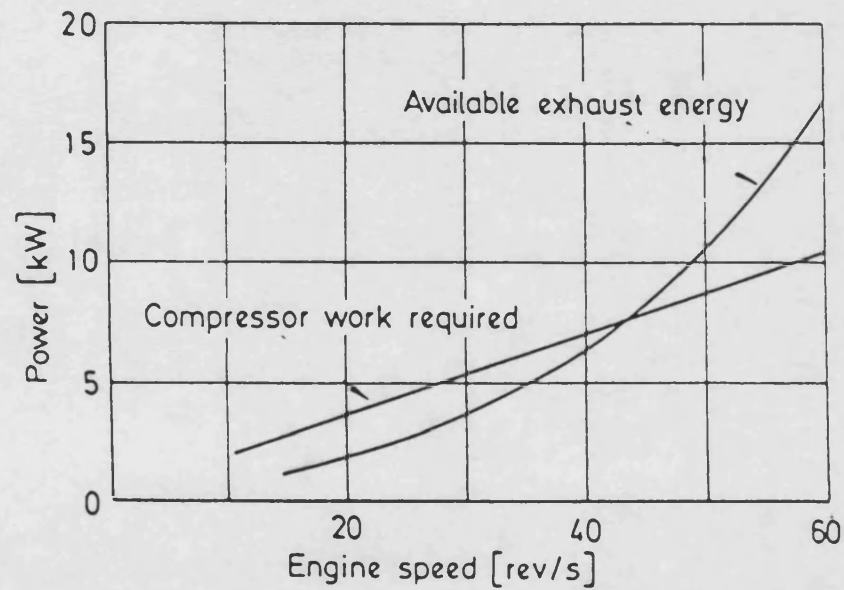
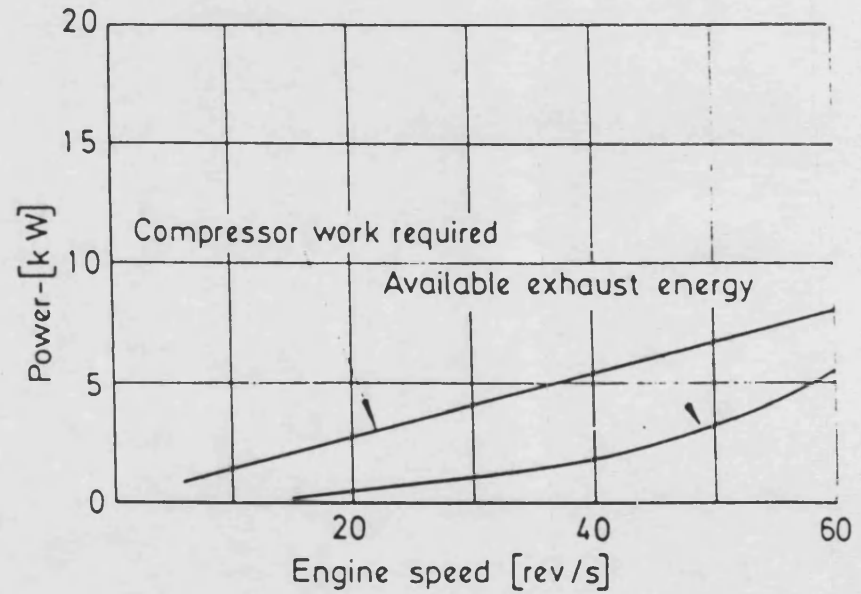


Fig-1.9 Turbine characteristics



a) at full load



b) at no load

Fig-1.10 Available exhaust energy and compressor work with 2:1 BDR
(3.61 diesel engine)

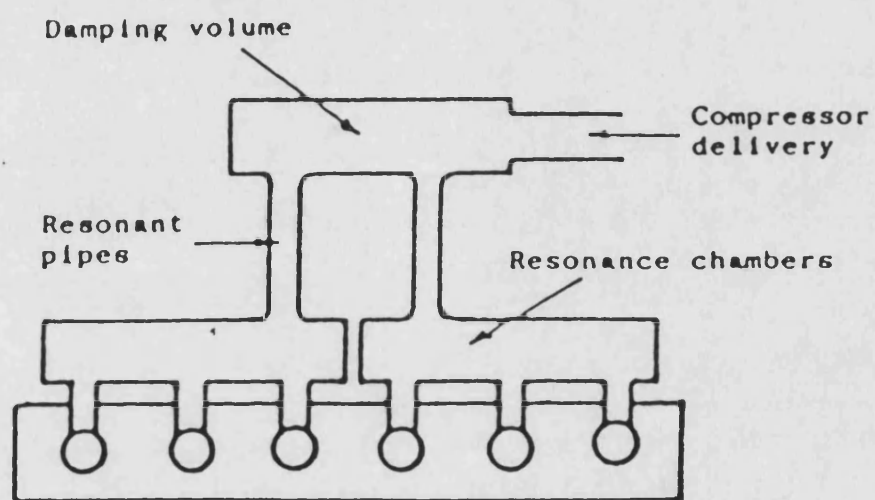


Fig-1.11 A schematic of resonant intake system

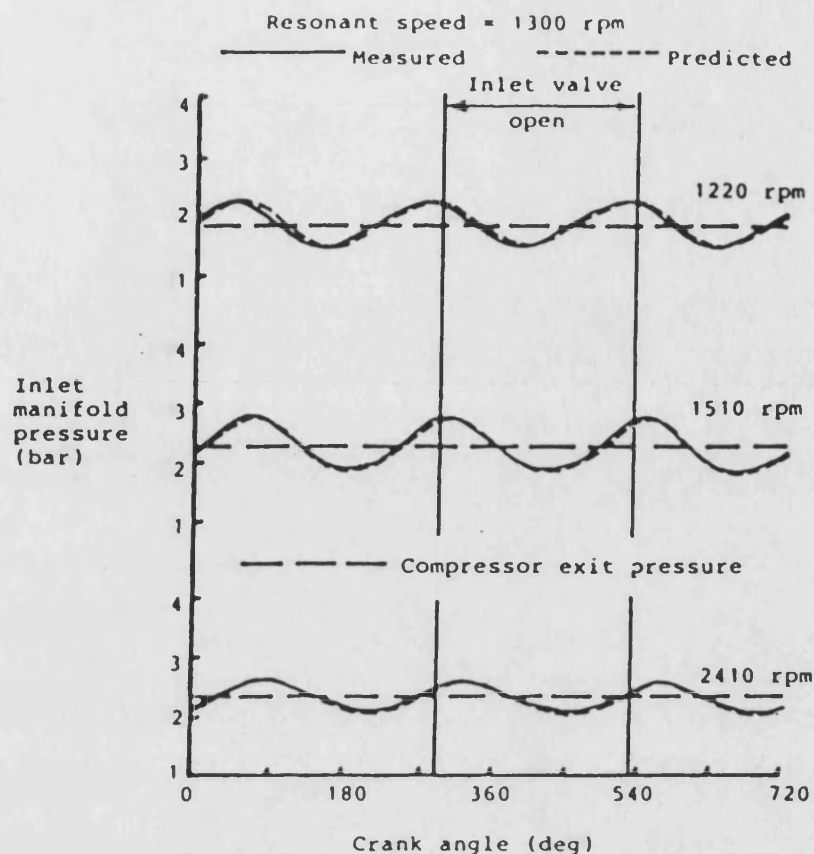


Fig-1.12 Measured and predicted pressure oscillations with a resonant inlet system on a 6-cylinder engine.

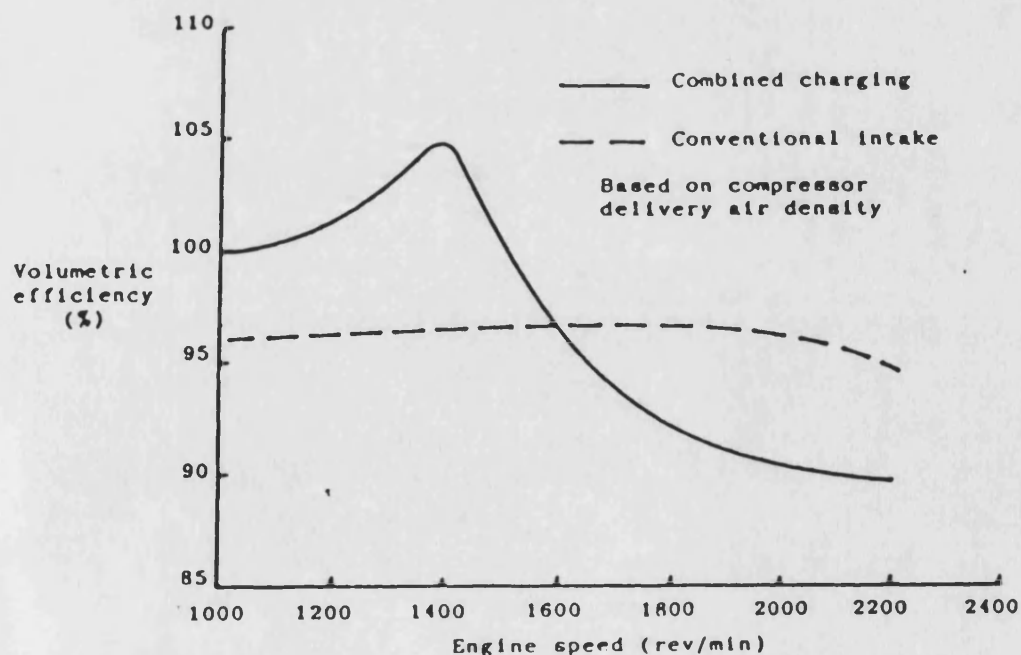
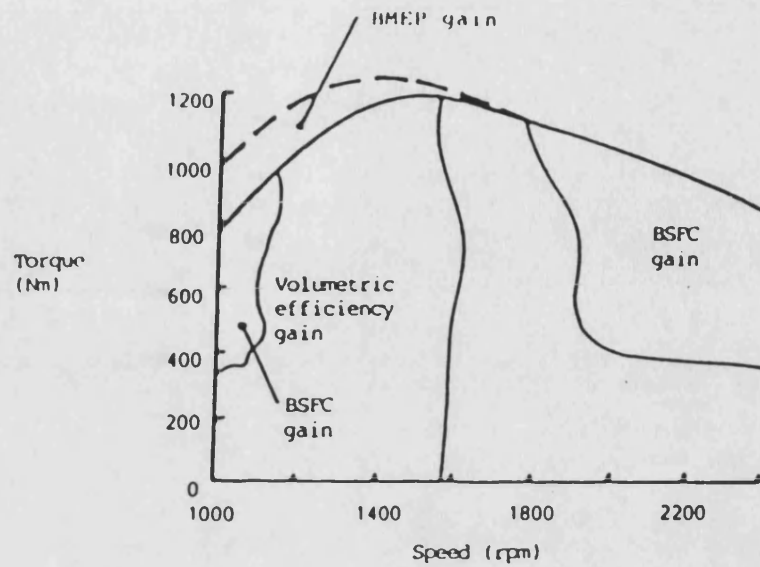
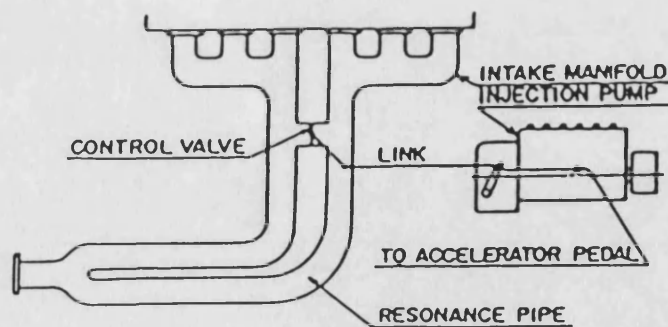


Fig-1.13 The effect of the resonant intake system on the volumetric efficiency

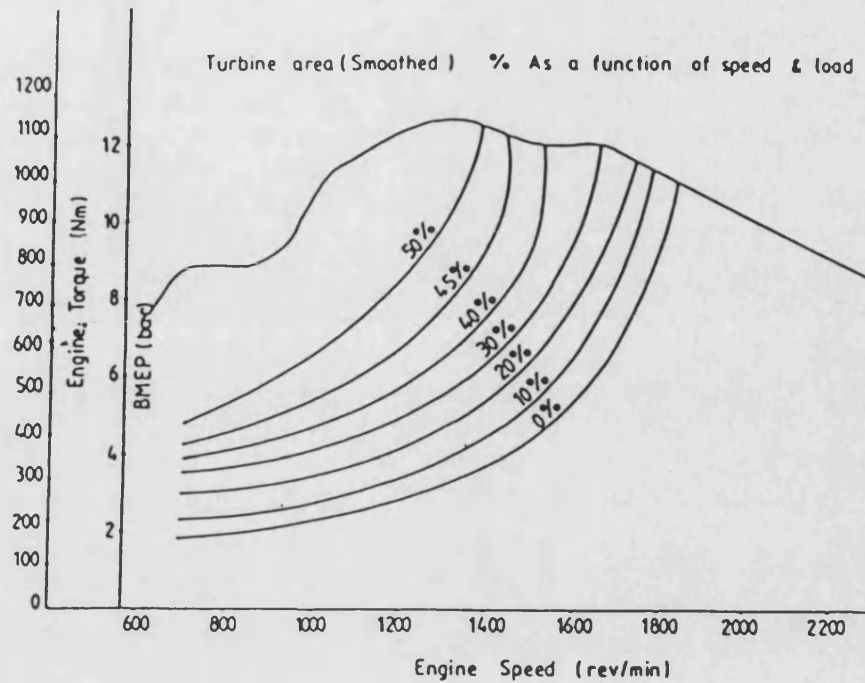


- a) Volumetric efficiency, BMEP and BSFC gains with resonant intake system on highly rated 6-cylinder engine (18.5 bar BMEP at 1250 rev/min).

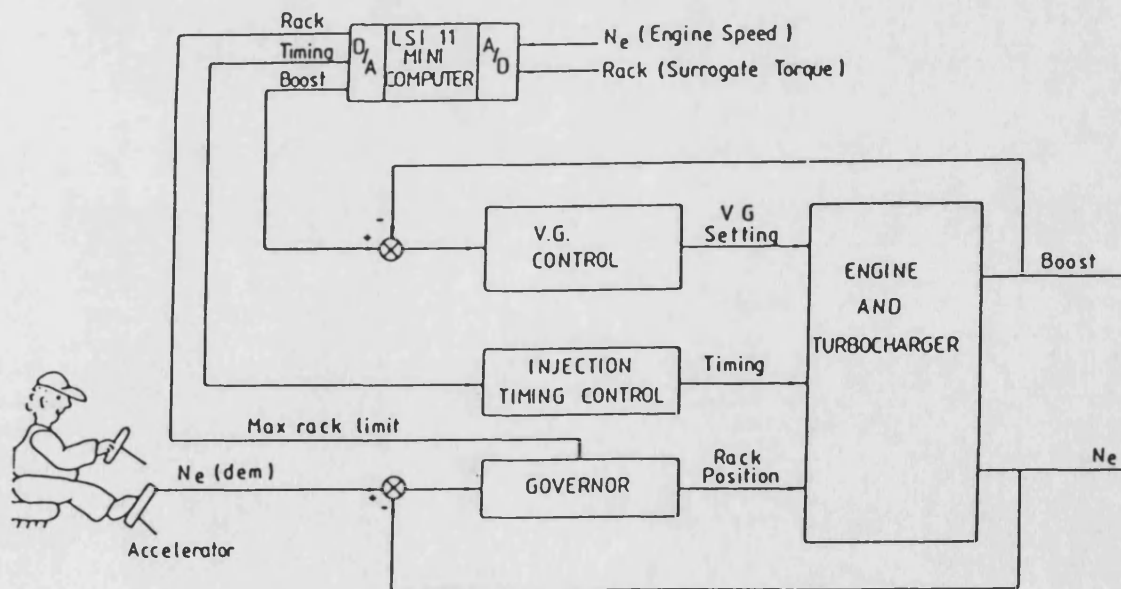


- b) Variable controlled inertia charging system

Fig-1.14 The resonant intake system by Hino and its performance

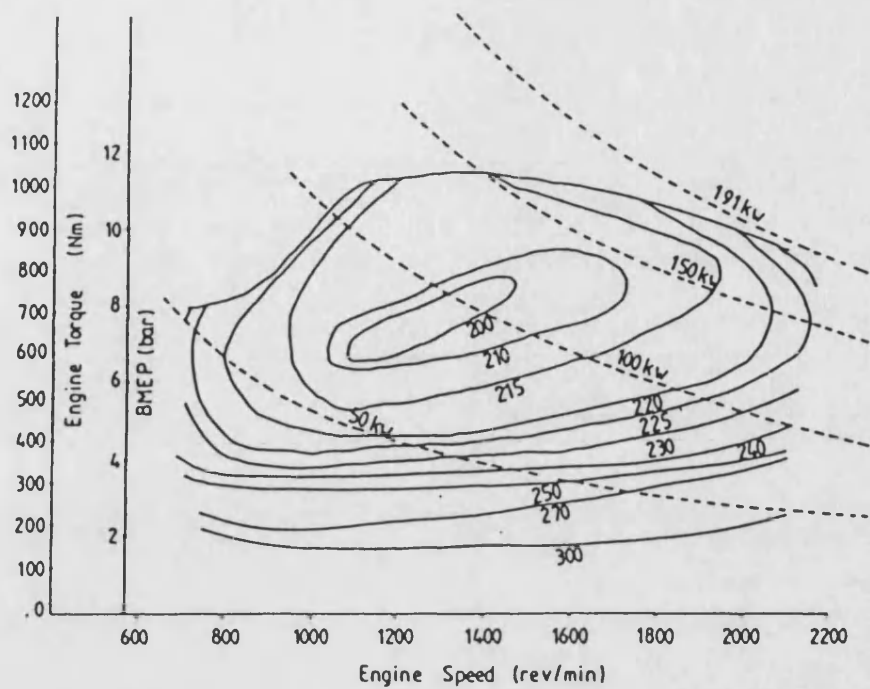


a) Steady state optimization — lines of constant variable geometry setting

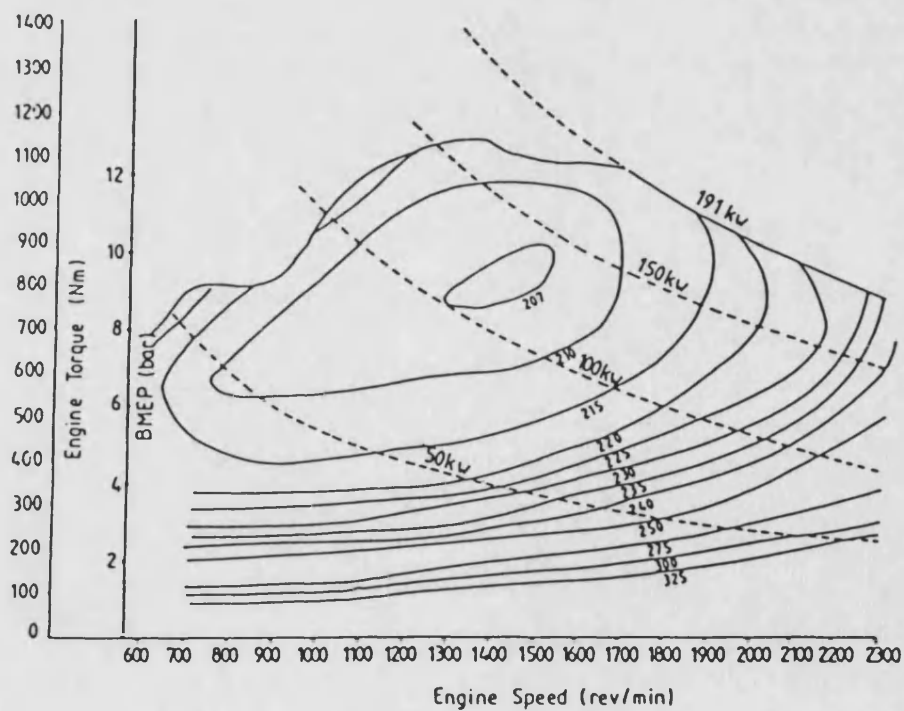


b) Schematic of computer control

Fig-1.15 The performance and control of a VG turbocharged engine system



a) Baseline engine performance map



b) Steady state optimization (fully optimized system)

Fig-1.16 Comparison between the base line (turbocharged) and optimised VG turbocharged engine performance

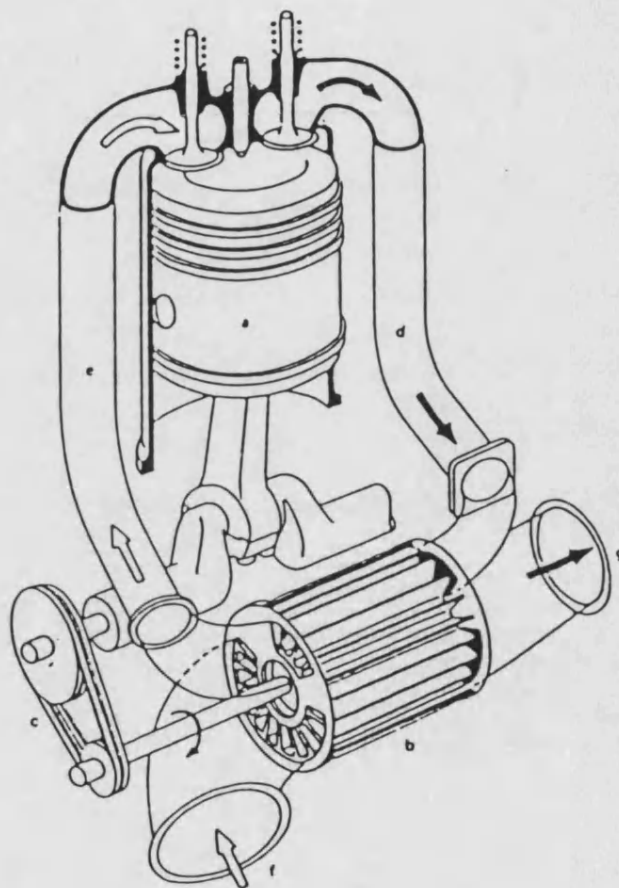


Fig-1.17 The schematic of the Complex

- a) Engine
- b) Cell-wheel
- c) Belt-drive
- d) High pressure gas
- e) High pressure air
- f) Low pressure air
- g) Low pressure gas

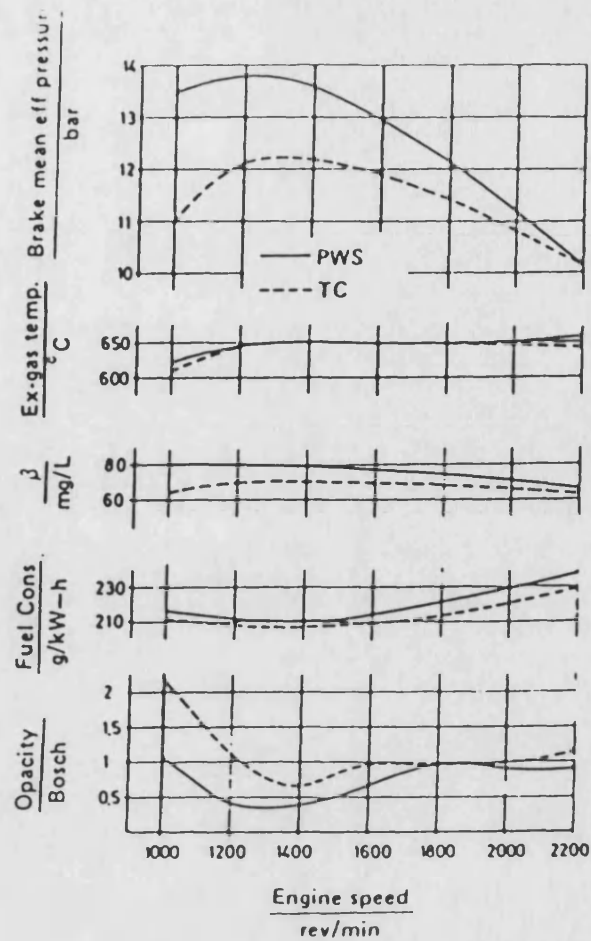
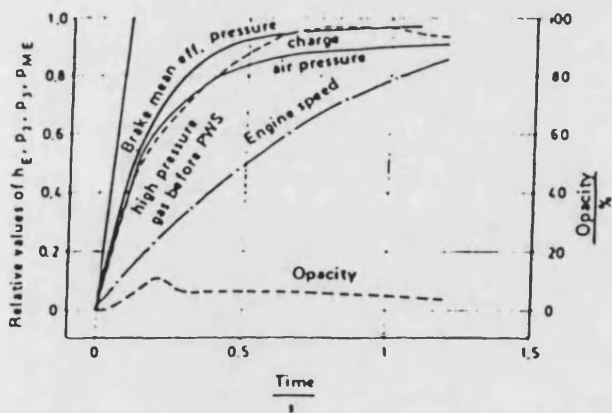
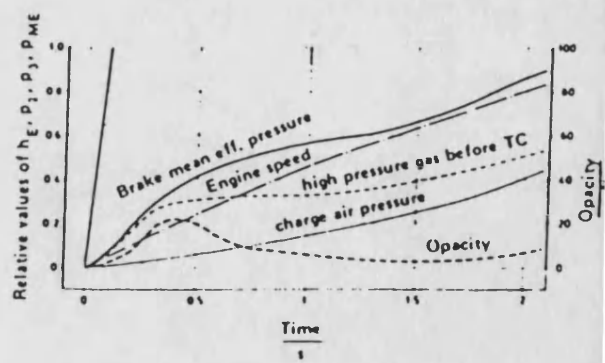


Fig-1.18 Limiting torque curve of TC and PWS systems



On-load acceleration with PWS



On-load acceleration with TC

Fig-1.19 The transient characteristics of TC and PWS systems

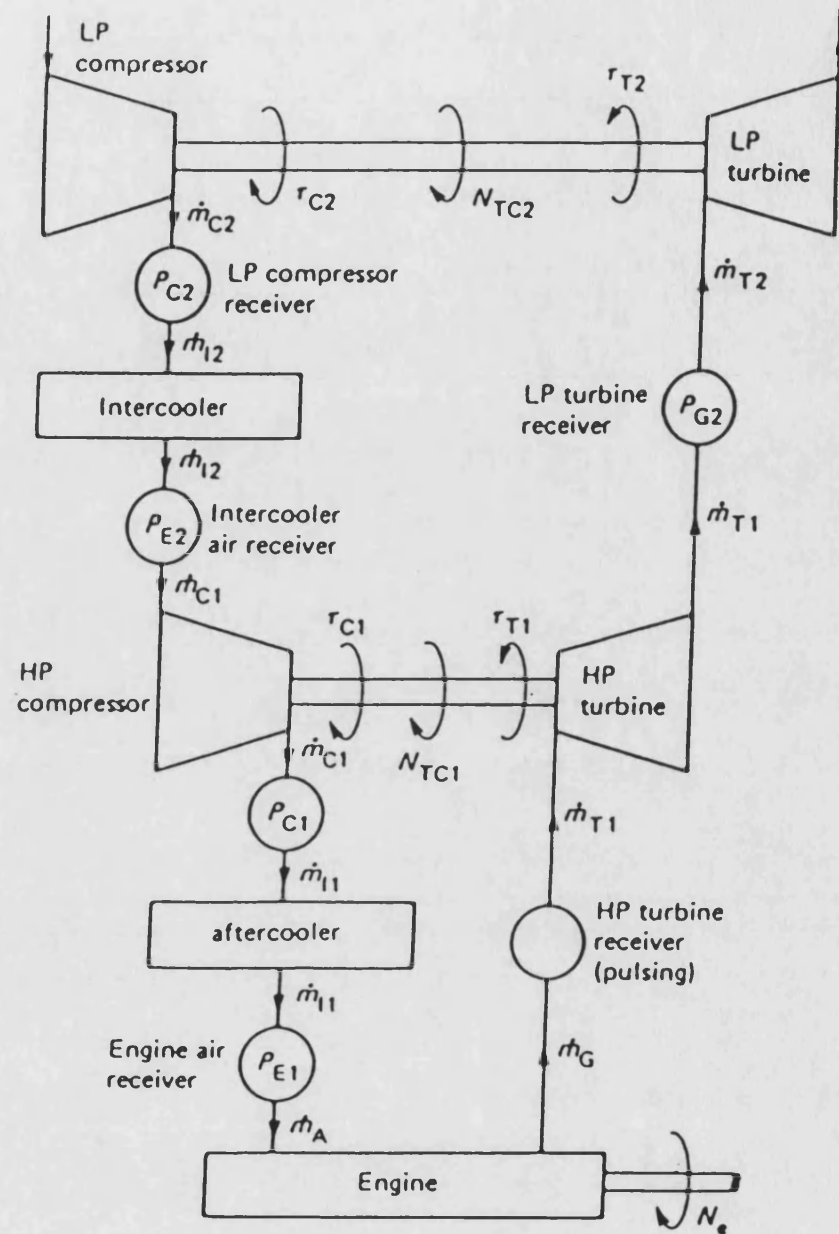
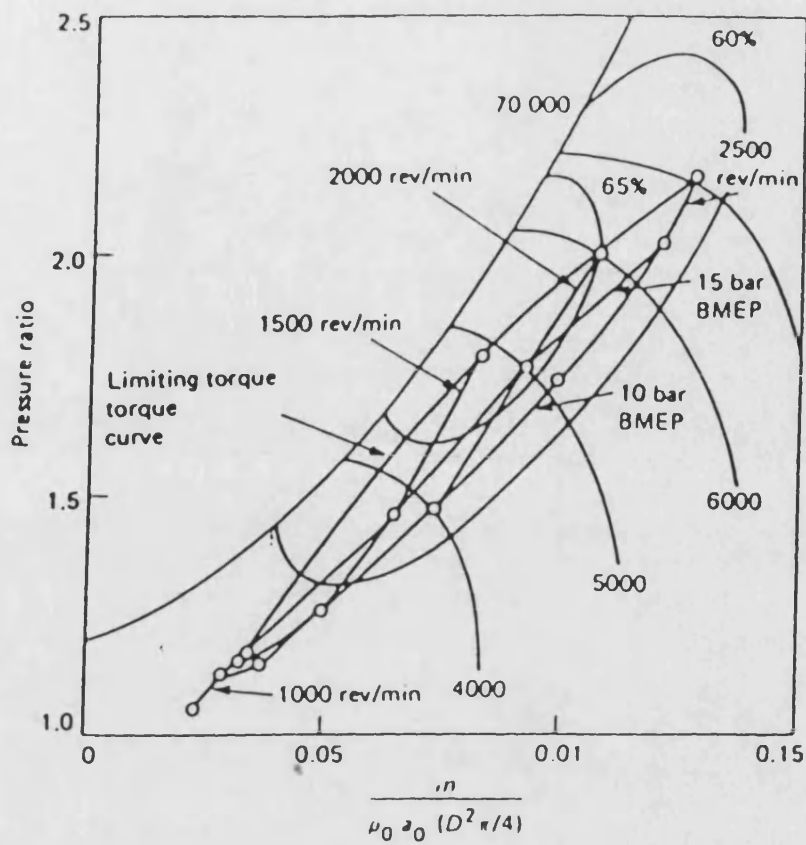
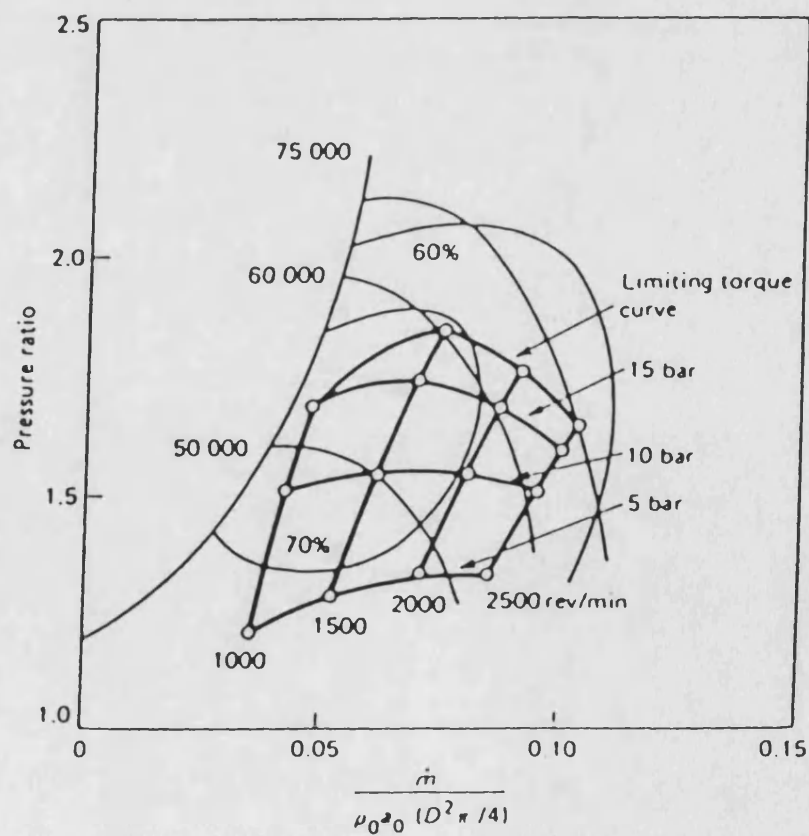


Fig-1.2o The layout of two stage turbocharged engine



(a) LP compressor map (two stage turbocharging)



(b) HP compressor map (two stage turbocharging)

Fig-1.21 The operating points on the LP and HP compressor map

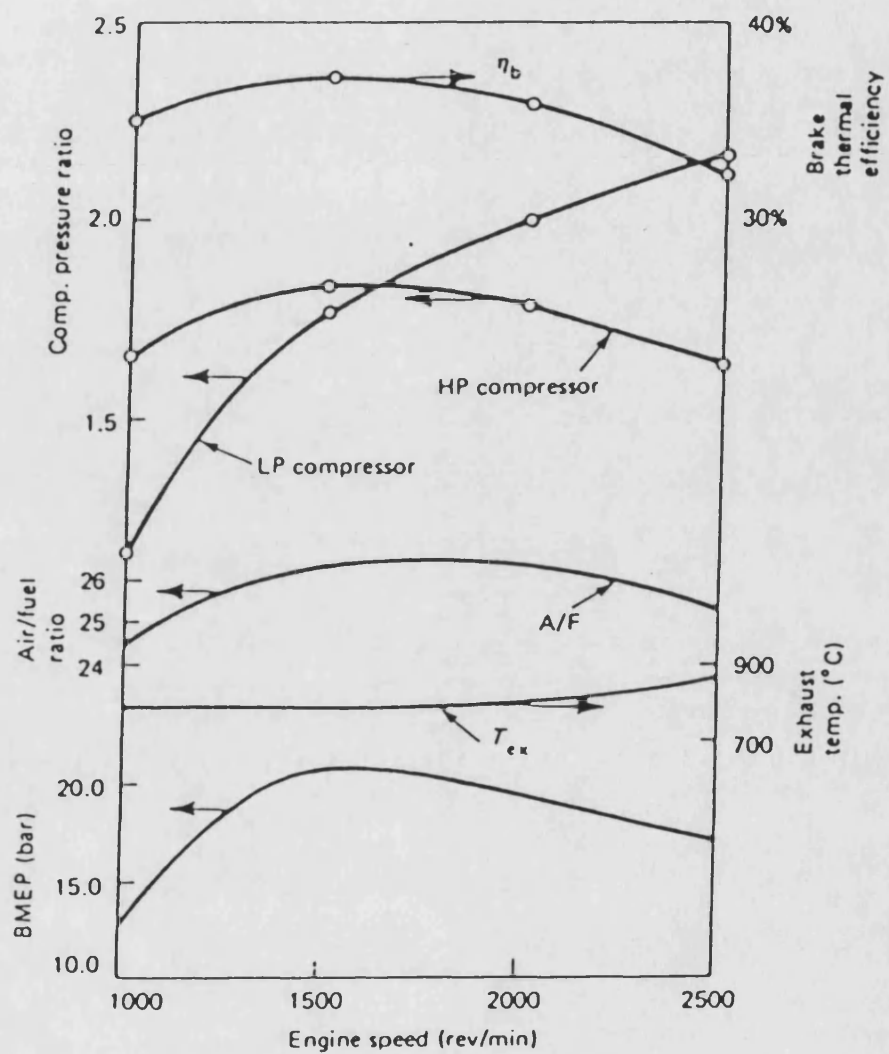


Fig-1.22 The limiting torque curve performance of two stage turbocharged engine

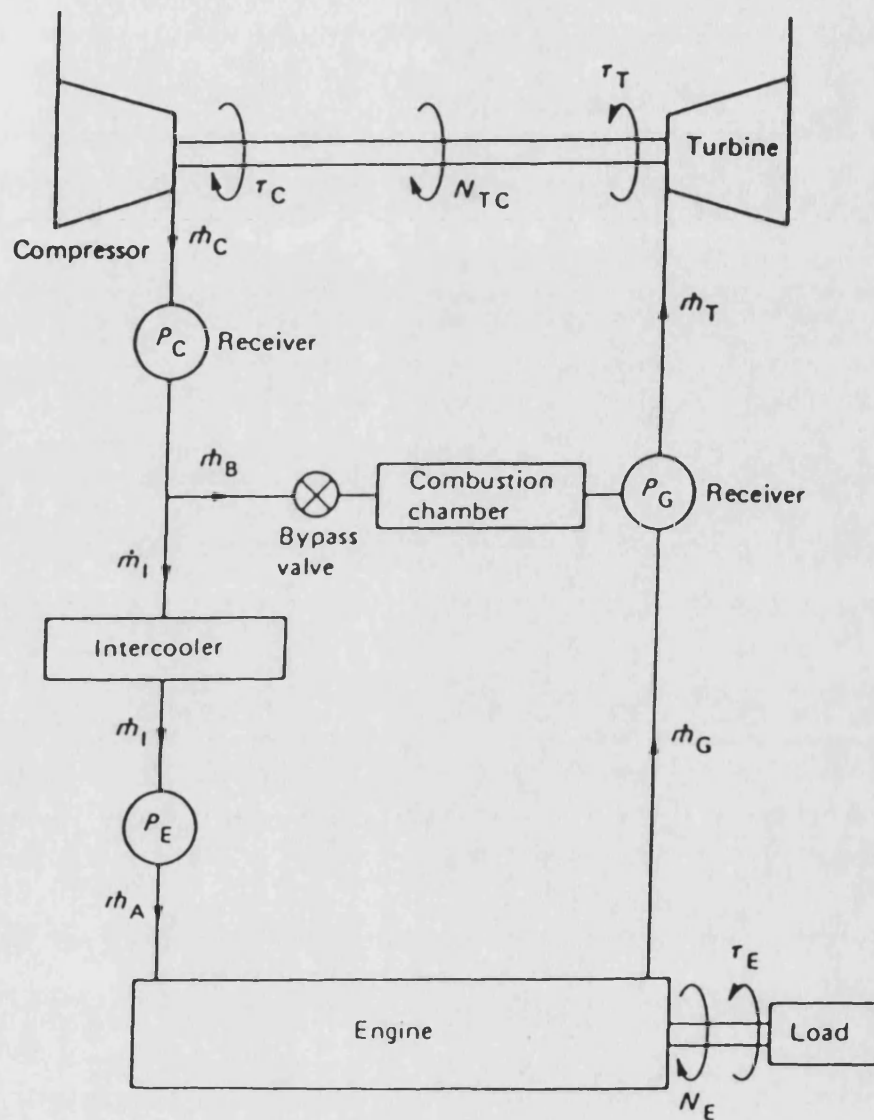


Fig-1.23 The layout of Hyperbar turbocharging system

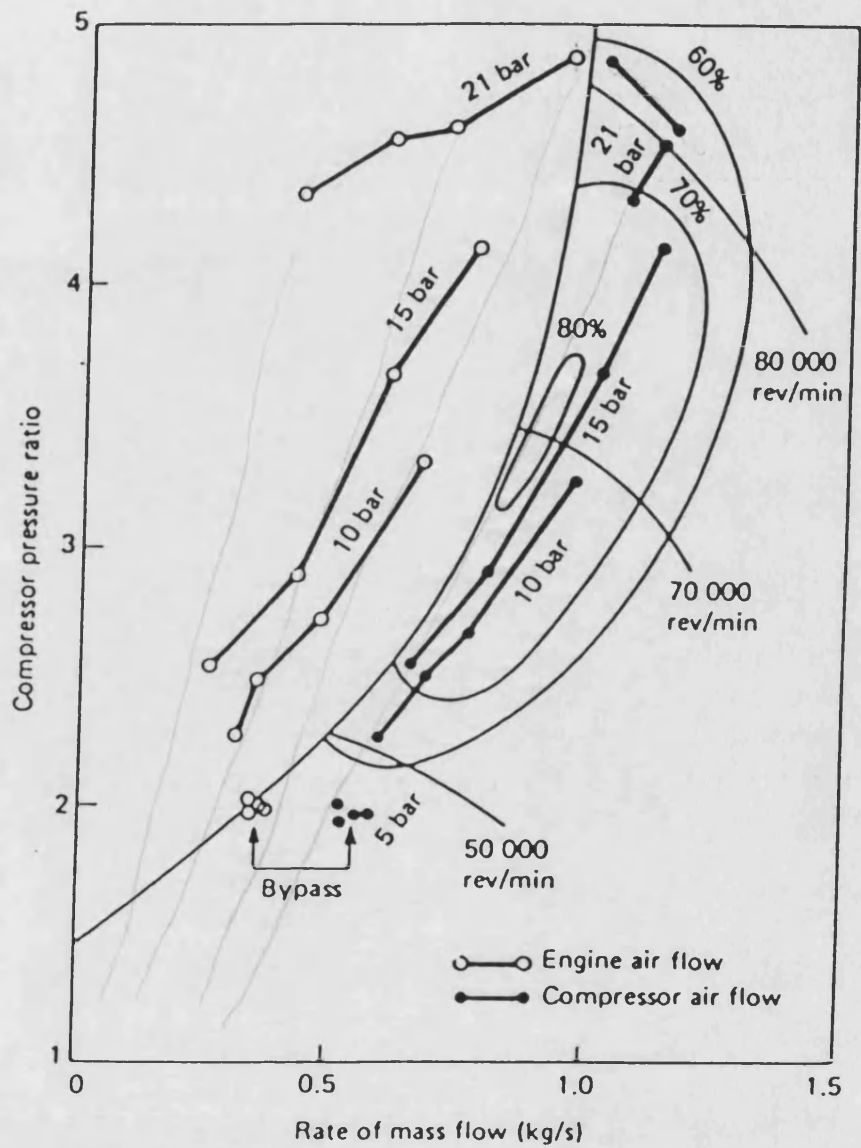


Fig-1.24 The operating points of the Hyperbar system on the compressor map

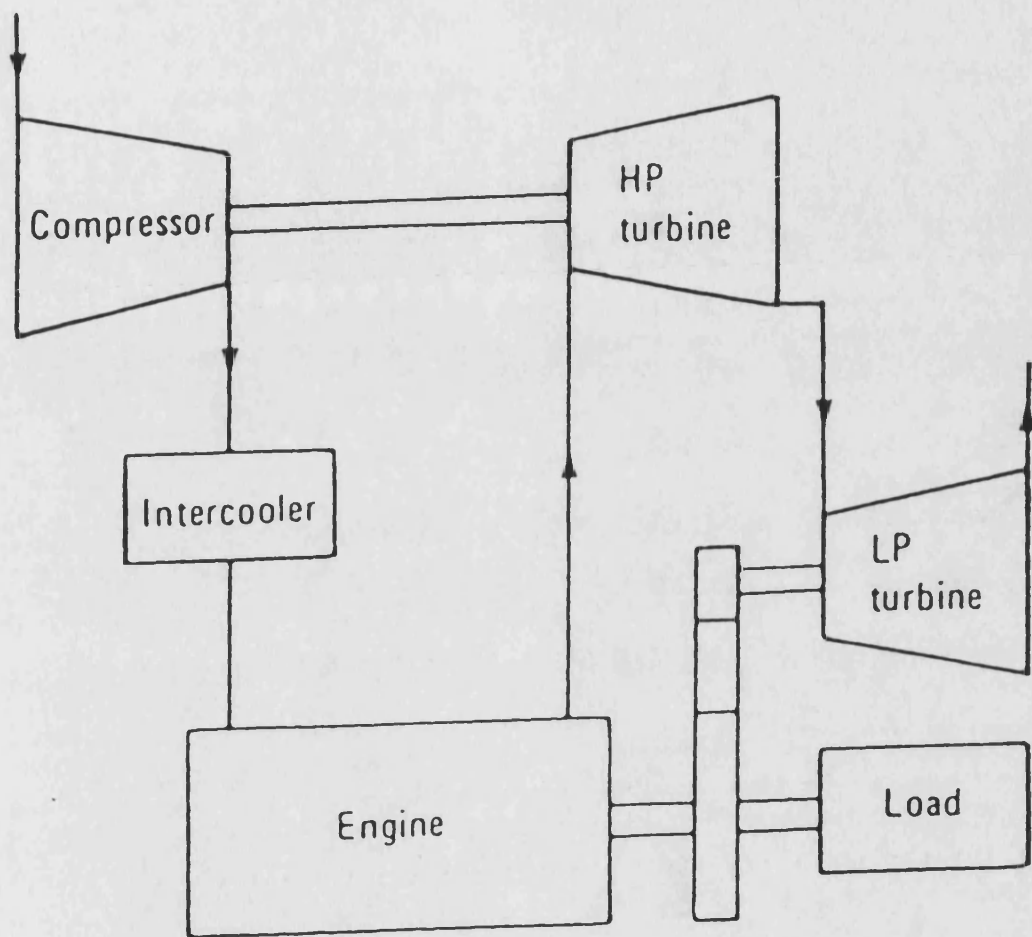


Fig-1.25 Cummins compound engine scheme

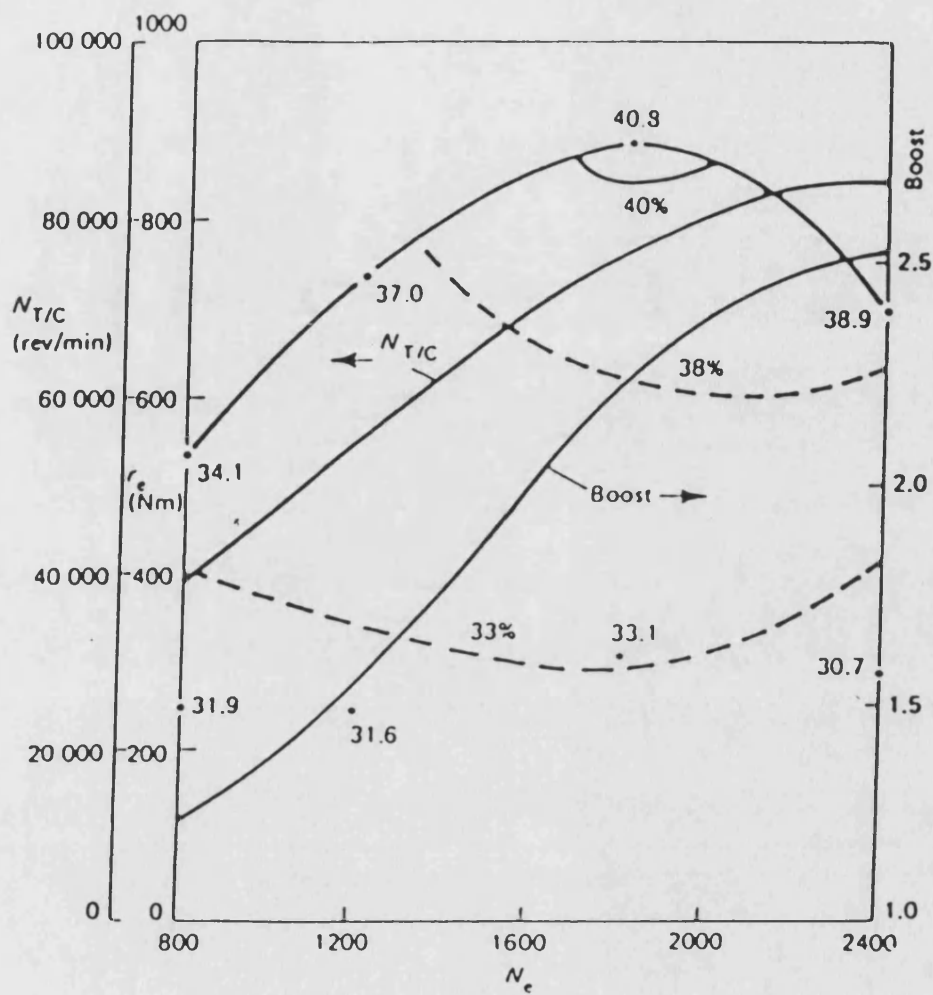
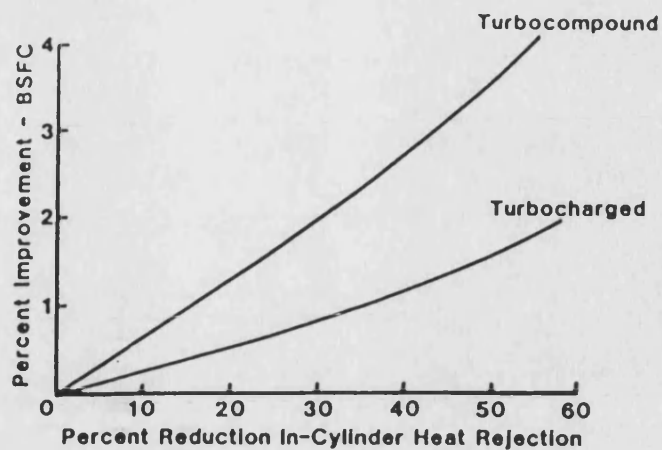
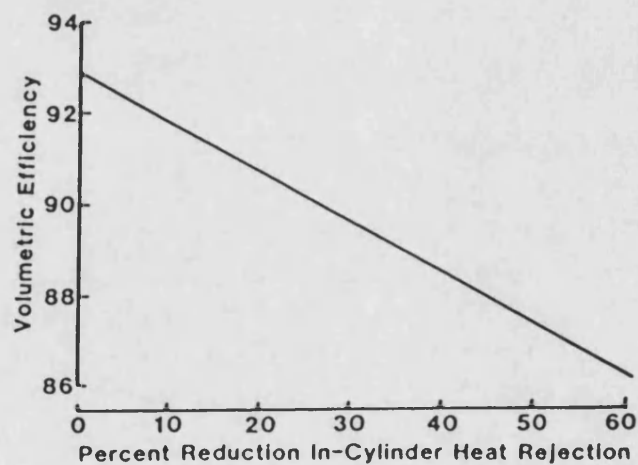


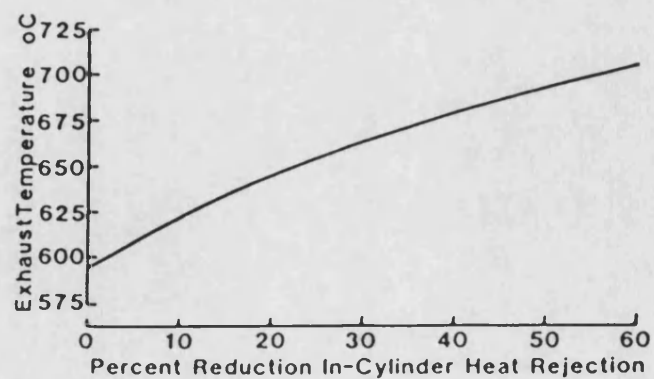
Fig-1.26 Operating characteristics of Cummins compound engine



Effect of insulation under turbocharged turbocompound conditions (liner insulation is 1/2 thickness of piston, head insulation).



Effect of insulation on volumetric efficiency



Effect of insulation on exhaust temperature.

Fig-1.27 The effects of insulation on engine performance

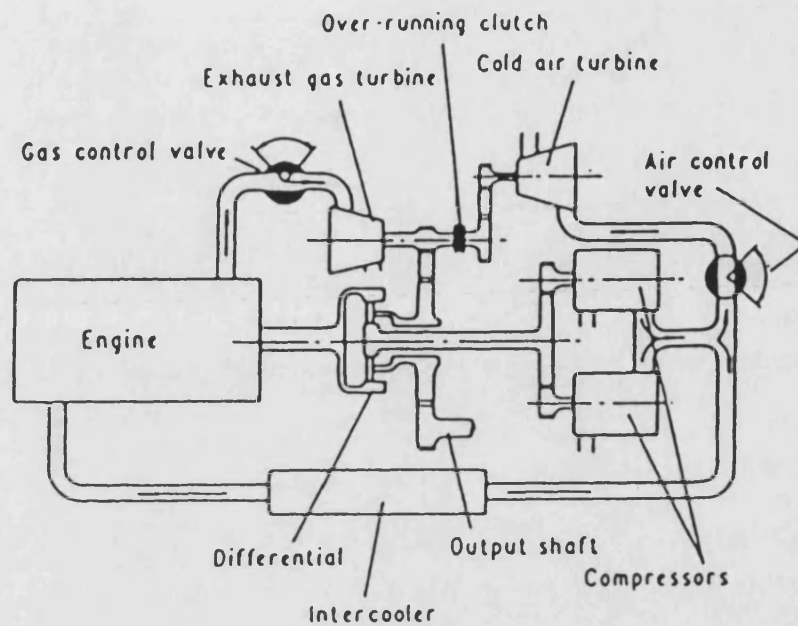
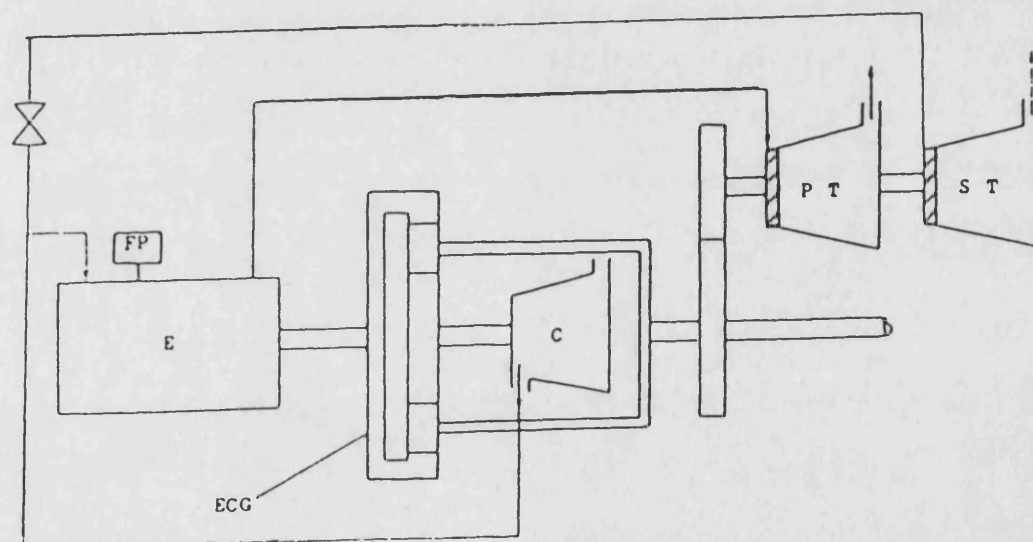
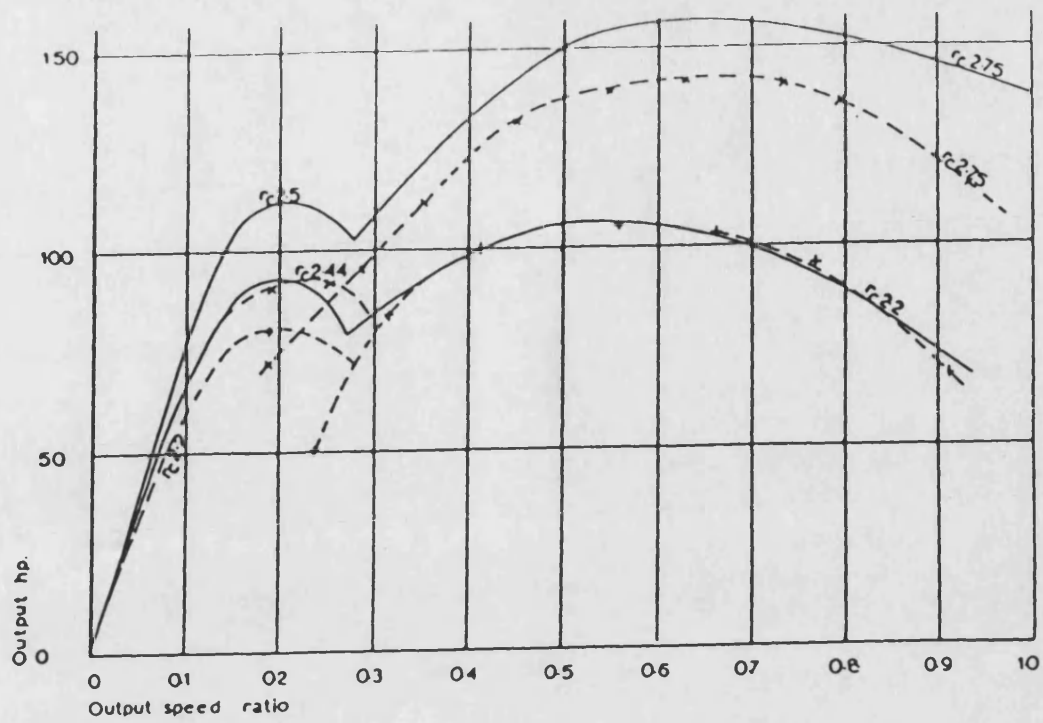


Fig-1.28 The original schem of the DCE

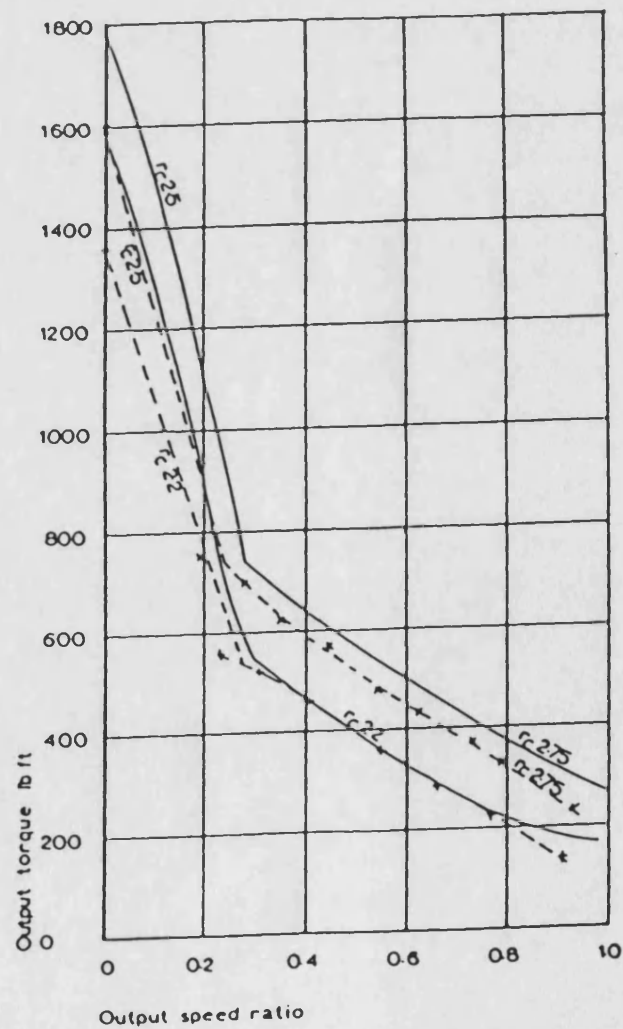


E	: ENGINE	C	: COMPRESSOR
FP	: FUEL PUMP	PT	: POWER TURBINE
ECG	: EPICYCLIC GEARTRAIN	ST	: STALL TURBINE

Fig-1.29 Modified DCE scheme (variable nozzle turbine)



Output power at 2400 rpm engine speed



Torque at output engine speed of 2400 rpm

Fig-1.3o The performance of the modified DCE

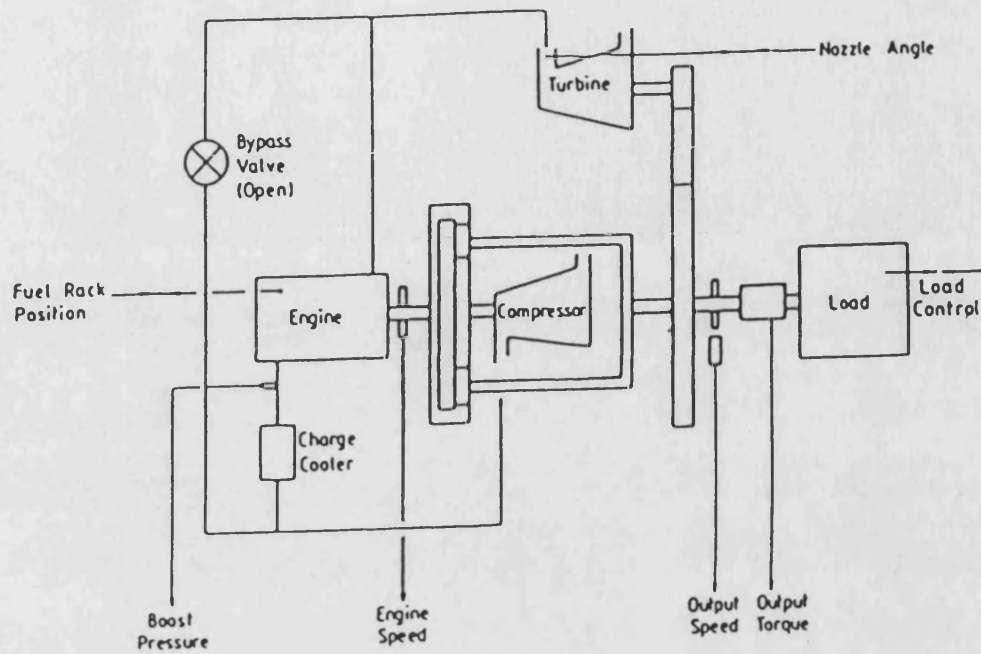
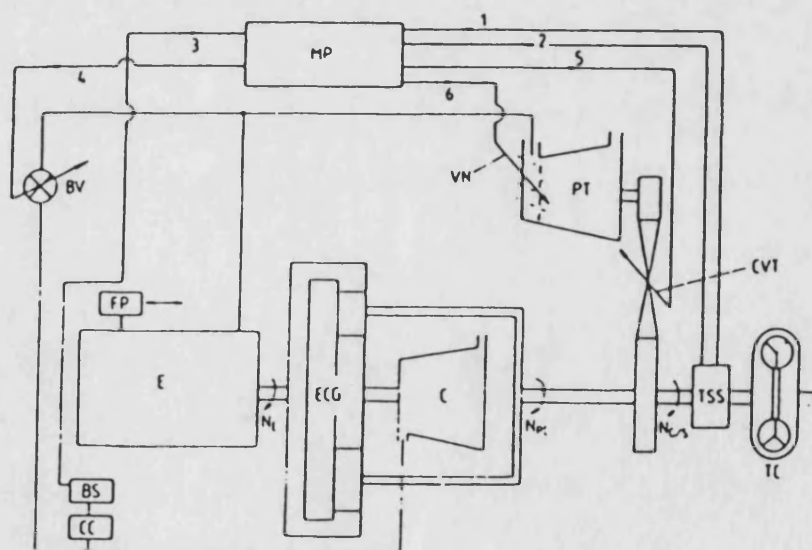


Fig-1.31 The present state of the DCE system



BV bypass valve; BS boost sensor; C compressor; CC charge cooler; E semi-adiabatic engine; ECG epicyclic gear train; FP fuel pump; PT power turbine; TC torque converter; VN variable turbine nozzles; TSS output torque and speed sensor; N_e engine speed; N_{os} output shaft speed; N_{pc} planet carrier speed; MP microprocessor;
 Input signals: 1 torque transducer; 2 speed transducer; 3 boost transducer
 Output signals: 4 bypass valve control; 5 CVT control; 6 nozzle control

Fig-1.32 The ultimate version of the DCE system

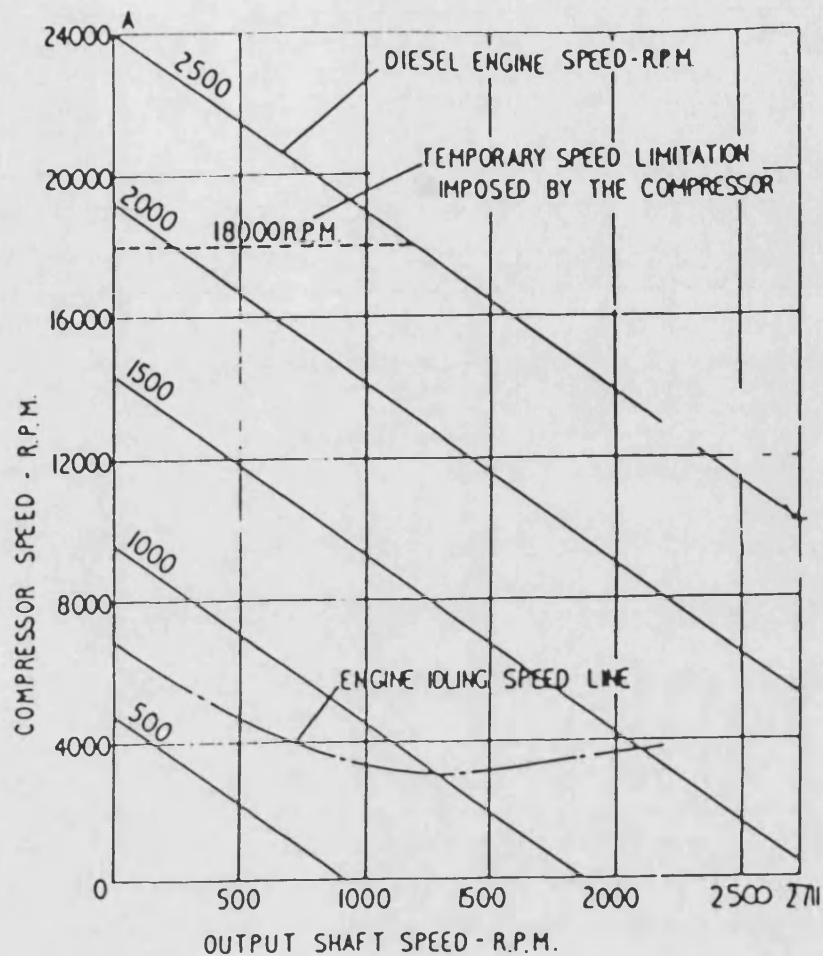


Fig-1.33 The engine, output shaft and compressor speed relationship in the DCE

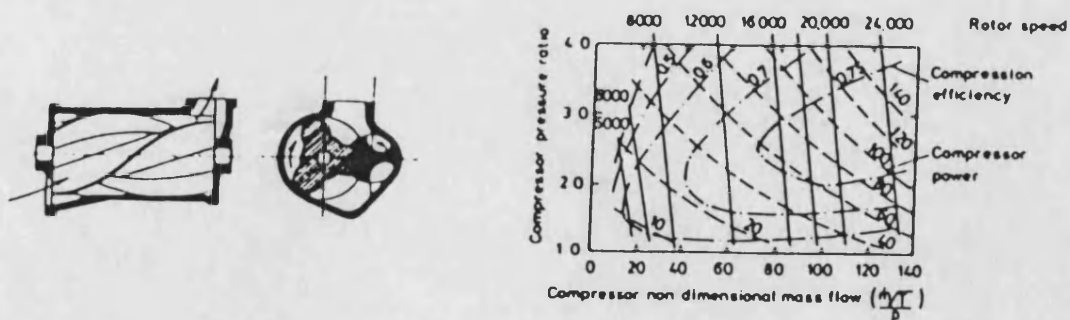


Fig-1.34 Typical screw (Lysholm) compressor and its performance

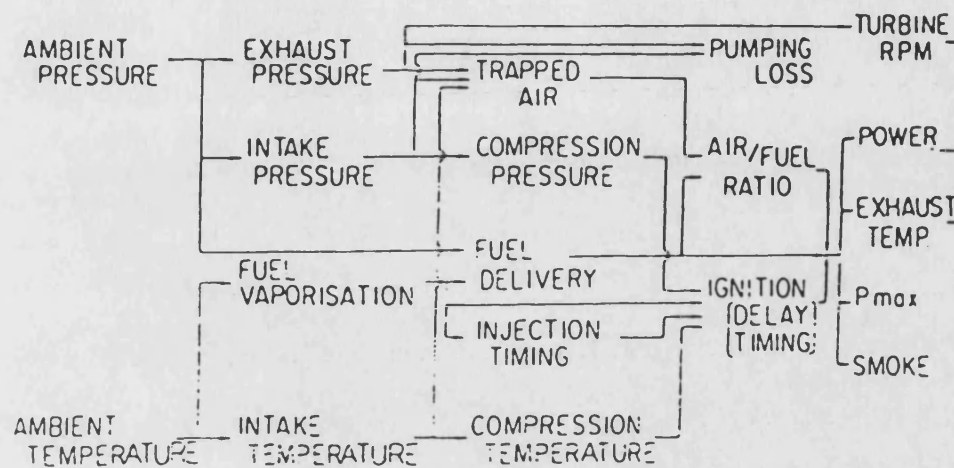


Fig-1.35 The flow of influence of ambient pressure and temperature on engine performance

CHAPTER 2

SURVEY OF THE THEORETICAL WORK

This chapter describes the major simulation programs used in the performance assessment of turbocharged and differentially compounded systems based on the Cummins L10 engines.

2.1 Simulation of the Turbocharged Cummins L10 Engine

Using Program EMAT

2.1.1 The Matching Program EMAT[34,35]

In simulating the turbocharged Cummins L10 engine, the program EMAT was used. EMAT is a quasi-steady state simulation program for engine/turbocharger matching and performance prediction purposes. In the program, the three major components, the engine, turbine and the compressor are represented by separate analytical models, while the main program links them to simulate the whole system. Although the component models are relatively simple, for speed of computation, great emphasis is placed on treating the interrelationships between the different components. With sufficient empirical data, acceptably accurate results can be obtained. EMAT has proved to be a very effective tool for matching calculations. The advantage of this program compared with the more comprehensive step-by-step type is its fast running speed. The overall characteristics of an engine/turbocharger combination under various operating condition can be investigated with great economy.

2.1.1.1 Main Program

The function of the main program is to link the various components of the system. The input of the basic data and operating data, and the output of the results are also performed in this part. A sample of the data file is shown in Table-2.1 while Table-2.2 shows a list of variables relevant to the data file. Various

compatibilities are checked and convergence is obtained using iterative loops(see section c below 'Program Structure).

a)Input The input data include engine geometry, valve timing, turbine geometry; some empirical data, such as engine diagram efficiency, fmep, as functions of engine speed, and delivery ratio as a function of both the engine speed and exhaust/inlet pressure ratio, etc. These data are used with interpolation routines under the relevant operating conditions.

b)Output The final results including all the major performance parameters of the engine, compressor and turbine, are output systematically as numerical arrays. For checking purposes, some intermediate data can also be recorded. Table-2.3 shows a typical output data file of EMAT.

c)Program Structure The flow chart of the EMAT is shown on Fig-2.1. As is well known, in turbocharged engine operation, several major compatibilities have to be satisfied between various components of the system. The compressor and the engine are connected thermodynamically through gas flow, therefore these two flows must be in balance. A similar situation occurs between the engine and the turbine. The connection between the compressor and the turbine requires that the power balance be satisfied at the specified speed, with due allowance for mechanical(bearing) losses.

In EMAT, the balance of the mass flow between the engine and the compressor is accomplished by adjusting the compressor mass flow rate so that the delivery ratio obtained according to this mass flow is compatible with that by interpolation from the empirical data at the relevant engine speed and the exhaust/inlet pressure ratio.

A five-step pulse model is used to simulate the exhaust process. The length of these steps is adjusted by iteration on an initially assumed value of minimum pulse pressure so that the total crank angle period occupied by these five steps equals that of the exhaust process which is determined by valve timing. Thus the mass flow balance between the engine and the turbine is satisfied. Fig-2.2 shows the pulse model schematically. Two cylinders are involved, one being at the start and the other the end, of the exhaust process. Instant mixing of the gases in these two cylinders and in the exhaust manifold is assumed. Dealing with 6 cylinder engine, two exhaust manifold structure is assumed, each manifold connecting three selected cylinders. Therefore the exhaust period is 240deg. However, in the actual

calculation, the exhaust process is carried out in five pressure ratios each covering a certain crank angle interval, rather than a continuous process.

Finally, the matching is completed when the power of the turbine and the compressor has converged. In this case, turbocharger speed is used as the iterating variable, the whole process of calculation having to be repeated until all compatibility conditions are satisfied, within specified tolerance.

2.1.1.2 Engine Subroutine

In the engine model the cycle is divided into a relatively small number of steps. It uses findings based on detailed experimental investigations into heat release and heat transfer and hence gives a relatively realistic representation of the cycle. The heat release is related to injection timing and duration, and modified by heat transfer. The gas exchange process takes details of valve timing and valve lift curves into account, and can deal realistically with pressure differences across the engine.

The cycle P-V diagram of the model is presented in Fig-2.3. The closed period starts from the assumed trapped condition, point 1, 15 degrees before nominal IVC. The compression process 1-2 is assumed adiabatic. The heat release is divided into proportion α in the constant volume process 2-3, which is from the start of injection up to 5 degrees ATDC and in which an allowance for work over TDC is taken into account; and β , half of which is at constant pressure 3-4, half on a constant slope 4-5 to match the isentropic expansion 5-6. The calculated heat transfer is subtracted first from β to give β_1 , the remainder from α to give α_1 if β is not sufficient.

Open period includes blowdown 6-7 which is taken as starting from 15 degrees after nominal EVO, exhaust process 7-8 and intake 9-10. In the calculation, inlet and exhaust pressures allow for a calculated pressure difference across the valves, assuming steady incompressible flow with valves fully open.

The combustion period is covered by the adoption of the fuel preparation rate equation:

$$dm_f = xk \cdot (m_{f, inj} - m_f) d\theta$$

xk combustion rate factor

m_f fuel prepared

$m_{f, inj}$ fuel injected

$d\theta$ crank angle increment

This is shown in Fig-2.4, where X_{inj} denotes the start of injection, D_{inj} duration of injection, and XA the injection period covered by the constant volume burning phase which ended at 5 deg. ATDC. The fuel burned in various periods of combustion is obtained by integration of this equation over the relevant crank angle intervals.

Strictly, this equation is only appropriate for the diffusion burning phase; the combustion in the pre-mixed phase is of a different nature. In order to simulate the cycle reasonably in terms of overall performance (thermal efficiency, BMEP, cylinder pressure, exhaust temperature, etc.), it is very important that a suitable value of xk is specified. The variation of xk directly dictates the distribution of heat release in the various parts of the combustion. Higher xk values will result in more fuel being burnt in the 'constant volume' period, resulting in increased maximum cylinder pressure and temperature and cycle efficiency while the exhaust temperature will be lower. However, too high a value of xk will also result in poor efficiency due to excessive compression work. Usually a value of around 0.1 is used.

The significance of another parameter used in the engine model is worth emphasising, viz. the heat transfer factor qlf . The function of qlf is to control the amount of heat transfer to coolant, affecting both engine efficiency and exhaust condition. Therefore it is also important to specify a proper value of qlf when applying the model to a particular engine. The value of heat transfer to coolant is calculated from an empirical equation relating to air flow rate, air/fuel ratio, temperature difference based on the inlet air and coolant temperature. Fig-2.5 shows the variation of this heat transfer against engine fuel flow, which appears to be quite representative for diesel engine cycle.

The input data include inlet mass flow, pressure and temperature, and the operating data: engine speed and fuelling in the form of fuel/rev. The injection timing, fmep etc are interpolated from empirical data. Output include all major performance data, such as power, bmep, sfc, thermal efficiency and exhaust temperature which is of special importance in the subsequent turbine calculation.

Generally, relatively realistic prediction can be obtained with the program.

2.1.1.3 Turbine Subroutine[36,37,38,39]

The turbine subroutine currently used is due to Way[39]. A one-dimensional treatment is applied to the flow analysis. The only explicit loss included is the incidence loss while a polytropic correlation is used throughout with a constant polytropic efficiency to cover all other forms of losses both in the fixed and rotating passages, i.e. skin friction, leakage and secondary flow losses. The model can deal with turbines of either nozzled or nozzleless design. The input data are speed and pressure ratio as well as turbine geometry. Output data are mass flow, power, efficiency and torque, etc.

2.1.1.4 Compressor Subroutine

The compressor map is presented as a series of numerical arrays of efficiency and pressure ratio based on mass flow rate and compressor speed; the data at a specific point can be obtained by interpolation from known values of mass flow and speed. The input data are speed and mass flow; at the start of the calculation the mean mass flow between surge and choke at the initial assumed speed is used as a first approximation. The output data are power, efficiency, pressure ratio, torque and outlet condition.

2.1.1.5 Charge Cooler Subroutine

The effectiveness and pressure loss through the cooler are calculated from empirical equations, based on mass flow rate and known inlet temperature of coolant and air. The input data include mass flow rate and inlet temperature. The output includes exit pressure ratio and temperature.

2.1.1.6 Other Features

In all these calculations, the effects of composition and state on gas properties have been taken into account. Fig-2.6 shows the variations of specific heat C_p and the ratio of specific heat, with air/fuel ratio and temperature. Use of this correlation will make the simulation more realistic.

2.1.2 VG Turbocharging Simulation

An important additional facility of EMAT is its ability to simulate variable geometry turbocharging. Because turbine nozzle angle is input as an operating parameter, turbine matching is easily accomplished by specifying various values of turbine nozzle angle. This is equivalent to operating the system with turbines of

various sizes, therefore the best combination can be selected. Further, it is particularly flexible in that the turbine nozzle angle can be varied at will in theoretical investigations, i.e. it can be scheduled at different operating points so that the best value of sfc or torque backup can be obtained for all these points. Therefore it is possible to synthesize an optimised performance map for any VG turbocharged engines.

2.1.3 Derating for Altitude and Temperature

As stated earlier, variations in ambient conditions will affect the operation of the system in a very complex manner. This is difficult to describe in detail, even with a very comprehensive program. Furthermore, more detailed programs will incur greater computing cost.

The ambient conditions are represented by two parameters, viz. pressure and temperature. In the present case, the effect of changing ambient conditions on the performance of the system is assessed by varying the values of these two variables, and ensuring that limiting conditions such as maximum cylinder pressure, exhaust temperature, air fuel ratio, turbocharger speed etc. are never exceeded.

In the present investigation, the main emphasis is placed on the effect of varying ambient conditions on the overall performance of the system, such as the variation of system mass flow rate, and changes in output power subject to the various operating limits already described. Specific measures taken so that the value of these critical parameters are not exceeded include changes in turbine nozzle angle, injection timing and reduced fuelling. The program EMAT is obviously very suitable for this purpose.

Most of the programs can be used directly while some correction is necessary when using the compressor subroutine. As mentioned earlier, the compressor is presented as arrays of pressure ratio and efficiency based on speed and mass flow rate. Clearly, as the inlet(ambient) conditions vary, for the same speed(N) and pressure ratio(Pr), the mass flow rate will change accordingly. In dealing with this matter, it is assumed that under any conditions, for the same dimensionless speed(N/\sqrt{T}) and pressure ratio, the mass flow parameter($\dot{M}\sqrt{T}/P$) and efficiency(η) will be the same, i.e. the method of similarity is applicable in the operation of the compressor(which is the basis on which the conventional compressor map using dimensionless parameters is obtained):

$$\text{if } Pr_x = Pr_o \text{ and } N_x / \sqrt{T_x} = N_o / \sqrt{T_o} ,$$

then $\dot{M}_x \sqrt{T_x} / P_x = \dot{M}_o \sqrt{T_o} / P_o$ and $\eta_x = \eta_o$

Pr	pressure ratio
P	(ambient) pressure
N	speed
T	temperature
\dot{M}	mass flow rate
η	efficiency

where o and x represent base and derated conditions respectively.

In calculations, the compressor speed and mass flow are first transferred to their respective equivalent under standard conditions. After the pressure ratio and efficiency are obtained, the mass flow and speed are transferred back to their original value.

2.2 Simulation of L10 DCE Using Program DCE

2.2.1 The Matching Program DCE2

(Variable Turbine Nozzle Build)

Like EMAT, DCE2 is also a simple quasi-steady state program. Most of the subroutines, such as engine, turbine and charge cooler, are identical to those in EMAT. However, a different compressor subroutine is adopted, not only because a different type of compressor (of rotary positive displacement rather than aerodynamic or centrifugal type) is used, but a different approach is adopted in constructing the program. Here, the compressor is represented as numerical arrays of volume flow rate and power, based on its speed and pressure ratio (which are the experimental data available). Other parameters such as mass flow rate and efficiency, etc. are obtained using the normal thermodynamic relationships.

The function of the main program is similar to that of the main program in EMAT. Most of the input variables are the same while for the DCE, additional data for the epicyclic geartrain and gear losses are included. The injection timing and duration of injection are presented as numerical arrays based on fuel/rev and engine speed rather than as operating data, as in the case in EMAT. The operating data include output shaft speed, engine speed, engine torque and turbine gear ratio. The output data include all the major parameters such as output shaft power, efficiency, etc. as well as all relevant operating variables for engine, compressor and turbine. A sample of the data file for the DCE2 is shown in Table-2.4 while Table-2.5 lists the

various items in the file. Table-2.6 is a typical output data file for DCE2.

2.2.1.1 The Structure of the Original Program DCE2

The flow chart for DCE2 is shown in Fig-2.7. Being constructed in great detail, it appears very complex.

As stated earlier, the DCE system is substantially complicated by the incorporation of an epicyclic gear train, variable geometry turbine, turbine CVT and bypass duct, but equally its flexibility is greatly enhanced. This has a significant effect on theoretical simulation of the system, in that the analytical representation is not as complex as would be expected, because, for instance, a compatibility requirement can be satisfied by adjusting several variables simultaneously. As a result, the simulation involves only several small separate loops rather than large nested loops as in the simulation program for the turbocharging system, EMAT.

In the DCE, the epicyclic gear dictates the torque and speed relationships between engine, output shaft and compressor. Although these relationships cannot be easily visualised, they are fixed for a specific geartrain. If the known variables are sufficient, then the solution is unique. For instance, in the DCE program, the input operating data include engine speed, engine torque and output shaft speed. From analysing the characteristics of the epicyclic geartrain(Fig-2.8), its operation is determined: the compressor speed and torque, the part of the output shaft torque contributed by the engine torque, are all fixed. This is shown below[40]:

Defining:

N_c compressor speed

N_e engine speed(known)

N_{os} output shaft speed(known)

τ_e engine torque(known)

N_t turbine speed

τ_t turbine torque

N_{pc} planet carrier speed

N_s sun gear speed

$EGR = R_a / R_s$ annulus/sun diameter ratio

$CGR = N_c / N_s . EGR$ overall compressor gear ratio

$TGR = N_t / N_{os}$ turbine(to output shaft) gear ratio

$OGR = N_{os} . EGR / [N_{pc} . (EGR + 1)]$ overall output shaft gear ratio

then, the unknowns can be determined as follows:

a)compressor speed

$$N_c = CGR (N_e - N_{os} / OGR)$$

b)compressor and output torque

$$\tau_c = \tau_e / CGR$$

$$\tau_{os} = \tau_e / OGR + \tau_t . TGR$$

c)compressor and output power

$$W_c = W_e [1 - N_{os} / (OGR . N_e)]$$

$$W_{os} = [W_e / (N_e . OGR) + \tau_t . TGR] . N_{os}$$

Clearly, these equations have to be employed in the simulation procedure. In the following, the outline of the program is described.

As mentioned earlier, the operating data include engine speed and torque, and output shaft speed.

The program starts with the compressor calculation. From the input operating data, compressor speed and torque are predetermined. An iterative loop is formed and the compressor pressure ratio (r_c) is taken as the iterating variable whose initial value is interpolated from an arbitrary array based on engine torque. The loop will be completed when a proper pressure ratio is obtained so that at the specified speed, the compressor torque calculated with the subroutine matches that from the gear relation. Meanwhile, other compressor operating parameters, such as mass flow rate, are determined.

The second loop deals with the mass flow balance between the compressor and the engine. Due to the presence of the bypass, this compatibility is easily satisfied. In the program, the air flow through the engine is determined from an empirical array of delivery ratio based on engine speed and exhaust/inlet pressure ratio, while the rest goes through the bypass, mixing with the exhaust gas before the turbine.

Engine performance is calculated by varying the parameter fuel/rev to match the required engine torque which is specified in the input data together with engine and output shaft speed.

The turbine is presented as constant inlet pressure operation. The mass flow balance is satisfied by adjusting the turbine nozzle angle. A further complication is the optimisation of the gear ratio between the turbine and the output shaft. This is done by running the turbine over a series of speeds(gear ratio). The optimum value

is obtained when system efficiency reaches a maximum.

Finally, the simulation is completed by a simple calculation of the output shaft torque: as the sum of the torque contributed from the engine through the planet carrier and the turbine torque transmitted through the turbine CVT.

As can be seen from the flow chart Fig-2.7, the analytical representation of the DCE is quite straightforward.

It should be mentioned that because of the epicyclic gear and the bypass duct, the pipe system will be longer and more complex. The flow losses will be greater and have to be taken into account. The assumed loss distribution is shown in Fig-2.9. However, the actual structure of the pipe system is unknown, as is the actual losses. In simulation, the situation is simplified and all the losses are taken as constant regardless of system operating conditions.

2.2.1.2 Modified Program DCE-VG(see flow chart Fig-2.10)

There are several difficulties in using the original program DCE2. In the following, these will be assessed separately.

a)Reverse Bypass Flow In the program, it is required that the mass flow in the bypass should always be positive and the occurrence of reverse flow is prohibited condition. Therefore, once a negative bypass flow is detected(air flow through the engine greater than compressor mass flow), the program will stop.

Obviously, an additional constraint is thus imposed on the system. It is necessary to examine the cause of reverse flow in order to ensure normal operation of the system.

The DCE is usually matched at the design point of the engine. Minimum bypass flow is required at this point for economy. The match of the system not only involves selection of turbine and compressor, it may also require determination of gear ratios including the ratio between the sun gear and the compressor, the ratio between the planet carrier and the output shaft, and the individual ratios within the epicyclic geartrain. Having established these various gear ratios, other characteristics of the system will be apparent, because the speed relationships between the different components are now fixed(Fig-1.31).

When operating the system under fixed engine power conditions, the engine speed and torque can vary over a very wide range. For a fixed output shaft speed,

the compressor speed will increase with increasing engine speed and vice versa. The engine mass flow and the compressor mass flow will vary in a similar fashion, due to the positive displacement action of the two devices.

However, as can be seen in Fig-1.31, as engine speed decreases, the compressor speed will decrease at a much greater rate. At a particular engine speed, a situation will occur such that the mass flow of the engine exactly matches that of the compressor, i.e. zero bypass flow. If the engine speed is further decreased, the mass flow capacity of the engine will exceed that of the compressor. When such a combination of engine, output shaft and compressor speed is encountered in the program, reverse bypass flow will be predicted. This phenomenon can be explained by further examining Fig-1.31. For a fixed output shaft speed, as the engine speed decreases, there is a unique value which results in the compressor speed of zero (along the abscissa of the figure). If the engine speed is further decreased, then the rotation of the compressor will be reversed. It can also be deduced that for certain higher values of engine speed, the mass flow of the compressor will be higher than that of the engine, and the higher the engine speed, the higher the bypass flow.

From the above discussion, it can be seen that the only remedy to the problem of reverse bypass flow is to increase the engine speed. In the original program, this may be done by altering the input data, but only in a manner of 'trial and error', and this may be rather tedious. The modified program DCE-VG automatically adjusts engine speeds.

b) Failure of the Turbine Subroutine Difficulties also arise frequently because of the failure of the turbine routine. In order to find out the reason for this the turbine subroutine and its interaction with the main program are examined.

In the program, when calling the turbine routine, the following variables, apart from the turbine geometric data, should be specified: the gas state at the turbine inlet and the turbine speed. The mass flow rate of the turbine, as well as other performance parameters, are calculated. However, the mass flow is already known as the sum of engine exhaust and bypass flow. The turbine nozzle angle is taken as an iterating variable and is adjusted so that the mass flow calculated matches that from the exhaust system.

Generally failure of the turbine subroutine is the result of too high a turbine speed relative to a low inlet pressure (pressure ratio).

A typical turbine performance map is shown in Fig-2.11. Notice the dashed

line in this map. It defines two different types of operation. In simple terms, if the operating point lies above this line, positive work will be produced by the turbine whereas if the operating point lies under this line, negative torque will appear on the turbine shaft. On the line itself, turbine torque is zero.

Fig-2.12 shows the variation of the turbine efficiency versus the blade speed ratio(u/c), which is defined as the rotor tip velocity(u) divided by the velocity(c) that would be achieved by the gas following isentropic expansion from the inlet condition to the pressure at the exit from the turbine. It can be seen that as the blade speed ratio increases from the value of 0.8, the turbine efficiency decreases sharply, reaching zero at a value of a little over 1.1.

Both these figures suggest that for a fixed pressure ratio across the turbine, there exists a maximum speed, above which the turbine can not work normally.

The reason for this may be explained as follows. For a specific inlet condition, the available energy of the gas is limited(the maximum being the isentropic expansion work over the pressure ratio available). When the turbine is running, a centrifugal field will be generated, which will result in an adverse pressure gradient. Clearly, before obtaining any useful work, this adverse pressure has to be overcome. However, if the turbine speed is too high, this adverse pressure could exceed the inlet pressure, i.e. the turbine is pushing the gas rather than otherwise. (At an extremely high speed, the turbine could be functioning as a compressor.) Therefore a negative torque is produced. Further, due to the various losses incurred over the turbine passage, this becomes more likely to occur. Moreover, the centrifugal field will be strengthened as the turbine speed increases, thus higher inlet pressure is required to overcome the incurred adverse pressure. This can be seen on Fig-2.11, the dashed line showing relation of increasing speed with pressure ratio.

In the program, the turbine speed (turbine gear ratio) is somewhat arbitrarily specified and too high a value can be supplied hence resulting in negative torque. Likewise, if too high a CVT ratio is implemented in real operation, a certain amount of work will be extracted by the turbine from the output shaft. This is clearly undesirable.

The turbine subroutine is so constructed that whenever a negative torque is detected zero mass flow will be initialised and failure is signaled. Subsequently, the program will stop. It is clear that the choice of the turbine gear ratio, particularly at

the first run, is very important for normal operation of the program, although this problem can be solved simply by reducing the turbine gear ratio.

Two cases can be distinguished. If the system is working at relatively high engine power and low output shaft speed, the relatively low turbine inlet pressure may be caused by an improper specification of the engine speed and torque in the input data(arbitrary). For fixed engine power, if the speed is high the torque will be relatively low. Low engine torque will result in low compressor torque and pressure ratio, thus low turbine inlet pressure(boost being controlled by turbine nozzle angle). Usually, under too high an engine speed, massive excess air is supplied by the compressor with very high bypass flow. If the engine speed is reduced, then the bypass flow can be reduced, thus leading to a gain in overall efficiency. At the same time, boost pressure and turbine inlet pressure can be increased. This may avoid the failure of the turbine subroutine and the system is further improved due to the operation of the turbine.

However, the problem often occurs under low load and high output shaft speed conditions. The available exhaust energy becomes insufficient to overcome the resistance of the turbine passage. Under these circumstances, the turbine becomes rather an energy-consuming device. It would appear more advantageous that the turbine is bypassed and the exhaust gas is directly discharged to atmosphere.

c)Other Shortcomings In the original program, the optimisation of the turbine gear ratio is performed by running the system with eight equally spaced values between the input data tgr1 and tgr2. The choice of tgr1 and tgr2 is arbitrary and the optimisation process itself is rather tedious. The results for all the tgr values have to be printed out for inspection. Then improved values of tgr1 and tgr2 are obtained. The program has to be run repeatedly until the two converge, even for only one operating point.

In order to overcome these problems, the original program DCE2 was modified. Relevant measures are taken regarding the problems discussed above. The new program is designated as DCE-VG and its flow chart is shown in Fig-2.10. The modification includes the following features:

*a)*In the input operating data, the engine torque is replaced by engine power. This allows one to compute the performance of the system in a neater order over the operating range. The engine power is fixed while the speed and torque can be varied as required.

b) If reverse bypass flow is detected, the engine speed is adjusted automatically so that the program can proceed normally, rather than stop as in the original scheme.

c) Turbine operation is checked. If failure occurs in running the turbine routine the turbine gear ratio will be adjusted immediately.

d) The optimisation of turbine gear ratio is accomplished automatically and the optimum operating data are first output to a special file. The final results can be obtained subsequently using the optimum data. Further, the optimisation process is only performed in the turbine loop, while in the original program, for every value of tgr, the whole program had to be run from the start, which involved much unnecessary calculation.

All these points can be seen by comparing Fig-2.7 and Fig-2.10. With DCE-VG, major economies in run time have been achieved compared with DCE2 in spite of the fact that the structure of the program DCE-VG is more complex than that of DCE2.

2.2.2 Simulation of the DCE with Fixed Nozzle Turbine (Program DCE-FG)

For a conventionally turbocharged engine system, implementation of a VG turbine can greatly enhance the system performance, as been shown in numerous publications. The DCE system embodies the VG turbine as an essential component. Since its adoption, VG turbine setting has been one of the important control parameters and the determination of this parameter an important aspect of system optimisation, both for steady state and transient performance. It is obvious that the availability of variable turbine geometry as a control parameter confers an additional degree of freedom on the system. However, it has also been exhibited from ealier work[23] that the DCE can be run with a fixed geometry turbine (but with two turbines). This raises the question of how the operation of the system and its simulation are affected by substituting a fixed geometry (FG) turbine for a variable geometry (VG) turbine.

The operation of the DCE with a fixed nozzle turbine implies that, in an analytical sense, one more constraint is placed on the system. This is significant in that the flexibility in turbine matching is lost. Further, because the turbine is at the end of the system flow path, if the mass flow balance at this point is not satisfied, the calculation may have to start again from the beginning. This makes the

simulation more difficult.

An earlier program was available for this purpose, but was found not to be ideal. It should be possible to compare the results obtained for FG operation directly with those for VG operation in order to assess the merits and demerits of the two systems. The existing program could not fulfil this task for the following reasons:

a) The strategy of the program is quite different from that of program DCE-VG. In the former, the input operating data include output shaft speed and torque, i.e. the output power is fixed while the engine operating condition is predicted. In the latter, however, the engine power is fixed and so is the engine speed (except in some unusual circumstances). The output results are the natural outcome of synthesising the performance of the various components. Further, because the engine rating is fixed, the choice of the engine operating conditions as input data will be more realistic. If on the other hand the output shaft operating conditions are taken as input data, it is possible that the predicted engine performance exceeds its maximum rating or alternatively that this maximum rating is not reached. It is obviously difficult to obtain relevant data for comparison of the two systems.

b) In the existing program, no losses are taken into account in the various part of the flow path. This will undoubtedly alter the system flow balance. Although it is not strictly accurate in the program DCE2 or DCE-VG to assume fixed pressure losses in the pipes, it can be considered relatively more realistic. Further, as stated earlier, for meaningful comparisons, it is desirable that similar considerations are applied to both cases.

Owing to these considerations, a new program was written, DCE-FG, based on program DCE-VG. Much of the process is the same as that of DCE-VG, e.g. the system operating condition is fixed by engine power and the output shaft speed. In addition, it has the following distinct features:

a) The engine speed is taken as an iterating variable. The mass flow balance between the compressor and the turbine can no longer be achieved by adjusting the turbine nozzle angle, therefore the operation of the compressor has to be altered instead. As seen, for fixed output shaft speed, the compressor speed is proportional to the engine speed. Therefore iterating the engine speed is obviously the appropriate approach.

b) Reverse bypass flow treatment. Reverse bypass flow is avoided in program DCE-VG by increasing the engine speed to increase the mass flow rate of the

compressor, but this is accompanied by an increase in the turbine nozzle angle as a result. In FG turbine operation this possibility is eliminated. This means that the mass flow balance of the system cannot always be achieved under the condition of no reverse bypass flow. Consequently, the restriction on reverse bypass flow has to be lifted.

In the event of reverse bypass flow, the gas state and composition at the engine inlet have to be adjusted accordingly, i.e. in the inlet manifold there will be a mixture of air from the compressor and exhaust gas from the bypass. Fig-2.13 shows the relationship between the various quantities.

It is postulated that the pressure loss across the bypass become zero under reverse flow condition. Defining the following variables (for reverse bypass flow only):

- cmf** compressor mass flow
- omf** bypass flow(reverse)
- tmf** turbine flow
- exmf** engine exhaust flow
- f** overall fuel/air ratio in the engine
- f_i** fuel/air ratio at the engine inlet
- f_{prev}** fuel per rev.
- Ne** engine speed

the calculation can be carried out as follows:

the fuel flow through the engine:

$$omf \cdot f / (1 + f) + f_{prev} \cdot Ne \\ \approx omf \cdot f + f_{prev} \cdot Ne$$

the air through the engine:

$$= cmf + omf (1 - f)$$

the overall fuel/air ratio of the engine:

$$f = (omf \cdot f + f_{prev} \cdot Ne) / [cmf + (1 - f) omf]$$

solving this equation:

$$f = \frac{cmf - \sqrt{cmf^2 - 4 \cdot omf \cdot f_{prev} \cdot Ne}}{2 \cdot omf}$$

therefore the fuel/air ratio at the engine inlet:

$$f = \frac{omf \cdot f}{[omf(1-f) + cmf]}$$

the state of the mixture(P, T , etc.) can be obtained from the usual mixing calculation.

Further, the effect of the reverse bypass flow is subsequently taken into consideration through the engine calculation.

In order to obtain an accurate solution, this part of the program is run five times.

The program for simulating the DCE with a fixed nozzle turbine is designated DCE-FG and the flow chart for the program is shown in Fig-2.14.

2.2.3 Simulation of the DCE under Changing Ambient Conditions

Similar to the case with the turbocharged engine system, the compressor performance has to be modified for changes in ambient conditions. As mentioned earlier, the compressor map is represented as numerical arrays of volume flow rate and power, based on speed and pressure ratio. Because the compressor is now of the positive displacement type, it is assumed that its volume flow characteristic, i.e. the relation between speed, pressure ratio and volume flow rate is unchanged. Consequently, the original volume flow data can be adopted directly. In the following the effects of the changes in ambient pressure and temperature on the compressor power are examined (noting that the compressor map is presented as arrays of power and volume flow rate), under conditions of the same volume flow rate and pressure ratio.

If the compression process is considered reversible, then the compression work will be:

$$\begin{aligned} W &= \frac{k}{k-1} \cdot P \cdot \dot{V} [Pr^{k/(k-1)} - 1] \\ &= \frac{k}{k-1} \cdot \dot{M} \cdot R \cdot T [Pr^{k/(k-1)} - 1] \end{aligned}$$

where \dot{V} volume flow rate

Using subscripts o and x for standard and modified ambient conditions, respectively, and assuming constant k but variable P , then

$$W_x / W_o = P_x / P_o$$

or $W_x = W_o \cdot P_x / P_o$ (for the same Pr)

If only T is changed, then

$$W_x / W_o = M_x.T_x / (M_o.T_o)$$

but

$$M_x.R.T_x = P.V \text{ and } M_o.R.T_o = P.V$$

then, due to constant volume flow and fixed inlet pressure(P),

$$W_x = W_o \text{ (for the same } P_r \text{)}$$

Therefore the compression work is proportional to ambient pressure but not affected by changes in ambient temperature.

The transformation is simply to obtain the compressor power by multiplying the interpolated value based on the standard data by a factor P_x / P_o , the rest of the procedure being unchanged.

2.3 Optimisation of the DCE System(with VG Turbine)

The DCE multi-variable system calls automatically for optimisation. However, this can only be realised through suitable control procedures. In the following, this aspect of the system is studied by examining the interrelations between the various variables and their effects on the overall performance of the system.

Optimisation with turbine nozzle angle and turbine gear ratio has been mentioned earlier. The turbine nozzle angle is obtained by satisfying other turbine operating parameters, such as mass flow rate, pressure ratio and speed, while by running the turbine at various speeds, the best turbine gear ratio is obtained.

Injection timing and duration of injection are input as numerical arrays of empirical data based on engine speed and fuel/rev. Obviously, the optimisation with these two parameters can be achieved by varying each parameter in turn.

Re-examining the various relationships involved in the epicyclic geartrain, a systematic optimisation procedure should be considered. As stated previously, for fixed engine power and output shaft speed, the engine speed can vary over a wide range. This will certainly influence the overall system operation. However, in both program DCE2 and DCE-VG, the engine speed is fixed(unless failure occurs), and is chosen arbitrarily.

It can be seen from the following equations for compressor and output power, derived previously:

$$W_c = W_e [1 - N_{os} / (OGR.N_e)]$$

$$W_{os} = [W_e / (N_e.OGR) + \tau t.TGR].N_{os}$$

that

a) An increase in engine speed will lead to an increase in compressor power but a reduction in output shaft power; although the turbine work can be somewhat increased, its inlet temperature will decrease, thus efficiency. Therefore engine speed should be as low as possible.

b) A decrease in engine speed will result in a reduction in system mass flow rate. Hence the engine speed should not be so low that the engine is starved of air.

c) High engine speed will result in low compressor torque and low pressure ratio and vice versa. Under extreme pressure ratios (either too low or too high), the compressor efficiency will be poor.

Clearly, all these factors have to be taken into consideration during optimisation. For this purpose, an exploratory procedure is constructed based on program DCE-VG, instead of outputting data for any one engine speed, the program is run over a range of engine speeds, until the optimum value has been obtained.

6.0	0.125	0.136	0.21778	0.0566	0.0566	16.3			
3.0000	193.0000	495.0000	701.50000	0.0500	8.0000	1.5000			
1000.00	1200.00	1600.00	1800.00	2100.00					
0.800	0.9100	1.000	1.110	1.250					
.845	.850	.855	.860	.865	.845	.850	.855	.860	.865
.860	.865	.845	.850	.855	.860	.865	.845	.850	.855
0.9850	0.9700	0.9450	0.9300	0.9250					
0.9350	1.170	1.250	1.270	1.300					
40000.	50000.	60000.	80000.	100000.					
0.0976	0.09	0.07	0.02540	0.004600	1.5708	0.18			
0.01350	0.01350	0.01350	1.5708	0.7200	0.00400				
0.1840	0.097	0.0	0.0	0.000	0.000	0.000	0.000	0.0	
0.287	43150.0	0.8415	313.5	350.0	0.800	1.00			
0.00	2.0	1.5							
0.000136	346.0000	345.0000	344.0000	344.0000	345.0000				
0.0003175	343.0000	342.0000	341.0000	341.0000	342.0000				
0.0004536	340.0000	339.0000	338.0000	338.0000	339.0000				
0.000136	12.0000	12.0000	13.0000	14.0000	15.0000				
0.0003175	17.0000	18.0000	19.0000	20.0000	22.0000				
0.0004536	23.0000	24.0000	25.0000	26.0000	27.0000				
240.	115000.	160.	24.	0.000	1.000				
00011102									
CUMMINS L10 DIESEL ENGINE, HOLSET H2C TURBOCHARGER									
1000.0	0.0003492	342.	18.	23.0					
1260.0	0.0003612	341.	20.	23.0					
1500.0	0.0003532	340.	20.	23.0					
1800.0	0.0003303	341.	21.	23.0					
2100.0	0.0003042	342.	22.	23.0					
0.									
0.									

Table-2.1 A sample of input data file for the program EMAT

Table-2.2 The variable list for the input data Table-2.1

```

c-----data input cards
c
c      input data must be in metric units.
c
c-----cards 1 and 2 engine data      8f10.0
c      1      cyl      no of cylinders
c      bore      cylinder bore diameter
c      strk      stroke
c      conlen      connecting rod length
c      dvi      inlet valve diameter
c      dve      exhaust valve diameter
c      cr      nominal compression ratio
c      2      xevc      angle of exhaust valve closing      nominal.
c      xivc      angle of inlet valve closing      degrees after
c      xevo      angle of exhaust valve opening      top dead centre
c      xivo      angle of inlet valve opening      open period
c      xk      empirical combustion rate factor - approx value 0.1
c      rhm      ratio of manifold to cyl volume. empirical factor.
c      qlf      empirical heat loss factor.
c-----cards 3,4,5,6,7,8,9 arrays of engine empirical factors
c      3      ves      5 values of engine speed      8f10.0
c      4      arl      5 values of exhaust to inlet pressure ratio      8f10.0
c      5      vdrs      25 values of delivery ratio based on swept volume
c      6      as a function of ves and arl.      13f6.0
c      7      ved      5 values of engine diagram efficiency
c      8      fo      5 values of fmep as a function of ves.      8f10.0
c      9      vts      5 values of turbine speed as a function of ves.
c      first estimate to start iteration.      8f10.0
c-----card 10      turbine data      8f10.0
c      dl      nozzle outlet diameter
c      d2t      tip rotor diameter at entry.
c      d3o      outir diameter at exit.
c      d3i      inner (hub) diameter at exit.
c      al      volute throat area
c      not same for the two turbine models.if itu-
c      rb=1,immediate entry area.=0,min effective area
c      b2      blade angle at rotor entry.
c      bp3      blade pitch at exit.(distance advanced in 1 rev)
c      bt2      rotor entry blade thickness
c-----card 11      turbine data
c      bblmax      maximum nozzle width.zero for nozzlelessunit
c      bb2s      width just upstream of rotor entry
c      bb2r      width just downstream of rotor entry
c      psi      cone angle at rotor entry,usually pi/2
c      ff      flow loss polytropic efficiency
c      not same for the two turbine models.presently
c      =0.8 for iturb=1 and =0.4 for iturb=0
c      tfric      empirical bearing loss factor
c      bt3o      blade thickness at rotor exit,outside
c      bt3i      blade thickness at rotor exit,inside
c-----card 12      turbine data
c      d0      volute inlet diameter
c      dl1      nozzle outlet diameter
c      sk1      incidence gain multiplier (ar<1.0)
c      sk2      incidence gain multiplier (ar>1.0)
c      cfl      coefft. of friction of stationary ducts
c      fls      loss factor of stationary ducts

```

c	flr	loss factor of rotor	
c	flp	flow loss index	
c-----	card 13	turbine data	
c	nb	no. of blades,[[card 13 must be removed if blade	
c		thicknesses are not specified]]	
c-----	card 14	data common to all runs	8f10.0
c	r	gas constant kj/kg.k	
c	calval	calorific value of fuel	
c	pa	atmospheric pressure	
c	ta	atmospheric temperature	
c	tw	engine water temperature	
c	e	air cooler effectiveness	
c	sfca	no of turbochargers	
c-----	card 15	variable geometry specifications	
c	resmax	max. restriction required, set to zero for fixed	
c		geometry operation, but rmjfo & rmjfr must have some	
c		arbitrary non-zero values.	
c	rmjfo	boost ratio at which throat is required to be 'just'	
c		fully open	
c	rmjfr	boost ratio at which throat is required to be 'just'	
c		fully restricted	
c-----	card 16	control markers 8011	
c	imark	set to 1 for error diagnostic output on first run	
c	metout	set to 1 for british output data	
c	iout	marker for output. = 1 for array printout each run.	
c	ioutpt	no of final printout copies.	
c	icomp	code of compressor to be used. must be 1 or 2.	
c	iturb	0 or 1 , turbine selector	
c-----	card 17	ihead heading for printout over results 20a4.	
c-----	card 18 onwards	individual data for each run	8f10.0
c	es	engine speed	
c	fprev	fuel input per min * 10000 / rev per min	
c	xinj	angle atdco for start of injection. degrees	
c	dinj	crank angle duration of injection degrees	
c	a2	turbine nozzle angle	

(continued)

Table-2.3 A sample of output data file for the EMAT

CUMMINS L10 DIESEL ENGINE, HOLSET H2C TURBOCHARGER

149

119

595

number of cylinders	6.0	bore	(m)	0.13	stroke	(m)	0.13600	
con-rod length (m)	0.21778	inlet valve closing (degs)	193.0	compressor scale factor	1.00			
ambient temperature (deg k)	274.4	heat loss factor	1.0000	ambient pressure (bar)	0.99000			
compression ratio	16.30	combustion rate factor	0.0500	turbine flow loss factor	0.8000			
engine speed(r.p.m)	1000.00	1260.00	1500.00	1800.00	2100.00	0.00	0.00	0.00
boost pressure ratio	1.358	1.512	1.808	2.029	2.141	0.000	0.000	0.000
trapped a/f ratio	19.462	20.664	24.982	29.545	33.304	0.000	0.000	0.000
delivery ratio	0.847	0.847	0.852	0.855	0.855	0.000	0.000	0.000
manifold temp (deg k)	292.261	296.297	301.320	307.113	312.139	0.000	0.000	0.000
engine power (k w.)	114.88	151.40	178.03	186.17	192.57	0.00	0.00	0.00
engine torque (n.m.)	1097.07	1147.43	1133.40	987.64	875.68	0.00	0.00	0.00
b.m.e.p (bar)	13.7672	14.3991	14.2230	12.3939	10.9889	0.0000	0.0000	0.0000
s.f.c. (kgs/kw hr)	0.182	0.180	0.179	0.192	0.199	0.000	0.000	0.000
b.thermal eff.	0.4575	0.4626	0.4673	0.4354	0.4192	0.0000	0.0000	0.0000
fuel / rev (kg.)	3.492	3.612	3.532	3.303	3.042	0.000	0.000	0.000
max cyl pressure (bar)	112.31	121.69	133.75	137.42	131.31	0.00	0.00	0.00
max cyl temperature(deg k)	2222.91	2183.90	2002.89	1852.61	1741.82	0.00	0.00	0.00
exhaust temperature(deg k)	287.51	900.82	846.53	835.30	809.34	0.00	0.00	0.00
percentage heat to coolant	21.13	17.45	14.27	12.13	10.90	0.00	0.00	0.00
compressor pressure ratio	1.4075	1.5843	1.9056	2.1596	2.3049	0.0000	0.0000	0.0000
delivery temperature(deg k)	343.54	360.00	376.11	388.67	397.08	0.00	0.00	0.00
delivery pressure (bar)	1.391	1.569	1.883	2.135	2.278	0.000	0.000	0.000
compressor speed (r.p.m.)	50782.2	50508.6	74084.0	83506.2	90103.3	0.0	0.0	0.0
volume flow (cu ft / min)	5.80	8.03	11.30	14.99	18.16	0.00	0.00	0.00
compressor power (kw.)	5.581	10.310	18.072	27.668	36.499	0.000	0.000	0.000
compressor efficiency	0.618	0.635	0.734	0.773	0.778	0.000	0.000	0.000
turbine speed (r.p.m)	50782.2	50508.6	74084.0	83506.2	90103.3	0.0	0.0	0.0
turbine power (kw)	5.684	10.439	18.322	27.878	36.712	0.000	0.000	0.000
effective turbine efficiency.	0.658	0.664	0.646	0.623	0.601	0.000	0.000	0.000
fract of flow thro turbine.	1.000	1.000	1.000	1.000	1.000	0.000	0.000	0.000
first step. pressure ratio.	1.453	1.583	1.837	2.134	2.426	0.000	0.000	0.000
n.d. torque	1.8319	1.9235	1.9726	1.9801	1.9672	0.0000	0.0000	0.0000
n.d. mass flow.	264.5017	274.8977	279.5947	282.3611	282.2206	0.0000	0.0000	0.0000
n.d.speed	1572.4206	1863.4125	2451.8250	2886.5112	3192.7586	0.0000	0.0000	0.0000
efficiency.	0.664	0.673	0.667	0.639	0.612	0.000	0.000	0.000
final step. pressure ratio.	1.114	1.223	1.475	1.797	2.129	0.000	0.000	0.000
n.d. torque	0.0433	0.3746	0.8109	1.2220	1.4862	0.0000	0.0000	0.0000
n.d. mass flow.	83.8942	155.1191	211.5935	245.9831	262.3044	0.0000	0.0000	0.0000
n.d.speed	1622.8221	1921.5428	2518.3993	2948.3199	3245.4803	0.0000	0.0000	0.0000
efficiency.	0.191	0.515	0.568	0.586	0.583	0.000	0.000	0.000
compressor mass flow(kg/min).	6.80	9.40	13.24	17.57	21.28	0.00	0.00	0.00
delivered air to fuel ratio	12.46	20.66	24.98	29.54	33.30	0.00	0.00	0.00
v.g. nozzle width (mm.)	13.5000	13.5000	13.5000	13.5000	13.5000	0.0000	0.0000	0.0000
cooler effectiveness	0.9069	0.8726	0.8393	0.8022	0.7716	0.0000	0.0000	0.0000
engine diagram factor	0.9800	0.9667	0.9527	0.8900	0.8800	0.0000	0.0000	0.0000
start of injection(deg.)	342.36	340.89	340.43	340.75	342.25	0.00	0.00	0.00
duration of injection(deg.)	18.21	20.00	20.16	20.50	21.50	0.00	0.00	0.00
turbine nozzle angle(deg.)	23.00	23.00	23.00	23.00	23.00	0.00	0.00	0.00

6.0000	0.4102	0.4462	0.7145	0.1857	0.1857	16.3000	1700.0000
3.0000	193.0000	495.0000	701.0000	0.0100	110.0000	1.0000	
9.5500	14.6700	1.4450	0.9800	0.9310	0.9800	10.0000	10.0000
10.0000							
0.0000	1000.0000	1300.0000	1500.0000	1800.0000	2200.0000		
0.8000	0.8450	0.8450	0.8450	0.8450	0.8450		
0.9100	0.8500	0.8500	0.8500	0.8500	0.8500		
1.0000	0.8550	0.8550	0.8550	0.8550	0.8550		
1.1100	0.8600	0.8600	0.8600	0.8600	0.8600		
1.2500	0.8650	0.8650	0.8650	0.8650	0.8650		
0.0003	346.0000	345.0000	344.0000	344.0000	345.0000		
0.0007	343.0000	342.0000	341.0000	341.0000	342.0000		
0.0010	340.0000	339.0000	338.0000	338.0000	339.0000		
0.0003	12.0000	12.0000	13.0000	14.0000	15.0000		
0.0007	17.0000	18.0000	19.0000	20.0000	22.0000		
0.0010	23.0000	24.0000	25.0000	26.0000	27.0000		
1.0000	0.9600	0.9200	0.9000	0.8900			
7.0000	10.0000	13.0000	14.0000	16.0000			
0.0000	1.0000	1.5000	2.0000	3.0000			
3.0000	2.2000	1.2000	0.8000	0.6000			
0.0000	150.0000	300.0000	450.0000	600.0000			
1.0000	1.5000	2.0000	2.5000	3.0000			
0.6000	0.5815	0.4600	0.1200	20.0000	1.5708	0.8000	0.0000
0.0542	0.0542	0.0542	1.5708	0.8000	0.1000	0.0000	0.0000
53.300	18550.000	14.400	530.000	630.000	0.800	12.500	1.100
0001011							
200							
CUMMINS	L10	D C E					
0.0000000	0.0000000	0.0000000	1.5000000				
0.0000000	0.0000000	0.0000000	1.5000000				
0.0000000	0.0000000	0.0000000	1.5000000				
0.0000000	0.0000000	0.0000000	1.5000000				
440.0000	1259.0000	1350.0000	1.0000				
105.7	105.7						
440.0000	1020.0000	1250.0000	1.0000				
95	95						

Table-2.4 A sample of input data file for DCE2

Table-2.5 The variable list for the data file Table-2.4

```

c data input cards.
c
c cards 1 and 2 engine data      8f10.0
c -----
c
c 1  cyl      no of cylinders
c    bore     cylinder bore diameter
c    strk     stroke
c    conlen   connecting rod length
c    dvi      inlet valve diameter
c    dve      exhaust valve diameter
c    cr       nominal compression ratio
c    etmax    maximum engine torque
c
c 2  xevc     angle of exhaust valve closing      nominal.
c    xivc     angle of inlet valve closing        degrees after
c    xevo     angle of exhaust valve opening      top dead centre
c    xivo     angle of inlet valve opening        open period
c    xk       empirical combustion rate factor - approx value 0.1
c    aorif    bypass orifice area (sq in)
c    qlf      empirical heat loss factor.
c
c card 3 and 4      gearbox data
c -----
c
c    cgr      compressor gear ratio
c    tgr      turbine gear ratio
c    ogr      output shaft gear ratio
c    cge      compressor gear efficiency
c    tge      turbine gear efficiency
c    oge      output shaft gear efficiency
c    cgft     compressor gearing friction torque (lb.ft)
c    tgft     turbine gearing friction torque
c
c 4  ogft     output shaft gearing friction torque
c
c cards 5 - 22 arrays of engine empirical factors
c -----
c
c 5  v0       initial engine speed, preferably 0.0
c    ves      5 values of engine speed      8f10.0
c
c 6  arl      5 values of exhaust to inlet pressure ratio 8f10.0
c 7  vdrs     25 values of delivery ratio based on swept volume
c 8           as a function of ves and arl. 13f6.0
c 9
c 10
c
c 11 vfprev,  5 values of injection timing as a function of fprev
c 12 vxinj
c 13
c
c 14 vfprev,  5 values of injection duration as a function of
c 15 vdinj    fprev
c 16
c
c 17 ved      5 values of diagram factor as a function of ves

```



```

c
c 18 fo      5 values of fmep as a function of ves.  8f10.0
c
c 19 vosr    5 values of ratio of output shaft speed to engine speed
c
c 20 votr    5 values of ratio of output shaft torque to engine torque
c
c 21 vet      5 values of engine torque
c
c 22 vrc      5 values of boost pressure ratio
c
c card 23 , 24      turbine data                      8f10.0
c -----
c
c 23 d1      diameter at volute exit tongue or nozzle exit.
c      d2t    rotor tip diameter.
c      d3o    rotor outer exit diameter.
c      d3i    inner (hub) diameter at exit.
c      a      volute entry area (nozzleless) or nozzle angle.
c      b2     blade angle at rotor entry.
c      bp3    blade pitch at exit. (distance advanced in 1 rev)
c      bt2    rotor blade thickness at entry.
c
c 24 bbl      passage depth at rotor entry.
c      bb2s   stator passage width at rotor entry.
c      bb2r   rotor passage width at entry.
c      psi    cone angle with axis.
c      ff     fluid friction factor.
c      tfric  mechanical friction factor.
c      bt3o   blade thickness at rotor exit (outer).
c      bt3i   blade thickness at turbine exit (inner).
c
c card 24a      nb  number of turbine blades.
c               only input if any blade thickness values given
c
c card 25      data common to all runs                8f10.0
c -----
c
c      r      gas constant  lbf.ft/lbm.deg r
c      calval  calorific value of fuel
c      pa      atmospheric pressure
c      ta      atmospheric temperature
c      tw      engine water temperature
c      e       air cooler effectiveness
c      tim     delay in injection timing
c      scfa    compressor scale factor
c
c card 26      control markers 8011
c -----
c
c      imark   set to 1 for error diagnostic output on first run
c      jmark   set to 1 for diagnostic information from engine sub
c      metin   set to 1 for metric (si) input data
c      metout  set to 1 for metric (si) output data
c      iout    marker for output. = 1 for array printout each run.
c      ioutpt  no of final printout copies.
c
c card 27      format 15
c -----

```

continued

```

c      limit      limit on number of iterations for each loop
c
c      card 28      ihead      heading for printout over results 20a4.
c
c      card 29 onwards      individual data for each run      8f10.0
c      -----
c
c      os          output shaft speed
c      et          engine torque
c      es          engine speed
c      tgr1(2)     turbine gear ratio
c      tim         delay in injection timing

```

continued

Table-2.6 A sample of output data file for DCE2

COMBUSTION L10			30 26 24 24					
number of cylinders	6.0	bore	(m.m.)	125.03	stroke	(m.m.)	136.00	
con-rod length (m.m.)	217.78	inlet valve closing (degs)	193.0	compressor scale factor		1.18		
ambient temperature (deg k)	313.3	ambient pressure (bar)	0.84	cooler effectiveness		0.8635		
compression ratio	16.30	engine diagram factor	0.9263	turbine flow loss factor		0.8000		
----- compressor gear ratio	9.5500	output shaft gear ratio	1.4450	-----				
engine speed (r.p.m.)	1475.00	1305.00	1140.00	1000.00	1805.00	1655.00	1525.00	1375.00
boost pressure ratio	3.623	3.836	2.940	1.980	3.635	2.968	2.327	1.473
delivered air to fuel ratio	30.756	31.086	31.854	37.312	28.588	29.013	31.717	34.545
delivery ratio	0.854	0.854	0.854	0.853	0.853	0.852	0.852	0.852
manifold temp (deg k)	355.262	342.602	329.426	317.128	352.018	340.334	328.427	317.233
engine power (kw.)	240.29	180.19	120.07	59.98	240.07	180.01	119.99	59.88
engine torque (n.m.)	1555.81	1318.87	1006.50	573.71	1271.37	1039.95	752.40	417.24
b.m.e.p (bar)	12.5078	16.5361	12.6133	7.1328	15.9287	13.0259	9.4233	5.2158
s.f.c. (kg/kw hr)	0.196	0.197	0.201	0.211	0.205	0.208	0.214	0.232
b.thermal eff.	0.4251	0.4242	0.4157	0.3961	0.4076	0.4005	0.3900	0.3590
fuel / rev (kg.)	3.327	4.529	3.522	2.105	4.535	3.775	2.804	1.686
max cyl pressure (bar)	172.16	143.49	110.83	73.56	136.42	113.05	88.63	55.87
exhaust temperature (deg k)	903.19	870.32	825.26	713.31	949.60	916.05	840.42	755.82
mass flow (kg/min)	24.167	18.357	12.790	7.854	23.404	18.127	13.565	8.009
percentage heat to coolant	10.81	12.51	15.23	20.03	10.92	12.52	14.67	19.78
compressor speed (r.p.m.)	7146.8	5523.3	3947.6	2610.6	6663.4	5230.9	3989.4	2556.9
compressor pressure ratio	4.875	4.064	3.146	2.164	3.921	3.231	2.568	1.688
mass flow (kg/min)	25.373	19.261	13.590	8.511	24.537	19.119	14.369	8.537
compressor power (kw.)	118.50	77.54	42.12	15.73	90.11	57.74	31.66	11.11
compressor torque (n.m.)	152.27	134.00	101.84	57.53	129.08	105.37	75.75	41.46
delivery temperature (deg k)	588.69	551.42	497.37	423.64	530.87	492.74	444.64	391.10
compressor efficiency	0.641	0.641	0.656	0.700	0.681	0.691	0.736	0.651
turbine speed (r.p.m.)	54894.0	50922.5	44210.8	30411.5	52510.1	46917.1	39521.8	23099.7
turbine pressure ratio	4.752	3.941	3.023	2.041	3.798	3.109	2.445	1.566
mass flow (kg/min)	26.160	19.853	13.992	8.723	25.356	19.746	14.800	8.771
turbine power (kw)	106.60	68.23	36.03	11.41	94.01	59.14	30.91	6.09
turbine torque (n.m.)	18.54	12.77	7.78	3.54	17.09	12.03	7.47	2.52
inlet temperature (deg k)	889.79	856.90	807.91	692.84	932.55	896.65	820.65	735.47
turbine nozzle angle	0.950	5.467	4.919	4.615	7.519	7.119	6.716	8.153
turbine efficiency	0.760	0.750	0.737	0.724	0.760	0.751	0.741	0.732
output shaft speed (r.p.m.)	1050.00	1050.00	1050.00	1050.00	1600.00	1600.00	1600.00	1600.00
output shaft power (kw)	212.91	159.52	106.24	51.03	226.40	169.62	110.66	49.45
output shaft torque (n.m.)	1935.51	1459.12	965.76	463.86	1362.56	1011.95	660.17	295.00
output shaft sfc (kg/kw.hr)	0.221	0.222	0.227	0.248	0.215	0.221	0.232	0.281
output thermal efficiency	0.3767	0.3755	0.3678	0.3369	0.3878	0.3774	0.3597	0.2965
engine fuel flow (kg/min)	0.786	0.591	0.402	0.211	0.819	0.625	0.428	0.232
dynamic injection (degree ca)	337.3	349.0	342.9	345.8	339.0	340.6	342.6	345.1
duration of injection	28.4	24.0	18.4	13.9	26.0	22.1	17.8	13.4
turbine gear ratio	42.3	48.6	42.1	29.3	32.8	29.3	24.7	14.4
pressure loss in pipe a (bar)	0.10345	0.10345	0.10345	0.10345	0.10345	0.10345	0.10345	0.10345
pressure loss in pipe b (bar)	0.10345	0.10345	0.10345	0.10345	0.10345	0.10345	0.10345	0.10345
pressure loss in pipe c (bar)	0.10345	0.10345	0.10345	0.10345	0.10345	0.10345	0.10345	0.10345
pressure loss in pipe d (bar)	0.10345	0.10345	0.10345	0.10345	0.10345	0.10345	0.10345	0.10345
engine diagram factor	0.92111	0.92979	0.93562	0.94000	0.92985	0.91437	0.91898	0.92635
cooler effectiveness	0.82148	0.84095	0.87586	0.90200	0.79379	0.81420	0.83556	0.86346

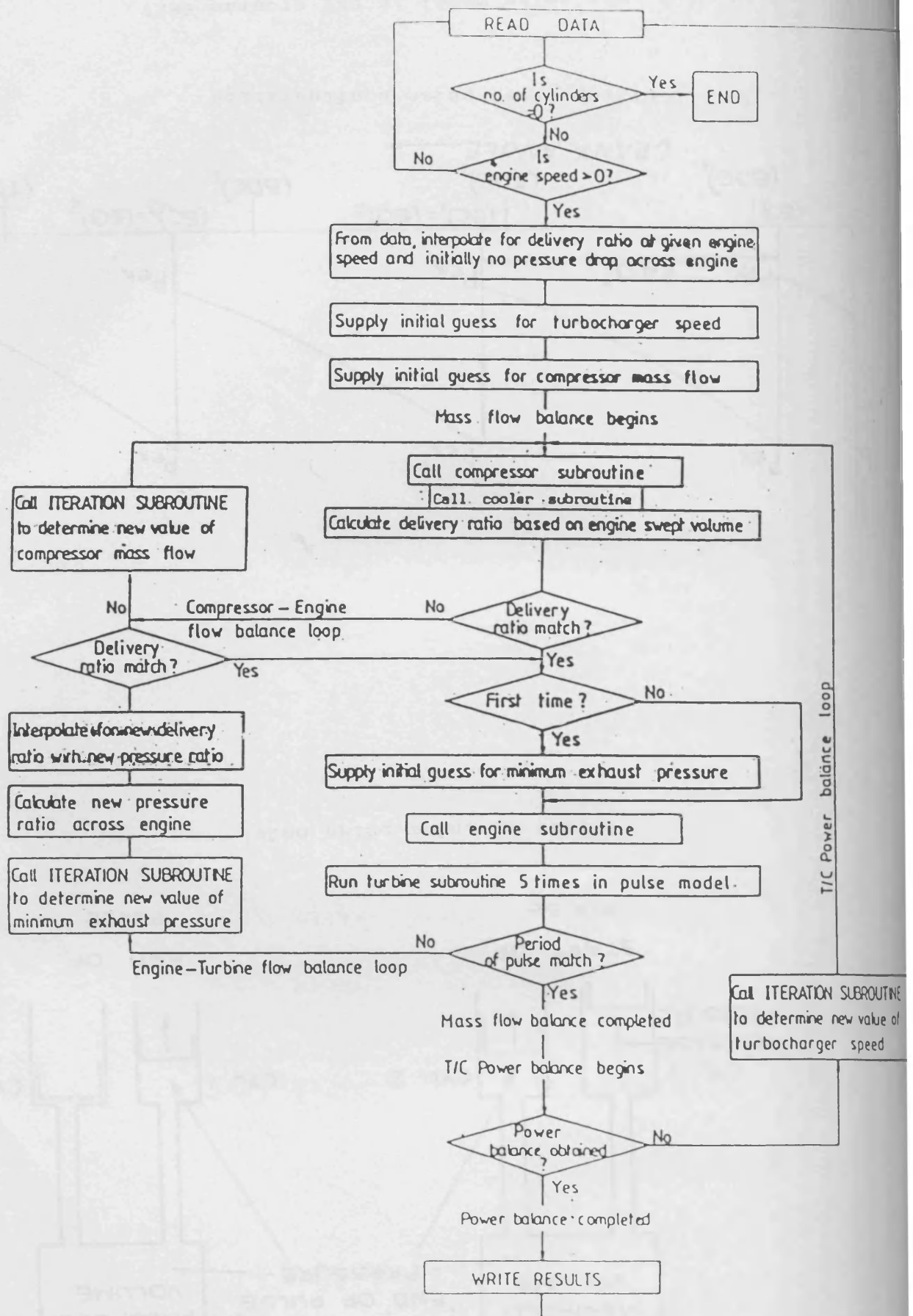
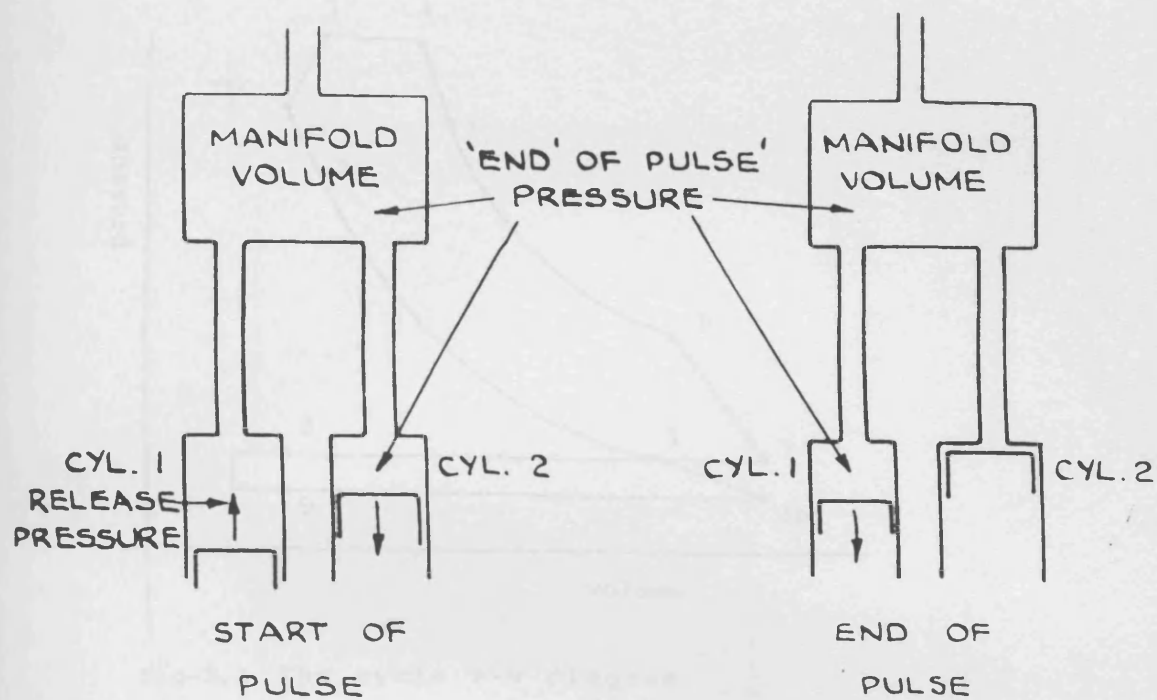
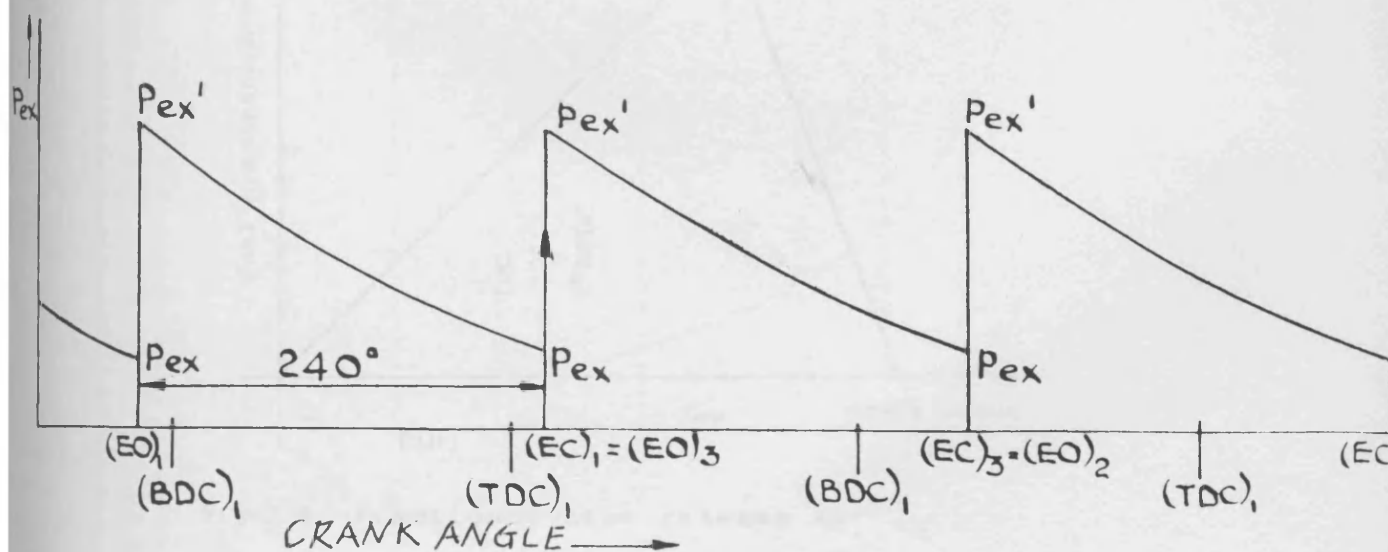


Fig-2.1 The flow chart for the program EMAT



a) Twin cylinder pulse model



b) Simplified pulse configuration

Fig-2.2 The pulse model in the program EMAT

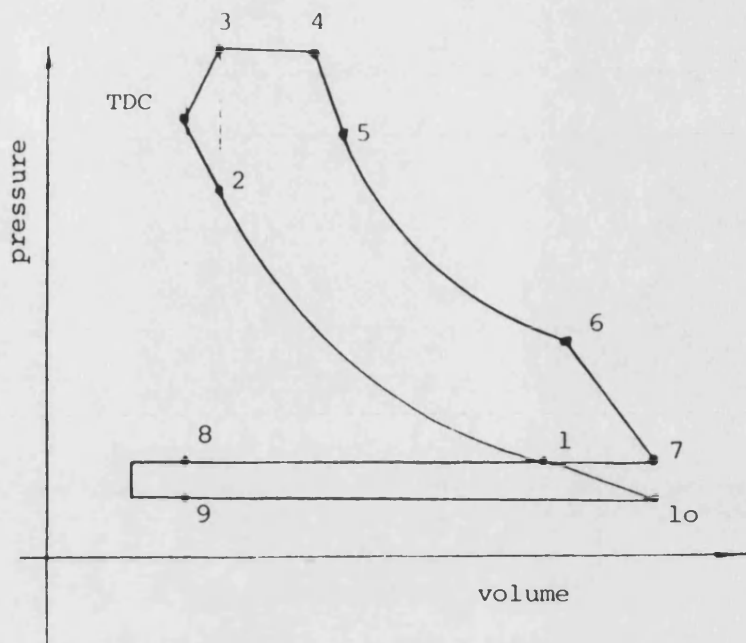


Fig-2.3 The cycle P-V diagram

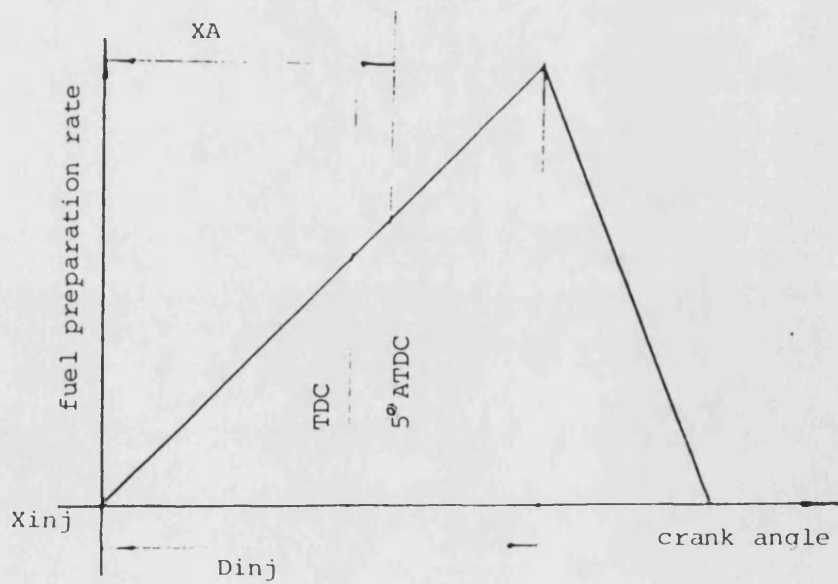


Fig-2.4 Fractional heat release as function of fuel injection

% age
HEAT LOSS

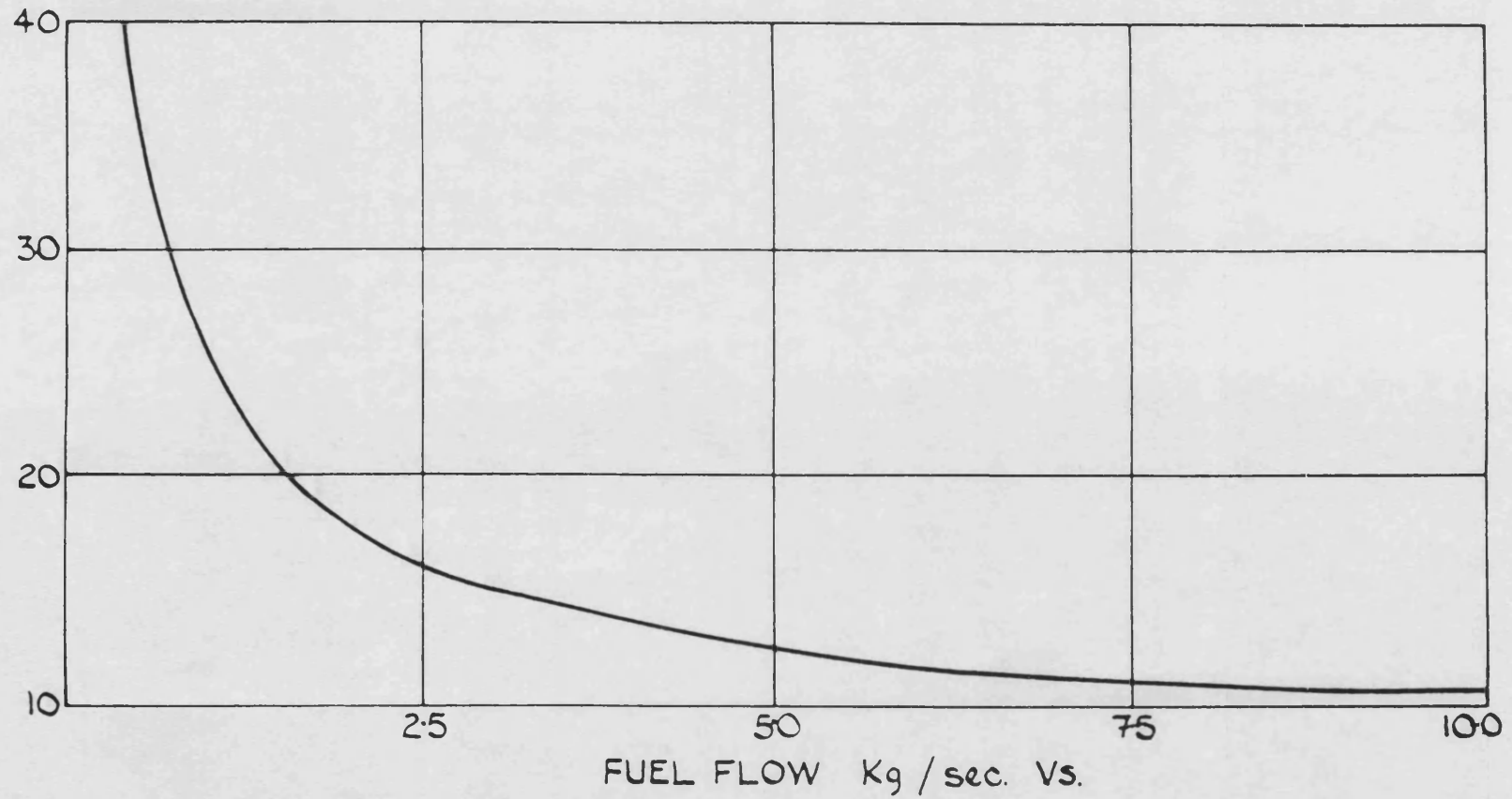


Fig-2.5 Cooling water heat loss

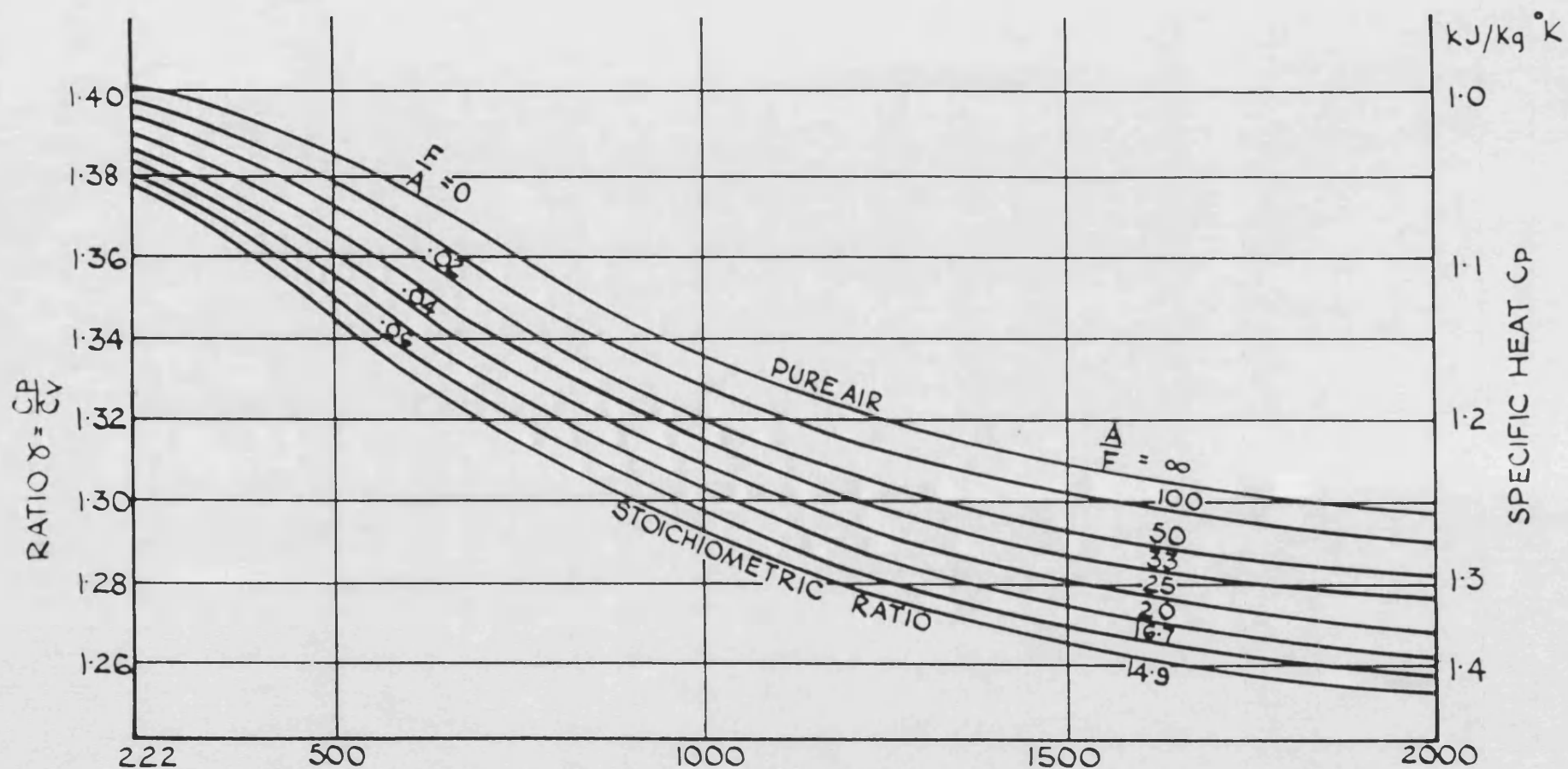


Fig-2.6 RATIO OF SPECIFIC HEATS $\gamma = \frac{C_p}{C_v}$ AND SPECIFIC HEAT C_p AS A FUNCTION OF TEMPERATURE & FUEL AIR RATIO.

FLOWCHART FOR DCE 2

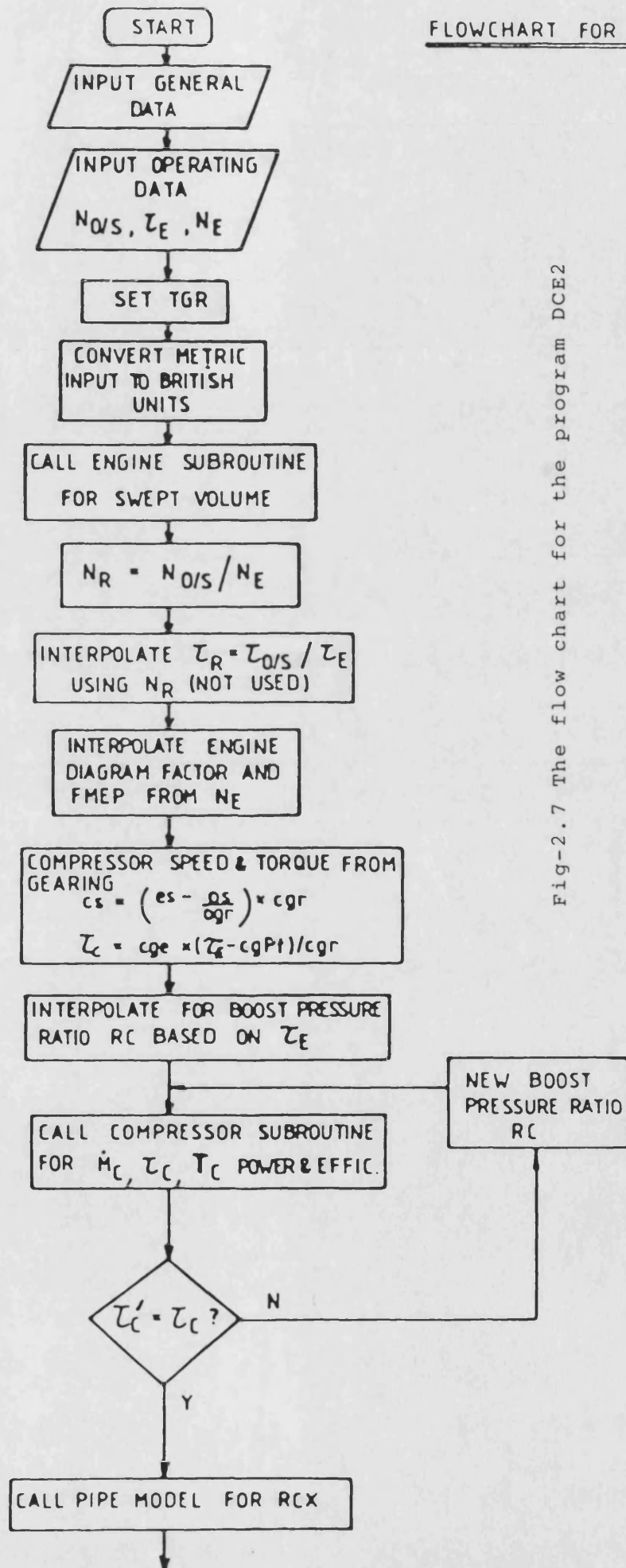
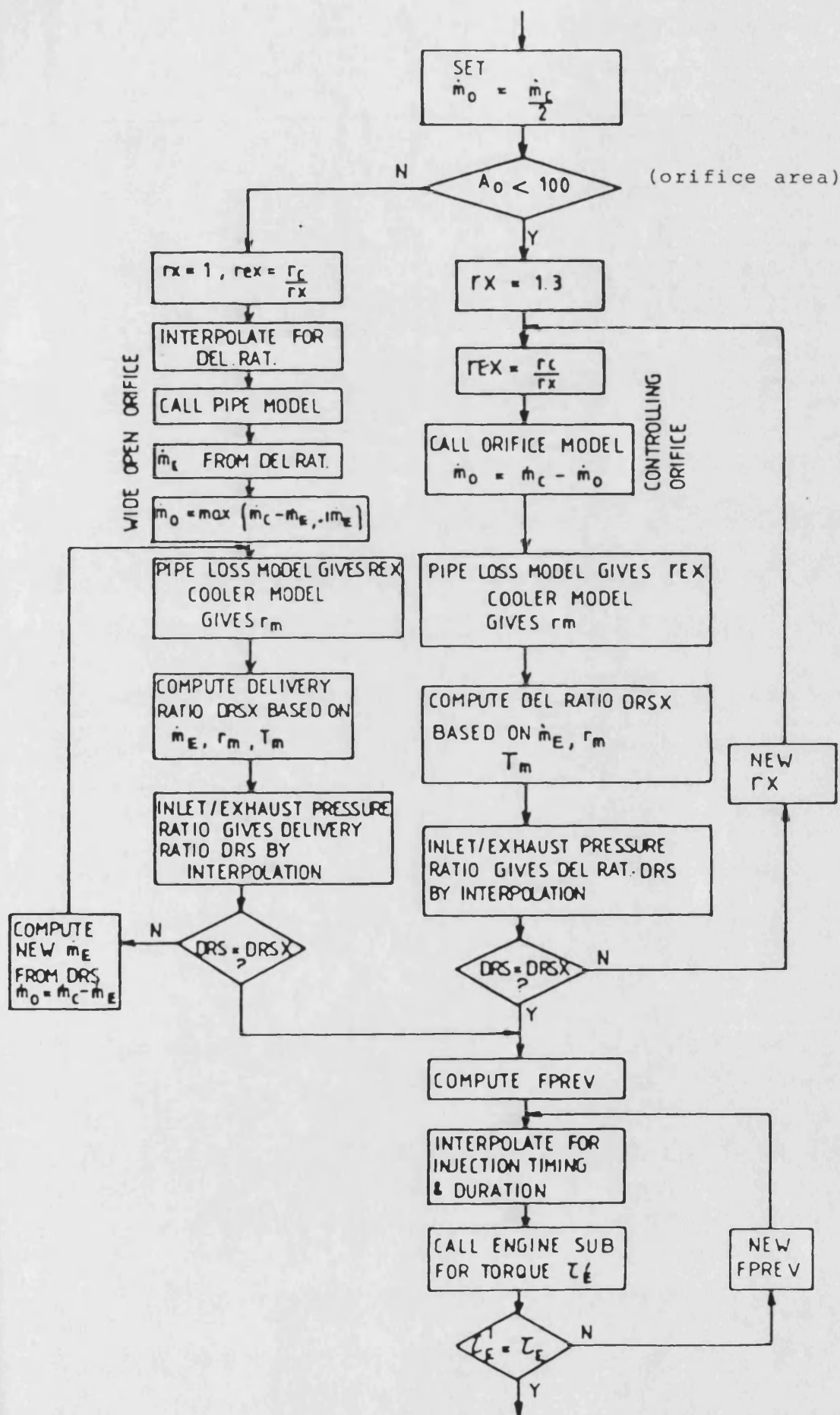
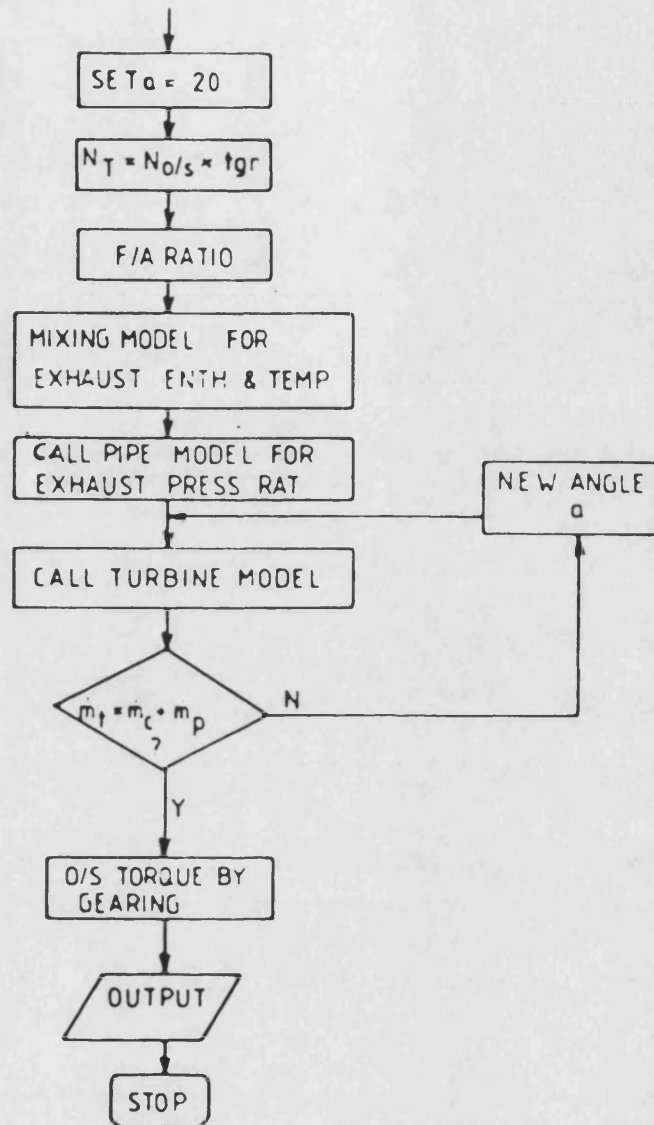


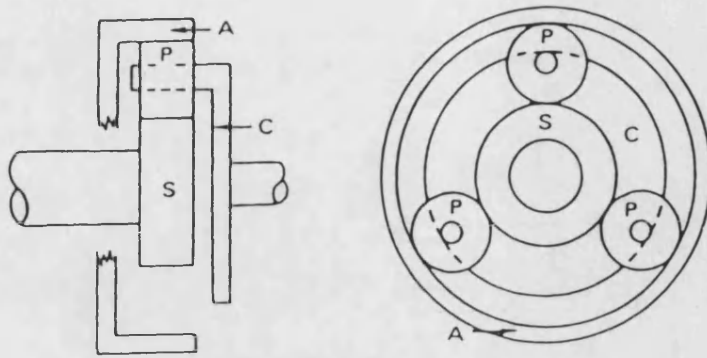
Fig-2.7 The flow chart for the program DCE2

CONTINUED: -

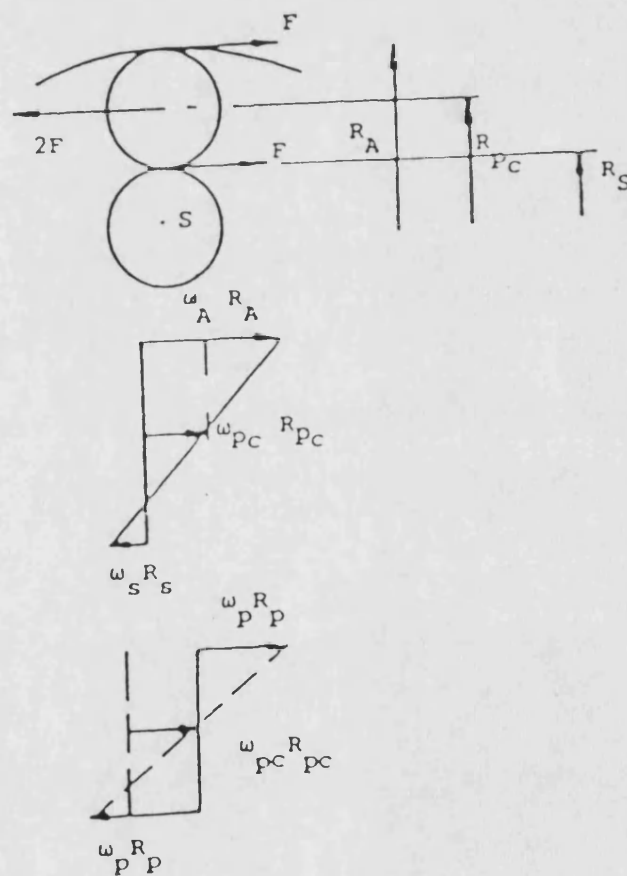


CONTINUED





a) The structure of an epicyclic gear train



b) The interacting force and the speed relationship in the epicyclic gear train

Fig-2.8 Epicyclic gear and its characteristics

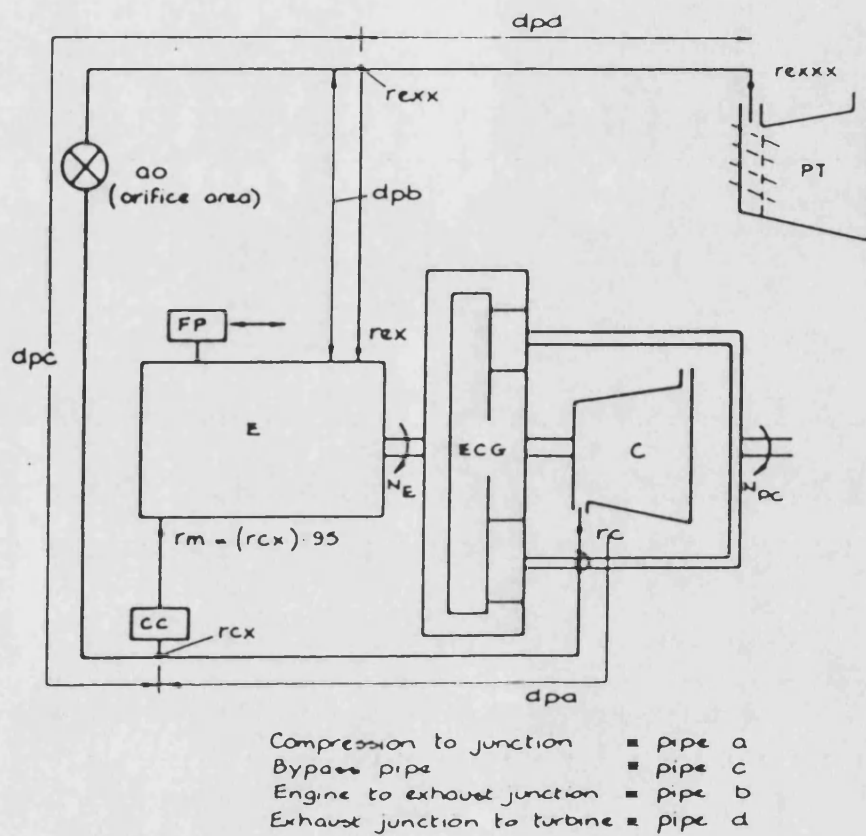


Fig-2.9 pressure loss distribution in the DCE

FLOW CHART FOR DCE-VG
=====

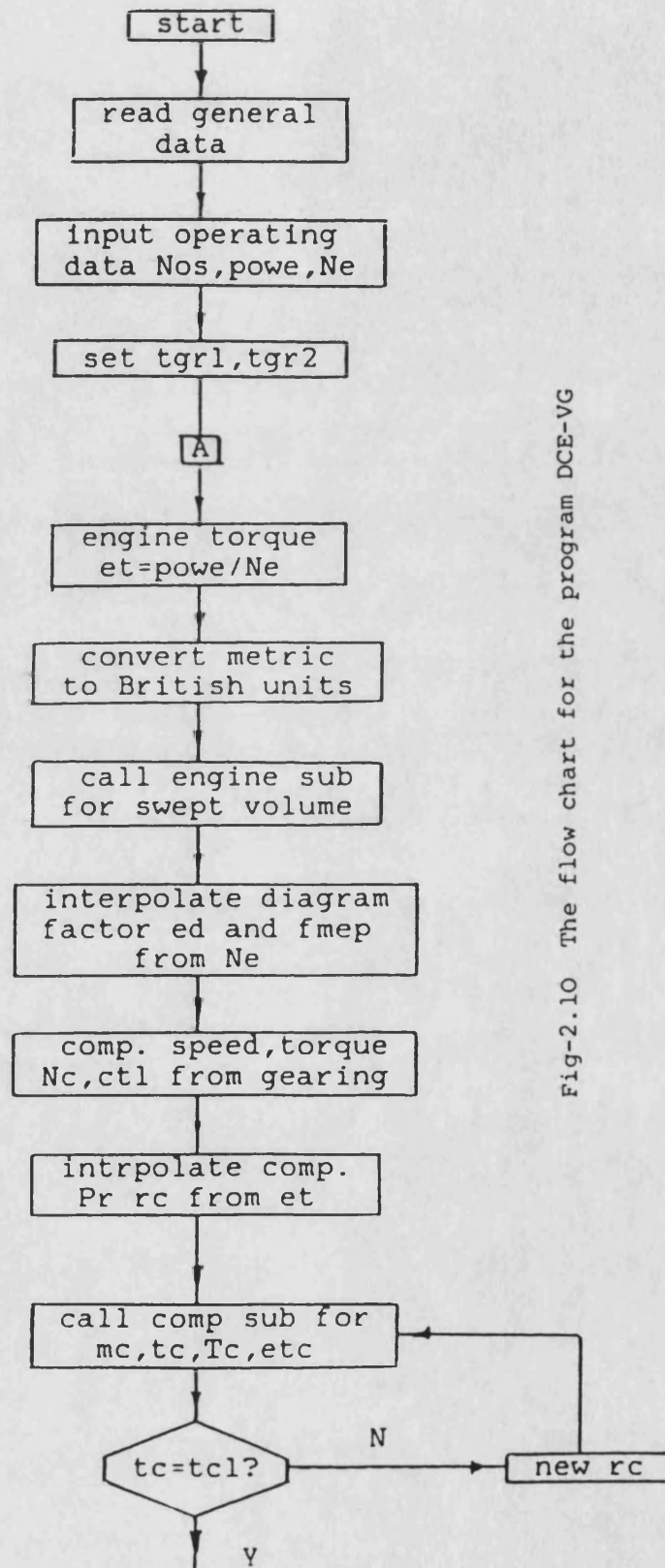
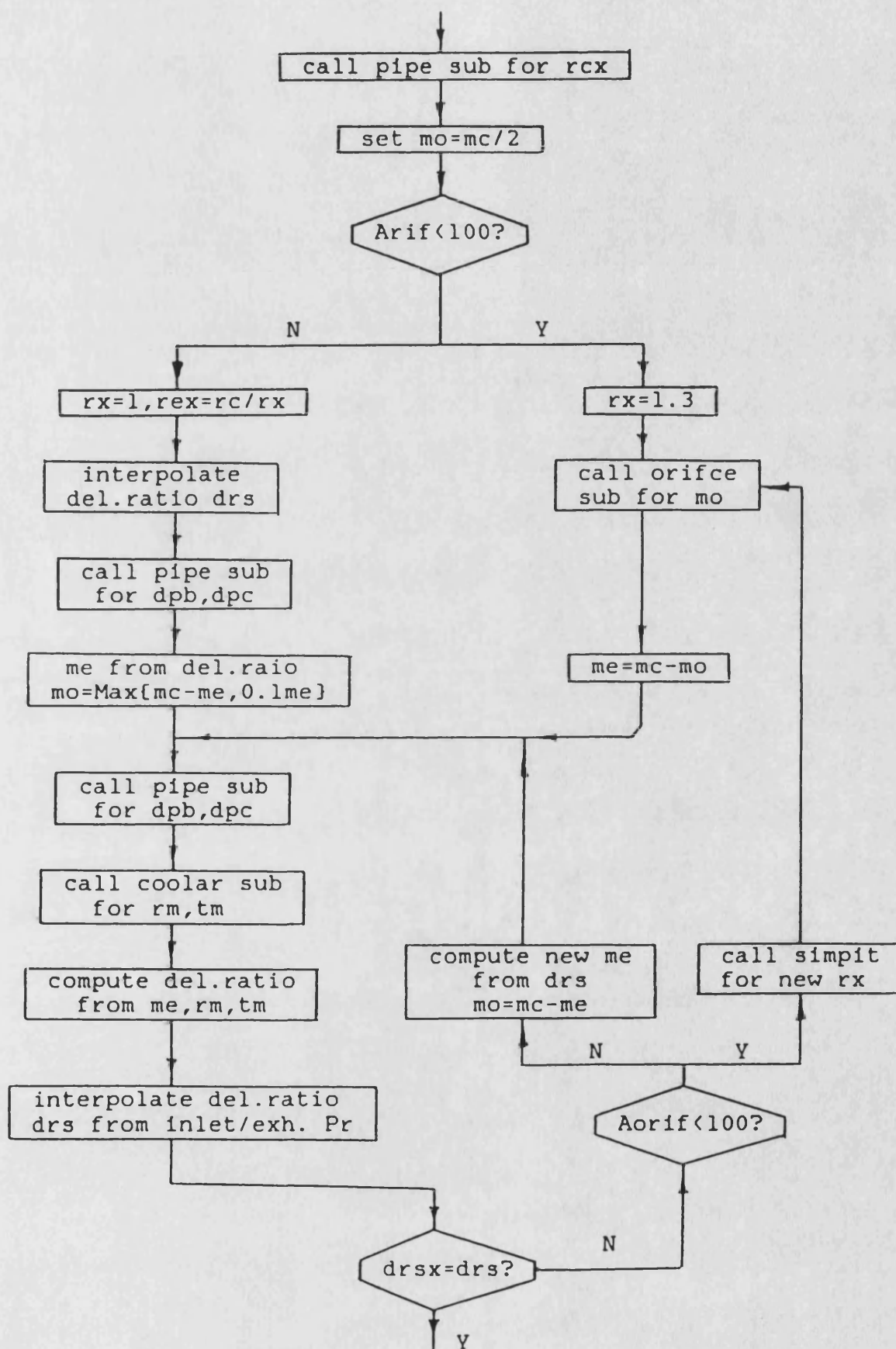
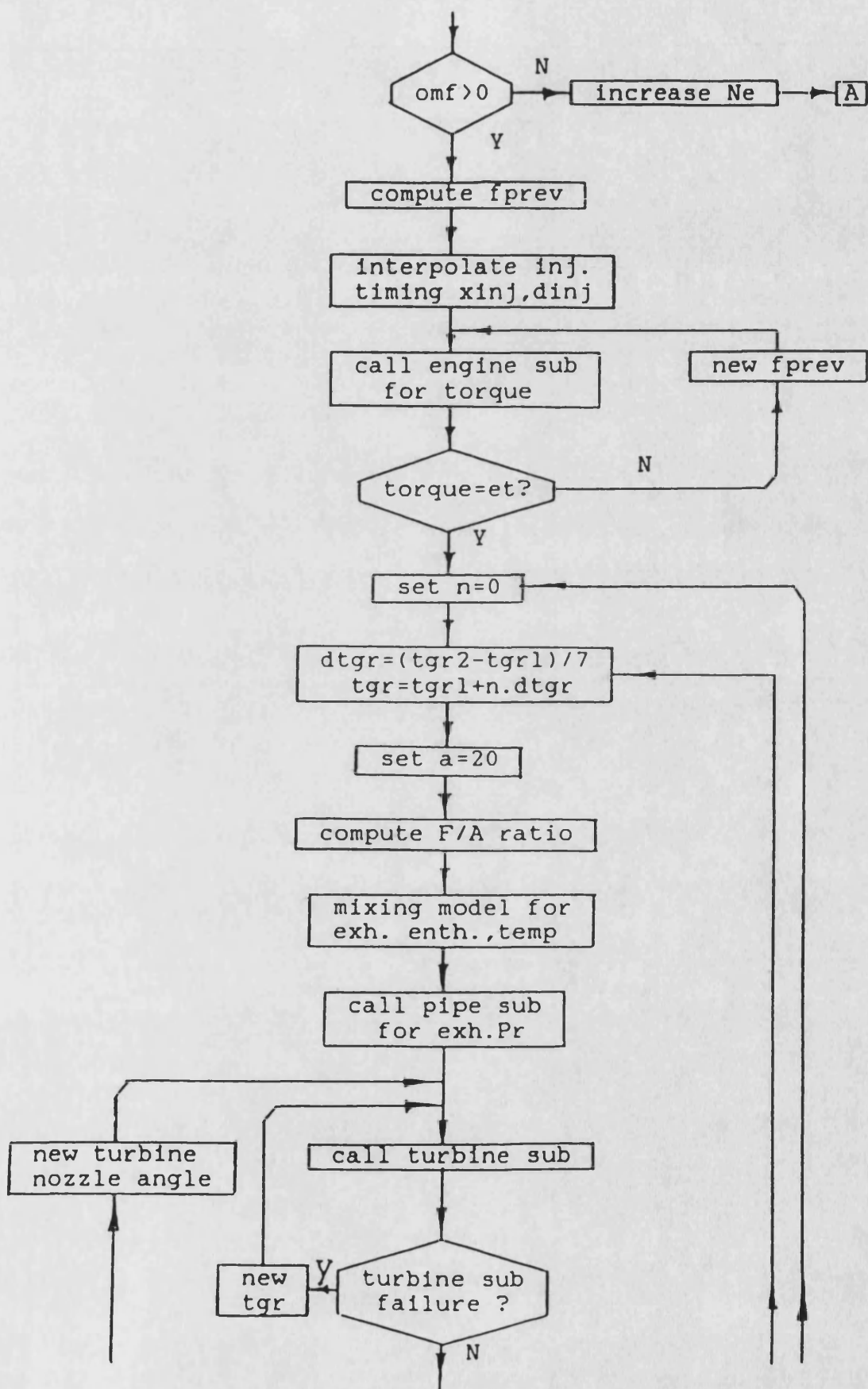


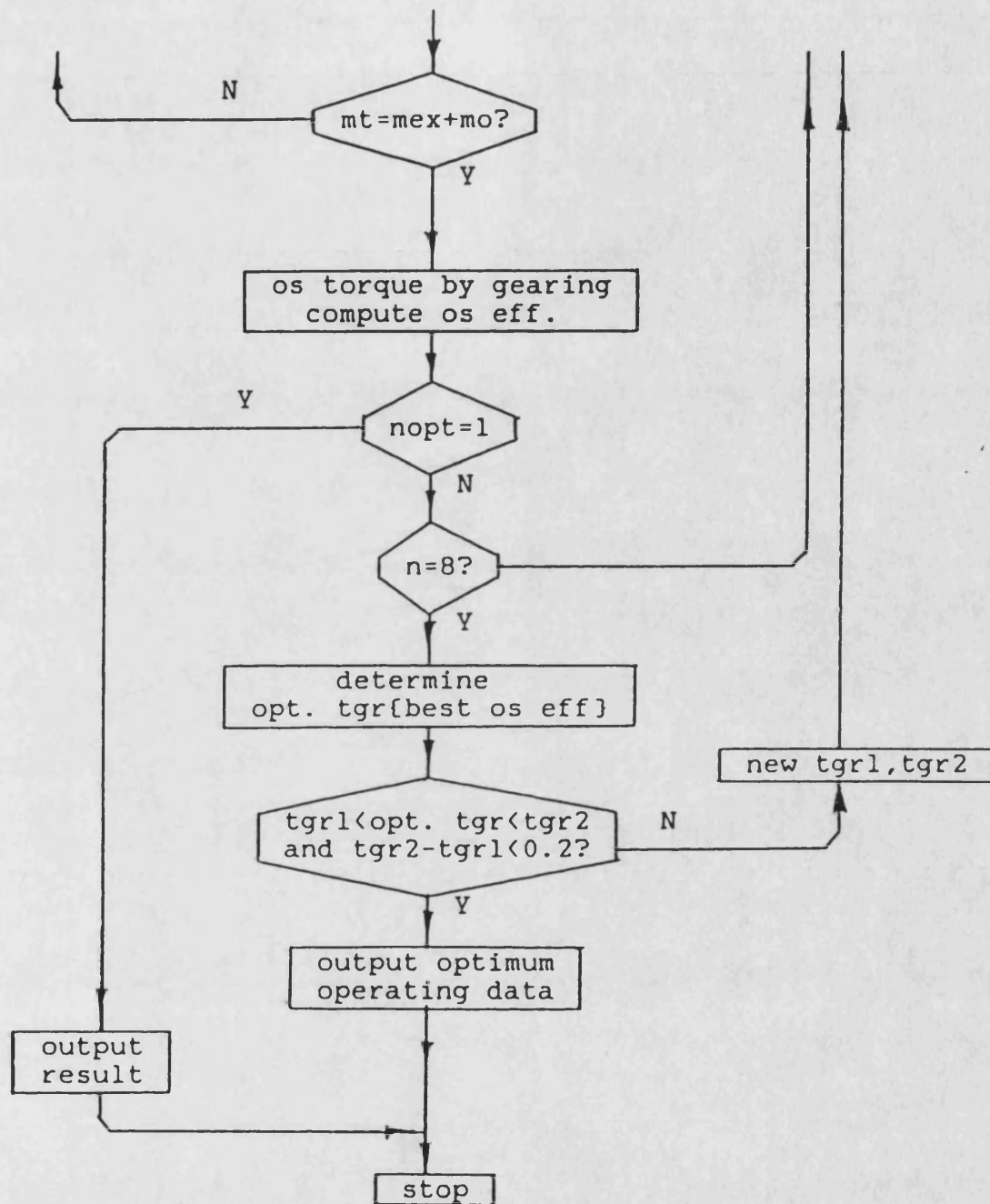
Fig-2.10 The flow chart for the program DCE-VG



continued



continued



continued

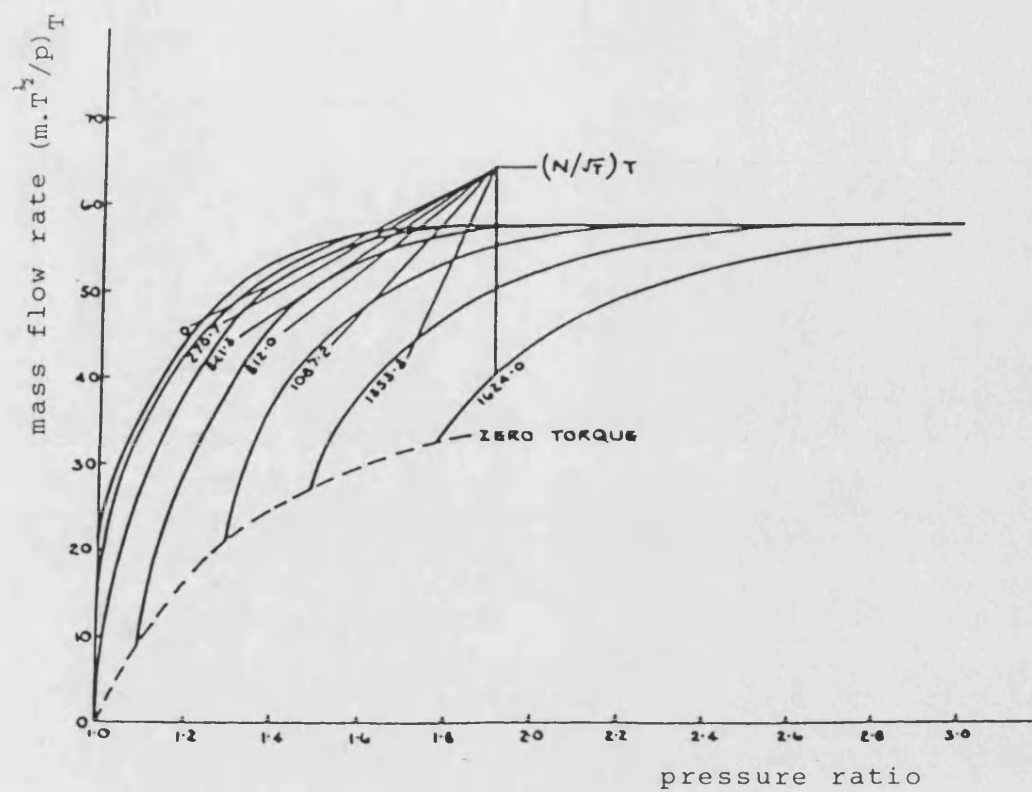


Fig-2.11 A typical turbine performance map (p_T/p_O)

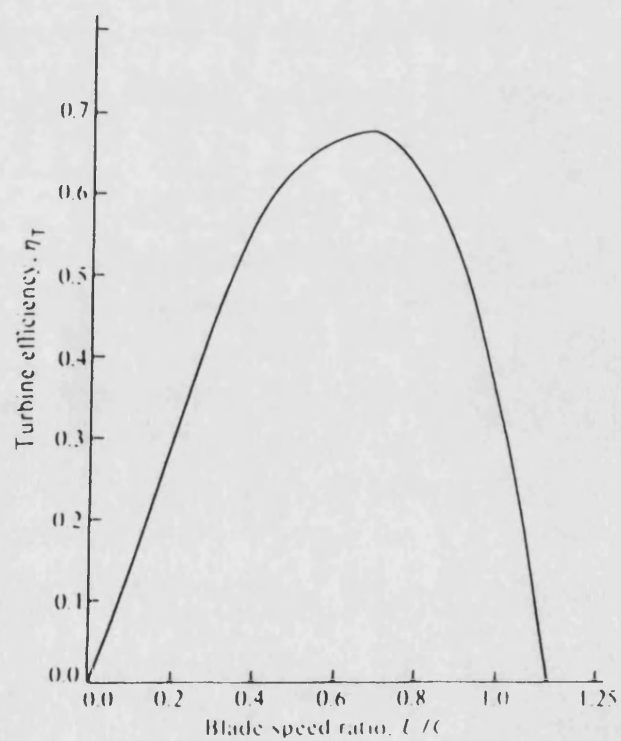


Fig-2.12 Turbine efficiency characteristic.

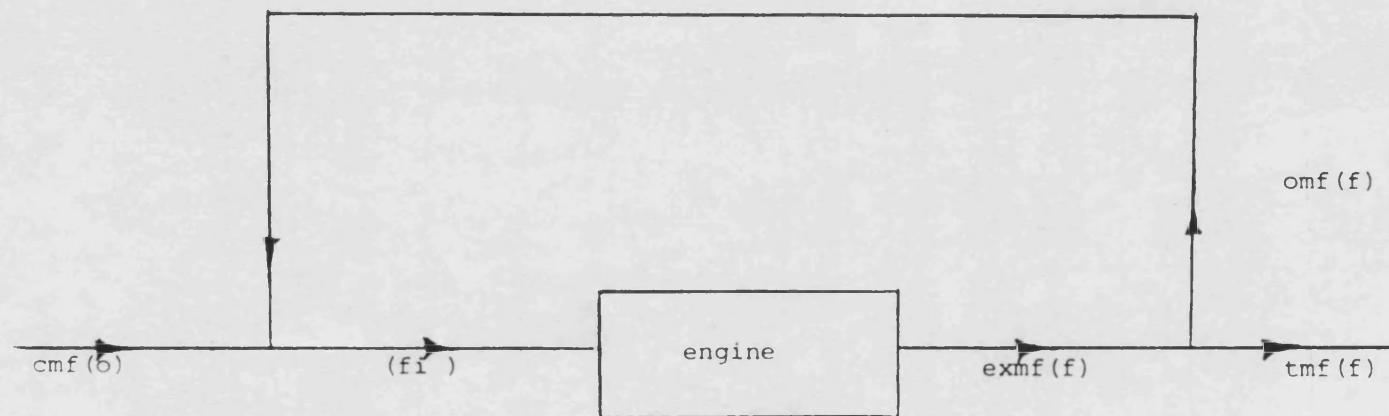


Fig-2.13 The flow diagram under reverse bypass flow

FLOW CHART FOR DCE-FG

=====

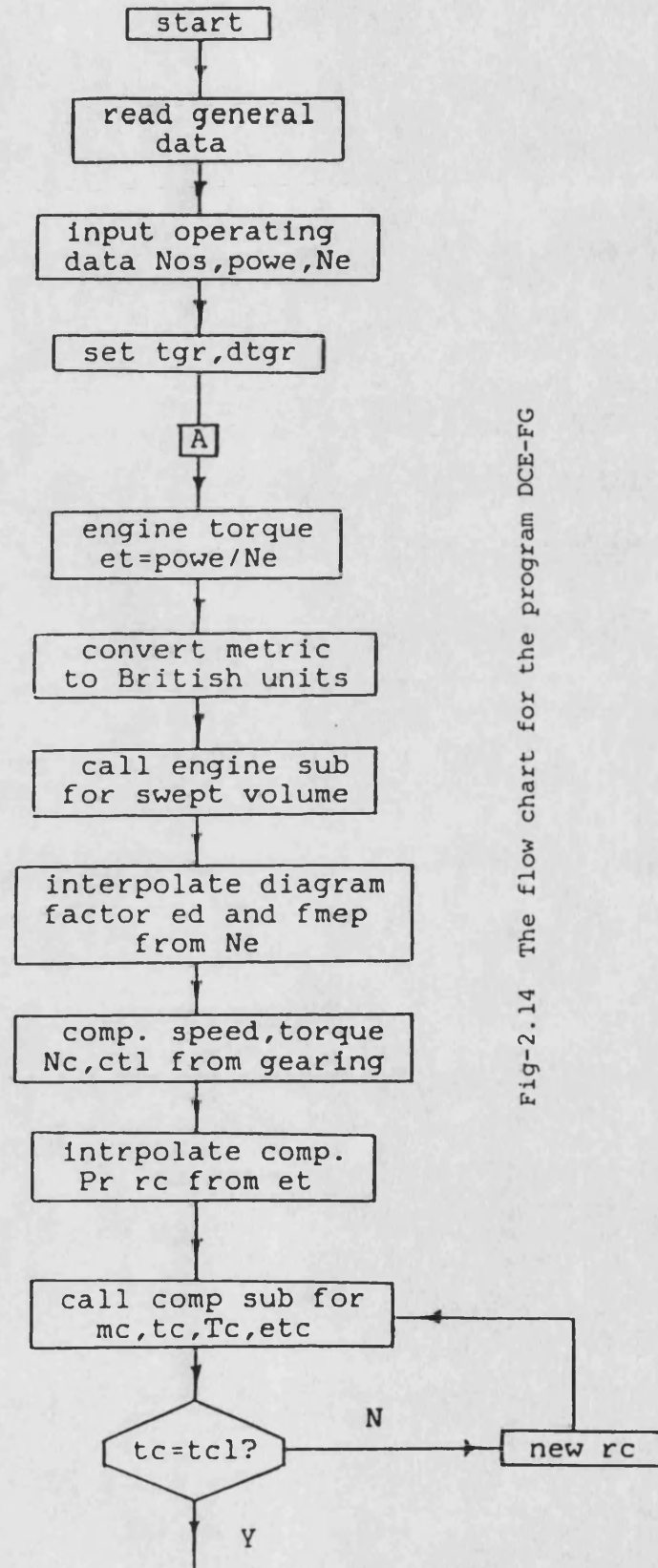
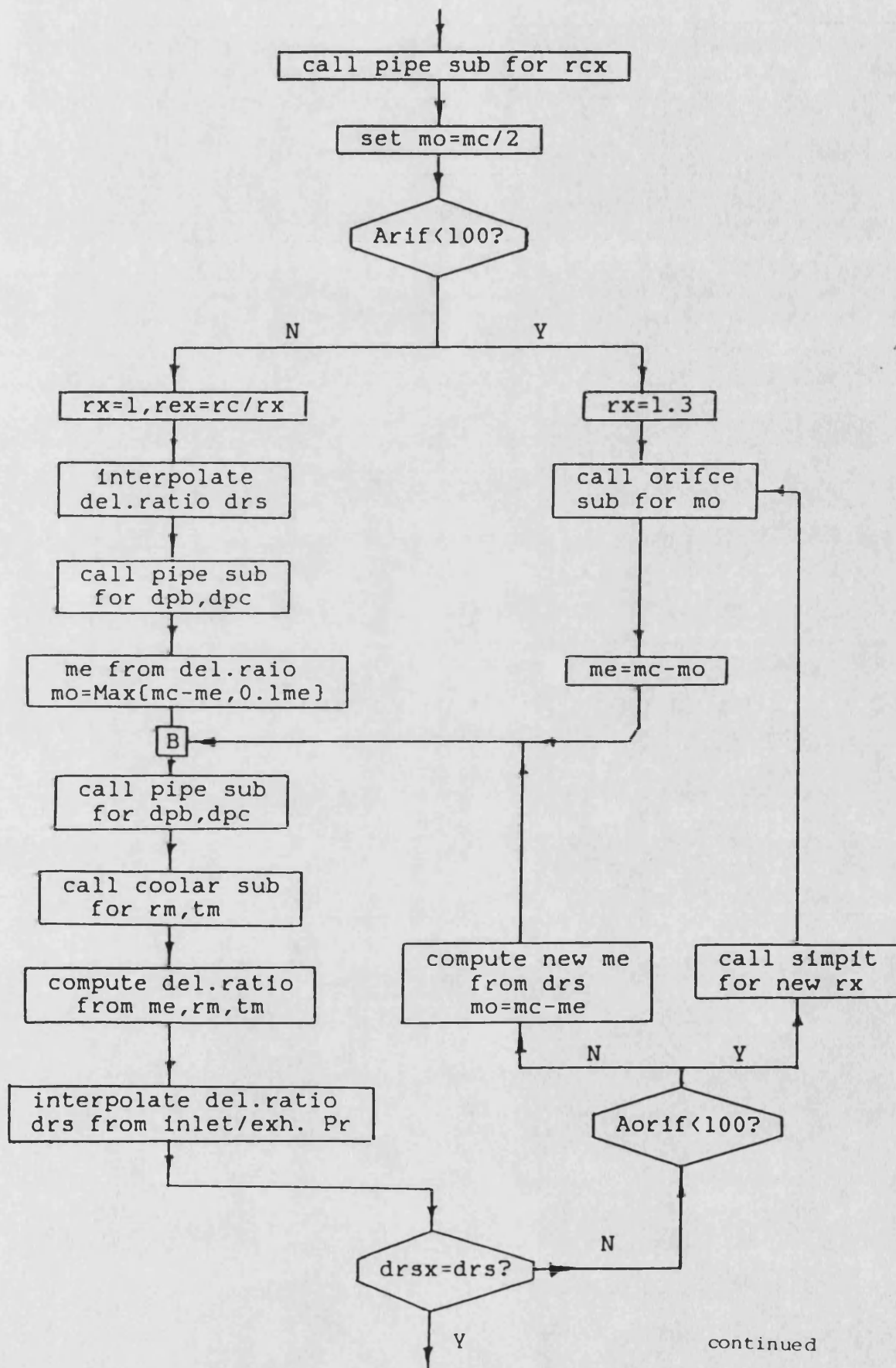
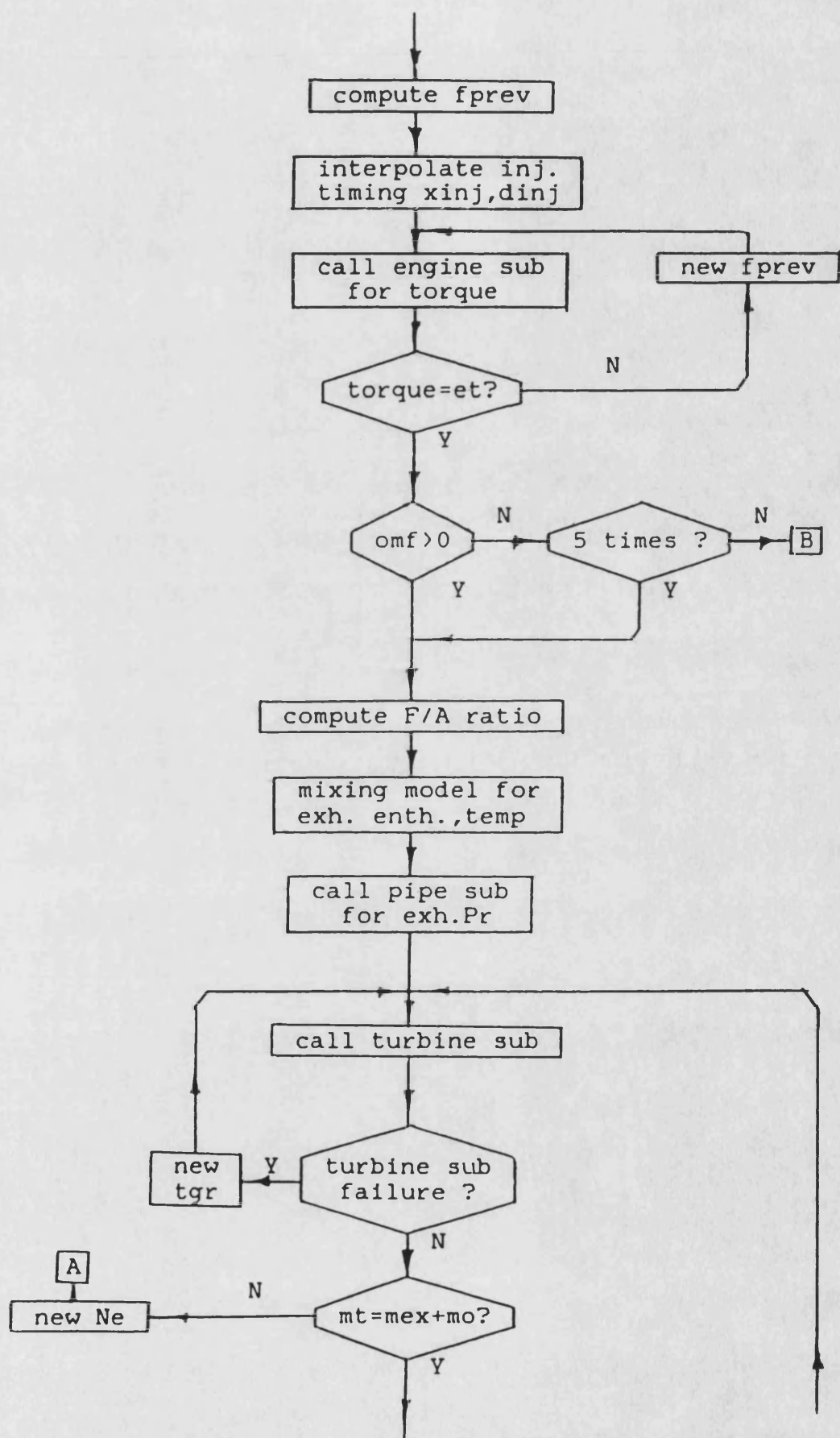


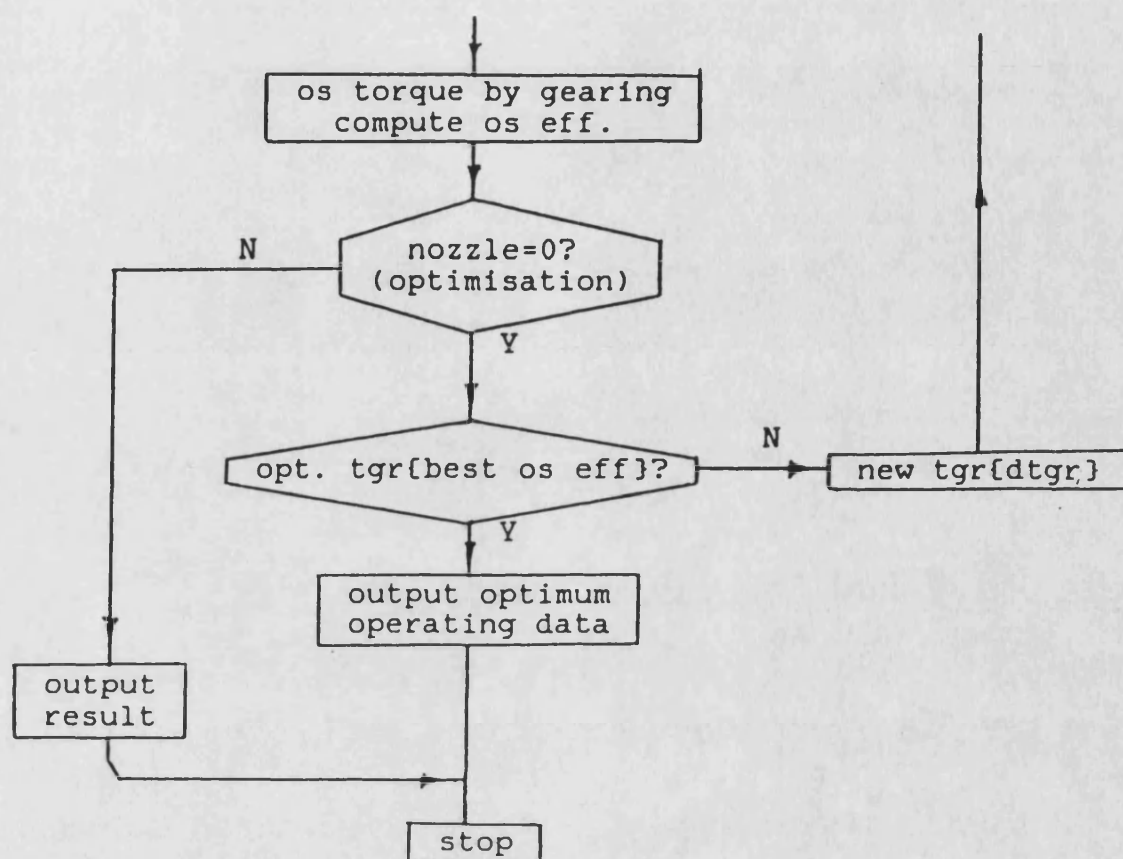
Fig-2.14 The flow chart for the program DCE-FG



continued



continued



continued

CHAPTER 3

DETAILED SIMULATION OF THE TURBOCHARGED CUMMINS L10 ENGINE USING PROGRAM EMAT

In the following extensive computer investigations, the performance of the L10 engine in standard build form is simulated, in the first place. Then using these results as the base data, the performance with variable geometry turbocharger is studied. Finally the effects of changing ambient conditions on the system operation are investigated in detail.

Some important data of the engine are listed in Table-3.1. The compressor map used is based on the Holset H2C 8650 turbocharger(Fig-3.1) while, for convenience, the turbine calculation is based on the Holset H2C 8640 turbocharger(dimensions being known and previously used with the Leyland engine TL11) which are scaled to suit the present need(with a turbine nozzle angle of 23deg. rather than 26deg.).

The experimental performance data on the limiting torque curve(Table-3.2) of this engine are based on data supplied by the company; and on simulations using program SPICE.

In view of the inherent nature of the program as described in chapter 2 some important empirical parameters have to be adjusted in simulating a specific engine. Calculations have been carried out with various values of the mixing rate constant x_k and the heat loss factor q_{lf} . the final choice is $x_k=0.05$ and $q_{lf}=1.5$, which gives most satisfactory results. In order to match the operation of the turbocharger with the highest possible accuracy, the turbine flow loss factor(polytropic efficiency) is altered to 0.72 instead of 0.80 as used in most earlier calculations.

It should be noted that in all the following cases, simulation is only performed on the limiting torque curve.

3.1 Base Line Results(Standard Ambient Conditions)

(Pa=0.99bar, Ta=294.4K)

The predicted performance data are shown in Table-3.3. The major operating parameters are engine speed and fueling(fuel/rev), i.e. 1000rpm-349.2mg/rev; 1260rpm-361.2mg/rev; 1500rpm-353.2mg/rev; 1800rpm-330.3mg/rev and 2100rpm-304.2mg/rev. In order to assess the quality of the prediction, relevant data from Table-3.2(experimental) and Table-3.3(predicted) are grouped together to form Table-3.4. The table is divided into five sets according to the different operating conditions. To assist analysis some selected parameters are plotted in Fig-3.2(a,b,c).

a) It can be seen that very good agreement has been achieved between experimental and predicted brake power, torque, BMEP(Fig-3.2a), bsfc and brake thermal efficiency(Fig-3.2b), all with differences of under 3%. Although slightly bigger differences are produced in terms of maximum cylinder pressure, exhaust temperature(Fig-3.2c) and heat(loss) to coolant(Table-3.4), they are still quite acceptable. Generally, experimental maximum cylinder pressure and heat to coolant are higher than predicted values while, conversely, exhaust temperature is lower.

b) Relatively significant discrepancies exist in turbocharger operating parameters, especially for turbocharger speeds(Fig-3.2c). At lower engine speeds predicted values are lower(52518rpm cf. 57790rpm at engine speed of 1000rpm). The difference decreases with increasing engine speed. Eventually predicted values exceed those from experiments.

As a direct result, compressor pressure ratio and boost ratio(Fig-3.2a) vary in a similar fashion, although not strictly in phase. However the variation of air/fuel ratio is comparatively irregular(Fig-3.2b).

c) Over the entire engine speed range, predicted compressor and turbine efficiencies are better than experimental ones. Also the calculated turbine pressure ratios exceed the experimental values(Table-3.4). However, the predicted values here represent the theoretical maximum pulse pressure ratio whereas the measured values are averaged over the complete cycle. As is known, in pulse turbocharging, turbine inlet pressure rises rapidly during the blowdown period. After reaching a peak value, it falls gradually to its minimum level at the beginning of the exhaust process unless pronounced pulse interference from other cylinders is present. In

general this is not the case with 6 cylinder in line engines. In the analytical model used in EMAT, instantaneous mixing of the gases in the cylinder and exhaust manifold at EVO is assumed; thereafter turbine inlet pressure falls progressively from its highest value in five steps to its lowest level at the end of the process. Therefore the pressure ratio in the first step will be higher than the averaged value. Obviously the variation of turbine pressure ratio is a continuous process and the simplified procedure adopted will inevitably introduce errors. Further, the program as a whole is a simplification of a very complex process, and inaccuracies can also be introduced in the numerical presentation of the compressor and turbine map, etc.

d) It also can be seen that the difference in inlet manifold temperature is relatively significant. This may be due to the specification of charge cooler medium temperature. Lower predicted values of inlet temperature suggests that a higher charge coolant temperature is required. However, in view of the very accurate prediction regarding other important parameters, no further attempt was made.

The engine operating lines based on experiment and prediction are located in the compressor map Fig-3.1. It can be seen that the two lines are in substantial agreement.

At this stage, it is necessary to stress clearly some criteria with which the system performance obtained in the ongoing sections will be judged. Firstly, the base line data will be used as the standard data and the ambient conditions under which this base line results are obtained will be designated standard ambient conditions, which are temperature of 294K(21deg.C) and pressure of 0.99bar. Secondly, the values of some critical parameters under these standard conditions, such as maximum cylinder pressure, maximum exhaust temperature and maximum turbocharger speed, will be used as their respective limiting values under the same conditions when some other parameters of the system are varied(e.g. in turbine matching), although these values may not be realistic. In the present case, the maximum cylinder pressure is 131bar, the maximum exhaust temperature is 817K and the maximum turbocharger speed is 85320rpm.

3.2 Effects of Variable Geometry Turbocharging

(under Standard Ambient Conditions)

3.2.1 Effects of Turbine Match

a) In the following, calculations are carried out for two cases, each with a

different turbine nozzle angle(turbine size), one smaller(18deg. cf. 23deg.) than the standard value and the other larger(28deg. cf. 23deg.), with other data being fixed. In particular, the standard fuelling schedule as set out in Table-3.3, as well as the standard ambient conditions, are retained. The results are shown in Table-3.5(small turbine) and Table-3.6(large turbine). Some performance data from these two tables together with those from the standard results are graphically presented in Fig-3.3(a,b,c).

In Fig-3.3a the brake power and BMEP are increased with the smaller turbine but decreased with the large turbine over the greater part of the operating region, especially in the low speed region. At the high speed end, differences are small, the standard build having the highest value, followed by the large build and then the small build(power: 187.12kw, 188.27kw, 185.77kw; BMEP: 10.677bar, 10.74bar, 10.601bar; in order of decreasing turbine nozzle angle). However, the more significant point is that as turbine nozzle angle decreases, the maximum BMEP increases and moves toward lower engine speed(12.7bar, 1500rpm; 13.0bar, 1300rpm; 13.4bar, 1260rpm again in decreasing nozzle angle order, with resultant torque backup of 19.8%, 21% and 25.5%). It can also be seen from Fig-3.3a that boost pressure ratio increases with decrease of turbine nozzle angle over the entire engine operating range becoming more significant at high speeds. In Fig-3.3b, The variation of thermal efficiency is similar to that of power and BMEP due to constant fuelling, while bsfc varies in the opposite sense(minimum bsfc: 197 g/kw.hr, 1550rpm; 195 g/kw.hr, 1350rpm; 192 g/kw.hr, 1300rpm). The variation of air/fuel ratio is very similar to that of boost ratio. From all these results, it seems that the match with the small turbine is the best one in terms of bsfc, torque back up and air fuel ratio. In Fig-3.3c the variation of exhaust temperature from the three matches gives the same indication(low exhaust temperature implying low thermal load). However, when looking at the plots of maximum cylinder pressure and turbocharger speed, this is no longer the case. With the small turbine the maximum cylinder pressure increases to 146bar at 1750rpm from the standard value of 132bar at 1700rpm, and the turbocharger speed from 85320 to 95163rpm at rated engine speed. As stated earlier(section 3.1), this is not allowed. Therefore appropriate measures have to be taken to ensure that the limits are not exceeded. The match with the large turbine results in very poor performance, with lowest economy, highest exhaust temperature, and lowest torque(BMEP). The only favourable features are lowest cylinder pressure and turbocharger speed with the potential of increasing the fuelling at high speed to produce more power, although it

may not be realistic, for a reasonable torque backup is always necessary for an automotive engine.

At this stage it is appropriate to discuss the fundamental reasons for these results in some detail. For this purpose, the performance data for the three matches at engine speeds of 1000rpm and 2100rpm are selected in Table-3.7.

As turbine nozzle angle decreases, the pressure ratio across the turbine increases(1.411, 1.448, 1.548 for the first pulse step at 1000rpm). This results in increased turbine power and hence turbocharger speed, compressor pressure ratio and mass flow. As a consequence, the following changes take place in engine performance: Air/fuel ratio is increased(17.7, 18.4 and 19.95 at 1000rpm), resulting in lower cycle temperature and lower heat loss to coolant; higher boost leads to higher cylinder pressure and higher back pressure. If the effects of higher cylinder pressure and lower heat loss outweigh those of lower cycle temperature and higher pumping work due to high back pressure, engine efficiency will increase and vice versa. It can be observed that at low speeds favourable effects are produced with decreasing nozzle angle, engine efficiency increasing from 0.3842 to 0.3968 and then to 0.4225 at 1000rpm. However, at high speed the results are not very clear cut, but usually excessive back pressure will increase the pumping work substantially with the smaller turbine.

b) To make the comparison more realistic, the fuelling with the smallest turbine match is modified so that turbocharger speed and maximum cylinder pressure are confined within the limits set by the standard match(giving a maximum turbocharger speed of 85320rpm at 2100rpm engine speed and maximum cylinder pressure of 132bar at 1700rpm engine speed, Table-3.3), i.e. the fuelling at some operating points is reduced if necessary. The results are presented in Table-3.8 and Fig-3.4(a,b,c)(together with the results for the other two unchanged matches). Clearly, the system performance at high speeds has deteriorated significantly. The BMEP is reduced with substantial loss of power(134kw at 2100rpm cf. 188kw for the standard rated) and the economy is poor(bsfc of 216g/kw.hr cf. 204g/kw.hr at 2100rpm). The maximum cylinder pressure can also be adjusted by varying the injection timing. However, this can also affect turbocharger speed due to its influence on exhaust energy. In this preliminary study, only fuelling is adjusted.

c) The above analyses show that with different turbine matches, the performance characteristics of the system will be significantly altered. For a specific fixed geometry turbine match, the quality of operation of the system will vary over

the entire speed range. At a particular engine speed, if the turbine selected is too small, excessive boost and pumping work will result. There is also the possibility of excessive cylinder pressure(at high load) and of turbocharger overspeed(at high engine load and speed). However, if the turbine is too large, it will not be possible to extract sufficient power from the exhaust for the necessary boost. The air/fuel ratio may be too low(especially at low speed), with increased smoke emission, and the exhaust temperature too high. Therefore a better match can be obtained with a variable geometry turbine whose swallowing capacity can be adjusted continuously as required by controlling its effective flow area.

3.2.2 Synthesized VG Turbocharged Engine Operation

In the following, the performance of the system with a variable nozzle turbine is explored. In the calculation, the engine is also run under the same conditions(standard as in Table-3.3; defined by speed and fuelling) and only the turbine nozzle angle is varied. The nozzle angles at different speeds are obtained so that best performance is achieved while maximum cylinder pressure and turbocharger speed do not exceed the highest in the standard operation. Since in the previous calculations, change of turbine nozzle angle at the high speed end did not lead to any appreciable improvement in system operation(not as expected that larger turbine would lead to better results, probably because the fuelling is matched to the standard turbine), no alterations were made to the turbine nozzle angle at engine speeds of 1800rpm and 2100rpm. The synthesized results are shown in Table-3.9. As can be seen the turbine nozzle angle is reduced gradually with decreasing engine speed, limited by maximum cylinder pressure rather than turbocharger speed. The results are also shown in Fig-3.5(a,b,c)(with standard ones). As a consequence of rematching, the performance at low speeds is improved. Maximum BMEP is increased to 13.35bar at 1260rpm with a nozzle angle of 19 deg. from 13bar at 1300rpm. Very high BMEP is retained all the way down to the lowest speed of 1000rpm(13.13bar)(Fig-3.5a). Low speed boost was significantly increased(Fig-3.5a). The same is true for air/fuel ratio(23.72 cf. 18.4 at 1000rpm) and bsfc(191.2g/kw.hr cf. 210g/kw.hr at 1000rpm)(Fig-3.5b). On the other hand, maximum cylinder pressure has increased, to approximately its base line limiting value of 131bar all over the low speed region(Fig-3.5c). Turbocharger speed has also increased but remains well below the limiting value(Fig-3.5c). A very prominent feature of the results is that the engine efficiency actually increases in the direction of decreasing speed(Fig-3.5b).

Limiting torque operation under fixed and variable geometry turbocharging is plotted in Fig-3.6 on the compressor map. Selection of small nozzle angles at lower speeds causes the compressor pressure ratios and mass flows to rise. It appears that at an engine speed of 1000rpm the operating point is slightly closer to the compressor surge line but sufficient margin is still retained. However, if the application of variable turbocharging leads to unstable operation of the compressor(e.g. due to substantial uprating of the system), or the flow range of the compressor is too narrow, then a variable geometry compressor has to be adopted. However, some practical tests on compressors with variable diffuser guide vanes indicate that while the dangers of surge can be averted, there are no improvements in overall system efficiency[15].

3.3 System Performance under Varying Ambient Conditions

Vehicle engines are required to work under changing ambient conditions. This means that the properties of air before the compressor will vary, thus affecting the mass flow through the system. As is well known, the engine capacity is largely dictated by the air charge to be trapped in the cylinder, the engine performance will vary accordingly. In the following, the effects of changing ambient conditions, i.e. pressure(relating to altitude) and temperature, on engine operation are considered.

3.3.1 Operation at Altitude(1250m and 3000m)

a)Fixed Geometry Turbocharging When the engine is working at altitude, the ambient pressure will be lower, leading to reduction in mass flow due to lower air density. However, if the fuelling is unchanged, the air/fuel ratio will be lower, resulting in higher cycle temperature and exhaust temperature(within limits). In addition, low ambient pressure implies low turbine exit pressure, which contributes to increasing expansion ratio across the turbine. Under these circumstances, turbine specific power may increase. Ultimately turbocharger speed and compressor pressure ratio will increase. This increase in pressure ratio will result in higher air density at compressor discharge and, therefore, mass flow through the system. As a consequence, the effects of low ambient pressure will be partially offset.

It should be noted that in the usual matching process, allowance is made for the increase in turbocharger speed at altitude, so that the system will work within permissible limits under all possible conditions.

In this part of the investigations, calculations were performed with ambient pressures of 85% and 70% of that under standard conditions, corresponding to altitudes of 1250m and 3000m respectively; while the ambient temperature is retained at its standard value. Also, the fuelling schedule is retained. The results are shown in Table-3.10 and Table-3.11. Fig-3.7(a,b,c) show some important parameters, as set out before, under these two ambient pressures together with those for standard conditions. In Fig-3.8 the limiting torque operating lines of the system under different conditions are superimposed on the compressor map.

In order to investigate the changes in terms of system performance, the results at an engine speed of 2100rpm are discussed in detail. First, as expected, the compressor mass flow rate decreases with increasing altitude(18.87kg/m, 17.22kg/m and 15.53kg/m), although not by as much as the decrease in ambient pressure itself($17.22/18.87=0.912$ cf. 0.85 and $15.53/18.87=0.823$ cf. 0.70). The compensating effects of the turbocharger is clearly demonstrated. As can be seen, turbine pressure ratio is increased with decreasing ambient pressures(2.325, 2.553 and 2.871 at the first pulse step), as does the turbine power(30.8kw, 32.5kw and 34.1kw) and speed(85320rpm, 89844rpm and 97552rpm).

Due to the assumption of constant fuelling, the air/fuel ratio is decreased(29.5, 27.0 and 24.3, Fig-3.7b) but is still not critical. The decrease in cylinder pressure(124.5bar, 118.1bar and 111.4bar, Fig-3.7c), the increase in cycle temperature, the increasing exhaust temperature and back pressure, all interact with each other, resulting in slight deterioration in engine efficiency(0.4097, 0.4040 and 0.3972, Fig-3.7b). The performance of the system at this speed is quite acceptable, with little derating(power: 188.2kw, 185.62kw and 184.3kw, Fig-3.7a).

However, at lower speeds, low air/fuel ratio becomes critical(18.4, 16.5 and 16.0 at 1000rpm), and this has a strong influence on engine performance. These and other adverse effects lead to a noticeable reduction in engine efficiency(0.3968, 0.3663 and 0.2918 at 1000rpm).

Fig-3.7a shows that generally the power loss increases with decreasing ambient pressure, from small percentage reduction at high speed to significant reduction at low speed. The effect on the variation of BMEP is even more striking, the performance of the system being severely impaired. With decreasing ambient pressure maximum BMEP of 13.2bar at 1300rpm is reduced to 12.8bar at 1450rpm and then to 12.2bar at 1500rpm, the resultant torque backup being 22.9%, 20.75% and 17.2%, while at the same time the speed at which peak torque occurs, increases.

Fig-3.7b shows that system performance has severely deteriorated with decrease in ambient pressure (efficiency and bsfc), particularly at low engine speed, indicating the strong effects of low air/fuel ratio.

In Fig-3.7c, the increase of turbocharger speed is more marked at high engine speed. Boost pressure (Fig-3.7a) and air/fuel ratio (Fig-3.7b) follow similar patterns. The variations of maximum cylinder pressure on the one hand and exhaust temperature on the other, follows opposite trends (Fig-3.7c), with a particularly marked decrease in maximum cylinder pressure from 110 to 88 bar, accompanied by an increase in exhaust temperature from 790K to 920K, at the lowest engine speed (1000 rpm).

In Fig-3.8, it can be seen that the increase in compressor pressure ratio with altitude moves the operating point at the lowest engine speed (1000 rpm) towards the surge line, but the situation is not critical in the present case. Nevertheless, due attention has to be paid to this fact in the matching process.

It can be seen that the variation in ambient pressure has a profound effect on the operation of the system and proper consideration has to be given in the matching process in order to achieve the best compromise.

b) Variable Geometry Turbocharging at Altitude Referring the plots for BMEP in Fig-3.7a, if a rematch is considered in order to alleviate the effects of altitude, then a smaller turbine is needed. As a result, more power can be extracted at low engine speed with greater mass flow. However, at high speed the operation may suffer from excessive back pressure and overspeed of the turbocharger. Again, as an ideal solution, variable geometry turbocharging can overcome the associated problem. If sufficient turndown ratio is available, suitable mass flow can be obtained under all conditions. In Fig-3.7c, the maximum cylinder pressure decreases with altitude, and turbocharger speed decreases with decreasing engine speed, indicating increasing margin over which turbine rematch can be considered. This means that boost ratio and turbocharger speed can be increased to a varying extent as necessary at different operating points to increase mass flow, without exceeding any of the operating limits which have to be imposed.

In the following, variable geometry turbocharging at an altitude of 3000m is considered. As before, the limiting conditions are set such that the maximum cylinder pressure never exceeds that under standard conditions while the highest permissible turbocharger speed is set equal to that for the standard build

turbocharger at 3000m altitude.

A set of preliminary turbine nozzle angle schedules and the corresponding system performance are presented in Table-3.12. In Fig-3.9(a,b,c), the results for variable geometry turbocharging at sea level and at altitude are presented together with the base line results, i.e. for fixed geometry turbocharging at sea level, as set out in Table-3.3 and Fig-3.2(a,b,c). In order not to exceed the maximum turbocharger speed the nozzle angle at the maximum engine speed of 2100rpm is unchanged at 23deg. As can be seen in Fig-3.9a, system performance has been improved greatly, especially at low speeds, with power and BMEP exceeding the base line results over a significant operating range and being comparable to those with variable geometry turbocharging under standard condition. The variations of efficiency, bsfc and air/fuel ratio display similar characteristics(Fig-3.9b). These result from the very high turbocharger speed which is maintained over the entire operating range(Fig-3.9c) accompanied by the correspondingly high boost ratio(Fig-3.9a). It can be seen from the comparison between Table-3.12 and Table-3.11(fixed nozzle turbine) that maximum cylinder pressure has been increased due to the high boost ratio while exhaust temperature has been reduced due to high air/fuel ratio. The turbine nozzle angle has been reduced from 23deg. at 2100rpm to 13deg. at 1000rpm(Table-3.12).

Fig-3.10 shows the limiting torque operating lines of the system at 3000m in the compressor map, when FG and VG turbocharged. With the latter, the pressure ratio is much higher over the whole speed range. Although at an engine speed of 1000rpm, the running condition is near the surge line, an adequate margin is still retained.

It may be concluded that VG turbocharging provides a very effective means of largely compensating for the adverse effects of altitude operation.

3.3.2 Operation at Elevated Temperature

When ambient temperature varies, a change in air density results. This will reduce the mass flow through the system. In addition, this effect will be aggravated by the resultant shift in turbocharger operation. Since the specific power of a compressor is proportional to the inlet temperature, for the same pressure ratio this power will increase with increase in inlet temperature. Conversely, for the same amount of power supplied, compressor pressure ratio has to decrease in order to reach a power balance. Therefore the mass flow will be further reduced. On the

turbine side, inlet pressure is likely to be reduced due to the lower compressor pressure ratio. This will result in reduced turbine specific power. However, for constant fuelling, the exhaust temperature will increase and lead to higher turbine power. The ultimate result is a balance between these two factors. If the outcome is a reduction in turbine power, the mass flow through the system may suffer a still further reduction. Clearly, high ambient temperature is more detrimental to system operation than reduced ambient pressure.

a) In the following calculations the ambient temperature is increased from 294.4K(21deg.c) to 313.5K(40deg.c) while the ambient pressure retains the standard value. Further, the fuelling schedule is unchanged. The corresponding results are presented in Table-3.13 and Fig-3.11(a,b,c) in which the standard results are also shown. As can be seen, boost ratio(Fig-3.11a) and air/fuel ratio(Fig-3.11b) are decreased. Turbocharger speed is slightly increased due to a small increase in exhaust temperature(Fig-3.11c). It also can be seen, by comparing Table-3.3(standard) and Table-3.13, that compressor mass flow and turbine power have decreased(17.97kg/min cf. 18.87kg/min and 29.849kw cf. 30.812kw at 2100rpm). Owing to the resultant low cylinder pressure and other factors(e.g. lower air/fuel ratio), engine efficiency decreases over the entire operating range. Generally, however, the extent of deterioration in engine performance is very small. Output power is hardly affected(186.13kw cf. 188.22kw at 2100rpm, Fig-3.11a) while best efficiency is reduced from 0.4248 to 0.4203 at 1500rpm(Fig-3.11b). The greatest reduction in air/fuel ratio appears at 2100rpm(28.14 cf. 29.53) and the difference diminishes toward low engine speed. However, although the maximum BMEP is only reduced from 13.2bar at 1300rpm to 12.9bar at 1400rpm, the effect of this shift in peak torque speed on the system performance can be more significant.

As also can be seen, the effects of elevated temperature on engine performance are more or less uniform across the speed range.

Recalling the preceding analyses, the results appear to be surprisingly optimistic, with the effects of elevated temperature hardly felt by the system. This may be explained as follows. Firstly, because the ambient pressure is fixed in the present case, the variation in ambient air density follows a constant pressure process, i.e. density decreases proportionally with temperature rise. Therefore the fractional fall in air density at compressor inlet is $(1-294.4/313.5)=0.061$, a relatively small factor. Secondly, the same intercooler coolant temperature is used, which is not quite realistic, giving a relatively lower inlet manifold temperature.

b) Variable geometry turbocharging has also been applied under these conditions, the results being presented in Table-3.14 and Figs-3.12a-c. As expected, the data are very comparable to those for VG turbocharging under standard conditions. In Fig-3.12d, the operating lines with FG and VG are superimposed on the compressor map.

3.3.3 System Operation at Elevated Altitude and Temperature

a) As a relatively extreme case, the system operation is studied when a combination of high altitude and elevated ambient temperature takes place. In the calculation an altitude of 1250m and an ambient temperature of 40deg.c are assumed. The results for a fixed nozzle turbine(nozzle angle 23deg.) are presented in Table-3.15. This is also shown in Figs-3.13(a,b,c), together with the separate results for elevated altitude(1250m, standard ambient temperature) and elevated ambient temperature(40deg.c, standard ambient pressure). As expected, derating(power, BMEP in Fig-3.13a) occurs mainly at low engine speeds as a direct result of the decrease in air/fuel ratio. This trend is also reflected in the bsfc and efficiency curves. The maximum BMEP decreases and moves toward higher engine speed, which is comparatively more significant.

b) The results for the variable nozzle angle schedule are presented in Table-3.16. Figs-3.14(a,b,c) show the results for variable geometry turbocharging under standard conditions(Table-3.3 and Figs-3.2(a,b,c)) and under a combination of elevated altitude and temperature. Again, as expected, system performance has been substantially enhanced, particularly in the low speed region where the two sets of results are quite comparable. In Fig-3.14d, FG and VG operating lines are superimposed on the compressor map. At medium speeds boost ratio has been kept somewhat lower to avoid exceeding the maximum cylinder pressure limit.

3.4 Summary

a) The operation of the L10 engine under various ambient conditions has been studied. As can be seen, the change in ambient conditions can significantly affect the system performance. In the present study, only the effects of elevation in ambient temperature and of reduction in ambient pressure have been touched upon. Under both circumstances the system will be derated, which is of most concern. Under increased ambient pressure and elevated ambient temperature, the system will operate under favourable conditions in terms of the air mass which could be trapped, although it has to be made sure that the maximum cylinder pressure do not

exceed the limiting value.

Under reduced ambient pressure condition, the problem of the match between the engine and turbocharger in the conventional system becomes acute, i.e. under low speed operation, insufficient air supply becomes more severe, output power and torque backup deteriorating substantially. Due to the compensating effects of the turbocharger, derating at high speeds is not as serious as at low speeds.

Under elevated temperature, the system performance deteriorates across the entire speed range almost uniformly. Under the combination of reduced ambient pressure and elevated temperature, the problem will be aggravated.

b) The effects of VG turbocharging on system performance have also been studied. Within the limits set out in the base line data, introduction of VG turbocharging can significantly enhance the system performance, by increasing the low speed boost, hence power and efficiency. Most importantly, torque backup is substantially improved.

VG turbocharging becomes even more significant when the system is operating under changing ambient conditions. The adverse effects which occur with the conventional turbocharging system have almost been eliminated and high performance is retained.

The present investigations have been carried out for a fixed fuelling schedule and the objective has been limited to obtaining an improved limiting torque curve, hence torque backup. Undoubtedly, low load operation can also be improved with VG turbocharging, and this has indeed been shown to be the case[14]. Also, uprating can be achieved with VG turbocharging, with some modifications to the system. With the provision of a VG compressor, even higher power density can be achieved[17].

c) The program EMAT has been used throughout the investigation. It can be seen that EMAT is a very effective tool in simulating a turbocharged engine system with reliable accuracy and acceptable computing economy.

Cummins L10-250 engine data
=====

Number of cylinder	6
Cylinder bore	0.125m
Stroke	0.136m
Connecting rod length	0.21778m
Inlet valve diameter	0.0556m
Exhaust valve diameter	0.0556m
Compression ratio	16.3

Valve timing relative to TDC

in the open period:

EVC	3 degrees ATDC
IVC	193 degrees ATDC
EVO	495 degrees ATDC
IVO	701 degrees ATDC

Table-3.1 A list of important parameters of L10 engine

Table-3.2 COMPARISON BETWEEN EXPERIMENTL RESULTS AND SPICE PREDICTIONS
USING WIEBE FUNCTION AS HEAT RELEASE MODEL
(CUMMINS L10-250 T/C)

	EXP.	SPICE	EXP.	SPICE	EXP.	SPICE	EXP.	SPICE	EXP.	SPICE	
.....											
ENG. RUN. COND.											
Nom Speed RPM	1000.00	1000.00	1260.00	1260.00	1500.00	1500.00	1800.00	1800.00	2100.00	2100.00	
Load %	100.00	100.00	100.00	100.00	100.00	100.00	100.00	100.00	100.00	100.00	
Fuel Flow lb/h	46.34	46.34	60.20	60.20	70.10	70.10	78.67	78.67	84.50	84.50	
Fuel/Shot mg	116.40	116.40	120.40	120.40	117.74	117.74	110.10	110.10	101.40	101.40	
Timing BTDC deg		17.00		18.00		17.00		16.50		15.50	
Burn Dur Angle		52.50		62.50		62.50		62.50		62.50	
ENGINE RESULTS											
.....											
Torque kg.m	97.04	95.27	104.04	102.49	104.27	102.47	97.26	95.45	86.70	86.08	
Brk. Power kW	99.62	97.80	134.60	132.60	160.57	157.80	179.73	176.40	186.92	185.40	
BMEP bar	11.94	11.7	12.80	12.6	12.83	12.6	11.96	11.7	10.67	10.6	
Brk Th Eff %	39.95	39.14	41.56	40.87	42.51	41.81	42.42	41.63	41.05	40.67	
BSFC g/kWh	210.54	214.90	202.38	205.80	197.98	201.20	198.24	202.00	204.89	206.80	
Max Cyl P bar	119.97	132.00	127.76	132.00	132.04	136.00	132.04	131.00	129.21	127.00	
Max Cyl T K		2136.00		2028.00		1940.00		1834.00		1725.00	
Trap. Vol Eff %	77.00	96.60	93.00	96.10	95.00	95.40	94.00	94.20	92.00	92.60	
Air Flow kg/min	5.92	7.70	9.73	10.58	12.90	13.70	15.90	17.04	19.02	20.63	
Trap. A/F Ratio	17.07	21.90	20.64	23.20	24.08	25.80	26.60	28.60	29.48	32.30	
Inl Man P bar	1.47	1.46	1.59	1.61	1.73	1.77	1.83	1.86	1.93	1.97	
Exh Man P bar	1.27	1.25	1.38	1.40	1.46	1.55	1.57	1.69	1.70	1.88	
Inl Man T degK	324.00	322.00	326.00	323.00	330.00	325.00	333.00	325.00	337.00	327.00	
Exh Man T degK	787.00	739.00	805.00	770.00	796.00	758.00	792.00	749.00	784.00	729.00	
TURBOCHARGER											
.....											
Speed RPM	57790.00	57778.00	64987.00	65017.00	72568.00	72552.00	78047.00	78281.00	83863.00	83946.00	
Turb Power kW		6.6/6.7		11.6/11.3		17.5/17.4		24.8/23.7		32.1/32.4	
T/C Eff %	35.50	37.49	36.85	39.13	37.95	43.51	38.96	48.15	38.52	47.07	
Turb PR	1.27	1.36	1.35	1.53	1.47	1.68	1.57	1.80	1.70	1.96	
Turb Eff %	56.40	51.53	55.00	52.26	55.00	58.24	54.50	64.52	53.50	65.06	
Comp PR	1.43	1.52	1.56	1.67	1.71	1.84	1.85	1.93	1.96	2.04	
Comp Eff %	63.00	72.85	67.00	74.90	69.00	74.72	71.50	74.64	72.00	72.36	
BALLANCES											
.....											
Mass Flow	--	1.00	--	1.00	--	1.00	--	1.00	--	1.00	
T/C Power	--	0.99	--	1.03	--	1.00	--	1.04	--	0.99	
Energy :	--	1.00	--	1.00	--	1.00	--	1.00	--	1.00	
Coolant %	35.31	29.94	28.77	25.24	24.15	23.22	22.28	22.05	21.60	21.93	
Exhaust %	24.74	30.92	29.67	33.89	33.34	34.97	35.30	36.32	37.34	37.40	
Work %	39.95	39.14	41.56	40.87	42.51	41.81	42.42	41.63	41.06	40.67	

Table-3.3 Base line results (a=23deg.)

CUMMINS L10 DIESEL ENGINE, HOLSET H2C TURBOCHARGER

	152	109	545
number of cylinders	6.0	bore (m)	0.13
con-rod length (m)	0.21778	inlet valve closing (degs)	193.0
ambient temperature (deg k)	274.4	heat loss factor	1.5000
compression ratio	16.30	combustion rate factor	0.0500
stroke (m)		compressor factor	1.00
		ambient pressure (bar)	0.99000
		turbine flow loss factor	0.7200
engine speed(r.p.m.)	1000.00	1260.00	1500.00
boost pressure ratio	1.367	1.570	1.754
trapped a/f ratio	18.382	20.191	22.905
delivery ratio	0.850	0.848	0.852
manifold temp (deg k)	312.422	315.370	318.746
engine power (k w.)	77.64	137.47	161.84
engine torque (n.m.)	751.49	1042.01	1030.28
b.m.e.p (bar)	11.7402	13.0762	12.9290
s.f.c. (g/kw hr)	210.278	198.609	196.421
b.thermal eff.	0.3768	0.4201	0.4248
fuel / rev (kg.)	3.492	3.612	3.532
max cyl pressure (bar)	111.27	122.63	130.15
max cyl temperature(deg k)	2255.21	2191.05	2082.96
exhaust temperature(deg k)	795.76	815.15	816.88
percentage heat to coolant	33.50	27.11	23.06
compressor pressure ratio	1.4107	1.6355	1.8425
delivery temperature(deg k)	338.57	355.74	370.16
delivery pressure (bar)	1.398	1.618	1.812
compressor speed (r.p.m.)	52518.4	64277.3	73259.3
volume flow (cu ft / min)	5.48	7.84	10.36
compressor power (kw.)	4.739	9.421	15.363
compressor efficiency	0.693	0.729	0.746
turbine speed (r.p.m.)	52518.4	64277.3	73259.3
turbine power (kw)	4.848	9.603	15.579
effective turbine efficiency.	0.591	0.584	0.576
fract of flow thro turbine.	1.000	1.000	1.000
first step. pressure ratio.	1.448	1.621	1.825
n.d. torque	1.4953	1.6108	1.6898
n.d. mass flow.	244.1671	254.5593	261.3642
n.d.speed	1630.7065	2027.0258	2380.4644
efficiency.	0.614	0.612	0.599
final step. pressure ratio.	1.135	1.282	1.487
n.d. torque	0.0411	0.3374	0.7111
n.d. mass flow.	83.1574	152.7862	199.7163
n.d.speed	1677.4153	2085.5766	2440.8715
efficiency.	0.145	0.417	0.500
compressor mass flow(kg/min).	6.42	9.17	12.14
delevered air to fuel ratio	18.38	20.19	22.91
v.g. nozzle width (m.m.)	13.5000	13.5000	13.5000
cooler effectiveness	0.9152	0.8826	0.8513
engine diagram factor	0.9850	0.9660	0.9515
start of injection(deg.)	342.36	340.89	340.43
duration of injection(deg.)	18.21	20.00	20.16
turbine nozzle angle(deg.)	23.00	23.00	23.00

Table-3.4

EXPERIMENTAL AND PREDICTED LIMITING TORQUE CURVE OF CUMMINS L10-250 T/C ENGINE

SET NUMBER	1		2		3		4		5	
PARAMETERS	exp.	pred.	exp.	pred.	exp.	pred.	exp.	pred.	exp.	pred.
ENGINE	1000.00		1260.00		1500.00		1800.00		2100.00	
speed(rpm)	1000.00		1260.00		1500.00		1800.00		2100.00	
boost P. ratio	1.47	1.367	1.59	1.57	1.73	1.754	1.83	1.905	1.93	1.979
trapped A/F ratio	17.07	18.382	20.64	20.191	24.08	22.905	26.60	26.346	29.48	29.531
man. T(K)	324.00	312.42	326.00	315.37	330.00	318.95	333.00	323.53	337.00	327.77
power(kw)	99.62	99.64	134.6	137.49	160.57	161.84	179.73	178.57	186.92	188.22
torque(n.m.)	952.0	951.49	1020.2	1042.01	1022.9	1030.28	954.1	947.35	850.5	855.88
BMEP(bar)	11.94	11.94	12.80	13.08	12.83	12.93	11.96	11.89	10.67	10.74
bsfc(g/kw.hr)	210.54	210.00	202.38	199.00	197.98	196.00	198.24	200.00	204.89	204.00
b. thermal eff.(%)	39.95	39.68	41.56	42.00	42.51	42.48	42.42	41.76	41.05	40.97
fuel/rev (mg)	349.2		361.2		353.2		330.3		304.2	
max cyl P(bar)	119.97	111.27	127.76	122.63	132.04	130.15	132.04	131.28	129.21	124.45
exh. T(K)	787.00	795.76	805.00	815.15	796.00	816.88	792.00	809.69	784.00	794.36
heat to coolant(%)	35.31	33.50	28.77	27.11	24.15	23.06	22.28	19.95	21.60	18.00
COMPRESSOR										
P. ratio	1.43	1.4107	1.56	1.6355	1.71	1.8425	1.85	2.003	1.96	2.114
speed(rpm)	57790.00	52518.4	64987.00	64277.3	72568.00	73259.3	78047.00	80641.4	83863.00	85319.8
eff.(%)	63.00	69.3	67.00	72.9	69.00	74.6	71.50	74.7	72.00	73.5
TURBINE										
speed(rpm)	57790.00	52518.4	64987.00	64277.3	72568.00	73259.3	78047.00	80641.4	83863.00	85319.8
P. ratio	1.27	1.448	1.35	1.621	1.47	1.825	1.57	2.087	1.70	2.325
eff.(%)	56.40	59.1	55.00	58.4	55.00	57.6	54.50	56.4	53.50	55.2

Table-3.5 The results with small turbine (a=18deg.)

COMPIES L10 DIESEL ENGINE, HOULET H2C TURBOCHARGER

179

135

675

number of cylinders	6.0	bore	(m)	0.13	stroke	(m)	0.13600	
con-rod length (m)	0.21778	inlet valve closing (degs)	173.0	compressor factor	1.00	0.00	1.00	
ambient temperature (deg k)	299.4	heat loss factor	1.5000	ambient pressure (bar)			0.99000	
compression ratio	16.30	combustion rate factor	0.0500	turbine flow loss factor			0.7200	
engine speed(r.p.m)	1000.00	1200.00	1500.00	1800.00	2100.00	0.00	0.00	0.00
boost pressure ratio	1.488	1.811	2.053	2.234	2.330	0.000	0.000	0.000
trapped a/f ratio	19.951	23.146	26.625	30.584	34.116	0.000	0.000	0.000
delivery ratio	0.950	0.850	0.855	0.861	0.861	0.000	0.000	0.000
manifold temp (deg k)	313.559	318.089	322.969	328.820	334.007	0.000	0.000	0.000
engine power (k w.)	106.11	140.71	164.34	178.89	185.77	0.00	0.00	0.00
engine torque (n.m.)	1013.26	1066.45	1046.19	949.05	844.77	0.00	0.00	0.00
b.m.e.p (bar)	12.7155	13.3829	13.1297	11.9097	10.6010	0.0000	0.0000	0.0000
s.f.c. (g/kw hr)	197.458	194.057	193.134	199.407	206.322	0.000	0.000	0.000
b.thermal eff.	0.4225	0.4299	0.4313	0.4184	0.4044	0.0000	0.0000	0.0000
fuel / rev (kJ.)	3.492	3.612	3.532	3.303	3.042	0.000	0.000	0.000
max cyl pressure (bar)	116.33	132.59	142.66	144.99	138.52	0.00	0.00	0.00
max cyl temperature(deg k)	2171.19	2056.93	1946.19	1835.50	1740.70	0.00	0.00	0.00
exhaust temperature(deg k)	747.39	777.49	774.93	771.42	762.89	0.00	0.00	0.00
percentage heat to coolant	31.94	25.09	21.23	18.45	16.76	0.00	0.00	0.00
compressor pressure ratio	1.5336	1.8796	2.1501	2.3584	2.4870	0.0000	0.0000	0.0000
delivery temperature(deg k)	351.02	376.54	394.19	408.29	417.87	0.00	0.00	0.00
delivery pressure (bar)	1.518	1.858	2.128	2.339	2.469	0.000	0.000	0.000
compressor speed (r.p.m.)	59272.6	73945.4	83635.9	90510.8	95163.5	0.0	0.0	0.0
volume flow (cu ft / min)	5.95	8.99	12.94	15.52	18.60	0.00	0.00	0.00
compressor power (kw.)	6.592	14.459	23.519	34.599	44.951	0.000	0.000	0.000
compressor efficiency	0.680	0.713	0.726	0.723	0.714	0.000	0.000	0.000
turbine speed (r.p.m)	59272.6	73945.4	83635.9	90510.8	95163.5	0.0	0.0	0.0
turbine power (kw)	6.716	14.676	23.509	34.937	45.325	0.000	0.000	0.000
effective turbine efficiency.	0.617	0.613	0.604	0.593	0.581	0.000	0.000	0.000
fract of flow thro turbine.	1.000	1.000	1.000	1.000	1.000	0.000	0.000	0.000
first step. pressure ratio.	1.548	1.862	2.201	2.597	2.968	0.000	0.000	0.000
n.d. torque	1.3486	1.5233	1.6190	1.6747	1.7334	0.0000	0.0000	0.0000
n.d. mass flow.	206.5878	218.5037	224.1482	227.3516	228.2598	0.0000	0.0000	0.0000
n.d. speed	1884.8117	2423.3414	2828.7189	3147.0061	3363.6980	0.0000	0.0000	0.0000
efficiency.	0.646	0.638	0.621	0.603	0.586	0.000	0.000	0.000
final step. pressure ratio.	1.230	1.518	1.865	2.276	2.714	0.000	0.000	0.000
n.d. torque	0.2259	0.6737	1.0339	1.3330	1.5116	0.0000	0.0000	0.0000
n.d. mass flow.	113.7808	170.5989	198.5528	214.6867	221.6780	0.0000	0.0000	0.0000
n.d. speed	1933.9416	2485.1828	2887.6169	3195.9092	3402.0034	0.0000	0.0000	0.0000
efficiency.	0.415	0.539	0.568	0.577	0.574	0.000	0.000	0.000
compressor mass flow(kg/min).	6.97	10.53	14.11	18.18	21.79	0.00	0.00	0.00
delivered air to fuel ratio	19.95	23.15	26.62	30.58	34.12	0.00	0.00	0.00
v.g. nozzle width (n.m.)	13.5000	13.5000	13.5000	13.5000	13.5000	0.0000	0.0000	0.0000
cooler effectiveness	0.9132	0.8784	0.8460	0.8085	0.7775	0.0000	0.0000	0.0000
engine diagram factor	0.9859	0.9669	0.9515	0.9300	0.9250	0.0000	0.0000	0.0000
start of injection(deg.)	342.36	340.89	340.13	340.75	342.25	0.00	0.00	0.00
duration of injection(deg.)	18.21	20.90	20.16	20.50	21.50	0.00	0.00	0.00
turbine nozzle angle(deg.)	18.00	18.00	18.00	18.00	18.00	0.00	0.00	0.00

Table-3.6 The results with large turbine (a=28deg.)

COMPUTES C10 DIESEL ENGINE, HOLSET H2C TURBOCHARGER						137	120	600
number of cylinders	6.0	bore	(m)	0.13	stroke	(m)	0.13600	
con-rod length (m)	0.21778	inlet valve closing (degs)	193.0	compressor factor	1.00	0.00	1.00	
ambient temperature (deg k)	294.4	heat loss factor	1.5000	ambient pressure (bar)			0.99000	
compression ratio	16.30	combustion rate factor	0.0500	turbine flow loss factor			0.7200	
engine speed(r.p.m.)	1000.00	1260.00	1500.00	1800.00	2100.00	0.00	0.00	0.00
boost pressure ratio	1.311	1.423	1.563	1.683	1.741	0.000	0.000	0.000
trapped a/f ratio	17.665	18.368	20.578	23.454	26.187	0.000	0.000	0.000
delivery ratio	0.350	0.817	0.852	0.852	0.857	0.000	0.000	0.000
manifold temp (deg k)	311.883	313.872	316.426	319.890	323.459	0.000	0.000	0.000
engine power (k w.)	26.52	128.54	153.99	176.49	187.12	0.00	0.00	0.00
engine torque (n.m.)	221.66	974.20	1012.16	936.32	850.88	0.00	0.00	0.00
b.m.e.p. (bar)	11.5659	12.2252	12.7016	11.7499	10.6777	0.0000	0.0000	0.0000
s.f.c. (g/kw hr)	217.083	212.434	199.939	202.120	204.841	0.000	0.000	0.000
b.thermal eff.	0.3843	0.3927	0.4173	0.4128	0.4073	0.0000	0.0000	0.0000
fuel / rev (kJ.)	3.492	3.612	3.532	3.303	3.042	0.000	0.000	0.000
max cyl pressure (bar)	108.97	116.51	122.40	122.15	114.68	0.00	0.00	0.00
max cyl temperature(deg k)	2297.47	2291.02	2189.23	2062.22	1943.54	0.00	0.00	0.00
exhaust temperature(deg k)	829.03	876.59	851.19	845.96	829.72	0.00	0.00	0.00
percentage heat to coolant	34.29	28.63	24.50	21.25	19.17	0.00	0.00	0.00
compressor pressure ratio	1.3546	1.4869	1.6490	1.7982	1.8869	0.0000	0.0000	0.0000
delivery temperature(deg k)	332.46	343.73	354.23	364.79	373.31	0.00	0.00	0.00
delivery pressure (bar)	1.337	1.474	1.625	1.801	1.866	0.000	0.000	0.000
compressor speed (r.p.m.)	48956.4	57344.3	65607.1	72845.4	77406.3	0.0	0.0	0.0
volume flow (cu ft / min)	5.26	7.13	9.30	11.90	14.28	0.00	0.00	0.00
compressor power (kw.)	3.925	6.892	10.902	16.405	22.062	0.000	0.000	0.000
compressor efficiency	0.795	0.721	0.761	0.768	0.747	0.000	0.000	0.000
turbine speed (r.p.m.)	48956.4	57344.3	65607.1	72845.4	77406.3	0.0	0.0	0.0
turbine power (kw)	4.019	7.015	11.074	16.619	22.290	0.000	0.000	0.000
effective turbine efficiency.	0.564	0.552	0.543	0.533	0.524	0.000	0.000	0.000
fract of flow thro turbine.	1.000	1.000	1.000	1.000	1.000	0.000	0.000	0.000
first step. pressure ratio.	1.411	1.509	1.644	1.818	1.993	0.000	0.000	0.000
n.d. torque	1.6146	1.6976	1.7211	1.7560	1.8082	0.0000	0.0000	0.0000
n.d. mass flow.	279.2174	295.9350	291.3625	295.7512	299.2262	0.0000	0.0000	0.0000
n.d.speed	1502.3009	1757.4770	2067.5137	2368.7289	2575.9946	0.0000	0.0000	0.0000
efficiency.	0.574	0.576	0.568	0.550	0.535	0.000	0.000	0.000
final step. pressure ratio.	1.102	1.177	1.309	1.503	1.707	0.000	0.000	0.000
n.d. torque	-0.2154	0.1320	0.4299	0.8184	1.1485	0.0000	0.0000	0.0000
n.d. mass flow.	61.9216	120.5456	185.9464	233.6817	262.3072	0.0000	0.0000	0.0000
n.d.speed	1547.5105	1819.1968	2124.9935	2424.1312	2625.3322	0.0000	0.0000	0.0000
efficiency.	-0.287	0.258	0.411	0.477	0.500	0.000	0.000	0.000
compressor mass flow(kg/min).	6.17	8.36	10.90	13.94	16.73	0.00	0.00	0.00
delivered air to fuel ratio	17.66	18.37	20.58	23.45	26.19	0.00	0.00	0.00
v.g. nozzle width (m.m.)	13.5000	13.5000	13.5000	13.5000	13.5000	0.0000	0.0000	0.0000
cooler effectiveness	0.7162	0.8852	0.8547	0.8195	0.7874	0.0000	0.0000	0.0000
engine diagram factor	0.7850	0.9669	0.9515	0.9300	0.7250	0.0000	0.0000	0.0000
start of injection(deg.)	342.36	340.89	340.43	340.75	342.25	0.00	0.00	0.00
duration of injection(deg.)	18.21	20.00	20.16	20.50	21.50	0.00	0.00	0.00
turbine nozzle angle(deg.)	24.00	28.00	29.00	28.00	28.00	0.00	0.00	0.00

Table-3.7 The results with various turbines (a=28,23,18deg.) at 1000 & 2100rpm

CUMMINS L10 DIESEL ENGINE, HOLSET H2C TURBOCHARGER

	211		157		785			
number of cylinders	6.0	bore	(m)	0.13	stroke	(m)	0.13600	
con-rod length (m)	0.21778	inlet valve closing (degs)	173.0	compressor factor	1.00	0.00	1.00	
ambient temperature (deg k)	274.4	heat loss factor	1.5000	ambient pressure (bar)	0.99000			
compression ratio	16.30	combustion rate factor	0.0500	turbine flow loss factor	0.7200			
engine speed(r.p.m)	1000.00	1000.00	1000.00	2100.00	2100.00	2100.00	0.00	0.00
boost pressure ratio	1.311	1.367	1.488	1.741	1.979	2.330	0.000	0.000
trapped a/f ratio	17.665	18.382	19.951	26.187	29.531	34.116	0.000	0.000
delivery ratio	0.850	0.850	0.850	0.857	0.862	0.861	0.000	0.000
manifold temp (deg k)	311.883	312.422	313.557	323.459	327.770	334.007	0.000	0.000
engine power (k w.)	96.52	99.64	106.11	137.12	188.22	185.77	0.00	0.00
engine torque (n.m.)	921.66	951.47	1013.26	850.88	855.88	844.77	0.00	0.00
b.m.e.p (bar)	11.5659	11.9402	12.7155	10.6777	10.7405	10.6010	0.0000	0.0000
s.f.c. (g/kw hr)	217.083	210.278	197.458	204.841	203.643	206.322	0.000	0.000
b.thermal eff.	0.3843	0.3768	0.4225	0.4073	0.4097	0.4044	0.0000	0.0000
fuel / rev (kJ.)	3.492	3.492	3.492	3.042	3.042	3.042	0.000	0.000
max cyl pressure (bar .)	108.97	111.27	116.33	114.68	124.45	138.52	0.00	0.00
max cyl temperature(deg k)	2297.47	2255.21	2171.19	1943.54	1845.42	1740.70	0.00	0.00
exhaust temperature(deg k)	820.73	795.76	747.39	829.72	794.36	762.89	0.00	0.00
percentage heat to coolant	34.29	33.50	31.94	19.17	18.00	16.76	0.00	0.00
compressor pressure ratio	1.3546	1.4107	1.5336	1.8867	2.1302	2.4870	0.0000	0.0000
delivery temperature(deg k)	332.46	338.57	351.02	373.31	391.63	417.87	0.00	0.00
delivery pressure (bar)	1.337	1.378	1.513	1.866	2.114	2.469	0.000	0.000
compressor speed (r.p.m.)	48756.4	52518.4	59272.6	77406.3	85319.8	95163.5	0.0	0.0
volume flow (cu ft / min)	5.26	5.48	5.95	14.28	16.10	18.60	0.00	0.00
compressor power (kw.)	3.925	4.739	6.592	22.062	30.650	44.951	0.000	0.000
compressor efficiency	0.705	0.693	0.680	0.747	0.735	0.714	0.000	0.000
turbine speed (r.p.m)	48756.4	52518.4	59272.6	77406.3	85319.8	95163.5	0.0	0.0
turbine power (kw)	4.019	4.848	6.716	22.290	30.812	45.325	0.000	0.000
effective turbine efficiency.	0.564	0.591	0.617	0.524	0.552	0.581	0.000	0.000
fract of flow thro turbine.	1.000	1.000	1.000	1.000	1.000	1.000	0.000	0.000
first step. pressure ratio.	1.411	1.448	1.548	1.993	2.325	2.968	0.000	0.000
n.l. torque	1.6146	1.4753	1.3486	1.8082	1.7915	1.7334	0.0000	0.0000
n.l. mass flow.	278.2174	244.1671	206.5878	279.2262	267.7513	228.2598	0.0000	0.0000
n.l.speed	1502.3009	1630.7065	1884.8117	2575.8946	2926.7527	3363.6980	0.0000	0.0000
efficiency.	0.574	0.614	0.646	0.535	0.561	0.586	0.000	0.000
final step. pressure ratio.	1.102	1.135	1.230	1.707	2.045	2.714	0.000	0.000
n.l. torque	-0.0154	0.0411	0.2258	1.1485	1.3483	1.5116	0.0000	0.0000
n.l. mass flow.	61.9216	83.1574	113.9808	262.3072	248.4794	221.6780	0.0000	0.0000
n.l.speed	1547.5105	1679.4153	1938.9416	2625.3322	2973.8706	3402.0034	0.0000	0.0000
efficiency.	-0.087	0.145	0.415	0.500	0.537	0.574	0.000	0.000
compressor mass flow(kg/min).	6.17	6.42	6.97	16.73	18.87	21.79	0.00	0.00
delivered air to fuel ratio	17.66	18.38	19.95	26.19	29.53	34.12	0.00	0.00
v.g. nozzle width (mm.)	13.5000	13.5000	13.5000	13.5000	13.5000	13.5000	0.0000	0.0000
cooler effectiveness	0.9162	0.9152	0.9132	0.7874	0.7823	0.7775	0.0000	0.0000
engine diagram factor	0.9850	0.9850	0.9850	0.9250	0.9250	0.9250	0.0000	0.0000
start of injection(deg.)	342.36	342.36	342.36	342.25	342.25	342.25	0.00	0.00
duration of injection(deg.)	18.21	18.21	18.21	21.50	21.50	21.50	0.00	0.00
turbine nozzle angle(deg.)	28.00	23.00	18.00	28.00	23.00	18.00	0.00	0.00

Table-3.8 The results with small turbine (a=18deg.), with adjusted(reduced) fuelling

CUMMINS L10 DIESEL ENGINE, HOLSET H2C TURBOCHARGER:

	168	128	640
number of cylinders	6.0	bore (m)	0.13
con-rod length (m)	0.21778	inlet valve closing (degs)	193.0
ambient temperature (deg k)	274.4	heat loss factor	1.5000
compression ratio	16.30	combustion rate factor	0.0500
stroke (m)		compressor factor	1.00
		ambient pressure (bar)	0.99000
		turbine flow loss factor	0.7200
engine speed(r.p.m)	1000.00	1260.00	1500.00
boost pressure ratio	1.488	1.794	1.912
trapped a/f ratio	17.951	23.308	27.864
delivery ratio	0.850	0.850	0.855
manifold temp (deg k)	313.557	317.885	321.109
engine power (k w.)	106.11	138.24	144.66
engine torque (n.m.)	1013.26	1047.66	920.96
b.m.e.p (bar)	12.7155	13.1471	11.5572
s.f.c. (g/kw hr)	197.458	174.421	196.281
b.thermal eff.	0.4225	0.4291	0.4251
fuel / rev (kJ.)	3.492	3.555	3.155
max cyl pressure (bar)	116.33	131.05	130.78
max cyl temperature(deg k)	2171.19	2049.03	1898.12
exhaust temperature(deg k)	747.39	772.92	746.77
percentage heat to coolant	31.74	25.21	22.06
compressor pressure ratio	1.5336	1.8622	2.0025
delivery temperature(deg k)	351.02	375.01	383.09
delivery pressure (bar)	1.518	1.841	1.982
compressor speed (r.p.m.)	59272.6	73308.5	78887.1
volume flow (cu ft / min)	5.95	8.91	11.25
compressor power (kw.)	6.592	14.064	19.544
compressor efficiency	0.680	0.715	0.733
turbine speed (r.p.m)	59272.6	73308.5	78887.1
turbine power (kw)	6.716	14.276	19.791
effective turbine efficiency.	0.617	0.613	0.606
fract of flow thro turbine.	1.000	1.000	1.000
first step. pressure ratio.	1.548	1.846	2.056
n.d. torque	1.3486	1.5077	1.5415
n.d. mass flow.	206.5878	217.8841	220.7339
n.d.speed	1884.8117	2408.6701	2712.4274
efficiency.	0.646	0.638	0.625
final step. pressure ratio.	1.230	1.508	1.759
n.d. torque	0.2258	0.6634	0.9579
n.d. mass flow.	113.9808	169.5930	193.2500
n.d.speed	1738.7416	2469.6175	2766.0521
efficiency.	0.415	0.538	0.567
compressor mass flow(kg/min).	6.97	10.44	13.19
delevered air to fuel ratio	17.95	23.31	27.86
v.g. nozzle width (m.m.)	13.5000	13.5000	13.5000
cooler effectiveness	0.7132	0.8787	0.8480
engine diagram factor	0.9850	0.9660	0.7515
start of injection(deg.)	342.36	341.01	341.19
duration of injection(deg.)	18.21	19.75	18.63
turbine nozzle angle(deg.)	13.00	18.00	18.00

Table-3.9 The results for synthesized VG turbocharging operatio

CUMMINS L10 DIESEL ENGINE, HOLSET H2C TURBOCHARGER

	159	119	595
number of cylinders	6.0		
con-rod length (m)	0.21778		
ambient temperature (deg k)	274.4		
compression ratio	16.30		
bore (m)	0.13		
inlet valve closing (degs)	193.0		
heat loss factor	1.5000		
combustion rate factor	0.0500		
stroke (m)	0.13600		
compressor factor	1.00	0.00	1.00
ambient pressure (bar)			0.99000
turbine flow loss factor			0.7200
engine speed(r.p.m)	1000.00	1260.00	1500.00
boost pressure ratio	1.784	1.775	1.802
trapped a/f ratio	23.720	22.709	23.391
delivery ratio	0.850	0.850	0.848
manifold temp (deg k)	316.172	317.657	319.563
engine power (k w.)	109.58	140.40	162.32
engine torque (n.m.)	1046.45	1064.08	1033.34
b.m.e.p (bar)	13.1320	13.3531	12.9674
s.f.c. (g/kw hr)	191.195	174.470	195.840
b.thermal eff.	0.4364	0.4290	0.4260
fuel / rev (kg.)	3.492	3.612	3.532
max cyl pressure (bar)	128.44	131.07	131.80
max cyl temperature(deg k)	2006.23	2074.93	2063.16
exhaust temperature(deg k)	712.55	782.15	810.54
percentage heat to coolant	20.71	25.35	22.80
compressor pressure ratio	1.8320	1.8426	1.8909
delivery temperature(deg k)	373.00	373.28	374.26
delivery pressure (bar)	1.813	1.821	1.859
compressor speed (r.p.m.)	71916.1	72580.9	74991.9
volume flow (cu ft / min)	7.07	8.82	10.58
compressor power (kw.)	11.572	13.624	16.538
compressor efficiency	0.669	0.717	0.741
turbine speed (r.p.m)	71916.1	72580.9	74991.9
turbine power (kw)	11.778	13.659	16.745
effective turbine efficiency.	0.642	0.606	0.582
fract of flow thro turbine.	1.000	1.000	1.000
first step. pressure ratio.	1.860	1.815	1.875
n.d. torque	1.2107	1.5423	1.6789
n.d. mass flow.	165.4347	226.5064	254.5124
n.d.speed	2396.4788	2366.5507	2450.6306
efficiency.	0.664	0.633	0.604
final step. pressure ratio.	1.538	1.471	1.536
n.d. torque	0.5980	0.6151	0.7715
n.d. mass flow.	134.4360	170.4894	200.8334
n.d.speed	2454.4538	2428.6317	2511.1080
efficiency.	0.583	0.519	0.516
compressor mass flow(kg/min).	8.28	10.34	12.39
delevered air to fuel ratio	23.72	22.71	23.39
v.g. nozzle width (m.m.)	13.5000	13.5000	13.5000
cooler effectiveness	0.9092	0.8790	0.8512
engine diagram factor	0.9850	0.9660	0.9515
start of injection(deg.)	342.36	340.89	340.43
duration of injection(deg.)	19.21	20.00	20.16
turbine nozzle angle(deg.)	13.00	17.00	22.00
			23.00
			23.00

131

100

500

[illegible]

CUMMINS L10 DIESEL ENGINE, HOLSET H2C TURBOCHARGER

COMBUSTION L10 DIESEL ENGINE, HOLSET H2C TURBOCHARGER						174	119	595
number of cylinders	6.0	bore	(m)	0.13	stroke	(m)	0.13600	
con-rod length (m)	0.21778	inlet valve closing (degs)	193.0	compressor factor	1.00	0.00	1.00	
ambient temperature (deg k)	294.4	heat loss factor	1.5000	ambient pressure (bar)		0.69300		
compression ratio	16.30	combustion rate factor	0.0500	turbine flow loss factor		0.7200		
engine speed(r.p.m)	1000.00	1200.00	1500.00	1800.00	2100.00	0.00	0.00	0.00
boost pressure ratio	1.452	1.886	2.130	2.294	2.375	0.000	0.000	0.000
trapped a/f ratio	16.000	16.736	19.056	21.768	24.306	0.000	0.000	0.000
delivery ratio	0.847	0.846	0.847	0.855	0.863	0.000	0.000	0.000
manifold temp (deg k)	313.353	319.113	324.051	330.026	335.120	0.000	0.000	0.000
engine power (k w.)	73.27	120.38	152.77	173.16	182.47	0.00	0.00	0.00
engine torque (n.m.)	699.69	912.34	972.59	918.64	829.76	0.00	0.00	0.00
b.m.e.p (bar)	8.78004	11.4490	12.2051	11.5280	10.4127	0.0000	0.0000	0.0000
s.f.c. (g/kw hr)	285.952	226.837	208.071	206.009	210.054	0.000	0.000	0.000
bthermal eff.	0.2918	0.3678	0.4010	0.4050	0.3972	0.0000	0.0000	0.0000
fuel / rev (ky.)	3.492	3.612	3.532	3.303	3.042	0.000	0.000	0.000
max cyl pressure (bar .)	88.27	111.36	118.26	118.49	111.43	0.00	0.00	0.00
max cyl temperature(deg k)	2393.14	2403.63	2283.19	2152.79	2031.21	0.00	0.00	0.00
exhaust temperature(deg k)	926.25	939.17	898.05	882.23	871.18	0.00	0.00	0.00
percentage heat to coolant	40.12	30.41	25.84	22.46	20.32	0.00	0.00	0.00
compressor pressure ratio	1.5155	1.9825	2.2587	2.4672	2.5938	0.0000	0.0000	0.0000
delivery temperature(deg k)	347.47	385.84	403.08	416.81	424.74	0.00	0.00	0.00
delivery pressure (bar)	1.050	1.371	1.557	1.708	1.802	0.000	0.000	0.000
compressor speed (r.p.m.)	58359.4	77532.3	86779.2	93283.7	97551.8	0.0	0.0	0.0
volume flow (cu ft / min)	5.80	9.29	12.31	15.78	18.93	0.00	0.00	0.00
compressor power (k w.)	4.379	11.639	10.332	26.463	33.805	0.000	0.000	0.000
compressor efficiency	0.679	0.700	0.715	0.713	0.712	0.000	0.000	0.000
turbine speed (r.p.m)	58359.4	77532.3	86779.2	93283.7	97551.8	0.0	0.0	0.0
turbine power (kw)	4.533	11.923	18.629	26.798	34.142	0.000	0.000	0.000
effective turbine efficiency.	0.587	0.579	0.566	0.550	0.532	0.000	0.000	0.000
fract of flow thro turbine.	1.000	1.000	1.000	1.000	1.000	0.000	0.000	0.000
first step. pressure ratio.	1.527	1.894	2.184	2.537	2.871	0.000	0.000	0.000
n.d. torque	1.6364	1.9103	1.9448	1.9721	1.9585	0.0000	0.0000	0.0000
n.d. mass flow.	252.8064	269.7622	272.5534	273.2740	271.2435	0.0000	0.0000	0.0000
n.d.speed	1750.4938	2309.6059	2666.4607	2953.4498	3154.3188	0.0000	0.0000	0.0000
efficiency.	0.612	0.600	0.581	0.557	0.533	0.000	0.000	0.000
final step. pressure ratio.	1.162	1.416	1.707	2.095	2.477	0.000	0.000	0.000
n.d. torque	0.0655	0.5267	0.9624	1.3658	1.5915	0.0000	0.0000	0.0000
n.d. mass flow.	94.4778	181.0954	223.2679	249.1840	259.3351	0.0000	0.0000	0.0000
n.d.speed	1806.0364	2389.0881	2745.4792	3022.0749	3211.2573	0.0000	0.0000	0.0000
efficiency.	0.185	0.453	0.513	0.533	0.528	0.000	0.000	0.000
compressor mass flow(kg/min).	4.76	7.62	10.10	12.94	15.53	0.00	0.00	0.00
delevered air to fuel ratio	13.62	16.74	19.06	21.77	24.31	0.00	0.00	0.00
v.g. nozzle width (m.m.)	13.5000	13.5000	13.5000	13.5000	13.5000	0.0000	0.0000	0.0000
cooler effectiveness	0.9151	0.8798	0.8490	0.8125	0.7811	0.0000	0.0000	0.0000
engine diagram factor	0.9850	0.9660	0.9515	0.9300	0.9250	0.0000	0.0000	0.0000
start of injection(deg.)	342.36	340.89	340.43	340.75	342.25	0.00	0.00	0.00
duration of injection(deg.)	18.21	20.00	20.16	20.50	21.50	0.00	0.00	0.00
turbine nozzle angle(deg.)	23.00	23.00	23.00	23.00	23.00	0.00	0.00	0.00

Table-3.12 The results of VG turbocharging under reduced ambient pressure (altitude of 3000m)

CUMMINS L10 DIESEL ENGINE, HOLSET H2C TURBOCHARGER

	235	161	805
number of cylinders	6.0	bore (m)	0.13
con-rod length (m)	0.21778	inlet valve closing (degs)	193.0
ambient temperature (deg k)	274.4	heat loss factor	1.5000
compression ratio	16.30	combustion rate factor	0.0500
stroke (m)		compressor factor	1.00
		ambient pressure (bar)	0.69300
		turbine flow loss factor	0.7200
engine speed(r.p.m.)	1000.00	1260.00	1500.00
boost pressure ratio	2.187	2.375	2.402
trapped a/f ratio	20.096	20.753	21.429
delivery ratio	0.848	0.847	0.855
manifold temp (deg k)	319.837	324.546	327.980
engine power (k w .)	106.26	137.56	159.03
engine torque (n.m.)	1014.75	1042.51	1012.42
b.m.e.p (bar)	12.7341	13.0825	12.7049
s.f.c. (g/kw hr)	197.170	198.513	199.885
b.thermal eff.	0.4231	0.4203	0.4174
fuel / rev (kg.)	3.492	3.612	3.532
max cyl pressure (bar .)	117.51	125.68	126.69
max cyl temperature(deg k)	2172.70	2175.98	2164.07
exhaust temperature(deg k)	747.76	813.71	846.84
percentage heat to coolant	32.02	26.94	24.23
compressor pressure ratio	2.2607	2.4777	2.5370
delivery temperature(deg k)	414.44	424.71	425.00
delivery pressure (bar)	1.567	1.715	1.758
compressor speed (r.p.m.)	36218.7	92518.8	94427.7
volume flow (cu ft / min)	3.56	11.52	13.84
compressor power (kw.)	14.072	20.558	24.765
compressor efficiency	0.648	0.673	0.692
turbine speed (r.p.m.)	36218.7	92518.8	94427.7
turbine power (kw)	14.365	21.067	25.122
effective turbine efficiency.	0.643	0.621	0.591
fract of flow thru turbine.	1.000	1.000	1.000
first step. pressure ratio.	2.248	2.460	2.553
n.d. torque	1.4107	1.6915	1.8612
n.d. mass flow.	172.6585	208.9701	237.8880
n.d.speed	2741.6879	2930.0124	2996.6233
efficiency.	0.662	0.638	0.603
final step. pressure ratio.	1.793	1.977	2.077
n.d. torque	0.7763	1.0276	1.2117
n.d. mass flow.	148.3105	184.7527	215.5720
n.d.speed	2819.1402	3008.8588	3072.1928
efficiency.	0.590	0.580	0.561
compressor mass flow(kg/min).	7.02	9.44	11.35
delevered air to fuel ratio	20.10	20.75	21.43
v.g. nozzle width (m.m.)	13.5000	13.5000	13.5000
cooler effectiveness	0.9058	0.8732	0.8436
engine diagram factor	0.9850	0.9660	0.9515
start of injection(deg.)	342.36	340.89	340.43
duration of injection(deg.)	18.21	20.00	20.16
turbine nozzle angle(deg.)	13.00	16.00	17.00

Table-3.13 The results under elevated temperature(40deg.C; sea level; a=23deg.)

CUMMINS L10 DIESEL ENGINE, HOLSET H2C TURBOCHARGER

	152	118	590
number of cylinders	6.0		
con-rod length (m)	0.21778		
ambient temperature (deg k)	313.5		
compression ratio	16.30		
bore (m)	0.13		
inlet valve closing (degs)	193.0		
heat loss factor	1.5000		
combustion rate factor	0.0500		
stroke (m)	0.13600		
compressor factor	1.00	0.00	1.00
ambient pressure (bar)			0.99000
turbine flow loss factor			0.7200
engine speed(r.p.m)	1000.00	1260.00	1500.00
boost pressure ratio	1.346	1.532	1.702
trapped a/f ratio	17.990	19.639	21.761
delivery ratio	0.847	0.852	0.850
manifold temp (deg k)	314.175	317.869	321.958
engine power (k w.)	97.79	134.96	160.15
engine torque (n.m.)	733.04	1022.85	1019.58
b.m.e.p (bar)	11.7188	12.8358	12.7947
s.f.c. (g/kw hr)	214.251	202.329	198.483
b.thermal eff.	0.3874	0.4123	0.4203
fuel / rev (kg.)	3.492	3.612	3.532
max cyl pressure (bar.)	110.25	121.17	127.63
max cyl temperature(deg k)	2280.92	2224.07	2129.75
exhaust temperature(deg k)	310.45	833.27	834.29
percentage heat to coolant	33.99	27.63	23.72
compressor pressure ratio	1.3912	1.5995	1.7915
delivery temperature(deg k)	358.09	375.14	387.27
delivery pressure (bar)	1.373	1.585	1.765
compressor speed (r.p.m.)	53000.2	64782.3	73729.6
volume flow (cu ft / min)	5.71	8.12	10.57
compressor power (kw.)	4.687	9.219	14.747
compressor efficiency	0.699	0.734	0.754
turbine speed (r.p.m)	53000.2	64782.3	73729.6
turbine power (kw)	4.773	9.383	14.970
effective turbine efficiency.	0.591	0.582	0.574
fract of flow thro turbine.	1.000	1.000	1.000
first step. pressure ratio.	1.444	1.612	1.801
n.d. torque	1.4789	1.5898	1.6593
n.d. mass flow.	243.2542	253.4337	259.7744
n.d.speed	1633.8026	2023.4645	2362.1050
efficiency.	0.615	0.613	0.599
final step. pressure ratio.	1.134	1.276	1.466
n.d. torque	0.0352	0.3170	0.6657
n.d. mass flow.	81.1378	149.8063	195.5031
n.d.speed	1682.0028	2081.2823	2421.6975
efficiency.	0.128	0.406	0.491
compressor mass flow(kg/min).	6.28	8.94	11.63
delevered air to fuel ratio	17.79	19.64	21.96
v.g. nozzle width (mm.)	13.5000	13.5000	13.5000
cooler effectiveness	0.9128	0.8792	0.8471
engine diagram factor	0.9850	0.9660	0.9515
start of injection(deg.)	342.36	340.89	340.43
duration of injection(deg.)	18.21	20.00	20.16
turbine nozzle angle(deg.)	23.00	23.00	23.00

Table-3.14 The results of VG turbocharging under elevated ambient temperature(40deg.C; sea level)

CUMMINS L10 DIESEL ENGINE, BOLSER H2C TURBOCHARGER

						182	139	695
number of cylinders	6.0	bore	(m)	0.13	stroke	(m)	0.13600	
con-rod length (m)	0.21778	inlet valve closing (degs)	193.0	compressor factor	1.00	0.00	1.00	
ambient temperature (deg k)	313.5	heat loss factor	1.5000	ambient pressure (bar)	0.99000			
compression ratio	16.30	combustion rate factor	0.0500	turbine flow loss factor	0.7200			
engine speed(r.p.m.)	1900.00	1260.00	1500.00	1900.00	2100.00	0.00	0.00	0.00
boost pressure ratio	1.730	1.785	1.795	1.894	1.911	0.000	0.000	0.000
trapped a/f ratio	22.801	22.620	23.072	25.821	28.137	0.000	0.000	0.000
delivery ratio	0.847	0.851	0.850	0.856	0.862	0.000	0.000	0.000
manifold temp (deg k)	318.034	320.977	323.370	328.287	332.335	0.000	0.000	0.000
engine power (k w.)	199.45	139.53	161.19	176.95	186.13	0.00	0.00	0.00
engine torque (n.m.)	1935.58	1057.96	1026.14	938.91	846.40	0.00	0.00	0.00
b.m.e.p (bar)	12.2955	13.2751	12.9771	11.7824	10.6215	0.0000	0.0000	0.0000
s.f.c. (g/kw hr)	193.203	195.634	197.214	201.561	205.923	0.000	0.000	0.000
thermal eff.	0.4318	0.4265	0.4230	0.4139	0.4052	0.0000	0.0000	0.0000
fuel / rev (kg.)	3.492	3.612	3.532	3.303	3.042	0.000	0.000	0.000
max cyl pressure (bar)	125.95	131.40	131.42	130.59	121.52	0.00	0.00	0.00
max cyl temperature(deg k)	2946.24	2983.89	2982.58	1983.33	1894.02	0.00	0.00	0.00
exhaust temperature(deg k)	723.72	737.92	717.69	822.43	816.25	0.00	0.00	0.00
percentage heat to coolant	29.66	25.51	23.09	20.31	18.63	0.00	0.00	0.00
compressor pressure ratio	1.7792	1.8557	1.8867	2.0162	2.0647	0.0000	0.0000	0.0000
delivery temperature(deg k)	396.81	398.17	397.79	407.07	411.78	0.00	0.00	0.00
delivery pressure (bar)	1.761	1.838	1.858	1.995	2.049	0.000	0.000	0.000
compressor speed (r.p.m.)	72120.8	75469.1	77346.7	83068.8	86089.0	0.0	0.0	0.0
volume flow (cu ft / min)	7.24	9.36	11.11	13.95	16.34	0.00	0.00	0.00
compressor power (kw.)	11.996	14.591	17.213	24.028	29.549	0.000	0.000	0.000
compressor efficiency	0.677	0.719	0.744	0.747	0.738	0.000	0.000	0.000
turbine speed (r.p.m.)	72120.8	75469.1	77346.7	83068.8	86089.0	0.0	0.0	0.0
turbine power (kw)	11.303	14.831	17.461	24.297	29.849	0.000	0.000	0.000
effective turbine efficiency.	0.640	0.615	0.587	0.570	0.553	0.000	0.000	0.000
fract of flow thro turbine.	1.000	1.000	1.000	1.000	1.000	0.000	0.000	0.000
first step. pressure ratio.	1.033	1.872	1.907	2.122	2.285	0.000	0.000	0.000
n.l. torque	1.1889	1.4879	1.6390	1.7207	1.7734	0.0000	0.0000	0.0000
n.l. mass flow.	164.4882	213.2950	246.0846	257.7745	266.9968	0.0000	0.0000	0.0000
n.l. speed	2373.6411	2452.3020	2511.6286	2762.0033	2904.6756	0.0000	0.0000	0.0000
efficiency.	0.663	0.640	0.610	0.585	0.563	0.000	0.000	0.000
final step. pressure ratio.	1.515	1.533	1.573	1.814	2.009	0.000	0.000	0.000
n.l. torque	0.5679	0.6736	0.7930	1.1054	1.3130	0.0000	0.0000	0.0000
n.l. mass flow.	137.0488	168.0242	197.8436	227.6549	246.7439	0.0000	0.0000	0.0000
n.l. speed	2430.2374	2513.3972	2571.4449	2815.8438	2951.3086	0.0000	0.0000	0.0000
efficiency.	0.576	0.541	0.524	0.538	0.537	0.000	0.000	0.000
compressor mass flow(kg/min).	7.96	10.29	12.22	15.35	17.97	0.00	0.00	0.00
delivered air to fuel ratio	22.80	22.62	23.07	25.82	28.14	0.00	0.00	0.00
v.g. nozzle width (mm.)	13.5000	13.5000	13.5000	13.5000	13.5000	0.0000	0.0000	0.0000
cooler effectiveness	0.9074	0.8755	0.8475	0.8116	0.7806	0.0000	0.0000	0.0000
engine diagram factor	0.9850	0.9669	0.9515	0.9300	0.9250	0.0000	0.0000	0.0000
start of injection(deg.)	342.36	340.89	340.43	340.75	342.25	0.00	0.00	0.00
duration of injection(deg.)	18.21	20.00	20.16	20.50	21.50	0.00	0.00	0.00
turbine nozzle angle(deg.)	13.00	17.50	21.00	22.00	23.00	0.00	0.00	0.00

Table-3.15 The results under elevated temperature and reduced pressure (40deg.C; 12oom; a=23deg.)

CUMMINS L10 DIESEL ENGINE, HOLSET H2C TURBOCHARGER

COMBINS L10 DIESEL ENGINE, HOLSET H2C TURBOCHARGER				158	113	565		
number of cylinders	6.0	bore	(m)	0.13	stroke	(m)	0.13600	
con-rod length (m)	0.21778	inlet valve closing (degs)	193.0	compressor factor	1.00	0.00	1.00	
ambient temperature (deg k)	313.5	heat loss factor	1.5000	ambient pressure (bar)			0.84150	
compression ratio	16.30	combustion rate factor	0.0500	turbine flow loss factor			0.7200	
engine speed(r.p.m)	1000.00	1260.00	1500.00	1800.00	2100.00	0.00	0.00	0.00
boost pressure ratio	1.418	1.654	1.843	2.001	2.060	0.000	0.000	0.000
trapped a/f ratio	16.037	17.850	20.097	23.056	25.549	0.000	0.000	0.000
delivery ratio	0.847	0.848	0.851	0.856	0.862	0.000	0.000	0.000
manifold temp (deg k)	315.004	319.344	324.202	330.199	335.474	0.000	0.000	0.000
engine power (k w.)	89.60	125.90	157.82	174.39	183.74	0.00	0.00	0.00
engine torque (n.m.)	855.59	954.21	1004.72	925.18	835.51	0.00	0.00	0.00
b.m.e.p (bar)	10.7368	11.9743	12.6082	11.6102	10.4848	0.0000	0.0000	0.0000
s.f.c. (g/kw hr)	233.847	216.885	201.419	204.552	208.608	0.000	0.000	0.000
b.thermal eff.	0.3568	0.3847	0.4142	0.4079	0.3999	0.0000	0.0000	0.0000
fuel / rev (kg.)	3.492	3.612	3.532	3.303	3.042	0.000	0.000	0.000
max cyl pressure (bar .)	103.93	115.29	121.81	122.49	114.90	0.00	0.00	0.00
max cyl temperature(deg k)	2409.85	2330.54	2225.80	2094.99	1985.13	0.00	0.00	0.00
exhaust temperature(deg k)	876.94	877.47	864.40	862.50	852.83	0.00	0.00	0.00
percentage heat to coolant	36.43	29.28	25.05	21.73	19.76	0.00	0.00	0.00
compressor pressure ratio	1.4720	1.7342	1.9502	2.1446	2.2406	0.0000	0.0000	0.0000
delivery temperature(deg k)	367.07	387.16	403.34	417.23	425.94	0.00	0.00	0.00
delivery pressure (bar)	1.237	1.459	1.632	1.804	1.890	0.000	0.000	0.000
compressor speed (r.p.m.)	57883.5	70611.7	79597.8	87063.5	91464.7	0.0	0.0	0.0
volume flow (cu ft / min)	5.79	8.67	11.38	14.66	17.45	0.00	0.00	0.00
compressor power (kw.)	5.020	10.011	16.002	23.783	30.692	0.000	0.000	0.000
compressor efficiency	0.687	0.729	0.738	0.740	0.727	0.000	0.000	0.000
turbine speed (r.p.m)	57883.5	70611.7	79597.8	87063.5	91464.7	0.0	0.0	0.0
turbine power (kw)	5.155	10.235	16.248	24.078	30.998	0.000	0.000	0.000
effective turbine efficiency.	0.590	0.580	0.572	0.559	0.547	0.000	0.000	0.000
fract of flow thro turbine.	1.000	1.000	1.000	1.000	1.000	0.000	0.000	0.000
first step. pressure ratio.	1.512	1.714	1.937	2.228	2.474	0.000	0.000	0.000
n.d. torque	1.6139	1.7200	1.7871	1.8330	1.8587	0.0000	0.0000	0.0000
n.d. mass flow.	251.4752	260.6342	265.9848	268.8753	269.7899	0.0000	0.0000	0.0000
n.d.speed	1726.3499	2142.9513	2483.5593	2801.6247	2999.4941	0.0000	0.0000	0.0000
efficiency.	0.612	0.608	0.593	0.571	0.554	0.000	0.000	0.000
final step. pressure ratio.	1.152	1.322	1.548	1.865	2.149	0.000	0.000	0.000
n.d. torque	0.0413	0.3712	0.7686	1.1659	1.4074	0.0000	0.0000	0.0000
n.d. mass flow.	86.2845	159.7184	206.2877	237.5301	251.4720	0.0000	0.0000	0.0000
n.d.speed	1782.2577	2209.6837	2551.5691	2862.6116	3051.4850	0.0000	0.0000	0.0000
efficiency.	0.133	0.414	0.497	0.529	0.534	0.000	0.000	0.000
compressor mass flow(kg/min).	5.60	8.12	10.65	13.71	16.32	0.00	0.00	0.00
delevered air to fuel ratio	16.04	17.85	20.10	23.06	25.55	0.00	0.00	0.00
v.g. nozzle width (m.m.)	13.5000	13.5000	13.5000	13.5000	13.5000	0.0000	0.0000	0.0000
cooler effectiveness	0.9123	0.8789	0.8478	0.8116	0.7803	0.0000	0.0000	0.0000
engine diagram factor	0.7850	0.9660	0.9515	0.9300	0.9250	0.0000	0.0000	0.0000
start of injection(deg.)	342.36	340.87	340.43	340.75	342.25	0.00	0.00	0.00
duration of injection(deg.)	18.21	20.00	20.16	20.50	21.50	0.00	0.00	0.00
turbine nozzle angle(deg.)	23.00	23.00	23.00	23.00	23.00	0.00	0.00	0.00

Table-3.16 VG turbocharging under elevated temperature and reduced pressure (40deg.C; 1200m)

CUMMINS L10 DIESEL ENGINE, HOLSET H2C TURBOCHARGER

236 166 830

number of cylinders	6.0	bore	(m)	0.13	stroke	(m)	0.13600	
con-rod length (m)	0.21778	inlet valve closing (degs)	193.0	compressor factor	1.00	0.00	1.00	
ambient temperature (deg k)	313.5	heat loss factor	1.5000	ambient pressure (bar)	0.84150	0.84150	0.84150	
compression ratio	16.30	combustion rate factor	0.0500	turbine flow loss factor	0.7200	0.7200	0.7200	
engine speed(r.p.m)	1000.00	1260.00	1500.00	1800.00	2100.00	0.00	0.00	0.00
boost pressure ratio	2.188	2.111	2.090	2.225	2.060	0.000	0.000	0.000
trapped a/f ratio	24.339	22.556	22.660	25.307	25.549	0.000	0.000	0.000
delivery ratio	0.854	0.855	0.855	0.855	0.862	0.000	0.000	0.000
manifold temp (deg k)	322.687	325.130	327.813	334.072	335.474	0.000	0.000	0.000
engine power (k w.)	108.45	138.95	160.16	175.00	183.74	0.00	0.00	0.00
engine torque (n.m.)	1035.62	1053.06	1019.58	928.38	835.51	0.00	0.00	0.00
b.m.e.p (bar)	12.7960	13.2147	12.7948	11.6503	10.4848	0.0000	0.0000	0.0000
s.f.c. (g/kw hr)	193.196	176.524	198.482	203.847	208.608	0.000	0.000	0.000
b.thermal eff.	0.4318	0.4245	0.4203	0.4093	0.3999	0.0000	0.0000	0.0000
fuel / rev (kg.)	3.492	3.612	3.532	3.303	3.042	0.000	0.000	0.000
max cyl pressure (bar)	131.68	131.83	130.75	130.09	114.90	0.00	0.00	0.00
max cyl temperature(deg k)	1992.62	2092.95	2107.22	2011.14	1985.13	0.00	0.00	0.00
exhaust temperature(deg k)	718.52	792.97	827.72	837.00	852.83	0.00	0.00	0.00
percentage heat to coolant	28.71	25.68	23.46	20.71	19.76	0.00	0.00	0.00
compressor pressure ratio	2.2476	2.1776	2.2013	2.3716	2.2406	0.0000	0.0000	0.0000
delivery temperature(deg k)	437.02	427.38	423.64	435.72	425.94	0.00	0.00	0.00
delivery pressure (bar)	1.893	1.849	1.852	1.994	1.890	0.000	0.000	0.000
compressor speed (r.p.m.)	38611.3	87256.2	87958.3	93774.0	91464.7	0.0	0.0	0.0
volume flow (cu ft / min)	7.09	10.98	12.84	16.09	17.45	0.00	0.00	0.00
compressor power (kw.)	17.940	19.551	22.114	30.750	30.692	0.000	0.000	0.000
compressor efficiency	0.655	0.678	0.724	0.722	0.727	0.000	0.000	0.000
turbine speed (r.p.m)	38611.3	87256.2	87958.3	93774.0	91464.7	0.0	0.0	0.0
turbine power (kw)	13.144	19.858	22.411	31.185	30.998	0.000	0.000	0.000
effective turbine efficiency.	0.651	0.623	0.594	0.580	0.547	0.000	0.000	0.000
fract of flow thro turbine.	1.000	1.000	1.000	1.000	1.000	0.000	0.000	0.000
first step. pressure ratio.	2.446	2.247	2.246	2.572	2.474	0.000	0.000	0.000
n.d. torque	1.1847	1.5354	1.7139	1.7887	1.8587	0.0000	0.0000	0.0000
n.d. mass flow.	142.5807	179.9377	235.2034	241.9263	269.7899	0.0000	0.0000	0.0000
n.d.speed	2756.4001	2826.9704	2835.5027	3087.3766	2999.4941	0.0000	0.0000	0.0000
efficiency.	0.667	0.643	0.612	0.590	0.554	0.000	0.000	0.000
final step. pressure ratio.	2.081	1.851	1.856	2.217	2.149	0.000	0.000	0.000
n.d. torque	0.8420	0.9135	1.0279	1.3365	1.4074	0.0000	0.0000	0.0000
n.d. mass flow.	132.5572	174.5395	204.8038	225.3048	251.4720	0.0000	0.0000	0.0000
n.d.speed	3017.1073	2875.2192	2902.2716	3143.9320	3051.4850	0.0000	0.0000	0.0000
efficiency.	0.623	0.578	0.553	0.562	0.534	0.000	0.000	0.000
compressor mass flow(kg/min).	8.50	10.27	12.01	15.05	16.32	0.00	0.00	0.00
delevered air to fuel ratio	24.34	22.56	22.66	25.31	25.55	0.00	0.00	0.00
v.g. nozzle width (m.m.)	13.5000	13.5000	13.5000	13.5000	13.5000	0.0000	0.0000	0.0000
cooler effectiveness	0.7017	0.8711	0.8432	0.8085	0.7803	0.0000	0.0000	0.0000
engine diagram factor	0.9850	0.9660	0.9515	0.9300	0.9250	0.0000	0.0000	0.0000
start of injection(deg.)	342.36	340.87	340.43	340.75	342.25	0.00	0.00	0.00
duration of injection(deg.)	18.21	20.00	20.16	20.50	21.50	0.00	0.00	0.00
turbine nozzle angle(deg.)	10.50	15.50	17.00	19.50	23.00	0.00	0.00	0.00

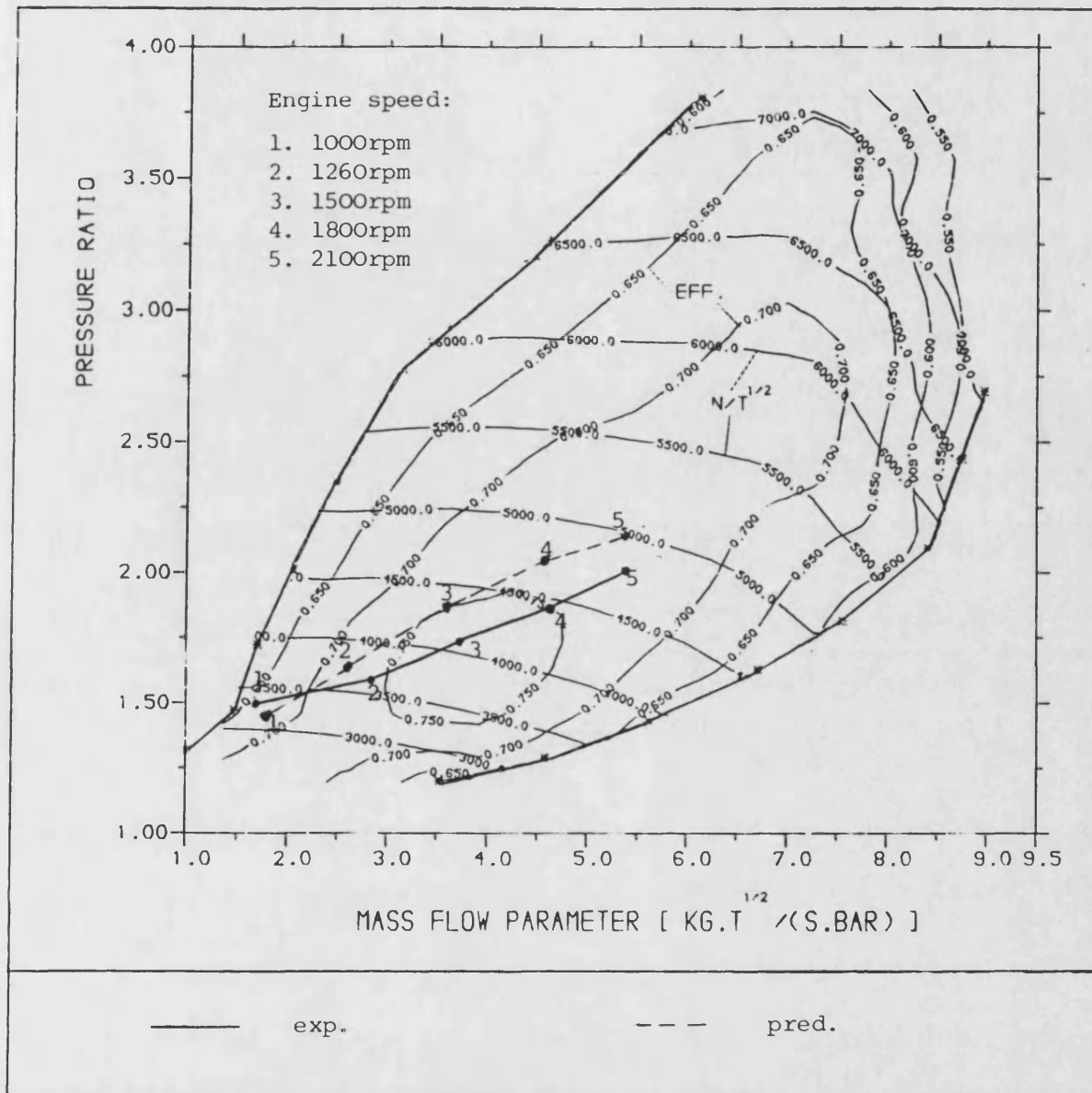


Fig-3.1 Experimental and predicted limiting torque curve on the compressor map

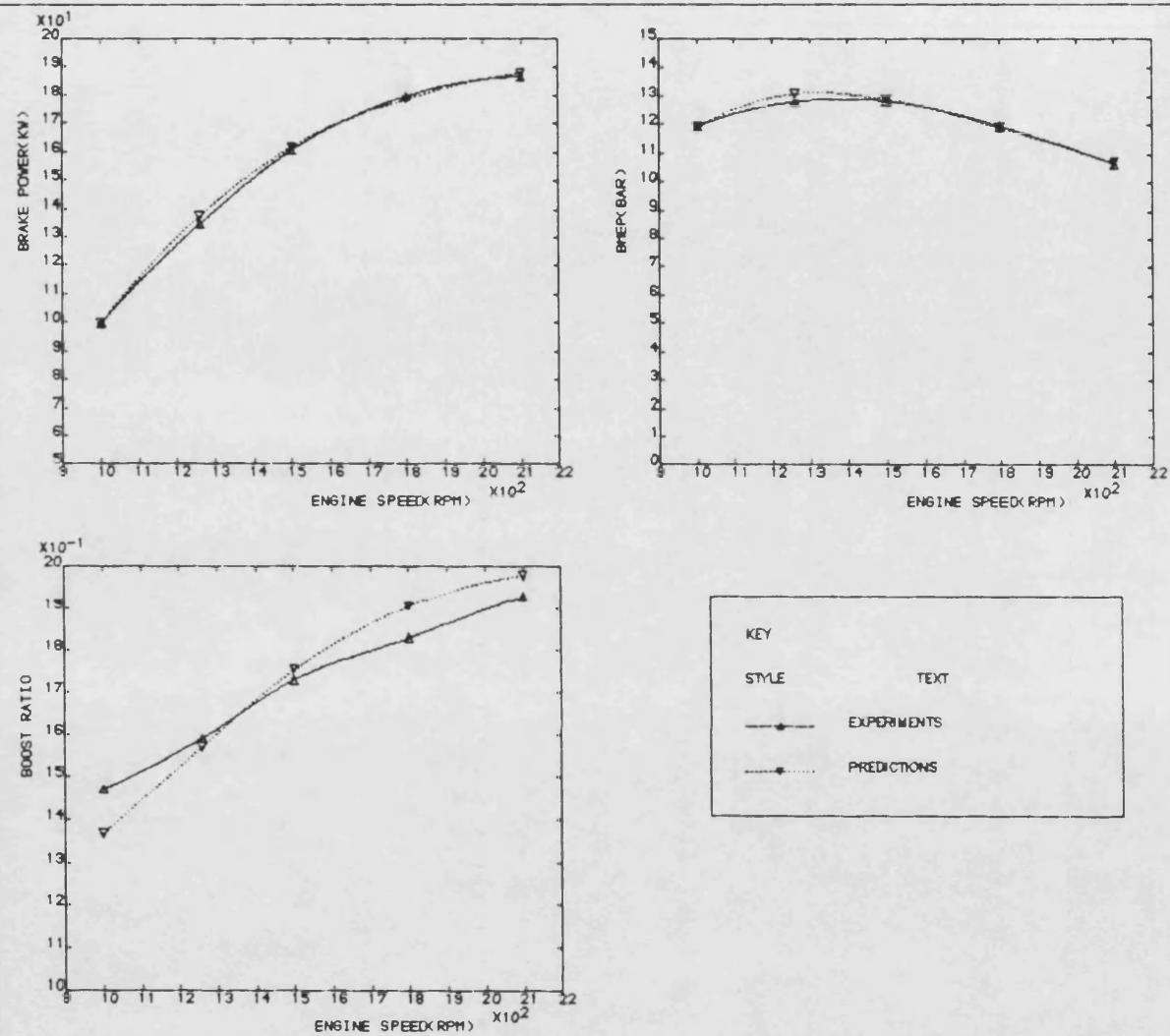


FIG-3.2a EXPERIMENTAL AND PREDICTED LIMITING TORQUE PERFORMANCE OF L10 ENGINE

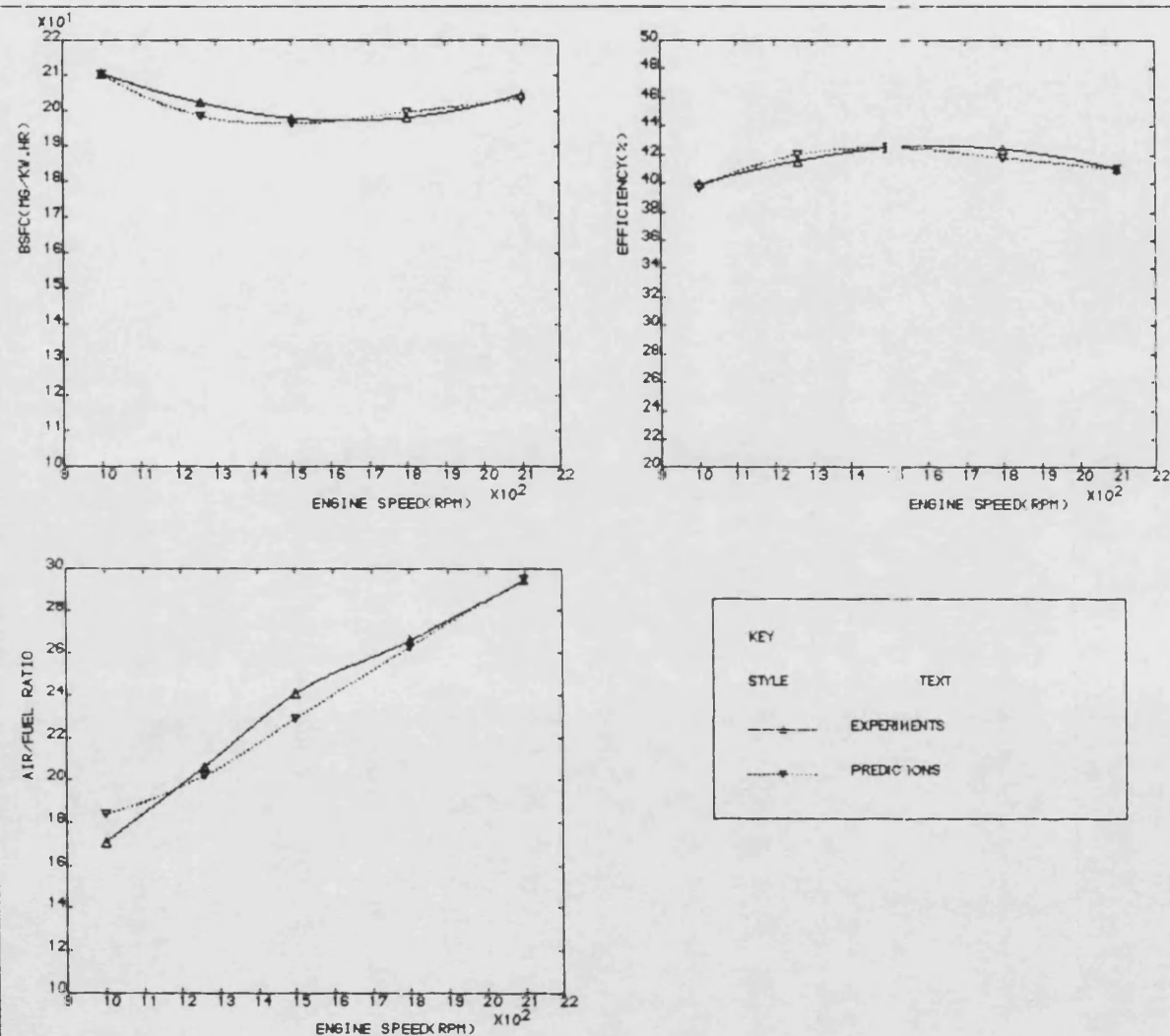


FIG-3.2b EXPERIMENTAL AND PREDICTED LIMITING TORQUE PERFORMANCE OF L10 ENGINE

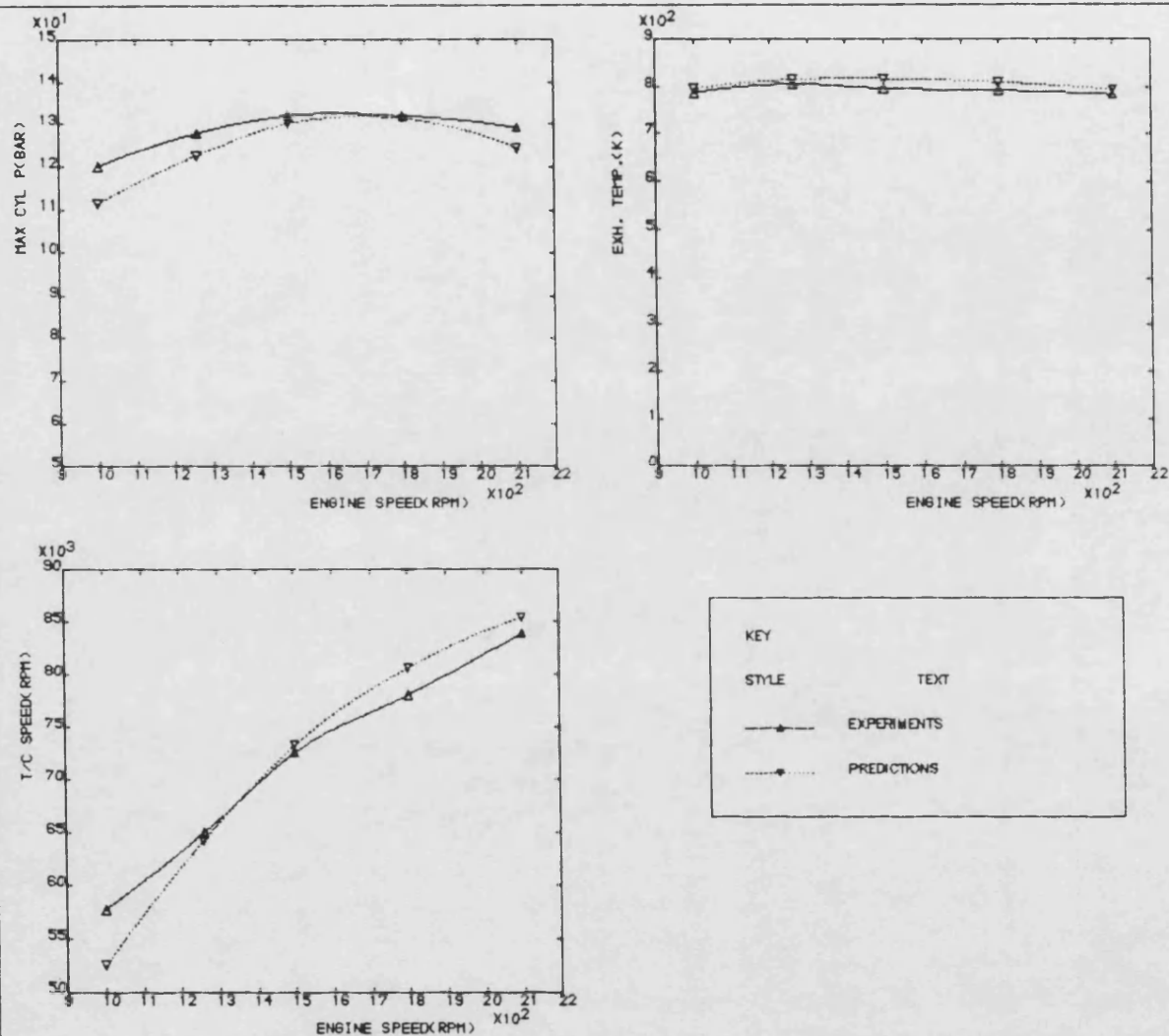


FIG-3.2c EXPERIMENTAL AND PREDICTED LIMITING TORQUE PERFORMANCE OF L10 ENGINE

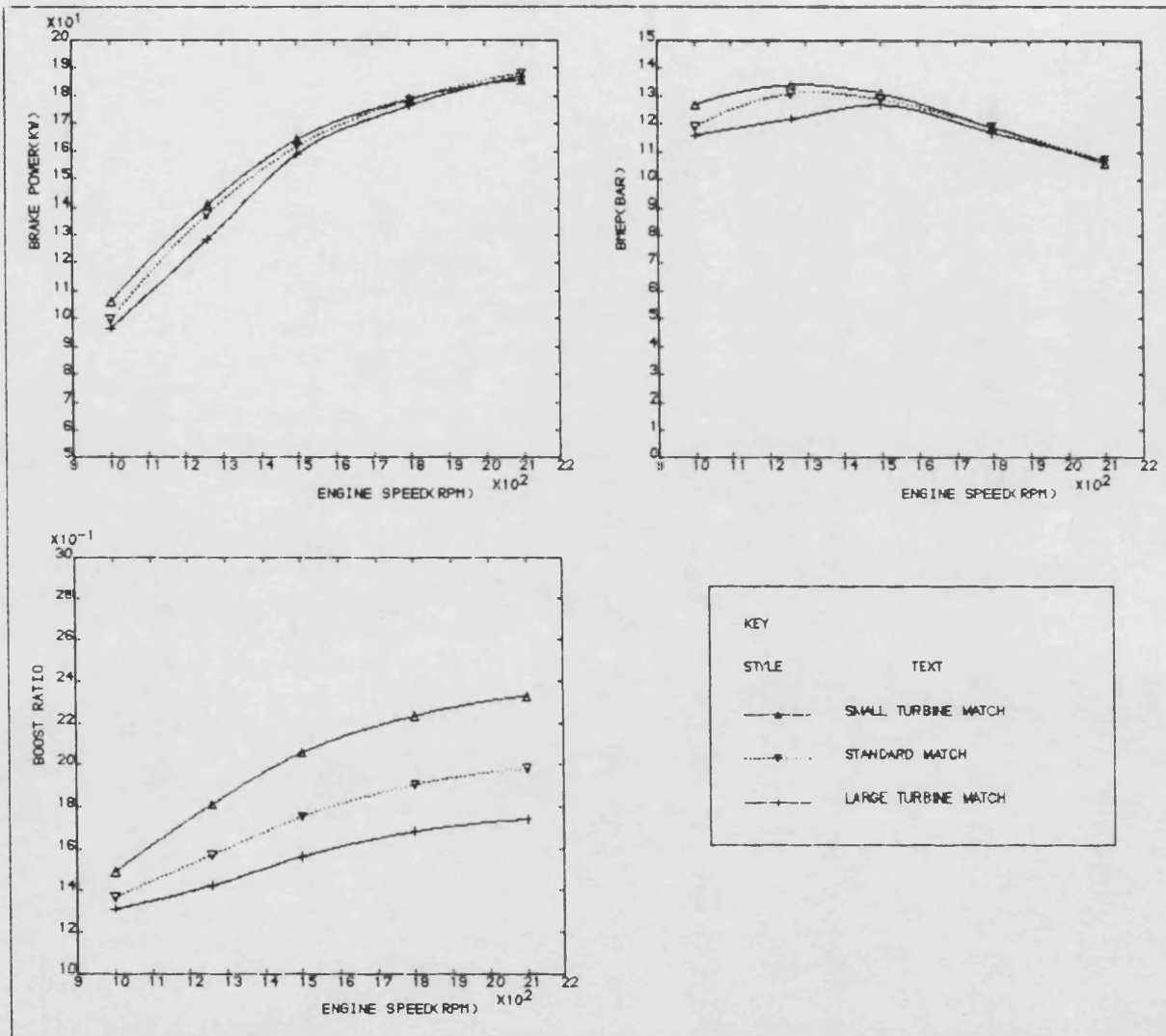


FIG-3.3a LIMITING TORQUE CURVE RESULTS WITH VARIOUS TURBINE MATCHES

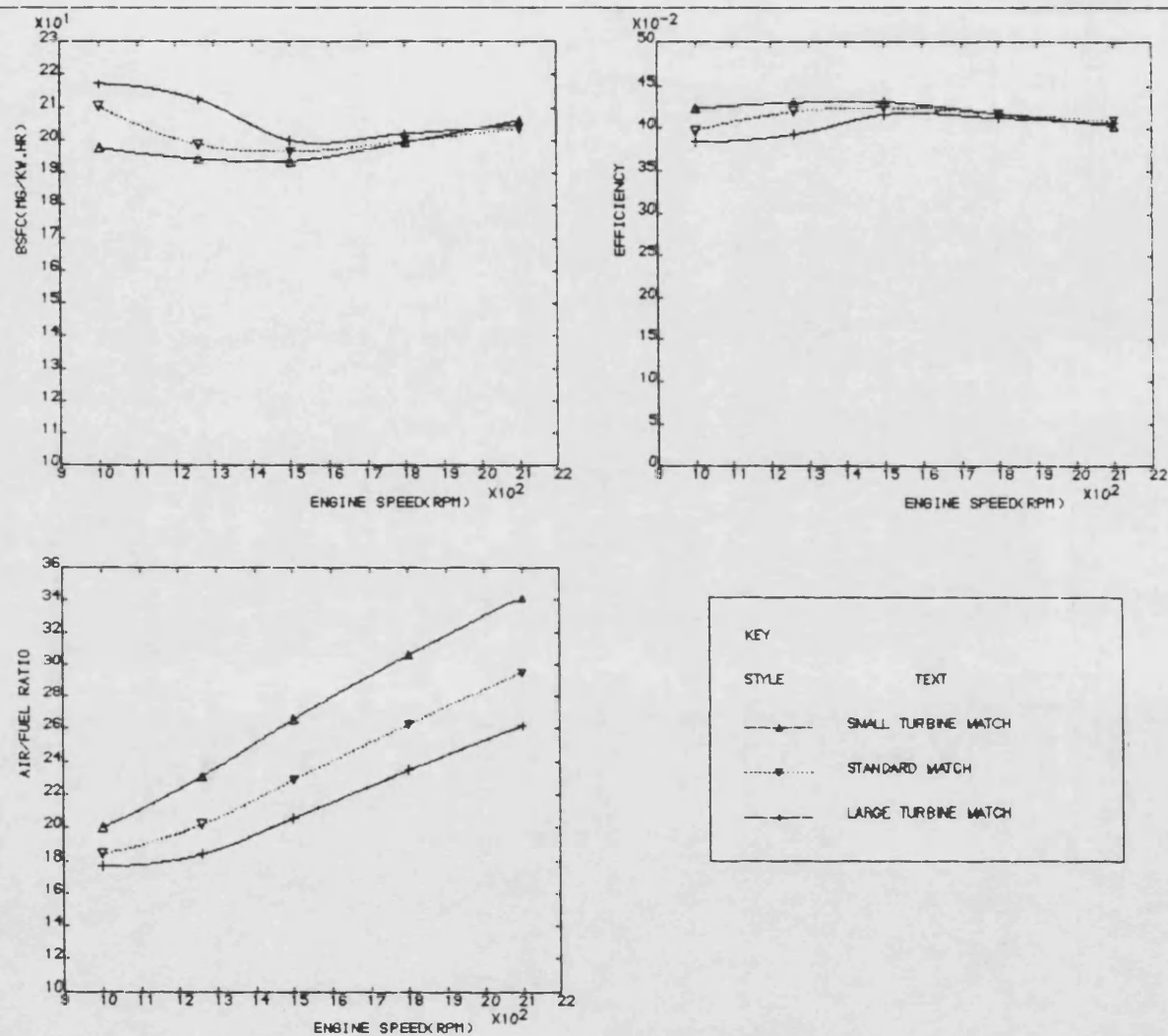


FIG-3.36 LIMITING TORQUE CURVE RESULTS WITH VARIOUS TURBINE MATCHES

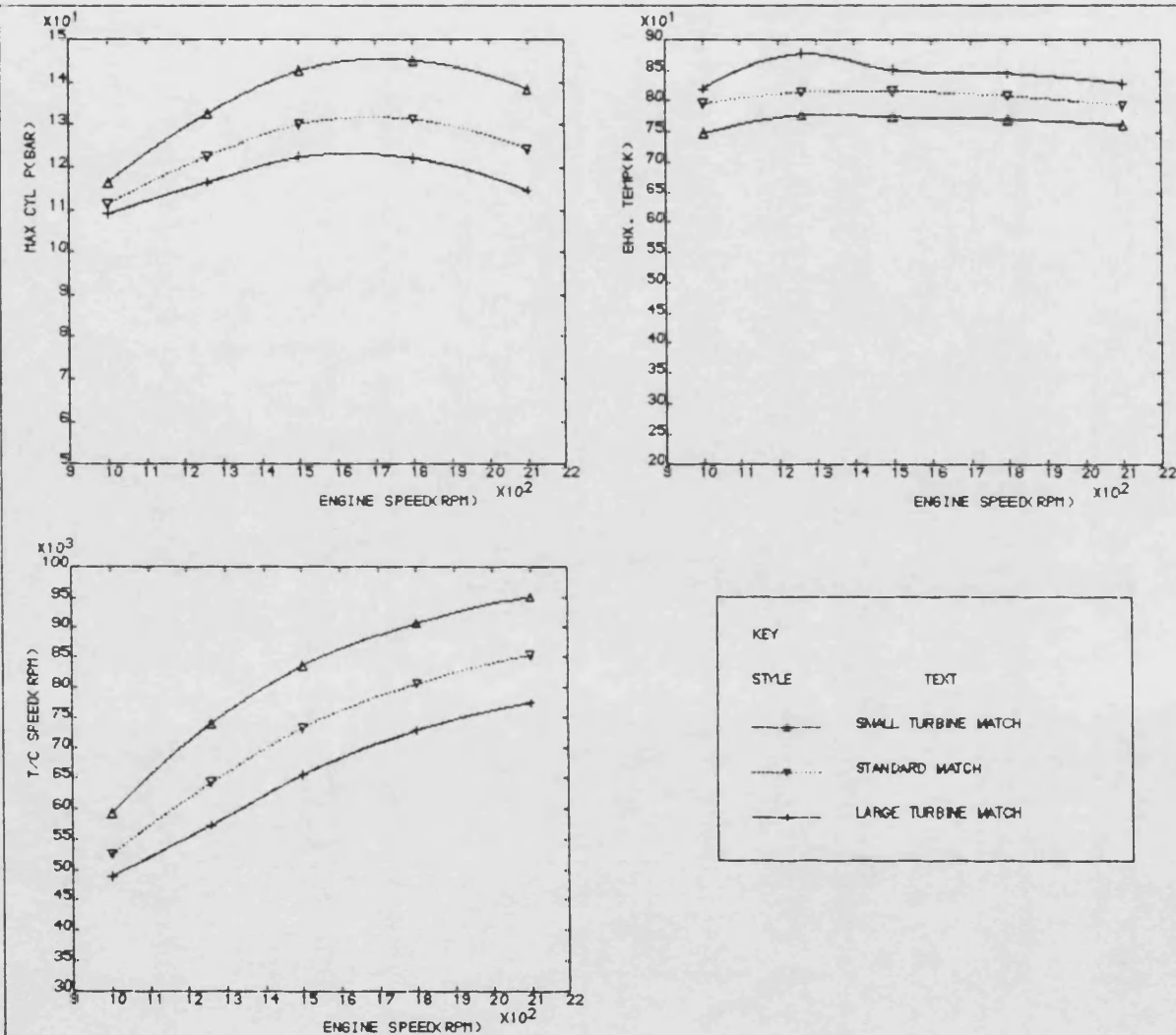


FIG-3.3c LIMITING TORQUE CURVE RESULTS WITH VARIOUS TURBINE MATCHES

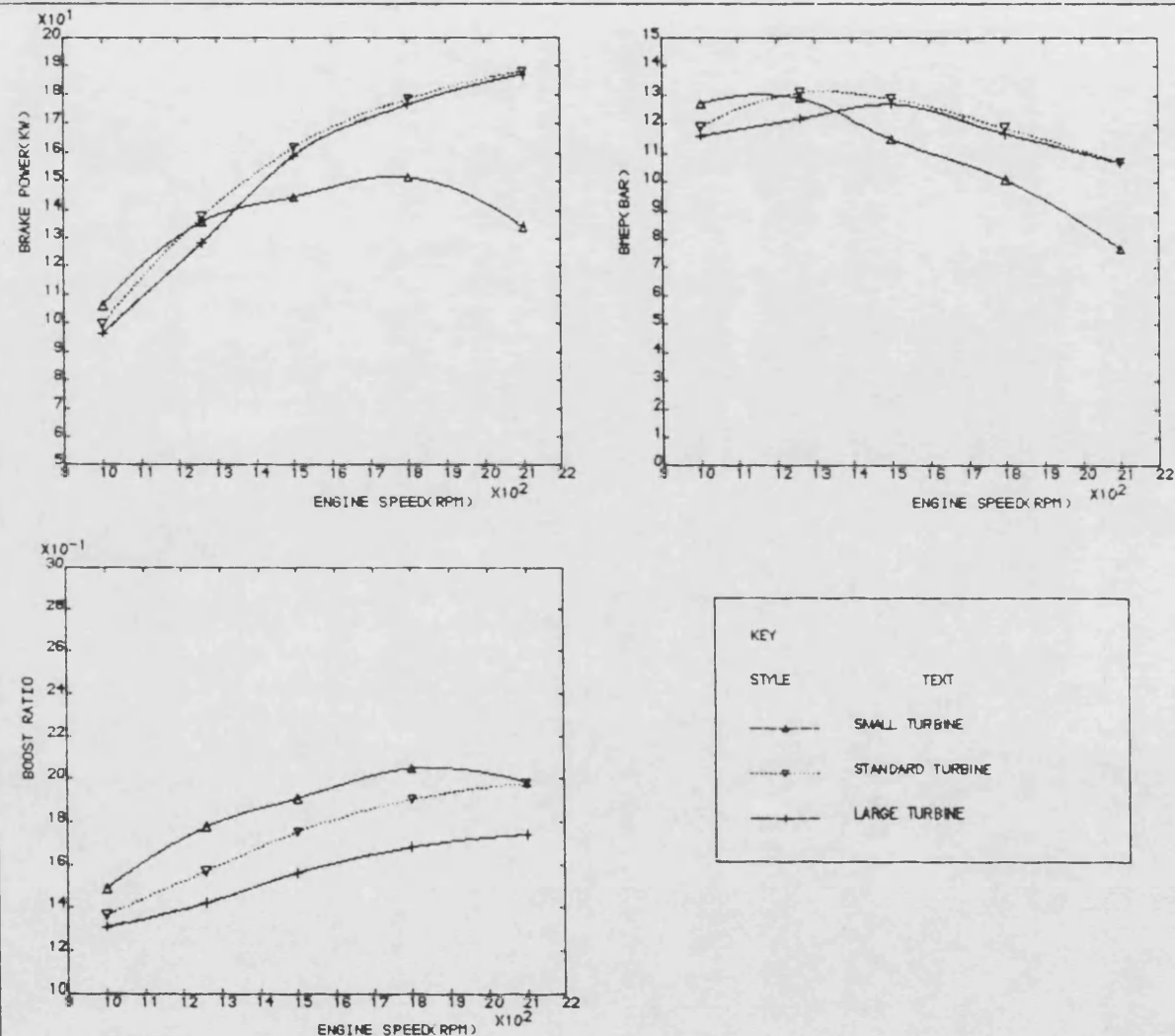
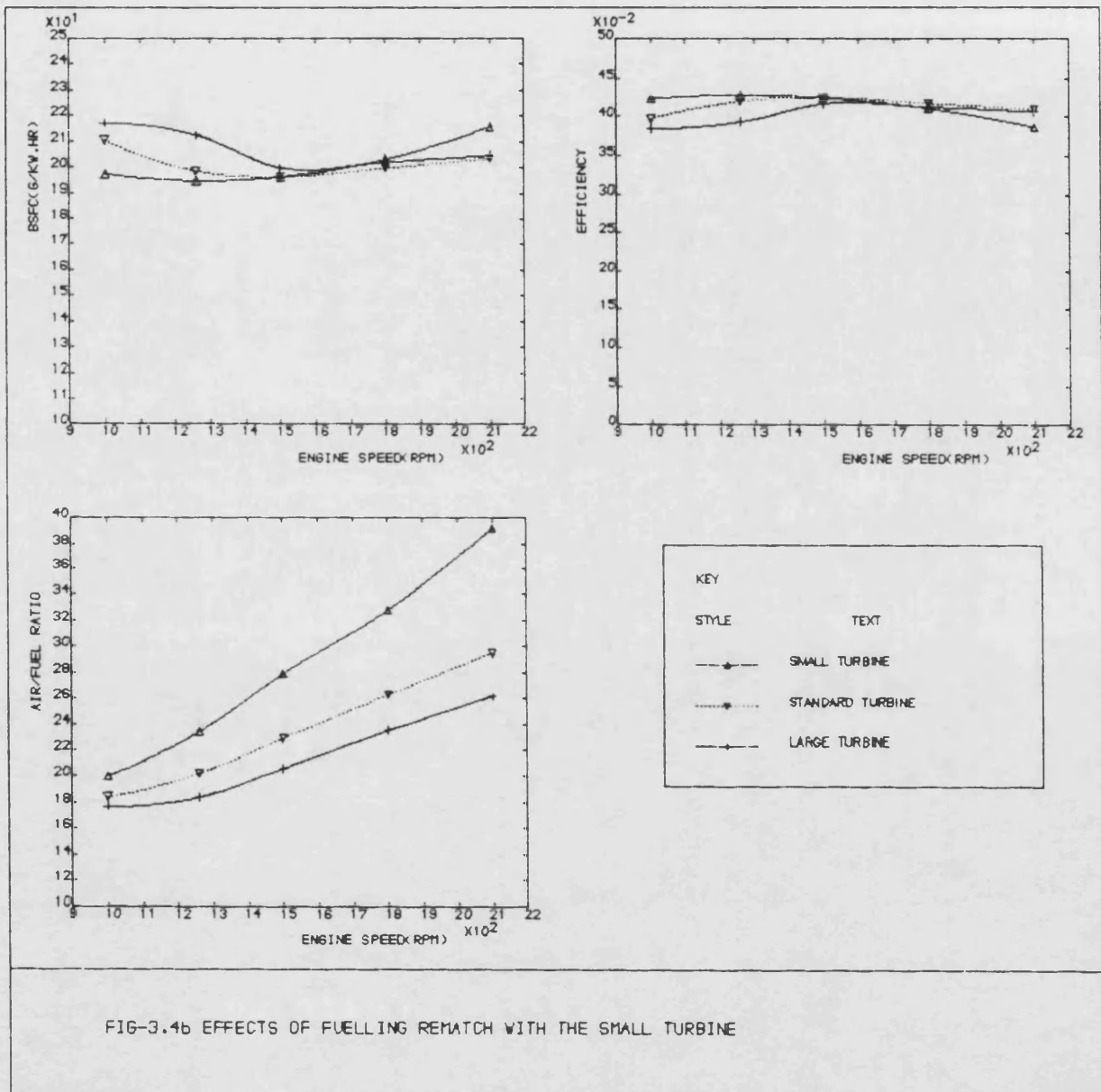


FIG-3.4a EFFECTS OF FUELLING REMATCH WITH THE SMALL TURBINE



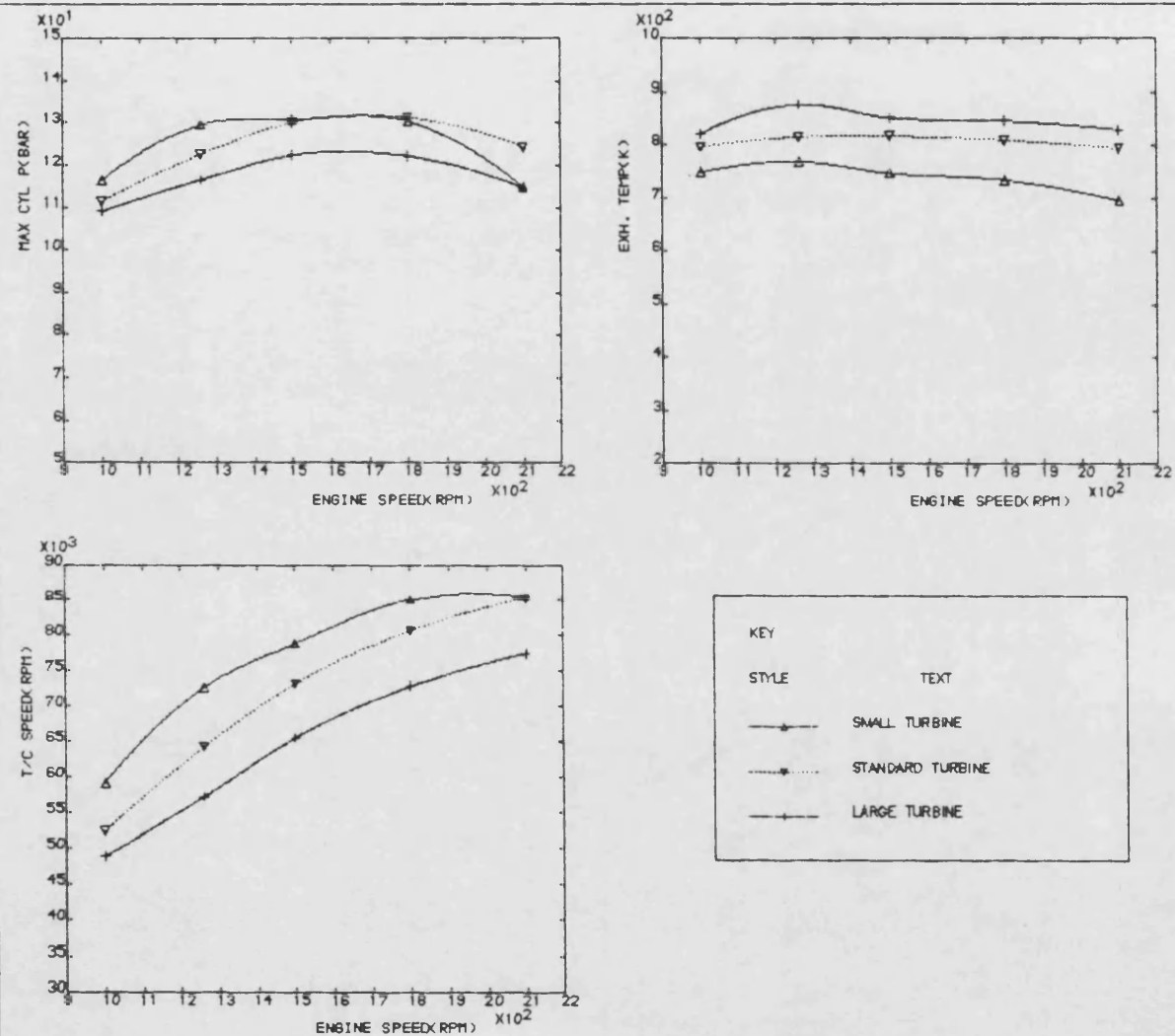
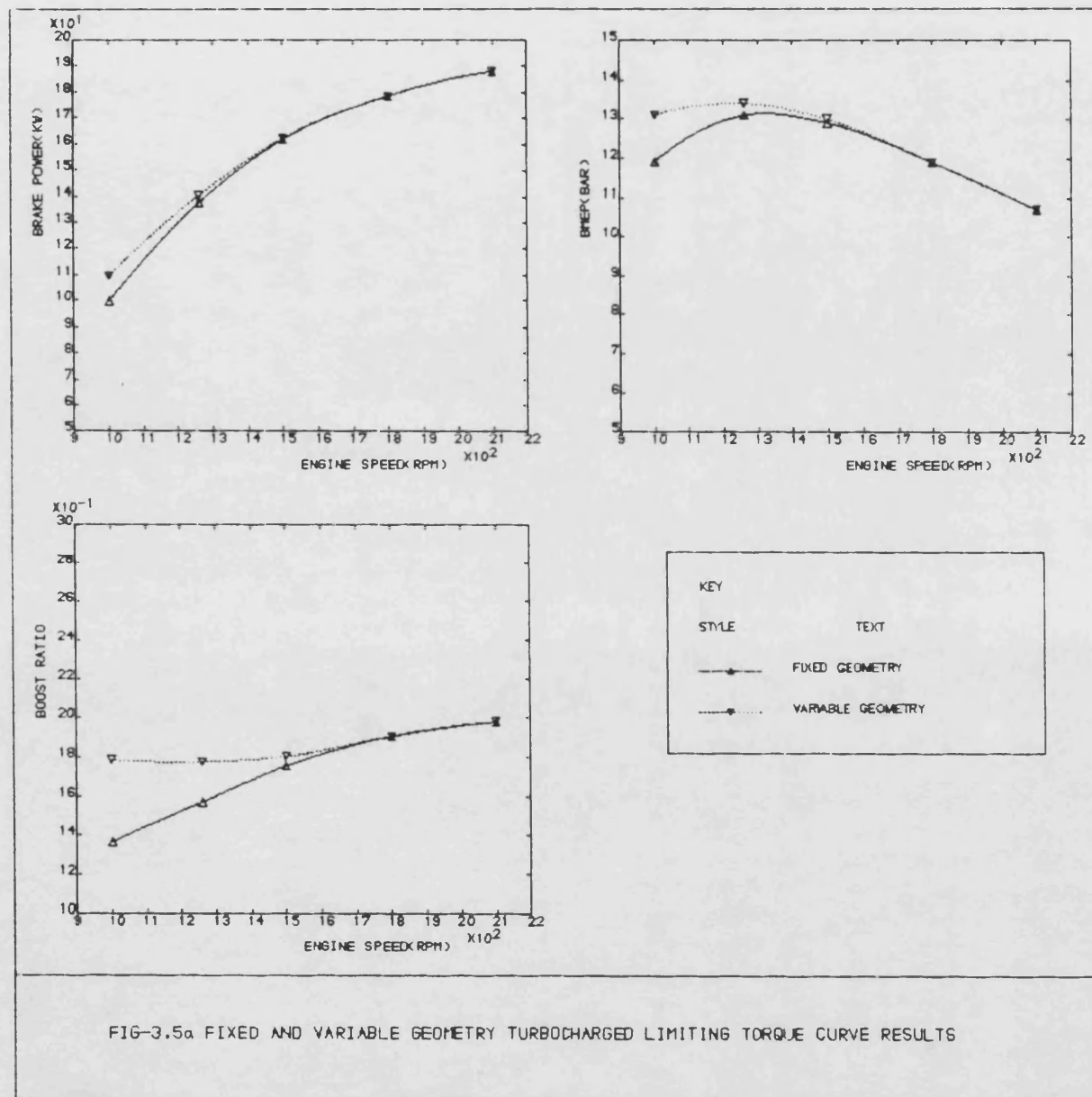


FIG-3.4c EFFECTS OF FUELLING REMATCH WITH THE SMALL TURBINE



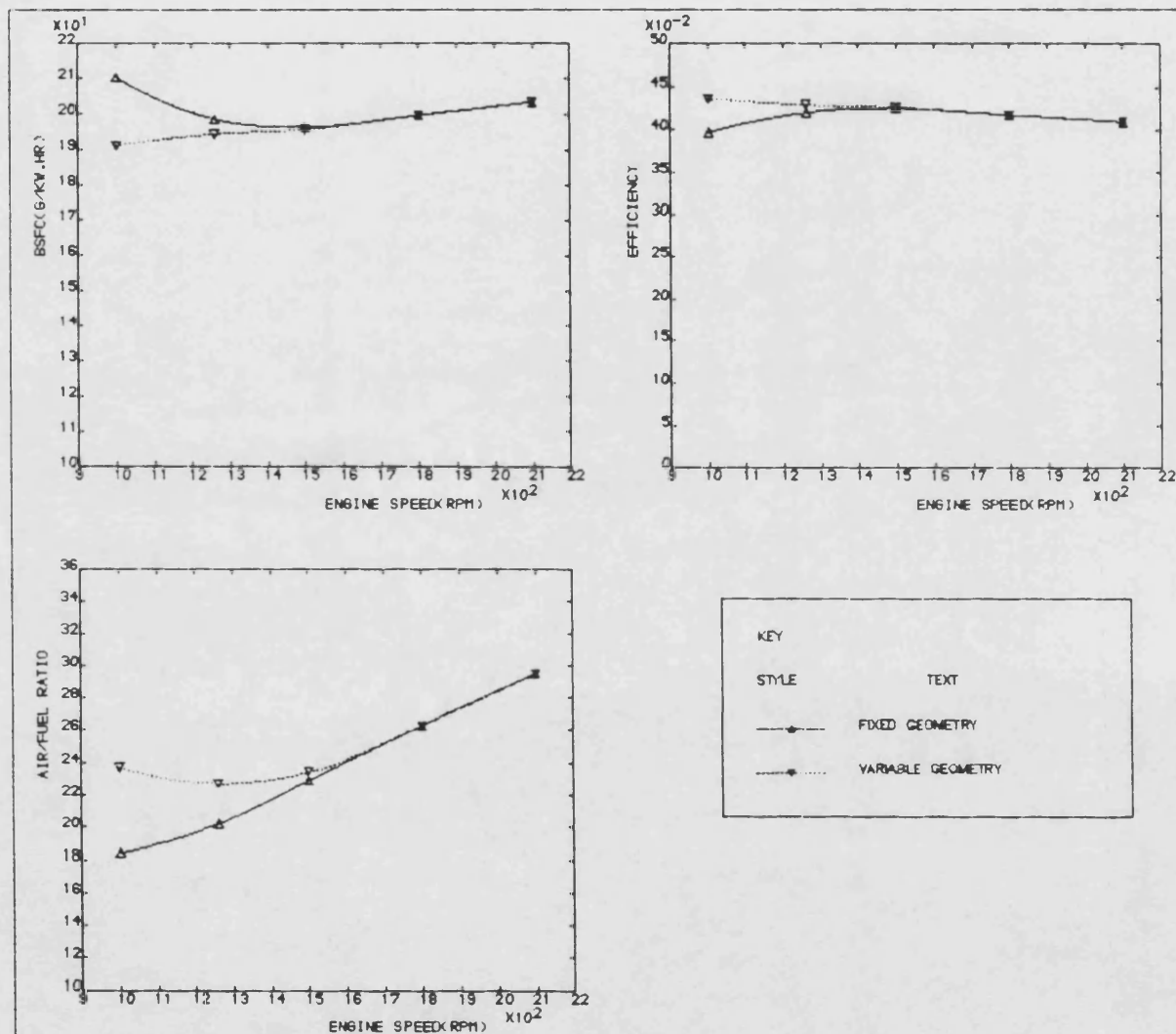
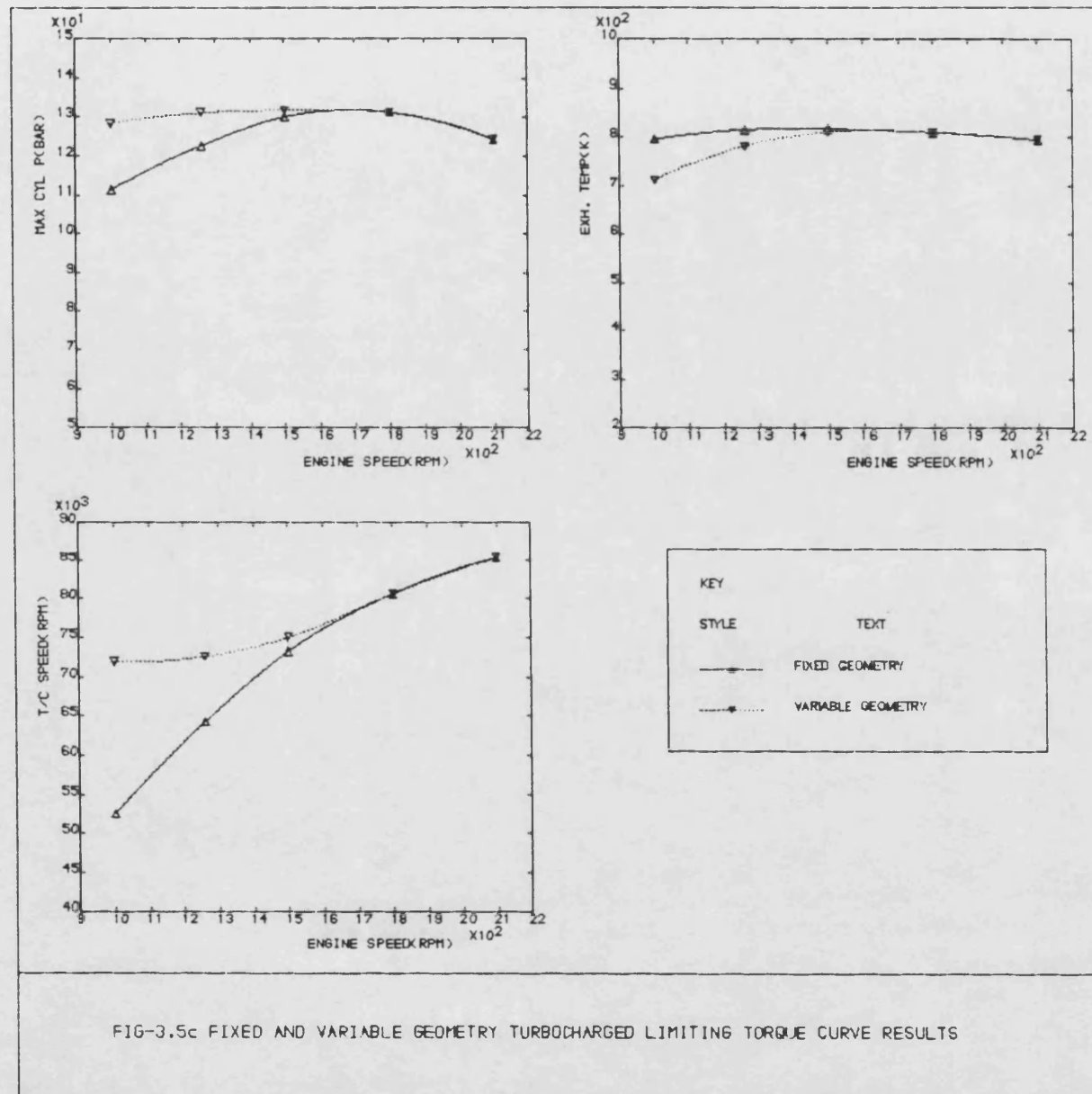


FIG-3.5b FIXED AND VARIABLE GEOMETRY TURBOCHARGED LIMITING TORQUE CURVE RESULTS



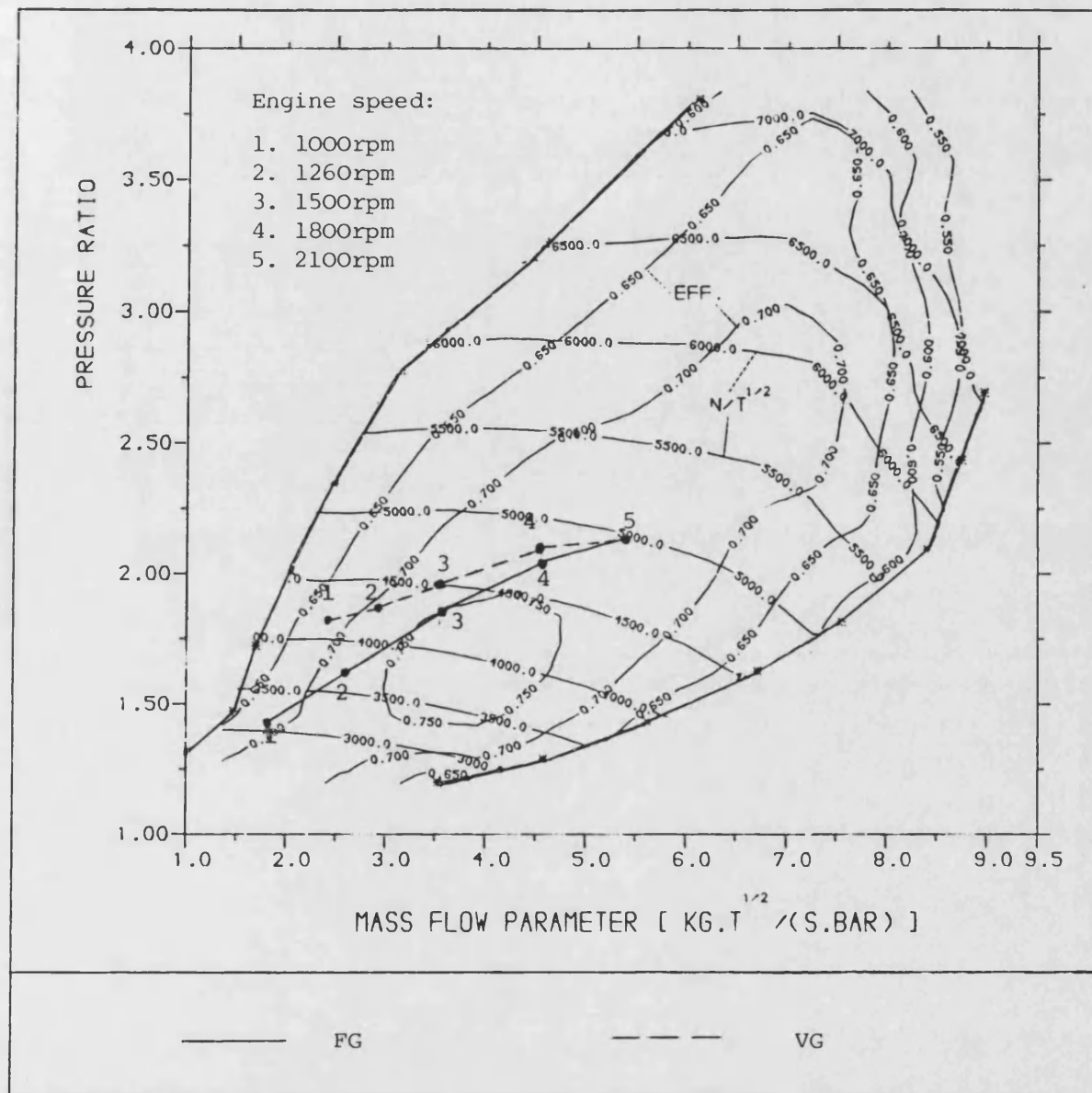
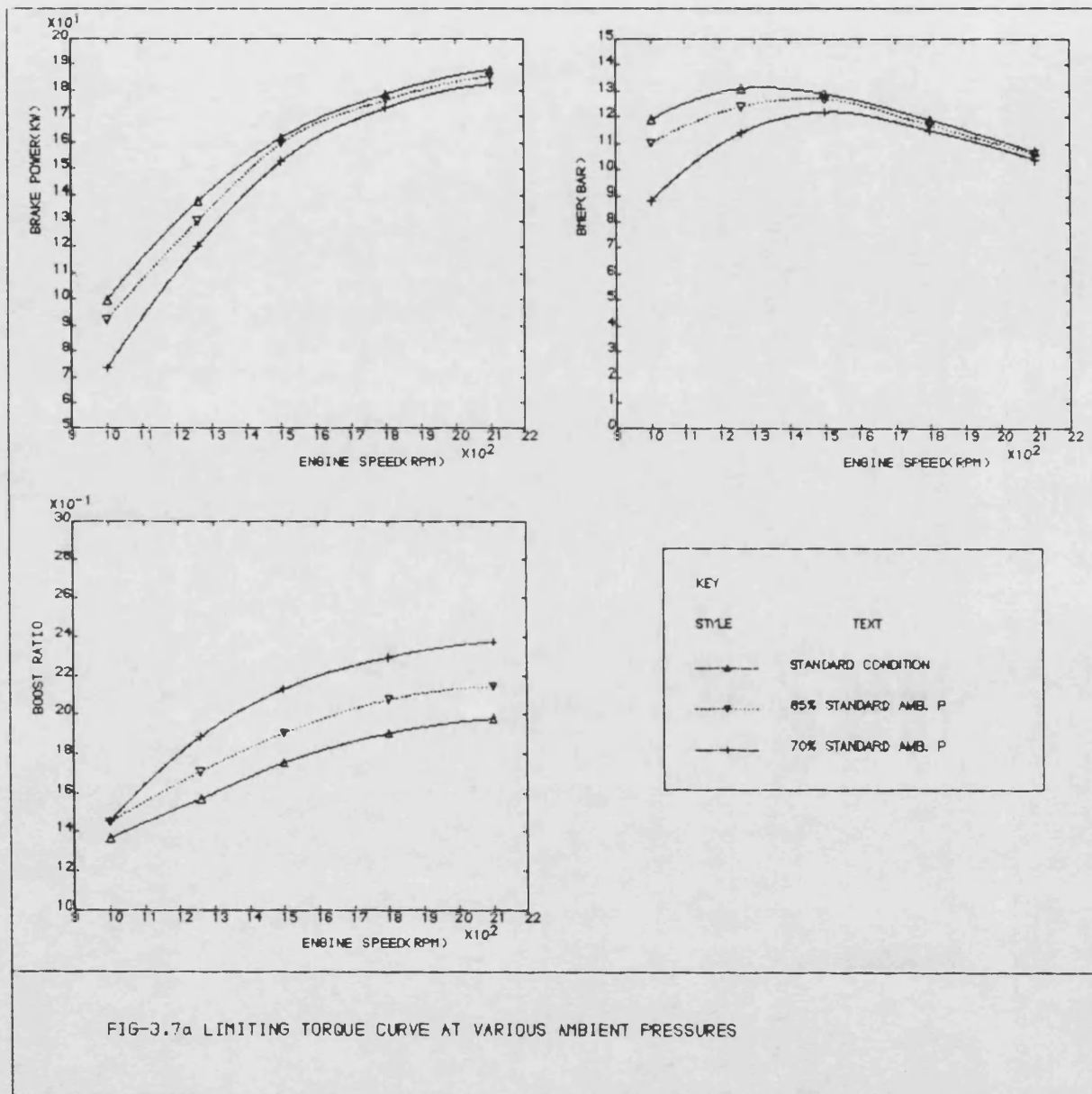


Fig-3.6 The effects of VG turbocharging



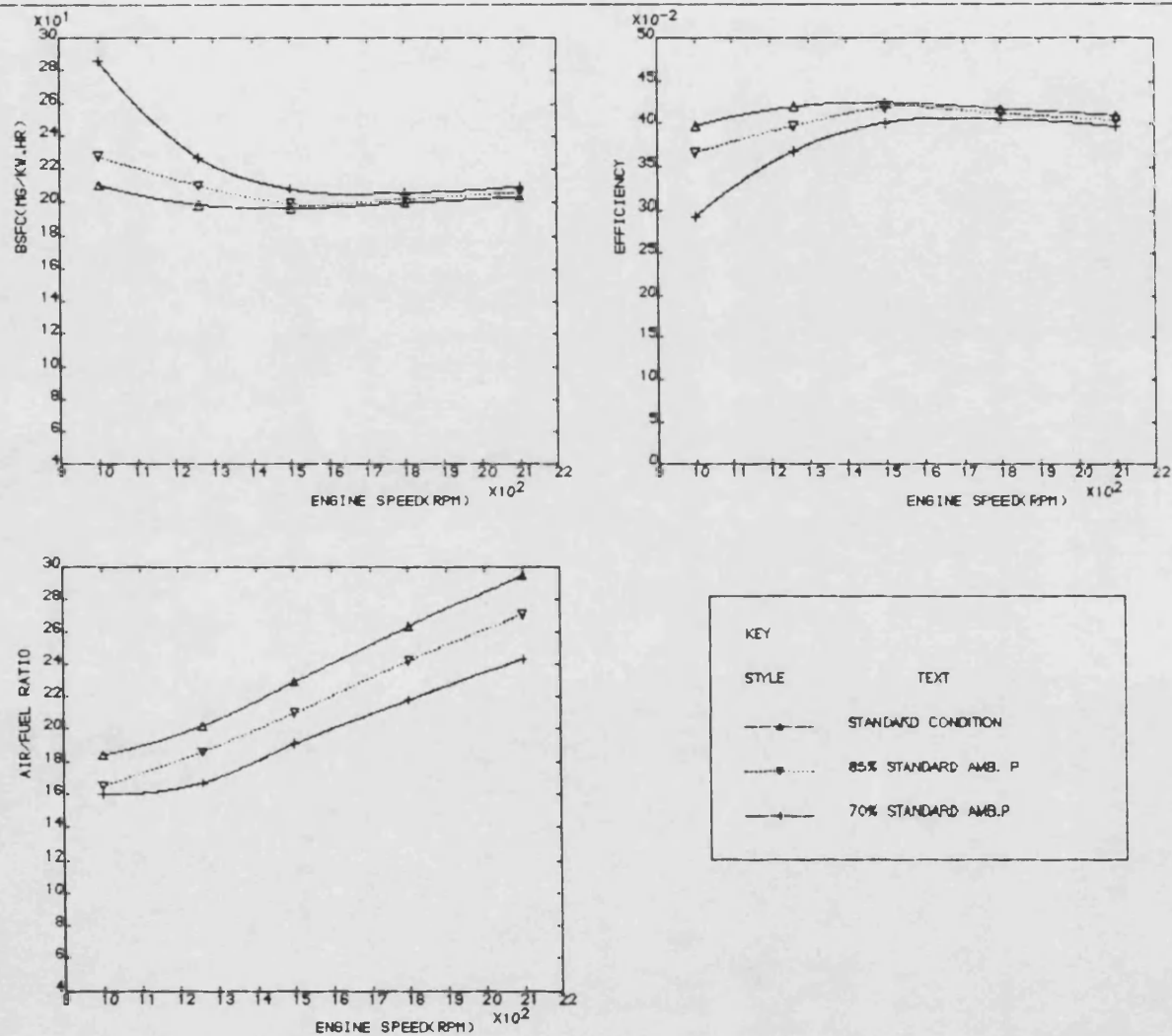


FIG-3.7b LIMITING TORQUE CURVE AT VARIOUS AMBIENT PRESSURES

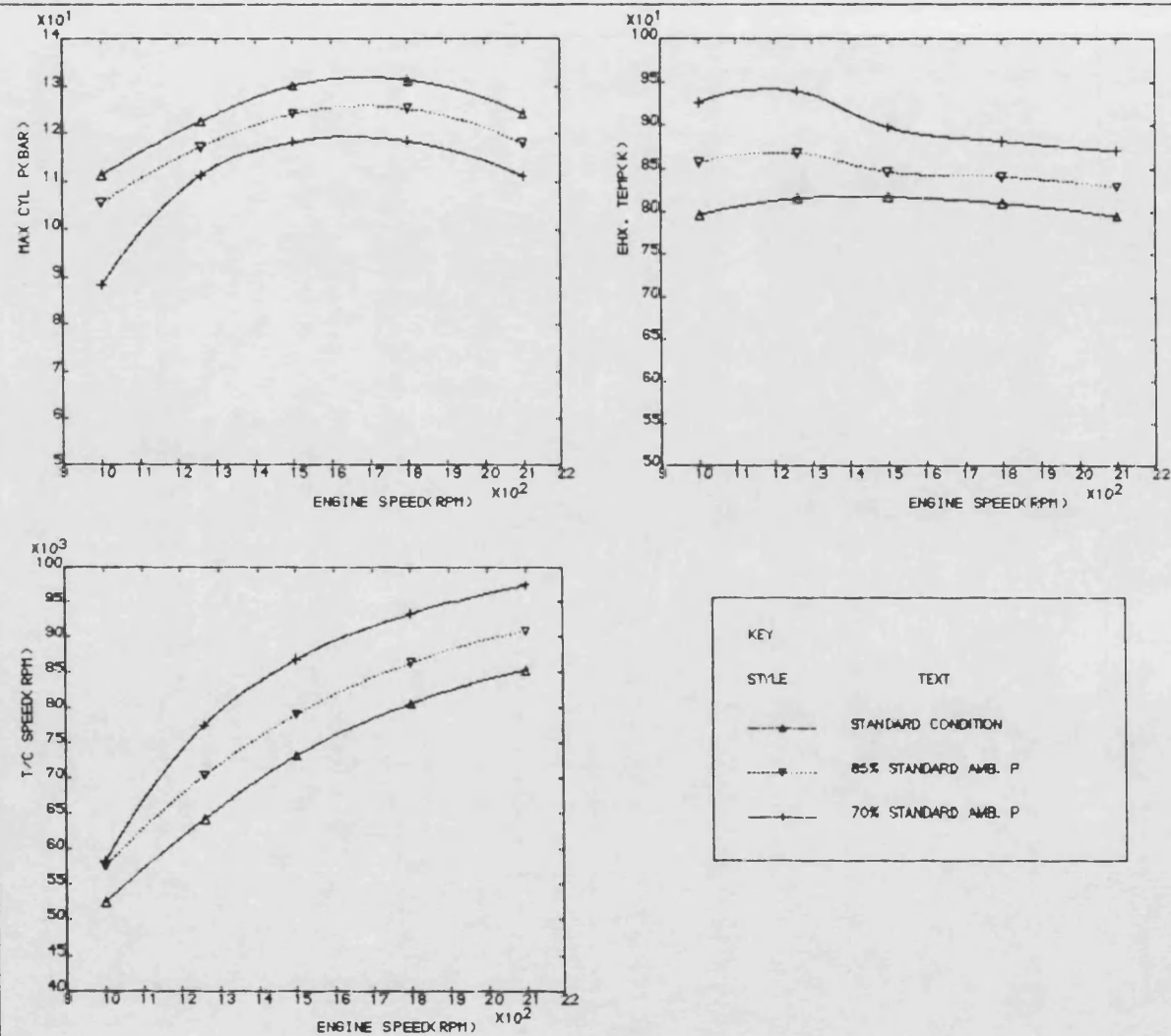


FIG-3.7c LIMITING TORQUE CURVE AT VARIOUS AMBIENT PRESSURES

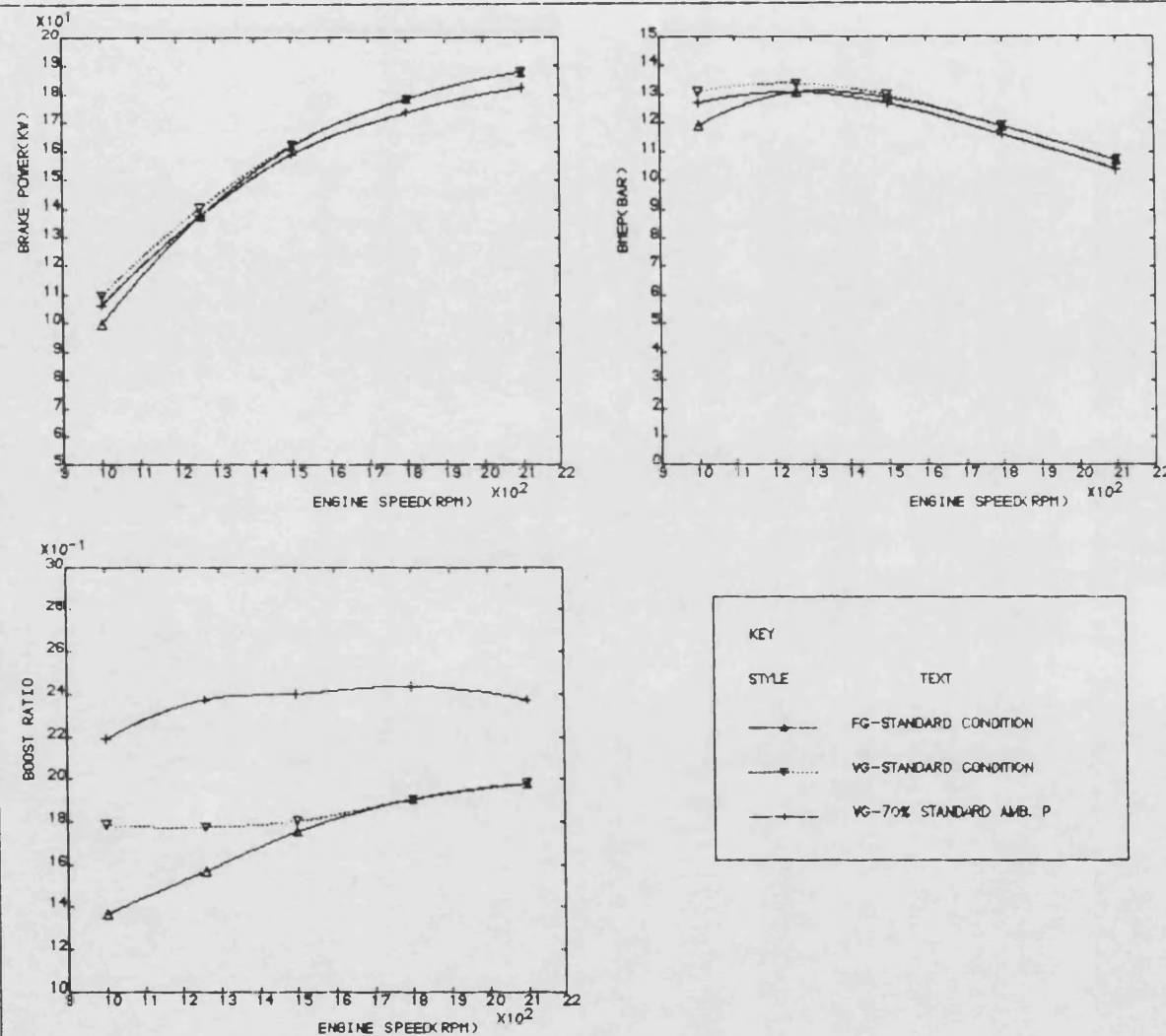
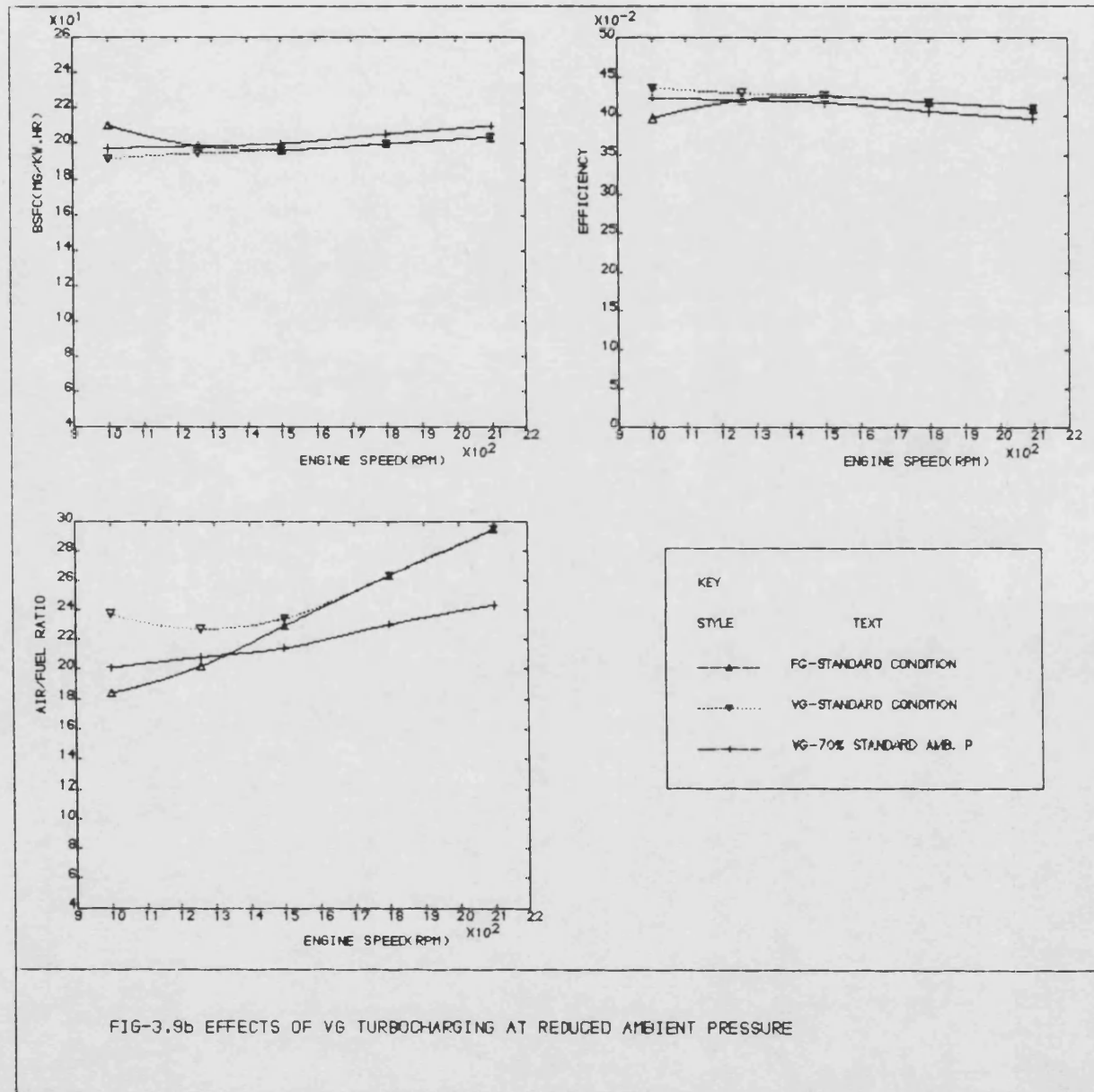


FIG-3.9a EFFECTS OF VG TURBOCHARGING AT REDUCED AMBIENT PRESSURE



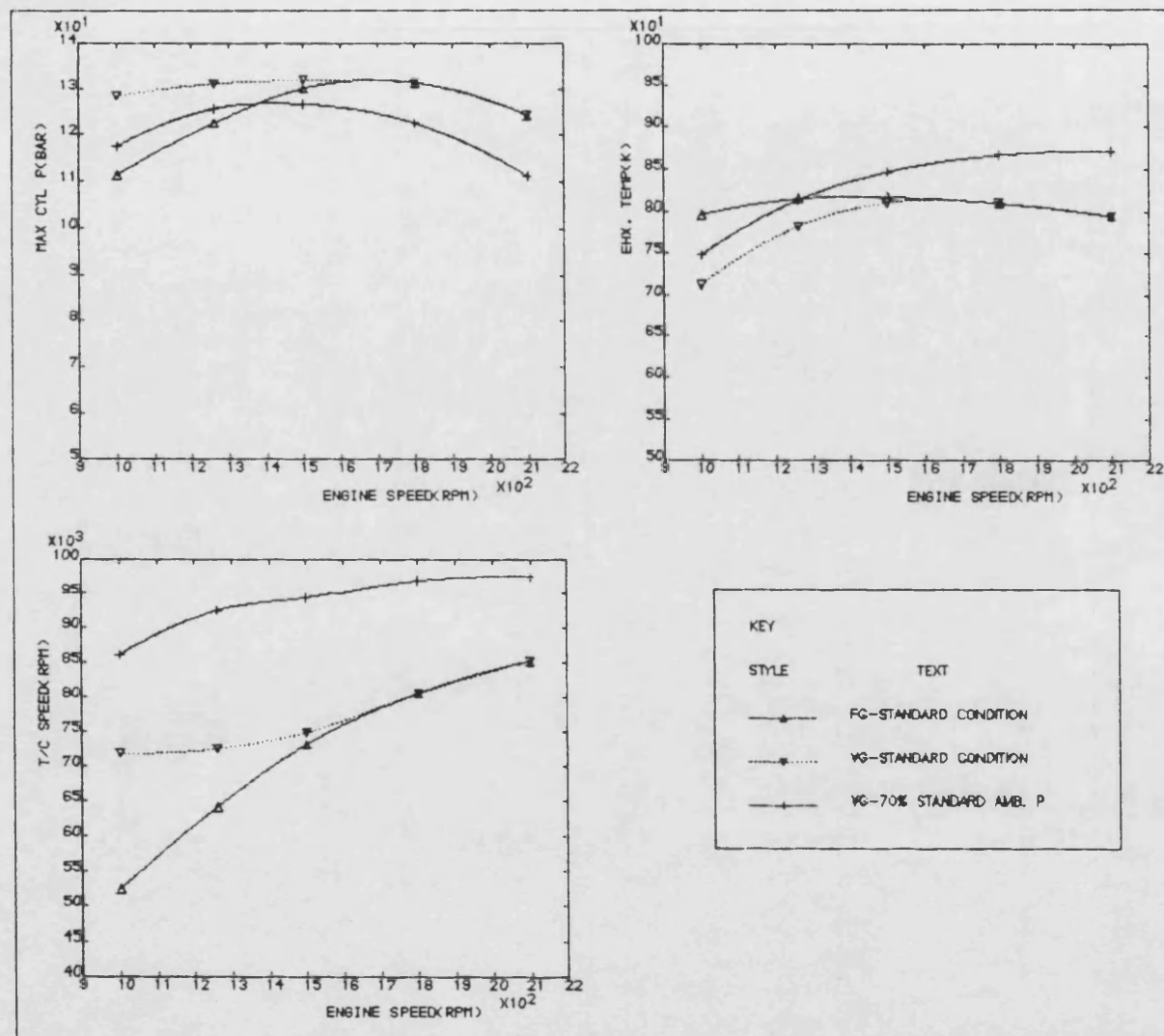


FIG-3.9c EFFECTS OF V6 TURBOCHARGING AT REDUCED AMBIENT PRESSURE

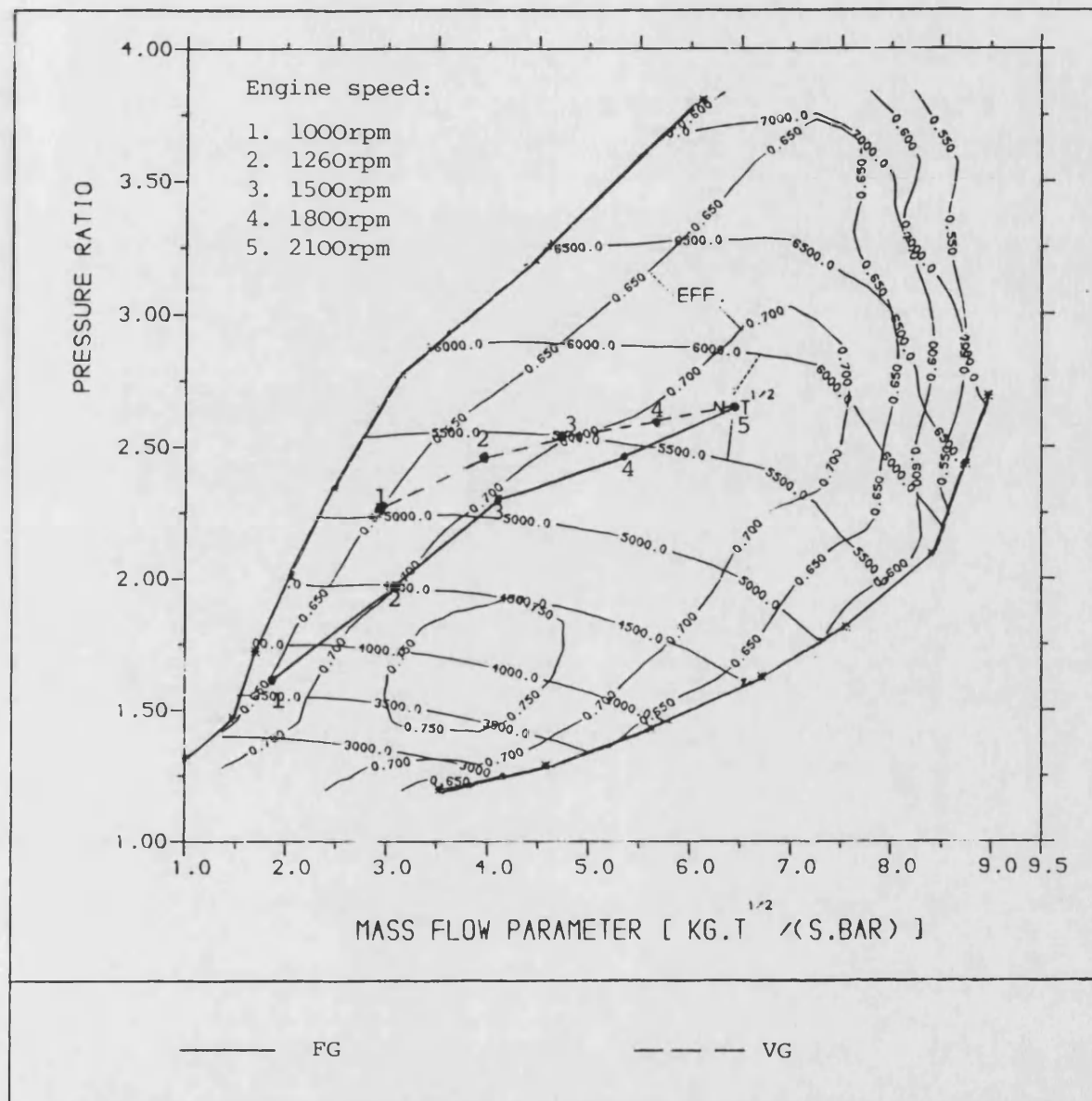
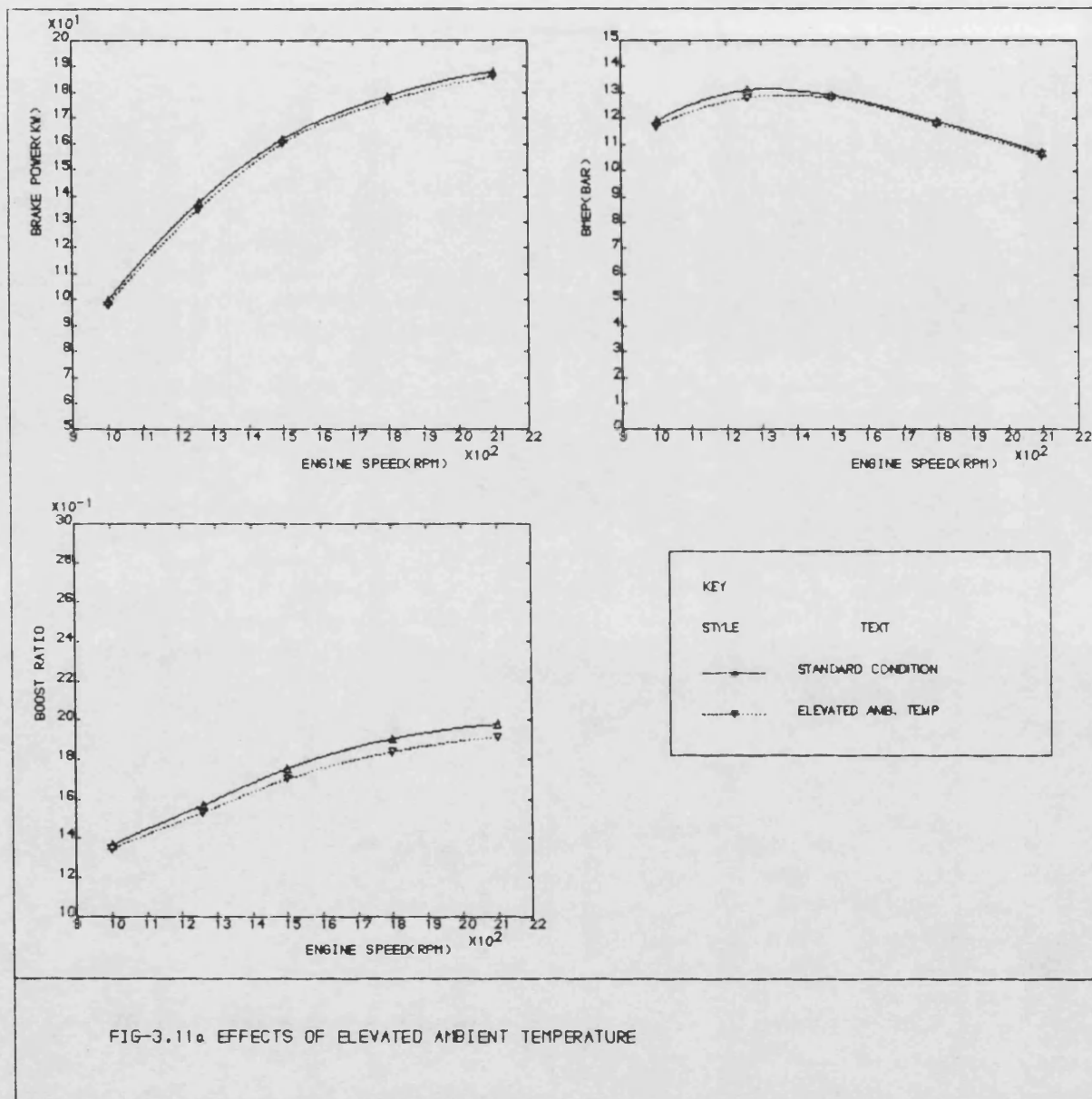


Fig-3.1o Effects of VG turbocharging at reduced ambient pressure



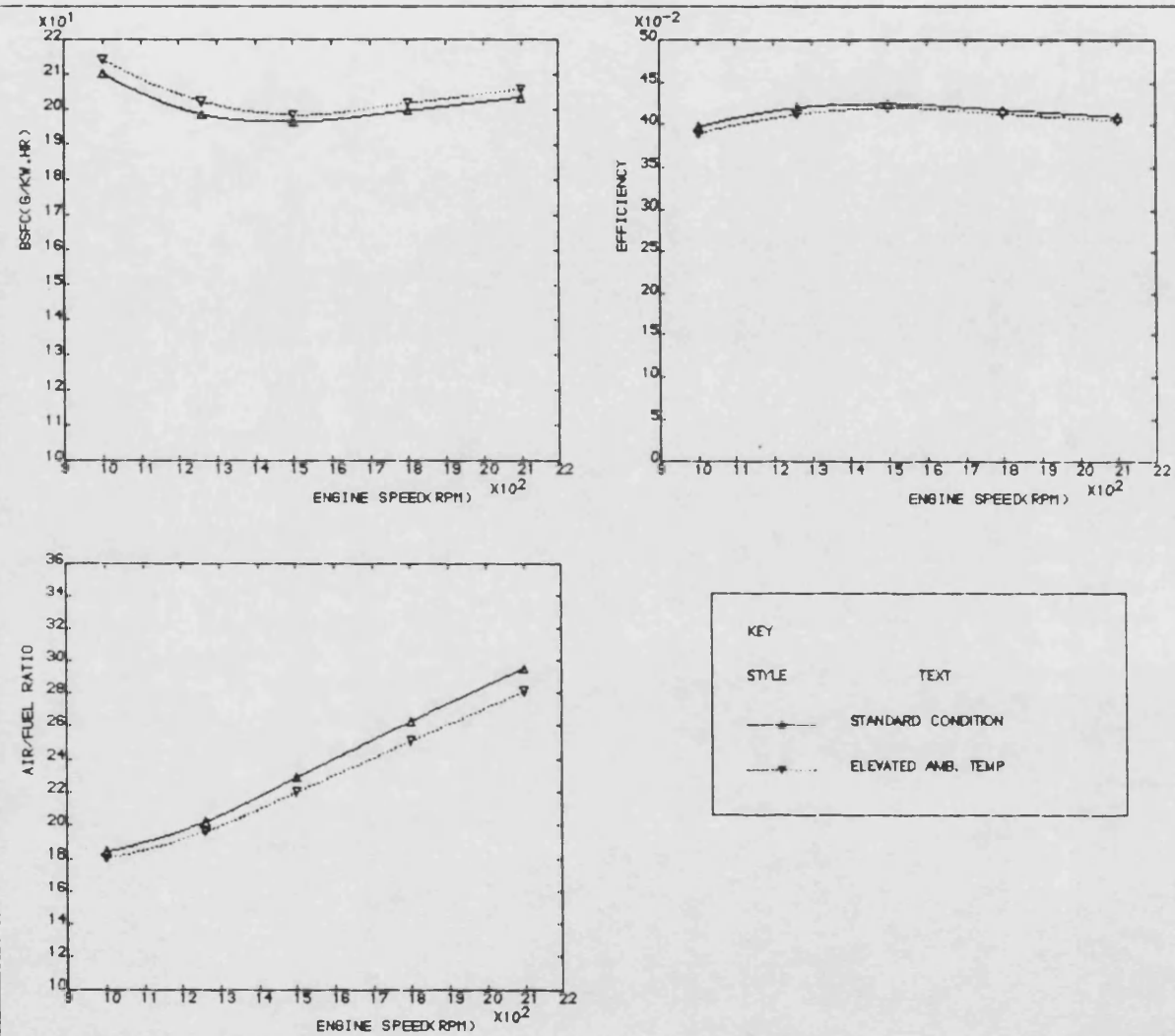


FIG-3.11b EFFECTS OF ELEVATED AMBIENT TEMPERATUTE

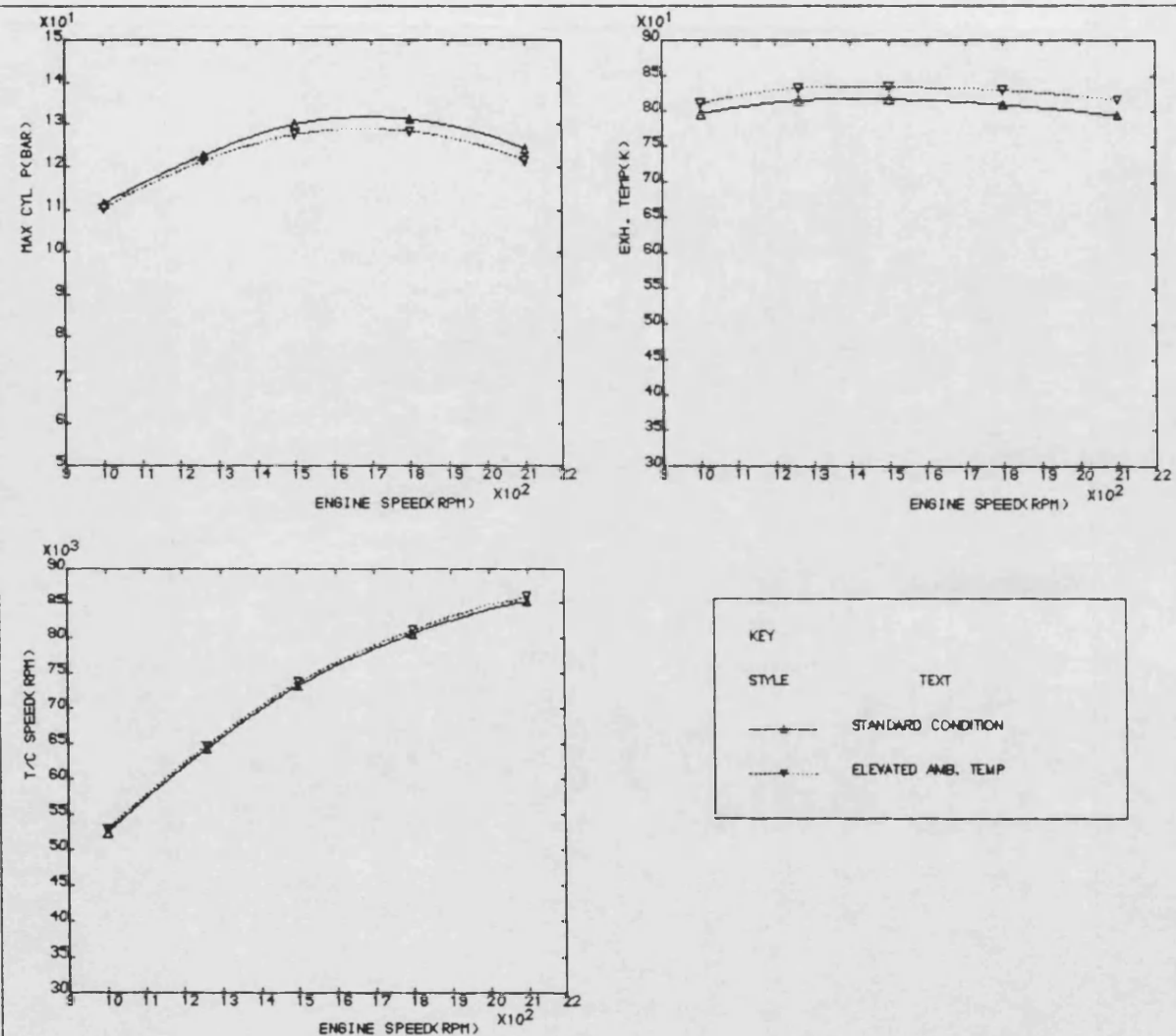


FIG-3.11c EFFECTS OF ELEVATED AMBIENT TEMPERATURE

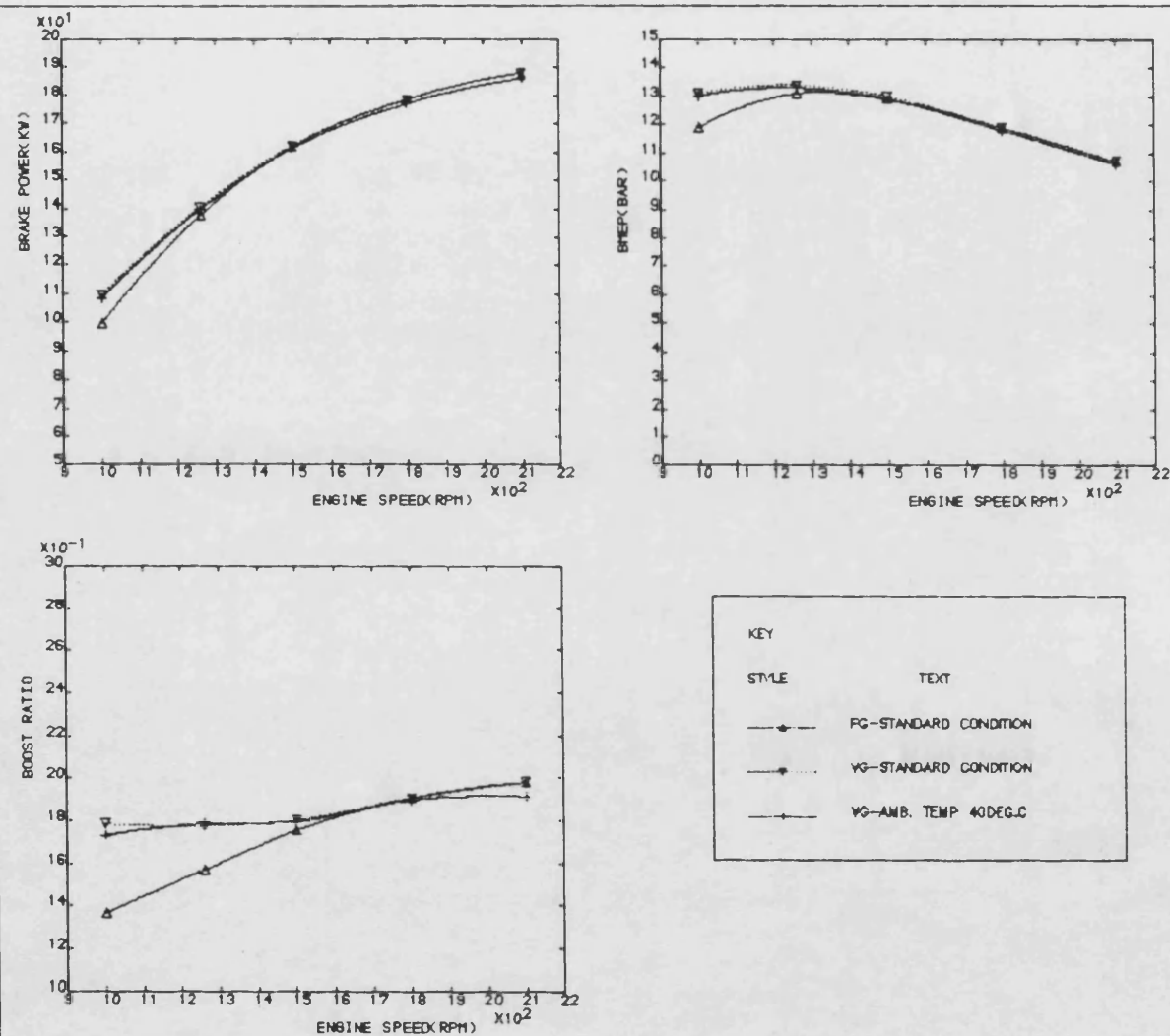


FIG-3.12a EFFECTS OF VG TURBOCHARGING AT ELEVATED AMBIENT TEMPERATURE

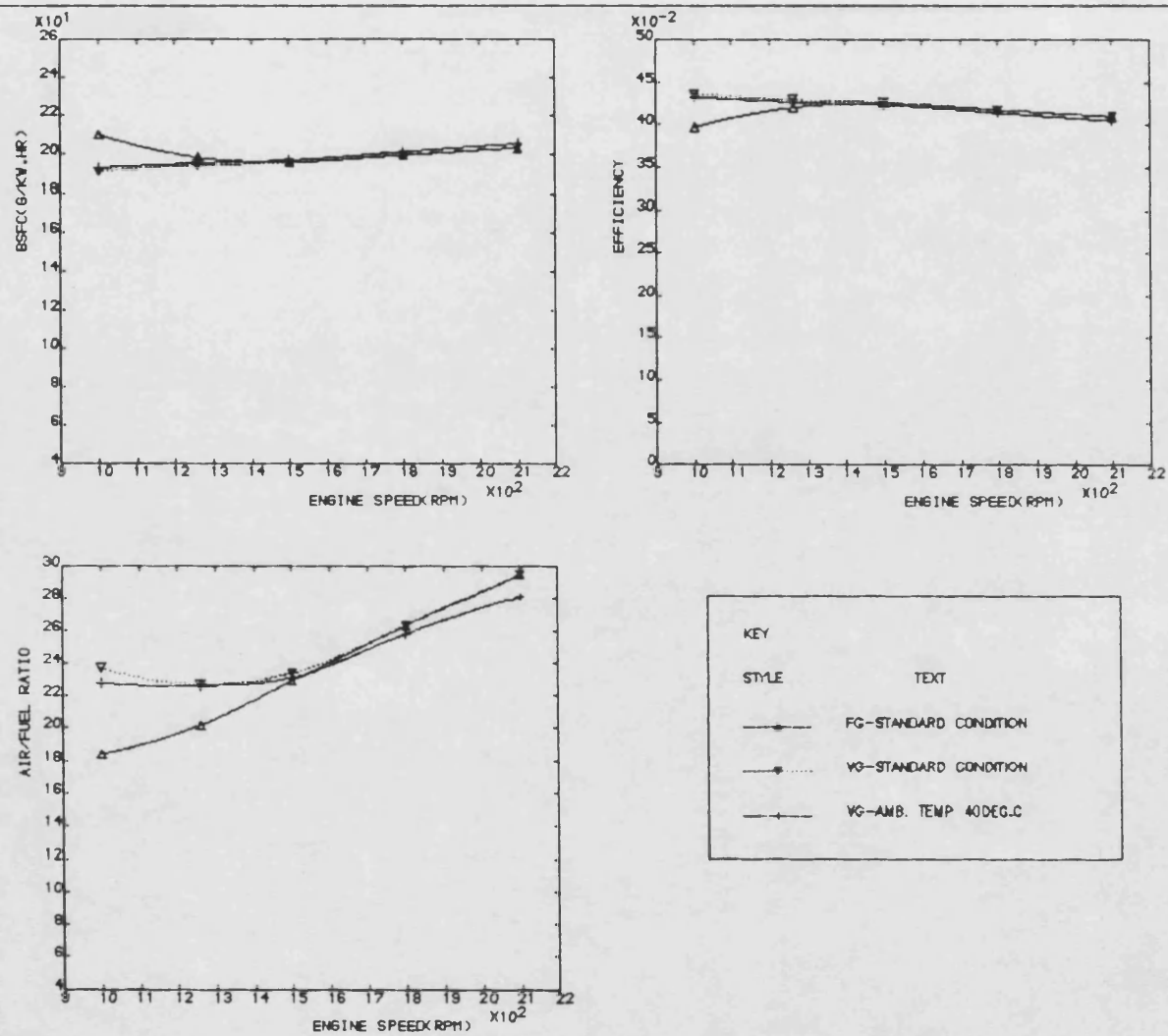


FIG-3.12b EFFECTS OF VG TURBOCHARGING AT ELEVATED AMBIENT TEMPERATURE

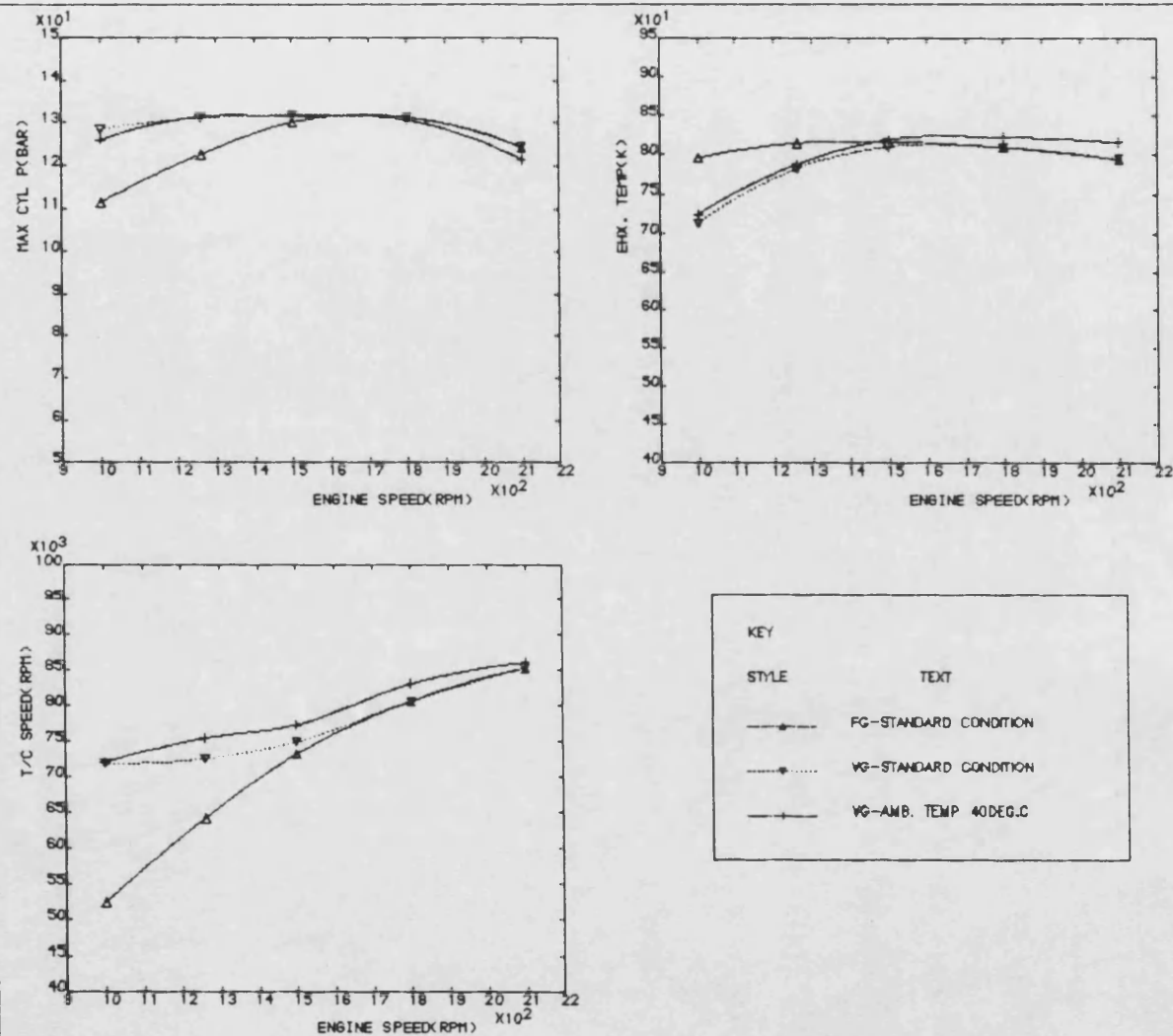


FIG-3.12c EFFECTS OF VG TURBOCHARGING AT ELEVATED AMBIENT TEMPERATURE

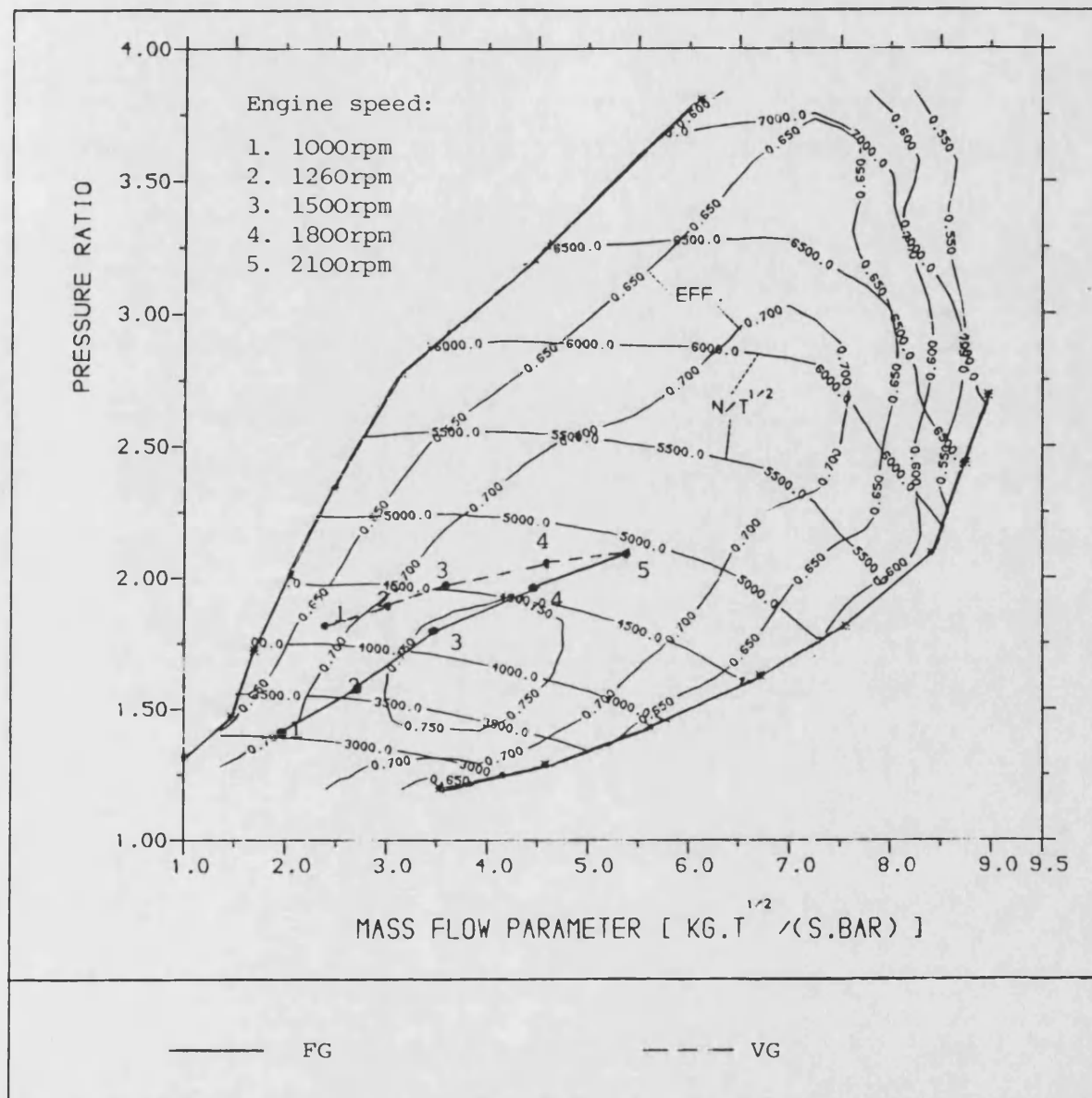


Fig-3.12d Effects of VG turbocharging at elevated ambient temperature

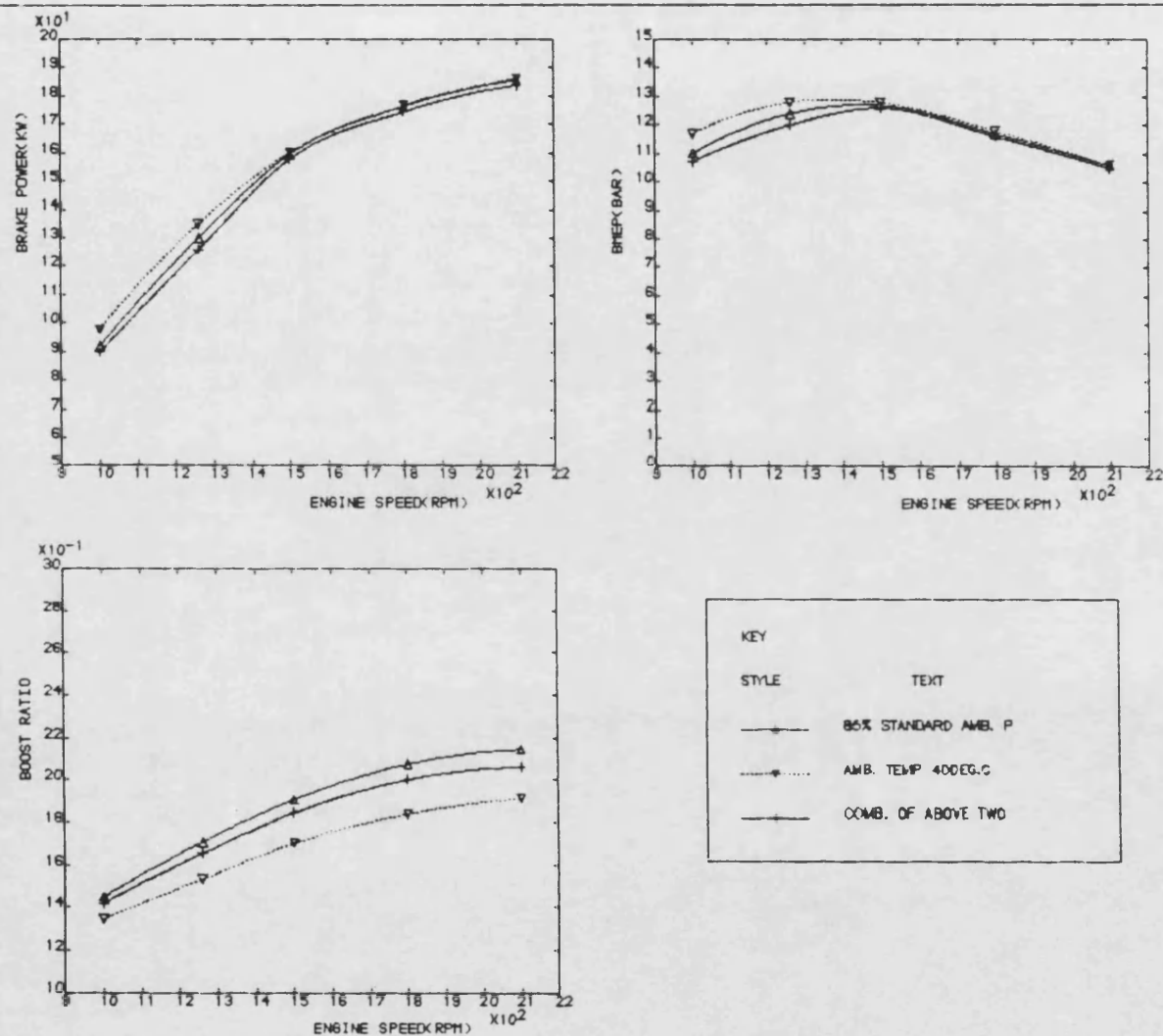
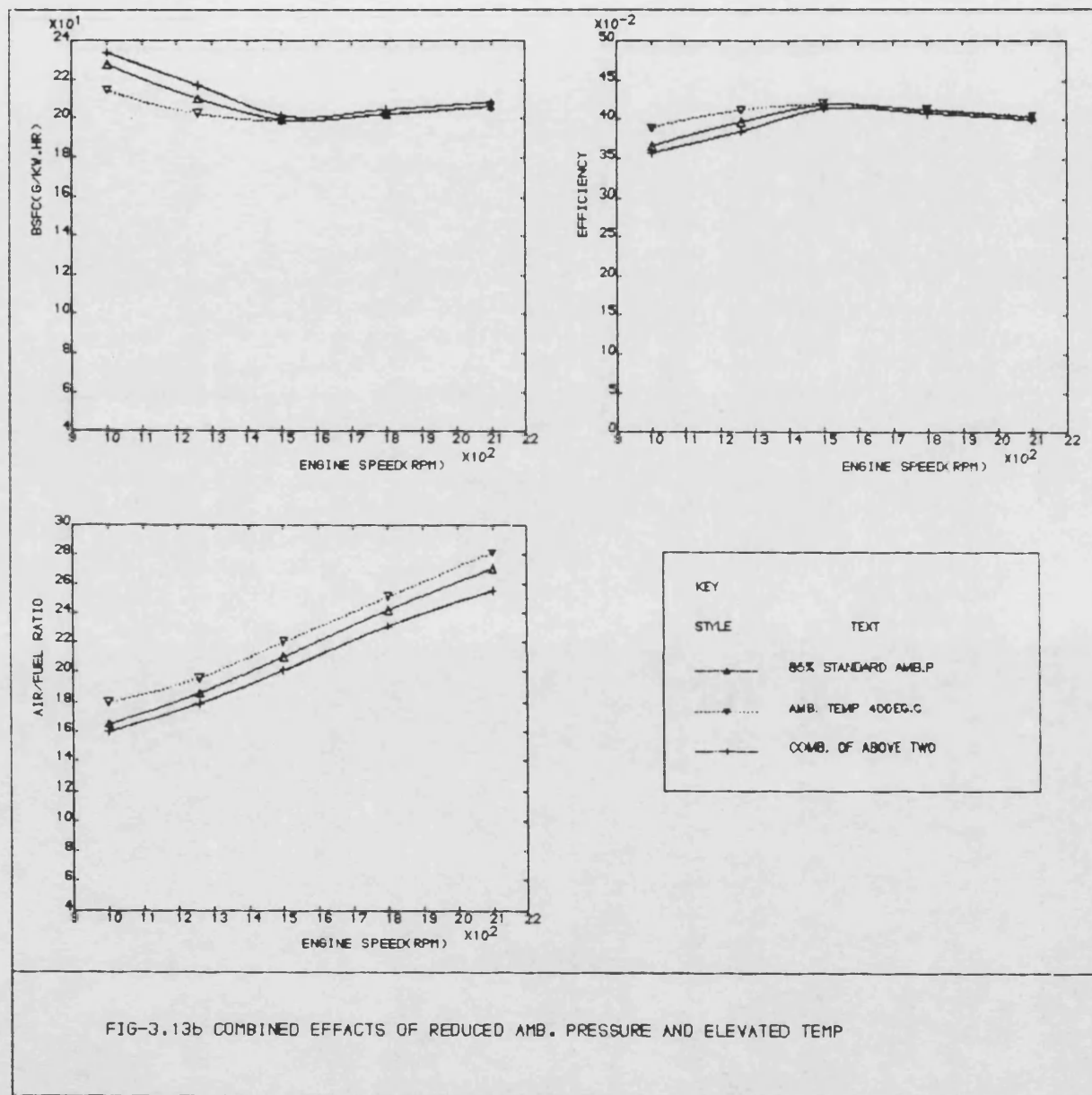


FIG-3.13a COMBINED EFFECTS OF REDUCED AMB. PRESSURE AND ELEVATED TEMP



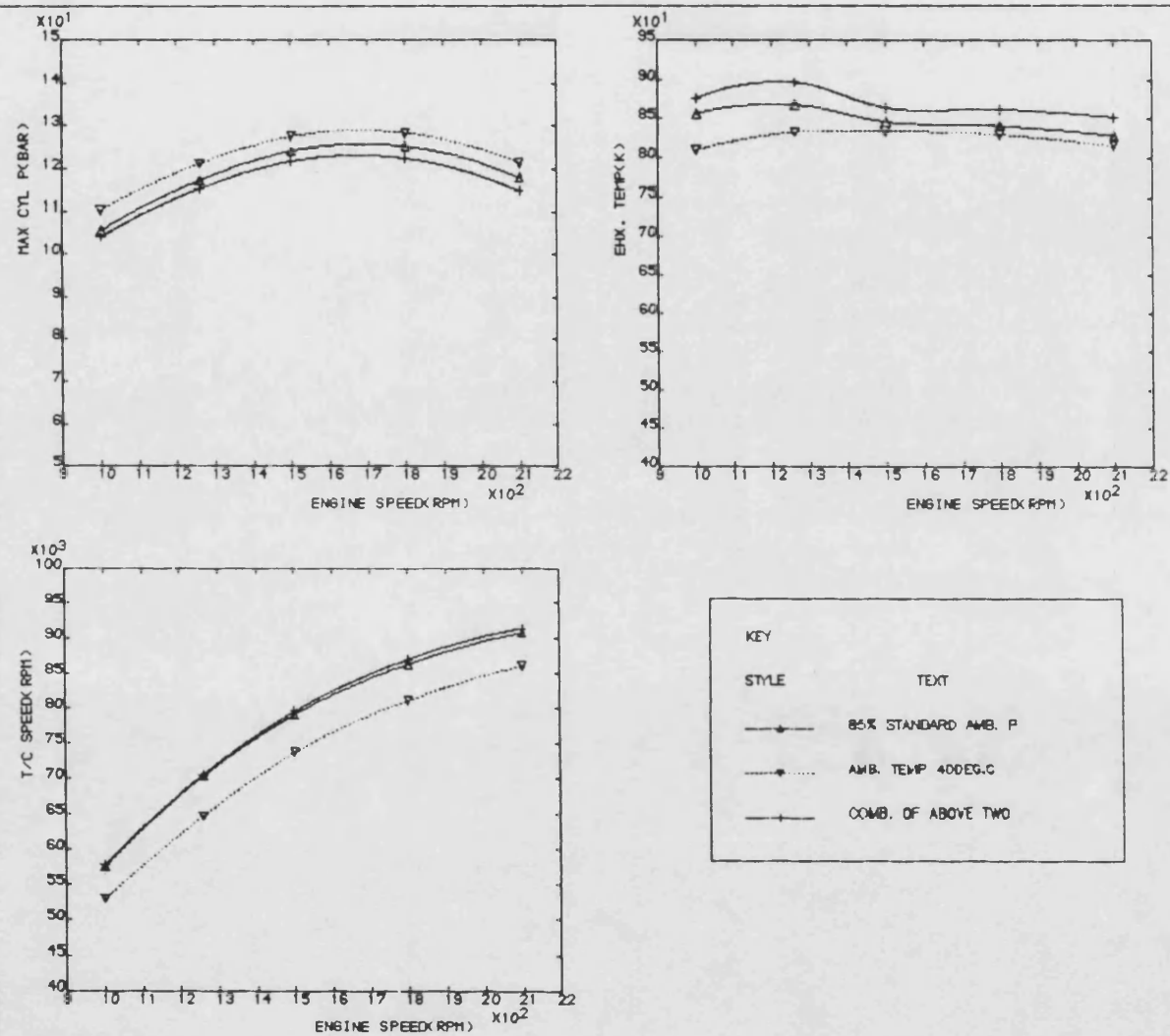


FIG-3.13c EFFECTS OF COMBINED EFFECTS OF REDUCED AMB. PRESSURE AND TEMP

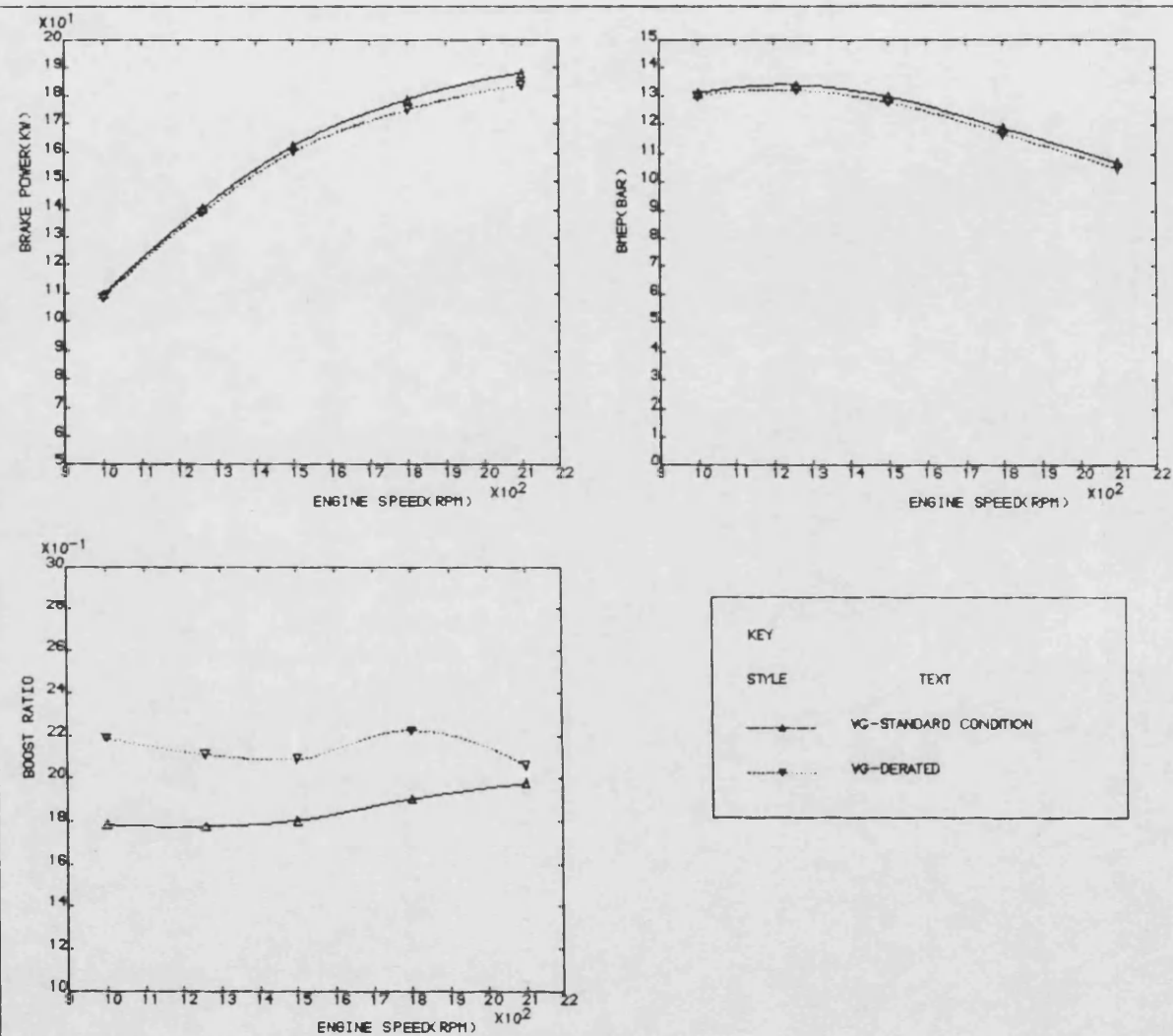


FIG-3.14a VG OPERATION AT REDUCED AMB. PRESSURE AND ELEVATED TEMPERATURE

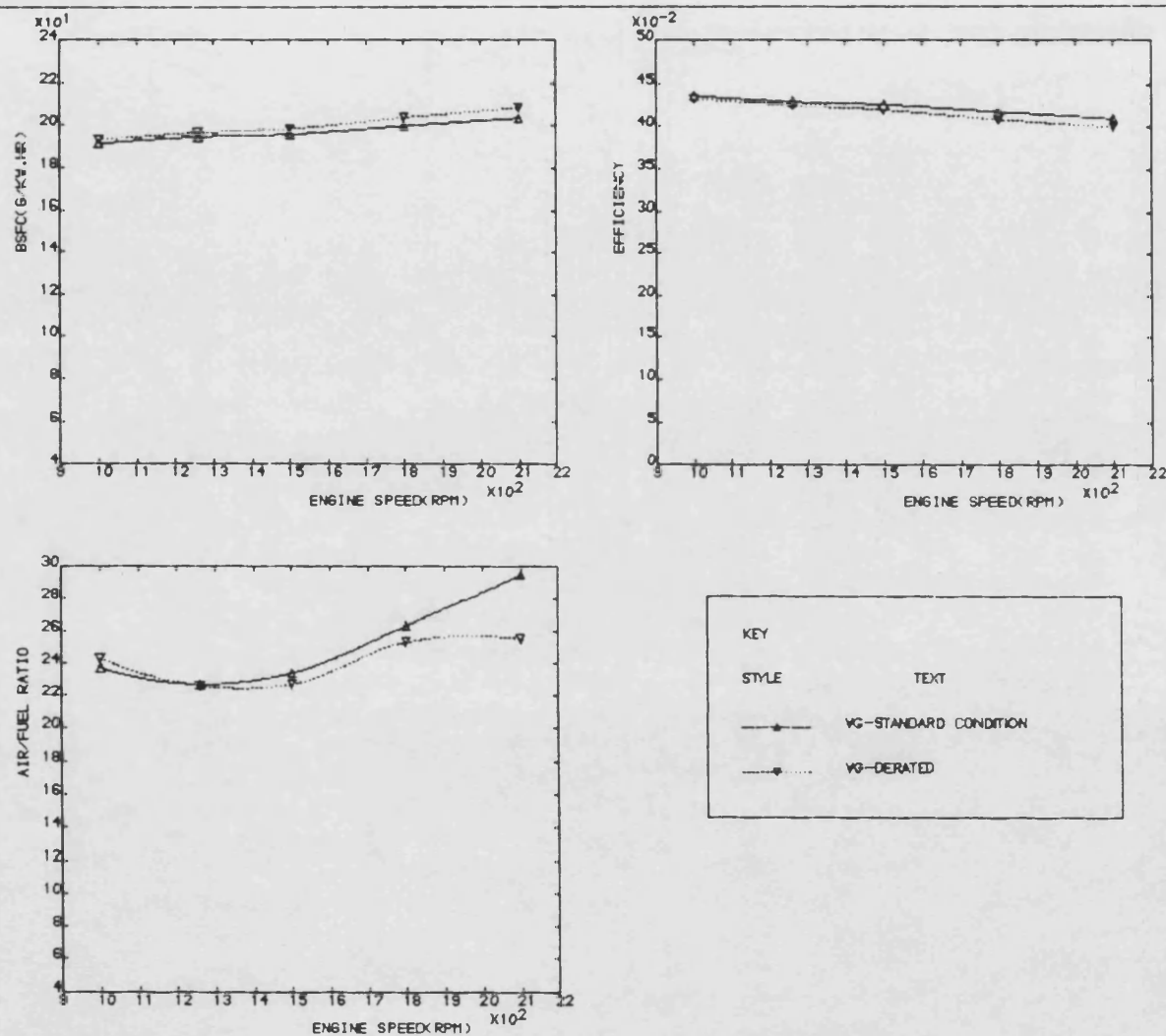


FIG-3.14b VG OPERATION AT REDUCED AMB. PRESSURE AND ELEVATED TEMPERATURE

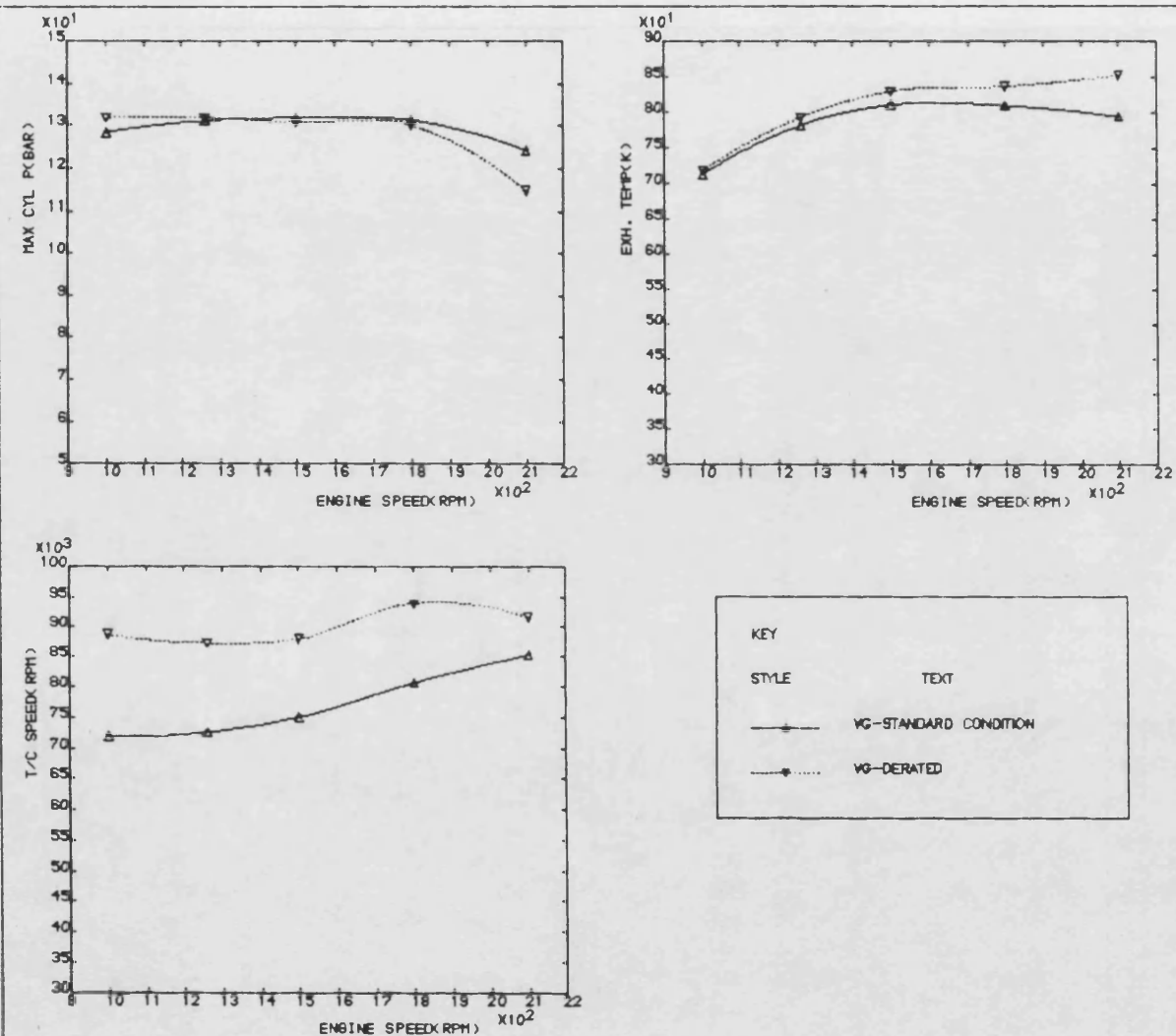


FIG-3.14C VG OPERATION AT REDUCED AMB. PRESSURE AND ELEVATED TEMPERATURE

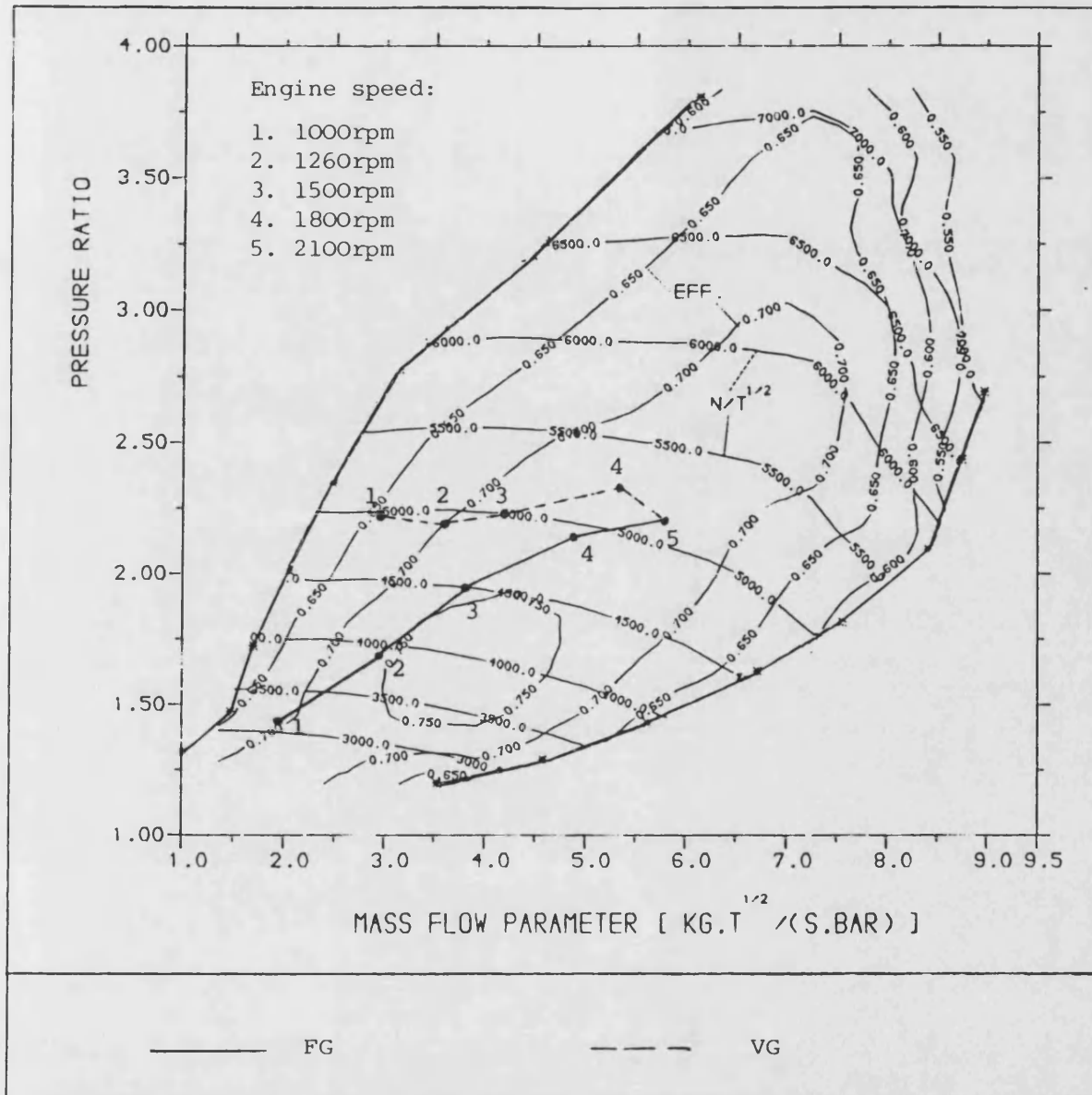


Fig-3.14d Effects of VG turbocharging at reduced ambient pressure and elevated temperature

CHAPTER 4

OPERATION OF THE DCE

WITH VARIABLE NOZZLE TURBINE

In this chapter, the detailed performance characteristics of the DCE and the effects of changing ambient conditions on the system operation are studied. In all these studies, particular attention has been paid to analysing the interrelation between the many operating variables and their effects on the overall system performance, the understanding of which is essential for grasping the behaviour of the system and hence for the development of a system optimisation strategy.

4.1 Design Consideration

As in the case of a conventional system, a proper match between the different components is of fundamental importance. Due to the greater flexibility of the DCE as compared with turbocharging systems, it is not difficult to obtain a 'match' from the point of view of the various compatibility requirements of the system. However, some factors specifically relevant to the DCE have to be taken into account. For instance, because the compressor is driven mechanically by the engine, part of the output power is thus consumed. Therefore, the compressor power should be as small as possible provided the demanded mass flow is satisfied. In the initial matching process, the following requirements have to be satisfied simultaneously at the design point:

a) The engine rating should be high, but not excessive, in order to allow an ample margin for the increase in boost and BMEP on the limiting torque curve without which the high torque ratio of the DCE cannot be realised. This in turn implies: air/fuel ratios of the order of 27 to 29:1; and boost ratios of the order of 2.8 to 3:1.

b) The ratio (engine-power/compressor-power), which is a function of the epicyclic gear train as well as of the choice of output shaft speed relative to engine speed, should be of the order of 3.0 to 3.8:1. If it is too low it implies excessive air

flow relative to the engine demand, if it is too high, the compressor will speed up excessively as output shaft speed is reduced. This in turn implies excessive bypass flows or the need to reduce engine speed excessively if the limiting compressor speed is not to be exceeded. For the Lysholm type blower a speed margin of between 1.8 and 2.1 as between rated and max. output shaft torque conditions is reasonable.

c) The bypass flow at the rated point should not be more than between 5% and 7%.

d) The compressor operating point should lie in such a position in the compressor map that the region of best efficiency is covered on the limiting torque curve.

In order to achieve these objectives, an appropriate combination of compressor, turbine and geartrain, with the engine has to be determined. The selection of the compressor is obtained by varying a scale factor using a given basic operating map, and no particular difficulty exists in matching the turbine because of the use of variable nozzles. The selection of a set of epicyclic geartrain ratios is of special importance because it has a very strong bearing on the speed and power relationship between the engine, compressor and the output shaft.

The matching process can be quite difficult because of the complex relationship between the various parameters. Obviously, a change in compressor scale factor will cause a change in compressor power as well as in mass flow in relation to its speed, while the variation of gear ratios will result in a change in the power flow in different components.

The important data for the L10 engine have been shown before in Table-3.1. The Holset H2C 8640 turbocharger turbine is adopted, i.e. its dimension is used in running the analytical program. A Compair screw compressor is used.

The initial work for matching the L10 DCE was carried out by Ghadiri[unpublished internal report]. The parameters adopted are as follows:

overall output shaft gear ratio:	1.445
overall compressor gear ratio:	9.55
compressor scale factor:	1.1

The compressor map with superimposed system operating points is shown in Fig-4.2.

4.2 Standard Operation

(sea level:Pa=0.99bar,Ta=294.4K)

The performance of the system under standard conditions is presented on Table-4.1 together with Fig-4.1 and Fig-4.2. The strategy is to allow the system to work at six different output shaft speeds, 440, 500, 1050, 1600, 1900, and 2200rpm; while at each speed, the system is allowed to operate at four power levels, full, three quarters, half and quarter load. In the following, the performance results will be examined in detail.

a)Design and Stall Points

Some major parameters at the design and stall points are listed below:

	design	stall
engine speed(rpm)	2100	1350
Eng.power(kw)	240.00	241.77
boost ratio	2.638	3.95
air/fuel ratio	30.575	32.438
BMEP(bar)	13.6868	21.4477
Eng.flow(kg/min)	25.628	24.306
Eng.eff.	0.3980	0.4485
comp.flow(kg/min)	25.756	48.93
comp.power(kw)	63.94	181.8
turb.power(kw)	74.96	144.13
O/S speed(rpm)	2200	440
O/S power(kw)	235.57	186.55
O/S eff.	0.3907	0.3461
gear loss(kw)	15.45	13.55

From the design point data, it can be seen that a very satisfactory match is obtained with an air/fuel ratio of 30.575, while the bypass flow is nearly eliminated(compressor mass flow equals the engine mass flow). The output shaft power is very close to the engine power and the output efficiency is comparable to the engine efficiency. This is quite remarkable considering that the transmission losses in the gear train have been taken into account. This is due to the compounding

feature of the system: the turbine power exceeds the compressor power(74.96kw cf. 63.94kw), therefore more power is fed to the output shaft.

At the stall point, the position appears to be a little different. As a result of the higher compressor speed, the compressor mass flow is substantially increased, so is the boost ratio and the compressor pressure ratio(4.219). The air/fuel ratio is acceptable and the engine performance is very good(eff.0.4485, due to the combination of low speed and high BMEP of 21.4477bar). However, the output results are not so encouraging, with an efficiency of 34.61%, as compared with 39.07% at the design point. This is due to the high power consumption of the compressor(181.77kw) and the relatively low power output of the turbine(144.13kw) which in turn is the result of the lower turbine inlet temperature arising from the large bypass flow. It can be seen that the bypass flow is even higher than the engine mass flow, therefore a substantial amount of energy is wasted. The large air flow is an inherent feature of the differential coupling between engine, output shaft and compressor, and reflects the fact that at low output shaft speeds and high torques, the circulating air fulfills the dual function of satisfying not only the combustion requirement of the engine, but also the torque conversion requirement of the system.

b)General

By examining the data from different power levels at a particular output shaft speed, it can be seen that as engine power decreases, the engine efficiency also decreases. At the same time the engine speed is reduced, and the compressor speed decreases at an even greater rate. Naturally, the lower the compressor speed, the less the power it consumes. However, due to the increasing imbalance between compressor and turbine power, the output shaft efficiency decreases steadily with decreasing engine power. This is most clear in Table-4.1a at the output shaft speed of 440rpm; at the 1/4 power level, the efficiency is very poor(0.1577). These trends can also be seen at other output shaft speeds and are a common feature of all compounding schemes.

Generally, the output efficiency is a function of engine efficiency, compressor and turbine efficiency, of the amount of bypass flow, and particularly of the boost level at which the plant operates.

c)Further Remarks

Fig-4.1(a-c) illustrate the operating characteristics of the DCE as contours of

the following parameters in a field of output torque and output shaft speed:

Fig-4.1a overall efficiency

b boost ratio

c BMEP

d turbine gear ratio

e turbine nozzle angle

In Fig-4.1a, overall efficiency of 40% has been reached and efficiency of over 37% covers a large area in the output torque/speed map, which indicates the system performance at high power level and high output shaft speeds is very good, because under these conditions, turbine power exceeds compressor power. However, as load decreases, compressor power will exceed turbine power, and this is always the case at lower output shaft speeds, therefore overall efficiency will be low. In Fig-4.1b, on the limiting torque curve, the boost ratio increases gradually as the output shaft speed decreases, accompanied by an increase in BMEP with decreasing output shaft speed, as shown in Fig-4.1c. Fig-4.1d shows that turbine gear ratio increases with decrease in output shaft speed and with increase in load in order to maintain an appropriate turbine speed (blade speed ratio), and therefore high turbine efficiency. Fig-4.1e shows the contours of turbine nozzle angle which is in line with the boost ratio and mass flow through the system. Clearly, for optimisation, these latter two parameters have to be carefully scheduled.

It also can be seen from Fig-4.1 that, on the limiting torque curve, a very high torque ratio of 3.96 over the speed range 2200 to 440rpm, i.e. a speed ratio of 5:1, is achieved (output shaft torque at sll of 4046Nm and at rated of 1022Nm). The maximum boost ratio (at stall) is rather high (3.95) and so is the compressor pressure ratio (4.219). The maximum BMEP (at stall) reaches the value of 21.4477bar at an engine speed of 1350rpm. Compared with the turbocharged version of the engine, although maximum engine power has not increased as much as expected (240 cf. 183kw), the performance characteristics have been enhanced significantly. With the latter, as the engine speed decreases, the power decreases as well. The torque rises only slightly over a narrow speed band (BMEP from 10.74bar at 2100rpm to 13bar at 1300rpm), with a torque ratio of 1.21, i.e. torque backup of 21% (chapter-3).

In Fig-4.2, the operating points of the engine are superimposed on the compressor map. It can be seen that although the match is acceptable, it is not ideal. If the system operating points can be moved to a higher compressor efficiency region, better results can be obtained.

4.3 Operation with New Compressor Map and Re-Optimization

(set-up of new base line)

4.3.1 General Approaches

a) Compressor Re-Match

In the previous section, it has been mentioned that if the operating points of the engine can be moved to a higher compressor efficiency area, the results can be improved, see Fig-4.2. Fig-4.3 shows the same compressor map in a slightly different form: mass flow rate(kg/min) is used instead of volume flow rate(cub.m/min). An associated study has been carried out by Ghadiri[unpublished report], by introducing a more suitable compressor which is shown in Fig-4.4. The change can be seen by comparing Fig-4.3 with Fig-4.4: the efficiency contours have moved towards a lower speed region and the area covered by a specific efficiency contour has been expanded in both the high and low pressure ratio directions. As expected, system performance has been generally improved by using the new compressor map. To show the full potential of the system, this new compressor map will be adopted in future investigations.

b) System Re-Optimization for Best Engine Speed

In setting up the new base line data, a further measure has been taken, i.e. re-optimization of the system for best engine speed. As discussed in chapter-2, selection of a suitable engine speed has strong effects on system performance under a specified operating condition. Further, in an investigation into the operation of the DCE with a fixed nozzle turbine it is revealed that under certain operating conditions, the system performance with a fixed nozzle turbine has been improved over that with a variable nozzle turbine(referring chapter-5), as a result of drastic decrease in engine speed, particularly at low load, accompanying the reduction in turbine nozzle angles. Investigations showed that by removal of the limit of 1100rpm on minimum engine speed (which was adopted for standard operation), the overall efficiency of the system can be substantially improved.

Clearly, the optimisation process is now carried out in a more complete sense. The program allows the engine speed, as well as the turbine nozzle angle and turbine gear ratio to vary, the latter two being the only independent variables in the previous calculations. Therefore optimal conditions can virtually be searched for over the entire operating field. Generally, if the engine speed is too low, the mass

flow requirement of the engine will exceed what the compressor can provide. This can be detected and subsequently corrected by modifying the input data by 'trial and error' in the earlier runs, but without necessarily arriving at a true optimal engine speed. In most such cases, the engine speed is higher than the optimal requirement. This means that power surplus to requirements is fed to the compressor and hence the system efficiency will suffer. The existing program DCE2 as previously used was modified to enable this shortcoming to be removed, i.e. by comparing the efficiencies at different engine speeds optimal conditions are achieved in an iterative manner. The engine speeds are selected such that the optimal system efficiency is reached and at the same time the air/fuel ratio is maintained above 26.

4.3.2 Presentation of Results

The calculation is carried out under the same(standard) ambient conditions as in the preceding section, and over the same operating range(Table-4.1). The results are presented in Table-4.2(a-c) together with Fig-4.5(a-e). In the following, the standard results will be used as the basis and the effects of the new approach will be assessed.

a)Regime at Output Shaft Speed of 2200rpm (Table-4.2c)

The data at the design point are presented in the following:

	standard	reoptimised
Eng.speed(rpm)	2100.	2100.
boost ratio	2.638	2.677
A/F ratio	30.58	31.383
power(kw)	240.	240.2
BMEP(bar)	13.687	13.696
efficiency	0.398	0.4052
air flow(kg/min)	25.63	25.86
Comp.power(kw)	63.94	64.08
speed(rpm)	5515	5515
mass flow(kg/min)	25.76	25.94
efficiency	0.724	0.724
Turb.power(kw)	74.96	74.07

	standard	reoptimised
speed(rpm)	49500	45860
nozzle angle(deg)	8.886	8.843
O/S speed(rpm)	2200.	2200.
power(kw)	235.57	234.74
efficiency	0.3907	0.3961

As can be seen, the engine speed remains unchanged and the compressor efficiencies are exactly the same. Little difference exists between the two sets. However, due to the slightly higher engine efficiency, resulting from the slightly high boost ratio and BMEP, the overall efficiency is slightly improved.

Similar changes can be seen at the 3/4 full load point. However, due to the improvement in compressor efficiency(0.749 cf. 0.679), there is a greater improvement in overall efficiency(0.3815 cf. 0.3652). Clearly this is essentially the result of compressor re-match (engine speed unchanged).

At the other load levels, in addition to the improvements in compressor efficiency(0.708 cf. 0.610 at 1/2 load) the engine speeds have been reduced(1880rpm cf. 1900rpm at 1/2 load). At the 1/2 load point, the change in engine speed is greater, this results in a greater improvement in overall system efficiency(0.3464 cf. 0.3232, being more than 2 percentage points).

b)Regime at Output Shaft Speed of 440rpm (Table-4.2a)

At the stall point, compressor efficiency is improved(0.713 cf. 0.675) and engine speed is slightly reduced(1340rpm cf. 1350rpm). The overall efficiency is subsequently improved, but the effect is not very strong(0.3486 cf. 0.3461). However, due to the improvement in output shaft torque (4233.3Nm cf. 4046.9Nm), the overall torque ratio(across the entire speed arnge) has been increased (4.158 cf. 3.96).

As load decreases, the change in engine speed increases. This leads to increased changes in system performance. At the 1/4 load, a drastic change in engine speed has taken place, resulting in a significant improvement in overall efficiency. The data at this point are shown below:

	standard	reoptimised
Eng.speed(rpm)	1100.	730.
boost ratio	1.337	2.198
A/F ratio	35.87	37.73
power(kw)	60.11	60.
BMEP(bar)	6.544	9.844
efficiency	0.4093	0.415
air flow(kg/min)	7.322	7.584
Comp.power(kw)	41.68	33.72
efficiency	0.54	0.75
speed(rpm)	7597	4064
mass flow(kg/min)	38.98	17.57
Turb.power(kw)	8.36	22.18
speed(rpm)	12584	30764
nozzle angle(deg)	36.66	6.16
O/S speed(rpm)	440.	400.
power(kw)	23.16	44.21
efficiency	0.1577	0.3057

As a result of the reduction in engine speed, BMEP and engine efficiency have increased. More significantly, compressor mass flow rate and power have been substantially reduced. The lower compressor power is also a result of higher compressor efficiency. The great increase in turbine power is attributed to higher pressure ratio and efficiency. Clearly, with lower compressor power and higher turbine power, the output power will be higher. All these lead to a much higher overall efficiency, the value being nearly doubled.

It also can be seen that the turbine nozzle angle is drastically reduced, which is in line with the reduction in system mass flow and the increase in boost ratio.

c)General Trend

By further comparing Table-4.1 and Table-4.2, it can be seen that with the adoption of the new approach, the system efficiency has been improved over the entire operating points. For a given output shaft speed, the greatest change usually occurs at the low load, where the reduction in engine speed is greatest.

Fig-4.5(a-e) shows the variations of various parameters over the entire operating range. The improvement in efficiency is substantial. As can be seen, the area embraced by the 0.39 efficiency contour in Fig-4.5a is almost as large as that embraced by the 0.372 efficiency contour in Fig-4.1a. Boost ratio, BMEP and turbine gear ratio have all increased while nozzle angle and its range have both been reduced.

In all the later studies, the approach adopted in this section will be applied and the results obtained with this approach, Table-4.2 and Fig-4.5 will be taken as the new base line data.

4.4 Operation under Changing Ambient Conditions

The differential link between the engine and the compressor imposes a unique torque and power relationship between them. If the engine operating point, i.e. its speed and torque, together with the output shaft speed are fixed, the compressor speed and hence the volume flow rate of the compressor will be fixed. Further, the power flow to the compressor will also be fixed(chapter-2).

As the ambient pressure is reduced, the specific power requirement per unit volume of the compressor will be reduced for the same pressure ratio. Consequently the total power requirement of the compressor will be reduced. However, as mentioned earlier, the power supply to the compressor is fixed, and as a result the pressure ratio of the compressor will be forced to increase, thus maintaining the equilibrium of the system. With this increase in pressure ratio a greater proportion of charge air will be forced into the cylinder. This implies a relatively lower bypass flow, therefore less additional power for compressing bypass air. In addition, the turbine will operate a little more favourably with increased inlet temperature and reduced back pressure. What is of the greatest importance is that the mass flow requirement by the engine can be easily met by varying the engine speed, owing to the fact that at a given output shaft speed, a relatively small increase in engine speed will lead to a substantial increase in compressor speed.

Elevation of ambient temperature has the effect of reducing the density of the air at compressor inlet. However, the specific power per unit volume will not be affected so that the epicyclic gear torque and power balance is preserved. On the other hand, the density of the air charge obtained will be reduced in proportion to the intake density with adverse effect on trapped air/fuel ratio.

The investigation of changes in ambient conditions is presented in three separate parts, dealing with the effects of reduced ambient pressure, elevated temperature and the combined effects of these two changes.

4.4.1 Derating for Reduced Ambient Pressure

($P_a=0.8415\text{bar}$, $T_a=294.4\text{K}$) Table-4.3(a-c)

4.4.1.1 General

In this section, the effects of a reduction in ambient pressure on system performance are studied. The computations are carried out again over the complete range of operating points as set out in Table-4.1(a-c) and Table-4.2(a-c) for standard ambient conditions. In the present calculations, the ambient pressure is reduced to 85% of the standard value, which corresponds to an altitude of about 1250m. The results are shown in Table-4.3(a-c). Again, the approach developed in section-4.3 is adopted, i.e, engine speed is fully optimised and the new compressor map is used. In the following, the new base line data (Table-4.2 and Fig-4.4) will be used as the basis for comparison.

4.4.1.2 Presentation of Results

The effects of reduced ambient pressure on the performance of the system can be seen by a comparison between the data in Table-4.2(a-c) (base line) and Table-4.3(a-c). As expected, the mass flow rate of the compressor is reduced and the pressure ratio increased. In most cases, engine speed has increased indicating higher volume flow through the system. For the engine, the air/fuel ratio is reduced but still sufficient. Reduction of the air/fuel ratio results in a higher exhaust temperature.

a) Regime at Output Shaft Speed of 2200 rev/min (Table-4.3c)

Some data at the design point are extracted below:

	baseline	derated
Eng.speed(rpm)	2100	2155
boost ratio	2.677	2.886
A/F ratio	31.383	28.05
power(kw)	240.2	239.76
BMEP(bar)	13.7	13.32
efficiency	0.4052	0.3892
air flow(kg/min)	25.86	24.02
Comp.power(kw)	64.08	68.31
mass flow(kg/min)	25.94	24.12
Turb.power(kw)	74.07	81.88
speed(rpm)	45860.	49300.
nozzle angle(deg)	8.844	9.205
O/S speed(rpm)	2200.	2200.
power(kw)	234.74	237.66
efficiency	0.3961	0.3858

As can be seen, at this point, the engine speed has to increase (2155rpm cf. 2100rpm) to satisfy the air demand of the engine from the compressor (engine mass flow and compressor mass flow are comparable, implying zero bypass flow). Compressor mass flow, and therefore engine air flow and air/fuel ratio have all decreased while boost ratio increased. BMEP has also slightly increased. These result in a slightly lower engine efficiency. Due to increase in engine speed, the compressor power has increased. However, the turbine power has also increased due to higher pressure ratio, higher speed and higher inlet temperature, and this leads to a increase in surplus power of the turbine over that of the compressor ($81.88 - 68.31 = 13.57\text{kw}$ cf. $74.07 - 64.08 = 9.99\text{kw}$). The final result is a slightly reduced overall efficiency, indicating the effects of lower engine efficiency.

A similar trend can be seen at other power levels.

b)Regime at Output Speed of 440 rev/min

Some important data at the stall point are shown below:

	baseline	derated
Eng.speed(rpm)	1340.	1320.
boost ratio	4.203	4.881
A/F ratio	33.48	31.853
power(kw)	239.92	240.11
BMEP(bar)	21.44	21.78
efficiency	0.4286	0.4354
air flow(kg/min)	26.05	24.42
Comp.power(kw)	180.62	179.84
mass flow(kg/min)	49.51	40.63
Turb.power(kw)	153.2	149.2
speed(rpm)	47293	50505
nozzle angle(deg)	9.457	8.047
O/S speed(rpm)	440.	440.
power(kw)	195.14	192.22
efficiency	0.3486	0.3485

At this point, there is a slight decrease in engine speed, hence a similar increase in BMEP. This results in a higher engine efficiency. However, an increased imbalance between the turbine and compressor power($149.17-179.84=-30.67\text{kw}$ cf. $153.17-180.62=-27.45\text{kw}$) has a negative effect on system performance. The interaction between these two factors leads to very similar overall efficiencies.

The engine speed at 1/2 load has also decreased while those at 3/4 and 1/4 loads increased. The interaction among various factors results in increased efficiencies for the 3/4 and 1/2 load points.

c)General Trend

Similar trends can be observed at other output shaft speeds.

It can be seen that the variation of turbine nozzle angle is not regular. Under reduced ambient pressure conditions, the boost ratio will be higher. This tends to

require a smaller nozzle angle. However, due to increase in engine speed, the volume flow rate through the system will be higher. This tends to demand a larger nozzle angle. Clearly, the variation of turbine nozzle angle will depend on the extent to which the pressure ratio and engine speed have varied.

Fig-4.6(a-e) shows the contours of efficiency, boost ratio, BMEP, turbine gear ratio and turbine nozzle angle. Compared with the corresponding plots in Fig-4.5, it can be seen that overall efficiency has only slightly deteriorated, e.g. the area encompassed by the 0.39 efficiency contour has only marginally reduced under the reduced ambient pressure conditions. The increase in boost ratio is clearly shown. In some cases (high load, low speed region), there is a slight decrease in BMEP. Also, the turbine gear ratio has increased and quite a similar pattern exists in the two turbine nozzle angle contour plots.

4.4.2 Derating for Elevated Temperature

($P_a=0.99\text{bar}$, $T_a=313.3\text{K}=40\text{deg.c}$)

4.4.2.1 General

In the present calculation, the ambient temperature is raised from 294.4K(21.2deg.c) to 313.3K(40deg.c) and the effects of this increase on the characteristics of the system are investigated. The results are shown in Table-4.4(a-c) and Fig-4.7(a-e)

4.4.2.2 Presentation of Results

Comparison of Table-4.4(a-c) with Table-4.2(a-c) demonstrates that the increase in the ambient temperature has brought about a shift in the balance of the system, although the extent of this shift is different under different operating regions. As can be seen, in the lower output shaft speed region, i.e. 440rev/min and 500rev/min, the engine speed remains almost unchanged at corresponding operating points, while at higher output shaft speeds, the engine speed is increased. In general the mass flow rate is decreased, coupled with a fall in air/fuel ratio. The compressor delivery temperature and hence the inlet manifold temperature rises, as expected. For all the operating points, the engine efficiencies deteriorate slightly. As for the boost ratio, decreases can be observed wherever the engine speed is increased. Finally, the overall efficiency is slightly lower over the entire operating range, but there is no loss of output power.

a) Regime at Output Shaft Speed of 2200rev/min(Table-4.4c)

At the design point, the engine speed is increased(2120rev/min cf. 2100rev/min) in order for the compressor to satisfy the demand for mass flow by the engine. In parallel, the engine BMEP together with engine torque decreases, hence boost ratio decreases(2.655 cf. 2.677). A closer examination of this change reveals the nature of the process, i.e. by increasing compressor flow rate(higher engine speed) together with shifting the distribution of the air flow between the engine and the bypass(lower boost ratio indicating less engine mass flow) a new balance is reached. In addition, with lower air density the air/fuel ratio will decrease. As shown in the table, the reduction in air/fuel ratio is substantial(28.806 cf. 31.383) but not critical. The high inlet manifold temperature together with a decrease in air/fuel ratio leads to a much higher exhaust temperature(948K cf. 884K), whereas the maximum pressure in the cylinder is slightly lower(116.29bar cf. 118.40bar). All these factors lead to lower engine efficiency(0.3965 cf. 0.4052).

As a result of the increase in engine speed, the compressor speed becomes higher(5706.2rev/min cf. 5515.2rev/min) and the compressor pressure ratio lower(2.925 cf. 2.953). These two factors interact with each other, resulting in very similar mass flow rate(25.914kg/min cf. 25.941kg/min). However, it is the pressure ratio that dictates the flow rate across the engine, which displays a greater difference(24.236kg/min cf. 25.856rev/min). Due to the dominant influence of the volume flow rate, compressor power is higher(65.63kw cf. 64.08kw), even though associated with a slight improvement in efficiency(0.729 cf. 0.724).

In line with the shift of the engine and compressor operation, the turbine expansion ratio decreases(2.820 cf. 2.849) and the turbine nozzle angle increases(9.007degree cf. 8.843degree). It should be noted that the turbine nozzle angle and the turbine gear ratio(turbine speed) are two important parameters for the operation of the variable nozzle turbine, for they can be properly selected to accommodate a specific set of expansion ratio and mass flow rate, which in turn are dictated by the engine and compressor operating condition. More importantly, appropriate pairs of nozzle angle and turbine gear ratio will result in the highest turbine efficiency for a prescribed expansion ratio and mass flow. In fact the program is so constructed that the optimum combination of these two parameters can always be obtained. Obviously a very complex interaction exists between the various operating parameters. In the present case, with reduced expansion ratio but similar mass flow rate, the nozzle angle has to increase(9.007degree cf. 8.843degree),

as already stated. Owing to the higher inlet temperature(928K cf. 882K), the turbine speed is increased(46420.4rev/min cf. 45859.9rev/min) and the turbine power is higher(75.80kw cf. 74.07kw).

All these factors lead to a slight deterioration in overall efficiency(0.3878 cf. 0.3961). Further examination of the data shows that at other power levels a similar pattern is followed.

b)Regime at Output Shaft Speed of 440rev/min(Table-4.4a)

As stated earlier, the engine speeds are almost identical at corresponding power levels. This shows that it is not necessary to increase the engine speed to meet the demand for mass flow by the engine. This is ascribed to the relatively higher compressor speed compared with that of the engine, as a result of a lower output shaft speed. In this region, a large proportion of compressor mass flow is bypassed, implying substantial amounts of surplus mass flow over the engine demand.

At the stall point, the boost ratio is slightly higher(4.212 cf. 4.203). The compressor mass flow is reduced(46.527kg/min cf. 49.514kg/min), as is the engine mass flow(24.406 cf. 26.051), as a result of lower air density. The engine efficiency is lower(0.4184 cf. 0.4286) and the exhaust temperature higher(911.97K cf. 846.09K). As expected, the compressor power remains unchanged. The turbine nozzle angle is slightly decreased(9.221degree cf. 9.457degree) to match the similarly slight increase in expansion ratio(4.306 cf. 4.303). The turbine power is higher(154.88kw cf. 153.17kw), for the inlet temperature is higher(747.63K cf. 696.47K); this latter effect outweighs that of smaller mass flow rate(47.331kg/min cf. 50.300kg/min). Overall, the effect of the engine efficiency exceeds that of the turbine, leading to a lower overall efficiency(0.3427 cf. 0.3486). The data at other power levels exhibit a similar pattern.

Another important point is that the output shaft torque at the stall point has increased (4267.9Nm cf. 4233.3Nm), implying the dynamic performance of the system has been improved.

c)General Trend

Fig-4.7(a-e) shows the contour plots for various parameters as before. Compared with Fig-4.5, the area encompassed by the corresponding efficiency contours has reduced. Boost ratio, BMEP and turbine gear ratio have decreased while nozzle angle has increased, with a shift of position, the smallest nozzle angle

contour has moved towards the lower speed and higher load region.

4.4.3 Combined Effects of Ambient Pressure and Temperature

($P_a=0.8415\text{bar}$, $T_a=313.3\text{K}$)(Table-4.8(a-c))

A further investigation has been carried out to obtain an insight into the combined effects of reduced ambient pressure and elevated ambient temperature. Table-4.5(a-c) shows the results obtained, under an ambient temperature of 313K(40deg.C) and an ambient pressure of 85% of the sea level value; It is again based on the improved compressor map and on engine speed optimisation. It can be seen by first comparing Table-4.2(base line, standard conditions) with Table-4.4(temperature derating) and then with Table-4.5(combined temperature and pressure derating) that the effect of elevation in ambient temperature is far more severe than that of reduction in ambient pressure. For example, at the design point, the elevation of the temperature reduces the air/fuel ratio from 31.383(Table-4.2) to 28.806(Table-4.4), while a drop of ambient pressure only reduces it from 28.806 to 27.239(Table-4.5).

In order to determine the combined effect of reduced ambient pressure and elevated ambient temperature, a comparison can be made of the important parameters between Table-4.2(standard ambient conditions) and Table-4.5(reduced ambient pressure and elevated ambient temperature).

Looking back to the previous separate investigations, i.e. the performance of the system under reduced ambient pressure (section-4.4.1) and elevated ambient temperature (section-4.4.2), it is clear that the effects of each will interact with those of the other in a very complex manner. They could lead to similar consequences in some cases but to opposite ones in others. Besides, the extent of the effects could be quite different. For instance, in both cases an increase in engine speed is required to achieve a new system equilibrium. In the present case, the increase in engine speed due to ambient pressure reduction is greater than for temperature elevation. The boost ratio will always increase in the case of lower ambient pressure, but the change of the turbine nozzle angle will depend on the extent of engine speed change. If the increase in engine speed is below a certain value, the nozzle angle may decrease due to higher boost ratio. However, if this increase is quite large, due to a higher resultant increase in mass flow, the nozzle angle has to be increased. On the other hand, the boost ratio will usually decrease with an increase in engine speed in the case of elevated ambient temperature, and

the turbine nozzle angle will increase to allow a greater volume flow. In the following some data at the design and stall points are selected from Table-4.2 (sea level), Table-4.4 (elevated ambient temperature) and Table-4.5 (reduced ambient pressure and elevated temperature) to illustrate these points.

	DESIGN POINT			STALL POINT		
	tables			tables		
	4.2	4.4	4.5	4.2	4.4	4.5
engine speed(rev/min)	2100	2120	2180	1340	1340	1320
boost ratio	2.677	2.655	2.904	4.203	4.212	4.976
air/fuel ratio	31.383	28.806	27.239	33.480	30.586	29.401
max.cylinder p(bar)	118.40	116.29	126.14	160.96	157.8	158.04
exh. temp.(K)	883.83	947.83	968.74	846.09	911.97	939.08
engine eff.	0.4052	0.3965	0.4007	0.4286	0.4184	0.4154
engine mass flow(kg/min)	25.856	24.236	22.752	26.051	24.406	23.626
comp. mass flow(kg.min)	25.941	25.419	23.816	49.514	46.527	38.180
comp. power(kw)	64.08	65.63	70.19	180.62	180.61	179.84
turbine gear ratio	20.8	21.1	22.4	107.5	109.6	119.4
turb.nozzle angle(deg.)	8.843	9.007	9.184	9.457	9.221	7.906
turbine power(kw)	74.07	75.80	79.29	153.17	154.88	153.10
output power(kw)	234.74	234.74	233.33	195.14	196.73	195.89
output eff.	0.3961	0.3878	0.3883	0.3486	0.3427	0.3388

It will be observed that although the air/fuel ratio decreases continuously, it is still sufficient. The variation in overall efficiency and output power is very small. At the design point the compounding effect, i.e. excess of turbine power over compressor power, remains virtually constant at approximately 10kw, while at the stall point, the adverse power balance associated with the inevitable high degree of bypassing, is again almost constant at approximately 26kw.

At these two points, efficiency has deteriorated by less than 1 percentage point. However, at some other points, this is no longer true, the deterioration approaching 2 percentage points. To demonstrate this, the efficiencies at all operating points are tabulated below (base line efficiency/derated efficiency):

stand/ derat.	100% load	75% load	50% load	25% load
440 rpm	0.3486 0.3388	0.3448 0.3377	0.3302 0.3224	0.3158 0.3061
500 rpm	0.3511 0.3432	0.3493 0.3420	0.3493 0.3345	0.3260 0.3140
1050 rpm	0.3832 0.3732	0.3920 0.3755	0.3865 0.3678	0.3559 0.3369
1600 rpm	0.4018 0.3878	0.3945 0.3774	0.3767 0.3597	0.3137 0.2965
1900 rpm	0.3998 0.3881	0.3917 0.3748	0.3637 0.3502	0.2892 0.2704
2200 rpm	0.3961 0.3883	0.3815 0.3684	0.3464 0.3359	0.2919 0.2737

The contours of various parameters are shown in Fig-4.8(a-e). Compared with Fig-4.5 (base line), there is a clear deterioration in efficiency, which is just above 1 percentage point in a certain area of high loads. Boost ratio and BMEP have decreased while turbine gear ratio has increased. Maximum nozzle angle has reduced while the pattern remains almost unaffected.

However, the output shaft torque has been slightly increased (4249.5Nm cf. 4233.3Nm), indicating the overall output torque ratio has been maintained.

Considering the extent of the change in ambient conditions this can be considered satisfactory, particularly when compared with turbocharged engines.

4.4.4 Discussion

It is clear from the cases studied so far that the system can operate under elevated altitude and temperature with virtually no derating, and without exceeding normal operating limits of maximum cylinder pressure(160bar) and

exhaust temperature(700deg.c). Due to the differential linkage of the system, adjustment can always be made for it to adapt to lower ambient pressures by raising the boost ratio. This is further illustrated in Table-4.6, in which the ambient pressure is reduced to 70% of the standard sea level value which corresponds to an altitude of about 3000m. Only the data at two operating points are shown, i.e. the stall point and the design point. It can be seen clearly that the DCE can still work at full power without appreciable loss of output shaft efficiency (0.3398 cf. 0.3486 at the stall point, and 0.3868 cf. 0.3961 at the design point compared with Table-4.6). Other parameters are also satisfactory. This should be considered excellent provided the compressor pressure ratio of 6.175(extrapolated) at the stall point is obtainable, with a reasonable efficiency; and the engine speed can be increased to 2255rpm at the design point. Further, while ambient pressure decreases with altitude, so does ambient temperature. Therefore the negative effects of the former will be partially offset by the compensating effects of the latter, so far as air density and its effects on system performance is concerned.

These characteristics are inherent in the system. Under reduced ambient pressure conditions, at a certain operating point, typically at full power and a high output shaft speed, the pressure ratio will rise. Under these circumstances the air demand by the engine will exceed compressor supply and a new balance is reached with an increase in engine speed. Therefore the compressor speed and hence the compressor mass flow rate(and power supply) will increase. At this new equilibrium, the mass flow across the engine is relatively higher while the fuel per revolution becomes lower because of the fixed engine power condition. As a result, the air/fuel ratio will increase relatively. In addition, the gear train selected and the match between different components lead to high air/fuel ratios under sea level conditions(31.383). This guarantees, to some extent, that the reduction of air/fuel will not become critical with decreases in ambient pressure.

The ambient temperature only varies within a very narrow range from a practical point of view, and within this range the highest value is limited. Probably 40 degree C may be considered a reasonable limiting value.

Theoretically, optimisation for the best engine speed is as essential as for other parameters, such as turbine nozzle angle and turbine gear ratio. However, in the present investigation, significant effects only appear at lower power conditions, associated with very low engine speeds. If these values are within practical limits, these results can be accepted. Otherwise, further adjustment has to be made. At

higher power conditions only a slight improvement has been produced through engine speed optimisation. This implies that the original engine speeds at these points are very close to the true optimal values (Table-4.1). Under these optimal conditions, the best combinations of engine speed, turbine nozzle angle and turbine gear ratio have been achieved. Probably the most significant factors are bypass flow and compressor and turbine efficiencies. The better the component efficiencies and the smaller the bypass flow, the better the overall efficiency. However, these parameters can vary in opposite directions, therefore a compromise has to be made. For example, the bypass flow at higher output shaft speeds is required to be as small as possible, but this is not the case at lower output speeds when high compressor speeds and hence air flow in excess of engine demand are inevitable. Furthermore, once a compressor and turbine has been selected, there is very little subsequent control over the manner in which efficiencies vary with operating conditions.

Table-4.1 Standard map, standard conditions

CUMMINS L10 D C E		STALL POINT				45	20	15	27
number of cylinders	6.0	bore	(m.m.)	125.03	stroke	(m.m.)	136.00		
con-rod length (m.m.)	217.78	inlet valve closing (degs)		173.0	compressor scale factor		1.10		
ambient temperature (deg k)	274.4	ambient pressure (bar)		0.99	cooler effectiveness		0.8104		
compression ratio	16.30	engine diagram factor		0.9874	turbine flow loss factor		0.8000		
----- compressor gear ratio	9.5500	output shaft gear ratio		1.4450	-----				
engine speed(r.p.m)	1350.00	1250.00	1150.00	1100.00	1400.00	1350.00	1200.00	1100.00	
boost pressure ratio	3.950	3.346	2.400	1.328	3.831	3.148	2.329	1.340	
delivered air to fuel ratio	32.438	35.505	35.349	35.882	32.089	35.305	35.598	36.069	
delivery ratio	0.853	0.853	0.853	0.854	0.853	0.853	0.853	0.854	
manifold temp (deg k)	324.959	314.943	306.695	297.499	324.809	314.018	305.326	297.607	
engine power (k w.)	241.77	181.62	120.98	59.64	241.78	181.42	120.95	59.94	
engine torque (n.m.)	1706.75	1382.92	1002.11	519.76	1646.89	1280.69	960.45	522.25	
b.m.e.p (bar)	21.4477	17.4010	12.5990	6.4928	20.6997	16.0937	12.0709	6.5258	
s.f.c. (kg/kw hr)	0.186	0.183	0.187	0.204	0.189	0.188	0.188	0.204	
b.thermal eff.	0.4485	0.4561	0.4466	0.4088	0.4411	0.4443	0.4427	0.4096	
fuel / rev (kg.)	5.550	4.428	3.274	1.844	5.447	4.204	3.165	1.849	
max cyl pressure (bar .)	174.31	148.47	107.29	59.74	171.70	140.38	104.11	60.20	
exhaust temperature(deg k)	835.89	765.79	737.15	687.09	847.85	777.61	737.04	685.61	
mass flow (kg/min)	24.306	19.654	13.310	7.277	24.471	20.038	13.519	7.337	
percentage heat to coolant	10.29	11.50	14.30	20.17	10.24	11.34	14.13	20.08	
compressor speed (r.p.m.)	9784.5	9029.5	8074.5	7597.0	10065.5	9588.0	8155.5	7200.5	
compressor pressure ratio	4.219	3.570	2.573	1.464	4.103	3.378	2.506	1.476	
mass flow (kg/min)	48.939	44.257	39.879	39.001	49.469	47.435	40.346	36.775	
compressor power (kw.)	181.77	133.09	85.94	41.34	176.74	130.56	83.11	39.38	
compressor torque (n.m)	173.77	140.69	101.59	51.95	167.61	129.98	97.27	52.20	
delivery temperature (deg k)	515.03	473.54	423.17	357.96	506.75	458.53	417.53	358.61	
compressor efficiency	0.675	0.719	0.710	0.536	0.685	0.745	0.719	0.542	
turbine speed (r.p.m)	46508.0	41800.0	30800.0	12584.0	45000.0	39300.0	31450.0	12850.0	
turbine pressure ratio	4.115	3.466	2.469	1.360	3.999	3.274	2.401	1.372	
mass flow (kg/min)	49.696	44.818	40.271	39.188	50.240	48.012	40.746	36.964	
turbine power (kw)	144.13	101.99	57.56	7.82	143.47	103.19	56.18	8.22	
turbine torque (n.m)	29.58	23.29	17.84	5.93	30.43	25.06	17.05	6.11	
inlet temperature (deg k)	683.20	610.48	534.96	424.14	685.12	601.30	531.71	428.80	
turbine nozzle angle	7.698	9.901	12.113	38.690	10.123	11.199	12.719	34.230	
turbine efficiency	0.774	0.768	0.761	0.707	0.774	0.771	0.765	0.729	
output shaft speed (rpm)	440.00	440.00	440.00	440.00	500.00	500.00	500.00	500.00	
output shaft power (kw)	186.55	137.18	83.91	22.52	190.94	140.43	85.28	25.07	
output shaft torque (n./m)	4046.89	2976.00	1820.31	488.56	3645.13	2680.86	1628.07	478.52	
output shaft sfc (kg/kw.hr)	0.241	0.242	0.269	0.540	0.240	0.243	0.267	0.487	
output thermal efficiency	0.3461	0.3445	0.3098	0.1544	0.3480	0.3439	0.3122	0.1713	
engine fuel flow (kg/min)	0.749	0.554	0.377	0.203	0.763	0.568	0.380	0.203	
dynamic injection(degree ca)	337.5	340.4	343.3	345.9	337.4	340.5	343.4	345.9	
duration of injection	28.7	23.3	17.8	13.3	28.5	22.7	17.6	13.3	
turbine gear ratio	105.7	95.0	70.0	28.6	90.0	78.6	62.9	25.7	
pressure loss in pipe a (bar)	0.10345	0.10345	0.10345	0.10345	0.10345	0.10345	0.10345	0.10345	
pressure loss in pipe b (bar)	0.10345	0.10345	0.10345	0.10345	0.10345	0.10345	0.10345	0.10345	
pressure loss in pipe c (bar)	0.10345	0.10345	0.10345	0.10345	0.10345	0.10345	0.10345	0.10345	
pressure loss in pipe d (bar)	0.10345	0.10345	0.10345	0.10345	0.10345	0.10345	0.10345	0.10345	

Table-4.1a

number of cylinders	6.0	bore	(m.m.)	125.03	stroke	(m.m.)	136.00	
con-rod length (m.m.)	217.78	inlet valve closing (degs)	193.0	compressor scale factor		1.10		
ambient temperature (deg k)	294.4	ambient pressure (bar)	0.99	cooler effectiveness		0.8301		
compression ratio	16.30	engine diagram factor	0.9392	turbine flow loss factor		0.8000		
----- compressor gear ratio	9.5500	output shaft gear ratio	1.4450	-----				
engine speed(r.p.m.)	1500.00	1350.00	1250.00	1100.00	1700.00	1600.00	1460.00	1400.00
boost pressure ratio	3.535	3.113	2.268	1.450	3.167	2.690	1.977	1.277
delivered air to fuel ratio	30.441	34.564	35.776	39.420	29.993	32.846	33.335	40.834
delivery ratio	0.852	0.853	0.853	0.854	0.852	0.852	0.853	0.853
manifold temp (deg k)	325.734	315.835	305.586	298.783	326.065	316.472	306.788	295.031
engine power (k w.)	241.48	181.42	120.95	60.33	241.33	181.09	121.51	60.05
engine torque (n.m.)	1537.48	1281.23	922.49	524.15	1356.61	1081.25	795.18	411.89
b.m.e.p (bar)	19.2797	16.0944	11.5877	6.5684	17.0010	13.5550	9.9676	5.1366
s.f.c. (kg/kw hr)	0.196	0.189	0.190	0.200	0.202	0.203	0.206	0.220
b.thermal eff.	0.4253	0.4424	0.4380	0.4179	0.4128	0.4117	0.4039	0.3799
fuel / rev (kg.)	5.262	4.222	3.071	1.824	4.781	3.822	2.864	1.569
max cyl pressure (bar .)	159.48	139.01	101.61	64.28	142.85	121.20	90.09	57.05
exhaust temperature(deg k)	887.52	788.53	739.43	656.75	906.98	837.49	795.58	669.28
mass flow (kg/min)	24.029	19.703	13.732	7.911	24.375	20.086	13.940	8.972
percentage heat to coolant	10.36	11.50	14.00	19.20	10.27	11.37	13.92	17.63
compressor speed (r.p.m.)	7385.6	5953.1	4993.1	3565.6	5660.6	4705.6	3368.6	2795.6
compressor pressure ratio	3.809	3.342	2.449	1.589	3.454	2.932	2.167	1.429
mass flow (kg/min)	35.126	27.803	23.322	16.430	26.105	21.382	14.596	12.425
compressor power (kw.)	120.94	81.01	48.63	19.55	81.75	53.97	28.36	11.97
compressor torque (n.m.)	156.30	129.90	92.86	52.32	137.86	109.49	80.36	40.88
delivery temperature (deg k)	499.15	468.04	417.02	365.70	480.87	445.05	410.59	352.19
compressor efficiency	0.666	0.697	0.690	0.587	0.669	0.703	0.628	0.550
turbine speed (r.p.m.)	42000.0	43470.0	32550.0	17115.0	48480.0	43200.0	35680.0	11200.0
turbine pressure ratio	3.705	3.238	2.345	1.485	3.350	2.828	2.063	1.325
mass flow (kg/min)	35.919	28.377	23.712	16.637	26.921	21.996	15.019	12.649
turbine power (kw)	107.30	69.35	35.95	7.19	85.82	55.11	23.66	2.83
turbine torque (n.m.)	24.39	15.23	10.54	4.01	16.90	12.18	6.33	2.41
inlet temperature (deg k)	774.91	701.94	615.38	512.11	881.95	816.20	780.06	586.68
turbine nozzle angle	8.355	7.232	8.131	11.673	7.455	7.020	6.995	14.516
turbine efficiency	0.751	0.754	0.747	0.743	0.756	0.748	0.736	0.728
output shaft speed (rpm)	1050.00	1050.00	1050.00	1050.00	1600.00	1600.00	1600.00	1600.00
output shaft power (kw)	212.20	157.74	99.89	43.40	230.46	170.57	108.77	45.80
output shaft torque (n.m.)	1929.07	1434.02	908.12	394.52	1374.91	1017.58	648.90	273.22
output shaft sfc (kg/kw.hr)	0.223	0.217	0.231	0.277	0.212	0.215	0.231	0.288
output thermal efficiency	0.3737	0.3847	0.3618	0.3006	0.3942	0.3877	0.3616	0.2898
engine fuel flow (kg/min)	0.789	0.570	0.384	0.201	0.813	0.612	0.418	0.220
dynamic injection(degree ca)	337.4	340.5	343.4	345.9	338.3	340.5	342.7	345.1
duration of injection	28.2	22.8	17.4	13.3	26.8	22.1	17.7	13.1
turbine gear ratio	40.0	41.4	31.0	16.3	30.3	27.0	22.3	7.0
pressure loss in pipe a (bar)	0.10345	0.10345	0.10345	0.10345	0.10345	0.10345	0.10345	0.10345
pressure loss in pipe b (bar)	0.10345	0.10345	0.10345	0.10345	0.10345	0.10345	0.10345	0.10345
pressure loss in pipe c (bar)	0.10345	0.10345	0.10345	0.10345	0.10345	0.10345	0.10345	0.10345
pressure loss in pipe d (bar)	0.10345	0.10345	0.10345	0.10345	0.10345	0.10345	0.10345	0.10345

Table-4.1b

CUMMINS L10 D C E

DESIGN POINT 42 32 23 23

number of cylinders	6.0	bore	(m.m.)	125.03	stroke	(m.m.)	136.00	
con-rod length (m.m.)	217.78	inlet valve closing (degs)	193.0	compressor scale factor		1.10		
ambient temperature (deg k)	294.4	ambient pressure (bar)	0.99	cooler effectiveness		0.7853		
compression ratio	16.30	engine diagram factor	0.9000	turbine flow loss factor		0.8000		
----- compressor gear ratio	9.5500	output shaft gear ratio	1.4450	-----				
engine speed(r.p.m)	1700.00	1775.00	1670.00	1570.00	2100.00	2000.00	1900.00	1800.00
boost pressure ratio	2.932	2.316	1.745	1.225	2.638	2.073	1.548	1.211
delivered air to fuel ratio	31.074	30.478	31.807	41.516	30.575	30.146	31.619	38.363
delivery ratio	0.851	0.852	0.852	0.853	0.851	0.851	0.852	0.852
manifold temp (deg k)	322.578	315.418	306.618	295.463	319.090	312.374	304.462	297.216
engine power (k w.)	240.01	180.88	122.02	59.63	240.00	180.86	120.49	71.47
engine torque (n.m.)	1207.34	974.41	693.91	366.34	1092.77	865.27	607.13	379.90
b.m.e.p (bar)	15.1282	12.2041	9.7500	4.5484	13.6868	10.8300	7.5950	4.7549
s.f.c. (kg/kw hr)	0.205	0.209	0.217	0.234	0.210	0.215	0.225	0.237
b.thermal eff.	0.4069	0.3983	0.3844	0.3569	0.3980	0.3873	0.3715	0.3518
fuel / rev (kg.)	4.315	3.557	2.642	1.479	3.792	3.246	2.373	1.569
max cyl pressure (bar .)	131.14	105.31	77.85	54.71	117.56	93.57	70.46	54.21
exhaust temperature(deg k)	392.53	881.11	831.63	679.34	904.25	892.47	841.16	725.91
mass flow (kg/min)	25.478	19.242	14.037	9.642	25.628	19.571	14.257	10.832
percentage heat to coolant	9.95	11.64	13.86	16.90	9.86	11.46	13.68	15.85
compressor speed (r.p.m.)	5587.9	4394.2	3391.4	2436.4	5515.2	4560.2	3605.2	2650.2
compressor pressure ratio	3.240	2.559	1.941	1.385	2.965	2.331	1.752	1.384
mass flow (kg/min)	25.745	19.917	14.810	10.498	25.756	21.030	16.360	11.687
compressor power (kw.)	71.64	45.22	24.99	9.24	63.94	41.78	22.98	10.44
compressor torque (n.m)	122.38	98.23	70.33	36.20	110.66	87.45	60.85	37.59
delivery temperature (deg k)	457.06	430.02	395.37	347.21	442.58	413.18	378.55	347.98
compressor efficiency	0.713	0.669	0.610	0.546	0.724	0.679	0.610	0.537
turbine speed (r.p.m)	47310.0	41610.0	30970.0	10830.0	49500.0	40700.0	30800.0	11220.0
turbine pressure ratio	3.136	2.455	1.837	1.280	2.861	2.226	1.648	1.280
mass flow (kg/min)	26.768	20.554	15.256	10.732	26.604	21.692	16.821	11.947
turbine power (kw)	81.13	46.97	20.21	1.75	74.76	43.34	16.08	2.08
turbine torque (n.m)	16.37	10.77	6.23	1.54	14.46	10.16	4.98	1.77
inlet temperature (deg k)	885.64	867.62	811.39	654.44	902.24	863.12	787.98	700.76
turbine nozzle angle	7.976	7.990	8.596	17.737	8.886	9.639	12.312	20.740
turbine efficiency	0.756	0.748	0.741	0.752	0.750	0.748	0.725	0.755
output shaft speed (rpm)	1700.00	1900.00	1900.00	1900.00	2200.00	2200.00	2200.00	2200.00
output shaft power (kw)	234.18	170.93	108.82	46.74	235.57	170.57	104.85	56.29
output shaft torque (n./m)	1176.48	858.72	546.71	234.83	1022.10	740.06	454.91	244.21
output shaft sfc (kg/kw.hr)	0.210	0.222	0.243	0.298	0.213	0.228	0.258	0.301
output thermal efficiency	0.3970	0.3764	0.3428	0.2798	0.3907	0.3652	0.3232	0.2771
engine fuel flow (kg/min)	0.820	0.631	0.441	0.232	0.838	0.649	0.451	0.282
dynamic injection(degree ca)	339.7	341.2	342.8	344.7	341.0	342.3	343.6	344.7
duration of injection	25.3	21.5	17.7	13.7	24.6	21.2	17.6	14.7
turbine gear ratio	24.9	21.9	16.3	5.7	22.5	18.5	14.0	5.1
pressure loss in pipe a (bar)	0.10345	0.10345	0.10345	0.10345	0.10345	0.10345	0.10345	0.10345
pressure loss in pipe b (bar)	0.10345	0.10345	0.10345	0.10345	0.10345	0.10345	0.10345	0.10345
pressure loss in pipe c (bar)	0.10345	0.10345	0.10345	0.10345	0.10345	0.10345	0.10345	0.10345
pressure loss in pipe d (bar)	0.10345	0.10345	0.10345	0.10345	0.10345	0.10345	0.10345	0.10345

Table-4.1c

Table-4.2 New baseline: new map, opt. speed, standard conditions

CUMMINS L10 D C E		STALL POINT				38	19	34	24
number of cylinders	6.0	bore	(m.m.)	125.03	stroke	(m.m.)	136.00		
con-rod length (m.m.)	217.78	inlet valve closing (deg)	193.0	compressor scale factor		1.18			
ambient temperature (deg k)	274.4	ambient pressure (bar)	0.99	cooler effectiveness		0.9287			
compression ratio	16.30	engine diagram factor	0.9487	turbine flow loss factor		0.8000			
----- compressor gear ratio	9.5500	output shaft gear ratio	1.4450	-----					
engine speed(r.p.m)	1340.00	1190.00	1020.00	730.00	1340.00	1150.00	850.00	740.00	
boost pressure ratio	4.203	3.553	2.807	2.195	4.197	3.693	3.418	2.199	
delivered air to fuel ratio	33.480	35.652	37.051	42.093	33.227	35.530	38.035	42.773	
delivery ratio	0.854	0.854	0.854	0.854	0.854	0.854	0.854	0.854	
manifold temp (deg k)	320.542	310.976	301.010	291.665	320.860	311.715	302.617	291.854	
engine power (kw.)	239.92	180.39	120.09	59.85	240.36	180.07	120.44	59.88	
engine torque (n.m.)	1712.56	1446.32	1124.92	785.90	1712.56	1496.63	1349.90	775.28	
b.m.e.p (bar)	21.4426	18.1540	14.1000	9.8182	21.4818	18.7523	16.9691	9.6902	
s.f.c. (kg/kw hr)	0.195	0.188	0.190	0.194	0.195	0.189	0.186	0.194	
b.thermal eff.	0.4286	0.4443	0.4382	0.4297	0.4272	0.4412	0.4482	0.4305	
fuel / rev (kg.)	5.807	4.743	3.735	2.652	5.837	4.934	4.395	2.612	
max cyl pressure (bar.)	160.96	157.88	125.46	96.60	159.47	155.74	150.93	96.54	
exhaust temperature(deg k)	846.09	777.75	734.63	644.73	851.34	784.27	721.58	640.00	
mass flow (kg/min)	26.051	20.122	14.116	8.150	25.987	20.159	14.209	8.269	
percentage heat to coolant	9.80	11.25	13.64	18.51	9.82	11.25	13.63	18.35	
compressor speed (r.p.m.)	9889.0	8456.5	6833.0	4063.5	9492.5	7678.0	4813.0	3762.5	
compressor pressure ratio	4.407	3.739	2.974	2.334	4.401	3.875	3.572	2.339	
mass flow (kg/min)	49.514	41.636	33.506	18.693	47.140	36.821	21.172	16.991	
compressor power (kw.)	180.62	130.27	81.77	33.72	173.37	122.42	68.92	30.78	
compressor torque (n.m)	174.34	147.04	114.23	79.20	174.34	152.20	136.69	78.09	
delivery temperature (deg k)	511.14	480.70	440.09	402.31	512.90	492.22	488.15	402.77	
compressor efficiency	0.713	0.721	0.738	0.750	0.706	0.701	0.664	0.748	
turbine speed (r.p.m)	47293.3	41583.3	35733.1	29011.2	46221.5	42955.6	41109.4	29554.9	
turbine pressure ratio	4.303	3.635	2.869	2.230	4.297	3.771	3.468	2.234	
mass flow (kg/min)	50.300	42.206	33.894	18.890	47.929	37.392	21.546	17.188	
turbine power (kw)	153.17	102.88	60.51	21.93	148.04	97.25	50.55	20.34	
turbine torque (n.m)	30.92	23.61	16.16	7.22	30.57	21.61	11.74	6.57	
inlet temperature (deg k)	696.47	631.64	571.02	512.69	708.66	659.28	649.28	522.79	
turbine nozzle angle	9.457	9.013	8.853	6.293	9.103	7.844	4.895	5.772	
turbine efficiency	0.775	0.767	0.758	0.737	0.773	0.763	0.743	0.734	
output shaft speed (rpm)	440.00	440.00	440.00	440.00	500.00	500.00	500.00	500.00	
output shaft power (kw)	195.14	139.97	90.49	43.98	197.52	142.57	93.87	45.33	
output shaft torque (n./m)	4233.29	3036.87	1963.18	954.19	3770.87	2721.74	1792.08	865.40	
output shaft sfc (kg/kw.hr)	0.239	0.242	0.253	0.264	0.238	0.239	0.239	0.256	
output thermal efficiency	0.3486	0.3448	0.3302	0.3158	0.3511	0.3493	0.3493	0.3260	
engine fuel flow (kg/min)	0.778	0.564	0.381	0.194	0.782	0.567	0.374	0.193	
dynamic injection(degree ca)	372.0	339.9	342.8	345.8	369.4	344.7	341.8	345.9	
duration of injection	29.8	24.5	19.3	14.7	29.9	25.2	21.9	14.6	
turbine gear ratio	107.5	94.5	81.2	65.9	92.4	85.9	82.2	59.1	
pressure loss in pipe a (bar)	0.10345	0.10345	0.10345	0.10345	0.10345	0.10345	0.10345	0.10345	
pressure loss in pipe b (bar)	0.10345	0.10345	0.10345	0.10345	0.10345	0.10345	0.10345	0.10345	
pressure loss in pipe c (bar)	0.10345	0.10345	0.10345	0.10345	0.10345	0.10345	0.10345	0.10345	
pressure loss in pipe d (bar)	0.10345	0.10345	0.10345	0.10345	0.10345	0.10345	0.10345	0.10345	

Table-4.2a

CUMMINS L10 D C E

39 22 20 24

number of cylinders	6.0	bore	(m.m.)	125.03	stroke	(m.m.)	136.00	
con-rod length (m.m.)	217.78	inlet valve closing (degs)	193.0	compressor scale factor		1.18		
ambient temperature (deg k)	294.4	ambient pressure (bar)	0.99	cooler effectiveness		0.8595		
compression ratio	16.30	engine diagram factor	0.9274	turbine flow loss factor		0.8000		
----- compressor gear ratio	9.5500	output shaft gear ratio	1.4450	-----				
engine speed(r.p.m)	1430.00	1210.00	1090.00	965.00	1705.00	1590.00	1480.00	1355.00
boost pressure ratio	4.027	3.496	2.737	1.829	3.298	2.753	2.152	1.373
delivered air to fuel ratio	33.492	35.031	37.994	44.663	32.758	34.673	38.252	43.072
delivery ratio	0.854	0.854	0.854	0.853	0.853	0.853	0.852	0.852
manifold temp (deg k)	324.418	315.016	304.141	293.791	323.517	313.488	303.430	293.874
engine power (k w.)	240.01	180.07	120.11	59.89	239.75	179.84	119.88	59.69
engine torque (n.m.)	1604.77	1422.41	1052.67	594.51	1345.94	1082.47	775.28	423.40
b.m.e.p (bar)	20.1007	17.8225	13.1969	7.4327	16.8402	13.5459	9.7006	5.2760
s.f.c. (kg/kw hr)	0.196	0.189	0.191	0.199	0.197	0.199	0.203	0.218
b.thermal eff.	0.4258	0.4414	0.4363	0.4189	0.4237	0.4192	0.4103	0.3823
fuel / rev (kg.)	5.479	4.687	3.511	2.060	4.613	3.751	2.745	1.602
max cyl pressure (bar .)	157.79	155.12	121.53	79.74	147.54	123.68	96.35	60.81
exhaust temperature(deg k)	848.72	789.34	728.72	633.79	852.65	804.80	737.38	657.29
mass flow (kg/min)	26.241	19.867	14.540	8.877	25.765	20.680	15.538	9.348
percentage heat to coolant	9.82	11.42	13.48	17.64	9.91	11.12	12.94	17.13
compressor speed (r.p.m.)	6717.1	4616.1	3470.1	2276.3	5708.4	4610.1	3559.6	2365.9
compressor pressure ratio	4.241	3.685	2.910	1.986	3.538	2.976	2.358	1.559
mass flow (kg/min)	30.420	19.983	14.643	8.901	26.019	20.878	15.831	9.674
compressor power (kw.)	114.92	69.93	38.74	14.22	81.68	53.00	29.12	10.32
compressor torque (n.m)	163.30	144.60	106.55	59.64	136.57	109.74	78.08	41.64
delivery temperature (deg k)	518.74	502.46	452.20	390.06	481.31	445.89	404.42	358.38
compressor efficiency	0.666	0.636	0.665	0.669	0.683	0.710	0.745	0.626
turbine speed (r.p.m)	49056.1	45765.4	38206.0	26880.9	48361.3	43460.6	35805.3	19032.0
turbine pressure ratio	4.137	3.581	2.806	1.882	3.434	2.871	2.253	1.455
mass flow (kg/min)	31.206	20.551	15.027	9.101	26.808	21.478	16.240	9.893
turbine power (kw)	105.98	60.39	32.52	9.59	83.74	53.54	27.50	4.83
turbine torque (n.m)	20.62	12.60	8.12	3.41	16.53	11.76	7.33	2.42
inlet temperature (deg k)	507.51	787.84	726.95	633.19	849.42	801.73	731.79	648.03
turbine nozzle angle	6.593	4.991	4.545	4.280	7.088	6.677	6.427	8.404
turbine efficiency	0.759	0.744	0.733	0.720	0.755	0.747	0.737	0.732
output shaft speed (rpm)	1050.00	1050.00	1050.00	1050.00	1600.00	1600.00	1600.00	1600.00
output shaft power (kw)	215.99	159.94	106.40	50.88	227.31	169.25	110.08	48.97
output shaft torque (n./m)	1963.51	1453.96	967.30	462.57	1356.09	1009.69	656.74	292.15
output shaft sfc (kg/kw.hr)	0.218	0.213	0.216	0.234	0.208	0.211	0.221	0.266
output thermal efficiency	0.3832	0.3920	0.3865	0.3559	0.4018	0.3945	0.3767	0.3137
engine fuel flow (kg/min)	0.784	0.567	0.383	0.199	0.787	0.596	0.406	0.217
dynamic injection(degree ca)	352.2	340.0	343.0	346.0	338.7	340.7	342.8	345.3
duration of injection	28.8	24.3	18.6	13.8	26.1	21.7	17.4	13.0
turbine gear ratio	46.7	43.6	36.4	25.6	30.2	27.2	22.4	11.9
pressure loss in pipe a (bar)	0.10345	0.10345	0.10345	0.10345	0.10345	0.10345	0.10345	0.10345
pressure loss in pipe b (bar)	0.10345	0.10345	0.10345	0.10345	0.10345	0.10345	0.10345	0.10345
pressure loss in pipe c (bar)	0.10345	0.10345	0.10345	0.10345	0.10345	0.10345	0.10345	0.10345
pressure loss in pipe d (bar)	0.10345	0.10345	0.10345	0.10345	0.10345	0.10345	0.10345	0.10345

Table-4.2b

CUMMINS L10 D C E

DESIGN POINT 38 32 20 24

number of cylinders	6.0	bore	(m.m.)	125.03	stroke	(m.m.)	136.00	
con-rod length (m.m.)	217.78	inlet valve closing (degs)		193.0	compressor scale factor		1.18	
ambient temperature (deg k)	294.4	ambient pressure (bar)		0.99	cooler effectiveness		0.8143	
compression ratio	16.30	engine diagram factor		0.9102	turbine flow loss factor		0.8000	
----- compressor gear ratio	9.5500	output shaft gear ratio		1.4450	-----			
engine speed(r.p.m.)	1895.00	1795.00	1680.00	1565.00	2100.00	2000.00	1880.00	1793.00
boost pressure ratio	2.940	2.476	1.889	1.250	2.677	2.220	1.670	1.236
delivered air to fuel ratio	31.681	34.519	36.831	42.457	31.383	33.479	35.054	39.798
delivery ratio	0.852	0.852	0.852	0.851	0.852	0.851	0.851	0.850
manifold temp (deg k)	322.173	312.654	303.178	294.055	320.678	311.703	302.805	295.697
engine power (k w.)	240.24	179.57	119.57	59.55	240.16	180.13	120.04	70.84
engine torque (n.m.)	1210.99	958.84	682.98	366.59	1092.77	860.56	610.33	381.38
b.m.e.p (bar)	15.1825	11.9807	8.5235	4.5568	13.6960	10.7860	7.6469	4.7318
s.f.c. (kg/kw hr)	0.201	0.203	0.210	0.233	0.206	0.209	0.218	0.235
b.thermal eff.	0.4143	0.4105	0.3963	0.3585	0.4052	0.3990	0.3829	0.3553
fuel / rev (kg.)	4.253	3.387	2.497	1.475	3.923	3.137	2.318	1.546
max cyl pressure (bar .)	131.18	110.64	84.76	55.57	118.40	98.70	74.98	55.08
exhaust temperature(deg k)	873.98	812.04	759.05	670.94	883.83	832.15	786.63	708.67
mass flow (kg/min)	25.535	20.988	15.449	9.803	25.856	21.008	15.278	11.030
percentage heat to coolant	9.94	11.00	12.98	16.66	9.84	10.98	13.07	15.62
compressor speed (r.p.m.)	5540.2	4585.2	3486.9	2388.7	5515.2	4560.2	3414.2	2583.4
compressor pressure ratio	3.197	2.717	2.112	1.452	2.953	2.481	1.910	1.460
mass flow (kg/min)	25.701	21.067	15.649	9.915	25.941	21.256	15.433	11.048
compressor power (kw.)	71.55	46.61	25.08	9.11	64.08	41.49	21.85	10.22
compressor torque (n.m.)	123.28	97.03	68.67	36.42	110.91	86.85	61.08	37.77
delivery temperature (deg k)	460.39	426.58	390.35	349.54	441.85	411.13	379.19	349.90
compressor efficiency	0.698	0.737	0.733	0.604	0.724	0.749	0.708	0.608
turbine speed (r.p.m.)	47113.4	42079.3	33574.1	15189.0	45859.9	39939.9	30665.4	16086.4
turbine pressure ratio	3.093	2.613	2.008	1.348	2.849	2.376	1.806	1.355
mass flow (kg/min)	26.511	21.680	16.074	10.150	26.771	21.891	15.875	11.329
turbine power (kw)	78.04	49.67	23.50	3.11	74.07	45.89	19.58	3.88
turbine torque (n.m.)	15.81	11.27	6.68	1.95	15.42	10.97	6.09	2.30
inlet temperature (deg k)	871.62	810.75	754.80	667.61	882.55	827.78	782.97	708.15
turbine nozzle angle	7.951	7.555	7.626	11.980	8.843	8.660	9.120	13.484
turbine efficiency	0.755	0.748	0.739	0.742	0.756	0.750	0.742	0.746
output shaft speed (rpm)	1900.00	1900.00	1900.00	1900.00	2200.00	2200.00	2200.00	2200.00
output shaft power (kw)	231.79	171.34	109.74	48.04	234.74	172.21	108.60	58.19
output shaft torque (n./m)	1164.49	860.79	551.31	241.35	1018.48	747.17	471.20	252.49
output shaft sfc (kg/kw.hr)	0.209	0.213	0.229	0.288	0.211	0.219	0.241	0.286
output thermal efficiency	0.3998	0.3917	0.3637	0.2892	0.3961	0.3815	0.3464	0.2919
engine fuel flow (kg/min)	0.806	0.608	0.419	0.231	0.824	0.627	0.436	0.277
dynamic injection(degree ca)	339.8	341.6	343.1	344.7	341.1	342.5	343.6	344.7
duration of injection	25.0	20.8	17.2	13.6	24.4	20.8	17.4	14.6
turbine gear ratio	24.8	22.1	17.7	8.0	20.8	18.2	13.9	7.3
pressure loss in pipe a (bar)	0.10345	0.10345	0.10345	0.10345	0.10345	0.10345	0.10345	0.10345
pressure loss in pipe b (bar)	0.10345	0.10345	0.10345	0.10345	0.10345	0.10345	0.10345	0.10345
pressure loss in pipe c (bar)	0.10345	0.10345	0.10345	0.10345	0.10345	0.10345	0.10345	0.10345
pressure loss in pipe d (bar)	0.10345	0.10345	0.10345	0.10345	0.10345	0.10345	0.10345	0.10345

Table-4.2c

Table-4.3 New map, opt. speed, reduced Pa(0.8415bar)

CUMMINS L10 D C E		STALL MAP				31 30 34 24			
number of cylinders	6.0	bore	(m.m.)	125.03	stroke	(m.m.)	136.00		
con-rod length (m.m.)	217.78	inlet valve closing (deg)	193.0	compressor scale factor		1.18			
ambient temperature (deg k)	294.4	ambient pressure (bar)	0.84	cooler effectiveness		0.3427			
compression ratio	16.30	engine diagram factor	0.9870	turbine flow loss factor		0.8000			
----- compressor gear ratio	9.5500	output shaft gear ratio	1.4450	-----					
engine speed(r.p.m)	1320.00	1210.00	1010.00	740.00	1340.00	1230.00	930.00	760.00	
boost pressure ratio	4.881	4.052	3.279	2.489	4.811	3.986	3.635	2.442	
delivered air to fuel ratio	31.853	34.862	35.432	28.235	31.645	34.699	33.628	29.872	
delivery ratio	0.853	0.853	0.854	0.855	0.853	0.853	0.854	0.855	
manifold temp (deg k)	332.116	321.161	320.899	384.578	332.330	320.999	339.024	372.441	
engine power (k w.)	240.11	180.83	120.53	59.84	240.09	130.79	120.27	59.90	
engine torque (n.m.)	1738.51	1422.41	1136.05	775.28	1712.56	1399.28	1233.78	754.88	
b.m.e.p (bar)	21.7846	17.8973	14.2921	9.6838	21.4581	17.6027	15.4871	9.4391	
s.f.c. (kg/kw hr)	0.192	0.182	0.183	0.215	0.193	0.183	0.187	0.211	
b.thermal eff.	0.4354	0.4572	0.4567	0.3887	0.4324	0.4551	0.4470	0.3952	
fuel / rev (kg.)	5.808	4.543	3.632	2.892	5.760	4.490	4.022	2.772	
max cyl pressure (bar.)	158.42	151.85	122.70	90.19	156.21	149.49	134.55	88.81	
exhaust temperature(deg k)	865.73	775.46	737.22	838.58	871.77	778.98	778.64	807.84	
mass flow (kg/min)	24.419	19.165	12.999	6.042	24.426	19.163	12.577	6.293	
percentage heat to coolant	10.38	11.81	14.90	25.73	10.38	11.80	15.67	24.82	
compressor speed (r.p.m.)	9698.0	8647.5	6737.5	4159.0	9492.5	8442.0	5577.0	3953.5	
compressor pressure ratio	5.204	4.315	3.477	2.617	5.136	4.251	3.822	2.575	
mass flow (kg/min)	40.632	35.648	27.186	16.032	39.560	34.644	21.090	15.114	
compressor power (kw.)	179.84	130.94	81.46	34.04	173.39	125.74	73.21	31.48	
compressor torque (n.m)	177.01	144.53	115.41	78.13	174.35	142.17	125.31	76.00	
delivery temperature (deg k)	556.50	512.63	472.90	421.30	553.99	510.07	500.82	418.89	
compressor efficiency	0.669	0.696	0.704	0.735	0.669	0.695	0.663	0.735	
turbine speed (r.p.m)	50504.7	45284.1	39932.2	32203.6	50550.0	45166.4	43988.8	32239.3	
turbine pressure ratio	5.082	4.193	3.354	2.495	5.013	4.129	3.700	2.452	
mass flow (kg/min)	41.403	36.202	27.556	16.248	40.337	35.200	21.465	15.327	
turbine power (kw)	149.17	101.28	59.24	24.74	145.73	98.17	54.89	22.85	
turbine torque (n.m)	28.19	21.35	14.16	7.33	27.52	20.75	11.91	6.77	
inlet temperature (deg k)	750.46	660.28	605.58	591.36	758.51	665.34	673.24	592.36	
turbine nozzle angle	8.047	8.070	7.457	6.039	7.997	8.008	5.515	5.827	
turbine efficiency	0.775	0.768	0.757	0.736	0.774	0.767	0.749	0.735	
output shaft speed (rpm)	440.00	440.00	440.00	440.00	500.00	500.00	500.00	500.00	
output shaft power (kw)	192.22	137.76	89.67	46.26	195.37	139.96	93.79	46.95	
output shaft torque (n./m)	4170.02	2988.46	1945.21	1003.60	3729.72	2671.99	1790.57	896.33	
output shaft sfc (kg/kw.hr)	0.239	0.239	0.245	0.278	0.237	0.237	0.239	0.269	
output thermal efficiency	0.3485	0.3483	0.3397	0.3005	0.3519	0.3523	0.3486	0.3098	
engine fuel flow (kg/min)	0.767	0.550	0.367	0.214	0.772	0.552	0.374	0.211	
dynamic injection(degree ca)	357.1	340.3	343.0	345.4	357.1	340.4	342.4	345.5	
duration of injection	29.7	23.7	18.8	15.3	29.6	23.5	20.4	15.1	
turbine gear ratio	114.8	102.9	90.8	73.2	101.1	90.3	88.0	64.5	
pressure loss in pipe a (bar)	0.10345	0.10345	0.10345	0.10345	0.10345	0.10345	0.10345	0.10345	
pressure loss in pipe b (bar)	0.10345	0.10345	0.10345	0.10345	0.10345	0.10345	0.10345	0.10345	
pressure loss in pipe c (bar)	0.10345	0.10345	0.10345	0.10345	0.10345	0.10345	0.10345	0.10345	
pressure loss in pipe d (bar)	0.10345	0.10345	0.10345	0.10345	0.10345	0.10345	0.10345	0.10345	

Table-4.3a

CUMMINS L10 D C E

29 27 22 24

number of cylinders	6.0	bore	(m.m.)	125.03	stroke	(m.m.)	136.00	
con-rod length (m.m.)	217.78	inlet valve closing (degs)		193.0	compressor scale factor		1.18	
ambient temperature (deg k)	294.4	ambient pressure (bar)		0.84	cooler effectiveness		0.8312	
compression ratio	16.30	engine diagram factor		0.9459	turbine flow loss factor		0.8000	
----- compressor gear ratio	9.5500	output shaft gear ratio		1.4450	-----			
engine speed(r.p.m)	1475.00	1320.00	1115.00	985.00	1780.00	1630.00	1510.00	1370.00
boost pressure ratio	4.528	3.794	2.978	2.050	3.659	3.012	2.361	1.513
delivered air to fuel ratio	31.330	34.452	35.440	42.009	30.098	30.916	34.649	40.482
delivery ratio	0.852	0.853	0.853	0.854	0.852	0.852	0.853	0.853
manifold temp (deg k)	336.924	324.166	315.460	311.439	332.552	322.244	309.648	297.632
engine power (k w.)	239.93	180.56	120.45	59.70	240.09	180.07	120.09	59.77
engine torque (n.m.)	1555.81	1303.88	1029.07	582.44	1289.23	1055.90	759.88	418.76
b.m.e.p (bar)	19.4809	16.3817	12.9375	7.2580	16.1535	13.2302	9.5248	5.2246
s.f.c. (kg/kw hr)	0.199	0.188	0.186	0.195	0.204	0.206	0.209	0.217
b.thermal eff.	0.4200	0.4446	0.4482	0.4266	0.4088	0.4047	0.4000	0.3838
fuel / rev (kg.)	5.383	4.277	3.351	1.975	4.586	3.795	2.764	1.580
max cyl pressure (bar .)	155.51	142.77	112.11	75.47	138.99	115.72	90.45	57.31
exhaust temperature(deg k)	890.26	793.24	740.63	645.22	913.27	873.39	785.25	670.41
mass flow (kg/min)	24.877	19.450	13.240	8.171	24.570	19.124	14.460	8.763
percentage heat to coolant	10.34	11.76	14.59	19.35	10.32	11.81	13.68	18.00
compressor speed (r.p.m.)	7146.8	5666.6	3708.8	2467.3	6424.6	4992.1	3846.1	2509.1
compressor pressure ratio	4.869	4.070	3.187	2.212	4.014	3.296	2.592	1.691
mass flow (kg/min)	27.009	21.129	13.308	8.340	24.784	19.151	14.588	8.848
compressor power (kw.)	118.50	78.61	40.49	15.09	88.09	56.05	30.83	10.87
compressor torque (n.m)	158.27	132.43	104.20	58.40	130.89	107.18	76.51	41.37
delivery temperature (deg k)	554.24	515.40	475.61	402.68	505.68	468.82	420.71	368.06
compressor efficiency	0.642	0.653	0.636	0.694	0.676	0.684	0.730	0.650
turbine speed (r.p.m)	53465.3	48446.2	41327.2	30049.7	52282.2	47373.6	38798.1	22115.5
turbine pressure ratio	4.746	3.947	3.064	2.089	3.892	3.174	2.469	1.569
mass flow (kg/min)	27.806	21.695	13.682	8.535	25.603	19.772	15.008	9.067
turbine power (kw)	110.33	67.24	32.50	10.73	94.15	58.64	30.22	5.76
turbine torque (n.m)	19.70	13.25	7.51	3.41	17.19	11.82	7.43	2.48
inlet temperature (deg k)	866.42	773.13	739.41	640.69	910.16	872.88	782.40	667.76
turbine nozzle angle	6.255	5.593	4.526	4.186	7.303	6.872	6.562	7.985
turbine efficiency	0.762	0.751	0.736	0.723	0.760	0.751	0.741	0.732
output shaft speed (rpm)	1050.00	1050.00	1050.00	1050.00	1600.00	1600.00	1600.00	1600.00
output shaft power (kw)	216.39	157.47	104.63	51.04	230.56	170.97	110.86	49.31
output shaft torque (n./m)	1967.16	1431.54	951.20	463.98	1375.49	1020.00	661.36	294.16
output shaft sfc (kg/kw.hr)	0.220	0.215	0.214	0.229	0.212	0.217	0.226	0.263
output thermal efficiency	0.3788	0.3877	0.3893	0.3648	0.3926	0.3842	0.3693	0.3166
engine fuel flow (kg/min)	0.794	0.565	0.374	0.195	0.816	0.619	0.417	0.216
dynamic injection(degree ca)	347.2	340.5	343.3	346.1	338.9	340.5	342.7	345.3
duration of injection	28.6	22.9	18.0	13.6	26.2	22.1	17.6	13.0
turbine gear ratio	50.9	46.1	39.4	28.6	32.7	29.6	24.2	13.8
pressure loss in pipe a (bar)	0.10345	0.10345	0.10345	0.10345	0.10345	0.10345	0.10345	0.10345
pressure loss in pipe b (bar)	0.10345	0.10345	0.10345	0.10345	0.10345	0.10345	0.10345	0.10345
pressure loss in pipe c (bar)	0.10345	0.10345	0.10345	0.10345	0.10345	0.10345	0.10345	0.10345
pressure loss in pipe d (bar)	0.10345	0.10345	0.10345	0.10345	0.10345	0.10345	0.10345	0.10345

Table-4.3b

CUMMINS L10 D C E

DESIGN POINT 34 34 24 24

number of cylinders	6.0	bore	(m.m.)	125.03	stroke	(m.m.)	136.00	
con-rod length (m.m.)	217.78	inlet valve closing (degs)		193.0	compressor scale factor		1.18	
ambient temperature (deg k)	294.4	ambient pressure (bar)		0.84	cooler effectiveness		0.7832	
compression ratio	16.30	engine diagram factor		0.8992	turbine flow loss factor		0.8000	
----- compressor gear ratio	9.5500	output shaft gear ratio		1.4450	-----			
engine speed(r.p.m)	1965.00	1840.00	1720.00	1585.00	2155.00	2050.00	1925.00	1818.00
boost pressure ratio	3.231	2.689	2.109	1.358	2.886	2.442	1.877	1.353
delivered air to fuel ratio	29.021	30.682	34.058	38.141	28.052	30.578	32.955	35.933
delivery ratio	0.851	0.852	0.852	0.853	0.850	0.851	0.851	0.852
manifold temp (deg k)	327.874	319.259	308.910	297.477	324.159	315.757	307.191	299.349
engine power (k w.)	239.93	179.97	120.00	59.95	239.76	179.88	119.90	71.40
engine torque (n.m.)	1167.85	935.39	667.10	361.96	1064.88	839.57	596.06	376.13
b.m.e.p (bar)	14.6230	11.7136	8.3556	4.5294	13.3242	10.5082	7.4594	4.7034
s.f.c. (kg/kw hr)	0.209	0.211	0.216	0.238	0.214	0.217	0.224	0.241
b.thermal eff.	0.3989	0.3948	0.3854	0.3498	0.3892	0.3852	0.3723	0.3457
fuel / rev (kg.)	4.255	3.444	2.516	1.503	3.973	3.166	2.326	1.579
max cyl pressure (bar .)	123.05	103.12	80.84	51.95	109.64	92.75	71.86	51.84
exhaust temperature(deg k)	935.89	883.22	803.12	712.39	958.02	889.12	824.33	754.23
mass flow (kg/min)	24.265	19.441	14.741	9.087	24.020	19.847	14.755	10.316
percentage heat to coolant	10.32	11.64	13.51	17.63	10.31	11.43	13.46	16.42
compressor speed (r.p.m.)	6208.7	5014.9	3868.9	2579.7	6040.5	5037.7	3844.0	2822.1
compressor pressure ratio	3.598	2.986	2.349	1.543	3.270	2.757	2.126	1.555
mass flow (kg/min)	24.394	19.642	14.942	9.297	24.116	19.977	15.024	10.492
compressor power (kw.)	77.05	49.62	27.20	9.65	68.31	44.75	24.10	10.99
compressor torque (n.m)	118.46	94.45	67.10	35.72	107.94	84.79	59.84	37.16
delivery temperature (deg k)	482.46	445.17	403.29	356.66	463.25	428.22	390.41	357.19
compressor efficiency	0.689	0.716	0.749	0.627	0.701	0.740	0.740	0.633
turbine speed (r.p.m)	50694.1	45222.5	36604.1	17271.8	49299.6	43230.2	34071.2	18363.2
turbine pressure ratio	3.476	2.863	2.226	1.421	3.147	2.634	2.003	1.432
mass flow (kg/min)	25.233	20.279	15.380	9.539	24.976	20.631	15.478	10.784
turbine power (kw)	87.65	55.15	27.52	3.81	81.88	51.88	23.85	4.87
turbine torque (n.m)	16.50	11.64	7.18	2.10	15.85	11.46	6.68	2.53
inlet temperature (deg k)	933.79	879.29	798.30	705.10	956.31	886.49	817.42	748.23
turbine nozzle angle	8.241	7.927	7.791	12.061	9.205	8.925	9.293	13.633
turbine efficiency	0.760	0.752	0.743	0.743	0.761	0.754	0.746	0.748
output shaft speed (rpm)	1900.00	1900.00	1900.00	1900.00	2200.00	2200.00	2200.00	2200.00
output shaft power (kw)	234.92	173.28	111.34	48.06	237.66	174.51	110.35	58.30
output shaft torque (n./m)	1180.20	870.51	559.35	241.47	1031.14	757.16	478.78	252.94
output shaft sfc (kg/kw.hr)	0.214	0.219	0.233	0.297	0.216	0.223	0.243	0.295
output thermal efficiency	0.3906	0.3801	0.3576	0.2804	0.3858	0.3738	0.3426	0.2823
engine fuel flow (kg/min)	0.836	0.634	0.433	0.238	0.856	0.649	0.448	0.287
dynamic injection(degree ca)	340.0	341.5	343.1	344.6	341.2	342.6	343.7	344.7
duration of injection	25.3	21.2	17.4	13.8	24.8	21.2	17.6	14.8
turbine gear ratio	26.7	23.8	19.3	9.1	22.4	19.7	15.5	8.3
pressure loss in pipe a (bar)	0.10345	0.10345	0.10345	0.10345	0.10345	0.10345	0.10345	0.10345
pressure loss in pipe b (bar)	0.10345	0.10345	0.10345	0.10345	0.10345	0.10345	0.10345	0.10345
pressure loss in pipe c (bar)	0.10345	0.10345	0.10345	0.10345	0.10345	0.10345	0.10345	0.10345
pressure loss in pipe d (bar)	0.10345	0.10345	0.10345	0.10345	0.10345	0.10345	0.10345	0.10345

Table-4.3c

Table-4.4 New map, opt. speed, elevated Ta(313K)

CUMMINS L10 D C E		STALL POINT				38 17 39 24			
number of cylinders	6.0	bore	(m.m.)	125.03	stroke	(m.m.)	136.00		
con-rod length (m.m.)	217.78	inlet valve closing (degs)	193.0	compressor scale factor		1.18			
ambient temperature (deg k)	313.3	ambient pressure (bar)	0.99	cooler effectiveness		0.9327			
compression ratio	16.30	engine diagram factor	0.9487	turbine flow loss factor		0.8000			
----- compressor gear ratio	9.5500	output shaft gear ratio	1.4450	-----					
engine speed(r.p.m)	1340.00	1190.00	1020.00	730.00	1340.00	1190.00	850.00	740.00	
boost pressure ratio	4.212	3.560	2.812	2.198	4.206	3.560	3.423	2.202	
delivered air to fuel ratio	30.586	32.809	33.675	37.731	30.491	32.772	34.808	38.364	
delivery ratio	0.854	0.854	0.854	0.854	0.854	0.854	0.854	0.854	
manifold temp (deg k)	342.647	333.036	322.907	313.632	342.971	333.325	324.589	313.818	
engine power (k w.)	240.15	179.93	120.13	60.00	240.15	179.92	119.86	60.01	
engine torque (n.m.)	1712.56	1446.32	1124.92	785.90	1712.56	1446.32	1349.90	775.28	
b.m.e.p (bar)	21.4630	18.1075	14.1043	9.8441	21.4628	18.1068	16.8873	9.7125	
s.f.c. (kg/kw hr)	0.199	0.192	0.195	0.201	0.200	0.192	0.191	0.201	
b.thermal eff.	0.4184	0.4349	0.4270	0.4150	0.4181	0.4348	0.4370	0.4159	
fuel / rev (kg.)	5.955	4.833	3.834	2.753	5.959	4.834	4.486	2.711	
max cyl pressure (bar .)	157.80	156.94	124.49	95.98	157.55	156.92	149.75	95.91	
exhaust temperature(deg k)	911.97	833.37	792.22	698.61	913.91	834.13	775.15	693.30	
mass flow (kg/min)	24.406	18.869	13.171	7.584	24.348	18.853	13.272	7.695	
percentage heat to coolant	10.54	12.15	14.82	20.32	10.56	12.16	14.81	20.15	
compressor speed (r.p.m.)	9889.0	8456.5	6833.0	4063.5	9492.5	8060.0	4813.0	3762.5	
compressor pressure ratio	4.410	3.742	2.975	2.335	4.404	3.741	3.574	2.339	
mass flow (kg/min)	46.527	39.123	31.485	17.565	44.295	36.929	19.892	15.967	
compressor power (kw.)	180.61	130.27	81.77	33.72	173.37	124.15	68.94	30.78	
compressor torque (n.m)	174.34	147.04	114.23	79.20	174.34	147.03	136.73	78.09	
delivery temperature (deg k)	543.07	510.87	467.88	427.84	544.93	512.76	518.82	428.33	
compressor efficiency	0.713	0.721	0.738	0.750	0.706	0.714	0.664	0.748	
turbine speed (r.p.m)	48218.9	43792.4	37824.2	30764.1	48235.5	43917.5	43571.2	30992.9	
turbine pressure ratio	4.306	3.637	2.871	2.231	4.300	3.637	3.470	2.235	
mass flow (kg/min)	47.331	39.703	31.882	17.770	45.100	37.509	20.274	16.170	
turbine power (kw)	154.88	103.56	61.05	22.18	149.41	99.14	51.01	20.57	
turbine torque (n.m)	30.66	22.57	15.41	6.88	29.57	21.55	11.17	6.33	
inlet temperature (deg k)	747.63	675.21	611.98	550.74	758.72	685.58	695.30	561.88	
turbine nozzle angle	9.221	8.767	8.629	6.159	8.864	8.345	4.768	5.641	
turbine efficiency	0.774	0.766	0.757	0.736	0.772	0.764	0.742	0.734	
output shaft speed (rpm)	440.00	440.00	440.00	440.00	500.00	500.00	500.00	500.00	
output shaft power (kw)	196.73	140.62	91.00	44.21	198.80	142.54	94.30	45.55	
output shaft torque (n./m)	4267.86	3050.63	1974.04	959.07	3795.17	2721.19	1800.28	869.55	
output shaft sfc (kg/kw.hr)	0.243	0.245	0.258	0.273	0.241	0.242	0.243	0.264	
output thermal efficiency	0.3427	0.3399	0.3234	0.3057	0.3461	0.3444	0.3438	0.3156	
engine fuel flow (kg/min)	0.798	0.575	0.391	0.201	0.799	0.575	0.381	0.201	
dynamic injection(degree ca)	361.7	339.7	342.5	345.7	361.7	339.7	341.6	345.7	
duration of injection	30.4	24.9	19.8	15.0	30.5	24.9	22.3	14.9	
turbine gear ratio	109.6	99.5	86.0	69.9	96.5	87.8	87.1	62.0	
pressure loss in pipe a (bar)	0.10345	0.10345	0.10345	0.10345	0.10345	0.10345	0.10345	0.10345	
pressure loss in pipe b (bar)	0.10345	0.10345	0.10345	0.10345	0.10345	0.10345	0.10345	0.10345	
pressure loss in pipe c (bar)	0.10345	0.10345	0.10345	0.10345	0.10345	0.10345	0.10345	0.10345	
pressure loss in pipe d (bar)	0.10345	0.10345	0.10345	0.10345	0.10345	0.10345	0.10345	0.10345	

Table-4.4a

CUMMINS L10 D C E

39 20 31 24

number of cylinders	6.0	bore	(m.m.)	125.03	stroke	(m.m.)	136.00	
con-rod length (m.m.)	217.78	inlet valve closing (degs)	193.0	compressor scale factor		1.18		
ambient temperature (deg k)	313.3	ambient pressure (bar)	0.99	cooler effectiveness		0.8653		
compression ratio	16.30	engine diagram factor	0.9271	turbine flow loss factor		0.8000		
----- compressor gear ratio	9.5500	output shaft gear ratio	1.4450	-----				
engine speed(r.p.m)	1400.00	1235.00	1105.00	975.00	1720.00	1595.00	1485.00	1360.00
boost pressure ratio	4.221	3.472	2.711	1.801	3.270	2.752	2.147	1.374
delivered air to fuel ratio	31.394	32.611	34.725	39.889	29.978	31.751	34.777	38.948
delivery ratio	0.854	0.854	0.854	0.854	0.853	0.853	0.853	0.852
manifold temp (deg k)	347.831	336.726	325.721	315.528	345.466	335.451	325.231	315.700
engine power (k w.)	240.17	179.84	119.71	60.02	240.19	180.15	120.09	59.98
engine torque (n.m.)	1639.16	1393.62	1038.38	588.42	1334.20	1079.07	772.67	421.84
b.m.e.p (bar)	20.5450	17.4390	12.9738	7.3721	16.7240	13.5266	9.6849	5.2818
s.f.c. (kg/kw hr)	0.200	0.193	0.196	0.206	0.201	0.203	0.209	0.225
b.thermal eff.	0.4170	0.4319	0.4248	0.4039	0.4148	0.4102	0.4000	0.3704
fuel / rev (kg.)	5.719	4.686	3.545	2.118	4.680	3.828	2.811	1.655
max cyl pressure (bar)	157.47	152.69	119.07	78.15	144.99	122.56	95.35	60.52
exhaust temperature(deg k)	903.89	840.33	783.23	688.05	916.17	864.38	794.93	709.25
mass flow (kg/min)	25.137	18.874	13.602	8.239	24.131	19.386	14.516	8.767
percentage heat to coolant	10.45	12.22	14.62	19.42	10.65	11.98	14.05	18.71
compressor speed (r.p.m.)	6430.6	4854.8	3613.3	2371.8	5851.6	4657.9	3607.4	2413.6
compressor pressure ratio	4.427	3.659	2.881	1.955	3.503	2.969	2.347	1.556
mass flow (kg/min)	26.697	19.986	14.542	8.893	25.250	19.876	15.138	9.355
compressor power (kw.)	112.38	72.03	39.80	14.66	83.01	53.38	29.41	10.56
compressor torque (n.m)	166.82	141.63	105.14	59.01	135.40	109.38	77.81	41.77
delivery temperature (deg k)	562.08	526.89	476.10	411.79	508.40	473.07	429.21	380.86
compressor efficiency	0.659	0.652	0.677	0.672	0.687	0.712	0.746	0.626
turbine speed (r.p.m)	52675.9	48065.5	41203.8	27984.3	49293.6	44769.9	36934.9	19825.1
turbine pressure ratio	4.322	3.554	2.777	1.851	3.399	2.865	2.243	1.452
mass flow (kg/min)	27.499	20.566	15.355	9.101	26.057	20.489	15.558	9.583
turbine power (kw)	105.29	63.11	34.37	9.82	85.73	54.46	27.98	4.93
turbine torque (n.m)	19.08	12.53	7.96	3.35	16.60	11.61	7.23	2.38
inlet temperature (deg k)	885.99	824.60	757.44	669.34	900.17	855.80	781.40	690.38
turbine nozzle angle	5.819	5.155	4.802	4.555	7.179	6.606	6.408	8.512
turbine efficiency	0.756	0.745	0.735	0.721	0.755	0.746	0.737	0.732
output shaft speed (rpm)	1050.00	1050.00	1050.00	1050.00	1600.00	1600.00	1600.00	1600.00
output shaft power (kw)	217.92	160.32	107.07	50.64	227.83	169.72	110.23	48.09
output shaft torque (n./m)	1981.02	1457.44	973.34	460.34	1359.20	1012.50	657.60	291.68
output shaft sfc (kg/kw.hr)	0.220	0.217	0.219	0.245	0.212	0.216	0.227	0.276
output thermal efficiency	0.3783	0.3851	0.3800	0.3408	0.3934	0.3864	0.3671	0.3019
engine fuel flow (kg/min)	0.801	0.579	0.392	0.207	0.805	0.611	0.417	0.225
dynamic injection(degree ca)	361.8	339.9	342.9	345.9	338.6	340.5	342.7	345.2
duration of injection	29.7	24.4	18.8	13.9	26.4	22.1	17.6	13.2
turbine gear ratio	50.2	45.8	39.2	26.7	30.8	28.0	23.1	12.4
pressure loss in pipe a (bar)	0.10345	0.10345	0.10345	0.10345	0.10345	0.10345	0.10345	0.10345
pressure loss in pipe b (bar)	0.10345	0.10345	0.10345	0.10345	0.10345	0.10345	0.10345	0.10345
pressure loss in pipe c (bar)	0.10345	0.10345	0.10345	0.10345	0.10345	0.10345	0.10345	0.10345
pressure loss in pipe d (bar)	0.10345	0.10345	0.10345	0.10345	0.10345	0.10345	0.10345	0.10345

Table-4.4b

CUMMINS L10 D C E

DESIGN POINT

39 32 24 24

number of cylinders	6.0	bore	(m.m.)	125.03	stroke	(m.m.)	136.00	
con-rod length (m.m.)	217.78	inlet valve closing (degs)		193.0	compressor scale factor		1.18	
ambient temperature (deg k)	313.3	ambient pressure (bar)		0.99	cooler effectiveness		0.8210	
compression ratio	16.30	engine diagram factor		0.9099	turbine flow loss factor		0.8000	
----- compressor gear ratio	9.5500	output shaft gear ratio		1.4450	-----			
engine speed(r.p.m.)	1715.00	1815.00	1690.00	1575.00	2120.00	2015.00	1890.00	1803.00
boost pressure ratio	2.913	2.450	1.876	1.238	2.655	2.202	1.671	1.231
delivered air to fuel ratio	29.083	31.451	33.342	37.930	28.806	30.568	32.129	35.780
delivery ratio	0.852	0.852	0.852	0.851	0.852	0.851	0.851	0.850
manifold temp (deg k)	344.075	334.399	324.885	315.606	342.650	333.535	324.631	317.288
engine power (k w.)	240.07	180.08	120.02	59.94	239.97	179.97	119.92	71.41
engine torque (n.m.)	1198.34	948.28	678.94	364.26	1082.47	854.15	607.10	379.26
b.m.e.p (bar)	15.0137	11.8826	8.5048	4.5576	13.5562	10.6966	7.5989	4.7435
s.f.c. (kg/kw hr)	0.206	0.208	0.216	0.240	0.210	0.214	0.223	0.242
b.thermal eff.	0.4054	0.4009	0.3861	0.3469	0.3965	0.3897	0.3736	0.3451
fuel / rev (kg.)	4.298	3.441	2.556	1.525	3.969	3.186	2.361	1.596
max cyl pressure (bar .)	128.71	108.55	83.53	54.72	116.29	96.97	74.27	54.43
exhaust temperature(deg k)	937.22	874.89	820.12	728.36	947.83	895.11	843.70	767.34
mass flow (kg/min)	23.940	19.641	14.405	9.110	24.236	19.621	14.337	10.293
percentage heat to coolant	10.66	11.86	14.09	18.27	10.55	11.84	14.11	17.03
compressor speed (r.p.m.)	5731.2	4776.2	3582.4	2484.2	5706.2	4703.5	3509.7	2678.9
compressor pressure ratio	3.163	2.686	2.093	1.436	2.925	2.455	1.904	1.448
mass flow (kg/min)	25.209	20.816	15.235	9.862	25.419	20.754	15.024	10.920
compressor power (kw.)	73.24	48.00	25.62	9.37	65.63	42.47	22.47	10.54
compressor torque (n.m.)	121.98	95.92	68.26	36.00	109.79	86.19	61.10	37.56
delivery temperature (deg k)	486.00	450.69	413.73	370.18	466.99	435.36	402.67	371.09
compressor efficiency	0.703	0.742	0.733	0.601	0.729	0.750	0.709	0.606
turbine speed (r.p.m.)	47727.4	42621.4	33715.5	14612.9	46420.4	40459.5	31197.8	15791.2
turbine pressure ratio	3.059	2.582	1.989	1.331	2.820	2.351	1.800	1.344
mass flow (kg/min)	26.036	21.446	15.671	10.106	26.266	21.403	15.476	11.212
turbine power (kw)	80.02	51.16	23.92	2.91	75.80	46.72	20.00	3.76
turbine torque (n.m.)	16.00	11.46	6.77	1.90	15.59	11.02	6.12	2.27
inlet temperature (deg k)	917.21	853.60	800.33	703.48	928.22	872.94	825.78	746.83
turbine nozzle angle	8.115	7.782	7.741	13.082	9.007	8.814	9.173	14.292
turbine efficiency	0.756	0.749	0.740	0.745	0.757	0.750	0.742	0.748
output shaft speed (rpm)	1900.00	1900.00	1900.00	1900.00	2200.00	2200.00	2200.00	2200.00
output shaft power (kw)	231.93	171.30	109.59	47.54	234.74	171.99	108.49	57.75
output shaft torque (n./m)	1165.16	860.60	550.54	238.83	1018.50	746.21	470.70	250.58
output shaft sfc (kg/kw.hr)	0.213	0.219	0.237	0.303	0.215	0.224	0.247	0.299
output thermal efficiency	0.3917	0.3813	0.3526	0.2752	0.3878	0.3725	0.3380	0.2791
engine fuel flow (kg/min)	0.823	0.624	0.432	0.240	0.841	0.642	0.446	0.288
dynamic injection(degree ca)	339.7	341.5	343.0	344.6	341.1	342.5	343.6	344.6
duration of injection	25.3	21.1	17.5	13.8	24.6	21.1	17.5	14.8
turbine gear ratio	25.1	22.4	17.7	7.7	21.1	18.4	14.2	7.2
pressure loss in pipe a (bar)	0.10345	0.10345	0.10345	0.10345	0.10345	0.10345	0.10345	0.10345
pressure loss in pipe b (bar)	0.10345	0.10345	0.10345	0.10345	0.10345	0.10345	0.10345	0.10345
pressure loss in pipe c (bar)	0.10345	0.10345	0.10345	0.10345	0.10345	0.10345	0.10345	0.10345
pressure loss in pipe d (bar)	0.10345	0.10345	0.10345	0.10345	0.10345	0.10345	0.10345	0.10345

Table-4.4c

Table-4.5 New map, opt. speed, reduced Pa, elevated Ta

CUMMINS L10 D C E	STALL POINT				32 18 39 24			
number of cylinders	6.0	bore	(m.m.)	125.03	stroke	(m.m.)	136.00	
con-rod length (m.m.)	217.78	inlet valve closing (degs)	173.0	compressor scale factor	1.18			
ambient temperature (deg k)	313.3	ambient pressure (bar)	0.84	cooler effectiveness	0.9308			
compression ratio	16.30	engine diagram factor	0.9487	turbine flow loss factor	0.8000			
----- compressor gear ratio	9.5500	output shaft gear ratio	1.4450	-----				
engine speed(r.p.m)	1320.00	1190.00	1020.00	730.00	1350.00	1210.00	940.00	740.00
boost pressure ratio	4.976	4.188	3.241	2.485	4.864	4.119	3.606	2.468
delivered air to fuel ratio	29.401	31.955	32.310	35.591	29.362	31.948	33.383	35.799
delivery ratio	0.854	0.854	0.854	0.854	0.854	0.854	0.854	0.854
manifold temp (deg k)	350.453	339.117	326.848	315.423	350.426	339.383	328.244	315.635
engine power (k w.)	240.13	179.76	120.09	59.97	239.99	179.74	120.12	59.97
engine torque (n.m.)	1738.51	1446.32	1124.92	785.90	1699.87	1422.41	1220.65	775.28
b.m.e.p (bar)	21.7862	18.0907	14.1003	9.8378	21.2901	17.7898	15.3043	9.7054
s.f.c. (kg/kw hr)	0.201	0.193	0.197	0.204	0.201	0.193	0.194	0.204
b.thermal eff.	0.4154	0.4320	0.4229	0.4092	0.4151	0.4311	0.4291	0.4091
fuel / rev (ky.)	6.088	4.861	3.870	2.791	5.953	4.790	4.140	2.753
max cyl pressure (bar .)	158.04	156.25	122.29	92.86	156.60	154.07	134.66	92.14
exhaust temperature(deg k)	939.08	850.76	813.66	720.77	938.82	851.60	798.26	719.12
mass flow (ky/min)	23.626	18.484	12.755	7.250	23.596	18.517	12.992	7.294
percentage heat to coolant	10.85	12.41	15.19	20.93	10.86	12.40	15.08	20.87
compressor speed (r.p.m.)	9698.0	8456.5	6833.0	4063.5	9588.0	8251.0	5672.5	3762.5
compressor pressure ratio	5.210	4.403	3.434	2.647	5.101	4.337	3.793	2.631
mass flow (kg/min)	38.180	32.427	26.062	14.612	37.688	31.493	20.268	13.295
compressor power (kw.)	179.84	130.21	81.65	33.73	173.83	124.93	73.63	30.79
compressor torque (n.m)	177.01	146.98	114.06	79.22	173.05	144.53	123.91	78.10
delivery temperature (deg k)	591.00	550.83	499.36	450.83	585.35	548.01	528.58	451.27
compressor efficiency	0.669	0.688	0.707	0.729	0.673	0.688	0.669	0.722
turbine speed (r.p.m)	52533.5	48085.1	41583.7	34298.4	52368.6	48419.5	44951.3	34381.0
turbine pressure ratio	5.087	4.281	3.312	2.525	4.979	4.214	3.670	2.509
mass flow (kg/min)	38.987	33.008	26.459	14.817	38.496	32.076	20.658	13.500
turbine power (kw)	153.10	103.46	61.64	22.87	149.47	100.12	55.25	21.08
turbine torque (n.m)	27.82	20.54	14.15	6.36	27.24	19.74	11.73	5.85
inlet temperature (deg k)	816.24	729.77	661.75	591.17	816.62	734.51	707.69	604.46
turbine nozzle angle	7.906	7.577	7.600	5.452	7.987	7.511	5.494	5.059
turbine efficiency	0.774	0.766	0.757	0.736	0.773	0.765	0.749	0.733
output shaft speed (rpm)	440.00	440.00	440.00	440.00	500.00	500.00	500.00	500.00
output shaft power (kw)	195.89	140.54	91.55	44.85	198.40	142.60	93.66	46.02
output shaft torque (n./m)	4249.51	3048.75	1986.06	973.05	3787.55	2722.26	1787.95	878.56
output shaft sfc (kg/kw.hr)	0.246	0.247	0.259	0.273	0.243	0.244	0.249	0.266
output thermal efficiency	0.3388	0.3377	0.3224	0.3061	0.3432	0.3420	0.3345	0.3140
engine fuel flow (kg/min)	0.804	0.578	0.395	0.204	0.804	0.580	0.389	0.204
dynamic injection(degree ca)	361.5	339.7	342.5	345.6	356.6	339.8	342.1	345.6
duration of injection	30.9	25.0	20.0	15.0	30.5	24.8	21.0	15.0
turbine gear ratio	119.4	109.3	94.5	78.0	104.7	96.8	89.9	68.8
pressure loss in pipe a (bar)	0.10345	0.10345	0.10345	0.10345	0.10345	0.10345	0.10345	0.10345
pressure loss in pipe b (bar)	0.10345	0.10345	0.10345	0.10345	0.10345	0.10345	0.10345	0.10345
pressure loss in pipe c (bar)	0.10345	0.10345	0.10345	0.10345	0.10345	0.10345	0.10345	0.10345
pressure loss in pipe d (bar)	0.10345	0.10345	0.10345	0.10345	0.10345	0.10345	0.10345	0.10345

Table-4.5a

CUMMINS L10 D C E

30 26 28 24

number of cylinders	6.0	bore	(m.m.)	125.03	stroke	(m.m.)	136.00	
con-rod length (m.m.)	217.78	inlet valve closing (degs)		193.0	compressor scale factor		1.18	
ambient temperature (deg k)	313.3	ambient pressure (bar)		0.84	cooler effectiveness		0.8635	
compression ratio	16.30	engine diagram factor		0.9263	turbine flow loss factor		0.8000	
----- compressor gear ratio	9.5500	output shaft gear ratio		1.4450	-----			
engine speed(r.p.m)	1475.00	1305.00	1140.00	1000.00	1805.00	1655.00	1525.00	1375.00
boost pressure ratio	4.623	3.836	2.940	1.980	3.635	2.968	2.327	1.473
delivered air to fuel ratio	30.114	31.086	31.854	37.312	28.588	29.013	31.717	34.545
delivery ratio	0.854	0.854	0.854	0.853	0.853	0.852	0.852	0.852
manifold temp (deg k)	355.252	342.692	327.426	317.128	352.018	340.334	328.427	317.233
engine power (k w.)	239.92	180.19	120.07	59.98	240.07	180.01	119.99	59.88
engine torque (n.m.)	1555.81	1318.87	1006.50	573.71	1271.37	1039.95	752.40	417.24
b.m.e.p (bar)	19.4799	16.5361	12.6133	7.1828	15.9287	13.0259	9.4233	5.2158
s.f.c. (kg/kw hr)	0.201	0.197	0.201	0.211	0.205	0.208	0.214	0.232
b.thermal eff.	0.4156	0.4242	0.4157	0.3961	0.4076	0.4005	0.3900	0.3590
fuel / rev (kg.)	5.441	4.525	3.522	2.105	4.535	3.775	2.804	1.686
max cyl pressure (bar .)	157.47	143.49	110.83	73.58	136.42	113.05	88.63	55.87
exhaust temperature(deg k)	925.26	870.32	825.26	713.31	949.60	916.05	840.42	755.82
mass flow (kg/min)	24.167	18.357	12.790	7.854	23.404	18.127	13.565	8.009
percentage heat to coolant	10.80	12.51	15.23	20.03	10.92	12.52	14.67	19.78
compressor speed (r.p.m.)	7146.8	5523.3	3947.6	2610.6	6663.4	5230.9	3989.4	2556.9
compressor pressure ratio	4.875	4.064	3.146	2.164	3.921	3.231	2.568	1.688
mass flow (kg/min)	25.373	19.261	13.590	8.511	24.537	19.119	14.369	8.537
compressor power (kw.)	118.50	77.54	42.12	15.73	90.11	57.74	31.66	11.11
compressor torque (n.m)	158.27	134.00	101.84	57.53	129.08	105.37	75.75	41.46
delivery temperature (deg k)	588.69	551.42	497.37	423.64	530.87	492.74	444.64	391.10
compressor efficiency	0.641	0.641	0.656	0.700	0.681	0.691	0.736	0.651
turbine speed (r.p.m)	54894.0	50982.5	44210.8	30811.5	52510.1	46917.1	39521.8	23099.7
turbine pressure ratio	4.752	3.941	3.023	2.041	3.798	3.109	2.445	1.566
mass flow (kg/min)	26.177	19.853	13.992	8.723	25.358	19.746	14.800	8.771
turbine power (kw)	109.31	68.23	36.03	11.41	94.01	59.14	30.91	6.09
turbine torque (n.m)	19.01	12.77	7.78	3.54	17.09	12.03	7.47	2.52
inlet temperature (deg k)	910.97	856.90	807.91	672.84	932.55	896.65	820.65	735.47
turbine nozzle angle	6.036	5.407	4.919	4.615	7.519	7.119	6.716	6.153
turbine efficiency	0.760	0.750	0.737	0.724	0.760	0.751	0.741	0.732
output shaft speed (rpm)	1050.00	1050.00	1050.00	1050.00	1600.00	1600.00	1600.00	1600.00
output shaft power (kw)	215.44	159.52	106.24	51.03	228.40	169.62	110.66	49.45
output shaft torque (n./m)	1958.49	1450.12	965.76	463.86	1362.56	1011.95	660.17	295.00
output shaft sfc (kg/kw.hr)	0.224	0.222	0.227	0.248	0.215	0.221	0.232	0.281
output thermal efficiency	0.3732	0.3755	0.3678	0.3369	0.3878	0.3774	0.3597	0.2965
engine fuel flow (kg/min)	0.803	0.591	0.402	0.211	0.819	0.625	0.428	0.232
dynamic injection(degree ca)	347.1	340.0	342.9	345.8	339.0	340.6	342.6	345.1
duration of injection	28.9	24.0	18.8	13.9	26.0	22.1	17.8	13.4
turbine gear ratio	52.3	48.6	42.1	29.3	32.8	29.3	24.7	14.4
pressure loss in pipe a (bar)	0.10345	0.10345	0.10345	0.10345	0.10345	0.10345	0.10345	0.10345
pressure loss in pipe b (bar)	0.10345	0.10345	0.10345	0.10345	0.10345	0.10345	0.10345	0.10345
pressure loss in pipe c (bar)	0.10345	0.10345	0.10345	0.10345	0.10345	0.10345	0.10345	0.10345
pressure loss in pipe d (bar)	0.10345	0.10345	0.10345	0.10345	0.10345	0.10345	0.10345	0.10345

Table-4.5b

CUMMINS L10 D C C

DESIGN POINT

34 33 32 24

number of cylinders	6.0	bore	(m.m.)	125.03	stroke	(m.m.)	136.00	
con-rod length (m.m.)	217.78	inlet valve closing (degs)		193.0	compressor scale factor		1.18	
ambient temperature (deg k)	313.3	ambient pressure (bar)		0.84	cooler effectiveness		0.8197	
compression ratio	16.30	engine diagram factor		0.9095	turbine flow loss factor		0.8000	
----- compressor gear ratio	9.5500	output shaft gear ratio		1.4450	-----			
engine speed(r.p.m)	1990.00	1860.00	1730.00	1585.00	2180.00	2065.00	1930.00	1818.00
boost pressure ratio	3.234	2.669	2.067	1.310	2.904	2.428	1.837	1.298
delivered air to fuel ratio	27.728	28.763	31.069	33.146	27.239	28.329	29.740	31.295
delivery ratio	0.852	0.852	0.851	0.851	0.851	0.851	0.851	0.850
manifold temp (deg k)	350.328	339.131	327.942	317.108	348.576	338.189	327.419	318.975
engine power (k w.)	240.82	179.92	117.92	59.81	240.79	179.80	119.79	71.25
engine torque (n.m.)	1153.18	925.33	663.24	361.96	1052.67	833.47	594.51	376.13
b.m.e.p (bar)	14.4925	11.5846	8.3015	4.5190	13.2279	10.4273	7.4332	4.6936
s.f.c. (kg/kw hr)	0.207	0.213	0.220	0.248	0.208	0.219	0.228	0.250
b.thermal eff.	0.4028	0.3918	0.3787	0.3361	0.4007	0.3814	0.3655	0.3343
fuel / rev (kg.)	4.176	3.432	2.544	1.561	3.832	3.174	2.361	1.630
max cyl pressure (bar .)	128.12	101.19	78.75	50.10	126.14	91.13	69.85	49.80
exhaust temperature(deg k)	964.66	926.42	856.83	782.49	968.74	941.04	884.98	826.25
mass flow (kg/min)	23.043	18.361	13.674	8.198	22.752	18.565	13.550	9.272
percentage heat to coolant	10.97	12.40	14.58	19.49	11.02	12.29	14.63	18.15
compressor speed (r.p.m.)	6447.4	5205.9	3964.4	2579.7	6279.2	5181.0	3891.7	2822.1
compressor pressure ratio	3.539	2.953	2.328	1.543	3.229	2.732	2.116	1.555
mass flow (kg/min)	24.105	19.340	14.490	8.737	23.816	19.424	14.346	9.860
compressor power (kw.)	78.99	50.94	27.71	9.65	70.19	45.68	24.33	10.99
compressor torque (n.m)	116.94	93.39	66.72	35.72	106.69	84.16	59.67	37.16
delivery temperature (deg k)	507.78	470.03	427.42	379.42	488.45	453.41	414.58	379.98
compressor efficiency	0.696	0.722	0.749	0.627	0.708	0.742	0.739	0.633
turbine speed (r.p.m)	51084.9	45533.5	37158.1	17968.1	49347.3	43948.7	34905.0	19023.8
turbine pressure ratio	3.417	2.830	2.205	1.421	3.107	2.609	1.994	1.432
mass flow (kg/min)	24.939	19.983	14.935	8.987	24.656	20.086	14.807	10.160
turbine power (kw)	86.69	55.39	27.58	3.87	79.29	52.01	23.84	4.92
turbine torque (n.m)	16.20	11.61	7.09	2.05	15.34	11.30	6.52	2.47
inlet temperature (deg k)	947.03	906.10	835.37	760.24	950.02	922.18	862.00	802.63
turbine nozzle angle	8.359	8.039	7.846	11.801	9.184	8.970	9.209	13.292
turbine efficiency	0.760	0.752	0.743	0.742	0.760	0.753	0.745	0.747
output shaft speed (rpm)	1900.00	1900.00	1900.00	1900.00	2200.00	2200.00	2200.00	2200.00
output shaft power (kw)	232.04	172.14	110.87	48.12	233.33	173.67	110.10	58.34
output shaft torque (n.m)	1165.72	864.81	557.01	241.74	1012.38	753.52	477.70	253.14
output shaft sfc (kg/kw.hr)	0.215	0.223	0.238	0.308	0.215	0.226	0.248	0.305
output thermal efficiency	0.3881	0.3748	0.3502	0.2704	0.3883	0.3684	0.3359	0.2737
engine fuel flow (kg/min)	0.831	0.638	0.440	0.247	0.835	0.655	0.456	0.296
dynamic injection(degree ca)	335.2	341.6	343.0	344.5	326.6	342.6	343.7	344.6
duration of injection	25.0	21.3	17.5	14.0	24.3	21.3	17.7	14.9
turbine gear ratio	26.9	24.0	17.6	9.5	22.4	20.0	15.9	8.6
pressure loss in pipe a (bar)	0.10345	0.10345	0.10345	0.10345	0.10345	0.10345	0.10345	0.10345
pressure loss in pipe b (bar)	0.10345	0.10345	0.10345	0.10345	0.10345	0.10345	0.10345	0.10345
pressure loss in pipe c (bar)	0.10345	0.10345	0.10345	0.10345	0.10345	0.10345	0.10345	0.10345
pressure loss in pipe d (bar)	0.10345	0.10345	0.10345	0.10345	0.10345	0.10345	0.10345	0.10345

Table-4.5c

Fig-4.6 Design and stall operation under extreme altitude de-rating

CUMMINS L10 D C E	STALL POINT	Design point	8	8	6	6
number of cylinders	6.0	bore (m.m.)	125.03	stroke (m.m.)	136.00	
con-rod length (m.m.)	217.75	inlet valve closing (deg)	173.0	compressor scale factor	1.18	
ambient temperature (deg k)	294.4	ambient pressure (bar)	0.70	cooler effectiveness	0.7512	
compression ratio	16.30	engine diagram factor	0.8886	turbine flow loss factor	0.8000	
----- compressor gear ratio	9.5500	output shaft gear ratio	1.4450	-----		
engine speed(r.p.m)	1320.00	2255.00				
boost pressure ratio	5.882	3.311				
delivered air to fuel ratio	31.200	27.411				
delivery ratio	7.954	0.851				
manifold temp (deg k)	338.347	333.970				
engine power (k w.)	240.30	240.00				
engine torque (n.m.)	1739.51	1017.66				
b.m.e.p (bar)	21.8016	12.7460				
s.f.c. (kg/kw hr)	0.192	0.213				
b.thermal eff.	0.4343	0.3917				
fuel / rev (kg.)	5.827	3.775				
max cyl pressure (bar.)	157.98	115.94				
exhaust temperature(deg k)	879.77	967.79				
mass flow (kg/min)	23.999	23.336				
percentage heat to coolant	10.58	10.64				
compressor speed (r.p.m.)	9698.0	6995.5				
compressor pressure ratio	6.175	3.729				
mass flow (kg/min)	33.306	23.352				
compressor power (kw.)	179.83	75.50				
compressor torque (n.m)	177.00	103.02				
delivery temperature (deg k)	612.65	486.84				
compressor efficiency	0.621	0.676				
turbine speed (r.p.m)	55595.9	52235.5				
turbine pressure ratio	6.027	3.582				
mass flow (kg/min)	34.078	24.207				
turbine power (kw)	144.68	99.01				
turbine torque (n.m)	24.84	16.27				
inlet temperature (deg k)	810.80	967.50				
turbine nozzle angle	6.988	9.529				
turbine efficiency	0.776	0.766				
output shaft speed (rpm)	440.00	2200.00				
output shaft power (kw)	188.04	236.91				
output shaft torque (n./m)	4079.35	1027.90				
output shaft sfc (kg/kw.hr)	0.245	0.216				
output thermal efficiency	0.3398	0.3869				
engine fuel flow (kg/min)	0.769	0.851				
dynamic injection(degree ca)	357.1	331.9				
duration of injection	27.8	24.5				
turbine gear ratio	126.4	23.7				
pressure loss in pipe a (bar)	0.10345	0.10345				
pressure loss in pipe b (bar)	0.10345	0.10345				
pressure loss in pipe c (bar)	0.10345	0.10345				
pressure loss in pipe d (bar)	0.10345	0.10345				

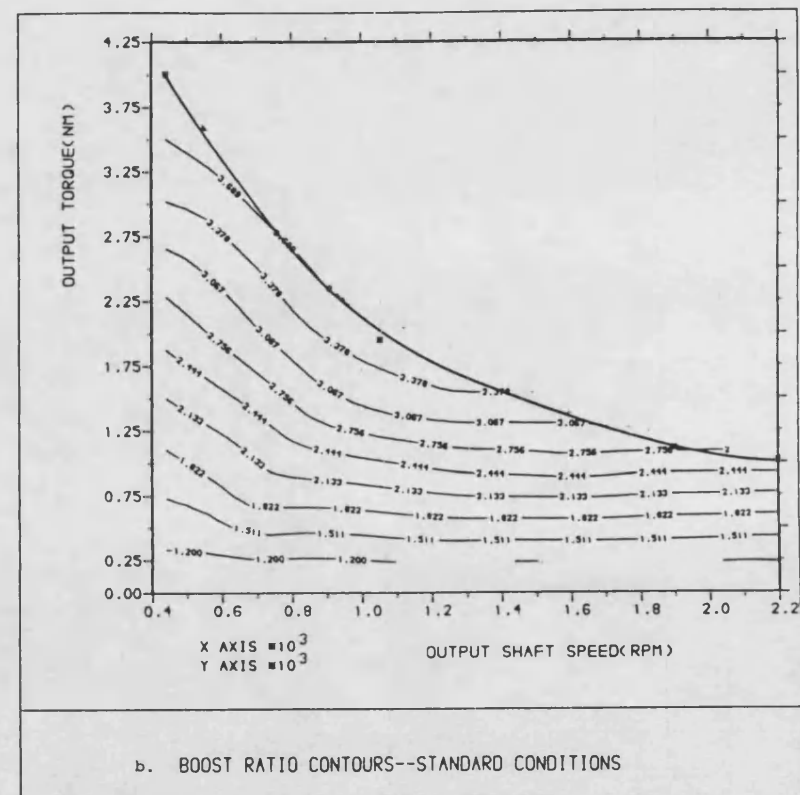
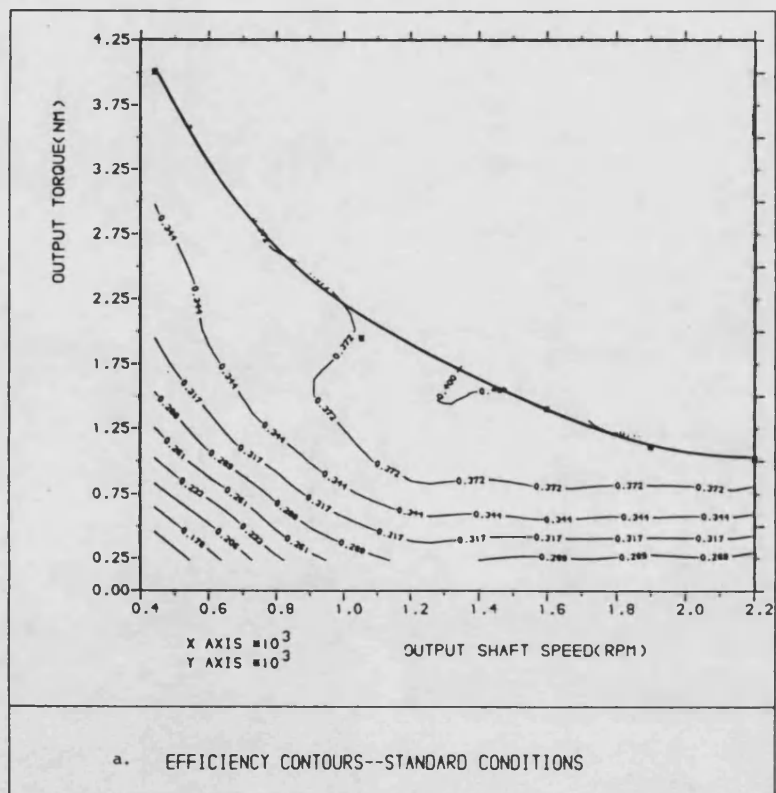
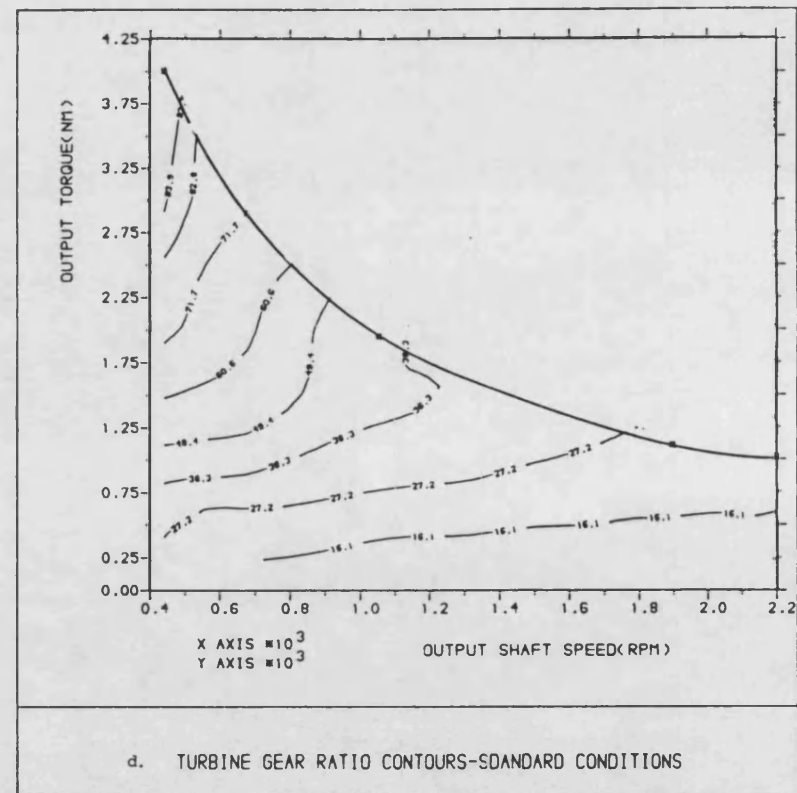
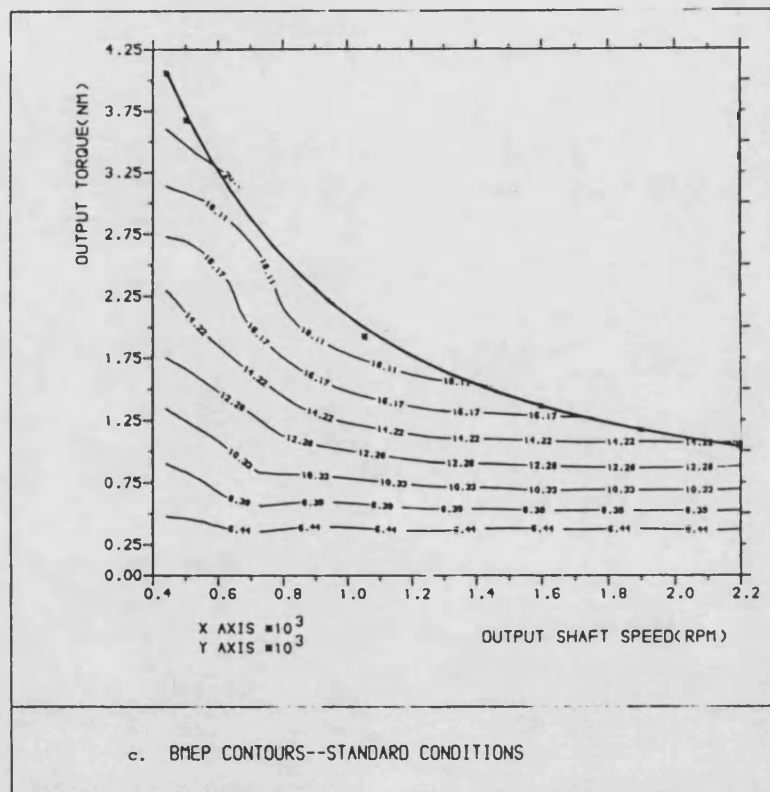


Fig-4.1(a-e) The characteristics of the DCE with variable nozzle turbine (standard map, standard conditions)



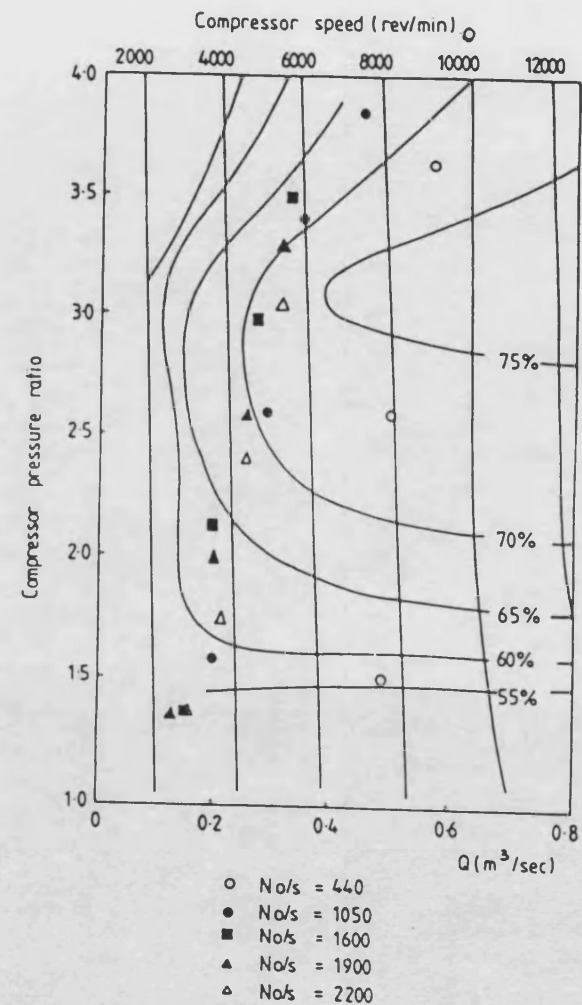
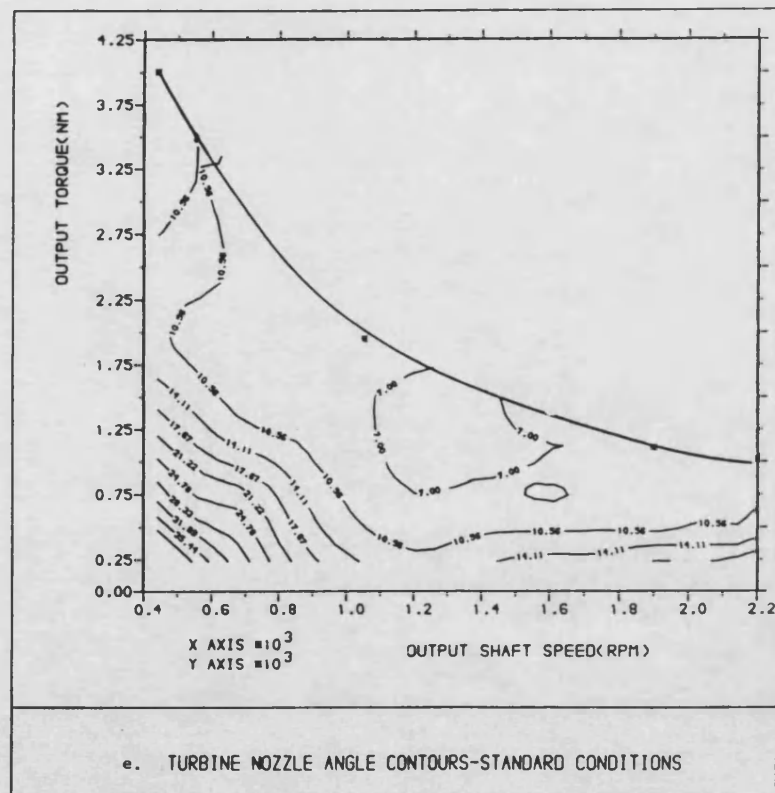
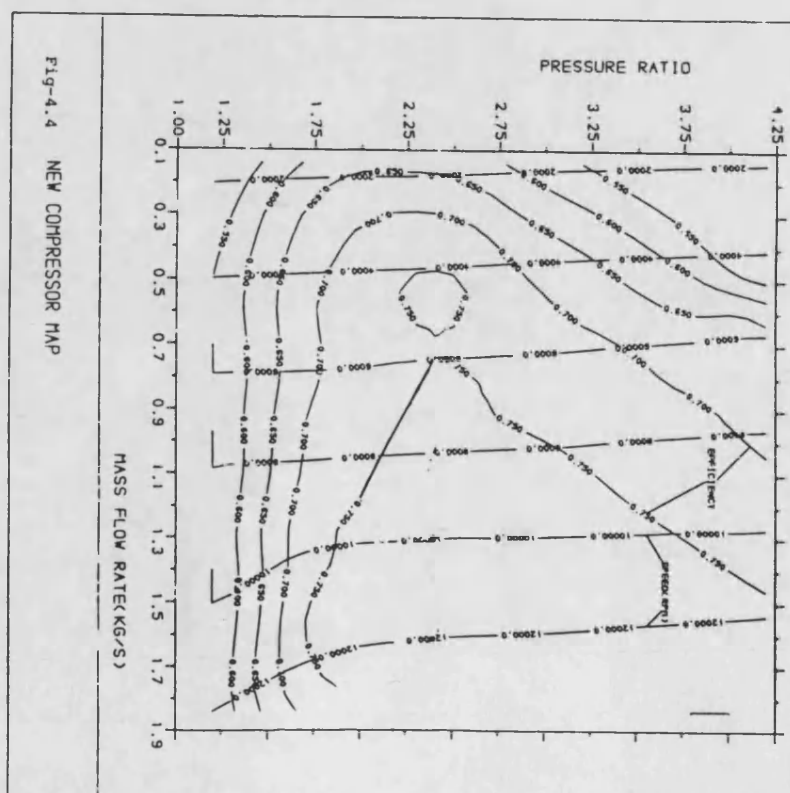
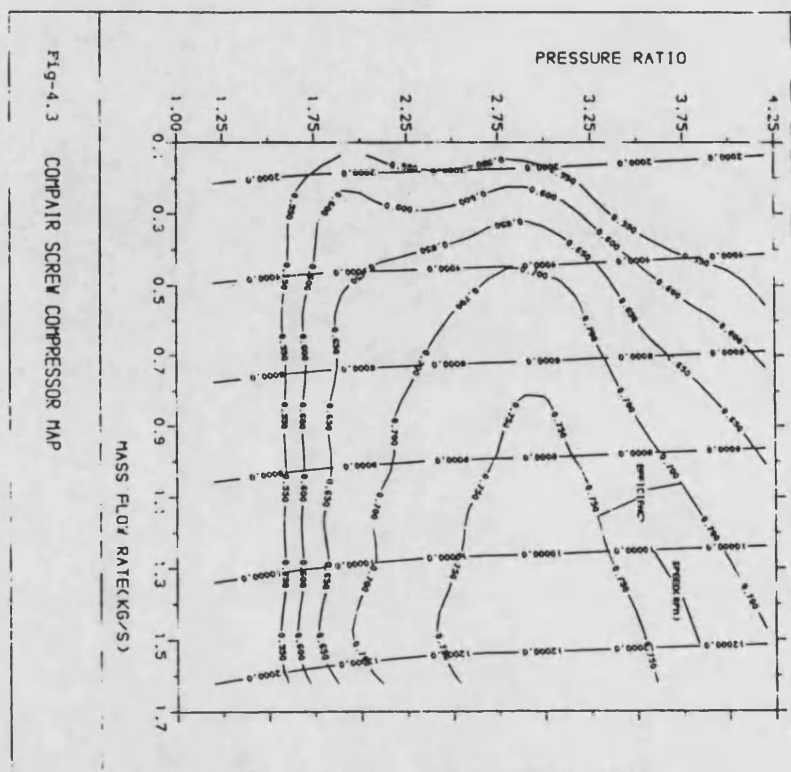


Fig-4.2 COMPRESSOR CHARACTERISTICS WITH OPERATING POINTS



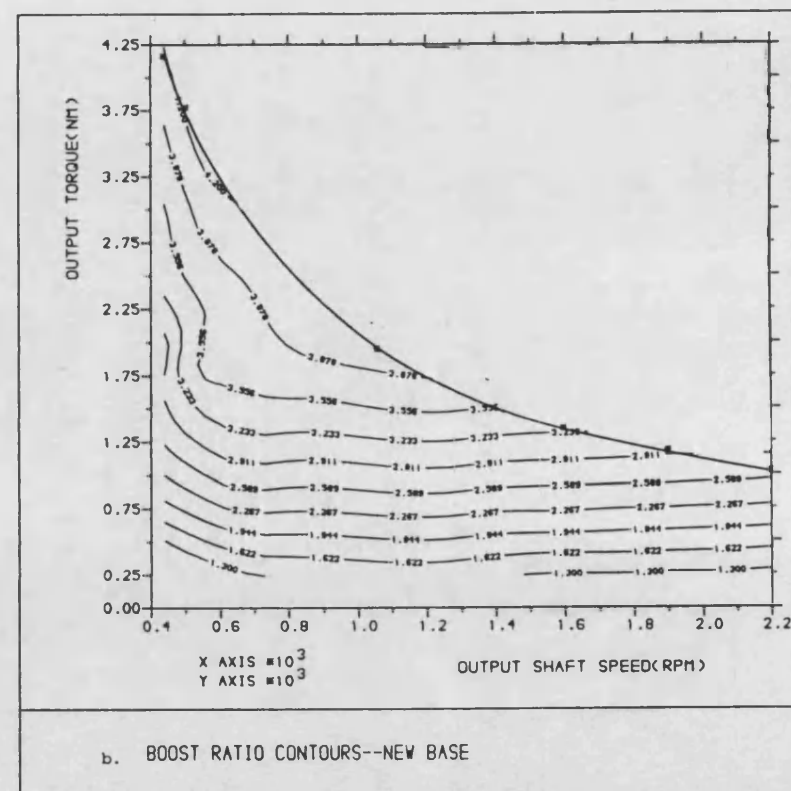
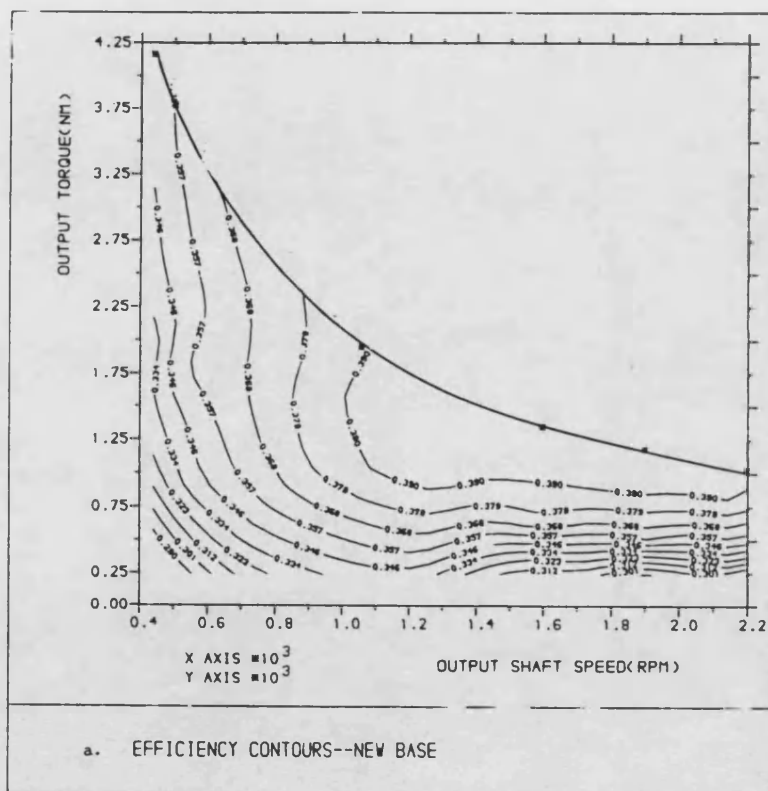
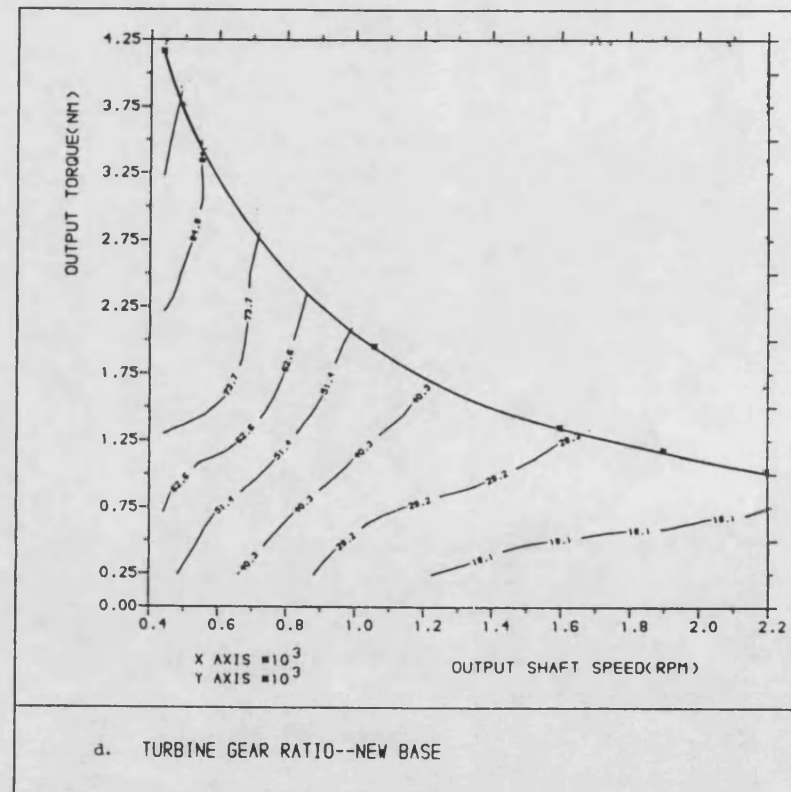
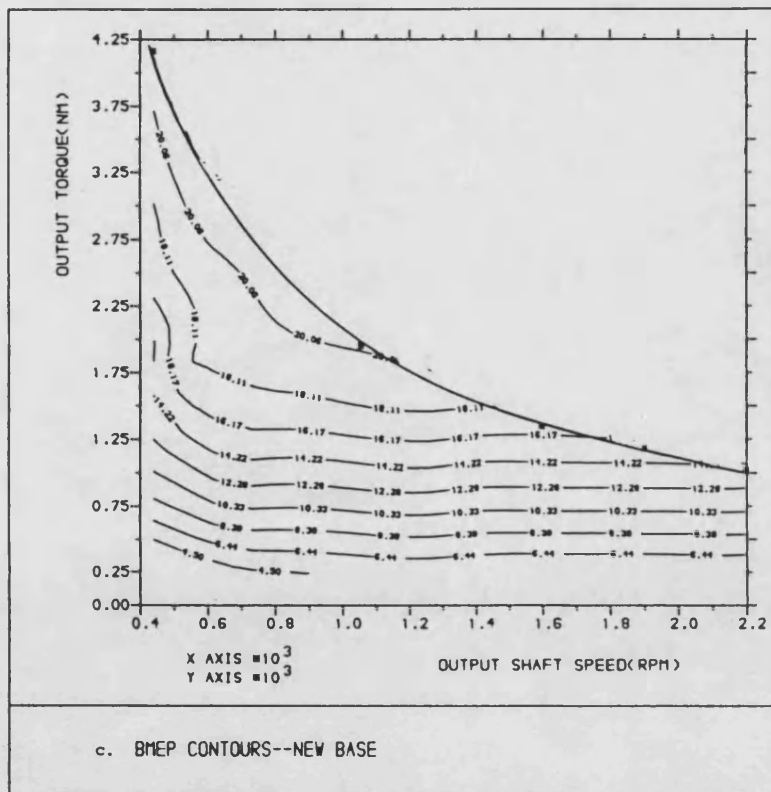


Fig-4.5(a-e) The characteristics of the DCE with variable nozzle turbine (new map, opt. speed, standard conditions)



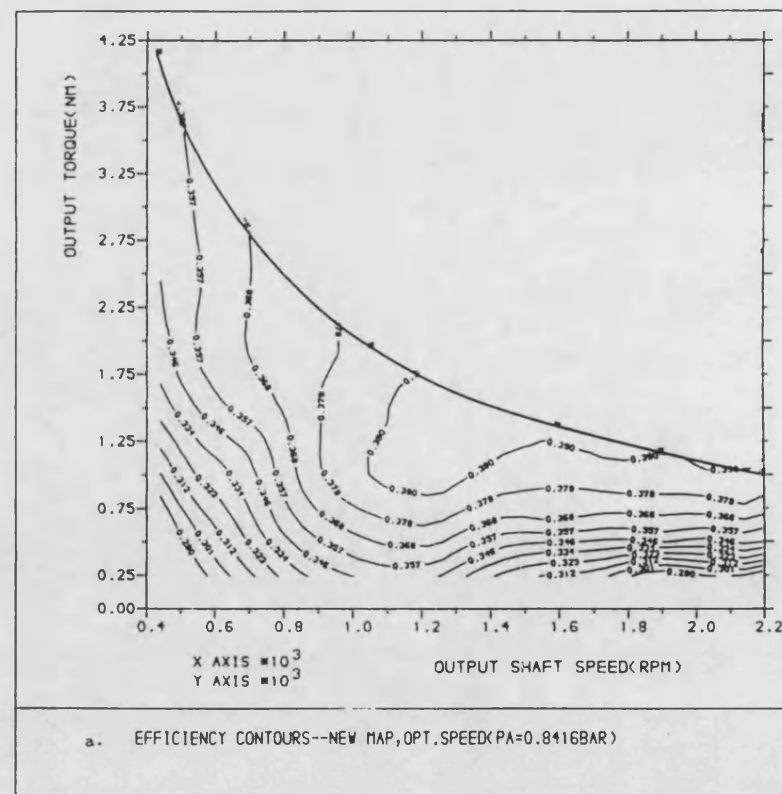
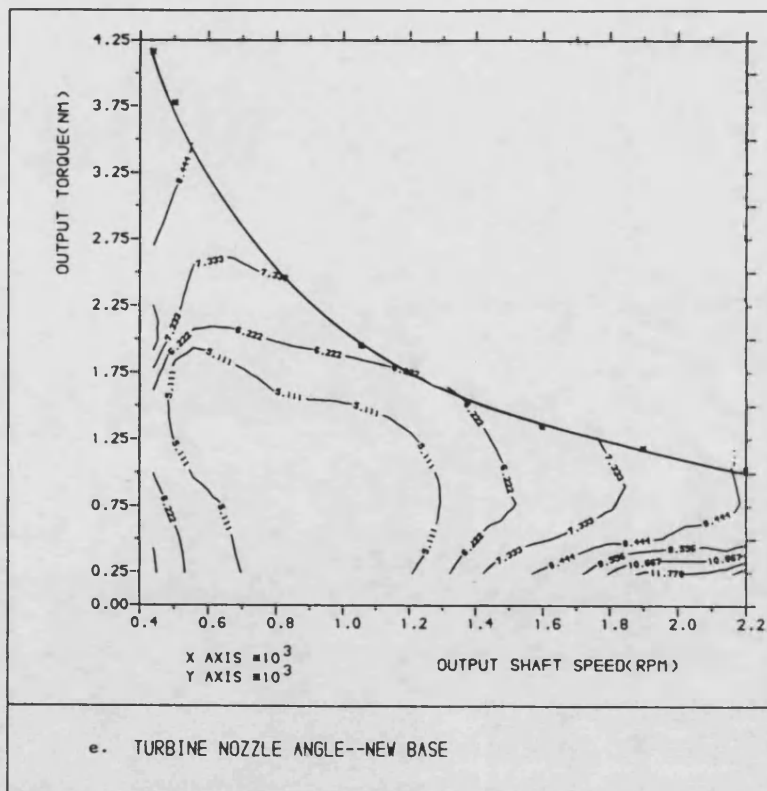
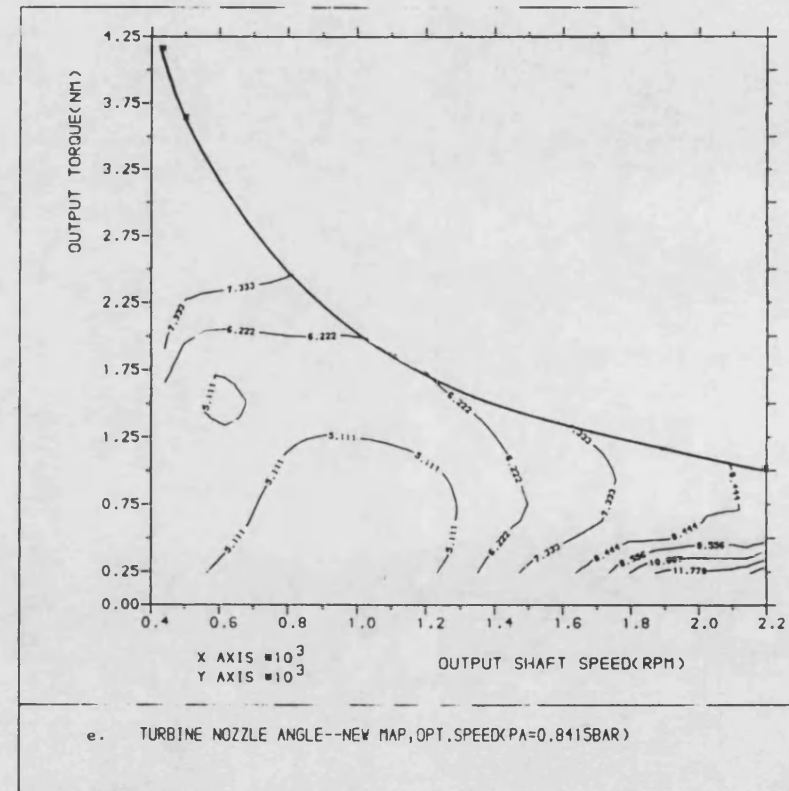
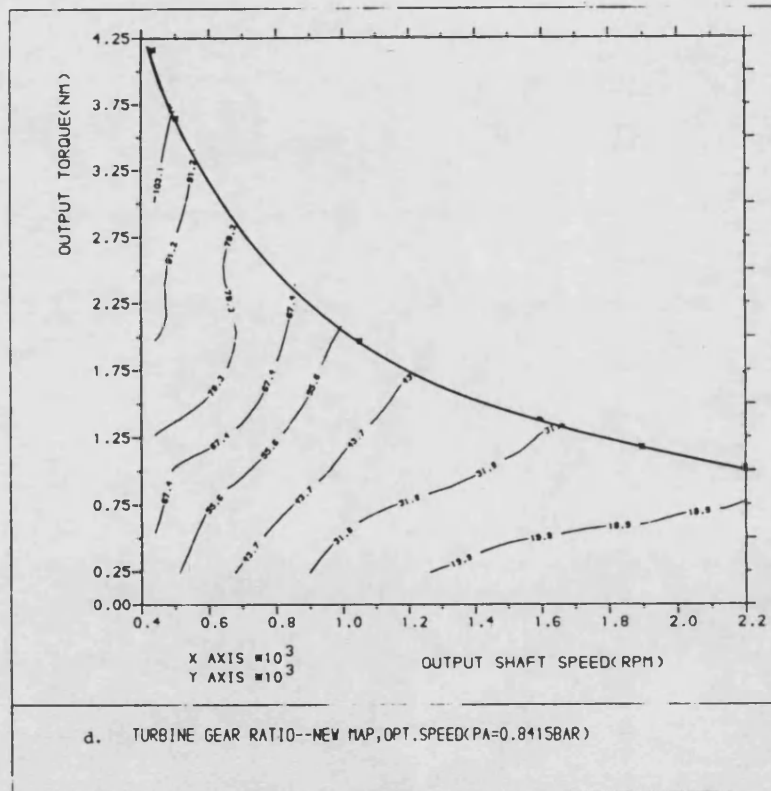


Fig-4.6(a-e) The characteristics of the DCE with variable nozzle turbine (new map, opt. speed, reduced Pa)



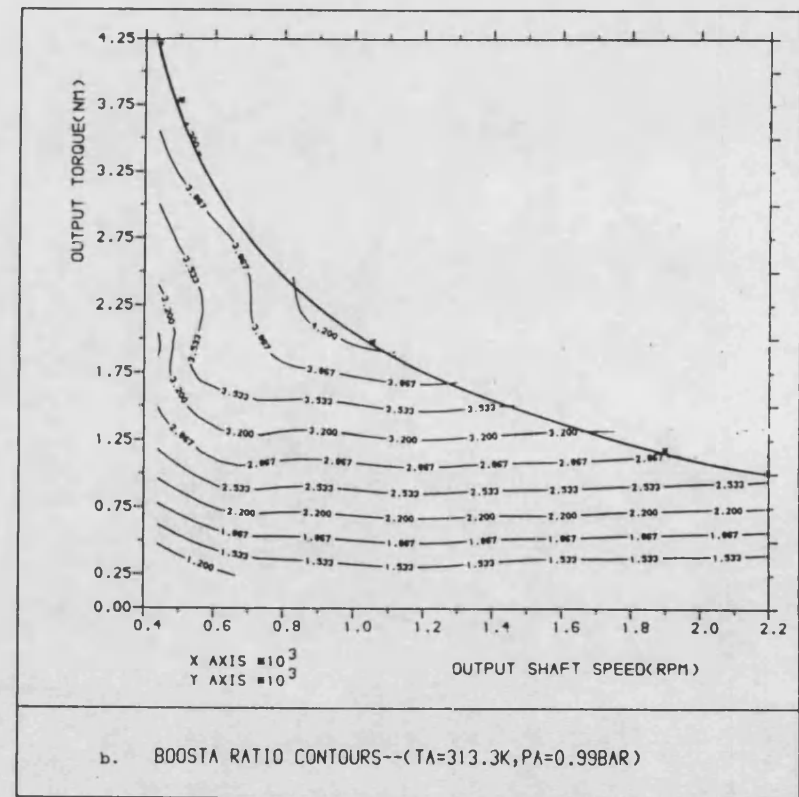
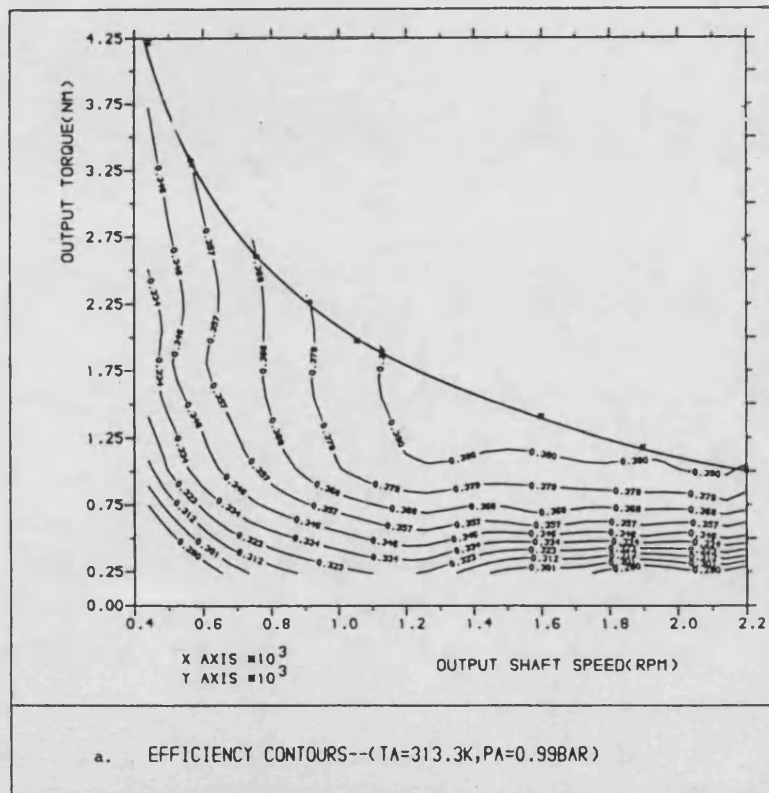
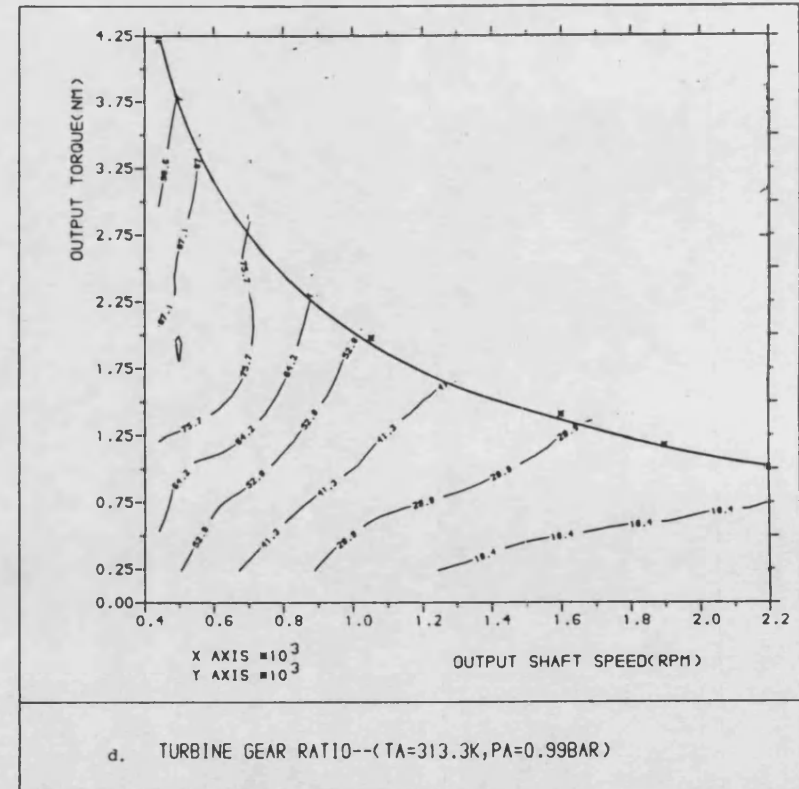
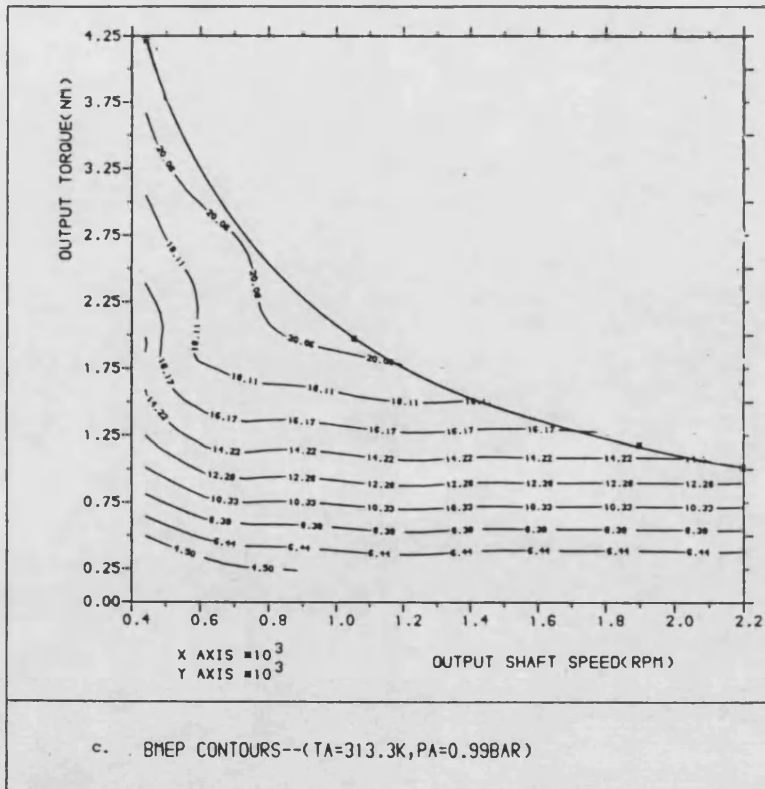


Fig-4.7(a-e) The characteristics of the DCE with variable nozzle turbine(new map, opt. speed, elevated T_a)



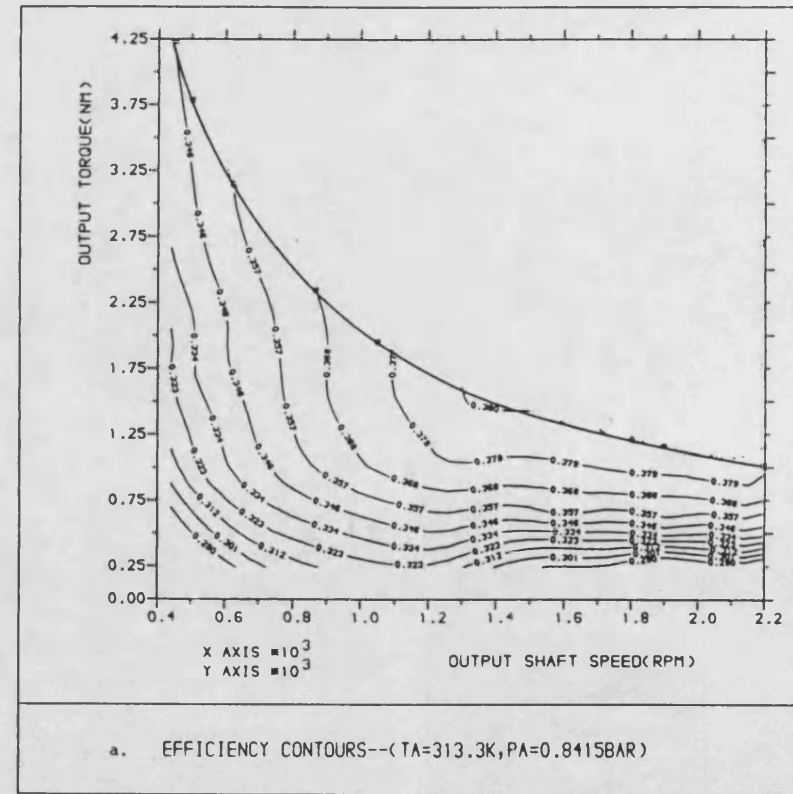
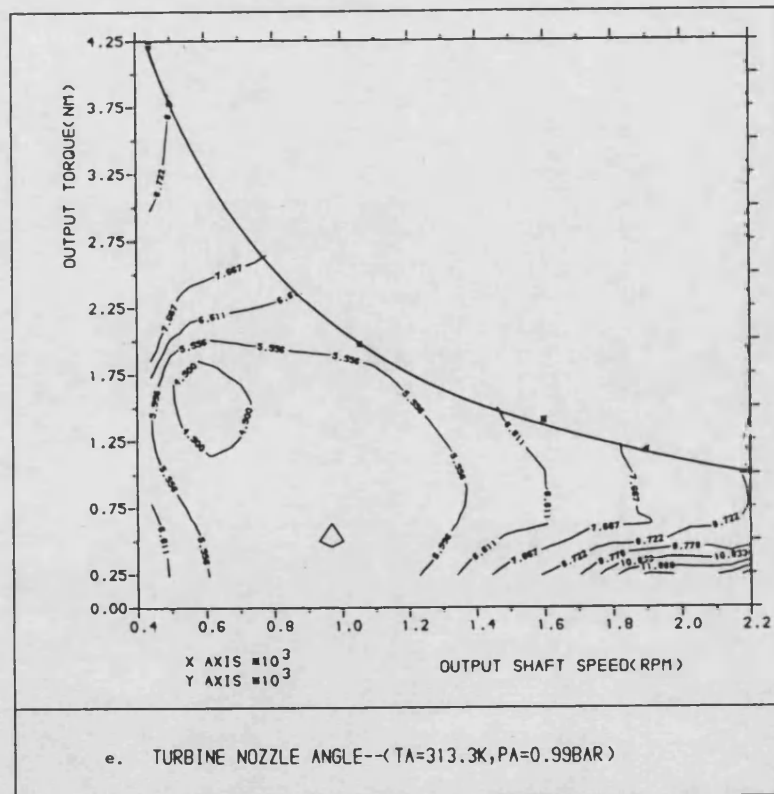
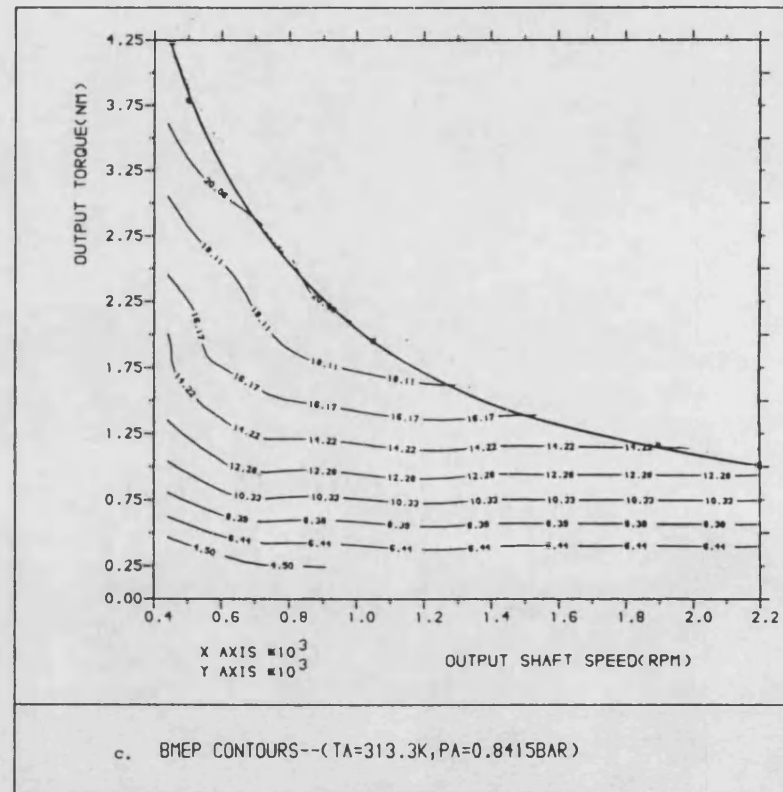
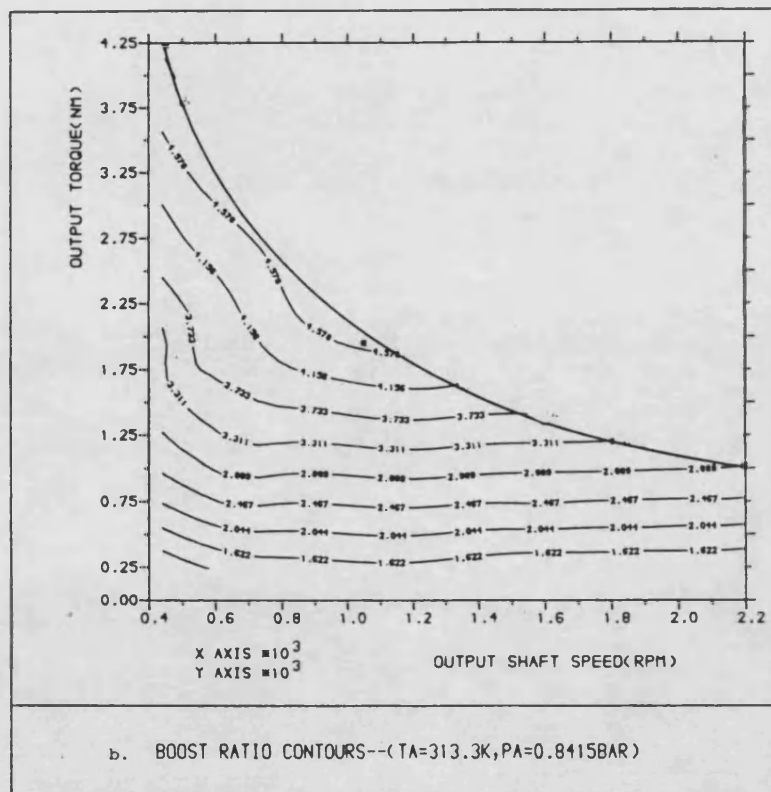
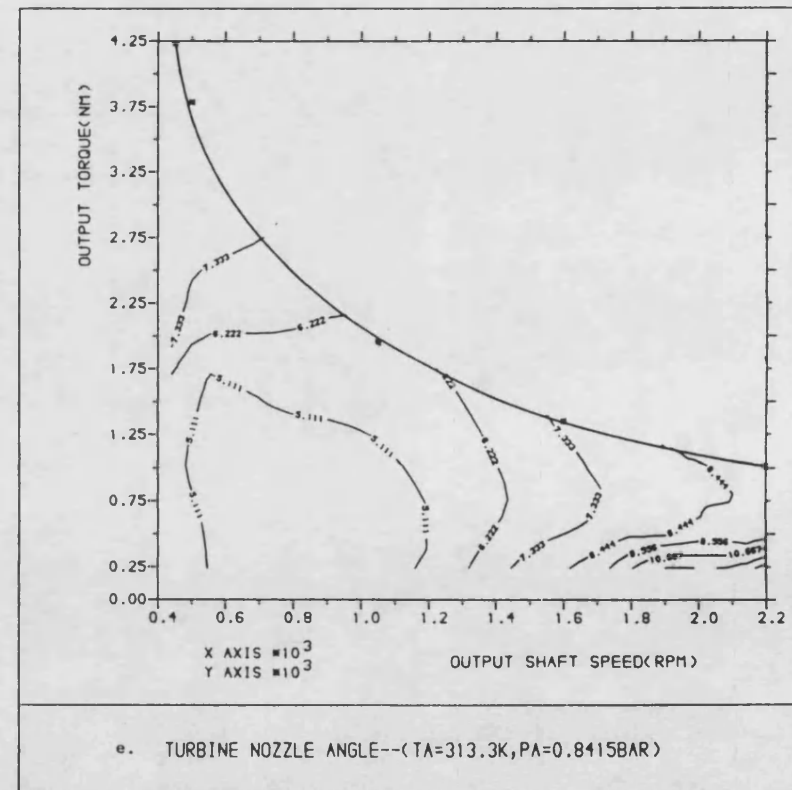
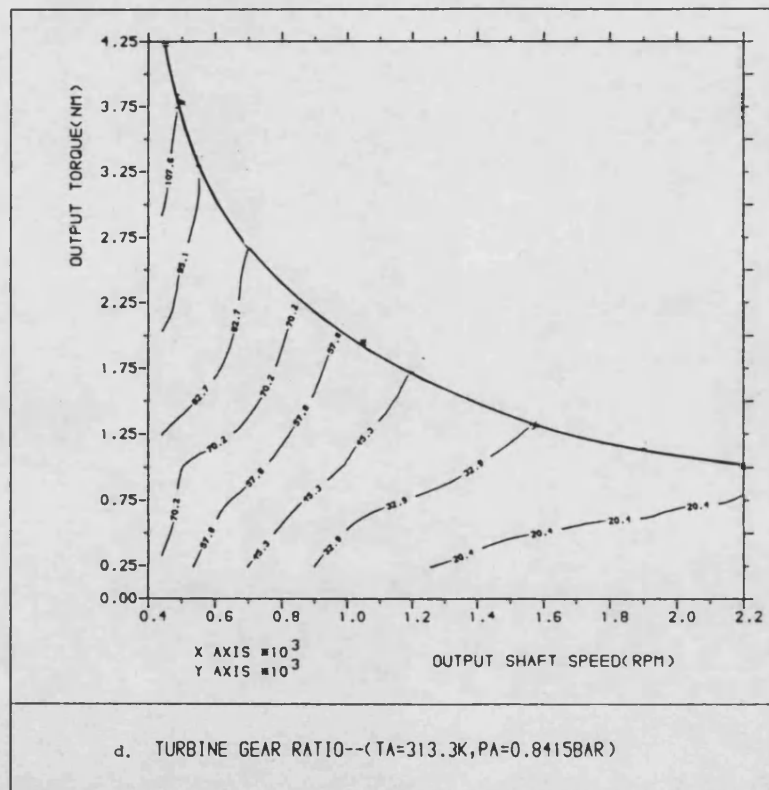


Fig-4.8(a-e) The characteristics of the DCE with variable nozzle turbine(new map, opt. speed, reduced Pa, elevated Ta)





CHAPTER 5

OPERATION OF THE DCE

WITH FIXED GEOMETRY(FG) TURBINE

The variable nozzle turbine was originally considered to be essential to achieve a satisfactory match under all operating conditions. However, detailed inspection of the results of section-4.2, and particularly of Fig-4.1e shows that the variation of turbine nozzle angle becomes significant only at low loads and speeds. This leads to the present study of the possibility of using a fixed geometry turbine.

5.1 Standard Steady State Operation

(standard condition, $P_a=0.99\text{bar}$, $T_a=294.4\text{K}$)

5.1.1 Performance Calculation

As indicated earlier, the present calculation is based on the steady (standard) state results of VG turbine scheme in section-4.2. The nozzle angle at the design point is used, Table-4.1c column 5, at an output shaft speed of 2200rpm and an engine power of 240kw, i.e. 8.886 degrees. The computation is carried out at the same output shaft speed points, i.e. 440, 500, ..., 2200rev/min. and the corresponding engine power, i.e. 240,180,120 and 60kw at each speed. Under these conditions relevant comparisons can be made of overall system efficiency(between the VG scheme and the FG scheme).

The program for this purpose has been described in chapter-2. It is obvious that with a fixed nozzle turbine the degrees of freedom of the system are reduced, i.e. only two variables, engine speed and turbine gear ratio have to be evaluated in the optimisation process. The strategy in the program is to take the engine speed as the iterating variable and execute the computation over a reasonable range of turbine gear ratios. For a specific turbine gear ratio, the correct engine speed will be reached when the mass flow balance between the engine, compressor, bypass and the turbine is satisfied. The combination of engine speed and turbine gear ratio, which

gives best overall efficiency, will be the optimal condition for that particular output shaft speed and load requirement.

The procedure outlined above is quite straightforward and the program performs very satisfactorily in most cases, particularly at high power and low output shaft speed. However in one or two cases at lower power and higher output shaft speed, i.e. engine power of 1/4 maximum value, output shaft speed of 2200 rev/min and/or 1900 rev/min, the engine speed and turbine gear ratio are very sensitive to each other. In such a situation the calculation has to be proceeded with by 'trial and error'.

The problem encountered is that at a higher output shaft speed and lower power, the available exhaust energy is very low. In order to ensure normal operation of the turbine a certain level of inlet pressure must be provided. This may be adjusted, to a certain extent, by decreasing the engine speed, which has a direct relation with BMEP under conditions of fixed power and also affects the boost level. On the other hand, the demand for air flow requires an increase in engine speed. Inspection of a typical radial turbine performance map shows that at low pressure ratio, the speed of the turbine has greater influence on its mass flow rate than at higher pressure ratio. As a result, the range of engine speed and turbine gear ratio is very narrow and the failure in turbine subroutine and engine subroutine can occur even with a very small degree of mismatch between them.

5.1.2 Presentation of Results

The performance results are tabulated in Table-5.1(a-c) and some important parameters are presented on Fig-5.1(a-d) contour plots. In assessing the system operation with fixed nozzle turbine, the present results will be compared with the standard(VG) ones (Table-5.1).

a) Limiting Torque Curve Results

On the limiting torque curve, the engine still operates at constant power over the entire output shaft speed range.

It would be expected that the data at the design point would be the same for both sets. However differences do exist (see Table-5.1c and Table-4.1c). It can be seen the engine speed is a little higher(2116rpm cf. 2100rpm). This is due to a slight difference in the engine power, and probably the accuracy of the nozzle angle. Moreover, engine speed is the iterating variable in the present case rather than

turbine nozzle angle as in the case with the variable nozzle turbine. This inevitably affects the numerical results. From the slightly higher mass flow rate, as well as the change in engine speed, it can be deduced that the exact turbine nozzle angle would be a little smaller.

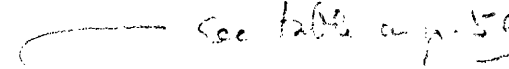
The air/fuel ratio is slightly lower(29.925 cf. 30.575). This stems from the lower boost(2.601 cf. 2.638) and delivery ratio. The output thermal efficiency is slightly higher(0.3914 cf. 0.3907), therefore the results can be considered optimal. Generally the two sets of data do not differ significantly.

At the stall point, because of the decrease in turbine nozzle angle(8.886 cf. 9.698deg.), the engine speed is substantially decreased(1292.6 cf. 1350rpm). Although the output power is lower(184.74 cf. 186.55), the output efficiency is higher(34.77% cf. 34.61%). This is due to higher engine efficiency(0.4552 cf. 0.4485), which is the result of higher BMEP(22.4073 cf. 21.4477bar) and lower engine speed, although it is probably an overestimate.

By examining the data at other output shaft speeds, it can be seen that the system performance over the limiting torque curve is almost unchanged, due to relatively small changes in the turbine nozzle angle(see Fig-4.4e) as already pointed out.

b)Part Load Results

The most significant differences occur at low speeds and low loads, because it is only under these conditions that, for the VG turbine scheme, nozzle angles become large, e.g. 36.664deg. at an output shaft speed of 440rpm and 1/4 load. The minimum engine speed chosen for that condition was 1100rpm. Obviously, if nozzle angle is to be held fixed at 8.886deg., the system operation will change drastically, as is indeed the case:



See table on p. 59

	VG	FG
O/S speed(rpm)	440	440
Eng.power(kw)	60.11	60.25
Nozzle angle(deg.)	36.664	8.886

	VG	FG
Eng.speed(rpm)	1100	771.2
Eng.eff.(%)	40.93	41.7
BMEP(bar)	6.54	9.36
A/F ratio	35.87	30.79
boost ratio	1.337	1.895
Comp.speed(rpm)	7597.	4456.9
Comp.power(kw)	41.68	35.19
Comp.mass flow(kg/min)	38.98	20.56
Turb.gear ratio	28.6	62.0
Turb.power(kw)	8.36	18.63
O/S power(rpm)	23.16	39.68
O/S eff.	0.1577	0.2747

Clearly, the engine speed has substantially decreased while BMEP and boost ratio have increased. The compressor speed, compressor mass flow rate hence compressor power have also decreased. Further, turbine power has increased substantially due to its higher speed(gear ratio) and pressure ratio(relating to boost ratio). These lead to a significant increase in output power and output efficiency(more than 10 percentage points). It may also be concluded that the VG operating point has not been truly optimised as a result of a lower limit being set for engine speed (1100rpm).

If such low engine speeds are admissible, at MEP levels which are still significant(BMEP of 9.36bar in the present case) the fixed nozzle scheme will prove acceptable.

At an engine power of 60kw and an output shaft speed of 2200rpm (Table-5.1c), the mass flow capacity of the engine exceeds that of the compressor(10.006 cf. 8.907), which results in a certain amount of reverse flow in the bypass duct. As can be seen, the turbine efficiency is extremely low(0.306). One of the reasons for this is to operate the turbine deliberately at a lower speed(smaller turbine gear ratio) to increase its mass flow capacity, therefore reducing circulation through the bypass. Nevertheless, since the energy available to the turbine is very low, this effect is not

significant(turbine power 1.34kw; still very low even with higher efficiency). It should also be noted that it is not correct to compare the two sets of data directly at this particular point, because the engine power level is different(60kw cf. 71kw). Due to the circulation of the exhaust gas, the inlet manifold temperature is increased and the delivery ratio is reduced, apart from the energy loss through the intercooler. However the delivered air/fuel ratio is higher(40.232), due to the comparatively lower fuel flow. More importantly, the output efficiency is quite acceptable(0.2668 at 47.74kw cf. 0.2771 at 56.29kw).

The overall efficiency of the system has been improved at certain operating points, particularly at low loads. This is clearly shown in Fig-5.1a. Compared with Fig-4.1a, it can be seen that efficiencies at high loads are comparable. The area covered by higher efficiency is slightly reduced but with higher efficiency extended to low loads. In fact, it is these findings that lead to the investigation on optimisation for engine speed.

Fig-5.1b to Fig-5.1d show the contours of boost ratio, BMEP and turbine gear ratio respectively. Generally, boost ratio and BMEP have increased at low loads, particularly at low speeds where nozzle angle has decreased more markedly. Turbine gear ratio has increased at lower speeds and decreased at higher speeds. These variations reflect two facts. One is to accommodate the change in nozzle angle and another is that the present results are more closely optimised.

5.1.3 Further Remarks

It should be noted that in the program DCE2 for the variable nozzle scheme, reverse bypass flow is not allowed. Therefore, at low load and high output shaft speed, a situation occurs where the system can no longer work, due to extremely low available exhaust energy, which leads to failure of the turbine subroutine. This is why in the calculations with the VG turbine an engine power of greater than 1/4 load is used at an output shaft speed of 2200rpm(71.47kw cf. 60kw, Table-4.1c).

If negative bypass flow is allowed, as in the present case with fixed nozzle angle, although the engine charge purity is affected, the air supply is still sufficient giving an acceptable trapped air/fuel ratio due to the low load operation.

Further, at an even lower load, because of the still lower available exhaust energy, the turbine can become an obstacle to the gas flow, even consuming a certain amount of energy. Therefore, the overall performance of the system will be affected. Certain measures can be taken to minimise this effect, e.g. the turbine can

be disconnected, i.e. brought to a stand-still, and act as an ordinary duct or bypass. Likewise, in the simulation, the turbine can be considered inoperative. Under this circumstance, the engine speed can be scheduled such that compressor mass flow exactly meets the engine demand, i.e. zero bypass flow, to maximise overall efficiency. This will, in addition, make the computation easier (without consideration of turbine mass flow balance).

5.2 Operation with New Compressor Map

(standard conditions, Pa=0.99bar,Ta=294.4K)

In section-4.3, the system (VG turbine) performance has been improved with a new compressor match. In this section, the system operation with FG turbine and with this new compressor (Fig-4.4) will be investigated. The results are shown in Table-5.2(a-c) and Fig-5.2(a-d), and these will be compared with the standard results in section-5.1.

a)Regime at Output Shaft Speed of 2200rpm

Some data at the design point are listed below:

	std.	new
Eng.speed(rpm)	2116	2097
boost ratio	2.601	2.631
A/F ratio	29.93	30.98
power(kw)	240.8	240.
BMEP(bar)	13.63	13.7
efficiency	0.3938	0.3978
air flow(kg/min)	25.43	25.54
Comp.power(kw)	65.45	63.92
efficiency	0.72	0.749
mass flow(kg/min)	26.6	25.83
Turb.power(kw)	79.66	75.42
speed(rpm)	46420	44549

	std.	new
O/S speed(rpm)	2200.	2200.
power(kw)	239.3	236.2
efficiency(%)	0.3914	0.3915

At this point, with the new match, engine speed has decreased, while boost ratio, BMEP and air/fuel ratio have increased, which is partly a result of an increase in compressor efficiency. This leads to higher engine efficiency.

With the change in engine speed, compressor power has decreased, but the reduction in turbine power is even greater.

With the increase in engine efficiency and reduction in surplus power of turbine over compressor, the overall efficiency remains unchanged.

At other power levels, engine speed has increased. Because of higher compressor efficiency (0.707 cf. 0.609 at 1/2 load), and therefore higher boost ratio, air/fuel ratio and higher engine efficiency, overall efficiency has been improved (0.3427 cf. 0.3293 at 1/2 load).

b)Regime at Output Shaft Speed of 440rpm

Some important parameter at the stall point are selected as follows:

	std.	new
Eng.speed(rpm)	1293	1313
boost ratio	4.08	4.215
A/F ratio	32.47	33.29
power(kw)	241.85	240.15
BMEP(bar)	22.41	21.91
efficiency	0.4552	0.4398
air flow(kg/min)	23.98	25.27
Comp.power(kw)	179.4	179.55
efficiency	0.656	0.704
mass flow(kg/min)	45.85	47.91

	std.	new
Turb.power(kw)	139.7	148.1
speed(rpm)	47212	47301
O/S speed(rpm)	2200.	2200.
power(kw)	184.74	191.53
efficiency(%)	0.3477	0.3507

At this point, engine speed has increased, while BMEP and engine efficiency have decreased. Due to the higher compressor efficiency, boost ratio and air/fuel ratio have increased. Turbine power has increased substantially because of the higher pressure ratio and mass flow, while the increase in compressor power is not significant. All these lead to a higher overall efficiency.

At 3/4 and 1/4 loads, engine speed has increased and overall efficiency also increased, while at 1/2 load, engine speed has decreased (1026 cf. 1045rpm) and overall efficiency slightly deteriorated (0.3381 cf. 0.3400).

c)General Trend

With the introduction of the new compressor, compressor efficiency has generally increased. In most cases, engine speed and overall efficiency have increased. Only at a couple of points, with a decrease in engine speed, has overall efficiency slightly deteriorated.

In Fig-5.2a, the area covered by the 0.376 efficiency contour is much greater than that by the 0.380 efficiency contour in Fig-5.1a. This becomes clearer comparing the area covered by the 0.361 efficiency contour in Fig-5.2a and that by 0.360 efficiency area in Fig-5.1a.

Boost ratio has increased over the entire operating area (Fig-5.2b cf. Fig-5.1a), while the change in BMEP (Fig-5.2c cf. Fig-5.1c) and turbine gear ratio (Fig-5.2d cf. Fig-5.1d) are not significant.

Comparing Table-5.2 with Table-4.2 (VG scheme), it can be seen that at certain low speed points, overall efficiency with the FG scheme has slightly increased. This shows that the VG results still deviate somewhat from the optimal. However, at certain high speed points, it is much lower (0.3285 cf. 0.3559 at 1/4 load and 1050rpm). Comparison between Fig-5.2a and Fig-4.5a (VG scheme) shows

that, with VG turbine, the area covered by the 0.39 efficiency contour is even greater than that by the 0.376 efficiency area with FG turbines.

As in the case with VG turbine, the results obtained in this section, Table-5.2 and Fig-5.2 will be taken as the new base line in later studies.

5.3 Operation under Changing Ambient Conditions

For a conventionally turbocharged engine, with a fixed nozzle turbine, its performance at altitude and/or at elevated temperature will deteriorate, particularly at low speeds(chapter-3), although certain compensating effects can be provided by the turbocharger as a result of increased speed and turbine inlet temperature. The characteristics of the DCE with a fixed geometry turbine under standard ambient conditions have been investigated previously and the outcome was quite acceptable. In the following investigation, its performance under changing ambient conditions is studied. Similar conditions to those with the VG turbine are applied under similar headings, i.e. a)ambient pressure of 85% standard value, b)ambient temperature of 40deg.c and c)a combination of both. The turbine nozzle angle adopted is still 8.886deg. In the following assessment the results are compared with those for the new base line results (section-5.2, new match, standard conditions). The relevant data will be identified as the analysis proceeds.

5.3.1 Effects of Reduced Ambient Pressure(Table-5.3a-c)

This set of data is obtained for an ambient pressure of 85% of the standard value, equivalent to an altitude of 1250m, Table-5.3(a-c) and Fig-5.3(a-d).

As the ambient pressure is reduced, the following changes take place: engine speed and boost ratio have increased, while mass flow, air/fuel ratio, BMEP and engine efficiency have decreased. Both compressor and turbine power have increased and a favourable shift of balance between the two has taken place, e.g. at the design point the surplus power of the turbine over compressor increased from 11.5kw to 13.55kw. Overall efficiency has generally deteriorated but in almost all cases by under 1 percentage point. The data at the design and stall points are listed below:

	design		stall	
	der.	base	der.	base
Eng.speed(rpm)	2139.	2097.	1386.	1313.
boost ratio	2.911	2.631	4.67	4.215
A/F ratio	27.2	30.44	31.7	33.29
power(kw)	239.7	240.	240.3	240.2
BMEP(bar)	13.42	13.7	20.74	21.91
efficiency	0.388	0.398	0.431	0.44
air flow(kg/min)	23.88	25.54	24.57	25.27
Comp.power(kw)	67.1	63.92	182.4	179.6
efficiency	0.697	0.723	0.691	0.704
mass flow(kg/min)	23.35	25.83	43.88	47.91
Turb.power(kw)	80.65	75.42	152.7	148.1
speed(rpm)	49308	44549	49731	47301
O/S speed(rpm)	2200.	2200.	440.	440.
power(kw)	237.7	236.2	192.9	191.5
efficiency(%)	38.49	39.15	34.59	35.07

Comparing Fig-5.3 with Fig-5.2(base line) efficiency has decreased only slightly, the area within the 0.37 efficiency contour in Fig-5.3a being comparable to that within the 0.376 efficiency contour in Fig-5.2a. The increase in boost ratio is clear but the decrease in BMEP and the increase in turbine gear ratio are not very noticeable.

Comparing Fig-5.3 with Fig-4.6 (VG scheme under the same conditions), there is a clear deterioration in overall efficiency, reaching over 1 percentage point at certain operating points at high load level. At certain low load points, an efficiency loss of 4 percentage points occurs, e.g. 0.3247 cf. 0.3648 at an output shaft speed of 1050rpm and 1/4 load, comparing Table-5.3 and Table-4.3 (for the VG scheme under the same conditions).

5.3.2 Effects of Elevated Temperature(Table-5.4a-c)

For this set of results, The ambient temperature is raised to 40deg.C, i.e. 313.5K. The results are shown in Table-5.4(a-c) and Fig-5.4(a-d). Generally, engine speed has increased while air flow decreased. In most cases, boost ratio has increased

but in some cases, it has decreased. In many cases, the deterioration in overall efficiency is over 1 percentage point with a couple of points with greater loss (at output shaft speed of 1050rpm and 1/4 load, a deterioration of over 2 percentage points has been reached: 0.3041 cf. 0.3285). The results at the design and stall points are shown below:

	design		stall	
	der.	base	der.	base
Eng.speed(rpm)	2113.	2098.	1330.	1313.
boost ratio	2.665	2.631	4.24	4.215
A/F ratio	28.84	30.46	30.68	33.29
power(kw)	240.	240.0	240.	240.2
BMEP(bar)	13.6	13.70	21.61	21.91
efficiency	0.397	0.398	0.42	0.440
air flow(kg/min)	24.24	25.54	24.4	25.27
Comp.power(kw)	65.14	63.92	180.2	179.6
efficiency	0.727	0.723	0.709	0.704
mass flow(kg/min)	25.09	25.83	45.99	47.91
Turb.power(kw)	75.47	75.42	150.9	148.1
speed(rpm)	45984	44549	48439	47301
O/S speed(rpm)	2200.	2200.	440.	440.
power(kw)	235.	236.2	193.4	191.5
efficiency(%)	38.85	39.15	33.82	35.07

Various parameters are plotted in Fig-5.4(a-d). Compared with Fig-5.2 (base line), it can be seen that the loss in efficiency is not very significant, e.g. the area covered by the 0.3678 efficiency contour in Fig-5.4a is nearly comparable to that by the 0.376 efficiency contour in Fig-5.2a. Changes in terms of boost ratio, BMEP and turbine gear ratio are very small.

Compared with Fig-4.7 (VG scheme under the same conditions), an efficiency loss of about 1 percentage point can be observed at high loads points. At medium speed and low load operating conditions, the deterioration is more severe, e.g. 0.3021 cf. 0.3408 at an output shaft speed of 1050rpm and 1/4 load(Comparing Table-5.4 and Table-4.4).

5.3.3 Combination of Altitude and Temperature Derating

(Table-5.5a-c)

This set of results is obtained at an ambient pressure of 85% of the standard value and a temperature of 40deg.c, Table-5.5 and Fig-5.5. Compared with Table-5.2(a-c) (base line under standard conditions), it can be seen that engine speed, boost ratio, compressor and turbine power have all increased while air/fuel ratio and BMEP have decreased. Generally, the loss in overall efficiency is around 1 percentage point at high loads. However, at certain high speed points, there is an improvement (e.g. design point), but at certain low load points, the loss has reached over 2 percentage points, e.g. 0.3173 cf. 0.3428 at an output shaft speed of 500rpm and 1/2 load. Compared with the results with temperature derating only (Table-5.4), the deterioration is quite small. The data at the design and stall points are shown below:

	design			stall		
	der.	der.	base	der.	der.	base
	Pa,Ta	Ta		Pa,Ta	Ta	
Eng.speed(rpm)	2155	2113.	2098.	1407	1330.	1313.
boost ratio	2.948	2.665	2.631	4.713	4.24	4.215
A/F ratio	27.3	28.84	30.46	29.84	30.68	33.29
power(kw)	240.2	240.	240.0	240.1	240.	240.2
BMEP(bar)	13.35	13.6	13.70	20.43	21.61	21.91
efficiency	0.402	0.397	0.398	0.418	0.42	0.440
air flow(kg/min)	22.8	24.24	25.54	23.84	24.4	25.27
Comp.power(kw)	68.3	65.14	63.92	183.1	180.2	179.6
efficiency	0.701	0.727	0.723	0.697	0.709	0.704
mass flow(kg/min)	22.66	25.09	25.83	42.03	45.99	47.91
Turb.power(kw)	79.27	75.47	75.42	155.4	150.9	148.1
speed(rpm)	50416	45984	44549	51269	48439	47301
O/S speed(rpm)	2200.	2200.	2200.	440.	440.	440.
power(kw)	235.2	235.	236.2	194.7	193.4	191.5
efficiency(%)	39.39	38.85	39.15	33.88	33.82	35.07

As can be seen, under derated conditions, all the important parameters are at their normal values and no loss of power has taken place, and at the stall points, output power has actually increased.

The variations of some parameters are shown in the contour plots, Fig-5.5(a-d). Compared with Fig-5.2(base line), only a little over 1 percentage point of efficiency loss can be observed, the area covered by the 0.3667 efficiency contour in Fig-5.5a being slightly smaller than that by the 0.376 efficiency contour in Fig-5.2a. The clear increase in boost ratio can also be seen.

Compared with Fig-4.8(VG scheme under the same conditions), about 1 percentage point of efficiency loss has been incurred at some high load points. At certain medium speed and low load points, the loss can be much greater, e.g. 0.229 cf. 0.3369 at output shaft speed of 1050rpm and 1/4 load(comparing Tabl-5.5 and Table-4.5). However, at certain high speed points, better results are obtained (0.3939 cf. 0.3883 at the design point).

5.4 Discussion

FG-turbine DCE operation under various ambient conditions has been studied. At most of the operating points the results are quite satisfactory with only about 1 percentage point efficiency loss and only at very few points at low loads do losses of 2 percentage points occur.

Compared with the VG scheme under the same ambient conditions, efficiency at high load is about 1 percentage points lower. While at certain medium speeds and low loads, the loss of overall efficiency can reach 4 percentage points. However, the VG scheme has its own disadvantages, such as complexity and possibly reduced reliability associated with its practical implementation. Further, in those cases where the efficiency difference between the two is highest, with the VG turbine, the calculated nozzle angle is very small, which may not be practical. Furthermore, the investigations carried out so far have been limited to steady state operation and a final conclusion can only be reached when other aspects of the system, such as transient response, have been examined. It should be expected that the VG scheme with its enhanced flexibility would have a superior transient performance.

5.5 Summary

The performance of the L10 DCE, with both VG and FG turbines, under various ambient conditions has been investigated. It can be seen that, due to its flexibility, the system can cope with changing ambient conditions excellently. The deterioration in performance is very small, particularly at high loads. As a result, the limiting torque curve of the system is only slightly affected and high torque ratio preserved. Even at low loads, only at certain points, are efficiency losses of 2 percentage points reached. This is outstanding compared with the conventional turbocharging system (with FG turbine). As shown in chapter-3, even on the limiting torque curve, the loss in efficiency can be as high as 4 percentage points. For a purely VG turbocharging system, the performance under changing ambient conditions is also outstanding (see chapter-3). However, in terms of the overall system characteristics the DCE is much superior.

A key disadvantage of the conventional system is its inability to obtain sufficient air at low speeds. VG turbocharging is a very good solution. The advantage of the DCE with VG turbine is obvious. However, with a FG turbine, the DCE achieves a variable function through the differential relationship between the engine and compressor imposed by the epicyclic geartrain. Therefore, an ample air supply is always available.

Table-5.1 Standard map, standard conditions

CUMMINS L10 D C I		STALL POINT		330		200		148		0	
number of cylinders	6.0	bore	(m.m.)	125.03	stroke	(m.m.)	136.00				
con-rod length	(m.m.) 217.78	inlet valve closing	(degs)	193.0	compressor scale factor	1.10					
ambient temperature	(deg k) 274.4	ambient pressure	(bar)	0.99	cooler effectiveness	0.4638					
compression ratio	16.30	engine diagram factor	1.0275		turbine flow loss factor	0.8000					
----- compressor gear ratio	9.5500	output shaft gear ratio		1.4450		-----					
engine speed(r.p.m)	1292.61	1183.77	1045.04	771.17	1315.46	1208.43	1054.74	793.60			
boost pressure ratio	4.080	3.476	2.805	1.895	4.011	3.416	2.704	1.849			
delivered air to fuel ratio	32.466	35.261	38.036	30.786	32.312	35.133	36.925	32.023			
delivery ratio	0.853	0.853	0.854	0.855	0.853	0.853	0.854	0.855			
manifold temp (deg k)	325.507	316.297	312.876	351.061	325.457	315.805	311.988	342.863			
engine power (k w.)	241.85	181.01	121.04	60.25	241.76	181.53	121.01	59.94			
engine torque (n.m.)	1781.74	1459.14	1101.92	746.61	1750.79	1429.40	1091.79	725.53			
b.m.e.p (bar)	22.4073	18.3121	13.8707	9.3565	22.0100	17.9899	13.7404	9.0458			
s.f.c. (kg/kw hr)	0.183	0.181	0.181	0.200	0.184	0.182	0.182	0.199			
b.thermal eff.	0.4552	0.4613	0.4613	0.4170	0.4524	0.4590	0.4580	0.4201			
fuel / rev (kg.)	5.714	4.608	3.490	2.604	5.648	4.549	3.482	2.499			
max cyl pressure (bar .)	181.56	153.80	123.24	82.23	178.80	151.30	119.63	80.35			
exhaust temperature(deg k)	829.29	764.39	706.06	756.36	833.95	767.58	717.29	737.47			
mass flow (kg/min)	23.980	19.233	13.873	6.183	24.005	19.313	13.562	6.352			
percentage heat to coolant	10.38	11.68	14.12	24.34	10.37	11.64	14.29	23.70			
compressor speed (r.p.m.)	9436.5	8397.3	7072.1	4456.9	9258.2	8236.0	6768.3	4274.3			
compressor pressure ratio	4.344	3.694	2.976	2.009	4.277	3.636	2.875	1.966			
mass flow (kg/min)	45.849	40.722	34.175	20.555	44.928	39.897	32.592	19.605			
compressor power (kw.)	179.38	130.34	82.68	35.19	172.91	125.22	78.17	32.74			
compressor torque (n.m)	181.45	148.16	111.60	75.36	178.27	145.13	110.25	73.12			
delivery temperature (deg k)	526.60	484.92	430.84	396.85	522.88	481.28	437.61	394.36			
compressor efficiency	0.656	0.697	0.745	0.636	0.659	0.701	0.724	0.629			
turbine speed (r.p.m)	47212.0	42240.0	35732.4	27280.0	47215.0	42135.0	35100.0	27000.0			
turbine pressure ratio	4.240	3.590	2.872	1.905	4.173	3.532	2.770	1.861			
mass flow (kg/min)	46.680	41.339	34.598	20.720	45.748	40.518	33.022	19.838			
turbine power (kw)	139.69	98.49	59.89	18.63	136.33	95.80	55.81	16.96			
turbine torque (n.m)	28.24	22.26	16.00	6.52	27.56	21.70	15.18	6.00			
inlet temperature (deg k)	693.04	623.75	553.11	513.64	697.51	626.96	560.33	513.71			
turbine nozzle angle	8.886	8.886	8.886	8.886	8.886	8.886	8.886	8.886			
turbine efficiency	0.772	0.766	0.759	0.741	0.772	0.766	0.757	0.738			
output shaft speed (rpm)	440.00	440.00	440.00	440.00	500.00	500.00	500.00	500.00			
output shaft power (kw)	184.74	136.30	89.20	39.68	187.98	138.82	89.60	40.42			
output shaft torque (n./m)	4007.82	2956.89	1935.10	860.82	3588.63	2650.24	1710.55	771.63			
output shaft sfc (kg/kw.hr)	0.240	0.240	0.245	0.304	0.237	0.238	0.246	0.294			
output thermal efficiency	0.3477	0.3474	0.3400	0.2747	0.3517	0.3510	0.3391	0.2833			
engine fuel flow (kg/min)	0.739	0.545	0.365	0.201	0.743	0.550	0.367	0.198			
dynamic injection(degree ca)	337.4	340.3	343.2	345.8	337.5	340.3	343.2	345.9			
duration of injection	29.2	23.9	18.4	14.7	29.0	23.7	18.4	14.5			
turbine gear ratio	107.3	96.0	81.2	62.0	94.4	84.3	70.2	54.0			
pressure loss in pipe a (bar)	0.10345	0.10345	0.10345	0.10345	0.10345	0.10345	0.10345	0.10345			
pressure loss in pipe b (bar)	0.10345	0.10345	0.10345	0.10345	0.10345	0.10345	0.10345	0.10345			
pressure loss in pipe c (bar)	0.10345	0.10345	0.10345	0.10345	0.10345	0.10345	0.10345	0.10345			
pressure loss in pipe d (bar)	0.10345	0.10345	0.10345	0.10345	0.10345	0.10345	0.10345	0.10345			

Table-5.1a

(CUMMINS L10 D C F

244 163 118 0

number of cylinders	6.0	bore	(m.m.)	125.03	stroke	(m.m.)	136.00	
con-rod length (m.m.)	217.78	inlet valve closing (degs)		193.0	compressor scale factor		1.10	
ambient temperature (deg k)	294.4	ambient pressure (bar)		0.99	cooler effectiveness		0.8342	
compression ratio	16.30	engine diagram factor		0.9506	turbine flow loss factor		0.8000	
----- compressor gear ratio	9.5500	output shaft gear ratio		1.4450	-----			
engine speed(r.p.m)	1535.44	1458.07	1282.68	1039.62	1799.36	1663.69	1507.94	1348.50
boost pressure ratio	3.475	2.980	2.216	1.547	3.052	2.439	1.881	1.361
delivered air to fuel ratio	30.535	34.806	35.675	40.032	30.697	30.498	32.505	42.384
delivery ratio	0.852	0.853	0.853	0.854	0.852	0.852	0.853	0.849
manifold temp (deg k)	325.434	314.983	305.032	302.457	323.567	315.291	305.971	295.804
engine power (k w.)	241.13	180.75	120.72	60.12	240.99	180.69	120.47	60.02
engine torque (n.m.)	1497.96	1184.66	897.77	553.83	1279.96	1038.25	763.66	426.97
b.m.e.p (bar)	18.8074	14.8458	11.2715	6.9255	16.0398	13.0071	9.5681	5.3305
s.f.c. (kg/kw hr)	0.197	0.195	0.192	0.196	0.203	0.207	0.211	0.216
b.thermal eff.	0.4227	0.4279	0.4342	0.4247	0.4106	0.4031	0.3962	0.3866
fuel / rev (kg.)	5.165	4.027	3.013	1.893	4.535	3.745	2.803	1.600
max cyl pressure (bar .)	156.79	133.60	99.42	68.05	137.13	111.24	86.23	60.36
exhaust temperature(deg k)	888.33	798.28	743.02	650.26	896.29	876.30	810.83	658.19
mass flow (kg/min)	24.215	20.437	13.789	7.878	25.048	19.003	13.740	9.147
percentage heat to coolant	10.30	11.23	13.95	19.39	10.07	11.72	14.02	17.44
compressor speed (r.p.m.)	7724.0	6985.2	5310.1	2988.9	6609.5	5313.8	3826.4	2303.8
compressor pressure ratio	3.752	3.217	2.398	1.685	3.349	2.675	2.071	1.514
mass flow (kg/min)	37.016	33.507	25.047	13.092	31.347	24.788	17.094	9.570
compressor power (kw.)	123.30	88.10	50.32	17.35	89.87	58.38	30.93	10.24
compressor torque (n.m)	152.37	120.39	90.46	55.39	129.79	104.87	77.16	42.42
delivery temperature (deg k)	492.58	451.26	414.51	373.78	465.28	435.05	402.66	358.56
compressor efficiency	0.679	0.743	0.697	0.598	0.709	0.680	0.630	0.580
turbine speed (r.p.m)	47250.0	41475.0	31500.0	24108.0	47040.0	41600.0	36800.0	27200.0
turbine pressure ratio	3.648	3.113	2.293	1.581	3.244	2.571	1.966	1.514
mass flow (kg/min)	37.882	34.158	25.447	13.279	32.218	25.381	17.542	9.775
turbine power (kw)	112.24	77.84	36.82	7.48	93.23	55.42	23.49	4.88
turbine torque (n.m)	22.67	17.92	11.16	2.96	18.92	12.72	6.09	1.71
inlet temperature (deg k)	762.31	671.63	603.51	545.71	818.15	783.11	738.10	646.00
turbine nozzle angle	8.886	8.886	8.886	8.886	8.886	8.886	8.886	8.886
turbine efficiency	0.766	0.761	0.749	0.708	0.761	0.752	0.719	0.625
output shaft speed (rpm)	1050.00	1050.00	1050.00	1050.00	1600.00	1600.00	1600.00	1600.00
output shaft power (kw)	214.00	158.45	98.85	45.88	228.65	165.97	105.02	49.42
output shaft torque (n./m)	1945.39	1440.45	898.65	417.07	1364.05	990.15	626.55	294.86
output shaft sfc (kg/kw.hr)	0.222	0.222	0.235	0.257	0.214	0.225	0.241	0.262
output thermal efficiency	0.3751	0.3751	0.3555	0.3241	0.3895	0.3703	0.3454	0.3184
engine fuel flow (kg/min)	0.793	0.587	0.387	0.197	0.816	0.623	0.423	0.216
dynamic injection(degree ca)	337.5	340.3	343.4	346.0	339.0	340.7	342.7	345.4
duration of injection	27.9	22.5	17.3	13.4	26.0	21.9	17.7	13.0
turbine gear ratio	45.0	39.5	30.0	23.0	29.4	26.0	23.0	17.0
pressure loss in pipe a (bar)	0.10345	0.10345	0.10345	0.10345	0.10345	0.10345	0.10345	0.10345
pressure loss in pipe b (bar)	0.10345	0.10345	0.10345	0.10345	0.10345	0.10345	0.10345	0.10345
pressure loss in pipe c (bar)	0.10345	0.10345	0.10345	0.10345	0.10345	0.10345	0.10345	0.10345
pressure loss in pipe d (bar)	0.10345	0.10345	0.10345	0.10345	0.10345	0.10345	0.10345	0.10345

Table-5.1b

CUMMINS L10 D C E		DESIGN POINT							
		135	105	87	0				
number of cylinders	6.0	bore	(m.m.)	125.03	stroke	(m.m.)	136.00		
con-rod length	(m.m.) 217.78	inlet valve closing	(degs)	193.0	compressor scale factor		1.10		
ambient temperature	(deg k) 294.4	ambient pressure	(bar)	0.99	cooler effectiveness		0.7866		
compression ratio	16.30	engine diagram factor		0.9023	turbine flow loss factor		0.8000		
----- compressor gear ratio	9.5500	output shaft gear ratio		1.4450	-----				
engine speed(r.p.m.)	1781.47	1838.13	1691.99	1561.31	2116.00	1993.70	1877.10	1747.00	
boost pressure ratio	2.859	2.244	1.700	1.241	2.601	2.078	1.571	1.190	
delivered air to fuel ratio	31.231	30.210	31.291	40.639	29.925	29.854	31.368	40.232	
delivery ratio	0.849	0.850	0.849	0.849	0.849	0.849	0.849	0.848	
manifold temp (deg k)	320.562	314.039	305.777	295.538	318.839	312.465	304.886	305.392	
engine power (k w.)	240.92	180.57	120.31	60.19	240.78	180.47	120.24	60.14	
engine torque (n.m.)	1162.32	939.72	680.59	368.78	1088.42	866.39	613.47	329.58	
b.m.e.p (bar)	14.5612	11.7644	8.5159	4.6169	13.6274	10.8406	7.6716	4.1225	
s.f.c. (kg/kw hr)	0.207	0.213	0.221	0.237	0.212	0.217	0.226	0.248	
b.thermal eff.	0.4021	0.3920	0.3780	0.3518	0.3938	0.3840	0.3684	0.3361	
fuel / rev (kg.)	4.203	3.483	2.615	1.524	4.016	3.277	2.417	1.424	
max cyl pressure (bar)	127.53	102.09	78.04	55.61	116.27	94.00	71.70	52.57	
exhaust temperature(deg k)	893.90	890.96	844.22	694.00	919.60	901.56	849.97	714.12	
mass flow (kg/min)	26.009	19.341	13.846	9.667	25.432	19.503	14.232	10.006	
percentage heat to coolant	9.80	11.57	13.95	16.88	9.90	11.49	13.70	16.91	
compressor speed (r.p.m.)	6365.9	4997.1	3601.4	2353.4	5668.0	4500.0	3386.5	2144.1	
compressor pressure ratio	3.177	2.490	1.894	1.400	2.927	2.334	1.774	1.361	
mass flow (kg/min)	30.206	23.273	16.038	10.013	26.598	20.704	15.110	8.907	
compressor power (kw.)	78.66	49.76	25.80	8.99	65.45	41.28	21.81	7.28	
compressor torque (n.m)	117.95	95.06	68.39	36.45	110.22	87.56	61.47	32.43	
delivery temperature (deg k)	449.78	422.18	390.72	348.25	441.29	413.60	380.85	386.69	
compressor efficiency	0.741	0.607	0.614	0.555	0.720	0.678	0.609	0.555	
turbine speed (r.p.m.)	46683.0	40660.0	34010.0	2790.0	46420.0	39600.0	22000.0	2200.0	
turbine pressure ratio	3.177	2.490	1.894	1.400	2.927	2.334	1.774	1.361	
mass flow (kg/min)	31.097	23.929	16.455	10.254	27.422	21.392	15.537	9.171	
turbine power (kw)	90.62	52.81	22.53	3.09	79.66	46.46	17.86	1.34	
turbine torque (n.m)	18.53	12.40	6.32	3.78	16.38	11.20	7.75	5.82	
inlet temperature (deg k)	338.64	820.09	788.72	683.08	901.17	876.64	825.82	714.12	
turbine nozzle angle	8.886	8.886	8.886	8.886	8.886	8.886	8.886	8.886	
turbine efficiency	0.761	0.752	0.739	0.534	0.757	0.750	0.683	0.306	
output shaft speed (rpm)	1900.00	1900.00	1900.00	1900.00	2200.00	2200.00	2200.00	2200.00	
output shaft power (kw)	236.94	171.68	108.51	48.31	239.27	173.65	107.49	47.74	
output shaft torque (n./m)	1190.33	862.51	545.15	242.72	1038.14	753.45	466.37	207.12	
output shaft sfc (kg/kw.hr)	0.211	0.224	0.245	0.295	0.213	0.226	0.253	0.313	
output thermal efficiency	0.3955	0.3728	0.3409	0.2823	0.3914	0.3695	0.3293	0.2668	
engine fuel flow (kg/min)	0.833	0.640	0.443	0.238	0.850	0.653	0.454	0.249	
dynamic injection(degree ca)	340.1	341.4	342.9	344.6	341.0	342.2	343.4	344.8	
duration of injection	25.1	21.4	17.7	13.8	24.8	21.3	17.7	14.1	
turbine gear ratio	24.6	21.4	17.9	4.1	21.1	18.0	10.0	1.0	
pressure loss in pipe a (bar)	0.10345	0.10345	0.10345	0.10345	0.10345	0.10345	0.10345	0.10345	
pressure loss in pipe b (bar)	0.10345	0.10345	0.10345	0.10345	0.10345	0.10345	0.10345	0.10345	
pressure loss in pipe c (bar)	0.10345	0.10345	0.10345	0.10345	0.10345	0.10345	0.10345	0.10345	
pressure loss in pipe d (bar)	0.10345	0.10345	0.10345	0.10345	0.10345	0.10345	0.10345	0.10345	

Table-5.1c

Table-5.2 New baseline: new map, standard conditions

CUMMINS L10 D C C		STALL		38		25		19		0							
NUMBER OF CYLINDERS		6.0		BORE		(M.M.)		125.03		STROKE		(M.M.)		136.00			
CON-ROD LENGTH		(M.M.)		217.78		INLET VALVE CLOSING		(DEGS)		193.0		COMPRESSOR SCALE FACTOR		1.10			
AMBIENT TEMPERATURE		(DEG K)		294.4		AMBIENT PRESSURE		(BAR)		0.99		COOLER EFFECTIVENESS		0.5236			
COMPRESSION RATIO		16.30		ENGINE DIAGRAM FACTOR		0.9900		TURBINE FLOW LOSS FACTOR		0.8000							
----- COMPRESSOR GEAR RATIO		9.5500		OUTPUT SHAFT GEAR RATIO		1.4450		-----									
ENGINE SPEED (R.P.M.)		1312.93		1190.77		1026.03		791.56		1335.03		1213.12		1053.21		818.35	
BOOST PRESSURE RATIO		4.215		3.517		2.790		1.994		4.143		3.448		2.729		1.941	
DELIVERED AIR TO FUEL RATIO		33.285		36.202		36.799		34.086		33.122		35.878		37.354		35.419	
DELIVERY RATIO		0.853		0.853		0.854		0.855		0.853		0.853		0.854		0.855	
MANIFOLD TEMP (DEG K)		324.254		315.590		314.204		340.481		324.320		315.189		311.714		332.521	
ENGINE POWER (K W.)		240.15		180.36		120.55		60.02		240.04		180.89		120.57		60.04	
ENGINE TORQUE (N.M.)		1747.86		1445.38		1118.30		724.78		1718.93		1418.75		1089.45		701.06	
B.M.E.P (BAR)		21.9056		18.1392		14.0705		9.0809		21.5334		17.8580		13.7101		8.7870	
S.F.C. (KG/KW HR)		0.190		0.180		0.183		0.202		0.191		0.181		0.182		0.200	
B.THERMAL EFF.		0.4398		0.4628		0.4570		0.4133		0.4377		0.4602		0.4577		0.4173	
FUEL / REV (KG.)		5.782		4.550		3.574		2.550		5.711		4.504		3.477		2.444	
MAX CYL PRESSURE (BAR)		159.94		155.13		122.97		86.14		158.71		152.33		120.57		84.00	
EXHAUST TEMPERATURE (DEG K)		837.63		753.04		721.60		733.61		841.48		758.34		714.02		714.38	
MASS FLOW (KG/MIN)		25.267		19.613		13.495		6.881		25.252		19.603		13.680		7.085	
PERCENTAGE HEAT TO COOLANT		10.05		11.53		14.39		22.57		10.05		11.52		14.20		21.91	
COMPRESSOR SPEED (R.P.M.)		9630.6		8463.9		6890.6		4651.4		9445.1		8280.8		6753.6		4510.7	
COMPRESSOR PRESSURE RATIO		4.488		3.737		2.958		2.112		4.417		3.669		2.900		2.062	
MASS FLOW (KG/MIN)		47.907		41.683		33.868		22.418		46.832		40.706		33.132		21.659	
COMPRESSOR POWER (KW.)		179.55		130.30		81.95		35.57		173.15		125.10		78.17		33.34	
COMPRESSOR TORQUE (N.M)		177.96		146.94		113.53		72.99		174.99		144.20		110.48		70.55	
DELIVERY TEMPERATURE (DEG K)		516.99		480.53		438.87		389.38		514.04		477.43		435.28		386.57	
COMPRESSOR EFFICIENCY		0.704		0.721		0.740		0.741		0.704		0.721		0.743		0.736	
TURBINE SPEED (R.P.M.)		47301.1		41789.9		34966.7		28767.7		47232.6		41631.1		35787.0		27751.5	
TURBINE PRESSURE RATIO		4.384		3.633		2.854		2.008		4.313		3.565		2.796		1.958	
MASS FLOW (KG/MIN)		48.291		42.156		34.224		22.664		47.298		41.171		33.441		21.899	
TURBINE POWER (KW)		148.11		99.95		59.32		21.98		144.53		96.82		56.67		20.24	
TURBINE TORQUE (N.M)		29.89		22.83		16.19		7.29		29.21		22.21		15.12		6.96	
INLET TEMPERATURE (DEG K)		694.72		615.23		557.89		502.67		699.45		619.50		556.61		500.96	
TURBINE NOZZLE ANGLE		8.886		8.886		8.886		8.886		8.886		8.886		8.886		8.886	
TURBINE EFFICIENCY		0.774		0.767		0.750		0.741		0.773		0.766		0.758		0.741	
OUTPUT SHAFT SPEED (RPM)		440.00		440.00		440.00		440.00		500.00		500.00		500.00		500.00	
OUTPUT SHAFT POWER (KW)		191.53		137.24		87.18		42.12		194.48		139.46		90.32		42.61	
OUTPUT SHAFT TORQUE (N.M)		4155.02		2977.22		1934.77		913.65		3712.82		2662.34		1724.27		813.39	
OUTPUT SHAFT SFC (KG/KW.HR)		0.238		0.237		0.247		0.288		0.235		0.235		0.243		0.282	
OUTPUT THERMAL EFFICIENCY		0.3507		0.3521		0.3381		0.2900		0.3546		0.3548		0.3428		0.2961	
ENGINE FUEL FLOW (KG/MIN)		0.759		0.542		0.367		0.202		0.762		0.546		0.366		0.200	
DYNAMIC INJECTION (DEGREE CA)		360.2		340.4		343.1		345.8		357.2		340.4		343.2		345.9	
DURATION OF INJECTION		29.6		23.7		18.7		14.6		29.3		23.5		18.3		14.4	
TURBINE GEAR RATIO		107.5		95.0		79.5		65.4		94.5		83.3		71.6		55.5	
PRESSURE LOSS IN PIPE A (BAR)		0.10345		0.10345		0.10345		0.10345		0.10345		0.10345		0.10345		0.10345	
PRESSURE LOSS IN PIPE B (BAR)		0.10345		0.10345		0.10345		0.10345		0.10345		0.10345		0.10345		0.10345	
PRESSURE LOSS IN PIPE C (BAR)		0.10345		0.10345		0.10345		0.10345		0.10345		0.10345		0.10345		0.10345	
PRESSURE LOSS IN PIPE D (BAR)		0.10345		0.10345		0.10345		0.10345		0.10345		0.10345		0.10345		0.10345	

Table-5.2a

CUMMINS L10 D C E

40 30 23 0

NUMBER OF CYLINDERS	6.0	BORE	(M.M.)	125.03	STROKE	(M.M.)	136.00	
CON-ROD LENGTH (M.M.)	217.78	INLET VALVE CLOSING (DEGS)	193.0	COMPRESSOR SCALE FACTOR	1.10			
AMBIENT TEMPERATURE (DEG K)	294.4	AMBIENT PRESSURE (BAR)	0.99	COOLER EFFECTIVENESS	0.8339			
COMPRESSION RATIO	16.30	ENGINE DIAGRAM FACTOR	0.9500	TURBINE FLOW LOSS FACTOR	0.8000			
----- COMPRESSOR GEAR RATIO	9.5500	OUTPUT SHAFT GEAR RATIO	1.4450	-----				
ENGINE SPEED(R.P.M)	1554.57	1431.28	1300.43	1064.43	1793.68	1695.46	1553.78	1351.60
BOOST PRESSURE RATIO	3.535	2.912	2.288	1.602	3.033	2.540	1.989	1.419
DELIVERED AIR TO FUEL RATIO	31.713	33.621	37.732	43.003	30.522	32.870	36.131	44.279
DELIVERY RATIO	0.852	0.853	0.853	0.854	0.852	0.852	0.853	0.850
MANIFOLD TEMP (DEG K)	324.844	314.562	304.498	300.659	323.396	314.539	304.803	296.304
ENGINE POWER (K W.)	240.29	180.08	120.37	60.16	240.12	180.13	119.54	59.88
ENGINE TORQUE (N.M.)	1476.19	1202.51	882.33	538.98	1279.40	1015.13	738.47	424.46
B.M.E.P (BAR)	18.5116	15.0679	11.0855	6.7683	16.0323	12.7236	9.2136	5.3059
S.F.C. (KG/KW HR)	0.197	0.195	0.191	0.195	0.203	0.205	0.209	0.214
B.THERMAL EFF.	0.4240	0.4287	0.4366	0.4282	0.4103	0.4070	0.3997	0.3891
FUEL / REV (KG.)	5.068	4.079	2.947	1.835	4.536	3.628	2.675	1.583
MAX CYL PRESSURE (BAR .)	158.62	131.21	101.94	69.97	136.47	114.50	89.75	62.41
EXHAUST TEMPERATURE(DEG K)	869.57	810.42	721.68	629.05	898.83	839.45	766.15	642.43
MASS FLOW (KG/MIN)	24.984	19.631	14.462	8.399	24.832	20.221	15.020	9.529
PERCENTAGE HEAT TO COOLANT	10.11	11.49	13.54	18.56	10.12	11.29	13.25	17.12
COMPRESSOR SPEED (R.P.M.)	7906.7	6729.3	5479.7	3225.8	6555.2	5617.3	4264.2	2333.4
COMPRESSOR PRESSURE RATIO	3.817	3.143	2.474	1.742	3.328	2.786	2.186	1.574
MASS FLOW (KG/MIN)	38.274	32.606	26.335	14.513	31.219	26.686	20.028	9.472
COMPRESSOR POWER (KW.)	124.33	86.22	51.14	18.23	89.19	60.47	33.23	10.31
COMPRESSOR TORQUE (N.M)	150.10	122.30	89.09	53.93	129.88	102.76	74.37	42.16
DELIVERY TEMPERATURE (DEG K)	487.74	452.14	410.54	369.66	464.70	429.76	393.69	361.43
COMPRESSOR EFFICIENCY	0.708	0.722	0.750	0.675	0.707	0.740	0.745	0.627
TURBINE SPEED (R.P.M)	46512.9	40126.3	32692.3	25115.4	45979.7	42379.0	34993.3	27615.5
TURBINE PRESSURE RATIO	3.713	3.039	2.370	1.638	3.224	2.682	2.082	1.574
MASS FLOW (KG/MIN)	39.014	33.143	26.767	14.718	31.986	27.253	20.446	11.559
TURBINE POWER (KW)	114.80	74.46	39.58	8.96	92.13	59.54	28.59	7.17
TURBINE TORQUE (N.M)	23.56	17.71	11.56	3.41	19.13	13.41	7.80	2.48
INLET TEMPERATURE (DEG K)	747.08	677.24	588.68	524.68	818.70	748.86	680.23	642.43
TURBINE NOZZLE ANGLE	8.886	8.886	8.886	8.886	8.886	8.886	8.886	8.886
TURBINE EFFICIENCY	0.767	0.760	0.752	0.709	0.761	0.753	0.739	0.672
OUTPUT SHAFT SPEED (RPM)	1050.00	1050.00	1050.00	1050.00	1600.00	1600.00	1600.00	1600.00
OUTPUT SHAFT POWER (KW)	214.61	156.63	100.27	46.15	227.56	167.18	106.91	51.27
OUTPUT SHAFT TORQUE (N./M)	1950.94	1423.93	911.53	419.56	1357.58	997.35	637.81	305.87
OUTPUT SHAFT SFC (KG/KW.HR)	0.220	0.224	0.229	0.254	0.215	0.221	0.233	0.250
OUTPUT THERMAL EFFICIENCY	0.3787	0.3729	0.3636	0.3285	0.3888	0.3778	0.3575	0.3332
ENGINE FUEL FLOW (KG/MIN)	0.788	0.584	0.383	0.195	0.814	0.615	0.416	0.214
DYNAMIC INJECTION(DEGREE CA)	337.7	340.3	343.4	346.0	339.0	340.9	342.8	345.4
DURATION OF INJECTION	27.6	22.6	17.2	13.3	26.0	21.5	17.4	12.9
TURBINE GEAR RATIO	44.3	38.2	31.1	23.9	28.7	26.5	21.9	17.3
PRESSURE LOSS IN PIPE A (BAR)	0.10345	0.10345	0.10345	0.10345	0.10345	0.10345	0.10345	0.10345
PRESSURE LOSS IN PIPE B (BAR)	0.10345	0.10345	0.10345	0.10345	0.10345	0.10345	0.10345	0.10345
PRESSURE LOSS IN PIPE C (BAR)	0.10345	0.10345	0.10345	0.10345	0.10345	0.10345	0.10345	0.10345
PRESSURE LOSS IN PIPE D (BAR)	0.10345	0.10345	0.10345	0.10345	0.10345	0.10345	0.10345	0.10345

Table-5.2b

CUMMINS L10 D C E

DESIGN

38 32 23 0

NUMBER OF CYLINDERS	6.0							
CON-ROD LENGTH (M.M.)	217.78							
AMBIENT TEMPERATURE (DEG K)	294.4							
COMPRESSION RATIO	16.30							
----- COMPRESSOR GEAR RATIO	9.5500							
BORE (M.M.)	125.03							
INLET VALVE CLOSING (DEGS)	193.0							
AMBIENT PRESSURE (BAR)	0.99							
ENGINE DIAGRAM FACTOR	0.9008							
STROKE (M.M.)	136.00							
COMPRESSOR SCALE FACTOR	1.10							
COOLER EFFECTIVENESS	0.7870							
TURBINE FLOW LOSS FACTOR	0.8000							
OUTPUT SHAFT GEAR RATIO	1.4450	-----						
ENGINE SPEED (R.P.M.)	1939.82	1844.96	1707.93	1565.02	2097.95	2004.77	1875.75	1781.68
BOOST PRESSURE RATIO	2.815	2.376	1.853	1.290	2.631	2.205	1.701	1.298
DELIVERED AIR TO FUEL RATIO	30.319	32.977	35.804	42.418	30.456	32.797	34.532	36.126
DELIVERY RATIO	0.851	0.852	0.852	0.849	0.851	0.851	0.852	0.849
MANIFOLD TEMP (DEG K)	321.358	313.628	305.114	295.829	318.981	311.791	304.589	297.803
ENGINE POWER (K.W.)	240.04	180.08	120.06	59.40	239.99	180.02	119.99	71.41
ENGINE TORQUE (N.M.)	1183.01	932.88	671.81	366.58	1093.84	858.51	611.71	383.80
B.M.E.P (BAR)	14.8197	11.6895	8.4185	4.5456	13.6998	10.7539	7.6606	4.8001
S.F.C. (KG/KW HP)	0.207	0.208	0.214	0.236	0.210	0.212	0.220	0.242
B.THERMAL EFF.	0.4037	0.4004	0.3901	0.3532	0.3978	0.3927	0.3790	0.3449
FUEL / REV (KG.)	4.261	3.389	2.505	1.494	3.997	3.179	2.346	1.615
MAX CYL PRESSURE (BAR)	126.28	106.59	83.27	57.34	117.32	98.27	76.26	57.83
EXHAUST TEMPERATURE (DEG K)	905.86	842.37	777.49	672.83	906.21	848.93	790.42	713.37
MASS FLOW (KG/MIN)	25.059	20.629	15.316	10.068	25.538	20.901	15.462	11.421
PERCENTAGE HEAT TO COOLANT	10.03	11.13	13.10	16.72	9.88	11.01	13.25	16.92
COMPRESSOR SPEED (R.P.M.)	5968.2	5062.2	3753.7	2388.9	5495.6	4605.8	3373.6	2475.3
COMPRESSOR PRESSURE RATIO	3.122	2.632	2.057	1.452	2.957	2.472	1.913	1.474
MASS FLOW (KG/MIN)	28.237	23.785	17.229	9.917	25.827	21.519	15.198	10.398
COMPRESSOR POWER (KW.)	75.27	50.03	26.56	9.12	63.92	41.81	21.58	9.86
COMPRESSOR TORQUE (N.M.)	120.38	94.33	67.54	36.42	111.02	86.64	61.06	38.01
DELIVERY TEMPERATURE (DEG K)	453.41	420.11	386.70	354.67	442.13	410.57	387.02	385.71
COMPRESSOR EFFICIENCY	0.711	0.747	0.732	0.604	0.723	0.749	0.707	0.610
TURBINE SPEED (R.P.M.)	45544.1	44243.8	34925.2	14567.9	44549.3	40673.4	31036.7	18878.4
TURBINE PRESSURE RATIO	3.018	2.527	1.953	1.452	2.852	2.368	1.809	1.474
MASS FLOW (KG/MIN)	29.030	24.440	17.685	11.044	26.657	22.171	15.411	10.706
TURBINE POWER (KW)	82.83	52.14	23.85	5.21	75.42	46.84	19.22	6.09
TURBINE TORQUE (N.M.)	17.36	11.25	6.52	3.41	16.16	10.99	5.91	3.08
INLET TEMPERATURE (DEG K)	860.55	791.93	738.14	672.83	901.66	837.75	790.42	713.37
TURBINE NOZZLE ANGLE	8.886	8.886	8.886	8.886	8.886	8.886	8.886	8.886
TURBINE EFFICIENCY	0.759	0.741	0.734	0.687	0.756	0.750	0.741	0.726
OUTPUT SHAFT SPEED (RPM)	1900.00	1900.00	1900.00	1900.00	2200.00	2200.00	2200.00	2200.00
OUTPUT SHAFT POWER (KW)	232.48	170.13	108.55	49.99	236.16	172.78	108.49	60.64
OUTPUT SHAFT TORQUE (N.M.)	1167.93	854.72	545.36	251.15	1024.67	749.64	470.69	263.08
OUTPUT SHAFT SFC (KG/KW.HR)	0.213	0.220	0.236	0.281	0.213	0.221	0.243	0.285
OUTPUT THERMAL EFFICIENCY	0.3910	0.3783	0.3528	0.2972	0.3915	0.3769	0.3427	0.2928
ENGINE FUEL FLOW (KG/MIN)	0.827	0.625	0.428	0.234	0.839	0.637	0.440	0.288
DYNAMIC INJECTION (DEGREE CA)	339.7	341.6	343.1	344.7	340.9	342.4	343.6	344.6
DURATION OF INJECTION	25.2	21.0	17.3	13.7	24.7	21.0	17.4	14.8
TURBINE GEAR RATIO	24.0	23.3	18.4	7.7	20.2	18.5	14.1	8.6
PRESSURE LOSS IN PIPE A (BAR)	0.10345	0.10345	0.10345	0.10345	0.10345	0.10345	0.10345	0.10345
PRESSURE LOSS IN PIPE B (BAR)	0.10345	0.10345	0.10345	0.10345	0.10345	0.10345	0.10345	0.10345
PRESSURE LOSS IN PIPE C (BAR)	0.10345	0.10345	0.10345	0.10345	0.10345	0.10345	0.10345	0.10345
PRESSURE LOSS IN PIPE D (BAR)	0.10345	0.10345	0.10345	0.10345	0.10345	0.10345	0.10345	0.10345

Table-5.2c

Table-5.3 New map, reduced Pa(0.8415bar)

CUMMINS L10 D C I		stall point		32		27		20		0	
number of cylinders	6.0	bore	(m.m.)	125.03	stroke	(m.m.)	136.00				
con-rod length (m.m.)	217.78	inlet valve closing (degs)	193.0	compressor scale factor	1.10						
ambient temperature (deg k)	294.4	ambient pressure (bar)	0.84	cooler effectiveness	0.6104						
compression ratio	16.30	engine diagram factor	0.9900	turbine flow loss factor	0.8000						
----- compressor gear ratio	9.5500	output shaft gear ratio	1.4450 -----								
engine speed(r.p.m)	1387.52	1253.51	1073.47	835.90	1405.80	1274.61	1097.14	861.46			
boost pressure ratio	4.670	3.889	3.051	2.152	4.590	3.823	2.985	2.095			
delivered air to fuel ratio	31.701	34.526	35.467	33.315	31.384	34.337	35.474	34.462			
delivery ratio	0.853	0.853	0.854	0.855	0.853	0.853	0.854	0.854			
manifold temp (deg k)	331.210	319.939	313.992	334.754	331.201	319.886	312.583	327.544			
engine power (k w.)	240.30	180.74	120.50	60.01	240.27	180.69	120.49	60.03			
engine torque (n.m.)	1653.70	1373.04	1068.88	686.34	1632.40	1350.31	1045.82	665.97			
b.m.e.p (bar)	20.7409	17.2683	13.4432	8.5978	20.4689	16.9774	13.1519	8.3458			
s.f.c. (kg/kw hr)	0.194	0.184	0.185	0.203	0.195	0.185	0.185	0.202			
b.thermal eff.	0.4310	0.4525	0.4520	0.4102	0.4284	0.4500	0.4504	0.4136			
fuel / rev (kg.)	5.586	4.429	3.452	2.433	5.545	4.379	3.389	2.342			
max cyl pressure (bar .)	158.38	146.56	115.12	79.68	156.99	144.29	112.74	77.84			
exhaust temperature(deg k)	870.38	782.31	736.35	738.01	877.14	786.58	736.51	720.71			
mass flow (kg/min)	24.569	19.168	13.144	6.774	24.466	19.166	13.191	6.953			
percentage heat to coolant	10.32	11.78	14.61	22.54	10.34	11.77	14.54	21.94			
compressor speed (r.p.m.)	10342.9	9063.1	7343.7	5074.9	10120.9	8868.0	7173.2	4922.4			
compressor pressure ratio	4.997	4.155	3.254	2.295	4.917	4.090	3.189	2.241			
mass flow (kg/min)	43.875	38.047	30.601	20.826	42.908	37.096	29.859	20.189			
compressor power (kw.)	182.40	132.45	83.38	36.74	176.15	127.44	79.67	34.55			
compressor torque (n.m)	168.34	139.49	108.37	69.10	166.13	137.17	106.01	67.00			
delivery temperature (deg k)	540.88	501.39	456.89	399.95	537.85	498.71	453.54	396.81			
compressor efficiency	0.691	0.711	0.726	0.749	0.691	0.711	0.726	0.748			
turbine speed (r.p.m)	49731.3	44405.5	38151.5	29362.0	49636.4	44323.1	37857.0	28153.8			
turbine pressure ratio	4.875	4.032	3.131	2.172	4.795	3.967	3.067	2.119			
mass flow (kg/min)	44.220	38.525	31.029	21.040	43.265	37.720	30.285	20.426			
turbine power (kw)	152.71	103.64	60.93	23.48	149.21	101.06	58.50	21.80			
turbine torque (n.m)	29.31	22.28	15.24	7.63	28.69	21.76	14.75	7.39			
inlet temperature (deg k)	734.52	649.95	583.56	517.77	740.81	654.71	585.33	515.77			
turbine nozzle angle	8.886	8.886	8.886	8.886	8.886	8.886	8.886	8.886			
turbine efficiency	0.777	0.770	0.761	0.748	0.776	0.770	0.760	0.747			
output shaft speed (rpm)	440.00	440.00	440.00	440.00	500.00	500.00	500.00	500.00			
output shaft power (kw)	192.87	138.41	87.13	42.31	195.76	140.91	90.47	42.81			
output shaft torque (n./m)	4184.06	3002.64	1933.68	917.90	3737.20	2690.14	1727.12	817.34			
output shaft sfc (kg/kw.hr)	0.241	0.241	0.249	0.288	0.239	0.238	0.247	0.283			
output thermal efficiency	0.3459	0.3466	0.3343	0.2893	0.3491	0.3509	0.3382	0.2950			
engine fuel flow (kg/min)	0.775	0.555	0.371	0.203	0.780	0.558	0.372	0.202			
dynamic injection(degree ca)	349.2	340.4	343.2	345.8	348.2	340.5	343.3	345.9			
duration of injection	29.1	23.3	18.3	14.4	29.0	23.2	18.1	14.3			
turbine gear ratio	113.0	100.9	86.7	66.7	99.3	88.6	75.7	56.3			
pressure loss in pipe a (bar)	0.10345	0.10345	0.10345	0.10345	0.10345	0.10345	0.10345	0.10345			
pressure loss in pipe b (bar)	0.10345	0.10345	0.10345	0.10345	0.10345	0.10345	0.10345	0.10345			
pressure loss in pipe c (bar)	0.10345	0.10345	0.10345	0.10345	0.10345	0.10345	0.10345	0.10345			
pressure loss in pipe d (bar)	0.10345	0.10345	0.10345	0.10345	0.10345	0.10345	0.10345	0.10345			

Table-5.3a

number of cylinders	6.0	bore	(m.m.)	125.03	stroke	(m.m.)	136.00	
con-rod length (m.m.)	217.78	inlet valve closing (degs)		173.0	compressor scale factor		1.10	
ambient temperature (deg k)	294.4	ambient pressure (bar)		0.84	cooler effectiveness		0.8312	
compression ratio	16.30	engine diagram factor		0.9460	turbine flow loss factor		0.8000	
----- compressor gear ratio	9.5500	output shaft gear ratio		1.4450	-----			
engine speed(r.p.m)	1622.60	1486.20	1343.86	1091.91	1858.74	1730.79	1597.14	1369.71
boost pressure ratio	3.755	3.252	2.524	1.745	3.412	2.793	2.197	1.513
delivered air to fuel ratio	30.246	31.526	35.255	40.315	29.254	30.266	33.467	40.505
delivery ratio	0.852	0.853	0.853	0.854	0.851	0.852	0.852	0.853
manifold temp (deg k)	331.680	320.170	307.745	301.177	329.043	319.548	308.364	297.639
engine power (k w.)	240.18	180.18	120.09	59.65	240.00	180.00	120.02	59.77
engine torque (n.m.)	1414.29	1158.07	853.82	525.42	1234.62	994.42	718.42	418.85
b.m.e.p (bar)	17.7271	14.5195	10.7022	6.5419	15.4633	12.4547	9.0000	5.2258
s.f.c. (ky/kw hr)	0.201	0.200	0.196	0.179	0.207	0.209	0.213	0.217
b.thermal eff.	0.4159	0.4165	0.4246	0.4193	0.4037	0.3989	0.3908	0.3839
fuel / rev (ky.)	4.947	4.046	2.926	1.811	4.446	3.624	2.673	1.580
max cyl pressure (bar .)	150.79	124.92	96.36	65.40	130.32	107.73	84.71	57.33
exhaust temperature(deg k)	903.61	852.17	756.74	650.37	928.87	886.18	805.35	670.18
mass flow (ky/min)	24.280	18.957	13.862	7.972	24.173	18.982	14.288	8.766
percentage heat to coolant	10.39	11.84	13.99	19.20	10.36	11.81	13.75	17.99
compressor speed (r.p.m.)	8556.4	7253.7	5894.4	3488.3	7176.5	5954.6	4678.3	2506.3
compressor pressure ratio	4.294	3.527	2.744	1.910	3.767	3.078	2.428	1.691
mass flow (ky/min)	35.191	29.688	24.041	13.480	28.927	23.999	18.693	8.834
compressor power (kw.)	128.82	89.29	53.23	19.03	94.22	62.68	35.46	10.86
compressor torque (n.m)	143.70	117.50	86.21	52.08	125.32	100.48	72.35	41.36
delivery temperature (deg k)	511.89	473.57	426.69	378.97	488.25	450.23	407.84	368.09
compressor efficiency	0.695	0.711	0.745	0.710	0.697	0.715	0.750	0.650
turbine speed (r.p.m)	50218.1	44031.0	34648.3	27316.2	49656.3	44433.1	38256.5	26515.5
turbine pressure ratio	4.171	3.404	2.621	1.787	3.645	2.956	2.306	1.569
mass flow (kg/min)	36.034	30.341	24.544	13.704	29.805	24.654	19.087	9.049
turbine power (kw)	121.72	80.14	42.86	10.08	99.67	63.52	32.33	5.32
turbine torque (n.m)	23.14	17.37	11.81	3.28	19.16	13.64	8.07	1.92
inlet temperature (deg k)	792.31	725.52	625.20	544.93	864.11	803.97	719.68	668.06
turbine nozzle angle	8.886	8.886	8.886	8.886	8.886	8.886	8.886	8.886
turbine efficiency	0.771	0.763	0.753	0.688	0.765	0.758	0.743	0.677
output shaft speed (rpm)	1050.00	1050.00	1050.00	1050.00	1600.00	1600.00	1600.00	1600.00
output shaft power (kw)	216.43	158.61	101.20	46.18	229.49	168.52	108.11	48.91
output shaft torque (n./m)	1767.51	1441.86	720.02	419.84	1369.09	1005.37	644.98	291.81
output shaft sfc (ky/kw.hr)	0.223	0.227	0.233	0.257	0.216	0.223	0.237	0.265
output thermal efficiency	0.3748	0.3667	0.3578	0.3247	0.3861	0.3735	0.3520	0.3142
engine fuel flow (kg/min)	0.803	0.601	0.393	0.198	0.826	0.627	0.427	0.216
dynamic injection(degree ca)	337.9	340.2	343.2	346.0	339.3	341.0	342.8	345.3
duration of injection	27.3	22.7	17.3	13.2	25.8	21.6	17.6	13.0
turbine gear ratio	47.8	41.9	33.0	27.9	31.0	27.8	23.9	16.6
pressure loss in pipe a (bar)	0.10345	0.10345	0.10345	0.10345	0.10345	0.10345	0.10345	0.10345
pressure loss in pipe b (bar)	0.10345	0.10345	0.10345	0.10345	0.10345	0.10345	0.10345	0.10345
pressure loss in pipe c (bar)	0.10345	0.10345	0.10345	0.10345	0.10345	0.10345	0.10345	0.10345
pressure loss in pipe d (bar)	0.10345	0.10345	0.10345	0.10345	0.10345	0.10345	0.10345	0.10345

Table-5.3b

COMPIHS L10 D C E

design point

34 68 84 0

number of cylinders	6.0	hore	(m.m.)	125.03	stroke	(m.m.)	136.00	
con-rod length (m.m.)	217.78	inlet valve closing (degs)	193.0	compressor scale factor	1.10			
ambient temperature (deg k)	294.4	ambient pressure (bar)	0.84	cooler effectiveness	0.7830			
compression ratio	16.30	engine diagram factor	0.9001	turbine flow loss factor	0.8000			
----- compressor gear ratio	9.5500	output shaft gear	ratio	1.4450	-----			
engine speed(r.p.m)	1796.20	1886.54	1749.42	1577.74	2139.21	2041.23	1915.78	1798.22
boost pressure ratio	3.155	2.608	2.045	1.369	2.911	2.454	1.894	1.380
delivered air to fuel ratio	28.760	30.431	33.420	36.794	27.195	30.114	32.532	32.150
delivery ratio	0.851	0.851	0.852	0.849	0.850	0.851	0.851	0.848
manifold temp (deg k)	326.584	317.892	300.298	298.355	327.168	317.487	308.867	305.696
engine power (k w.)	239.90	179.93	119.97	59.89	239.71	179.86	119.89	71.25
engine torque (n.m.)	1149.60	912.32	655.88	363.62	1072.75	843.18	598.93	380.27
b.m.e.p (bar)	14.3925	11.4225	8.2131	4.5462	13.4200	10.5525	7.4947	4.7453
s.f.c. (ky/kw hr)	0.210	0.213	0.218	0.244	0.215	0.217	0.224	0.250
b.thermal eff.	0.3972	0.3922	0.3827	0.3425	0.3881	0.3847	0.3719	0.3341
fuel / rev (ky.)	4.206	3.381	2.491	1.541	4.013	3.184	2.339	1.649
max cyl pressure (bar .)	120.22	100.03	78.59	52.48	110.74	93.49	72.60	52.89
exhaust temperature(deg k)	740.85	888.08	812.26	729.19	763.85	890.73	824.28	782.29
mass flow (kg/min)	24.148	19.408	14.563	9.038	23.880	19.832	14.778	10.127
percentage heat to coolant	10.32	11.62	13.59	17.92	10.62	11.62	13.67	17.88
compressor speed (r.p.m.)	6506.6	5459.4	4149.9	2510.4	5889.6	4954.0	3755.9	2633.3
compressor pressure ratio	3.523	2.906	2.284	1.555	3.297	2.771	2.145	1.583
mass flow (kg/min)	25.969	21.831	16.357	8.944	23.348	19.571	14.579	9.532
compressor power (kw.)	79.46	52.64	28.68	9.44	67.10	44.20	23.66	10.37
compressor torque (n.m)	116.57	92.03	65.97	35.89	108.74	85.16	60.14	37.59
delivery temperature (deg k)	476.65	438.35	399.32	361.82	477.96	435.93	397.90	386.35
compressor efficiency	0.698	0.729	0.749	0.628	0.697	0.738	0.740	0.636
turbine speed (r.p.m)	46294.1	43549.5	37905.8	17271.8	49308.2	49666.3	34071.2	22178.4
turbine pressure ratio	3.400	2.784	2.161	1.555	3.175	2.649	2.022	1.583
mass flow (kg/min)	26.883	22.477	16.784	10.151	24.245	20.197	15.008	9.847
turbine power (kw)	89.22	57.17	27.57	6.44	80.65	49.71	23.69	7.58
turbine torque (n.m)	18.40	12.53	6.74	3.56	15.61	9.55	6.64	3.26
inlet temperature (deg k)	712.19	843.65	771.50	729.19	763.85	890.73	824.28	782.29
turbine nozzle angle	8.886	8.886	8.886	8.886	8.886	8.886	8.886	8.886
turbine efficiency	0.758	0.756	0.740	0.695	0.760	0.730	0.745	0.730
output shaft speed (rpm)	1900.00	1900.00	1900.00	1900.00	2200.00	2200.00	2200.00	2200.00
output shaft power (kw)	233.91	172.05	109.87	50.74	237.74	173.05	110.65	61.47
output shaft torque (n./m)	1175.13	864.33	551.98	254.91	1031.52	750.84	480.08	266.70
output shaft sfc (ky/kw.hr)	0.215	0.222	0.238	0.287	0.217	0.225	0.243	0.289
output thermal efficiency	0.3873	0.3750	0.3505	0.2902	0.3849	0.3701	0.3432	0.2882
engine fuel flow (kg/min)	0.840	0.638	0.436	0.243	0.859	0.650	0.448	0.296
dynamic injection(degree ca)	340.2	341.7	343.1	344.6	341.0	342.5	343.7	344.5
duration of injection	25.1	21.2	17.4	13.9	24.9	21.2	17.6	14.9
turbine gear ratio	24.4	22.9	20.0	9.1	22.4	22.6	15.5	10.1
pressure loss in pipe a (bar)	0.10345	0.10345	0.10345	0.10345	0.10345	0.10345	0.10345	0.10345
pressure loss in pipe b (bar)	0.10345	0.10345	0.10345	0.10345	0.10345	0.10345	0.10345	0.10345
pressure loss in pipe c (bar)	0.10345	0.10345	0.10345	0.10345	0.10345	0.10345	0.10345	0.10345
pressure loss in pipe d (bar)	0.10345	0.10345	0.10345	0.10345	0.10345	0.10345	0.10345	0.10345

Table-5.3c

Table-5.4 New map, elevated Ta(313K)

CUMMINS L10 D C E		38 15 22 0						
		Stall point						
number of cylinders	6.0	bore	(m.m.)	125.03	stroke	(m.m.)	136.00	
con-rod length (m.m.)	217.78	inlet valve closing (degs)		193.0	compressor scale factor		1.10	
ambient temperature (deg k)	313.3	ambient pressure (bar)		0.99	cooler effectiveness		0.9246	
compression ratio	16.30	engine diagram factor		0.9458	turbine flow loss factor		0.8000	
----- compressor gear ratio	9.5500	output shaft gear ratio		1.4450	-----			
engine speed(r.p.m)	1330.18	1195.55	1031.24	799.44	1350.50	1218.32	1048.64	824.60
boost pressure ratio	4.241	3.543	2.782	1.946	4.173	3.473	2.748	1.901
delivered air to fuel ratio	30.681	32.783	33.628	35.827	30.504	32.619	33.703	35.951
delivery ratio	0.854	0.854	0.854	0.854	0.854	0.854	0.854	0.854
manifold temp (deg k)	342.747	332.983	322.835	313.338	342.727	333.030	322.961	313.430
engine power (k w.)	239.98	179.92	120.12	59.97	240.00	179.88	120.12	59.97
engine torque (n.m.)	1725.20	1439.60	1112.66	717.63	1699.24	1412.70	1094.19	695.74
b.m.e.p (bar)	21.6062	18.0227	13.9504	8.9833	21.2827	17.6817	13.7189	8.7093
s.f.c. (ky/kw hr)	0.197	0.192	0.196	0.205	0.199	0.193	0.196	0.206
b.thermal eff.	0.4196	0.4346	0.4263	0.4063	0.4190	0.4332	0.4257	0.4051
fuel / rev (ky.)	5.977	4.814	3.798	2.566	5.896	4.738	3.741	2.496
max cyl pressure (bar .)	159.61	156.21	123.18	85.56	158.14	153.19	121.63	83.49
exhaust temperature(deg k)	909.33	833.83	793.05	718.76	911.86	836.78	792.61	718.32
mass flow (ky/min)	24.395	18.866	13.171	7.351	24.291	18.828	13.221	7.398
percentage heat to coolant	10.54	12.15	14.82	20.68	10.57	12.16	14.79	20.61
compressor speed (r.p.m.)	9795.3	8509.5	6940.4	4726.7	9592.8	8330.5	6710.0	4570.5
compressor pressure ratio	4.439	3.725	2.945	2.087	4.372	3.656	2.913	2.043
mass flow (ky/min)	45.987	39.439	32.118	21.529	44.901	38.543	30.879	20.716
compressor power (kw.)	180.23	130.47	82.11	35.78	173.83	125.30	78.02	33.52
compressor torque (n.m)	175.63	146.35	112.93	72.26	172.97	143.58	110.99	70.01
delivery temperature (deg k)	545.23	509.61	465.48	412.57	542.46	506.27	463.73	409.97
compressor efficiency	0.709	0.723	0.742	0.739	0.709	0.723	0.742	0.734
turbine speed (r.p.m)	48438.5	43623.1	37512.4	29046.2	48419.4	43514.6	43571.2	28628.1
turbine pressure ratio	4.334	3.621	2.841	1.983	4.267	3.552	2.809	1.939
mass flow (kg/min)	45.892	40.094	32.550	21.768	45.016	39.186	31.323	20.914
turbine power (kw)	150.93	104.00	61.37	21.51	147.38	100.64	56.28	19.91
turbine torque (n.m)	29.74	22.76	15.62	7.07	29.06	22.08	12.33	6.64
inlet temperature (deg k)	749.20	673.57	608.31	523.81	753.33	676.85	613.16	526.98
turbine nozzle anyle	8.886	8.886	8.886	8.886	8.886	8.886	8.886	8.886
turbine efficiency	0.773	0.767	0.758	0.740	0.772	0.766	0.725	0.739
output shaft speed (rpm)	440.00	440.00	440.00	440.00	500.00	500.00	500.00	500.00
output shaft power (kw)	193.44	140.83	90.92	41.45	196.44	142.74	90.12	42.11
output shaft torque (n.m)	4196.51	3055.12	1972.34	899.27	3750.12	2724.92	1720.54	803.84
output shaft sfc (kg/kw.hr)	0.247	0.245	0.258	0.297	0.243	0.243	0.261	0.293
output thermal efficiency	0.3382	0.3402	0.3227	0.2809	0.3429	0.3438	0.3194	0.2844
engine fuel flow (kg/min)	0.795	0.575	0.392	0.205	0.796	0.577	0.392	0.206
dynamic injection(degree ca)	359.7	339.8	342.6	345.7	356.7	339.9	342.7	345.8
duration of injection	30.5	24.8	19.7	14.7	30.2	24.6	19.5	14.6
turbine gear ratio	110.1	99.1	85.3	66.0	96.8	87.0	87.1	57.3
pressure loss in pipe a (bar)	0.10345	0.10345	0.10345	0.10345	0.10345	0.10345	0.10345	0.10345
pressure loss in pipe b (bar)	0.10345	0.10345	0.10345	0.10345	0.10345	0.10345	0.10345	0.10345
pressure loss in pipe c (bar)	0.10345	0.10345	0.10345	0.10345	0.10345	0.10345	0.10345	0.10345
pressure loss in pipe d (bar)	0.10345	0.10345	0.10345	0.10345	0.10345	0.10345	0.10345	0.10345

Table-5.4a

number of cylinders	6.0	bore	(m.m.)	125.03	stroke	(m.m.)	136.00
con-rod length	(m.m.) 217.78	inlet valve closing	(degs)	193.0	compressor scale factor		1.10
ambient temperature	(deg k) 313.3	ambient pressure	(bar)	0.99	cooler effectiveness		0.8664
compression ratio	16.30	engine diagram factor		0.9276	turbine flow loss factor		0.8000
----- compressor gear ratio	9.5500	output shaft gear ratio		1.4450	-----		

engine speed(r.p.m.)	1571.07	1440.71	1307.56	1054.38	1809.80	1709.59	1560.42	1350.68
boost pressure ratio	3.560	2.923	2.273	1.604	3.056	2.536	1.966	1.395
delivered air to fuel ratio	30.429	31.118	33.490	37.556	29.236	30.991	32.867	39.318
delivery ratio	0.853	0.853	0.853	0.853	0.853	0.852	0.852	0.852
manifold temp	(deg k) 343.476	333.499	323.593	314.584	343.372	333.717	324.164	315.872
engine power	(k w.) 240.26	180.17	120.09	59.98	240.12	180.09	120.03	59.99
engine torque	(n.m.) 1460.67	1194.63	877.52	544.12	1268.00	1006.75	735.32	424.76
b.m.e.p	(bar) 18.3146	14.9766	10.9993	6.8127	15.8897	12.6160	9.2120	5.3189
s.f.c.	(kg/kw hr) 0.198	0.200	0.203	0.212	0.203	0.206	0.213	0.224
b.thermal eff.	0.4213	0.4160	0.4112	0.3934	0.4100	0.4041	0.3913	0.3722
fuel / rev	(ky.) 5.045	4.170	3.105	2.010	4.499	3.623	2.732	1.659
max cyl pressure	(bar) 158.06	130.61	101.08	70.36	135.63	113.08	88.20	61.16
exhaust temperature(deg k)	702.28	867.48	803.12	710.58	930.60	878.49	821.83	705.60
mass flow (kg/min)	24.120	18.697	13.595	7.959	23.804	19.197	14.014	8.808
percentage heat to coolant	10.62	12.20	14.56	19.77	10.68	12.01	14.30	18.66

compressor speed (r.p.m.)	8064.3	6819.4	5547.8	3129.9	6709.2	5752.2	4327.6	2324.6
compressor pressure ratio	3.779	3.125	2.457	1.763	3.297	2.762	2.172	1.576
mass flow (kg/min)	36.897	31.170	25.138	13.099	30.241	25.809	19.186	8.851
compressor power (kw.)	125.47	86.79	51.49	17.86	90.50	61.42	33.58	10.27
compressor torque (n.m)	148.51	121.49	88.60	54.45	128.75	101.92	74.06	42.19
delivery temperature (deg k)	515.01	478.91	435.48	394.80	491.12	455.06	417.79	382.76
compressor efficiency	0.712	0.725	0.750	0.677	0.712	0.743	0.744	0.627

turbine speed (r.p.m.)	47350.3	42074.4	30672.9	29730.5	46720.2	43188.3	35909.8	25325.1
turbine pressure ratio	3.674	3.021	2.353	1.659	3.193	2.658	2.067	1.472
mass flow (kg/min)	37.760	31.833	25.592	13.293	31.116	26.402	19.618	9.065
turbine power (kw)	115.02	76.06	40.36	8.78	91.95	59.48	28.78	4.61
turbine torque (n.m)	23.19	17.25	12.56	2.82	18.79	13.15	7.65	1.74
inlet temperature (deg k)	778.75	723.12	644.41	593.77	846.41	779.81	722.01	704.20
turbine nozzle angle	8.886	8.886	8.886	8.886	8.886	8.886	8.886	8.886
turbine efficiency	0.766	0.760	0.738	0.654	0.761	0.752	0.739	0.664
output shaft speed (rpm)	1050.00	1050.00	1050.00	1050.00	1600.00	1600.00	1600.00	1600.00
output shaft power (kw)	213.66	157.54	100.64	46.37	226.10	166.17	106.73	48.93
output shaft torque (n./m)	1942.30	1432.12	914.91	421.53	1348.86	991.32	636.73	291.88
output shaft sfc (kg/kw.hr)	0.223	0.229	0.242	0.274	0.216	0.224	0.240	0.275
output thermal efficiency	0.3747	0.3645	0.3446	0.3041	0.3860	0.3729	0.3480	0.3036
engine fuel flow (kg/min)	0.793	0.601	0.406	0.212	0.814	0.619	0.426	0.224
dynamic injection(degree ca)	337.8	340.1	343.1	345.8	339.1	341.0	342.7	345.3
duration of injection	27.5	23.1	17.8	13.7	25.9	21.5	17.6	13.2
turbine gear ratio	45.1	40.1	29.2	28.3	29.2	27.0	22.4	15.8
pressure loss in pipe a (bar)	0.10345	0.10345	0.10345	0.10345	0.10345	0.10345	0.10345	0.10345
pressure loss in pipe b (bar)	0.10345	0.10345	0.10345	0.10345	0.10345	0.10345	0.10345	0.10345
pressure loss in pipe c (bar)	0.10345	0.10345	0.10345	0.10345	0.10345	0.10345	0.10345	0.10345
pressure loss in pipe d (bar)	0.10345	0.10345	0.10345	0.10345	0.10345	0.10345	0.10345	0.10345

Table-5.4b

CUMMINS L10 D C E

design point 38 49 60 0

number of cylinders	6.0	bore	(m.m.)	125.03	stroke	(m.m.)	136.00	
con-rod length (m.m.)	217.78	inlet valve closing (degs)		173.0	compressor scale factor		1.10	
ambient temperature (deg k)	313.3	ambient pressure (bar)		0.99	cooler effectiveness		0.8200	
compression ratio	16.30	engine diagram factor		0.9105	turbine flow loss factor		0.8000	
----- compressor gear ratio	9.5500	output shaft gear ratio		1.4450	-----			
engine speed(r.p.m)	1756.46	1861.26	1684.90	1557.61	2113.64	2018.79	1875.59	1783.21
boost pressure ratio	2.843	2.363	1.886	1.259	2.665	2.195	1.680	1.254
delivered air to fuel ratio	28.734	30.907	33.454	36.472	28.837	30.505	32.035	33.456
delivery ratio	0.352	0.852	0.852	0.848	0.852	0.851	0.851	0.847
manifold temp (deg k)	343.225	333.722	324.767	317.062	342.773	333.469	324.960	320.903
engine power (k w.)	240.05	180.05	120.02	59.89	239.98	179.97	119.92	71.32
engine torque (n.m.)	1172.75	924.71	681.00	368.33	1085.72	852.55	611.76	383.47
b.m.e.p (bar)	14.6941	11.5848	8.5308	4.6044	13.5972	10.6762	7.6574	4.7901
s.f.c. (ky/kw hr)	0.207	0.210	0.216	0.245	0.210	0.214	0.223	0.248
b.thermal eff.	0.4035	0.3976	0.3866	0.3402	0.3968	0.3894	0.3742	0.3366
fuel / rev (ky.)	4.227	3.382	2.561	1.571	3.977	3.182	2.376	1.652
max cyl pressure (bar .)	125.59	104.80	83.95	55.85	116.73	96.66	74.80	55.76
exhaust temperature(deg k)	740.64	884.60	818.51	742.46	947.16	896.28	843.53	785.22
mass flow (ky/min)	23.929	19.455	14.437	9.100	24.242	19.596	14.309	10.255
percentage heat to coolant	10.64	11.91	14.07	18.69	10.55	11.85	14.17	17.86
compressor speed (r.p.m.)	6127.1	5217.9	3533.7	2318.1	5645.5	4739.6	3372.1	2489.9
compressor pressure ratio	3.097	2.602	2.103	1.456	2.934	2.448	1.913	1.472
mass flow (kg/min)	27.427	23.189	14.965	8.925	25.087	20.952	14.273	9.854
compressor power (kw.)	76.59	51.11	25.35	8.79	65.14	42.72	21.57	9.91
compressor torque (n.m)	119.33	93.49	68.47	36.20	110.14	86.03	61.05	37.97
delivery temperature (deg k)	477.39	444.67	414.46	379.85	467.85	434.90	404.81	390.84
compressor efficiency	0.716	0.748	0.733	0.603	0.727	0.750	0.707	0.610
turbine speed (r.p.m)	46605.7	42621.4	45596.0	17912.8	45984.2	38447.0	33397.8	15791.2
turbine pressure ratio	2.993	2.498	1.999	1.456	2.830	2.344	1.809	1.472
mass flow (kg/min)	28.301	23.861	15.424	10.224	25.950	21.667	14.703	10.688
turbine power (kw)	82.78	52.72	19.74	5.62	75.47	46.84	19.49	6.23
turbine torque (n.m)	16.75	11.81	4.13	3.00	15.67	11.63	5.57	3.76
inlet temperature (deg k)	880.43	821.00	805.78	742.46	733.02	869.87	843.53	785.22
turbine nozzle angle	8.886	8.886	8.886	8.886	8.886	8.886	8.886	8.886
turbine efficiency	0.750	0.750	0.610	0.718	0.756	0.748	0.737	0.679
output shaft speed (rpm)	1900.00	1900.00	1900.00	1900.00	2200.00	2200.00	2200.00	2200.00
output shaft power (kw)	231.07	169.58	105.97	50.62	234.95	171.85	108.74	60.71
output shaft torque (n./m)	1160.87	851.92	532.38	254.29	1019.38	745.61	471.81	263.41
output shaft sfc (ky/kw.hr)	0.215	0.223	0.244	0.290	0.215	0.224	0.246	0.291
output thermal efficiency	0.3884	0.3745	0.3413	0.2875	0.3885	0.3719	0.3393	0.2865
engine fuel flow (ky/min)	0.827	0.629	0.432	0.245	0.841	0.642	0.446	0.295
dynamic injection(degree ca)	340.0	341.7	343.0	344.6	341.0	342.5	343.5	344.5
duration of injection	25.1	21.1	17.5	13.9	24.6	21.1	17.5	14.9
turbine gear ratio	24.5	22.4	24.0	9.4	20.9	17.5	15.2	7.2
pressure loss in pipe a (bar)	0.10345	0.10345	0.10345	0.10345	0.10345	0.10345	0.10345	0.10345
pressure loss in pipe b (bar)	0.10345	0.10345	0.10345	0.10345	0.10345	0.10345	0.10345	0.10345
pressure loss in pipe c (bar)	0.10345	0.10345	0.10345	0.10345	0.10345	0.10345	0.10345	0.10345
pressure loss in pipe d (bar)	0.10345	0.10345	0.10345	0.10345	0.10345	0.10345	0.10345	0.10345

Table-5.4c

Table-5.5 New map, reduced Pa, elevated Ta

CUMMINS L10 I C C		stall point						
		32 14 24 0						
number of cylinders	6.0	bore	(m.m.)	125.03	stroke	(m.m.)	136.00	
con-rod length (m.m.)	217.78	inlet valve closing (degs)		193.0	compressor scale factor		1.10	
ambient temperature (deg k)	313.3	ambient pressure (bar)		0.84	cooler effectiveness		0.9197	
compression ratio	16.30	engine diagram factor		0.9448	turbine flow loss factor		0.8000	
----- compressor gear ratio	9.5500	output shaft gear ratio		1.4450	-----			
engine speed(r.p.m)	1407.17	1259.10	1078.10	842.54	1424.61	1282.57	1098.06	856.42
boost pressure ratio	4.713	3.917	3.044	2.103	4.630	3.843	2.988	2.088
delivered air to fuel ratio	29.836	31.302	31.774	33.799	29.594	31.175	31.714	34.082
delivery ratio	0.854	0.854	0.854	0.854	0.854	0.854	0.854	0.854
manifold temp (deg k)	349.528	338.020	326.257	314.879	349.441	338.131	326.375	314.994
engine power (k w.)	240.06	180.21	120.07	59.92	240.06	180.20	120.07	59.92
engine torque (n.m.)	1630.81	1366.94	1064.30	680.93	1610.85	1341.93	1044.95	669.89
b.m.e.p (bar)	20.4310	17.1407	13.3383	8.5167	20.1805	16.8263	13.0954	8.3794
s.f.c. (kg/kw hr)	0.200	0.195	0.199	0.210	0.200	0.196	0.200	0.210
b.thermal eff.	0.4177	0.4276	0.4189	0.3980	0.4167	0.4261	0.4178	0.3979
fuel / rev (kg.)	5.677	4.653	3.696	2.484	5.621	4.584	3.638	2.444
max cyl pressure (bar)	158.47	146.89	115.15	79.08	156.89	144.31	113.25	78.42
exhaust temperature(deg k)	925.25	861.79	822.26	742.91	929.36	864.55	823.73	740.30
mass flow (kg/min)	23.837	18.340	12.661	7.073	23.698	18.328	12.671	7.134
percentage heat to coolant	10.79	12.43	15.24	21.22	10.82	12.44	15.23	21.11
compressor speed (r.p.m.)	10530.5	9116.5	7387.9	5138.3	10300.5	8944.1	7181.9	4874.3
compressor pressure ratio	4.955	4.139	3.242	2.273	4.874	4.067	3.188	2.259
mass flow (kg/min)	42.025	36.031	28.982	19.905	41.121	35.257	28.102	18.719
compressor power (kw.)	183.10	132.63	83.52	36.90	176.89	127.73	79.69	34.42
compressor torque (n.m)	165.97	138.87	107.90	68.54	163.92	136.32	105.92	67.40
delivery temperature (deg k)	570.60	531.38	484.61	423.93	567.41	527.99	481.92	423.06
compressor efficiency	0.697	0.713	0.727	0.748	0.697	0.713	0.726	0.748
turbine speed (r.p.m)	51267.2	46870.5	39952.7	30399.1	51183.8	46202.5	44951.3	34381.0
turbine pressure ratio	4.832	4.017	3.117	2.150	4.752	3.944	3.066	2.136
mass flow (kg/min)	42.411	36.685	29.431	20.116	41.538	35.884	28.547	18.959
turbine power (kw)	155.44	107.56	63.40	23.20	151.60	104.41	59.32	20.91
turbine torque (n.m)	28.94	21.91	15.15	7.29	28.27	21.57	12.60	5.81
inlet temperature (deg k)	782.21	708.96	641.51	544.86	786.74	712.59	645.66	551.66
turbine nozzle angle	8.886	8.886	8.886	8.886	8.886	8.886	8.886	8.886
turbine efficiency	0.776	0.770	0.761	0.746	0.776	0.769	0.740	0.712
output shaft speed (rpm)	440.00	440.00	440.00	440.00	500.00	500.00	500.00	500.00
output shaft power (kw)	194.70	141.87	91.30	41.88	197.22	143.74	91.20	42.12
output shaft torque (n./m)	4223.71	3077.68	1980.56	908.60	3765.10	2744.01	1741.10	804.17
output shaft sfc (kg/kw.hr)	0.246	0.248	0.262	0.300	0.244	0.245	0.263	0.298
output thermal efficiency	0.3388	0.3366	0.3185	0.2782	0.3424	0.3399	0.3173	0.2797
engine fuel flow (kg/min)	0.799	0.586	0.398	0.209	0.801	0.588	0.400	0.209
dynamic injection(degree ca)	348.9	339.9	342.7	345.7	347.9	340.0	342.7	345.7
duration of injection	29.6	24.4	19.4	14.6	29.4	24.1	19.2	14.5
turbine gear ratio	116.5	106.5	90.8	69.1	102.4	92.4	89.9	68.8
pressure loss in pipe a (bar)	0.10345	0.10345	0.10345	0.10345	0.10345	0.10345	0.10345	0.10345
pressure loss in pipe b (bar)	0.10345	0.10345	0.10345	0.10345	0.10345	0.10345	0.10345	0.10345
pressure loss in pipe c (bar)	0.10345	0.10345	0.10345	0.10345	0.10345	0.10345	0.10345	0.10345
pressure loss in pipe d (bar)	0.10345	0.10345	0.10345	0.10345	0.10345	0.10345	0.10345	0.10345

Table-5.5a

number of cylinders	6.0	bore	(m.m.)	125.03	stroke	(m.m.)	136.00	
con-rod length (m.m.)	217.78	inlet valve closing (degs)		193.0	compressor scale factor		1.10	
ambient temperature (deg k)	313.3	ambient pressure (bar)		0.84	cooler effectiveness		0.8627	
compression ratio	16.30	engine diagram factor		0.9259	turbine flow loss factor		0.8000	
----- compressor gear ratio	9.5500	output shaft gear ratio		1.4450	-----			
engine speed(r.p.m)	1641.38	1501.27	1351.56	1088.92	1877.22	1747.69	1605.82	1383.32
boost pressure ratio	3.973	3.254	2.505	1.741	3.433	2.780	2.163	1.467
delivered air to fuel ratio	29.165	29.658	31.436	34.813	27.943	28.511	30.612	34.519
delivery ratio	0.853	0.853	0.853	0.853	0.852	0.852	0.852	0.852
manifold temp (deg k)	350.152	338.800	326.976	316.050	349.967	338.531	327.327	317.213
engine power (k w.)	240.17	180.09	120.02	59.92	240.00	179.95	119.93	59.88
engine torque (n.m.)	1390.11	1146.45	848.95	526.86	1222.46	984.80	714.53	414.73
b.m.e.p (bar)	17.5235	14.3662	10.6351	6.5899	15.3113	12.3309	8.9444	5.1843
s.f.c. (ky/kw hr)	0.201	0.204	0.207	0.217	0.207	0.211	0.218	0.233
b.thermal eff.	0.4149	0.4090	0.4025	0.3842	0.4034	0.3959	0.3832	0.3580
fuel / rev (ky.)	4.902	4.077	3.067	1.991	4.406	3.615	2.709	1.681
max cyl pressure (bar)	149.95	124.09	95.46	65.58	129.19	106.10	82.90	55.67
exhaust temperature(deg k)	932.29	898.27	836.24	740.66	962.95	926.89	859.24	756.54
mass flow (ky/min)	23.466	18.155	13.031	7.548	23.109	18.013	13.317	8.026
percentage heat to coolant	10.88	12.49	14.99	20.45	10.95	12.53	14.80	19.75
compressor speed (r.p.m.)	8735.8	7397.7	5968.0	3459.8	7353.0	6116.0	4761.2	2636.3
compressor pressure ratio	4.241	3.500	2.728	1.931	3.725	3.051	2.411	1.683
mass flow (ky/min)	34.032	28.615	22.936	12.519	28.079	23.324	17.959	8.908
compressor power (kw.)	130.00	90.41	53.59	19.10	95.57	63.73	35.89	11.49
compressor torque (n.m)	142.05	116.65	85.72	52.68	124.07	99.47	71.96	41.60
delivery temperature (deg k)	539.47	500.90	452.52	404.45	515.20	475.85	432.53	390.45
compressor efficiency	0.701	0.714	0.746	0.712	0.702	0.721	0.751	0.653
turbine speed (r.p.m)	50466.9	45391.5	33626.3	33078.1	50032.0	44061.0	39230.1	24935.2
turbine pressure ratio	4.118	3.378	2.606	1.809	3.603	2.929	2.288	1.560
mass flow (kg/min)	34.901	29.285	23.391	12.754	28.952	23.949	18.366	9.123
turbine power (kw)	121.18	81.06	43.70	10.45	99.14	63.51	32.44	6.05
turbine torque (n.m)	22.92	17.05	12.40	3.01	18.91	13.76	7.89	2.32
inlet temperature (deg k)	820.77	764.43	681.60	615.38	892.23	834.52	758.94	723.69
turbine nozzle angle	8.886	8.886	8.886	8.886	8.886	8.886	8.886	8.886
turbine efficiency	0.770	0.763	0.743	0.657	0.765	0.757	0.742	0.721
output shaft speed (rpm)	1050.00	1050.00	1050.00	1050.00	1600.00	1600.00	1600.00	1600.00
output shaft power (kw)	214.72	158.60	101.62	46.63	227.61	167.42	107.77	49.13
output shaft torque (n./m)	1951.97	1441.78	923.79	423.90	1357.90	998.82	642.95	293.08
output shaft sfc (ky/kw.hr)	0.225	0.232	0.245	0.279	0.218	0.226	0.242	0.284
output thermal efficiency	0.3710	0.3602	0.3408	0.2990	0.3826	0.3684	0.3444	0.2937
engine fuel flow (ky/min)	0.805	0.612	0.415	0.217	0.827	0.632	0.435	0.233
dynamic injection(degree ca)	338.0	340.0	342.9	345.7	339.4	341.0	342.7	345.0
duration of injection	27.1	22.9	17.8	13.7	25.6	21.6	17.7	13.4
turbine gear ratio	48.1	43.2	32.0	31.5	31.3	27.5	24.5	15.6
pressure loss in pipe a (bar)	0.10345	0.10345	0.10345	0.10345	0.10345	0.10345	0.10345	0.10345
pressure loss in pipe b (bar)	0.10345	0.10345	0.10345	0.10345	0.10345	0.10345	0.10345	0.10345
pressure loss in pipe c (bar)	0.10345	0.10345	0.10345	0.10345	0.10345	0.10345	0.10345	0.10345
pressure loss in pipe d (bar)	0.10345	0.10345	0.10345	0.10345	0.10345	0.10345	0.10345	0.10345

Table-5.5b

CUMMINS L10 D C E

design point

33 51 60 0

number of cylinders	6.0	bore	(m.m.)	125.03	stroke	(m.m.)	136.00	
con-rod length (m.m.)	217.78	inlet valve closing (degs)		193.0	compressor scale factor		1.10	
ambient temperature (deg k)	313.3	ambient pressure (bar)		0.84	cooler effectiveness		0.8196	
compression ratio	16.30	engine diagram factor		0.9101	turbine flow loss factor		0.8000	
----- compressor gear ratio	9.5500	output shaft gear		ratio	1.4450	-----		
engine speed(r.p.m)	2014.25	1901.40	1770.85	1569.39	2155.05	2056.44	1916.79	1795.30
boost pressure ratio	3.177	2.596	1.973	1.335	2.948	2.443	1.865	1.331
delivered air to fuel ratio	27.935	28.465	30.079	31.786	27.299	28.423	30.081	29.056
delivery ratio	0.852	0.852	0.851	0.847	0.851	0.851	0.851	0.847
manifold temp (deg k)	349.659	338.402	327.251	319.165	350.049	338.336	327.671	323.284
engine power (k w.)	240.20	179.88	119.86	59.73	240.20	179.81	119.81	71.11
engine torque (n.m.)	1139.30	905.19	647.94	365.56	1064.86	836.94	598.61	380.89
b.m.e.p (bar)	14.2815	11.3301	8.1061	4.5582	13.3486	10.4714	7.4459	4.7439
s.f.c. (kg/kw hr)	0.205	0.214	0.223	0.254	0.207	0.218	0.227	0.256
b.thermal eff.	0.4064	0.3893	0.3746	0.3290	0.4022	0.3820	0.3670	0.3255
fuel / rev (kg.)	4.079	3.379	2.512	1.608	3.852	3.182	2.368	1.692
max cyl pressure (bar)	133.21	98.41	75.49	51.33	129.09	91.70	70.82	51.06
exhaust temperature(deg k)	954.17	932.86	873.43	797.18	963.49	939.05	879.00	847.76
mass flow (kg/min)	22.947	18.286	13.380	8.216	22.796	18.597	13.652	9.203
percentage heat to coolant	11.00	12.41	14.74	19.99	11.10	12.28	14.58	19.11
compressor speed (r.p.m.)	6679.0	5601.3	4354.5	2430.6	6040.9	5099.2	3765.6	2605.3
compressor pressure ratio	3.484	2.883	2.237	1.569	3.271	2.747	2.143	1.588
mass flow (kg/min)	25.263	21.170	16.350	8.022	22.662	19.051	13.745	8.824
compressor power (kw.)	80.82	53.58	29.72	9.19	68.31	45.15	23.71	10.28
compressor torque (n.m)	115.50	91.30	65.15	36.10	107.94	84.52	60.11	37.66
delivery temperature (deg k)	503.23	463.97	421.76	372.44	495.47	454.49	416.31	403.82
compressor efficiency	0.702	0.732	0.747	0.629	0.701	0.741	0.740	0.636
turbine speed (r.p.m)	50223.5	45533.5	26975.8	16868.2	50415.6	48948.2	38136.8	19023.8
turbine pressure ratio	3.362	2.760	2.114	1.569	3.149	2.624	2.020	1.588
mass flow (kg/min)	26.471	21.784	16.806	10.067	24.034	19.676	14.191	9.951
turbine power (kw)	88.09	56.96	26.26	7.02	79.27	50.70	23.56	7.94
turbine torque (n.m)	16.74	11.94	9.29	3.97	15.01	9.89	5.90	3.99
inlet temperature (deg k)	917.74	876.19	799.63	797.18	963.49	928.96	876.25	847.76
turbine nozzle angle	8.886	8.886	8.886	8.886	8.886	8.886	8.886	8.886
turbine efficiency	0.762	0.754	0.703	0.673	0.759	0.739	0.737	0.690
output shaft speed (rpm)	1700.00	1900.00	1900.00	1900.00	2200.00	2200.00	2200.00	2200.00
output shaft power (kw)	231.47	170.88	107.58	51.55	235.23	173.00	110.48	61.91
output shaft torque (n.m)	1162.86	858.49	540.46	258.96	1020.59	750.60	479.34	268.59
output shaft sfc (kg/kw.hr)	0.213	0.226	0.248	0.294	0.212	0.227	0.246	0.294
output thermal efficiency	0.3917	0.3698	0.3362	0.2839	0.3939	0.3675	0.3384	0.2834
engine fuel flow (kg/min)	0.822	0.642	0.445	0.252	0.830	0.654	0.454	0.304
dynamic injection(degree ca)	329.5	341.8	343.1	344.5	325.4	342.6	343.6	344.5
duration of injection	24.7	21.3	17.6	14.1	24.3	21.3	17.7	15.1
turbine gear ratio	26.4	24.0	14.2	8.9	22.9	22.2	17.3	8.6
pressure loss in pipe a (bar)	0.10345	0.10345	0.10345	0.10345	0.10345	0.10345	0.10345	0.10345
pressure loss in pipe b (bar)	0.10345	0.10345	0.10345	0.10345	0.10345	0.10345	0.10345	0.10345
pressure loss in pipe c (bar)	0.10345	0.10345	0.10345	0.10345	0.10345	0.10345	0.10345	0.10345
pressure loss in pipe d (bar)	0.10345	0.10345	0.10345	0.10345	0.10345	0.10345	0.10345	0.10345

Table-5.5c

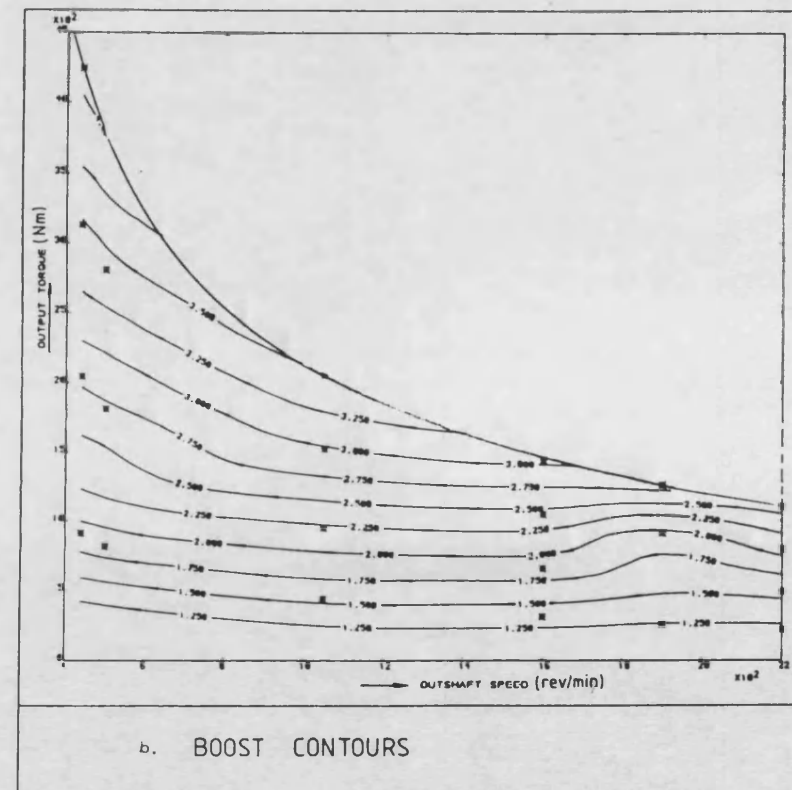
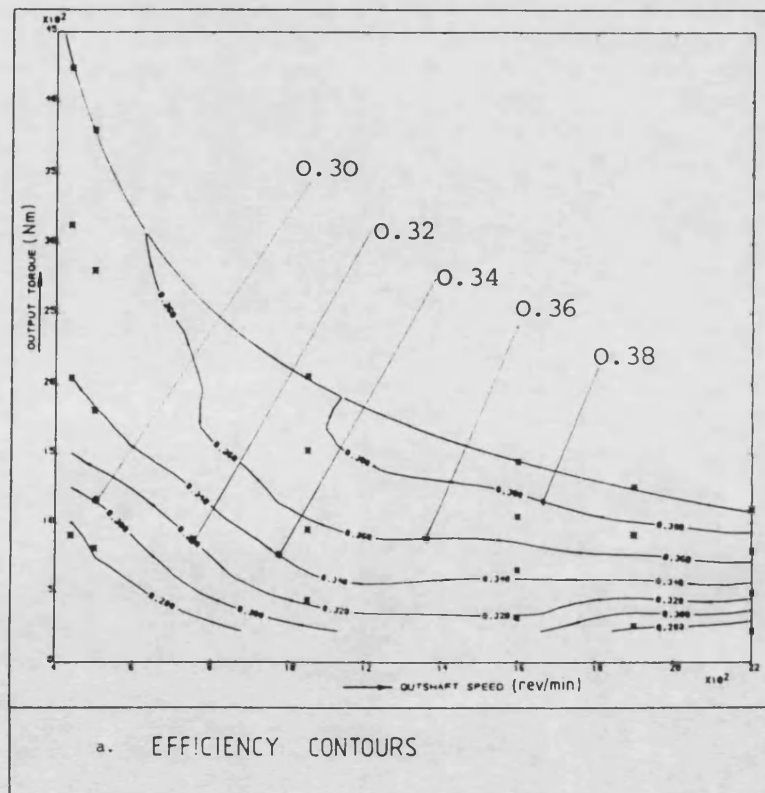
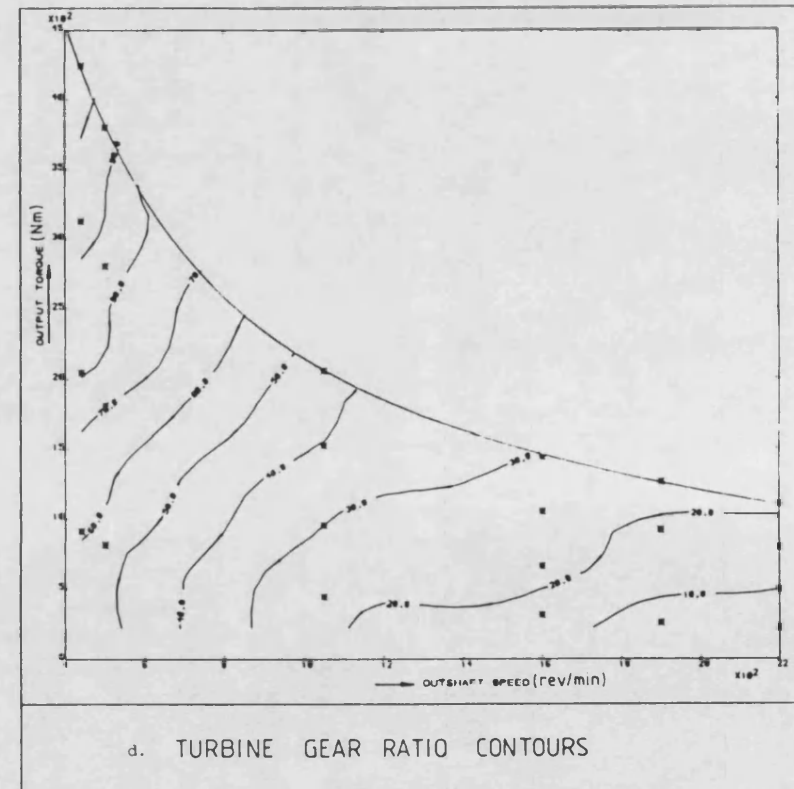
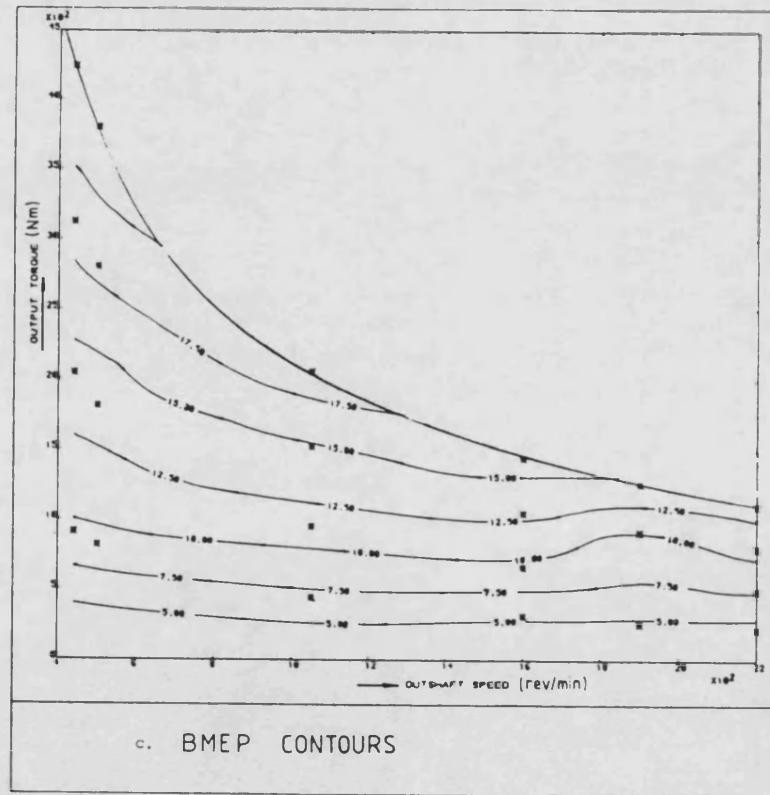


Fig-5.1(a-d) The characteristics of the DCE with fixed nozzle turbine (standard map, standard conditions)



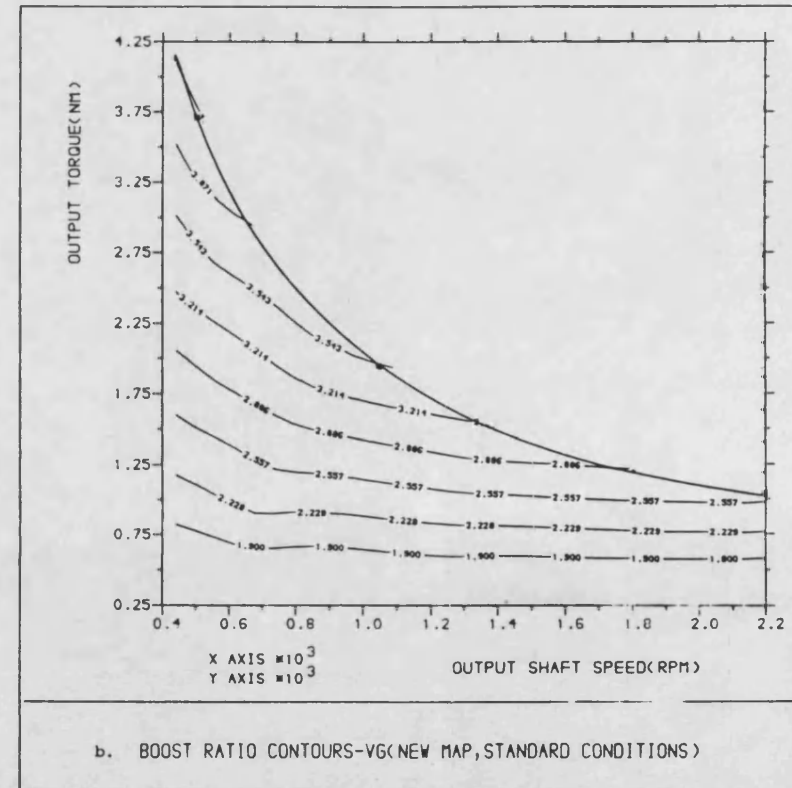
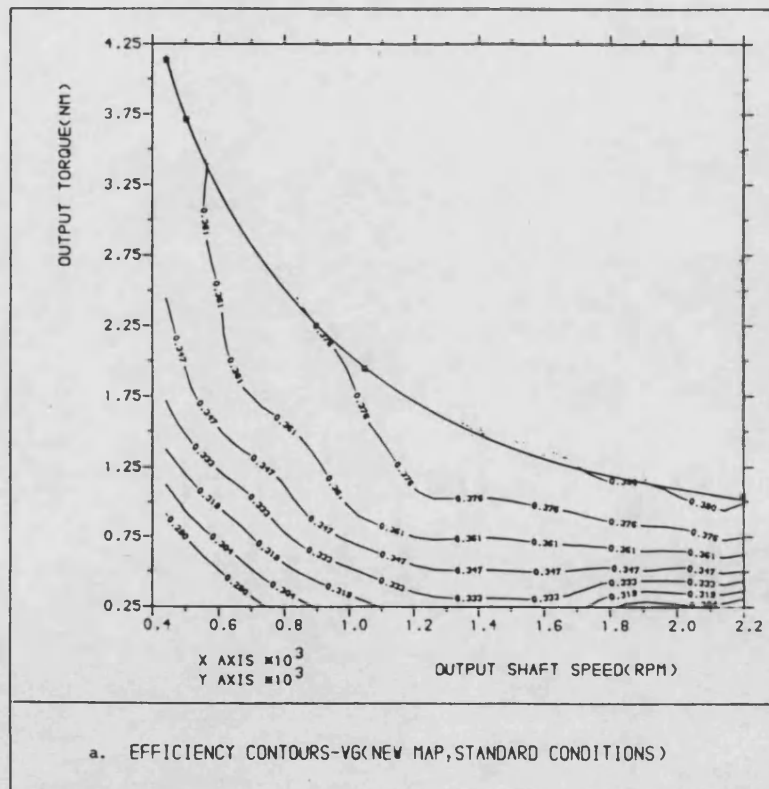
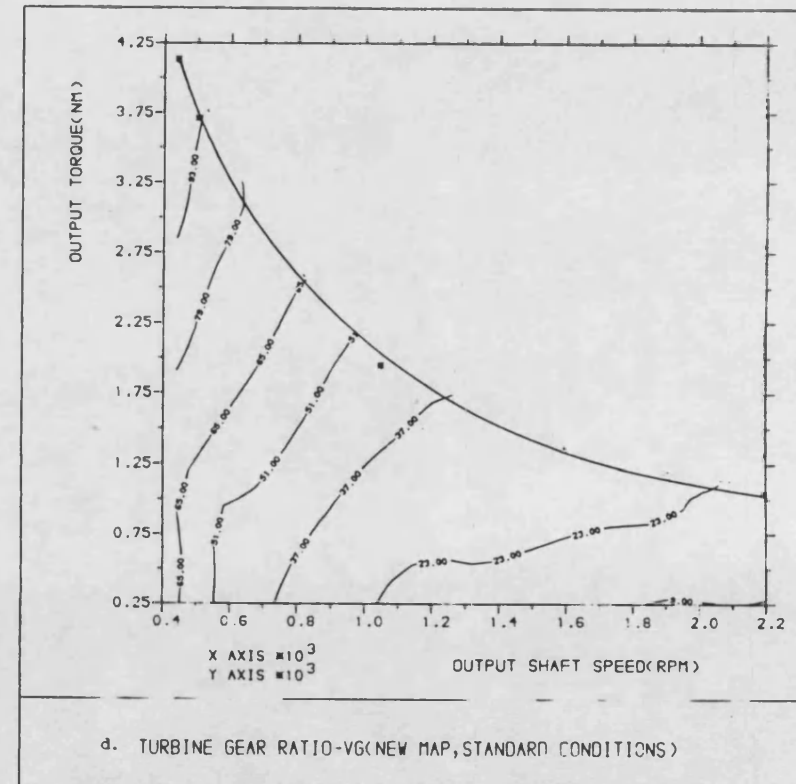
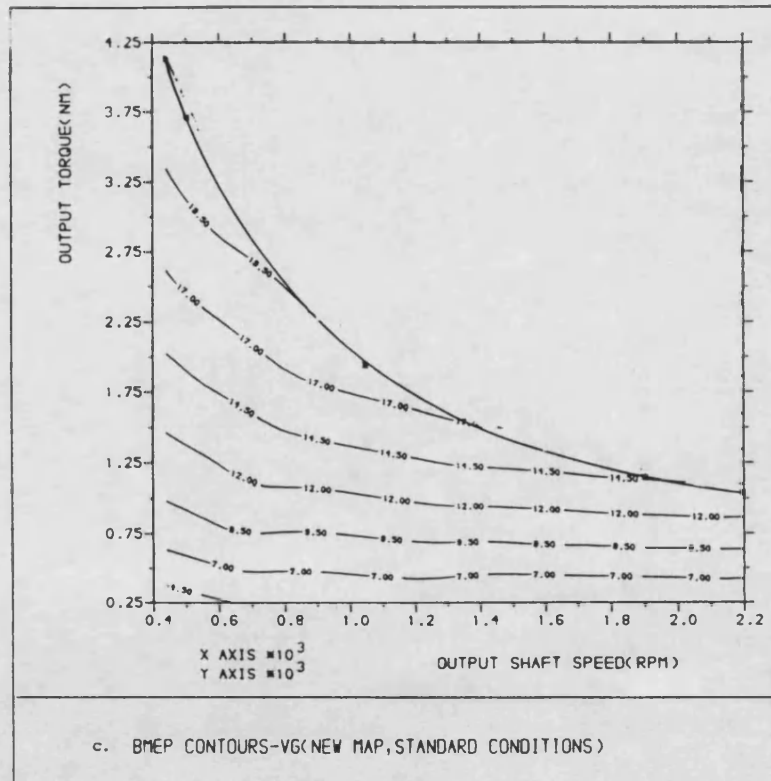
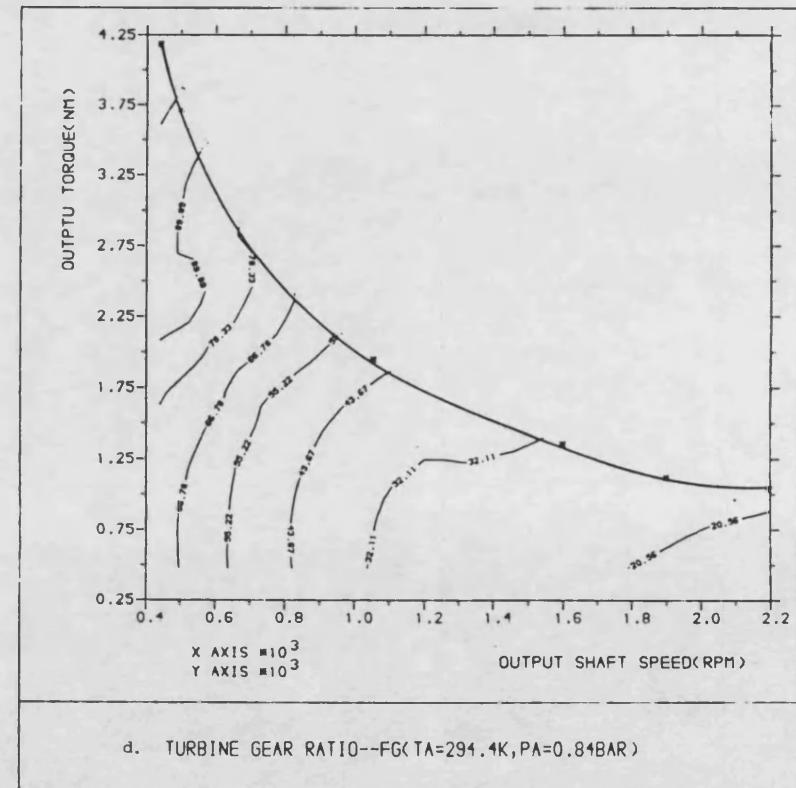
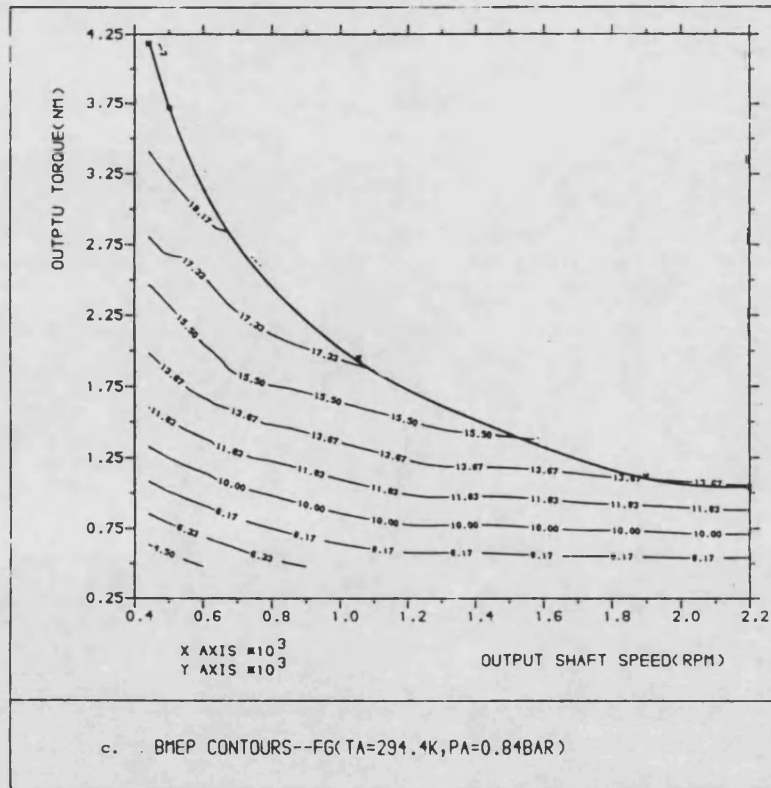


Fig-5.2(a-d) The characteristics of the DCE with fixed nozzle turbine(new map, opt. speed, standard conditions)





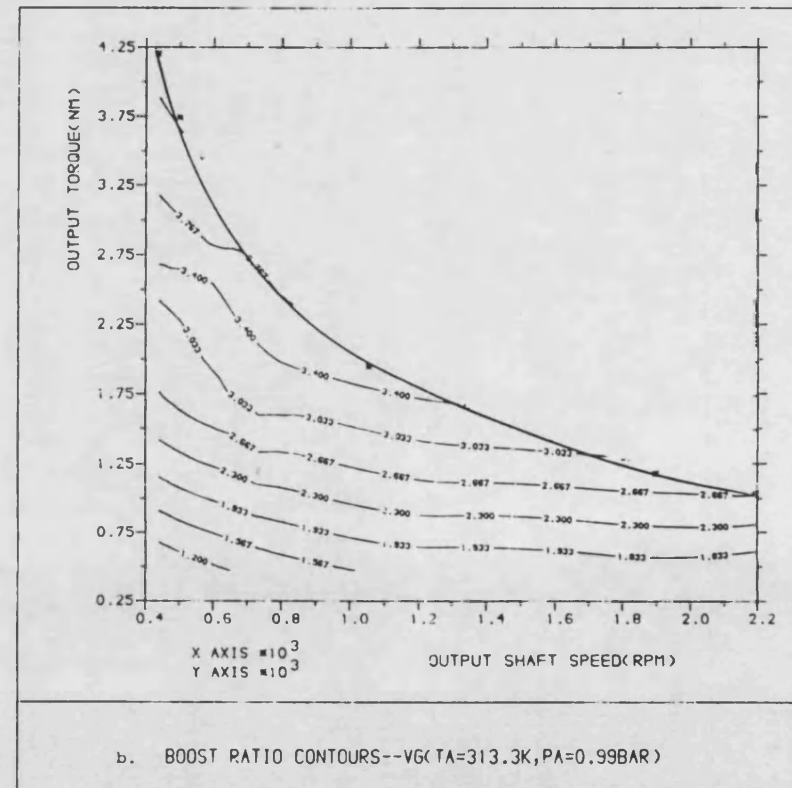
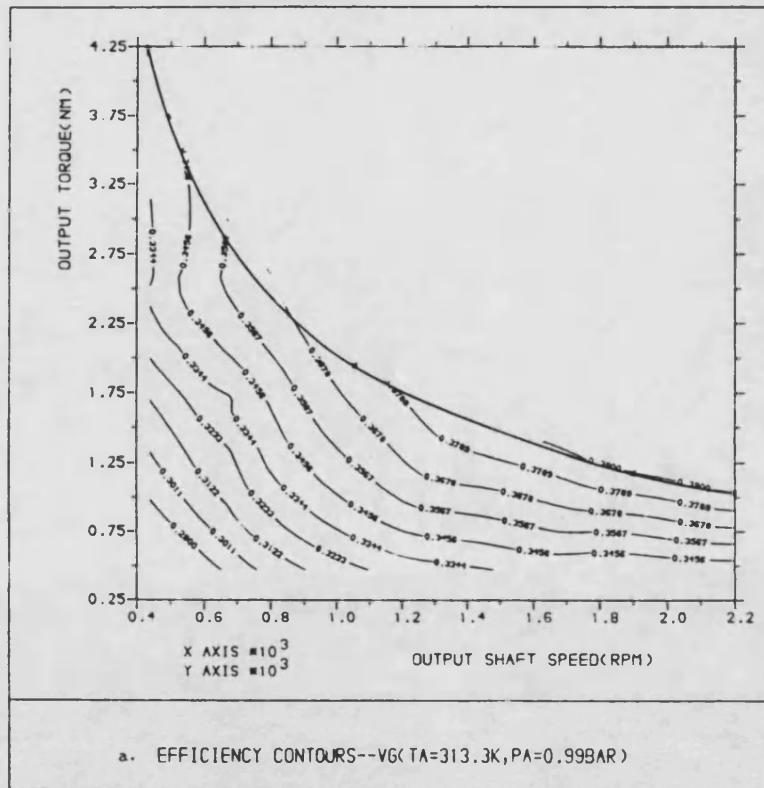
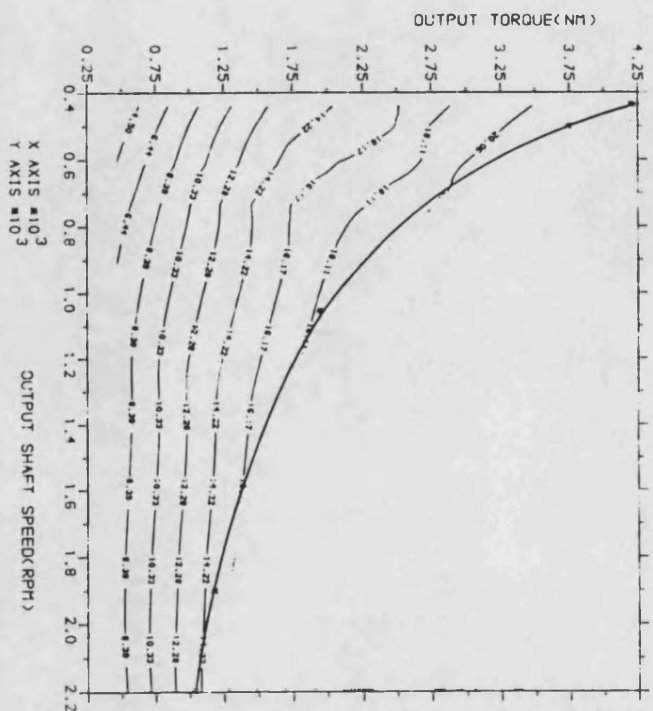
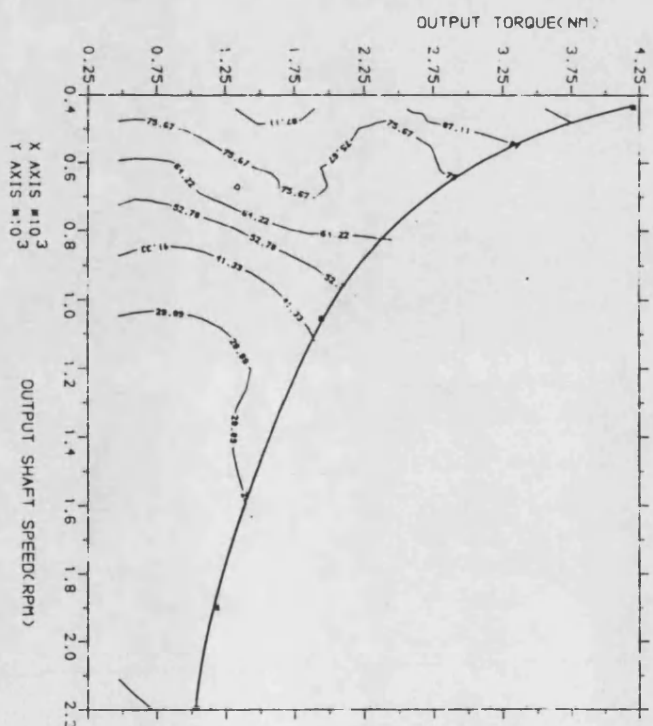


Fig-5.4(a-d) The characteristics of the DCE with fixed nozzle turbine (new map, opt. speed, elevated Ta)



c. BHP CONTOURS--VG(TA=313.3K, PA=0.99BAR)



d. TURBINE GEAR RATIO--VG(TA=313.3K, PA=0.99BAR)

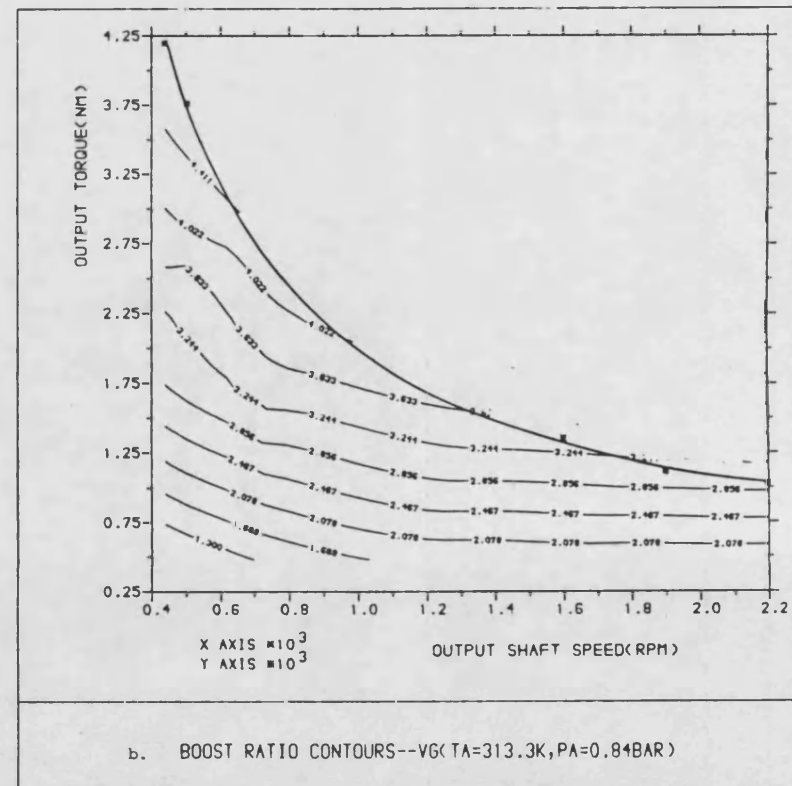
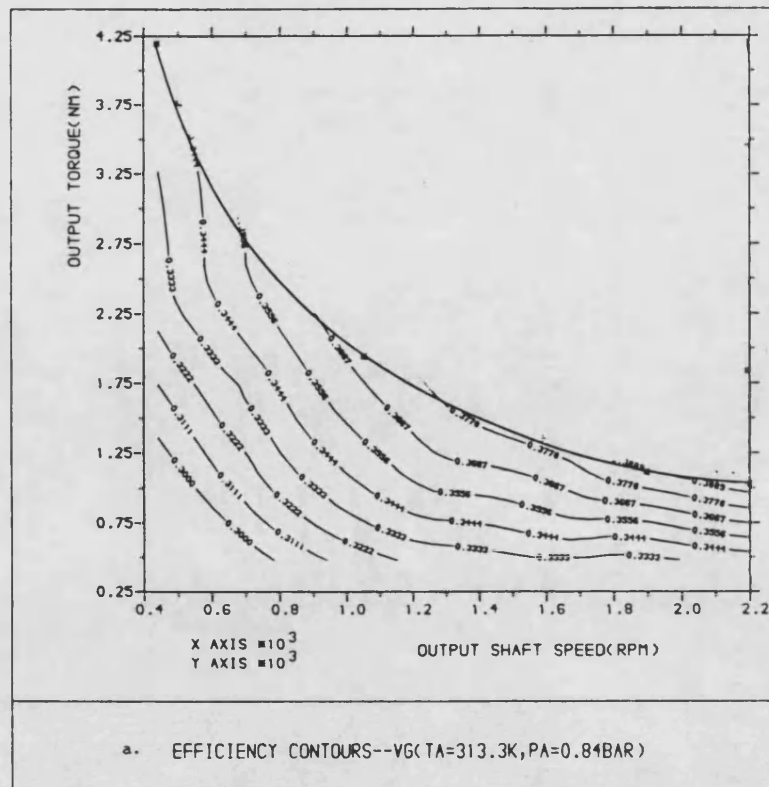
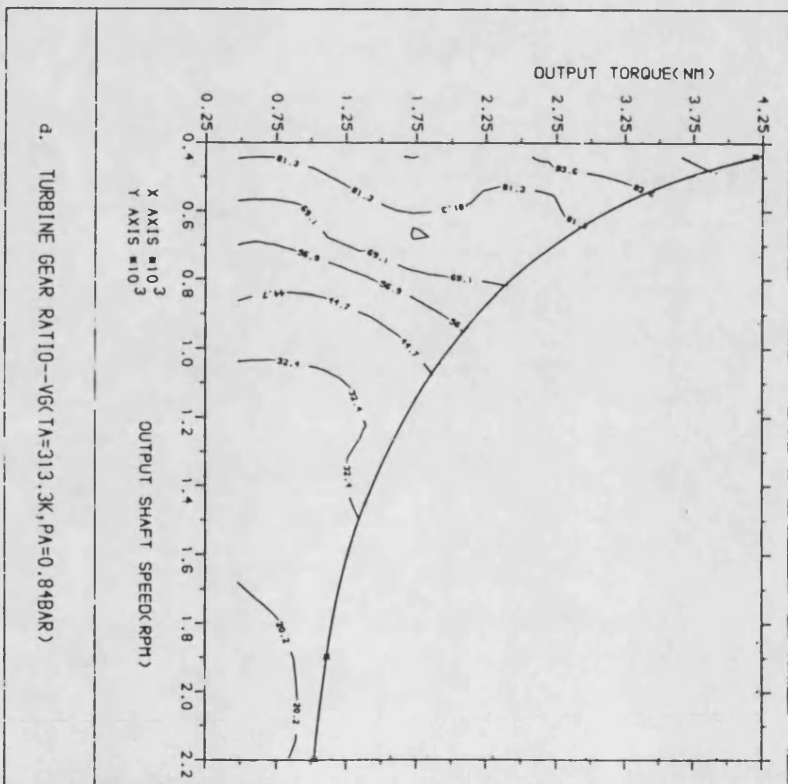
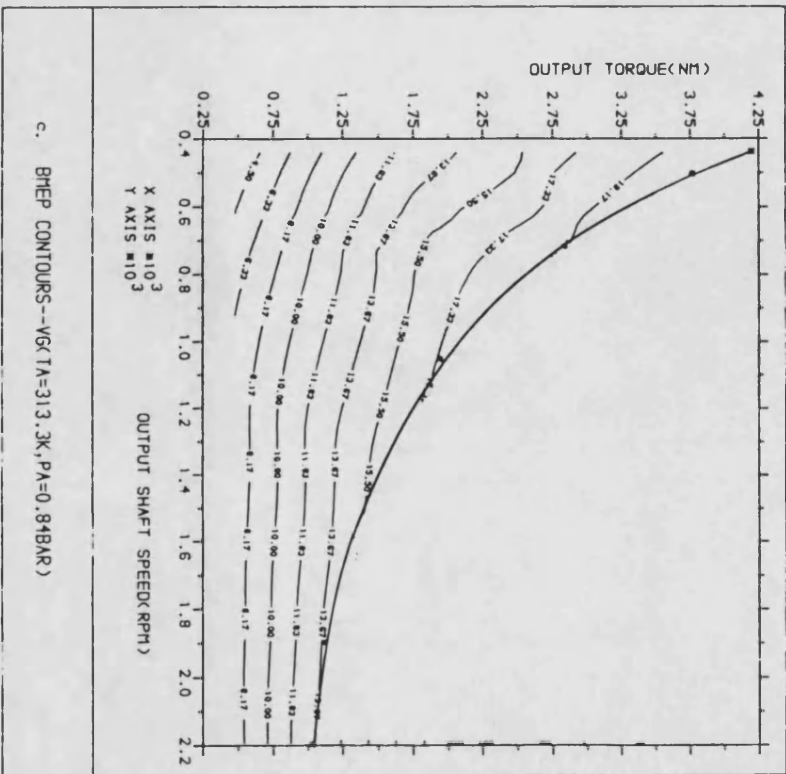


Fig-5.5(a-d) The characteristics of the DCE with fixed nozzle turbine(new map, opt. speed, reduced Pa, elevated Ta)



CHAPTER 6

EXPERIMENTS AND EVALUATION OF GEARBOX LOSSES OF THE LEYLAND 520 DCE

6.1 Background

The most recent prototype DCE, equipped with the Leyland 500 6-cylinder 8.21 DI engine, has been built up and fully instrumented. Steady state tests have been completed and the results at all the test points optimised.

Generally, these results are very encouraging. Fig-6.1 shows the overall system efficiency obtained by D. Prince[41], from some preliminary experiments. The significant effect of the optimisation can also be seen, the area embraced by constant efficiency lines being broadened.

Fig-6.2 shows the experimental overall efficiency contours obtained in the course of recent experiments. Certain improvement has been made over those by D. Prince. Further, the operation of the system has been pushed towards a higher load area, approaching the theoretically calculated limiting torque curve.

Although confidence can be placed in the accuracy of the overall system performance data from experiments(e.g overall efficiency), which are the results of direct measurements, uncertainty still exists in terms of the performance of some individual components. This uncertainty applies particularly to gearbox losses.

In the experiments, the engine speed and torque, the output shaft speed and torque, i.e. engine power and output power, are measured; the compressor power is interpolated(or extrapolated) from the manufacturer's limited experimental data, while the turbine power is calculated according to the enthalpy difference between the exit and inlet, based on measured temperature. The gearbox loss is subsequently calculated from a system energy balance, i.e.

$$W_{in} = W_{out}$$

$$W_e + W_t = W_c + W_o / s + W_l$$

i.e.

$$Wl = We + Wt - Wc - Wo / s \quad (1)$$

where

We engine power

Wt turbine power

Wc compressor power

Wo / s output shaft power

Wl (gearbox)loss

As is well known, gear train transmission systems are usually very efficient. However, the data from the experiments do not seem encouraging. As an approximate measurement, the overall transmission efficiency of the system can be defined as (actual output power)/(ideal output power), the ideal power being derived from the geartrain arrangement with zero transmission loss. In this investigation, six sets(A-F) of typical experimental data, Table-6.1, are examined in detail. The overall transmission efficiencies at these operating points can be calculated. These points are plotted on an output torque and speed map, together with their respective transmission efficiencies, Fig-6.3. It can be seen that these efficiencies are comparatively low, all under 80%.

Whether these data are realistic depends on the accuracy of the compressor power **Wc** and the turbine power **Wt**. The present investigation has been carried out experimentally. Accordingly, it is both necessary and informative to give a brief account of the experimental facilities and procedures in the first place.

6.2 Experimental Facilities

6.2.1 Mechanical Components

The general layout of the experimental plant is shown in Fig-6.4, and Fig-6.5 is a schematic of the gas flow paths connecting various components. As can be seen, the pipe lines are longer than those applicable to a practical application. However, efforts have been made to construct the best possible arrangement, consistent with the need for extensive flow, torque and other measurements. It should be noted that the experimental prototype, unlike the DCE discussed in earlier chapters, employs a fixed ratio step down gearbox between turbine and output shaft, rather than a CVT.

a)Engine

The engine used is a Leyland 520 6 cylinder in-line diesel, with certain modifications, i.e. integral block and head, low compression ratio pistons and uprated fuel pump. Some important parameters are listed below:

cylinder bore	118mm
stroke	125mm
connecting rod length	218.5mm
compression ratio	12.8:1
swept volume	8.2 litres
firing order	153624
valve timing:	
IVO	10deg. BTDC
IVC	50deg. ABDC
EVO	46deg. BBDC
EVC	14deg. ATDC
	(24deg. overlap)
rated speed	2600rpm
rated power	266kw at 3:1 boost
max torque speed	1673rpm
max torque power	229kw at 3.8:1 boost

There are two aspects which deserve special attention. One is that a variable injection timing device has been implemented. The basic design is a helically-splined shaft and a matching collar, Fig-6.6. As the collar is moved up the shaft, an angular displacement is produced between the two components and thus, being incorporated in the fuel pump drive, injection timing can be retarded. The collar can be moved by a yoke and arm driven by a jack which is connected up to its servovalve, giving a range of 22deg. crankshaft angular displacement.

Another aspect is that the mechanical governor has been removed from the fuel pump, while a jack and LVDT have been installed instead. Therefore, rack position can be controlled directly through an electronic system.

Fig-6.7 shows the servo-systems for timing and rack position, together with those for nozzle angle and a compressor brake(to prevent compressor reversal).

b)Compressor

A Compair rotary positive displacement compressor is adopted, which has the following specifications:

max output	0.870kg/sec
rated output	0.477kg/sec
max speed	11500rpm
rated speed	6606rpm
max P-ratio	3.95:1
rated P-ratio	3.171:1
max power absorption	173kw
rated power absorption	73.97kw

c)Turbine

The turbine is derived from a Napier Co-45 radial inflow type. Variable nozzles are implemented and the mechanism is shown in Fig-6.8. Each nozzle is mounted on a rod. The arms on the outside end of the rods are attached by a spring steel tab to a ring which can rotate, guided by three roller bearings fixed to the housing, thus varying the nozzle orientation and hence the flow area(0-5 square inch). This rotating ring is actuated by a hydraulic jack and an accompanying LVDT gives position feedback(Fig-6.7).

rated output	101.7kw at 50000rpm
rated inlet temp.	660deg.C
rated P-ratio	3.17:1
max torque output	156.4kw at 46500rpm
max torque inlet temp.	414deg.C
max torque P-ratio	3.95:1

d)Dynamometer

2 Sundstrand variable swash axial piston pumps in parallel driven by a splitter gearbox, are employed to dissipate energy through a relief valve by converting pressure into temperature. The associated hydraulic block is shown in Fig-6.9. Use of two pumps is matched by twin valves and twin coolers.

Load control is again implemented by use of electronics. The torque is controlled by adjusting the pump outlet pressure through a servovalve.

It is required that the two pumps are equally loaded at all times. The system adopted is shown in Fig-6.10, in which a single cone pilot stage is used to set the same max pressure limit for both pumps; a single pressure tapping is used to supply the servovalve and the same servo-pressure is applied to both loading valves. Some important parameters are shown below:

rated speed	2400rpm
rated power	at 35-bar(each)
rated flow	400l/min at rated speed(each)

The rating for the splitter gearbox is as follows:

rated speed input	3409rpm
rated speed output	2440rpm
rated speed ratio	1.392:1
rated power	275kw

e)Geartrains

The geartrains including the epicyclic geartrain, compressor and output shaft step-up gears and turbine geartrain are shown in Fig-6.11, in which the rated and stall speeds of all elements are indicated. The various ratios are listed below:

annulus to sun	3.074:1
sun to compressor	2.872:1
planet carrier to output shaft	2.44:1
turbine to output shaft	14.67:1

6.2.2 Instrumentation and Data Acquisition

All test data and controls are brought out to an instrumentation rack(Fig-6.12) and manometer board outside the test cell.

a)Speeds

Magnetic pick-ups and toothed wheels are used to measure the engine(120T), output shaft(120T) and compressor(60T) nominal speeds. The obtained signals are processed by f-V converter cards and subsequently displayed in the instrumentation panel.

Each of two sets of a once/rev marker and an optical pick-up is used to count the engine and output shaft revolutions. These and a time recording counter, are

operated simultaneously (with the fuel weighgear) to obtain average speeds.

The output shaft speed signal from the 120T wheel and the engine speed signal from a magnetic pick-up and another 154T wheel are used to obtain a compressor speed with a calculating card. This calculated compressor speed is used as an independent check on the measured one(from the 60T wheel). Turbine speed is calculated from the fixed gear ratio relative to the output shaft.

A dc tachogenerator is mounted on one of the hydraulic pumps for dynamometer control purpose.

b)Torque

Strain gauge torque transducers are used to measure the engine and output torques. The output torque meter is conditioned by its own bridge-amplifier box, which has a mechanical meter on it, and the output is passed through a gain/offset card to make it suitable for use as a feedback signal for the dynamometer controls. A digital readout in the controls gives the torque reading.

The engine torque meter is conditioned by an amplifier card and displayed on a DVM.

Compressor torque cannot be directly measured but is inferred from the manufacturer's experimental data. It is also impossible to obtain a direct measurement for the turbine torque; rather, turbine power is calculated from the temperature drop across the turbine, mass flow and pressure ratio.

c)Gas Pressures and Temperatures

A pressure transducer is used to measure the compressor delivery pressure in the plenum. The obtained signal is conditioned by instrument amplifier and displayed on a DVM. For other pressures, manometers(water or mercury as relevant) are employed to obtain the pressure differences against certain datum values(compressor delivery pressure in many cases), and the manometers are all displayed on a manometer board.

No.1 cylinder pressure is measured by a Kistler 6502 pressure transducer. The output is directed to a charge amplifier to convert it to a voltage and can be shown on an oscilloscope.

All temperatures, including inlet and exhaust manifold temperatures, the inlet and outlet temperatures of the turbine and compressor, etc. are measured by

thermocouples, which are connected to one of the two switching/display units, one up to 200deg.c('cold') and the other up to 1400deg.c('hot').

d)Gas Flows

Two mass flows are measured. An orifice plate is placed at the compressor inlet pipe section for the total system flow and another one is mounted on the pipe section between the compressor outlet plenum and engine inlet manifold for engine mass flow. From these two measurements the bypass flow can also be determined.

e)Fuel Flow

The fuel system is shown in Fig-6.13. The engine can be switched between the tank supply and a beaker. The steady state fuel flowrate can be measured accurately by the beaker on a set of scales. When a quantity of fuel(equivalent to the counter weight of the scale) is being consumed from the beaker, the time elapsed, and the engine and output shaft revolutions passed during the same period are recorded simultaneously. Therefore the fuel flowrate(and the average speeds of the engine and output shaft) are obtained.

An in-line positive displacement fuel flow meter mounted on the supply line can produce a pulse for every unit of fuel flow through a f-V converter device, to provide a flowrate feedback signal for governor constant fuel control purposes.

f)Injection Timing, Rack Position and Nozzle Angle

Three position transducers are used in parallel with the servo-driven jacks to provide position feedback signals for rack, nozzle angle and timing controls, Fig-6.7.

A 360T plate on the engine flywheel provides pulses every degree of crankshaft rotation. This can be combined with the once/rev marker on the flywheel at the TDC to give the instantaneous crankshaft position.

6.2.3 Control System

a)Engine Governor

This is a rack position loop around rack servo-valve, Fig-6.14. The rack demand comes through a limiting circuit which provides an adjustable maximum fuelling stop. There are three running modes, i.e. speed, rack and fuel demands. In speed and fuel modes, a rack demand is generated by the error between the demand and feedback signals. While in rack demand modes, the demand signal is set

directly.

b)Dynamometer Control

A torque control through an electro-hydraulic servo-valve is applied, which is capable of three modes, Fig-6.15. In speed demand mode, the torque demand is generated from the error between the demanded and feedback speeds. In torque demand mode, the demand signal is applied directly to the torque loop. In windage mode, a torque demand which increases linearly with speed feedback signal, is generated.

c)Injection Timing and Turbine Nozzle Angle

In both cases, a simple position demand loop is applied. For timing, the feedback signal comes from the carrier-amplifier card and the error voltage is converted to a current and used to drive the servovalve, while for nozzle angle, the feedback signal comes directly from the LVDT.

d)Bypass Flow

A butterfly valve is mounted in the bypass duct. However, in the steady state tests, the effects of bypass flow control is not particularly strong, therefore the bypass valve is always left wide open.

6.2.4 Data Processing

For effective control and experiment, a microprocessor has been commissioned. Run time data can be recorded via keyboard during tests. With special software, the records can be updated automatically. Further, all the system performance data can be calculated(using a data reduction program) and then systematically stored in discs, which can be printed out as needed. Fig-6.24 is a sample of data output.

6.3 Investigation of Gearbox Losses

Theoretical prediction of gearbox losses with reasonable accuracy is very difficult. In the present case, use of an epicyclic geartrain further complicates the matter, particularly considering that the operating condition of this geartrain (speed and load of individual gears) varies over a very wide range. On the other hand, experiments can be straightforward, provided accuracy can be assured. The uncertainty concerning gearbox losses arises from the fact that the physical arrangement of the components makes it impossible to fit torquemeters to the compressor and turbine shafts which account respectively for the sungear and part

of the planet carrier torque (see Fig-6.16).

The adopted experimental procedure is based on the assumption that the compressor performance data, deduced from the manufacturer's map, are accurate, while the major source of error is the turbine performance data. In order to eliminate this error term, the turbine has been dismantled, in an attempt to isolate the gear loss, by running the engine-compressor-gearbox combination, as far as possible, under similar conditions to those for the complete unit. Therefore the accuracy of the results can be improved.

Fig-6.16 shows the connection between various components, i.e. the engine, compressor, turbine and output shaft through the gear arrangement. If the turbine is disconnected, the torque contribution of the turbine to the output shaft will be eliminated. The following relationship will hold:

$$W_e = W_c + W_o / s + W_l$$

i.e.

$$W_l = W_e - W_c - W_o / s \quad (2)$$

Clearly, if the accuracy of W_c can be guaranteed, the gearbox losses thus obtained will be realistic.

Experiments were carried out against the steady state tests. Essentially, at a specific operating point, the engine and the compressor are brought to the same conditions as those when the turbine is fitted; and at the same time, the output shaft speed is maintained. In the absence of the turbine, the output shaft torque is equal to that part contributed by the engine. In the following investigation, only some typical data are used, Table-6.2. These data correspond to those in Table-6.1 in terms of operating conditions.

The gearbox losses with and without the turbine at the selected operating points are shown in Fig-6.17 on an engine torque(fixed) and output shaft speed map. Generally, the gearbox losses have been substantially reduced when the turbine is disconnected. As can be seen, some contradictory results have been obtained: at two operating points, negative loss values have been obtained, i.e. power was generated by the gearbox.

From equation(2), it can be seen that the reason for this anomaly can only result from inaccuracies in the compressor operating data. Obviously, if the deduced compressor power is too high, then the gearbox losses will be underestimated and

vice versa.

Before any further discussion, it is necessary to make clear the interaction between various components in the geartrain, particularly the turbine geartrain in relation to the epicyclic set, Fig-6.16. Because the turbine(when fitted) transmits power directly to the output shaft, it does not affect the power balance in the epicyclic; this is certainly true under steady state conditions. Consequently, if the engine torque and speed, and the output shaft speed are fixed, then the operating condition of the epicyclic will be fixed, and hence also the losses in it.

Further, assuming that the losses in the turbine geartrain are essentially speed dependent, i.e. not severely dependent on turbine torque, similar losses will be obtained whether the turbine is operative or not; therefore one would expect that the total losses with and without the turbine should be approximately the same, provided the system is working under the same conditions(fixed engine torque and speed, and fixed output shaft speed).

However, because of the errors which exist in both the compressor and turbine performance data, it is impossible to draw any sensible conclusion at this stage. Clearly, it is essential that these errors be identified and subsequently rectified if possible. For this purpose, operations of major individual components will be assessed.

a)Compressor Operation

In the following the deduced compressor power is compared with its ideal value(lossless) based on epicyclic gearbox torque and speed balance, thus gaining an insight as to how and to what extent the deduced data deviate from realistic values. As a matter of convenience, the data without turbine will be used in the analysis(Table-6.2).

Under ideal conditions, the compressor torque can be derived from the engine torque as follows:

$$(\tau_c)_i = \tau_e / cgr$$

and the power will be

$$(W_c)_i = K. \tau_c. N_c$$

where

τ_e	engine torque
K	constant(2π)

N_c	compressor speed
cgr	overall compressor gear ratio

If the transmission loss through the compressor geartrain is W_{lc} , then

$$(W_c)_i = (W_c)_a + W_{lc}$$

Where $(W_c)_a$ represents the actual compressor power. Clearly, under any circumstances, the actual power will be less than the ideal power (the compressor power consumption is less than that ideally provided by the engine through the geartrain). Unfortunately, direct measurement of compressor power is impossible. Instead it has to be deduced from manufacturer's data (Fig-6.19), where compressor power is expressed as function of speed and pressure ratio.

Fig-6.18 shows the ideal and deduced compressor power at the selected operating points (as in Fig-6.17) on the engine torque and output shaft speed map. These data show that the deduced values are very high, most of them being fairly close to the ideal values. Particularly in some cases (A, C and F), the deduced values exceed the ideal values. Obviously, these cannot represent the actual compressor power. The error may result from the way in which the manufacturer's map is used to calculate the compressor performance data.

The manufacturer's map is presented in two separate graphs. One represents power against speed, with pressure ratio as parameter, Fig-6.19. The other represents the volume flow rate against speed, again with pressure ratio as parameter, Fig-6.20. In these graphs, the compressor speed is limited to between 4600 and 9600 rpm, and the pressure ratio to between about 1.685 and 3.647. In the experiments, these two graphs are digitised in the form of numerical arrays and the compressor performance data at a specific operating point are obtained by interpolation if this point lies within the limits of the two manufacturer's graphs, or by extrapolation if otherwise. Usually, data from interpolation should be fairly accurate. Whilst error can rarely be incurred as a result of the speed lying outside the limits in the manufacturer's graphs, as can be seen, for fixed pressure ratio, both the power and flow rate are linearly related to speed; extrapolation outside the pressure ratio limit can certainly lead to inaccuracies, as can also be seen, the lines of constant pressure ratio on both graphs show very irregular patterns, as far as their spacing is concerned; however, in the data reduction program used in the experiments, simple linear interpolation (extrapolation) is applied, which is apparently inappropriate.

In Fig-6.21 the compressor geartrain efficiency c_{ge} defined as (deduced compressor power)/(ideal compressor power) as well as the gearbox losses at the selected operating points (without turbine) are shown in a synthesised compressor map derived from Fig-6.19 and Fig-6.20. From this plot, it can be seen that the operating points where major error occurs (deduced power greater than the ideal values and accompanied by negative gearbox losses), lie in the area far beyond the manufacturer's data limit in terms of pressure ratio (A and C). While within the pressure ratio limit, reasonable results can be obtained even if the speed lies in the area where extrapolation has to be carried out (B,D); if errors do occur, their magnitudes would be very small (F).

Of all the six points, only one (E) lies within the manufacturer's data limits, with a transmission efficiency of 98.6%. If the manufacturer's data are considered accurate, the deduced compressor performance data at this point should also be taken as accurate. If this is accepted, it could be concluded that c_{ge} is very high and W_{lc} very low. Points B and D may be similarly considered, though this might not be strictly correct.

It can be seen that c_{ge} 's at points B, D and E are very close, the differences between them being under 1%. If the accuracy of these values is taken as acceptable, then it should be expected that no significant error would result if an average value of 0.985 is assumed at those points where anomaly occurs (points A, C, F). From this the actual compressor power can be adjusted and further, overall gearbox losses can be corrected. Fig-6.22 compares the originally calculated losses and the corrected values. Clearly, anomalous negative losses have been eliminated. Further, it can be seen that the loss increases with engine torque and output shaft speed, and the losses appear to be more speed-dependent. Although at point A, the original negative value has been corrected, the very low loss tends to suggest that the assumed efficiency of 98.5% might still be too high; however, considering the very low output shaft speed at this point, this could be accepted. Generally this figure looks reasonable.

b) Output Shaft Operation

A procedure similar to that for the compressor analysis can be employed to deal with output shaft operation. Again the results without turbine will be considered (Table-6.2).

There is the following relationship between the ideal and the actual output

power:

$$(W_o / s)_i = (W_o / s)_a + W_{lo} / s$$

where

$(W_o / s)_i$ ideal output power

$(W_o / s)_a$ actual output power

W_{lo} / s represents the transmission loss through the output shaft geartrain (through the epicyclic set) (strictly, this should include the loss which occurs through the turbine geartrain which remains while the turbine is disconnected). Clearly, the ideal power is dependent on the engine torque and output shaft speed:

$$(\tau_o / s)_i = \tau_e / ogr$$

$$(W_o / s)_i = K. (\tau_o / s)_i . N_o / s$$

where

$(\tau_o / s)_i$ ideal output torque

ogr overall output shaft gear ratio

N_o / s output shaft speed

K constant(2π)

Fig-6.23 shows the output shaft geartrain loss and an arbitrary output shaft geartrain transmission efficiency defined as (measured power)/(ideal power), again on an engine torque/output speed map; it should be stressed that the output shaft geartrain efficiency only takes into account the engine power contribution and the loss incurred between the annulus and the output shaft. This figure also suggests that loss increases more rapidly with speed than with torque.

It can be seen that these values are considerably improved over those when the turbine is fitted, Fig-6.3, because the turbine geartrain loss is excluded. This indicates that the losses through the output shaft geartrain are comparatively small, while those in the turbine geartrain predominate.

c) Turbine Operation

As stated previously, the original assumption was that the major errors in the experimental results came from the turbine performance data. It is obviously necessary that this be clarified. The following analysis will therefore be based on Table-6.1, i.e. results with turbine.

There are indeed cases in which gross error occurs in the turbine data. For

example, the original data set C is shown in Fig-6.24. A turbine isentropic efficiency of 170.73% is reached, due to inaccurate measurement of outlet temperature. In order to carry out sensible evaluation, an arbitrary value of 65% was assumed for this point instead (Table-6.1), although this cannot be verified in the absence of a turbine torque meter.

In other cases, turbine efficiencies are generally very high, values of from 85% to 92% have been obtained, which shows that errors may also exist in these data, possibly for similar reasons.

Errors in measured temperatures at either turbine inlet or exit will result in errors in calculated enthalpy difference between these two points, on which the turbine efficiency calculations are based.

Suppose that the accuracy of turbine inlet temperature is acceptable, then turbine performance data can be adjusted by adopting a more realistic efficiency value. As is well known, a unique relationship exists between turbine blade speed ratio and efficiency (especially total-total efficiency). Accordingly the reliability of the experimental turbine efficiencies can be assessed. For this purpose, the following table is obtained.

set	A	B	C	D	E	F
eff(exp.)	0.479	0.851	0.65	0.909	0.770	0.926
U/C	0.143	0.276	0.312	0.604	0.546	0.779
(eff)(T-S)	0.209	0.399	0.45	0.651	0.633	0.617
(Wt)(kw)	30	10.4	39.9	24.8	58.1	34.2

note:

eff(exp.)	experimental efficiency
U/C	blade speed ratio
(eff)(T-S)	interpolated efficiency from the typical (eff)(T-S) curve based on U/C
(Wt)	turbine power based on (eff)(T-S)

Fig-6.25 shows the typical total-total and total-static efficiencies of radial inflow turbines, against blade speed ratio, with the experimental turbine efficiencies

at the selected operating points superimposed. As can be seen, these values are much higher even than the total-total efficiencies at the same blade speed ratio points.

Assuming that Fig-6.25 fits the actual characteristics of the turbine in the present case, more realistic turbine efficiency can be obtained by interpolation from the t-s efficiency curve, and hence more realistic turbine power can be calculated, as presented in the above table. In most cases, the turbine efficiency and power are substantially reduced, compared with the values given by the data reduction program(above table) using enthalpy drop.

Further, if the compressor power is also corrected[see section *a*)/Compressor Operation], the gearbox losses can be adjusted(here cge's are restricted under 98.5%). As shown in Fig-6.26, substantial differences exist between these and the original values, the reduction of these losses being mainly the results of the reduction in adjusted turbine power.

d)Distribution of Gearbox Losses

Having adjusted the compressor and turbine power, and the gearbox losses, it is possible to investigate the distribution of losses in greater detail. If the operating condition within the epicyclic(engine torque and speed, output shaft speed) are exactly the same whether the turbine is fitted or not, the turbine power contribution to the output when the turbine is fitted can be roughly calculated by subtracting the output power without turbine from the output power with turbine; and the turbine geartrain loss can be obtained from this power term and the actual turbine power. However, slight changes do occur in the operation within the epicyclic(e.g engine torque, compressor pressure ratio), which makes this procedure difficult. Therefore an alternative approach has to be adopted.

The compressor geartrain loss can be calculated as before, while the output shaft geartrain loss can be calculated by adopting the efficiencies in Fig-6.21, which only affect the engine contribution to the output. The turbine geartrain loss can finally be calculated from the above two terms and the total loss. The results are tabulated below (Wl=total gearbox loss):

set	A	B	C	D	E	F
Wl(kw)	12.5	11.2	18.3	17.0	37.2	32.0
Wlc(kw)	2.28	0.75	1.29	0.51	0.98	0.55
Wlo/s(kw)	1.72	3.12	4.58	8.1	10.3	11.3
Wlt(kw)	8.5	7.33	12.43	8.39	25.92	20.15

It can be seen that the losses in the turbine geartrain constitute the major part of the total loss. loss.

The turbine geartrain loss is plotted in Fig-6.27 on a turbine torque/speed diagram. This figure demonstrates the increased loss with load and speed, and again the speed is by far the predominant factor. Probably for this very reason, and also the fact that the magnitude of the turbine speed is much higher than those of output shaft and compressor speeds, the loss in the turbine geartrain is particularly high and becomes the dominant part of the total loss. There is a trend in this figure(though not strictly in all cases) which seems to suggest that the transmission efficiency increases with load. This is because if the load is too low, a greater proportion of power has to be consumed to overcome the loss.

The losses in the compressor geartrain in the above table appear to be very irregular(the losses being arranged in order of increasing output shaft speed). irregular(the losses being arranged in order of increasing output shaft speed). This is due to the differential relation in the epicyclic. It can be shown that, to that in Fig-6.27 will be obtained.

6.4 Discussion

The geartrain transmission loss from the experiments has been evaluated. Clearly this is composed of the loss in the gears, bearings, and of windage loss. D. Prince made a preliminary analysis of the gearbox loss and concluded that windage loss was the major part. Considering the bulk and the arrangement(e.g. the planet travels around the sun gear in a circle at high speed) of the epicyclic, and very high speed of revolution of the turbine gear, the resultant windage loss can be expected to be very high.

The present investigation confirms that the turbine geartrain loss is indeed the major part. This can be explained by a comparison between the losses when the turbine is either dismantled or fitted. As has been shown, the difference is substantial. However, the gear arrangements are exactly the same for the two cases,

indicating that windage losses in these two situations are the same and therefore this difference comes from the change in the turbine geartrain loss. Clearly if windage loss is the major part, then the differences of such magnitude as the experimental data show, would not have been possible.

Whether taking the typical turbine efficiency data(Fig-6.21) to adjust the experimental results is approximate, probably needs further investigation. However, if this procedure underestimates the turbine efficiency, then by assuming a higher value, the turbine power will be higher and therefore the resultant gearbox loss will increase(as the result of an increase in turbine geartrain loss). This would reinforce the conclusion reached above.

6.5 Computer Modelling of Gearbox Losses

Prediction of gearbox losses has to take all the individual losses, gear loss, bearing loss and windage loss, etc. into consideration. This will make the matter very complex, and in fact it is very difficult to ensure a reasonable accuracy.

In theoretical studies gearbox loss is usually resolved into two parts, one being speed-dependent and the other load dependent, i.e.

$$\tau = \tau_i - \tau_i.Kt - N.Kn$$

where

τ	transmitted torque
τ_i	input(ideal) torque
Kt	torque related loss coefficient
Kn	speed related loss coefficient
N	speed

this equation can be further transformed to:

$$\tau = [\tau_i - Kn.N / (1 - Kt)].(1 - Kt)$$

let

$$ge = 1 - Kt$$

and

$$ft = Kn.N / (1 - Kt)$$

then

$$\tau = (\tau_i - ft).ge \quad (3)$$

This is the form of equation used in the simple simulation program DCE2 and its other derivatives, where ft is designated friction torque, and ge the transmission

efficiency.

Fig-6.28 shows the contours of gearbox losses from the simulation results for the CUMMINS L10 engine DCE. The pattern in this figure bears some resemblance to that in Fig-6.26(corrected values), in terms of the variation of power losses against load and speed. Because f_t is taken as a constant, the influence of speed is not very strong as expected. However, in the prediction for CUMMINS L10 DCE, instead of fixed turbine gear ratio, an optimum value is obtained. This makes the variation of the turbine geartrain loss different from that if a fixed ratio is employed. In fact, the turbine is always working at relatively high speeds in a relatively narrower range, which will cause the turbine geartrain loss to vary similarly. Nevertheless, from the point of view of simulation it is not difficult to transfer f_t to a speed-dependent variable.

It must be concluded that the determination of gearbox losses in the present experimental DCE has not been fully resolved. An attempt has been made to interpret the results rationally and to allocate component losses.

Full resolution of the problem can be achieved only by fitting torquemeters to both the turbine and compressor shafts.

Since gearbox losses, as well as certain duct losses, have a very adverse effect on the performance of the DCE in its present form, an analysis is carried out in the next chapter with a view to predicting DCE performance if these losses are reduced to a level appropriate to a 'production' version of the DCE.

Table-6.1 THE EXPERIMENTAL DATA WITH TURBINE

SET	A	B	C	D	E	F
ENGINE-----						
speed(rpm)	1457.0	900.	1585	1700.	2107.0	2340.0
boost ratio	3.79	2.33	3.50	1.98	2.67	1.98
manifolt T(K)	334.4	318.	330.	320.	324.8	318.4
torque(Nm)	1350.9	735.2	1245.38	675.4	980.64	720.98
power(kw)	206.15	69.3	207.30	120.35	216.83	176.59
b MEP(bar)	20.79	11.26	19.08	10.34	15.02	11.04
th. effy(%)	39.76	40.53	39.22	39.66	39.24	37.27
max. cl. p(bar)	153.7	109.4	141.8	104.59	148.62	108.
exh. T(K)	883	665.	889.	740.	880.	607.
air flow(kg/m)	24.37	8.08	22.31	13.12	21.35	17.99
COMPRESSOR-----						
speed(rmp)	9502.0	2752.	5826.0	4279.	5618.0	4321.0
torque map(Nm)	161.54	80.66	146.36	75.6	110.32	80.76
power(kw)	161.18	23.25	89.70	34.0	65.37	36.82
isen effy TS(%)	77.26	76.65	78.62	80.8	79.11	78.17
overall effy(%)	61.85	60.93	60.24	64.57	66.52	64.76
mass orif(kg/m)	35.15	7.88	21.57	15.55	21.29	15.68
mass map(kg/m)	36.74	10.02	22.31	16.92	22.57	17.44
pr	4.57	2.42	3.95	2.23	3.17	2.39
inl. T(K)	297.	294.	300.6	300.	295.	300.
out T(K)	505	404.	283.	396.	440.	394.
TURBINE-----						
speed(rpm)	10266.9	15840.	24933.9	32766.	39600.9	49867.8
torque(Nm)	64.15	13.43	28.47	10.1	17.02	9.91
enthalpy(kw)	67.90	22.32	74.43	34.68	70.71	51.70
isen effy(%)	47.85	85.09	65.0	90.85	77.02	92.64
mass(kg/m)	38.61	10.94	24.15	18.03	24.33	18.88
pr	3.30	2.37	3.68	2.04	2.85	2.18
OUTPUT-----						
speed(rpm)	700.0	1080.	1700.0	2234.	2700.0	3400.0
torque(Nm)	1021.73	400.1	808.69	403.23	612.27	400.54
power(kw)	73.73	45.30	144.13	94.35	173.35	142.41
th effy(%)	14.22	26.5	27.27	31.1	31.37	30.06
hyp flow(kg/m)	12.37	1.93	0.	3.8	1.21	0.54
Gbox loss(kw)	39.13	23.06	47.9	26.68	48.82	49.04

Table-6.2 EXPERIMENTAL RESULTS WITHOUT TURBINE

SET	A	B	C	D	E	F
ENGINE						
speed(rpm)	1456.0	900.	1583.0	1702.	2111.0	2338.0
boost ratio	3.79	2.36	3.63	1.96	2.61	2.01
manifold T(K)	329.4	314.4	321.	317.	323.	317.3
torque(Nm)	1329.0	736.15	1262.6	667.91	977.27	722.5
power(kw)	202.63	69.38	209.3	119.04	216.03	176.89
bmepl(bar)	20.36	11.27	19.34	10.23	14.97	11.06
max. cl. p(bar)	149.66	116.6	148.	1.93	127.5	108.
exh. T(K)	913.	663.	913.	746.	928.	635.
air flow(kg/m)	22.88	8.64	22.72	12.54	20.94	18.11
vol effy(%)	99.22	91.22	92.1	84.51	87.62	88.85
COMPRESSOR						
speed(rmp)	9530.	2750.	5740.0	4342.	5689.0	4327.0
torque map(Nm)	163.17	82.14	154.6	74.73	109.41	83.64
power(kw)	162.96	23.68	92.95	33.8	64.99	37.92
isen effy TS(%)	79.71	75.85	77.66	80.88	77.41	79.71
overall effy(%)	60.42	60.37	57.83	64.29	66.65	64.27
mass orif(kg/m)	34.17	12.00	22.04	17.36	20.24	15.07
mass map(kg/m)	35.80	10.06	21.56	17.7	22.95	16.88
pr	4.62	2.45	4.13	2.21	3.15	2.45
in T(K)	299.	290.5	298.	289.5	291.	295.
out T(K)	503.	402.	488.	380.	436.	403
OUTPUT						
speed(rpm)	685.0	1081.	1713.0	2230.	2700.0	3399.0
torque(Nm)	698.9	372.56	660.06	328.78	495.12	360.94
power(kw)	50.13	42.17	118.4	76.78	139.99	128.47
byp flow(kg/m)	12.92	1.42	-1.16	5.16	2.01	-1.22
Gbox loss(kw)	-10.33	3.53	-2.05	8.46	11.05	10.5

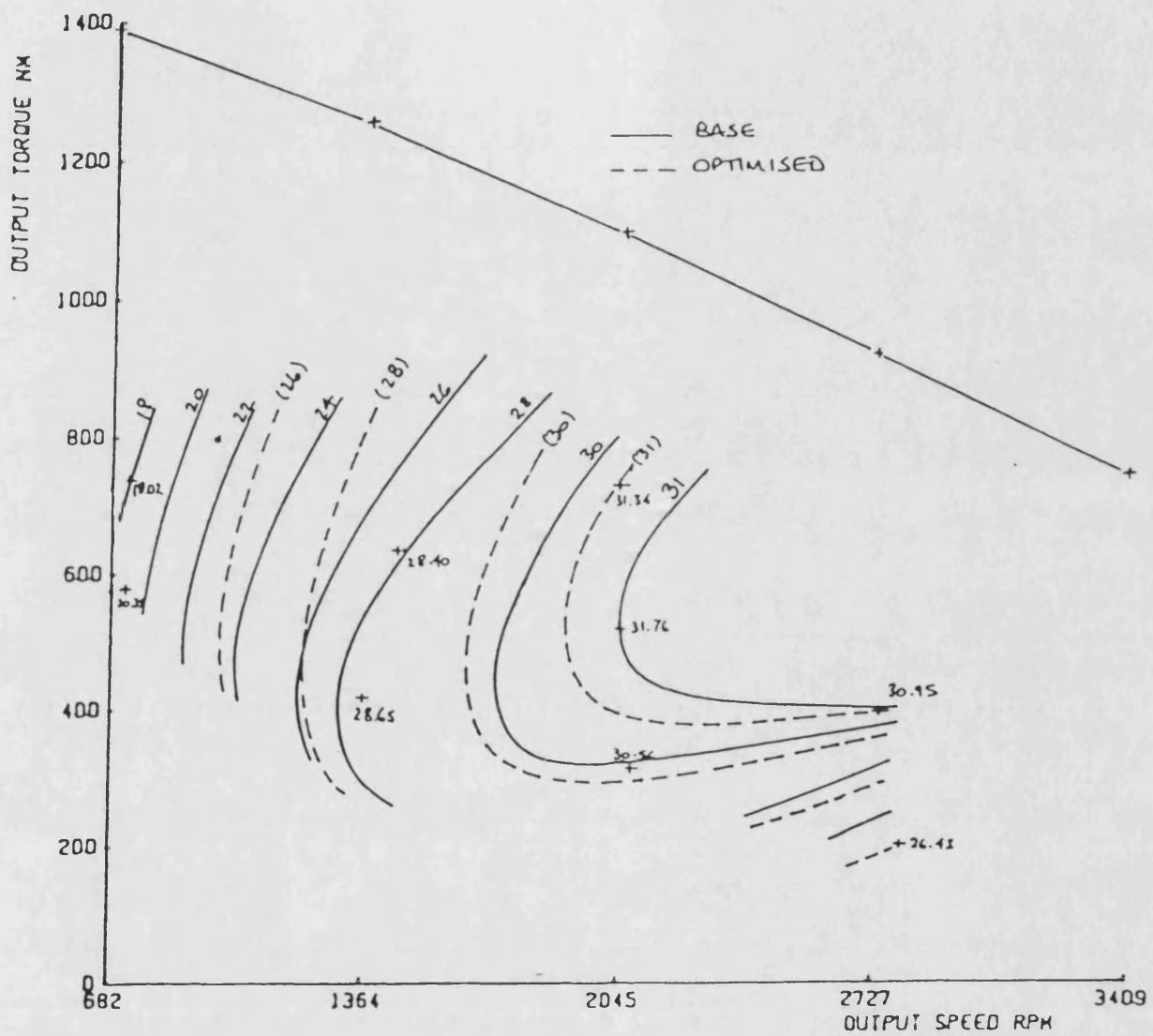
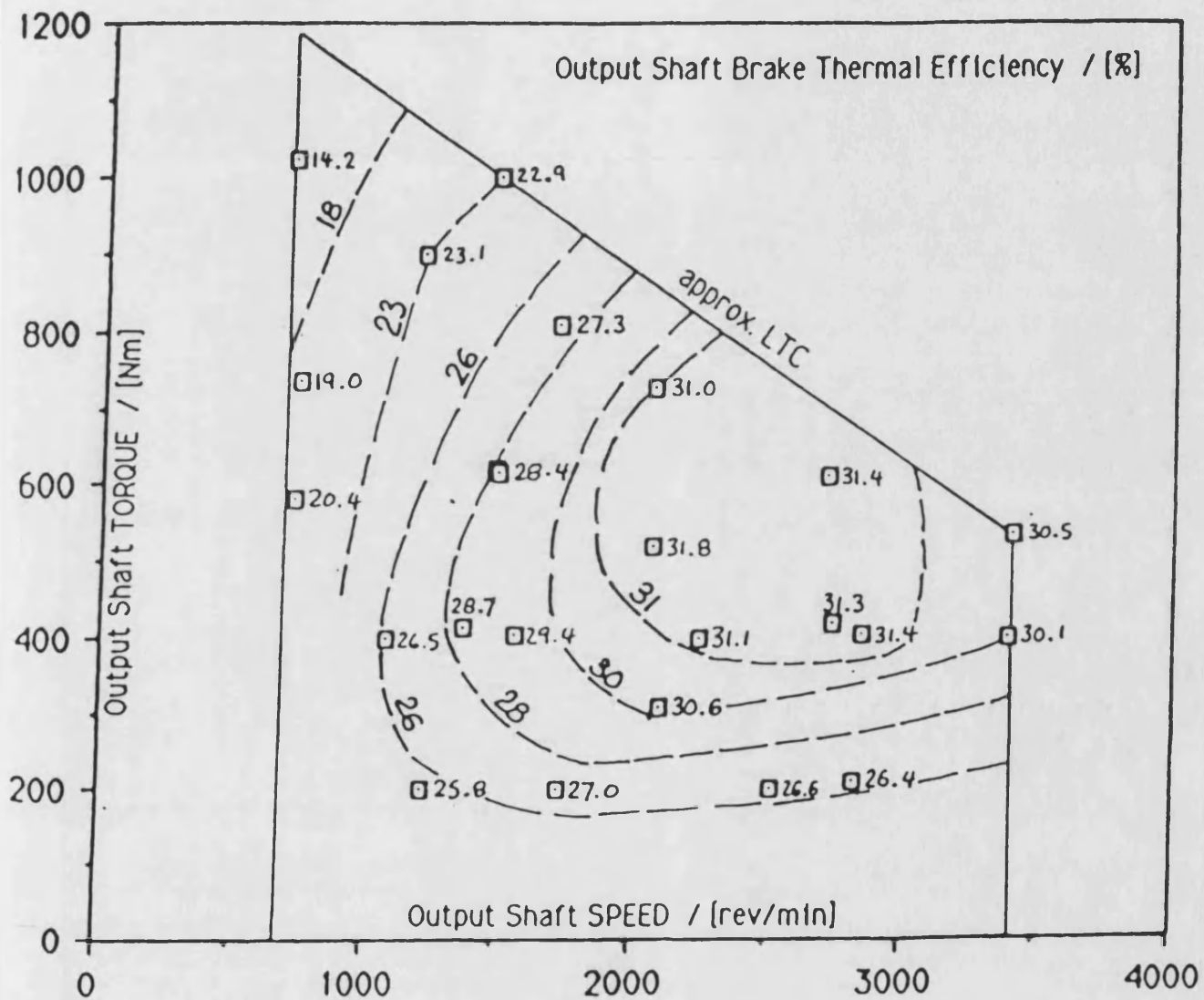


Fig-6.1 Some preliminary experimental results of the Leyland 520 DCE



notes: rated output shaft speed 3409 rev/min
 minimum output shaft speed 682 rev/min
 LTC = limiting torque curve.

Fig-6.2 Most recent experimental results of the
 Leyland 520 DCE

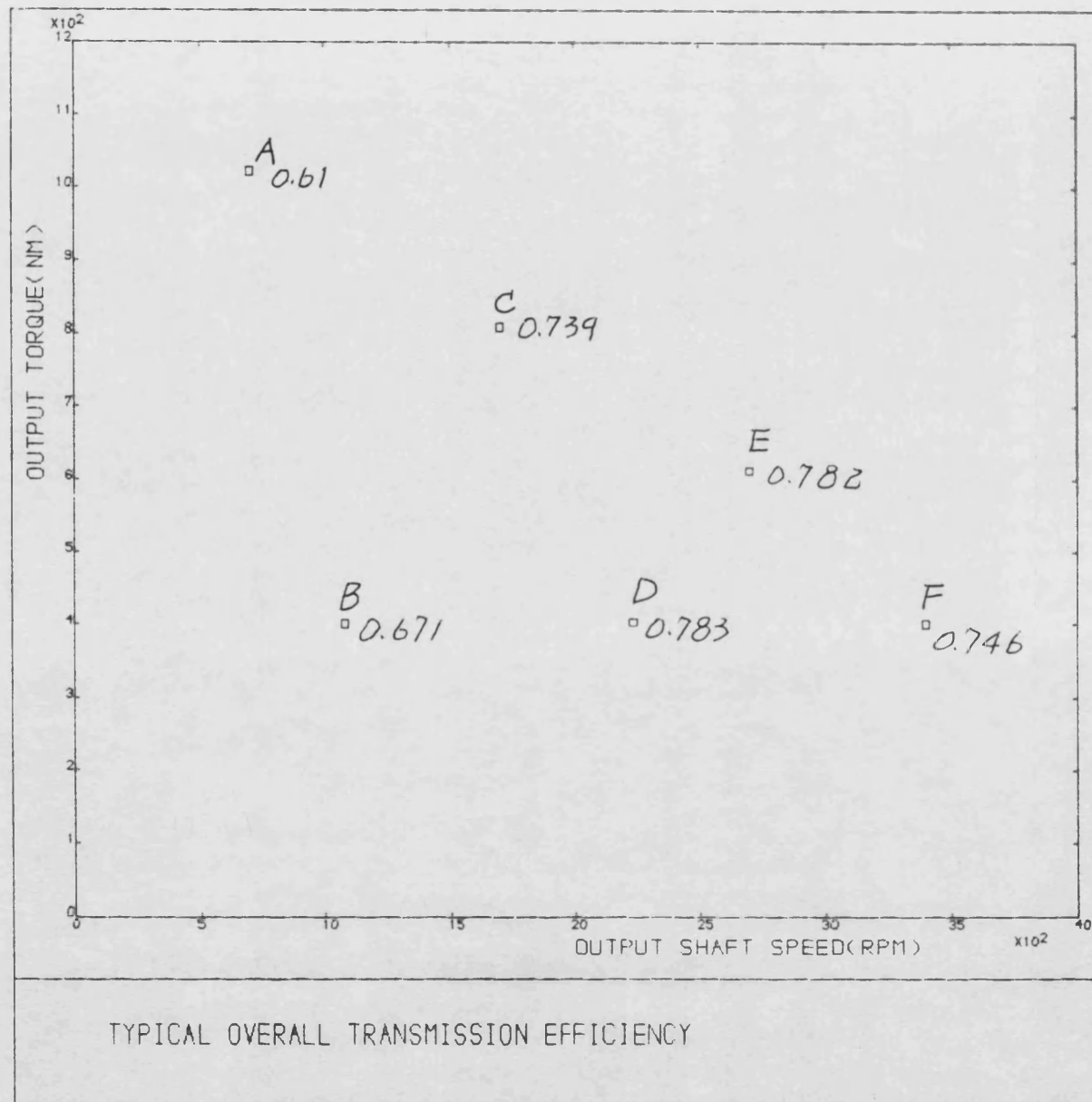


Fig-6.3

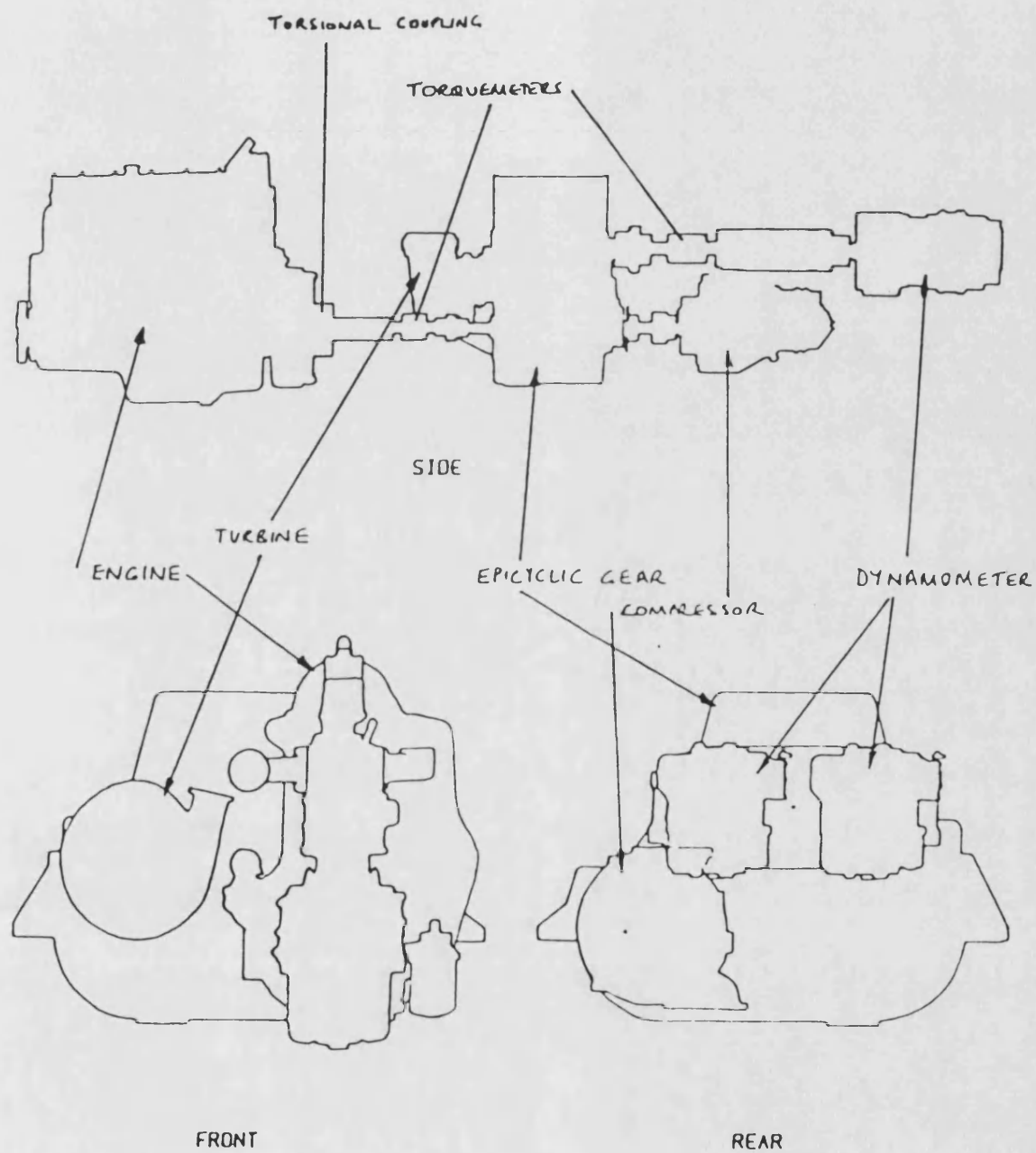


Fig-6.4 The general layout of the Levland 520 DCE in the experimental lab

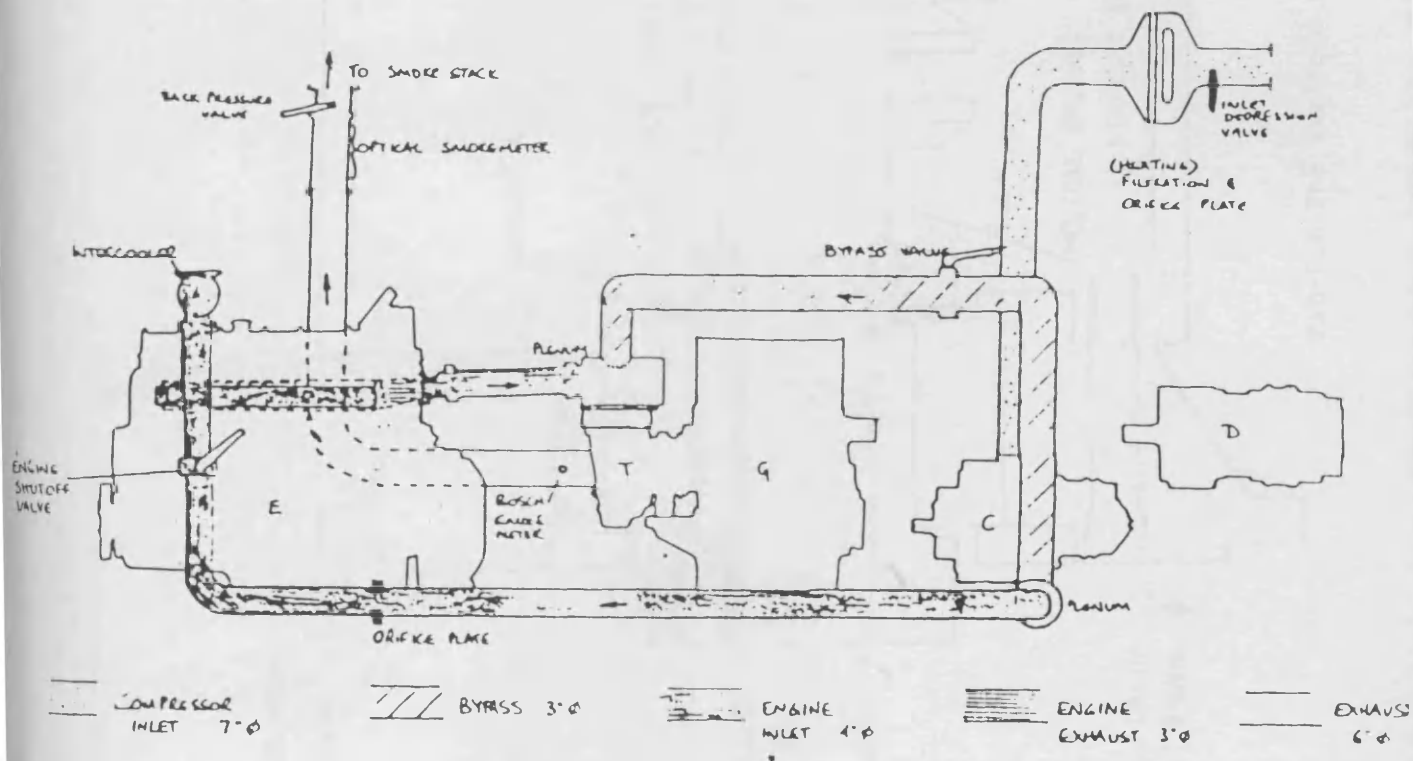
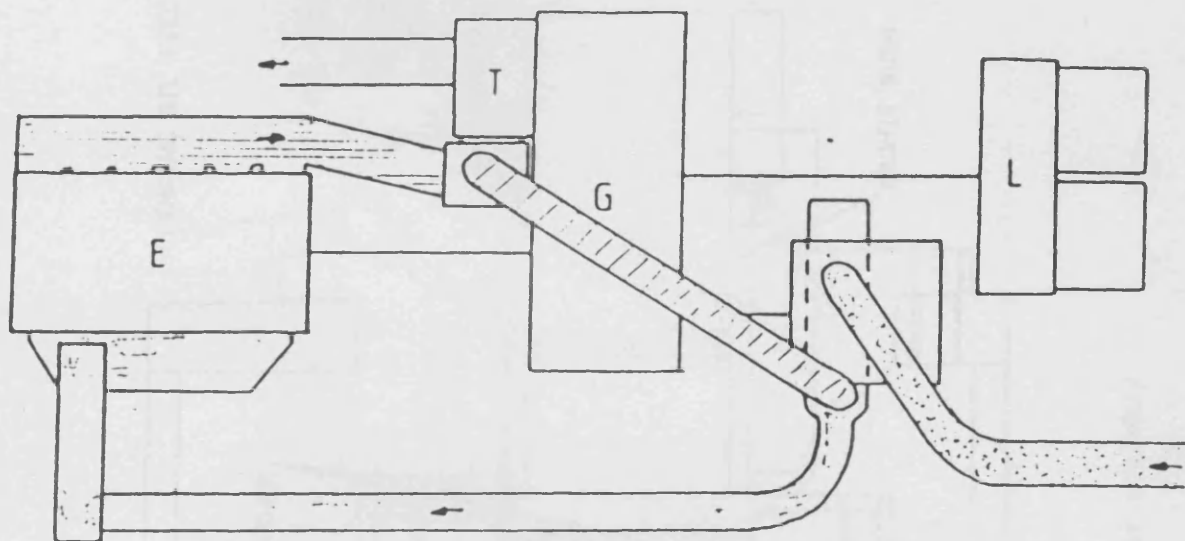


Fig-6.5 Pipe line arrangement of the Layland 520 DCE

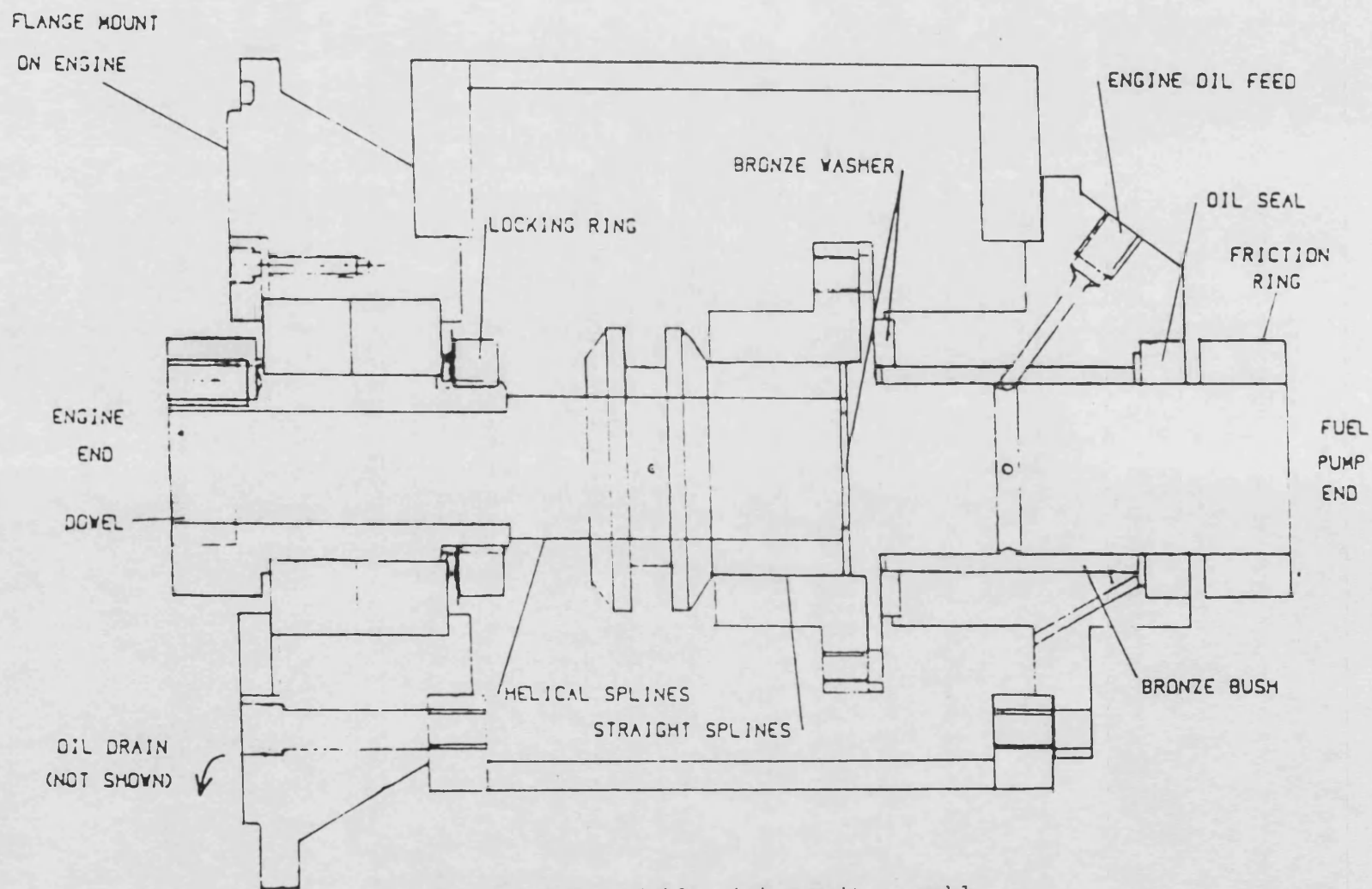


Fig-6.6 The variable timing unit assembly

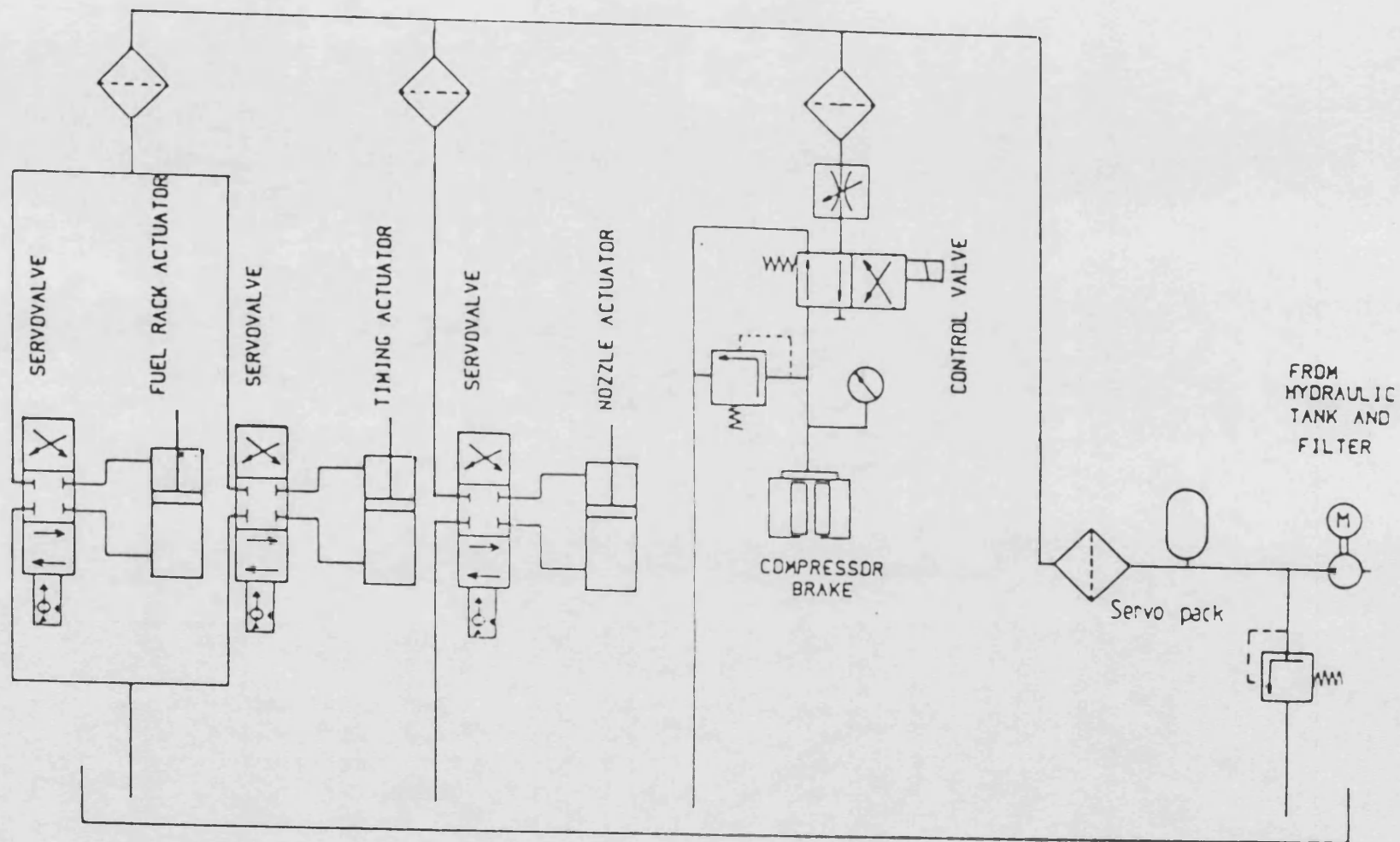


Fig-6.7 Servo system

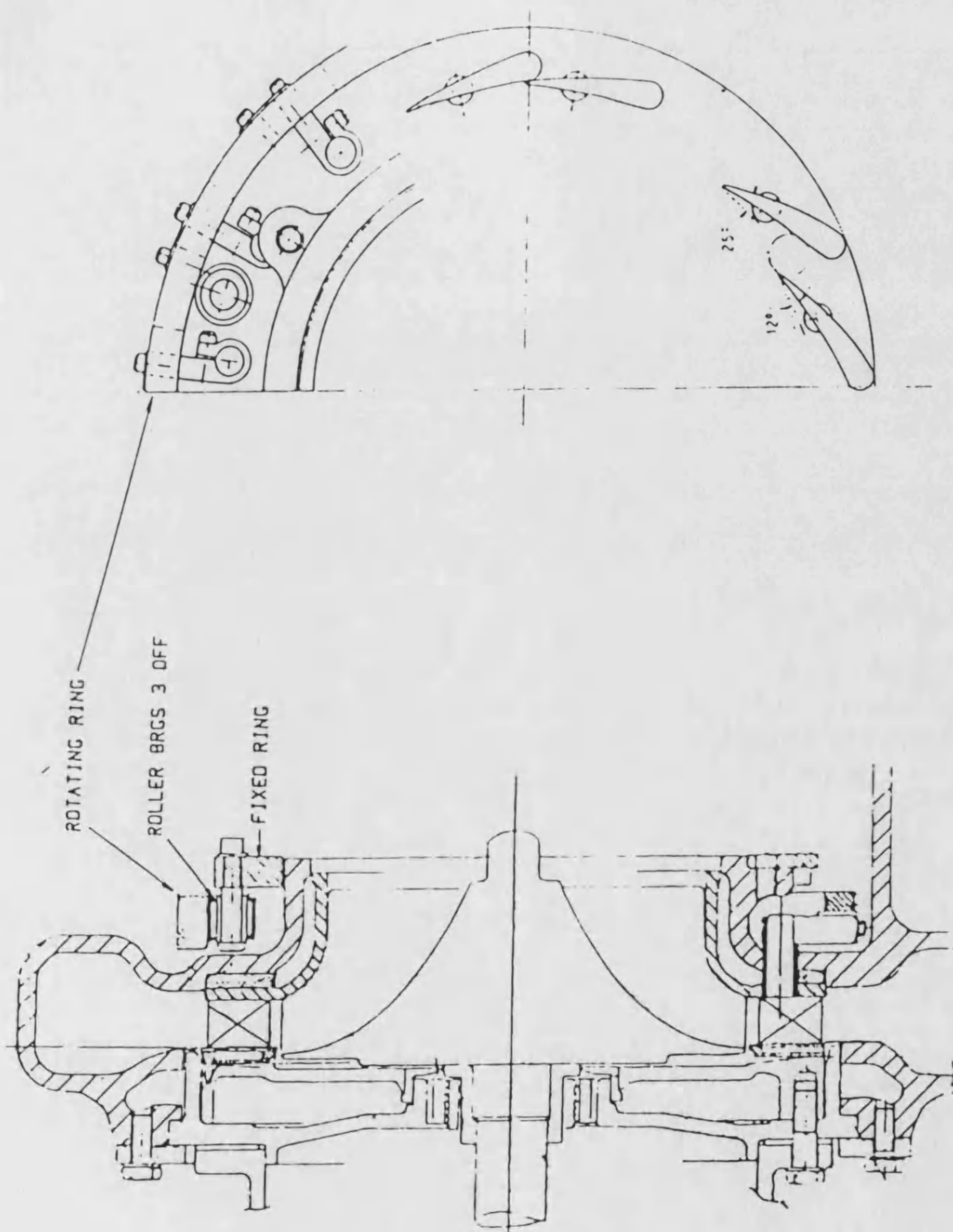


Fig-6.8 Turbine swivelling nozzle mechanism

Fig-6.9 Hydraulic charge circuit

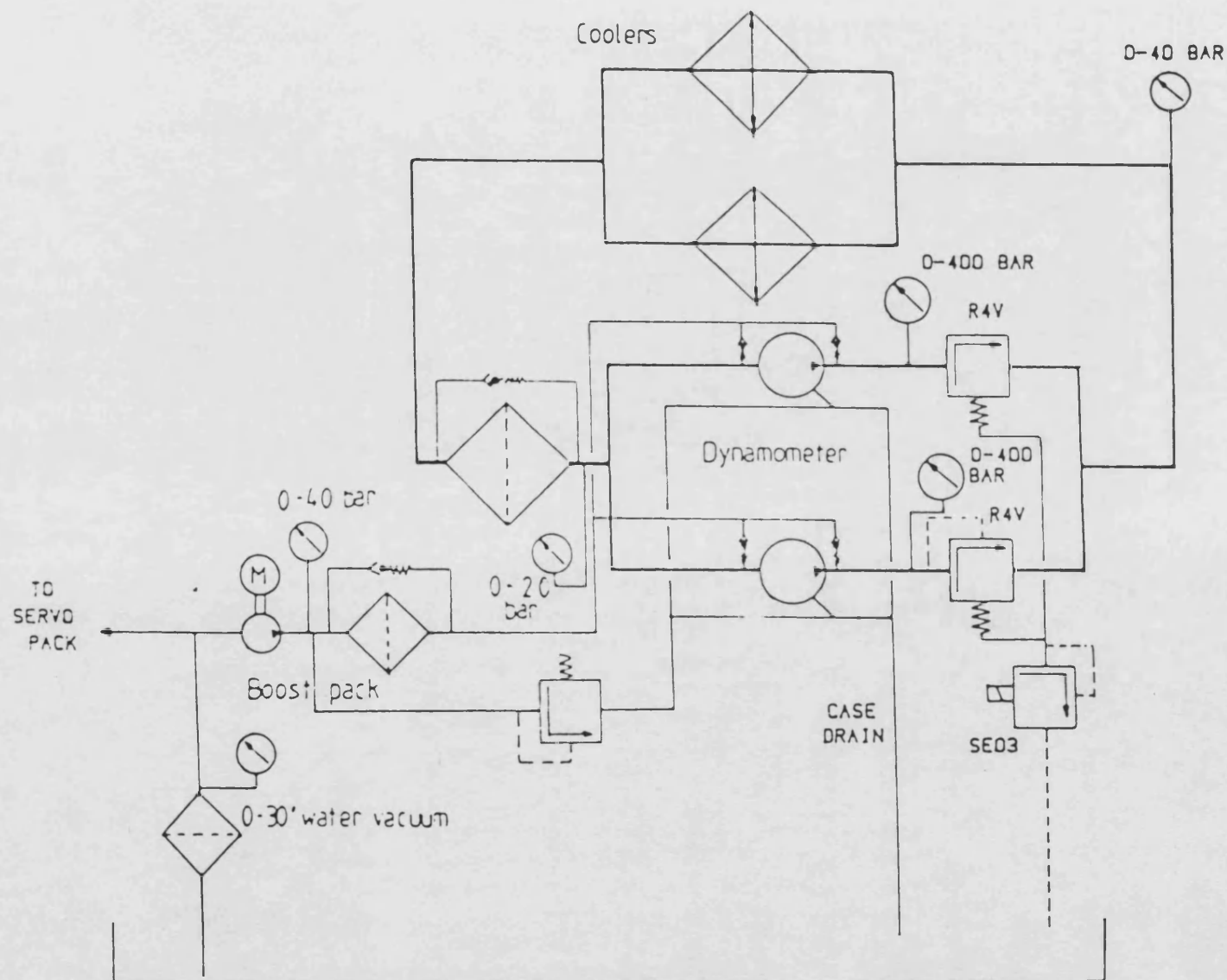
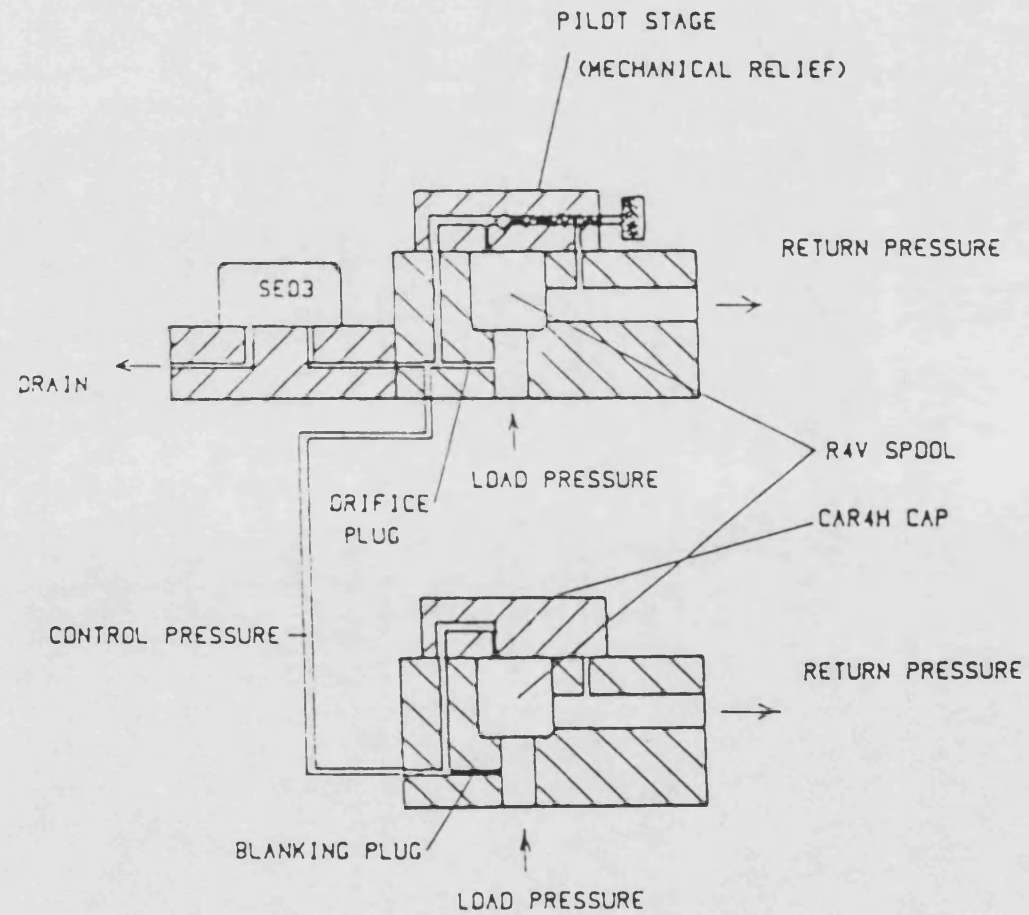
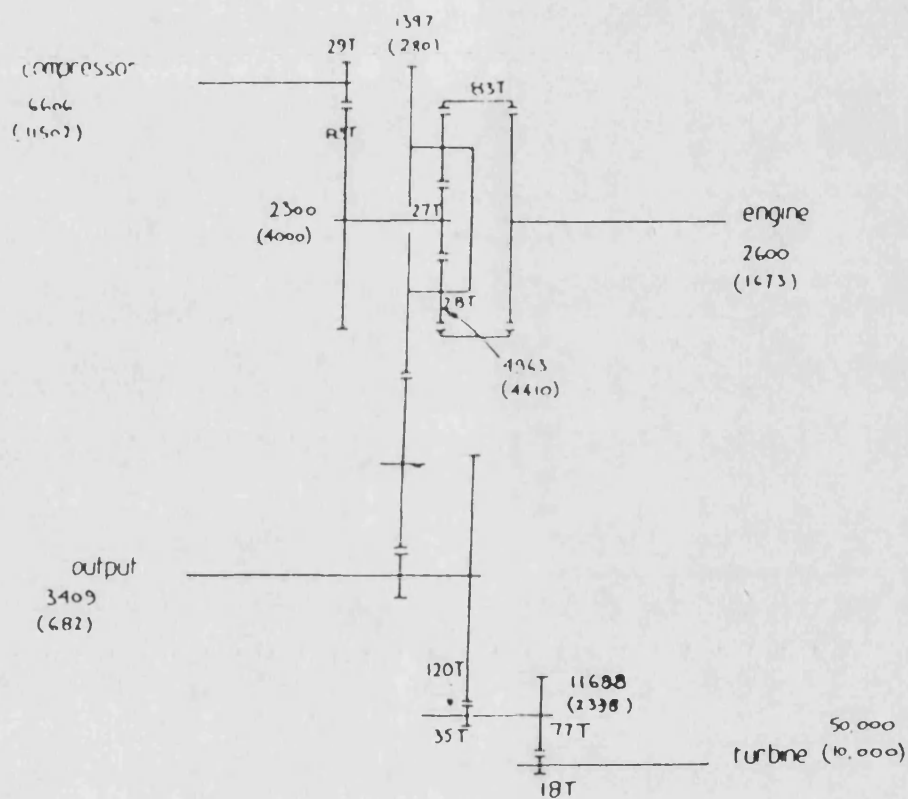


Fig-6.10 Dynamometer servo and loading valves





Speeds (RPM) at Rated and (Stall) conditions. T=no. of teeth

Fig-6.11 Epicyclic gear and turbine geartrain arrangement

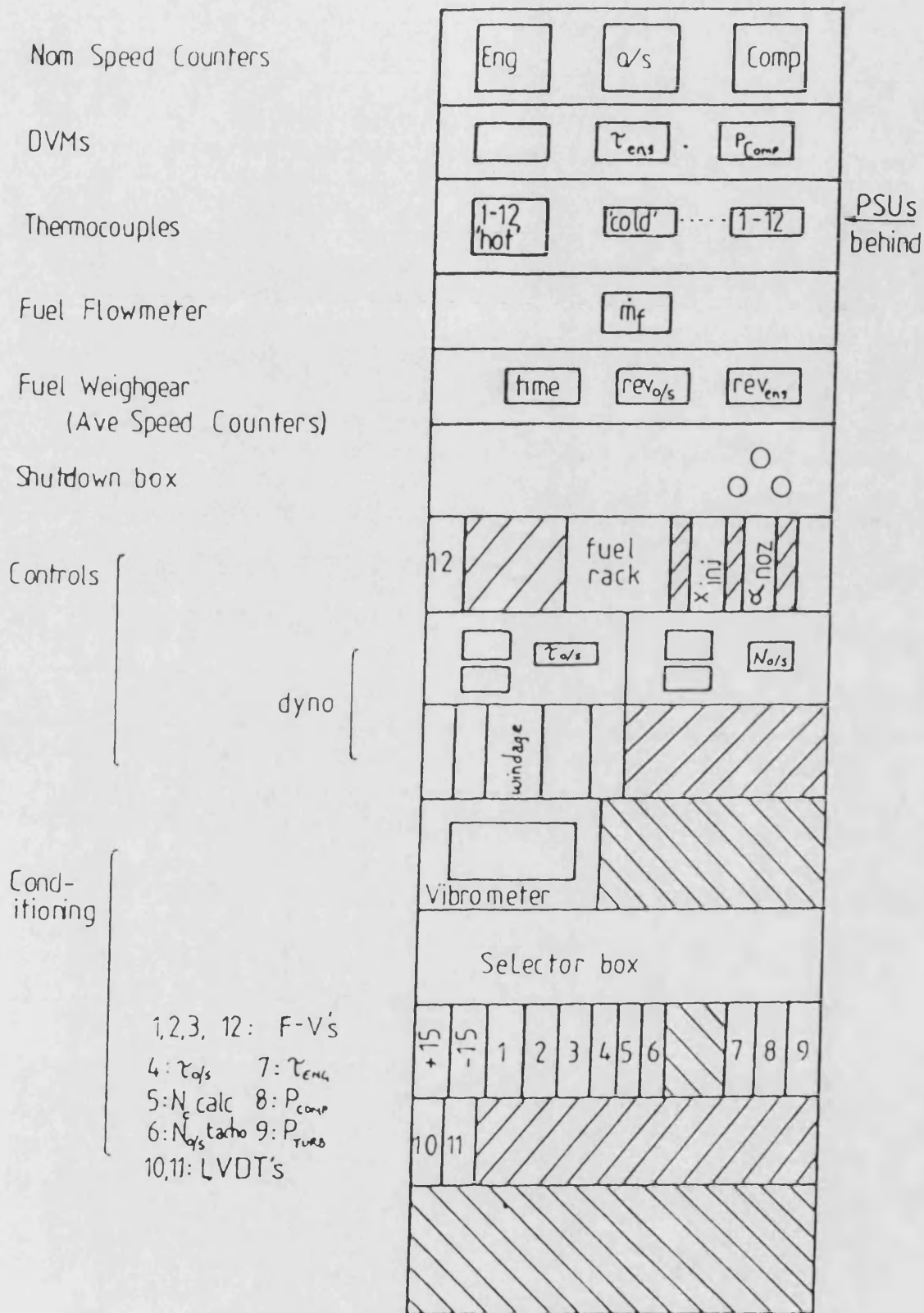


Fig-6.12 Layout of the instrumentation rack

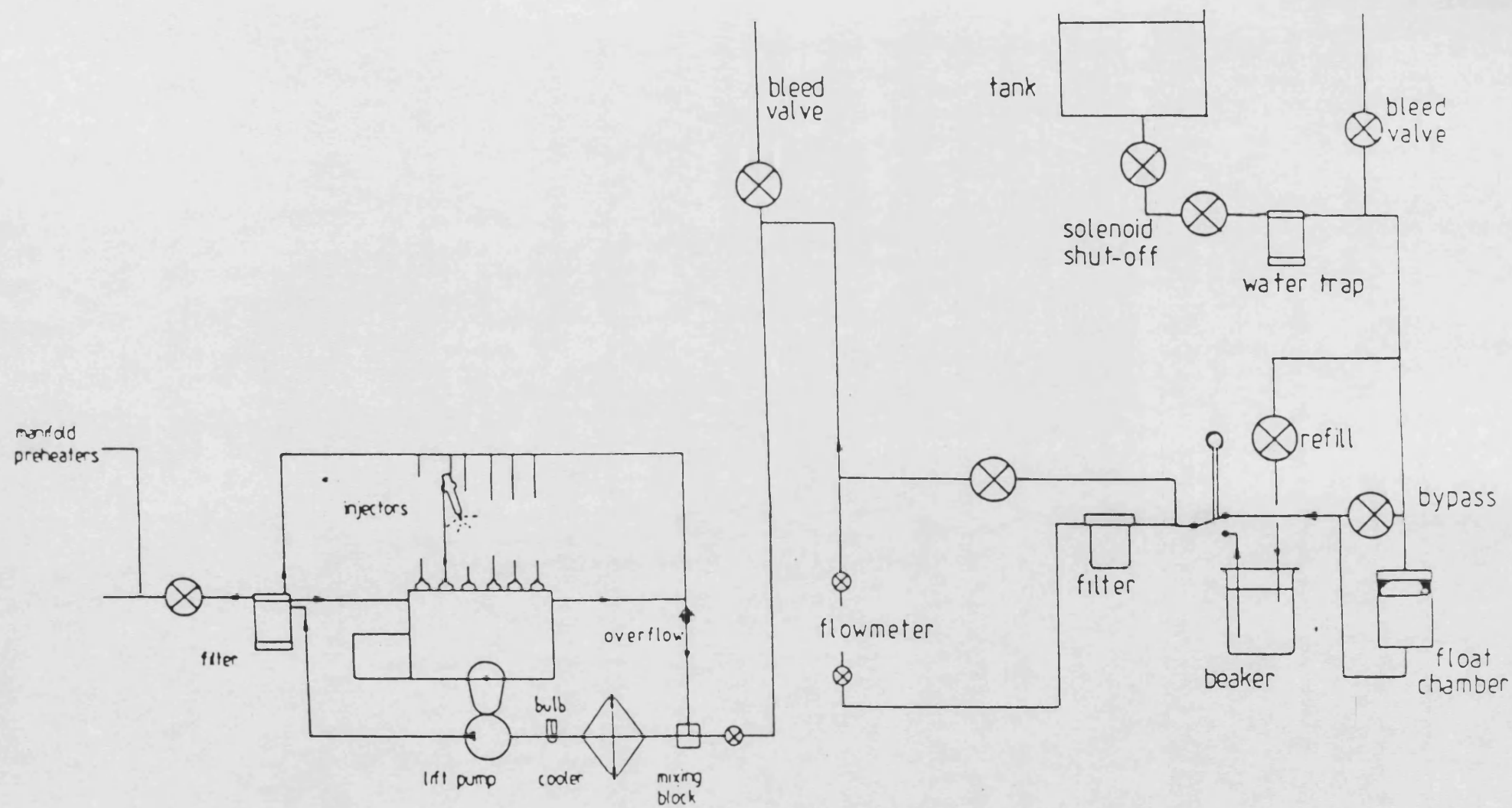


Fig-6.13 Fuel system and weighgear

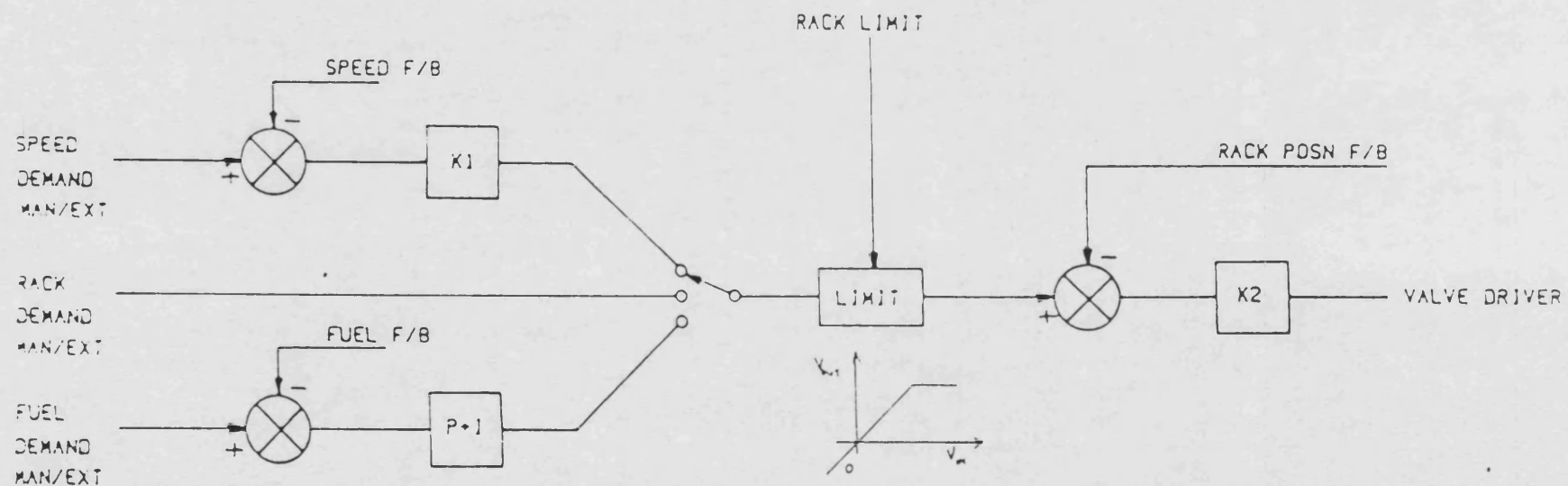


Fig-6.14 Engine governor controls

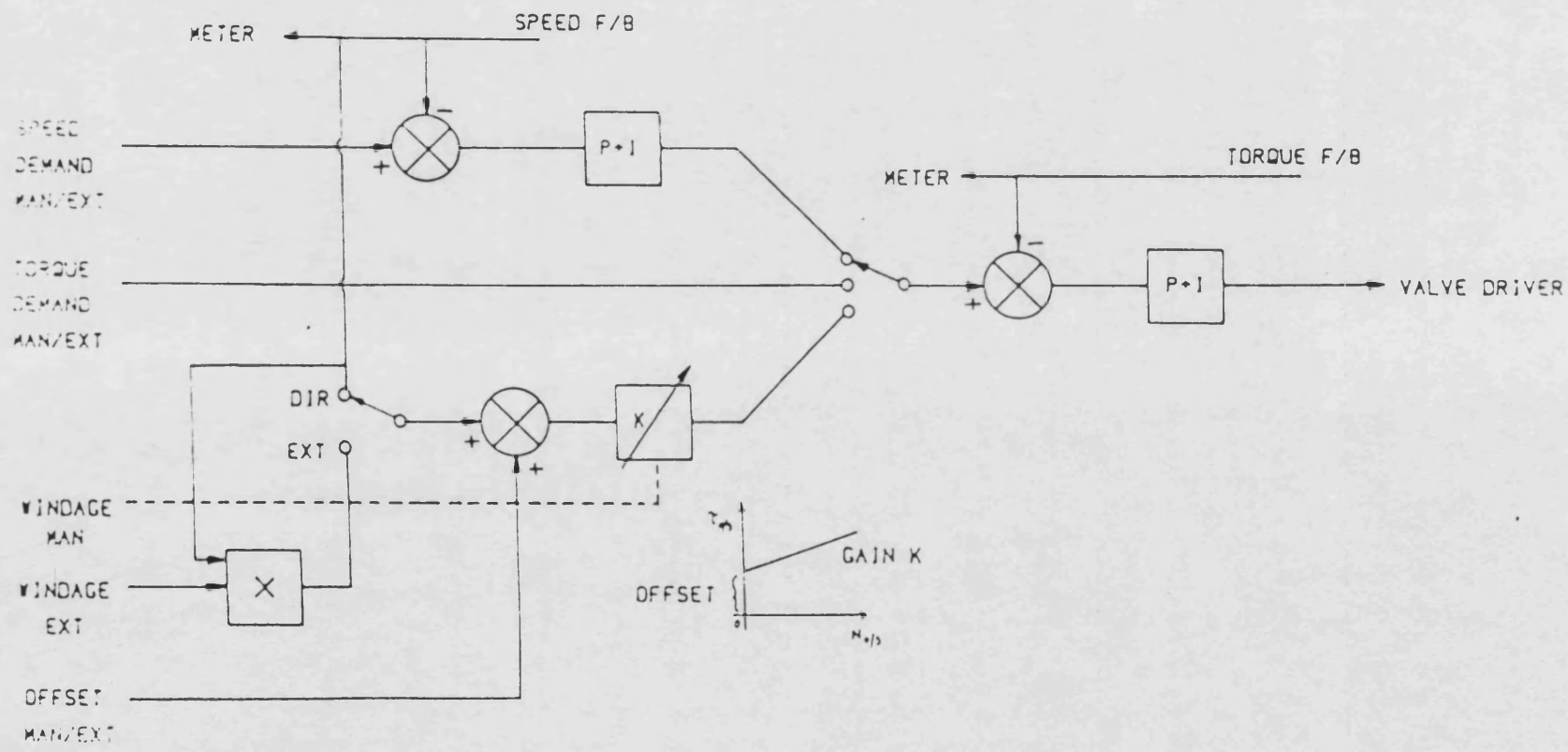


Fig-6.15 Dynamometer controls

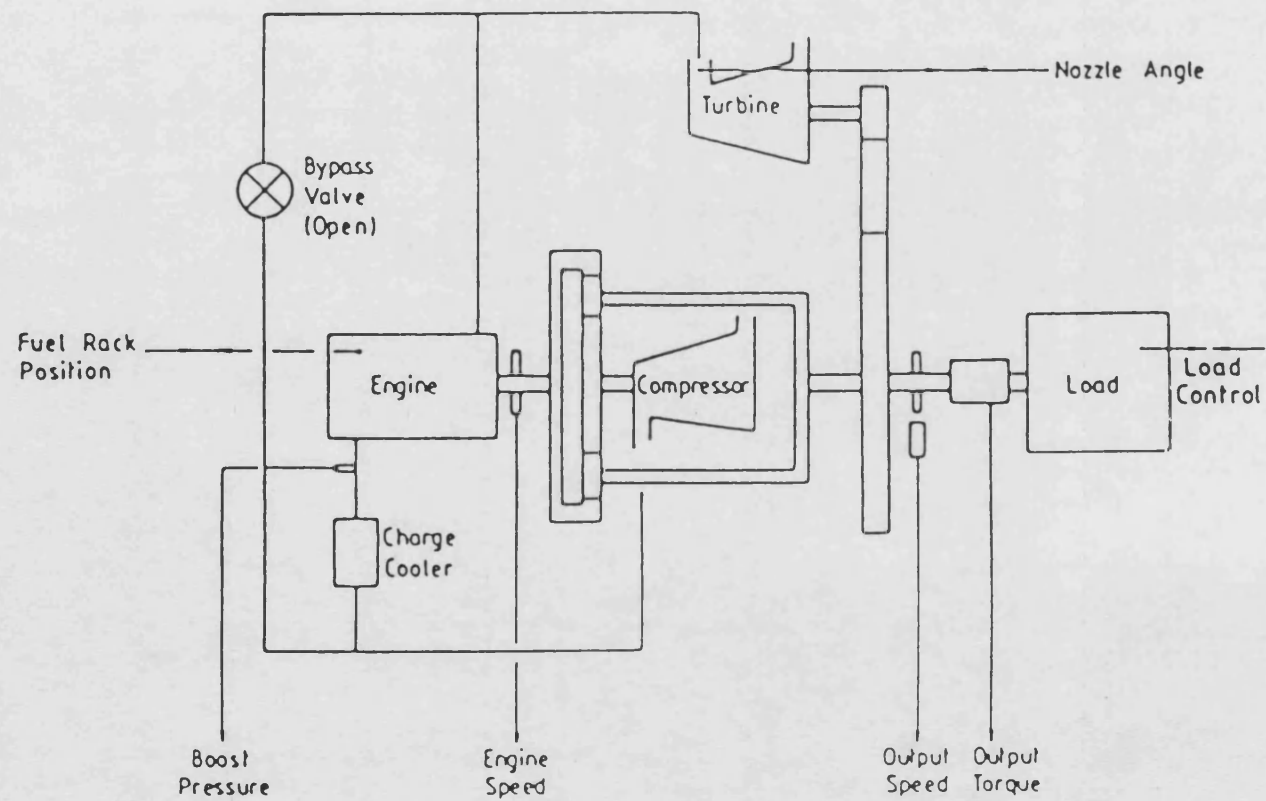


Fig-6.16 The connection of various components through geartrains

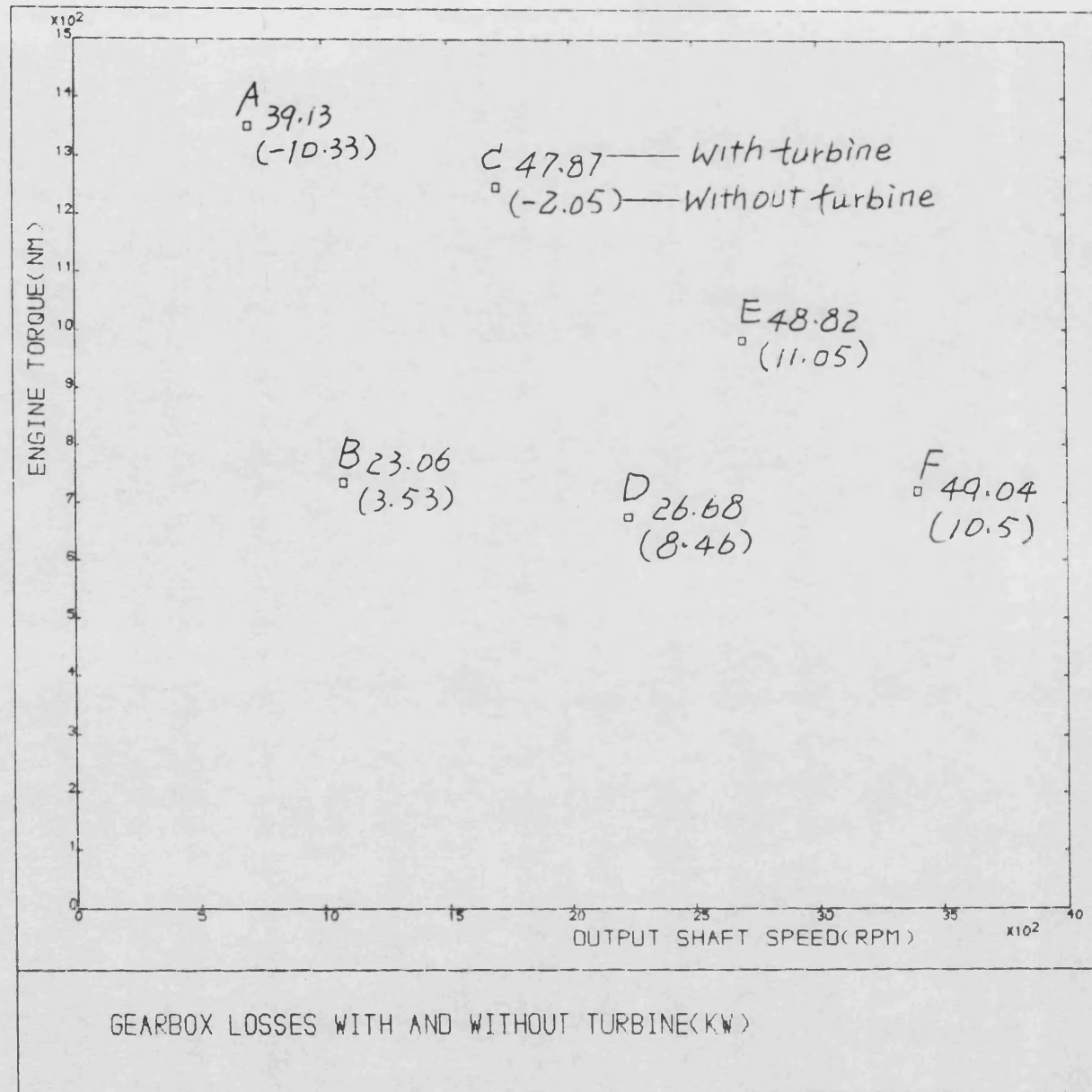


Fig-6.17

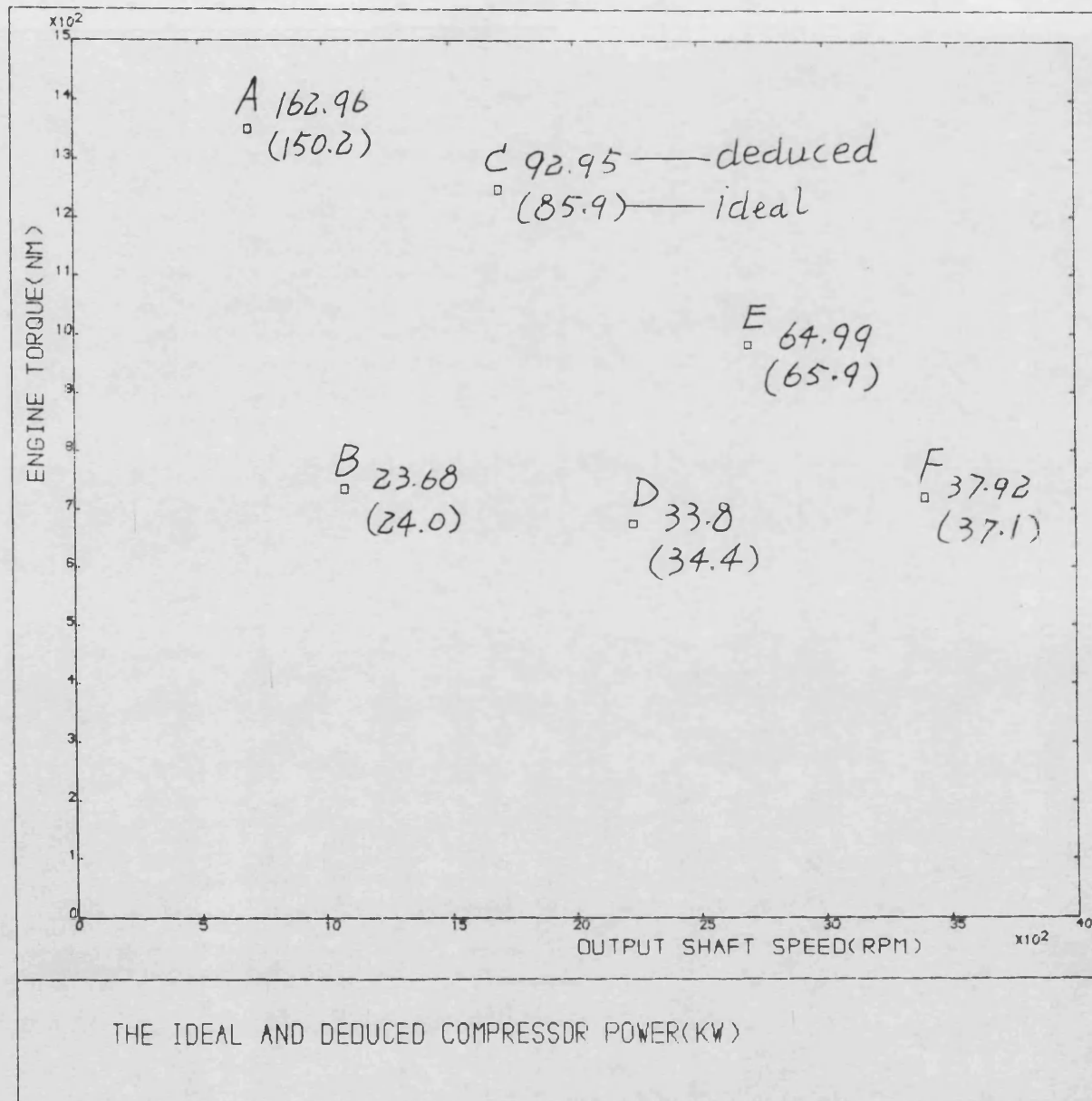


Fig-6.18

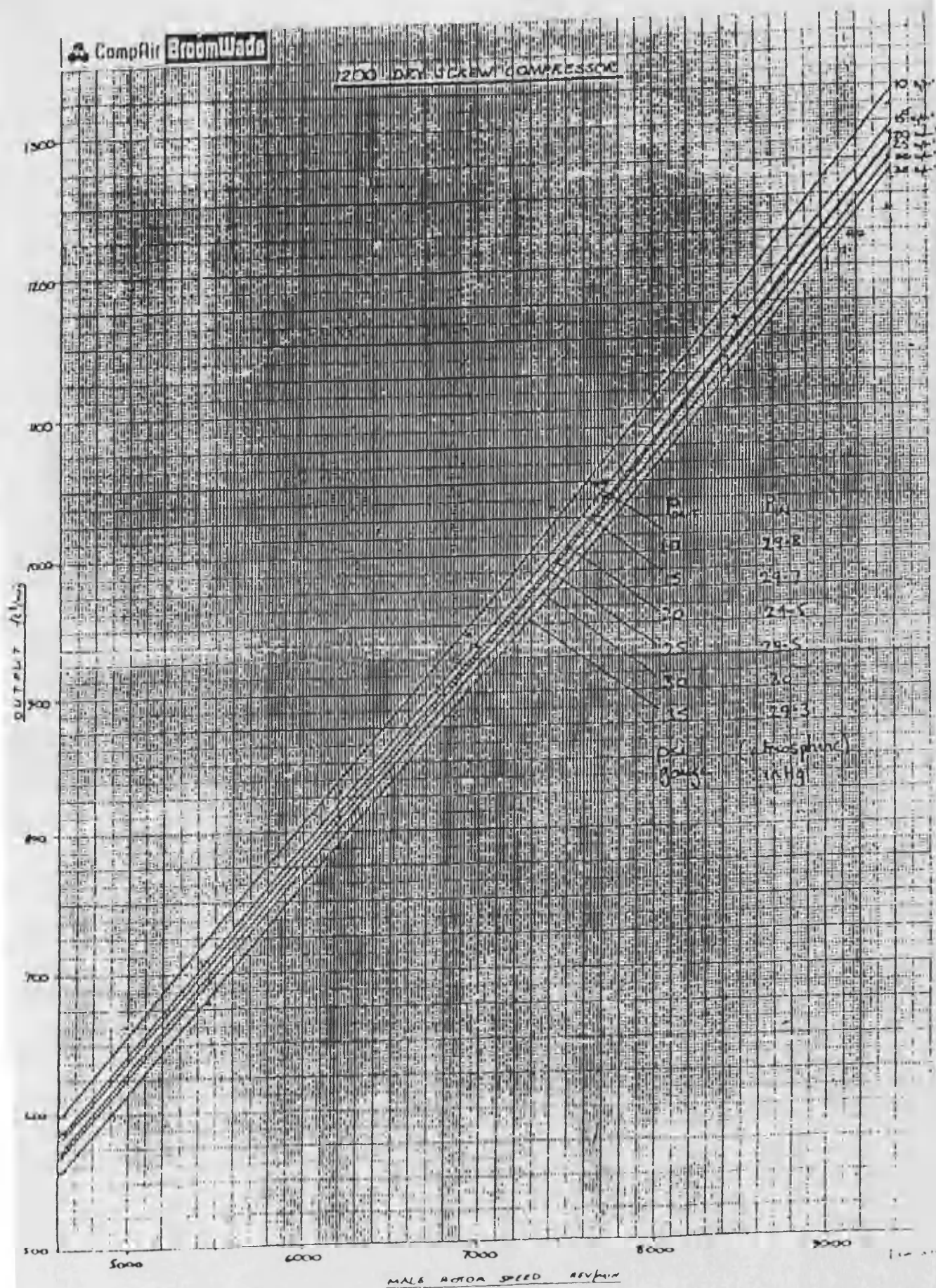
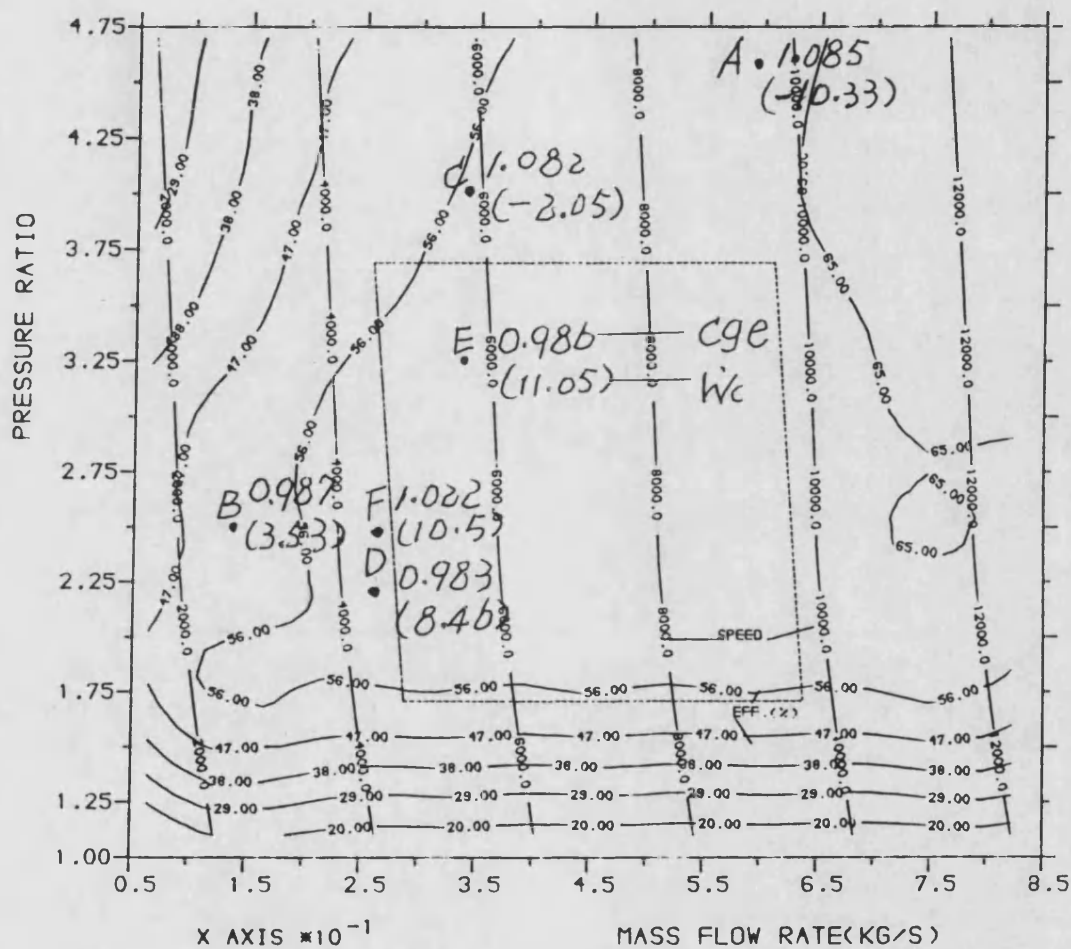


Fig-6.20 Compressor characteristics (volume flow rate vs. speed with P_r)



COMPRESSOR MAP

Fig-6.21 Measured compressor power and compressor geartrain transmission efficiency on the compressor map

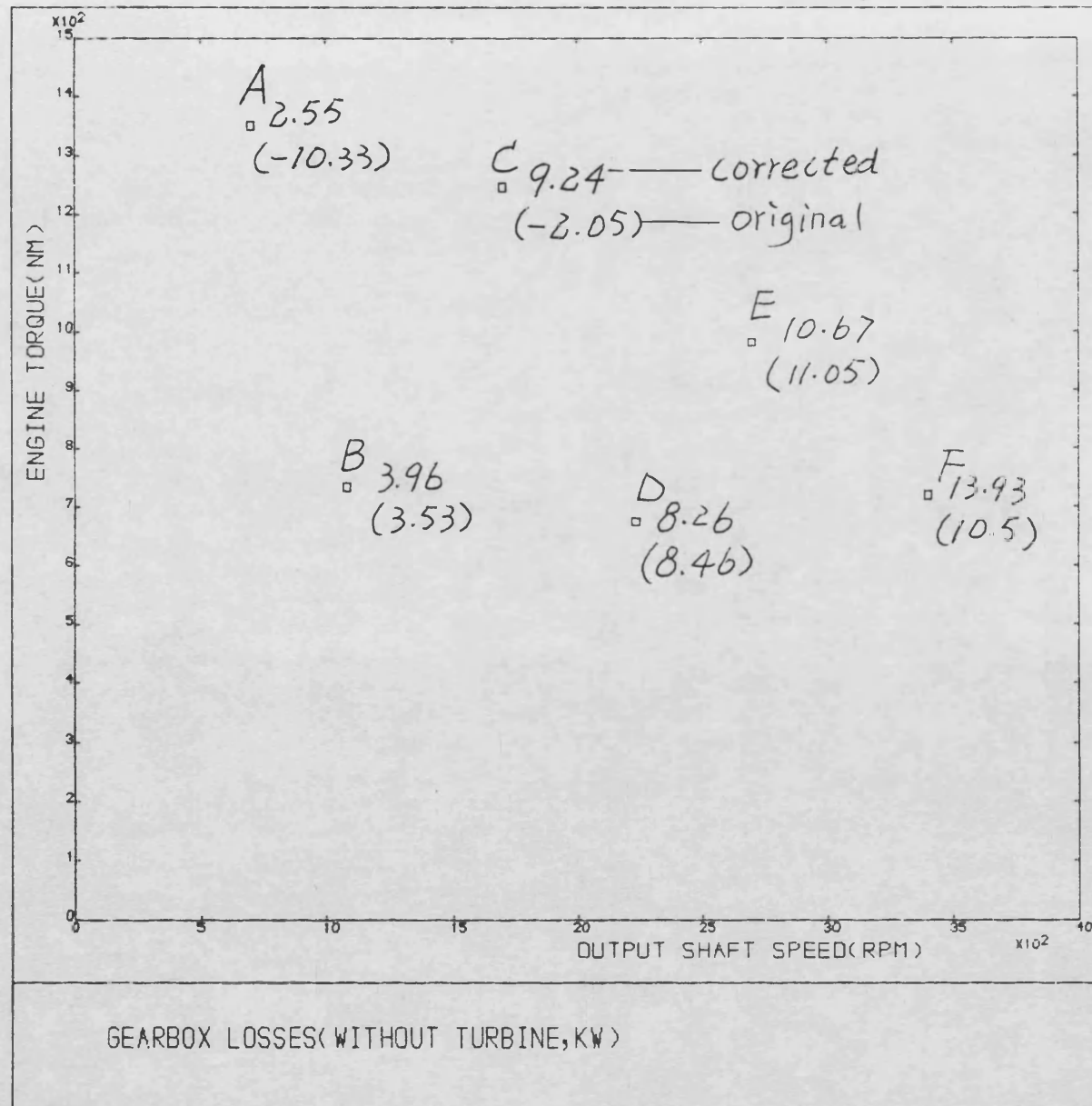


Fig-6.22

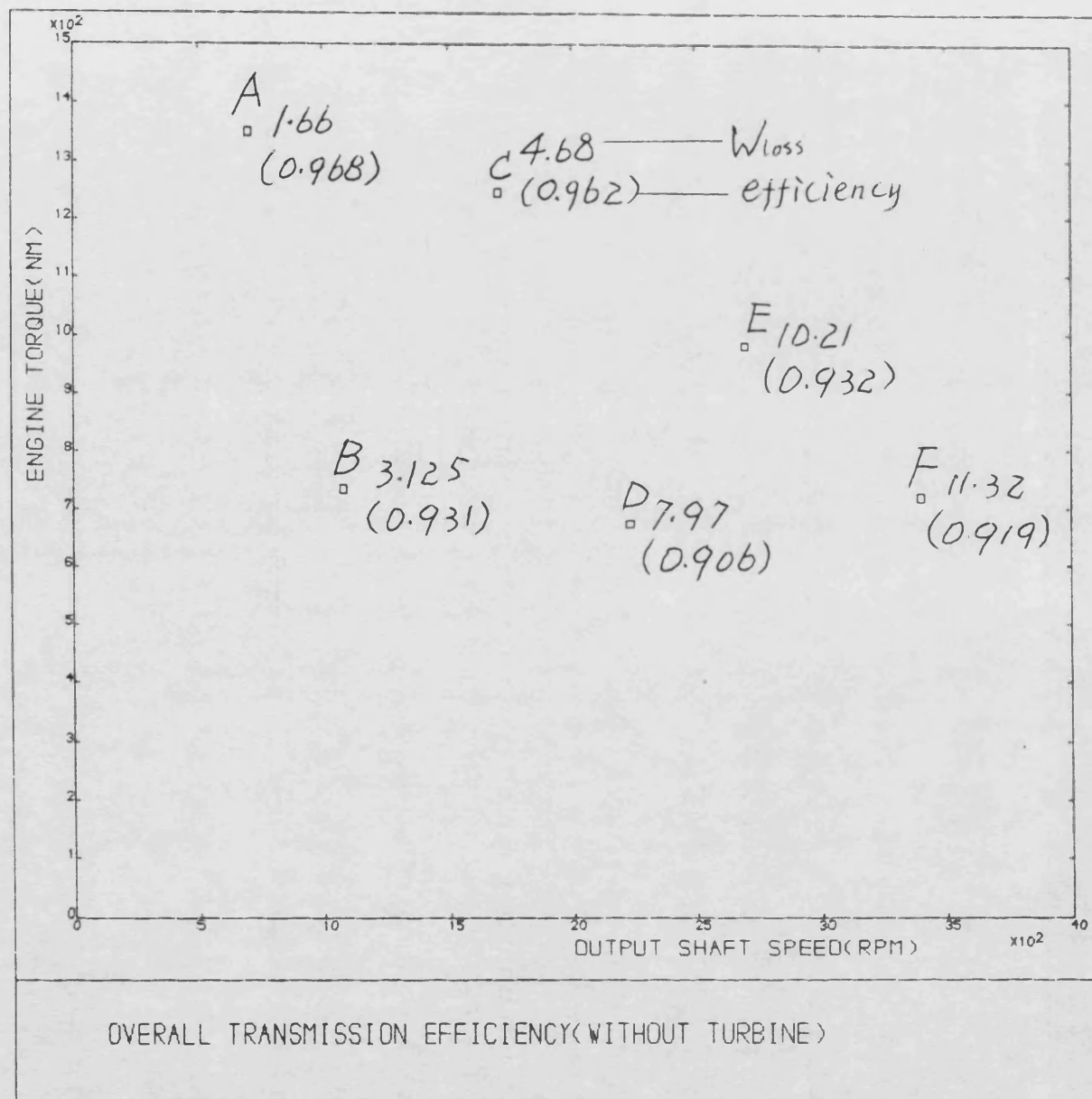


Fig-6.23

```

11.410
Flow Speed RPH 5826.00
Torque Nm 146.35
Power kW 89.70
Boost Ratio 1.410
Imper bar 19.48
Cyl Pr bar 141.79
Lyndt Coefficient 11.87
Inj Duration deg 39.71
Fuel Flow g/s 17.41
Fuel/Shot mg 156.28
Th Effv % 89.22
Air Flow kg/m 22.31
Vol Effv % 94.76
Air/Fuel 29.96
Inlet Air Pr bar 2.44
Exhaust Pr bar 2.76
Inlet Temp C 56.70
Exh Man Temp C 611.00
Exh Man Temp C 629.00

Compressor
Nom Speed RPH 5826.00
Rev Speed RPH 5852.56
Torque map Nm 146.35
Power map kW 89.70
Isen Effv % 78.62
Overall Effv % 60.24
Mass orif kg/m 21.57
Mass map kg/m 22.31
Press Ratio 3.95
Inlet Air Pr bar 2.44
Outlet Air Pr bar 2.72
Inlet Temp C 27.50
Outlet Temp C 210.00

Turbine
Nom Speed RPH 5826.00
Rev Speed RPH 5852.56
Wheel Torq Nm 74.18
Enthalpy kJ 195.51
Isen Effv % 179.13
Noz Angle V 8.30
Mass Flow kg/m 24.15
Press Ratio 3.68
Inlet Air Pr bar 2.70
Back Pr abar 2.79
Inlet Temp C 584.00
Inlet Temp C 587.90
Outlet Temp C 174.00

Output
Intercooler LH 57.79
Intercooler RH 83.92
Inj setting V 4.09
Bypass Flow kg/m 1.410

Smoke
Nom Speed RPH 1700.00
Rev Speed RPH 1702.04
Torque Nm 308.69
Power kW 144.15
Th Effv % 27.27
Vol Effv % 44.76

```

Fig-6.24 Typical printout of experimental results

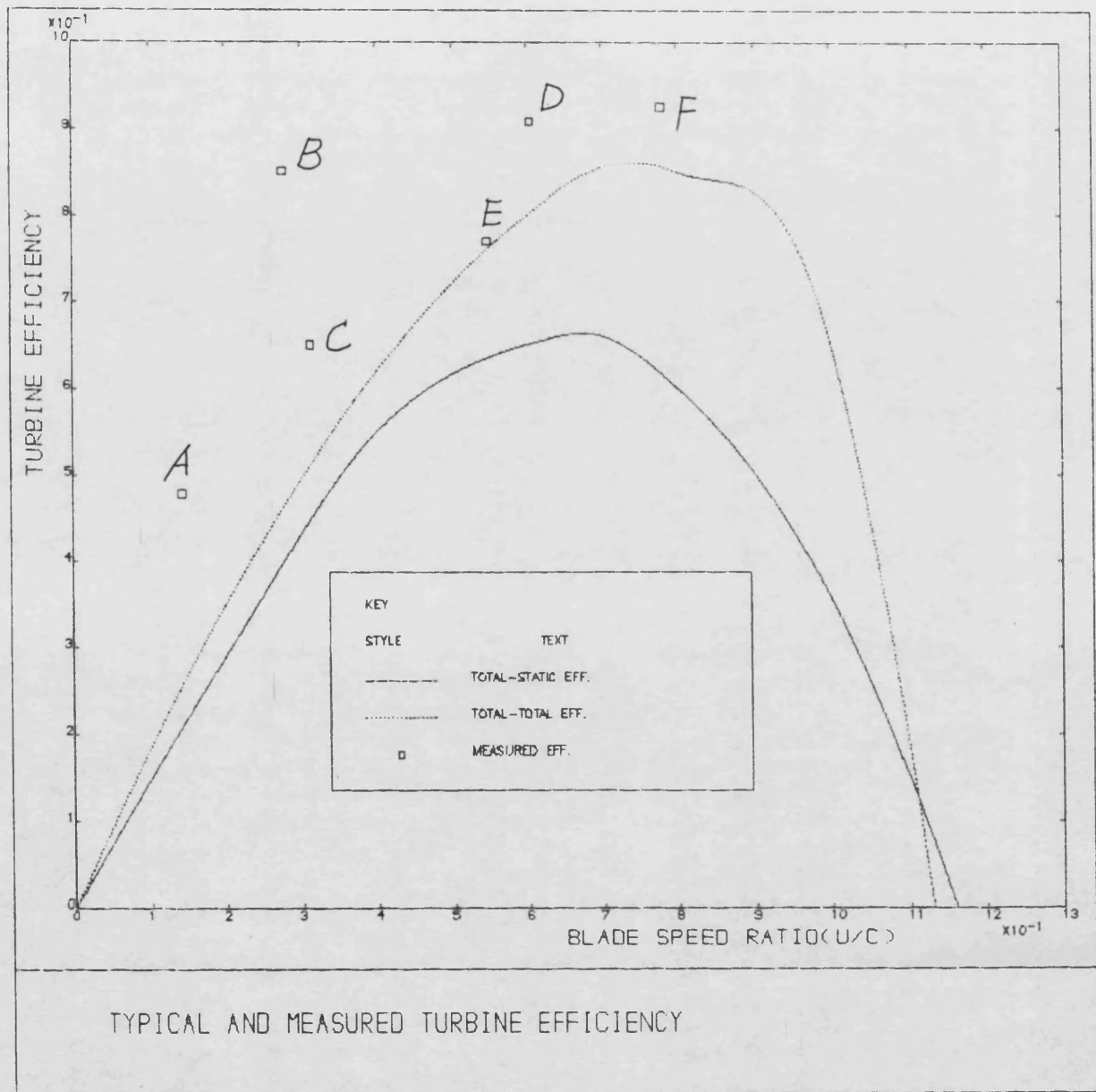


Fig-6.25

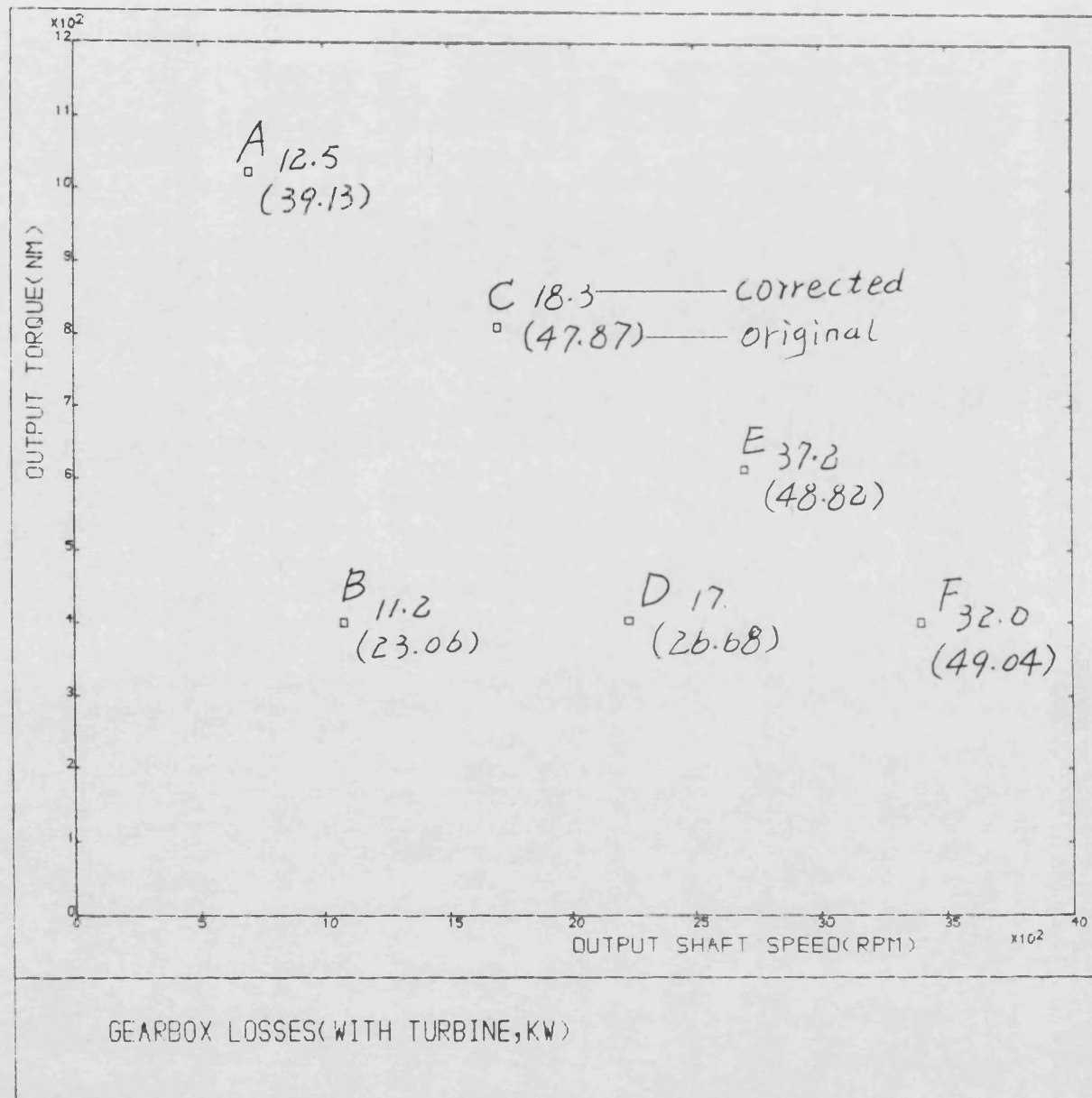


Fig-6.26

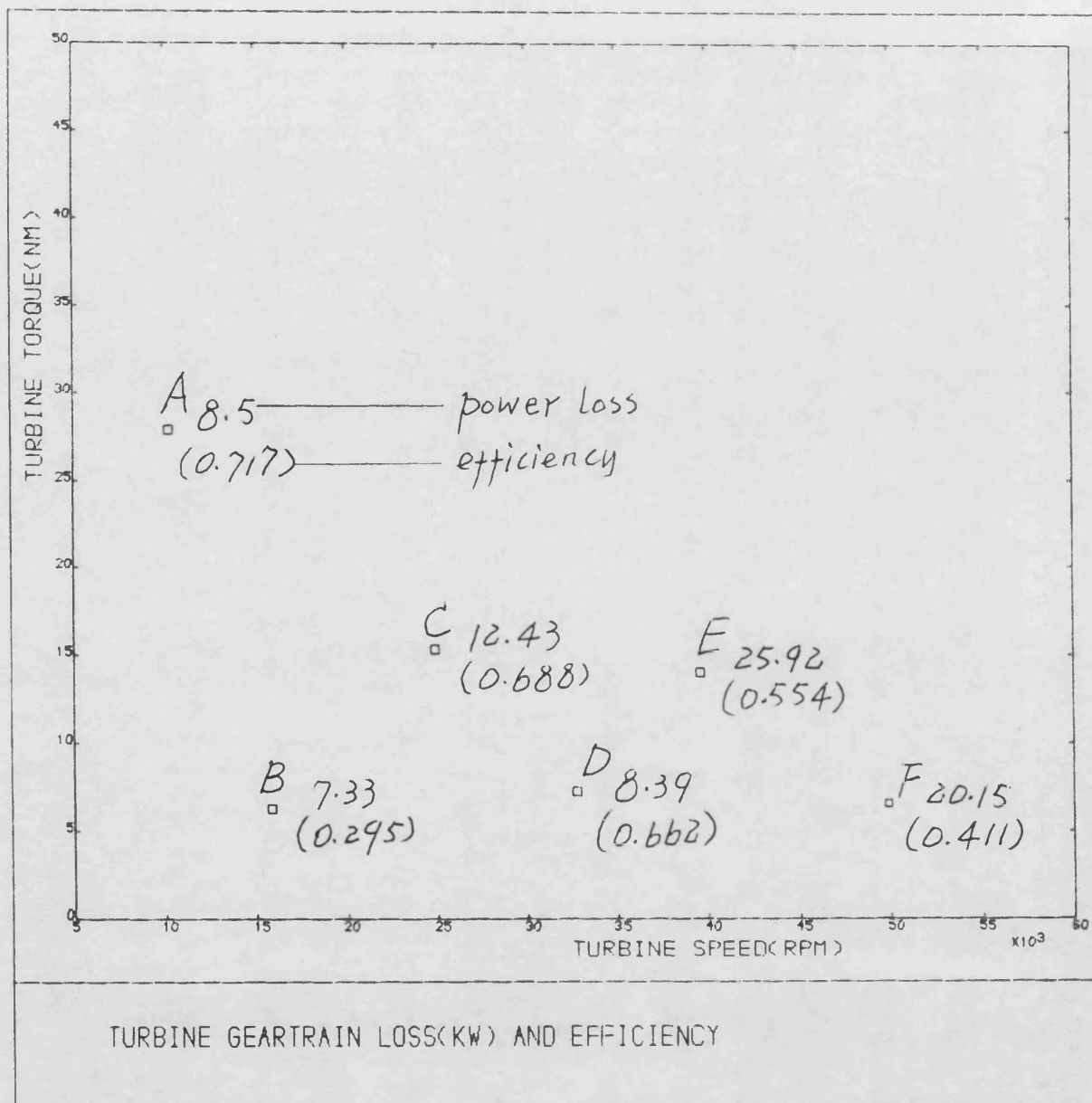


Fig-6.27

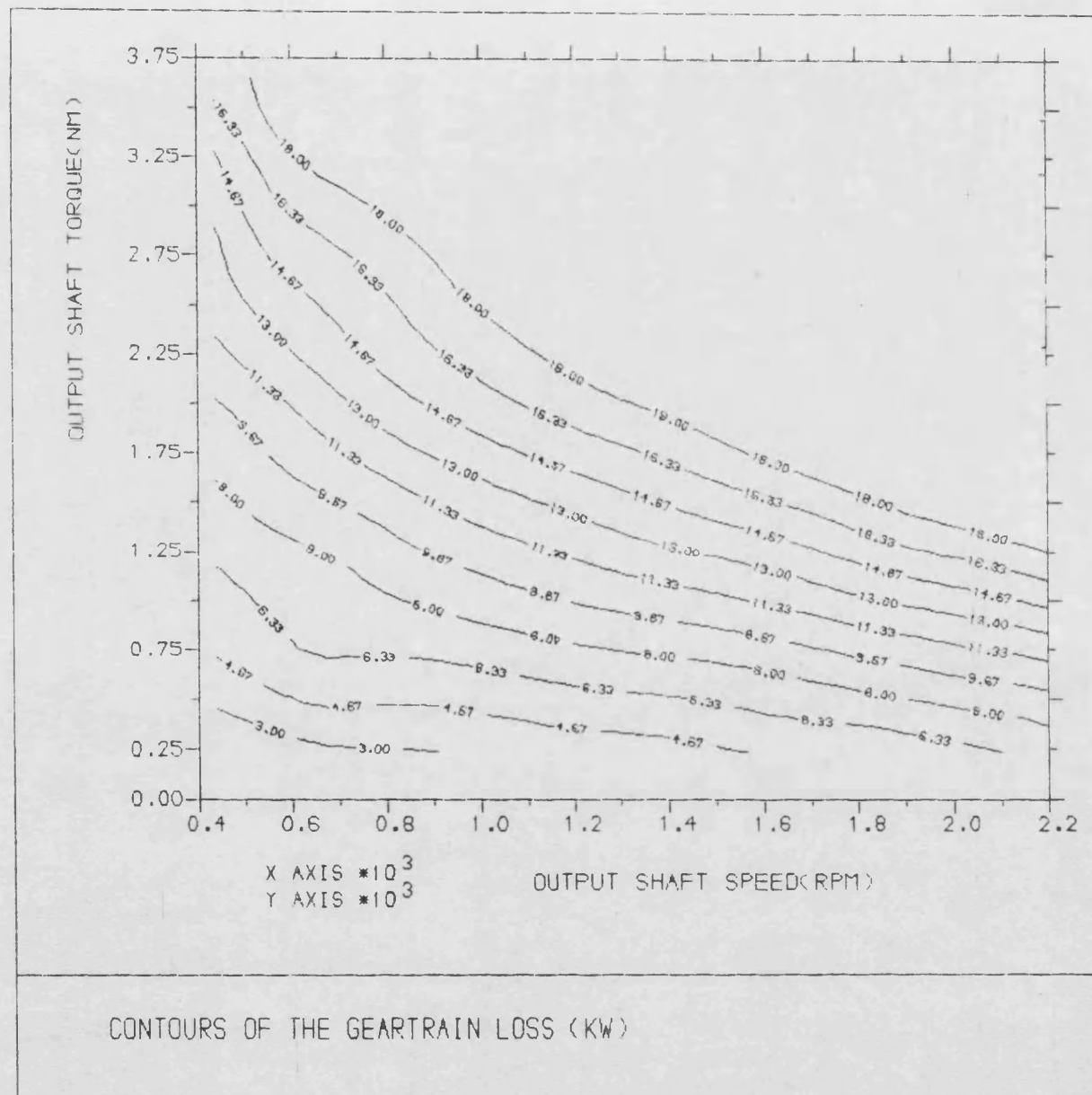


Fig-6.28

CHAPTER 7

SIMULATION OF THE LEYLAND 520 DCE

EXPERIMENTAL PLANT

In the following investigation, the program DCE2 is used to simulate the laboratory Leyland 520 DCE. This has been carried out in two parts, one in which more optimistic gearbox loss data are used and hypothetical pressure losses in various pipe sections are assumed, in an attempt to represent the system in a state as if it were implemented in a vehicle; the other in which the actual operating conditions of the system as measured from experiments are adopted, so that the performance of the system in the state of the present laboratory version is closely mimicked. Apart from examining the results of these simulations, further attempts will be made to assess the operations of the compressor and turbine.

7.1 Brief Presentation of the Experimental Results

Of the limited experimental results available, 16 sets were selected for the present investigations, Table-7.1. These data are all optimised and are reasonably distributed over the system operating range. These points are located in Fig-7.1, representing output shaft torque vs. output shaft speed, the accompanying numbers corresponding to the set numbers in Table-7.1. The relevant engine operating points are spotted on Fig-7.2, in order to assist the following analysis.

The optimisation was carried out under conditions of fixed engine speed and output shaft torque. The turbine nozzle angle is taken as the primary control variable. For a specific nozzle angle, a set of engine torques and output shaft speeds is determined; the best overall efficiency at this nozzle angle can be reached by varying the dynamic injection timing as a secondary control variable. Further, by running the system over a series of nozzle angles, an optimum combination of engine speed, output torque, and turbine nozzle angle is obtained.

The experimentally determined optimum engine speed distribution is presented in Fig-7.3, which shows the engine speed increases with output shaft

speed and torque. As output shaft speed decreases, the compressor mass flow will increase rapidly, and thus also the bypass flow. A decrease in engine speed will counteract this trend, reducing the compressor power and improving turbine efficiency. Engine air demand decreases with load, therefore engine speed can again be decreased.

Fig-7.4 shows the optimum boost ratio contours, while Fig-7.5 shows the engine BMEP, the patterns of the two figures being very similar. Generally boost ratio and BMEP increase with output torque. For constant output torque, higher boost ratios occur at the lower speed end, due to lower engine speed but higher engine torque, this relationship being dictated by torque balance in the epicyclic gearbox.

Fig-7.6 shows the optimum overall efficiency contours. These are not as good as would be expected. The reason for the poor system efficiencies has already been discussed in chapter-6. The highest value is about 32%. Along the limiting torque curve, efficiency deteriorates with decrease in output shaft speed, and clearly an efficiency of less than 14% can be expected at the stall point. The specific reasons for this are discussed in section-7.2.3(see also Fig-7.20 and Table-7.2a).

In Fig-7.7, engine torque and output torque are quoted at several low output shaft speed/high output torque points. At all these points, the output shaft torque is much lower than engine torque. Under these circumstances, it would be difficult to obtain the desired high torque rise. The main reasons for this are the high gearbox loss and low turbine efficiency, again as already discussed in chapter-6.

Fig-7.8 shows the bypass flow. Although these data are not regularly distributed, a general trend can be observed, i.e. bypass flow increases with decreasing output shaft speed.

A further feature is the excellent performance of the engine itself. Fig-7.9 shows the engine efficiency contours on an engine speed/torque map. For almost all the operating points, efficiency is above 37% and a value of 41% is reached. This is due to the combination of high BMEP operation and variable injection timing. The measured dynamic injection timing is shown in Fig-7.10. However, the pattern is not quite clear.

7.2 Preliminary Prediction (first simulation)

7.2.1 General

As mentioned earlier, this part of the simulation work is based on transmission and pressure losses which may be expected in a 'developed' DCE unit. This includes the following aspects:

a) Gearbox Losses (see chapter-6)

In the present laboratory prototype, the gearbox is relatively bulky, and suffers from exceptionally high losses. A 'developed' unit would have a more suitable gearbox, and the transmission efficiency would be higher. The data adopted in this part are intended to represent practical values for a purpose built automotive system and are as follows:

$$\begin{aligned}cge &= 0.98 & cgft &= 13.56 \text{ Nm} \\ oge &= 0.98 & ogft &= 13.56 \text{ Nm} \\ tge &= 0.931 & tgft &= 13.56 \text{ Nm}\end{aligned}$$

where	cge	compressor gear efficiency
	oge	output shaft gear efficiency
	tge	turbine gear efficiency
	cgft	compressor gear friction torque
	ogft	output shaft gear friction torque
	tgft	turbine gear friction torque

b) Pressure Losses

Because of the complex pipe arrangement required in the DCE, significant pressure losses in various sections can result and this has to be taken into account in the simulation process. In this investigation, an arbitrary value of about 0.1 bar is assumed for all sections (d_{pa} to d_{pd} as indicated in Fig-7.2). Further, fixed ambient conditions are adopted (T_a=293K and P_a=0.99bar) and ambient pressure is taken as compressor inlet and turbine back pressure.

It should be noted that no attempts were made in further optimisation. Rather, the program was run against the experimental operating points with respect to engine speed and torque, and output shaft speed. The input data therefore include output shaft speed, engine torque, engine speed and injection timing. The results are presented in Table-7.2, which is arranged in the same order as in Table-7.1.

7.2.2 Presentation of Results

As the input data implies, the engine operation is largely fixed, such as value of BMEP, power, etc. Particular attention has been paid to match the engine efficiency. This is shown in Fig-7.11. In most cases, the predicted values are very close to the experimental ones, with differences of under 2 percentage points. However, at a point denoted 9(set 9) the difference is higher than 3 percentage points, which is quite significant. Considering the operating conditions of the engine at this point and the general distribution of engine efficiency, the predicted value may be considered as acceptable.

The relatively good agreement in efficiency was obtained at the expense of inaccuracy in maximum cylinder pressure. As shown in Fig-7.12, the predicted value is generally much lower. Relatively significant discrepancy in exhaust temperature is shown in Fig-7.13, the data at point 5 being very poor.

The boost ratio(Fig-7.14) can be considered a very good match, except at point 10 where the difference is 0.17. In most other cases, the difference is under 0.07. A very good match was also obtained in terms of engine air mass flow(Fig-7.15), except at point 11, where a difference of about 6kg/min is obtained, possibly due to a measuring error.

7.2.3 Overall Performance

Having examined the engine operation, the overall performance can be assessed. As can be seen, in most cases, the predicted output torque and power are increased, therefore the overall efficiency is higher. This is plotted in Fig-7.16. At point 4, the predicted value is about 6.7 percentage points higher. However, at points 12 and 15, slightly lower values are predicted. The reason is an underestimation of turbine power. As can be seen in Table-7.2, set 12, the pressure ratio across the turbine is so low(relatively) that (possibly due to a subroutine failure) no power is developed from the turbine, but the presence of the turbine gear trains still requires that a certain amount of power be consumed in overcoming the friction. This further affects the overall efficiency.

Due to inaccuracies in certain measurements, significant anomalies have been observed in the experimental performance data of turbine and compressor, such as unreasonably high compressor power and turbine efficiency at certain points. This problem can be avoided in the simulation.

Due to the epicyclic connection, compressor power is largely fixed under a specific condition. Therefore it is the turbine performance which should be specially examined.

The predicted turbine efficiency is plotted in Fig-7.17. Generally, it deteriorates with decreasing output shaft speed, i.e. decreasing turbine speed due to the fixed ratio connection between the turbine and the output shaft. This is very clear in the region near the limiting torque curve. In the lower output shaft speed region, the turbine efficiency decreases with increasing output torque. Both these trends can be explained in terms of blade speed ratio. Fig-7.18 shows the bypass flow which is seen to increase rapidly with reducing output shaft speed, especially near the limiting torque curve. High bypass flow always has an adverse effect on overall system efficiency.

As mentioned earlier, lower transmission(gearbox) loss is assumed in the simulation procedure. This is shown in Fig-7.19, the effect of the output shaft speed is not as strong as expected from previous analysis.

Fig-7.20 compares the predicted engine torque and output shaft torque at four specially selected points(refer to Fig-7.7). Although certain improvements have been made over the experimental data, the predicted output torques are still very low. It can be seen that with a fixed ratio gear between the turbine and the output shaft, the DCE cannot take full advantage of the differential coupling of engine, compressor and turbine. Therefore a turbine CVT is required. To show this, a very preliminary calculation has been carried out for set 1 and 9(with highest load). The results are shown in Table-7.2a. Clearly, by adopting an appropriate turbine gear ratio, the system performance can be substantially enhanced. This is particularly demonstrated by the results for set 1, where by varying the turbine gear ratio from 14.7 to 60, turbine efficiency is improved from 24.4% to 66%, turbine power from 38.6kw to 104kw; also output torque from 1189Nm to 2020Nm and the overall efficiency from 17.4% to 29.5%.

7.3 Mimicking Experimental Performance

(second simulation)

In this part of the investigation, particular attention has been given to the following aspects:

a)The pressure losses in the various sections of the pipe line were deduced

from the experimental data and directly fed into the simulation program.

b) Ambient conditions, compressor inlet depression, turbine back pressure and pressure loss through the intercooler are also deduced from the experimental data and directly fed into the program.

c) The adopted data concerning the gearbox losses apply to the laboratory prototype and are largely deduced from the loss investigation of chapter-6. The data are as follows:

$$\begin{aligned}c_{ge} &= 0.99 & c_{gft} &= 2.71 \text{ Nm} \\o_{ge} &= 0.95 & o_{gft} &= 27.12 \text{ Nm} \\t_{ge} &= 0.61 & t_{gft} &= 27.12 \text{ Nm}\end{aligned}$$

The aim is to mimick the experimental operation as closely as possible.

Again, the calculations were performed at the selected points. The results are shown in Table-7.3.

In Fig-7.21, the mimicked engine efficiency is compared with the experimental values. In most cases, the difference is under 1 percentage point, and the greatest discrepancy occurs at point 9(set 9), with 2.3 percentage points. These have been improved, to some extent, over the previous prediction, which is further highlighted in terms of maximum cylinder pressure, Fig-7.22. Further examination shows that the accuracy of exhaust temperature, air/fuel ratio etc., are all generally improved.

The overall system efficiency is shown in Fig-7.23. In most cases, the difference is under 1.5 percentage points, while at point 14 and 15 it is 2.4 and 4.3 percentage points respectively. At point 15 this implies a difference of about 10kw in output power, which is quite significant compared with the engine power of 72kw.

Further examination shows that the data at point 15 seems to be somewhat contradictory. On the one hand, the experimental efficiency fits the general trend in Fig-7.23. However, if this is accepted, the output power should be about 50kw and this leads to a gearbox loss of 1.94kw, which does not seem to be reasonable. As shown in Fig-7.24, which shows the distribution of gearbox loss, at point 15, the mimicked gearbox loss is 11kw which fits the general trend. A value of 1.94kw can be a significant underestimate. Nevertheless, considering the results at other points the mimicked results are quite acceptable.

Comparing Fig-7.24 with Fig-7.19, it can be seen that gearbox loss in the laboratory prototype is generally high, and that it increases more rapidly with output shaft speed and torque than the 'idealised' values in Fig-7.19.

7.3.1 Compressor and Turbine Performance

Considering the general accuracy of the mimicked results, some confidence may be expressed in the mimicked compressor and turbine performance.

Fig-7.25 shows the comparison between the experimental and mimicked compressor pressure ratio. The two sets agree very well at lower load levels. However, as the operation moves towards the low output shaft speed/high torque corner, the difference is increasing. At point 11, the mimicked value is 0.637 lower, although the actual pipe loss has been fed into the program. However, calculation shows that the experimental compressor power is higher than the ideal value, which is obviously in error(see also chapter-6). From this standpoint, the accuracies of the mimicked value can be reconciled.

Fig-7.26 shows the experimental and mimicked compressor mass flowrate, good agreement is achieved(the experimental data adopted is derived from the compressor map).

Generally, the turbine pressure ratio does not agree as well as the compressor pressure ratio, Fig-7.27. At point 4 and 10, a difference of 0.4 is reached.

7.3.2 Effects of Pipe Losses

In the previous preliminary prediction, pipe losses are arbitrarily specified and no attention has been given to compressor inlet depression and the variation in turbine back pressure. This will certainly lead to differences in pressure ratio and therefore the performance of the compressor and turbine.

Although compressor power is largely fixed under a specific operating condition, due to the epicyclic gear connection, the variation in pressure ratio will induce changes in mass flow rate. In Fig-7.28, the preliminary prediction is compared with mimicked compressor mass flow. At low load level, the two agree relatively well, in spite of the different considerations mentioned above. In the high load/low speed corner, the two deviate significantly, the difference being approximately 6kg/min at point 1 and 3.5kg/min at point 9. This will have a marked effect on the overall system performance.

As can be seen in Tables-2 and 3, the assumed pressure losses for pipe a, b and d in the earlier prediction are generally too high, while for pipe c(bypass duct) the assumed value is sometimes higher and sometimes lower. Also the pressure loss through the intercooler calculated with the cooler subroutine is generally too low.

Unlike the compressor, turbine performance is dependent upon the gas flow state at the inlet. In Fig-7.29, the earlier predicted turbine power is compared with mimicked value. At point 12, turbine operation fails in the earlier run, which is a special case. For other points, a difference of up to 4kw is reached. It seems that at higher load, mimicked turbine power is lower and vice versa. Nevertheless, the difference in turbine power is not significant compared with the difference in gearbox loss.

7.4 Summary

The predicted performance has been assessed against experimental results, which show that if the true operating conditions of the system are properly taken into account, particularly the gearbox loss, reasonably accurate results can be predicted. Although the performance of the system in the form of the present prototype, can be further improved, to some extent, possibly by improving the gearbox design, limitations still exist. To take full advantage of the DCE concept, a turbine CVT should be adopted.

THE EXPERIMENTAL DATA

SET	1	2	3	4	5	6	7	8
ENGINE								
speed(rpm)	1457.0	1585	1700.	2107.0	2340.0	1200.0	2000.0	1250.
boost ratio	3.79	3.50	1.98	2.67	1.98	1.54	2.01	2.99
manifolt T(K)	334.4	330.	320.	324.8	318.4	317.6	321.0	323.
torque(Nm)	1350.9	1245.38	675.4	980.64	720.98	400.5	714.12	1025.85
power(kw)	206.15	207.30	120.35	216.83	176.59	50.33	149.47	134.17
bmeq(bar)	20.79	19.08	10.34	15.02	11.04	6.13	10.94	15.71
th. effy(%)	39.76	39.22	39.66	39.24	37.27	37.66	39.09	39.77
max. cl. p(bar)	153.7	141.8	104.59	148.62	108.	76.5	105.5	117.56
exh. T(K)	883	889.	740.	880.	607.	603.5	803.	791.
air flow(kg/m)	24.37	22.31	13.12	21.35	17.99	7.61	15.64	14.65
air/fuel ratio	33.35	29.96	30.67	27.42	26.94	40.41	29.03	30.83
inj tim(BTDC deg)	9.96	10.87	17.35	20.39	15.43	11.51	15.59	8.84
ch.clr Dp(mbar)	274.59	283.92	203.28	367.91	346.58	84.64	278.59	159.29
COMPRESSOR								
speed(rpm)	9502.0	5826.0	4279.	5618.0	4321.0	2334.	4043.	3954.
torque map(Nm)	161.54	146.36	75.6	110.32	80.76	46.45	78.83	113.6
power(kw)	161.18	89.70	34.0	65.37	36.82	11.32	33.38	47.16
isen effy TS(%)	77.26	78.62	80.8	79.11	78.17	76.26	80.58	74.87
overall effy(%)	61.85	60.24	64.57	66.52	64.76	54.98	65.02	62.84
mass orif(kg/m)	35.15	21.57	15.55	21.29	15.68	6.75	14.13	13.74
mass map(kg/m)	36.74	22.31	16.92	22.57	17.44	8.37	15.62	14.95
inlet Dp(mbar)	107.17	40.37	20.53	38.7	20.33	4.12	17.09	15.47
pr	4.57	3.95	2.23	3.17	2.39	1.63	2.34	3.20
inl. T(K)	297.	300.6	300.	295.	300.	297.	303.	300.
out T(K)	505	283.	396.	440.	394.	355.	405.	457.
TURBINE								
speed(rpm)	10266.9	24933.9	32766.	39600.9	49867.8	25227.2	41610.3	21598.82
torque(Nm)	64.15	28.47	10.1	17.02	9.91	2.67	10.03	16.5
inlet tep(K)	583.	857.	675.	850.	589.	586.	798.	766.
enthalpy(kw)	67.90	74.43	34.68	70.71	51.70	7.04	43.69	37.27
isen effy(%)	47.85	65.0	90.85	77.02	92.64	65.	96.22	63.48
mass(kg/m)	38.61	24.15	18.03	24.33	18.88	8.99	16.87	16.33
back p(mbar)	50.88	22.59	36.39	48.23	56.18	19.44	44.89	10.31
pr	3.30	3.68	2.04	2.85	2.18	1.57	2.17	3.07
OUTPUT								
speed(rpm)	700.0	1700.0	2234.	2700.0	3400.0	1720	2837.	1472.
torque(Nm)	1021.73	808.69	403.23	612.27	400.54	200.4	404.60	621.54
power(kw)	73.73	144.13	94.35	173.35	142.41	36.12	120.08	95.68
th effy(%)	14.22	27.27	31.1	31.37	30.06	27.	31.40	28.36
byp flow(kg/m)	12.37	0.	3.8	1.21	0.54	0.75	-0.01	0.3
Gbox loss(kw)	39.13	47.9	26.68	48.82	49.04	9.99	39.70	28.59

Table-7.1

THE EXPERIMENTAL DATA

SET	9	10	11	12	13	14	15	16
ENGINE-----								
speed(rpm)	1785.0	2435.0	1456.	1700.	900.0	1200.	1200.0	1200.
boost ratio	3.60	2.358	3.70	1.49	1.60	2.57	1.78	2.27
manifolt T(K)	335.	326.	330.	319.	319.	320.	318.	318.
torque(Nm)	1313.85	896.63	1319.91	423.07	401.98	888.14	575.21	730.51
power(kw)	244.93	228.89	201.44	75.29	37.92	111.70	72.31	91.94
bmepp(bar)	20.13	13.73	20.22	6.48	6.15	13.6	8.81	11.19
th. effy(%)	36.65	36.72	41.09	37.77	37.97	40.67	39.64	41.01
max. cl. p(bar)	153.56	135.25	149.73	80.89	79.23	138.19	94.58	124.51
exh. T(K)	970	964.	871.	663.	571.	720.	667.	686.
air flow(kg/m)	23.96	21.9	26.25	9.96	5.27	12.08	9.52	10.27
air/fuel ratio	25.44	24.93	37.99	35.45	37.51	31.21	37.05	32.52
inj tim(BTDC deg)	20.72	19.74	8.74	14.78	11.35	15.13	12.53	18.02
ch.clr Dp(mbar)	351.91	438.55	285.26	153.29	49.32	137.29	102.64	125.3
COMPRESSOR-----								
speed(rmp)	8642.	5165.	7085.	2908.	2056.	7300.	4857.	3069.
torque map(Nm)	155.92	100.59	155.4	50.03	46.04	101.61	66.09	81.31
power(kw)	141.24	54.9	115.44	15.26	9.97	78.08	33.69	26.69
isen effy TS(%)	80.24	78.53	79.25	76.84	76.65	82.06	78.5	80.82
overall effy(%)	63.67	65.7	62.56	56.08	54.38	67.26	61.51	62.73
mass orif(kg/m)	33.24	20.00	27.24	9.45	5.45	28.45	18.94	9.77
mass map(kg/m)	34.42	20.58	27.98	11.1	7.01	29.35	19.92	11.55
inlet Dp(mbar)	97.73	32.07	63.94	7.36	2.84	70.67	30.74	8.05
pr	4.37	2.91	4.26	1.66	1.65	2.92	1.94	2.42
inl. T(K)	298.	295.	301.	297.	299.	298.	297.	301.
out T(K)	490.	427.	290.	357.	359.	328.	376.	408.
TURBINE-----								
speed(rpm)	21633.8	49999.8	17600.4	36990.17	18025.74	10002.89	17527.1	22997.85
torque(Nm)	38.57	14.57	31.75	5.23	6.42	33.74	15.67	9.22
inlet tep(K)	847.	943.	783.	601.	554.	559.	525.	673.
enthalpy(kw)	86.93	76.06	58.46	20.26	12.1	35.02	28.69	22.07
isen effy(%)	54.49	87.19	48.17	127.99	130.99	65.58	142.41	72.65
mass(kg/m)	36.55	22.46	29.81	11.88	7.56	30.48	20.67	12.5
back P(mbar)	47.44	62.68	29.27	41.35	11.34	30.45	13.45	23.86
pr	2.71	2.60	3.59	1.56	1.62	2.05	1.50	2.30
OUTPUT-----								
speed(rpm)	1475.	3409.	1200.	2522.	1229.	682.	1195.	1568.
torque(Nm)	996.85	533.95	901.3	200.98	200.99	704.07	400.84	403.59
power(kw)	153.19	189.99	113.15	53.02	25.79	49.82	50.02	65.8
th effy(%)	22.92	30.48	23.08	26.6	25.83	18.14	27.42	29.35
byp flow(kg/m)	10.5	-1.32	1.73	1.41	1.74	17.27	10.4	1.28
Gbox loss(kw)	37.43	60.06	31.3	26.6	14.25	18.82	17.28	21.51

Table-7.1 (continued)

The results from the first simulation

LEYLAND 500 DCE

						32	34	31	24
number of cylinders	6.0	bore	(m.m.)	118.11	stroke	(m.m.)	124.97		
con-rod length (m.m.)	218.45	inlet valve closing (degs)	230.0	compressor scale factor	1.00				
ambient temperature (deg k)	294.4	ambient pressure (bar)	0.99	cooler effectiveness	0.8835				
compression ratio	12.80	engine diagram factor	0.9875	turbine flow loss factor	0.8000				
engine speed(r.p.m)	1457.00	1585.00	1700.00	2107.00	2340.00	1200.00	2000.00	1250.00	
boost pressure ratio	3.816	3.462	1.952	2.938	2.059	1.440	2.074	3.074	
delivered air to fuel ratio	30.763	29.112	31.192	31.468	27.297	38.321	30.443	34.108	
delivery ratio	0.054	0.054	0.052	0.053	0.049	0.053	0.052	0.054	
manifold temp (deg k)	314.616	316.914	302.207	317.433	313.595	291.372	307.403	305.345	
engine power (k w.)	206.05	206.93	117.02	215.72	176.58	49.95	149.07	133.89	
engine torque (n.m.)	1350.92	1248.15	675.46	980.65	721.01	400.77	714.10	1025.85	
b.m.e.p (bar)	20.6544	19.0680	10.2943	14.9533	11.0210	6.0790	10.8857	15.6437	
s.f.c. (kg/kw hr)	0.203	0.209	0.214	0.209	0.225	0.226	0.216	0.201	
b.thermal eff.	0.4110	0.3783	0.3897	0.3994	0.3708	0.3647	0.3862	0.4157	
fuel / rev (ky.)	4.784	4.556	2.514	3.564	2.829	1.565	2.683	3.582	
max cyl pressure (bar .)	127.12	116.45	106.42	123.57	107.72	76.05	111.08	112.44	
exhaust temperature(deg k)	858.99	876.81	787.25	848.01	891.26	643.56	824.24	766.77	
mass flow (kg/min)	21.441	21.023	13.334	23.629	18.523	7.196	16.335	15.272	
percentage heat to coolant	12.57	12.76	16.37	11.92	14.03	23.10	14.62	15.16	
compressor speed (r.p.m.)	9506.1	5837.4	4290.2	5647.7	4345.9	2341.9	4045.5	3973.5	
compressor pressure ratio	4.004	3.660	2.150	3.177	2.311	1.595	2.296	3.243	
mass flow (kg/min)	42.271	24.417	17.817	23.940	18.070	8.781	16.595	15.667	
compressor power (kw.)	147.82	83.80	33.00	63.45	35.84	10.54	33.09	46.77	
compressor torque (n.m)	148.43	137.03	73.43	107.23	78.72	42.98	78.08	112.34	
delivery temperature (deg k)	502.31	478.50	405.19	452.49	424.68	366.37	413.62	472.23	
compressor efficiency	0.685	0.644	0.651	0.728	0.672	0.587	0.663	0.660	
turbine speed (r.p.m)	10260.0	24939.0	32772.8	39609.0	49878.0	25232.4	41618.8	21594.2	
turbine pressure ratio	3.900	3.556	2.045	3.072	2.311	1.491	2.192	3.139	
mass flow (kg/min)	42.973	25.141	14.252	24.694	18.746	8.972	17.136	16.116	
turbine power (kw)	38.58	54.35	25.66	68.07	36.89	3.81	30.80	28.75	
turbine torque (n.m)	35.86	20.80	7.47	16.41	7.06	1.44	7.06	12.71	
inlet temperature (deg k)	693.73	847.26	700.08	843.45	891.26	597.03	818.54	760.05	
turbine nozzle angle	8.741	6.374	3.112	7.330	8.524	8.164	7.684	4.421	
turbine efficiency	0.244	0.510	0.742	0.736	0.677	0.615	0.726	0.520	
output shaft speed (rpm)	700.00	1700.00	2234.00	2700.00	3400.00	1720.00	2837.00	1472.00	
output shaft power (kw)	87.23	165.46	103.45	205.50	164.06	38.44	135.82	107.97	
output shaft torque (n./m)	1187.48	929.04	442.00	726.52	460.59	213.31	456.98	700.13	
output shaft sfc (kg/kw.hr)	0.479	0.262	0.240	0.219	0.242	0.293	0.237	0.249	
output thermal efficiency	0.1740	0.3185	0.3364	0.3905	0.3445	0.2845	0.3519	0.3352	
engine fuel flow (kg/min)	0.697	0.722	0.427	0.751	0.662	0.188	0.537	0.448	
dynamic injection(degree ca)	352.0	352.4	330.7	343.6	337.7	340.3	338.0	351.5	
duration of injection	25.9	26.5	17.2	25.7	24.3	10.0	20.2	18.3	
turbine gear ratio	14.7	14.7	14.7	14.7	14.7	14.7	14.7	14.7	
pressure loss in pipe a (bar)	0.10345	0.10345	0.10345	0.10345	0.10345	0.10345	0.10345	0.10345	
pressure loss in pipe b (bar)	0.10345	0.10345	0.10345	0.10345	0.10345	0.10345	0.10345	0.10345	
pressure loss in pipe c (bar)	0.10345	0.10345	0.10345	0.10345	0.10345	0.10345	0.10345	0.10345	
pressure loss in pipe d (bar)	0.10345	0.10345	0.10345	0.10345	0.10345	0.10345	0.10345	0.10345	
total gear box loss (kw)	2.581	12.022	2.036	14.846	13.564	4.778	10.957	7.908	
output shaft gear loss (kw)	1.606	3.702	3.400	5.058	5.364	2.086	4.453	2.833	
compressor gear loss (kw)	1.546	2.649	1.344	2.205	1.427	0.592	1.323	1.594	
turbine gear loss (kw)	3.588	5.998	4.725	8.268	7.041	2.538	5.877	3.931	

Table-7.2

number of cylinders	6.0	bore	(m.m.)	119.11	stroke	(m.m.)	124.97
con-rod length (m.m.)	218.45	inlet valve closing (degs)	230.0	compressor scale factor	1.00		
ambient temperature (deg k)	294.4	ambient pressure (bar)	0.99	cooler effectiveness	0.8748		
compression ratio	12.80	engine diagram factor	0.9900	turbine flow loss factor	0.8000		
engine speed(r.p.m)	1785.00	2438.00	1456.00	1700.00	700.00	1200.00	1200.00
boost pressure ratio	3.679	2.528	3.665	1.379	1.499	2.517	2.193
delivered air to fuel ratio	27.226	25.275	30.517	33.232	40.374	31.772	34.364
delivery ratio	0.853	0.850	0.854	0.852	0.854	0.854	0.854
manifold temp (deg k)	321.379	324.824	314.747	295.306	289.200	299.101	293.510
engine power (k w.)	245.43	228.46	201.23	74.70	37.83	111.54	71.84
engine torque (n.m.)	1313.71	876.57	1317.87	423.01	401.99	888.18	575.27
b.m.e.p (bar)	20.0814	13.6860	20.1853	6.4173	6.1386	13.5750	8.7435
s.f.c. (ky/kw hr)	0.208	0.226	0.201	0.236	0.222	0.208	0.214
b.thermal eff.	0.4018	0.3690	0.4153	0.3541	0.3753	0.4012	0.3903
fuel / rev (ky.)	4.756	3.530	4.626	1.725	1.557	3.220	2.132
max cyl pressure (bar .)	130.04	104.60	133.66	84.43	74.29	92.87	92.32
exhaust temperature(deg k)	705.70	957.24	853.21	735.16	601.40	783.32	712.68
mass flow (ky/min)	24.813	22.947	20.556	9.745	5.657	12.278	8.443
percentage heat to coolant	11.63	12.89	12.70	19.50	26.50	17.11	21.18
compressor speed (r.p.m.)	8683.2	5168.0	7097.8	2908.1	2049.1	7323.1	4861.3
compressor pressure ratio	3.895	2.795	3.853	1.589	1.636	2.679	1.859
mass flow (ky/min)	38.277	21.752	30.474	11.634	7.258	32.488	20.726
compressor power (kw.)	131.28	53.11	107.81	13.84	9.25	74.45	31.76
compressor torque (n.m)	144.32	78.07	144.78	45.44	43.11	97.05	62.36
delivery temperature (deg k)	498.37	467.08	504.70	365.73	370.81	431.28	385.28
compressor efficiency	0.682	0.670	0.655	0.587	0.585	0.700	0.630
turbine speed (r.p.m)	21638.3	50010.0	17604.0	36977.7	18029.4	10004.9	17530.6
turbine pressure ratio	3.791	2.795	3.749	1.485	1.532	2.575	1.755
mass flow (kg/min)	37.133	22.619	31.150	0.000	7.398	32.874	21.188
turbine power (kw)	71.92	65.71	47.08	0.00	3.85	23.04	14.80
turbine torque (n.m)	31.72	12.58	25.53	0.00	2.04	21.98	8.06
inlet temperature (deg k)	774.23	957.24	740.63	680.52	553.58	573.69	525.57
turbine nozzle angle	8.884	7.970	7.022	20.000	4.337	9.686	9.827
turbine efficiency	0.455	0.746	0.390	0.000	0.723	0.331	0.673
output shaft speed (rpm)	1475.00	3409.00	1200.00	2522.00	1229.00	682.00	1195.00
output shaft power (kw)	172.03	224.82	127.71	54.28	28.59	53.83	49.66
output shaft torque (n./m)	1113.24	629.51	1031.78	205.45	222.08	753.37	396.64
output shaft sfc (ky/kw.hr)	0.296	0.230	0.312	0.324	0.294	0.431	0.309
output thermal efficiency	0.2817	0.3631	0.2677	0.2573	0.2837	0.1936	0.2678
engine fuel flow (ky/min)	0.847	0.861	0.674	0.273	0.140	0.386	0.256
dynamic injection(degree ca)	347.3	343.7	347.6	331.5	344.1	352.8	341.4
duration of injection	30.1	30.3	25.1	13.0	8.7	16.4	12.2
turbine gear ratio	14.7	14.7	14.7	14.7	14.7	14.7	14.7
pressure loss in pipe a (bar)	0.10345	0.10345	0.10345	0.10345	0.10345	0.10345	0.10345
pressure loss in pipe b (bar)	0.10345	0.10345	0.10345	0.10345	0.10345	0.10345	0.10345
pressure loss in pipe c (bar)	0.10345	0.10345	0.10345	0.10345	0.10345	0.10345	0.10345
pressure loss in pipe d (bar)	0.10345	0.10345	0.10345	0.10345	0.10345	0.10345	0.10345
total gear box loss (kw)	14.036	16.436	10.787	6.567	3.826	6.289	5.226
output shaft gear loss (kw)	3.323	6.059	2.711	3.123	1.492	1.206	1.687
compressor gear loss (kw)	7.076	1.914	3.342	0.750	0.519	2.698	1.430
turbine gear loss (kw)	6.713	9.056	4.835	3.335	1.491	2.491	2.602

Table-7.2 (continued)

Table-7.2a The predicted results with CVT
for sets 1 and 9

	set-1	set-9
engine speed (rpm)	1457.0	1785.0
boost pressure ratio	3.816	3.679
delivered A/F ratio	30.763	29.226
delivery ratio	0.854	0.853
manifold temp (deg K)	314.6	321.4
engine power (kw)	206.05	245.43
engine torque (Nm)	1350.92	1313.91
BMEP (bar)	20.6544	20.0814
s.f.c. (kg/kw hr)	0.203	0.208
b.thermal eff.	0.4110	0.4019
fuel/rev (g)	4.784	4.756
max cyl pressure (bar)	129.12	130.03
exhaust temp (deg K)	859.	906.
mass flow (kg/min)	21.441	24.813
heat to coolant (%)	12.57	11.63
dynamic inj. (deg ca)	352.	349.
duration of inj. (deg)	25.9	30.1
compressor speed (rpm)	9506.1	8683.2
pressure ratio	4.004	3.895
mass flow (kg/min)	42.271	38.279
compressor power (kw)	147.82	131.28
compressor torque (Nm)	148.43	144.32
delivery temp (deg K)	502.31	498.37
compressor efficiency	0.685	0.682
turbine speed (rpm)	42000.	44250.
pressure ratio	3.900	3.791
mass flow kg/min)	42.974	39.134
turbine power (kw)	103.97	105.92
turbine torque (Nm)	23.63	22.85
inlet temp (deg K)	693.7	774.2
nozzle angle (deg)	8.941	8.884
turbine efficiency	0.658	0.670
turbine gear ratio	60.	30.
O/S speed (rpm)	700.	1475.
O/S power (kw)	148.1	203.7
O/S torque (Nm)	2019.6	1318.1
O/S s.f.c. (kg/kw hr)	0.282	0.250
output thermal eff.	0.2954	0.3335
O/S gear loss (kw)	1.606	3.323
comp. gear loss (kw)	4.546	4.076
turbine gear loss (kw)	8.099	9.259
total gear loss (kw)	14.1	16.4

The results from the second simulation

LEYLAND 500 DCF									
number of cylinders	6.0	hore	(m.m.)	118.11	stroke	(m.m.)	124.97		
con-rod length (m.m.)	218.45	inlet valve closing (degs)	230.0	compressor scale factor	1.00				
ambient temperature (deg k)	300.2	ambient pressure (bar)	0.97	cooler effectiveness	0.8863				
compression ratio	12.80	engine diagram factor	0.9750	turbine flow loss factor	0.8000				
ENGINE SPEED(r.p.m)	1457.00	1585.00	1700.00	2107.00	2340.00	1200.00	2000.00	1250.00	
boost pressure ratio	3.744	3.396	2.007	2.812	1.990	1.542	2.039	3.110	
delivered air to fuel ratio	26.424	26.259	30.597	27.264	26.193	42.387	28.069	32.812	
delivery ratio	0.860	0.850	0.850	0.848	0.847	0.852	0.848	0.852	
manifold temp (deg k)	318.711	318.969	303.357	317.174	308.733	291.880	308.479	306.737	
engine power (k w.)	205.95	206.25	120.09	215.92	176.27	50.25	149.24	134.20	
engine torque (n.m.)	1350.91	1245.38	675.41	980.65	720.98	400.73	714.12	1025.85	
b.m.e.p (bar)	20.6444	19.0050	10.3170	14.9668	11.0019	6.1156	10.8981	15.6805	
s.f.c. (kg/kw hr)	0.203	0.213	0.217	0.218	0.225	0.215	0.222	0.205	
b.thermal eff.	0.4116	0.3921	0.3852	0.3825	0.3706	0.3883	0.3752	0.4071	
fuel / rev (kg.)	4.774	4.614	2.549	3.724	2.826	1.499	2.765	3.666	
max cyl pressure (bar)	153.99	141.79	105.22	148.77	108.63	77.20	106.24	117.86	
exhaust temperature(deg k)	905.13	941.45	814.17	935.17	747.27	612.34	891.83	781.96	
mass flow (kg/min)	18.380	19.203	13.262	21.394	17.320	7.625	15.520	15.054	
percentage heat to coolant	14.72	14.53	17.73	13.59	15.24	23.95	16.27	16.53	
COMPRESSOR SPEED(r.p.m.)	9506.1	5837.4	4290.2	5647.7	4345.9	2341.9	4045.5	3973.5	
compressor pressure ratio	4.060	3.699	2.217	3.213	2.351	1.628	2.336	3.272	
mass flow (kg/min)	36.653	22.511	17.012	22.584	17.469	8.598	15.690	15.038	
compressor power (kw.)	150.54	85.21	33.99	64.75	36.48	10.95	33.68	47.73	
compressor torque (n.m)	151.16	139.33	75.63	109.43	80.12	44.63	79.46	114.67	
delivery temperature (deg k)	540.94	525.27	417.89	466.26	414.78	373.20	430.66	489.25	
compressor efficiency	0.597	0.602	0.644	0.683	0.644	0.584	0.648	0.638	
inlet pressure (bar)	0.8710	0.9366	0.9683	0.9414	0.9459	0.9855	0.9652	0.9738	
inlet temperature (deg k)	297.550	300.750	300.550	295.450	289.950	296.950	302.550	300.150	
bypass air flow (kg/min)	18.2726	3.3079	3.7501	1.1907	0.1496	0.9731	0.1700	-0.0163	
TURBINE SPEED(r.p.m)	10269.0	24939.0	32772.8	37609.0	49378.0	25232.4	41618.8	21594.2	
turbine pressure ratio	3.357	3.742	2.186	3.223	2.382	1.628	2.367	3.271	
mass flow (kg/min)	37.354	23.244	17.448	23.371	18.139	8.778	16.245	15.497	
turbine power (kw)	33.58	51.73	29.34	69.34	40.21	7.71	36.55	28.48	
turbine torque (n.m)	31.22	19.80	0.55	16.71	7.69	2.92	8.38	12.59	
inlet temperature (deg k)	735.58	807.19	735.23	913.55	743.34	507.10	887.47	781.96	
turbine nozzle angle	10.315	5.844	6.714	6.919	7.872	4.371	6.409	4.005	
turbine efficiency	0.284	0.491	0.733	0.724	0.702	0.737	0.746	0.494	
back pressure (bar)	1.0288	0.9996	1.0252	1.0283	1.0224	1.0094	1.0272	0.9996	
OUTPUT SHAFT SPEED(r.p.m)	700.00	1700.00	2234.00	2700.00	3400.00	1720.00	2837.00	1472.00	
output shaft power (kw)	69.39	140.63	92.37	176.87	146.24	36.48	122.80	94.34	
output shaft torque (n.m)	746.28	789.65	394.65	625.30	410.56	202.45	413.18	611.78	
output shaft sfc (kg/kw.hr)	0.601	0.312	0.282	0.266	0.271	0.296	0.270	0.291	
output thermal efficiency	0.1307	0.2673	0.2962	0.3133	0.3074	0.2819	0.3087	0.2862	
ENGINE FUEL FLOW(kg/min)	0.676	0.731	0.433	0.785	0.661	0.180	0.553	0.458	
dynamic injection(degree ca)	347.7	349.1	347.7	341.6	343.3	350.9	346.6	354.2	
duration of injection	25.8	26.8	17.3	26.6	24.2	9.8	20.6	18.7	
turbine gear ratio	14.7	14.7	14.7	14.7	14.7	14.7	14.7	14.7	
pressure loss in pipe a (bar)	0.00110	0.00044	0.00033	0.00045	0.00033	0.00010	0.00027	0.00020	
pressure loss in pipe b (bar)	0.07000	0.06000	0.04001	0.06000	0.06001	0.02379	0.05001	0.05001	
pressure loss in pipe c (bar)	0.68000	0.02000	0.07002	0.05000	0.03001	0.02379	0.02001	0.05001	
pressure loss in pipe d (bar)	0.00314	0.00110	0.00093	0.00142	0.00117	0.00025	0.00089	0.00051	
pressure loss in cooler (bar)	0.275	0.204	0.203	0.377	0.341	0.085	0.287	0.157	
total gear box loss (kw)	12.597	32.141	23.073	43.632	33.756	10.525	29.307	20.609	
output shaft gear loss (kw)	3.717	8.521	7.572	11.478	11.765	4.485	7.729	6.458	
compressor gear loss (kw)	1.026	1.048	0.480	0.837	0.510	0.186	0.472	0.610	
turbine gear loss (kw)	14.310	23.127	15.315	31.720	21.572	5.906	17.172	13.659	

Table-7.3

LEYLAND 500 DCE						34	30	33	24	
number of cylinders	6.0		bore	(m.m.)	118.11	stroke	(m.m.)	124.97		
con-rod length (m.m.)	218.45		inlet valve closing (degs)	230.0		compressor scale factor	1.00			
ambient temperature (deg k)	301.5		ambient pressure (bar)	0.90		cooler effectiveness	0.8474			
compression ratio	12.80		engine diagram factor	0.9800		turbine flow loss factor	0.8000			
ENGINE SPEED(r.p.m.)	1785.00	2435.00	1456.00	1700.00	900.00	1200.00	1200.00	1200.00		
boost pressure ratio	3.562	2.466	3.597	1.467	1.618	2.622	1.793	2.276		
delivered air to fuel ratio	24.934	23.524	27.641	35.637	44.864	32.023	35.146	34.283		
delivery ratio	0.852	0.846	0.854	0.849	0.853	0.863	0.862	0.852		
manifold temp (deg k)	323.560	322.124	317.048	295.938	289.888	301.203	294.409	299.326		
engine power (k w.)	245.54	227.82	201.04	75.17	37.52	111.44	72.18	91.74		
engine torque (n.m.)	1313.85	896.63	1317.71	423.07	401.98	888.14	575.21	730.51		
b.m.e.p (bar)	20.0904	13.6648	20.1662	6.4577	6.0887	13.5628	8.7852	11.1652		
s.f.c. (kg/kw hr)	0.214	0.227	0.206	0.224	0.216	0.198	0.205	0.208		
b.thermal eff.	0.3876	0.3681	0.4057	0.3727	0.3863	0.4207	0.4069	0.4018		
fuel / rev (kw.)	4.908	3.533	4.731	1.649	1.500	3.069	2.055	2.645		
max cyl pressure (bar)	153.47	135.72	150.09	81.56	79.73	139.02	95.25	125.20		
exhaust temperature(deg k)	787.53	1013.86	893.70	721.84	565.90	732.72	671.79	715.81		
mass flow (kg/min)	21.842	20.902	17.041	9.989	6.057	11.792	8.666	10.879		
percentage heat to coolant	13.53	14.33	14.58	20.67	27.30	18.94	22.45	19.79		
COMPRESSOR SPEED(r.p.m.)	8683.2	5141.6	7097.8	2908.1	2049.1	7323.1	4861.3	3071.3		
compressor pressure ratio	3.949	2.937	3.703	1.624	1.668	2.780	1.901	2.405		
mass flow (kg/min)	34.692	20.237	20.238	11.265	7.053	29.421	19.957	11.335		
compressor power (kw.)	133.72	53.85	107.81	14.36	9.61	76.22	32.73	26.17		
compressor torque (n.m)	147.00	79.97	147.68	47.13	44.75	99.35	64.27	81.32		
delivery temperature (deg k)	526.14	473.03	531.04	373.57	380.47	453.00	395.25	439.16		
compressor efficiency	0.620	0.668	0.615	0.581	0.579	0.655	0.611	0.623		
inlet pressure (bar)	0.9102	0.9312	0.9403	0.9749	0.9854	0.9136	0.9595	0.9772		
inlet temperature (deg k)	297.450	294.450	300.450	297.250	298.950	298.550	297.150	301.450		
bypass air flow (kg/min)	12.8499	-0.7449	9.1970	1.2754	0.9965	17.6291	11.2903	0.4558		
TURBINE SPEED(r.p.m.)	21638.3	50010.0	17604.0	36977.7	18029.4	10004.9	17530.6	23002.6		
turbine pressure ratio	3.772	3.012	3.647	1.634	1.668	2.177	1.546	2.394		
mass flow (kg/min)	35.573	21.100	28.727	11.550	7.188	29.774	20.209	11.653		
turbine power (kw)	68.44	67.51	44.98	8.60	5.60	18.17	12.49	17.83		
turbine torque (n.m)	30.19	12.87	24.39	2.22	2.97	17.34	6.80	7.40		
inlet temperature (deg k)	833.64	1013.86	785.70	685.87	541.20	572.08	521.68	705.70		
turbine nozzle angle	8.968	7.184	6.983	7.852	3.082	10.543	10.421	3.878		
turbine efficiency	0.482	0.752	0.405	0.557	0.652	0.369	0.702	0.606		
back pressure (bar)	1.0554	1.0261	1.0336	1.0236	0.9996	1.0147	1.0037	1.0091		
OUTPUT SHAFT SPEED(r.p.m.)	1475.00	3409.00	1200.00	2522.00	1229.00	682.00	1195.00	1568.00		
output shaft power (kw)	141.85	175.61	109.27	54.87	26.21	41.66	40.97	67.81		
output shaft torque (n.m)	717.78	547.70	867.20	207.76	203.55	583.14	327.28	412.82		
output shaft sfc (kg/kw.hr)	0.371	0.264	0.370	0.306	0.309	0.530	0.361	0.281		
output thermal efficiency	0.2251	0.3161	0.2205	0.2722	0.2699	0.1573	0.2310	0.2971		
ENGINE FUEL FLOW(kg/min)	0.876	0.860	0.689	0.280	0.135	0.368	0.247	0.317		
dynamic injection(degree ca)	346.1	338.9	349.4	347.3	351.4	346.3	349.4	347.3		
duration of injection	30.9	30.3	25.6	12.6	8.5	15.8	11.9	14.2		
turbine gear ratio	14.7	14.7	14.7	14.7	14.7	14.7	14.7	14.7		
pressure loss in pipe a (bar)	0.00101	0.00039	0.00066	0.00017	0.00007	0.00039	0.00050	0.00014		
pressure loss in pipe b (bar)	0.10003	0.07002	0.06002	0.02061	0.01000	0.03001	0.03001	0.03001		
pressure loss in pipe c (bar)	0.26007	0.03001	0.30004	0.01000	0.01000	0.58016	0.37010	0.04001		
pressure loss in pipe d (bar)	0.00273	0.00134	0.00167	0.00050	0.00015	0.00249	0.00130	0.00036		
pressure loss in cooler (bar)	0.351	0.437	0.285	0.153	0.049	0.144	0.103	0.125		
total gear box loss (kw)	33.403	45.878	26.734	14.519	7.308	11.722	10.965	15.583		
output shaft gear loss (kw)	7.680	13.702	6.267	6.737	3.209	2.725	3.710	5.561		
compressor gear loss (kw)	1.630	0.711	1.338	0.239	0.163	1.005	0.487	0.364		
turbine gear loss (kw)	27.248	32.237	19.622	7.726	4.315	8.268	6.740	9.669		

Table-7.3 (continued)

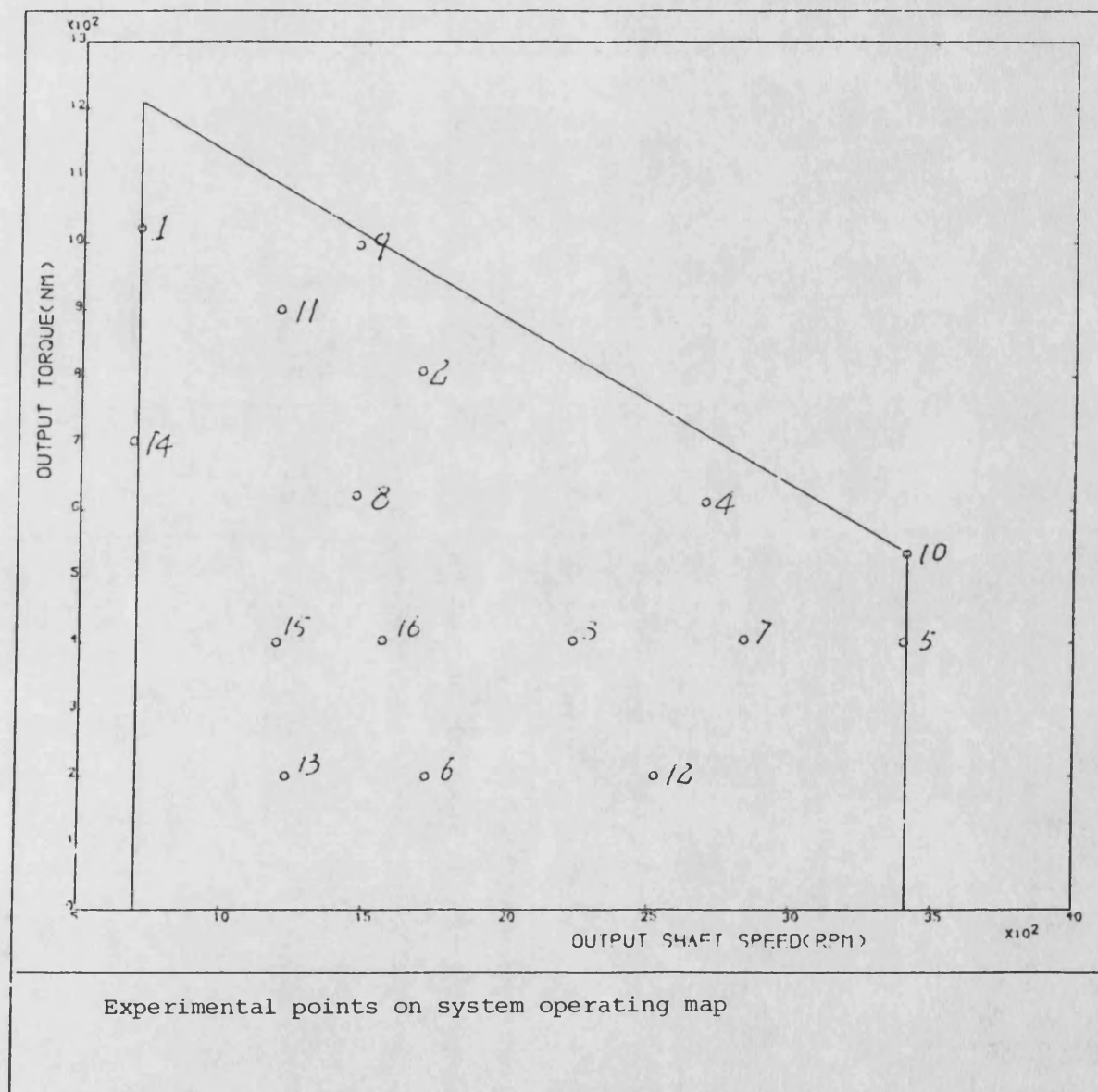


Fig-7.1

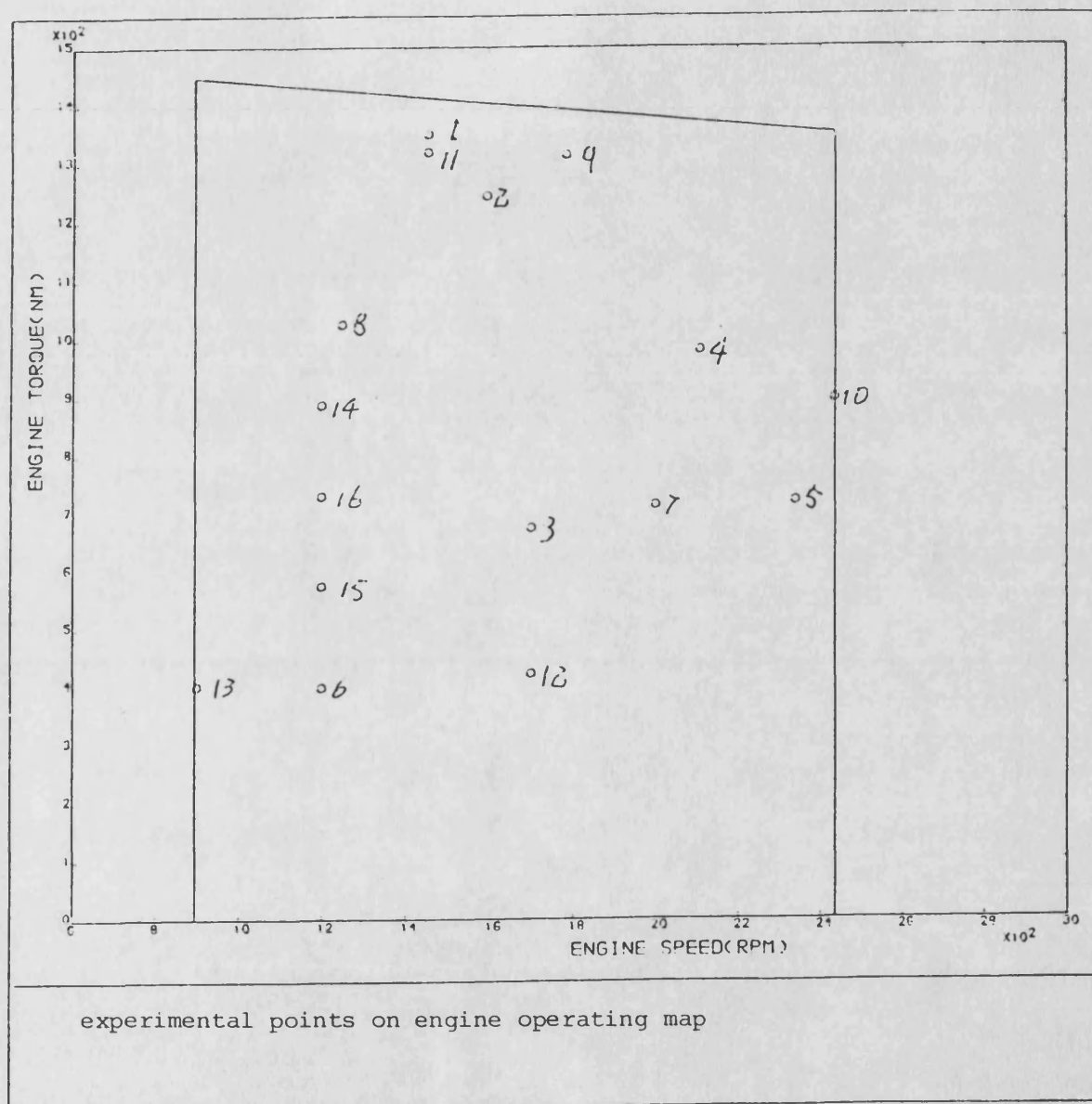


Fig-7.2

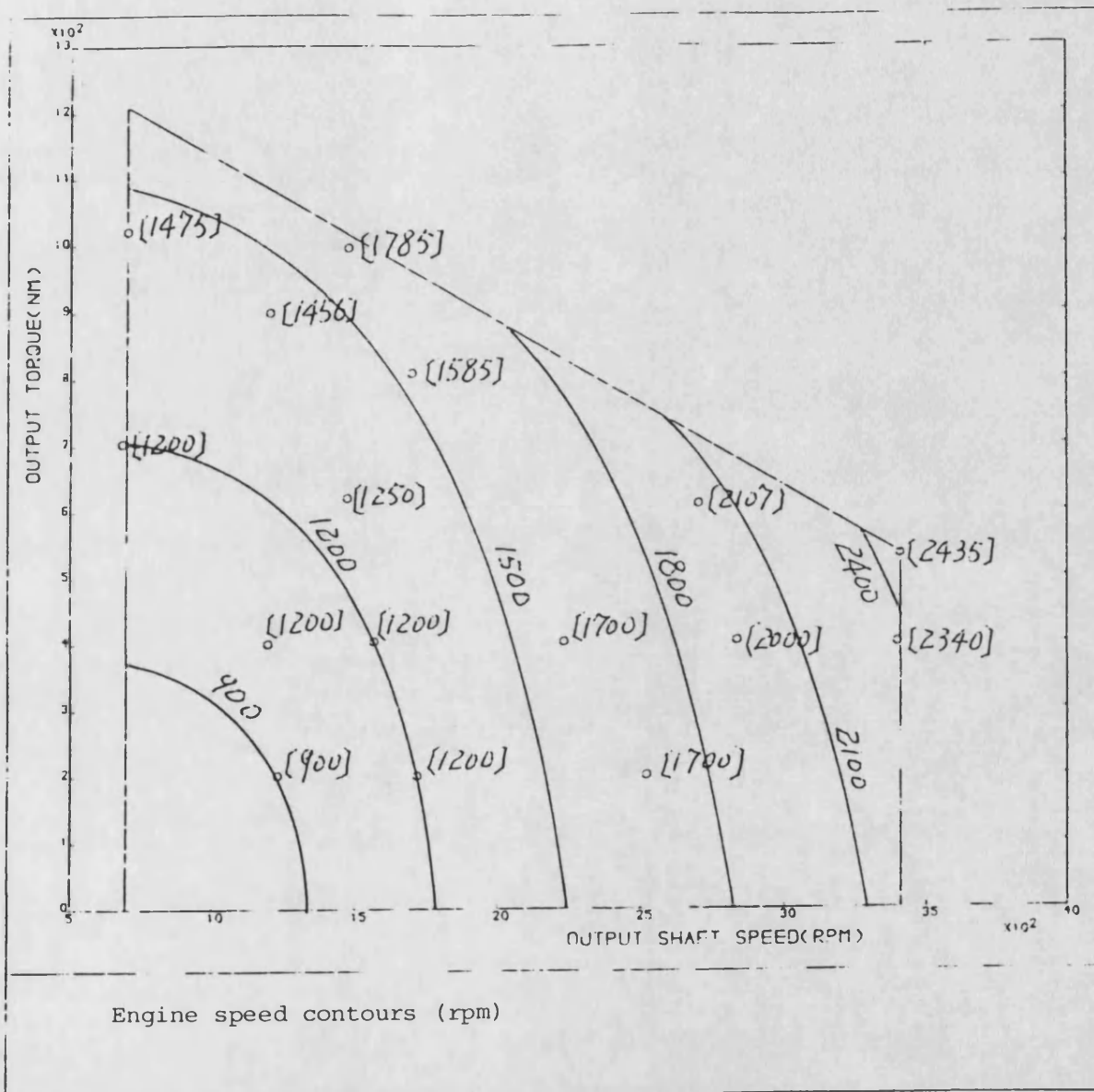


Fig-7.3

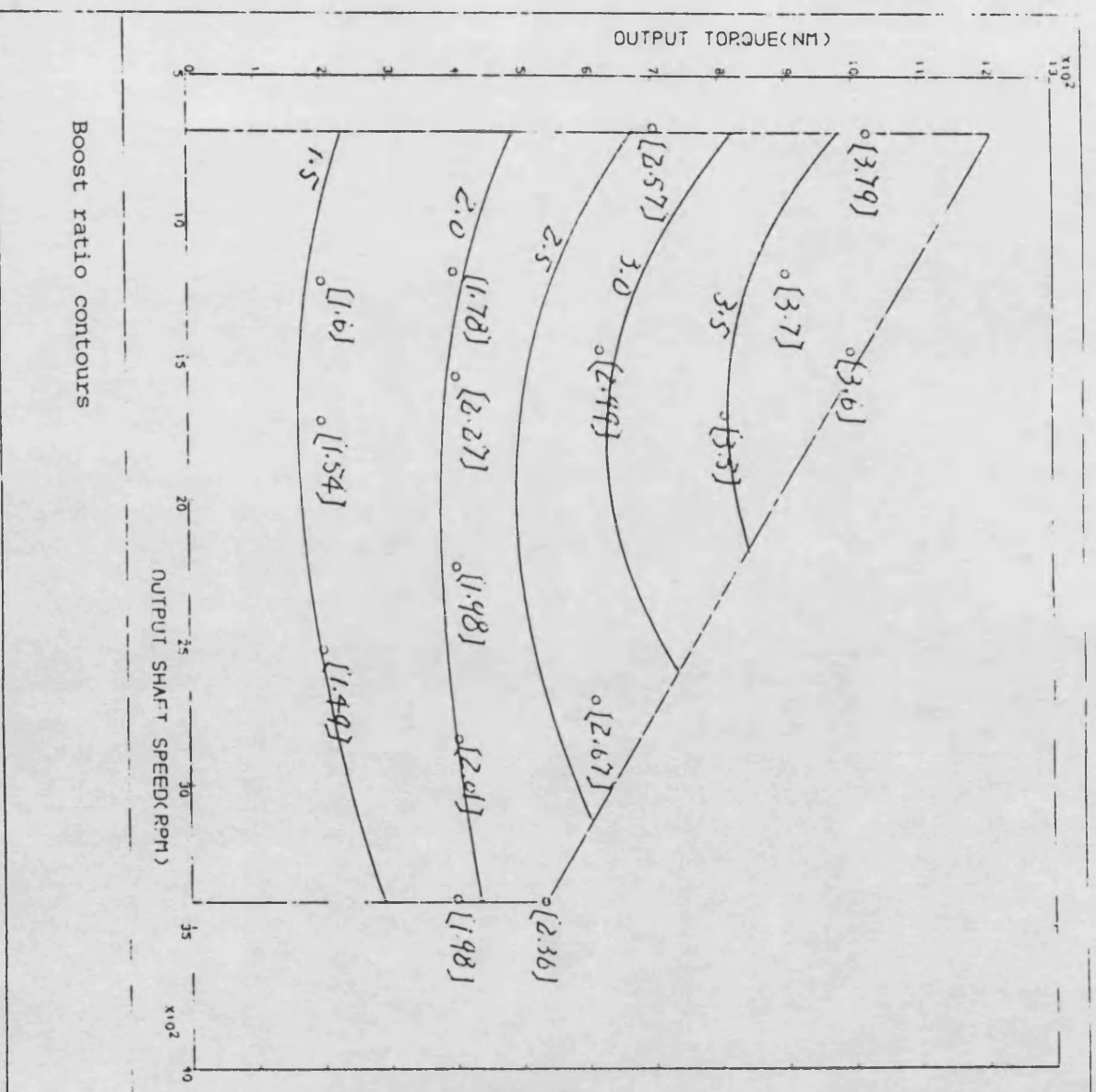


Fig-7.4

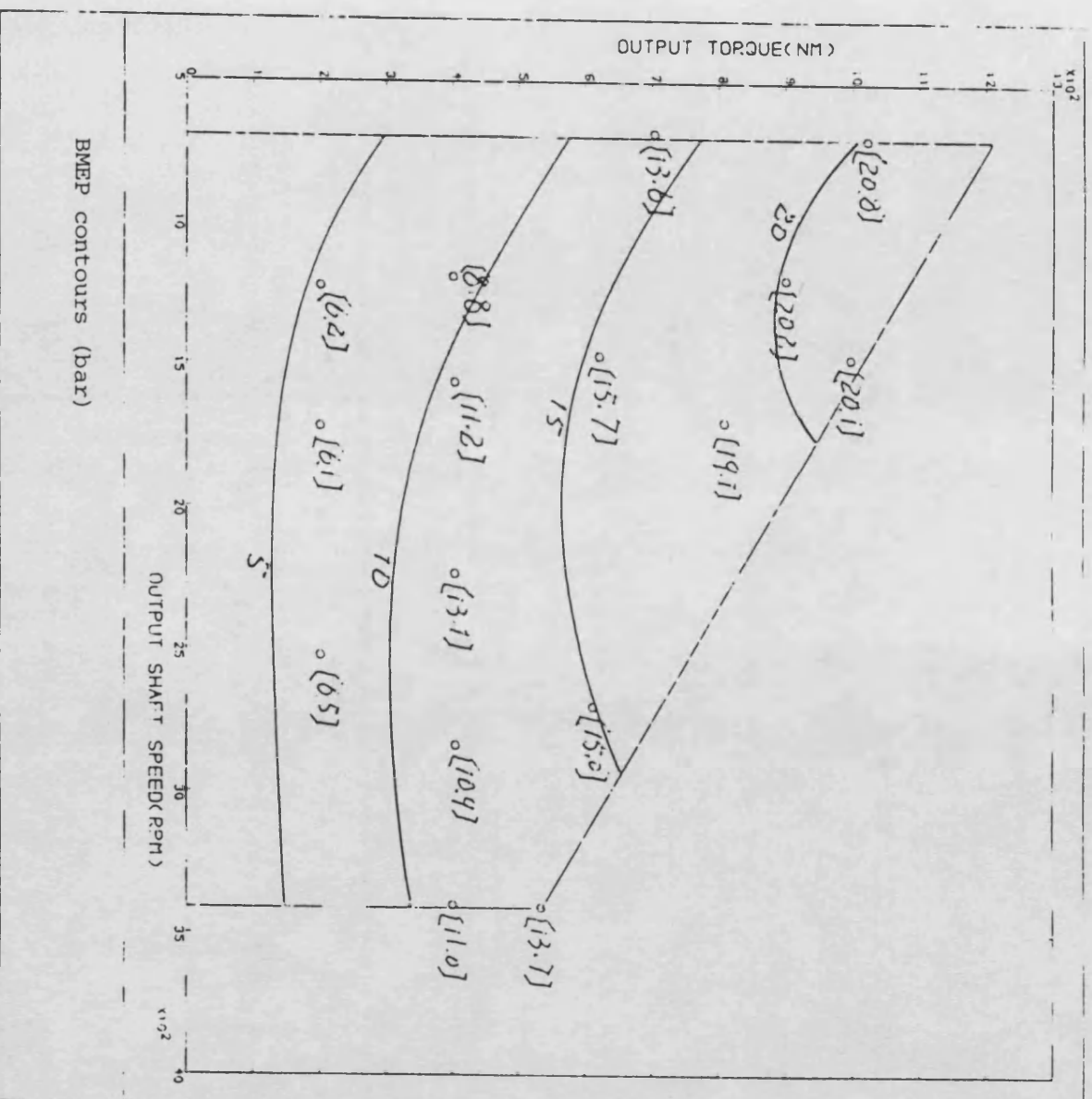
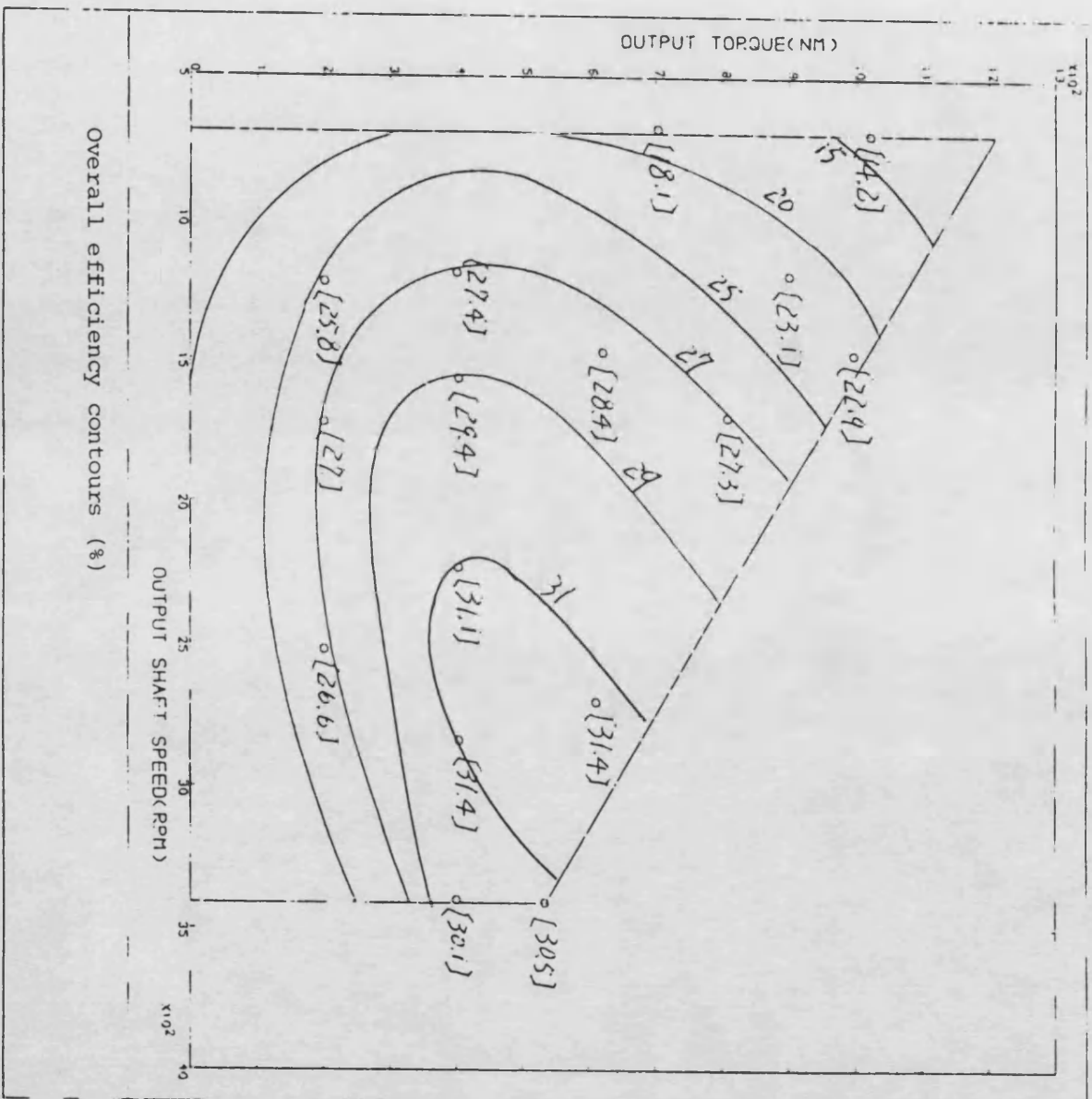


Fig-7.5



Overall efficiency contours (%)

Fig-7.6

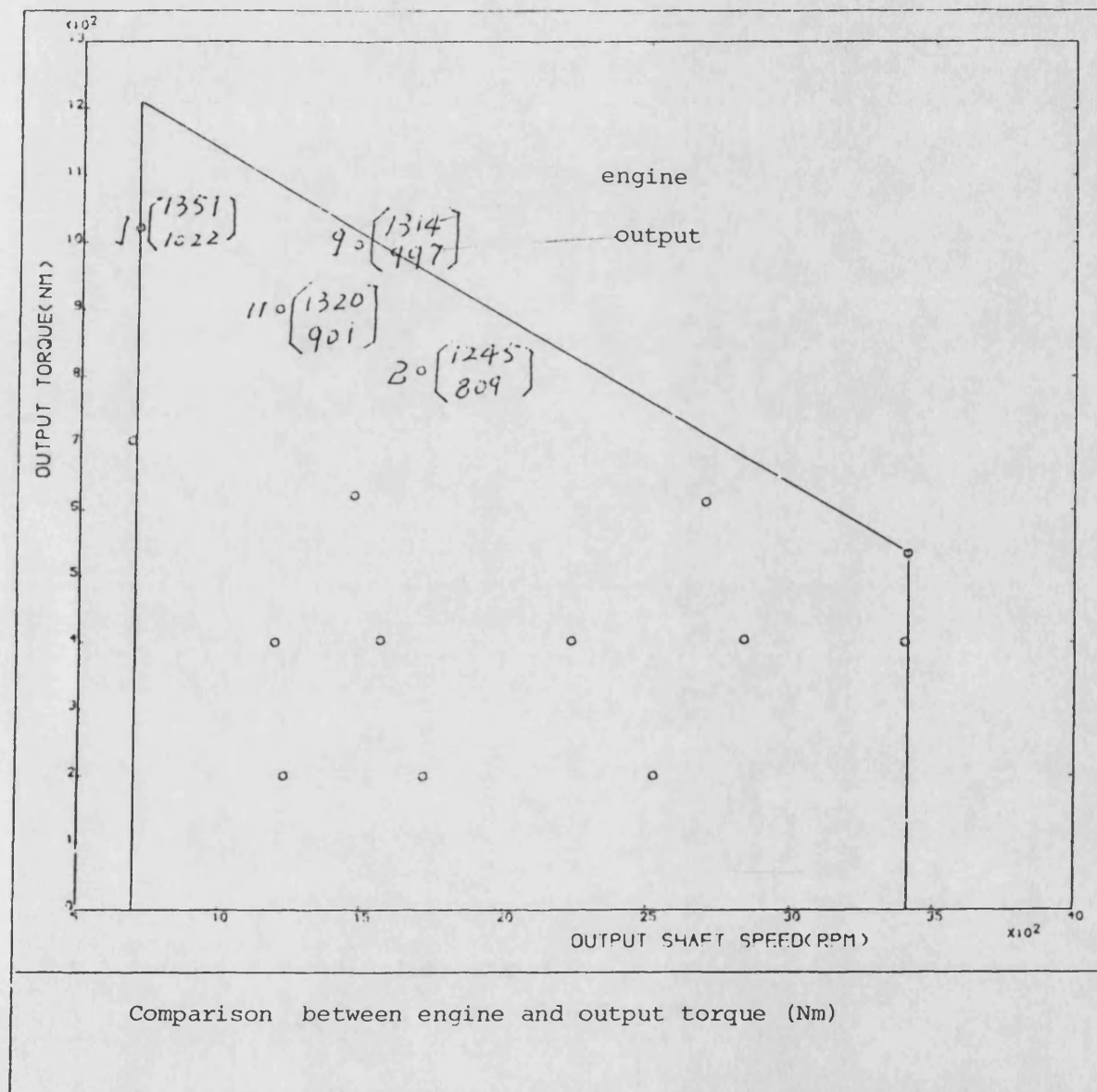


Fig-7.7

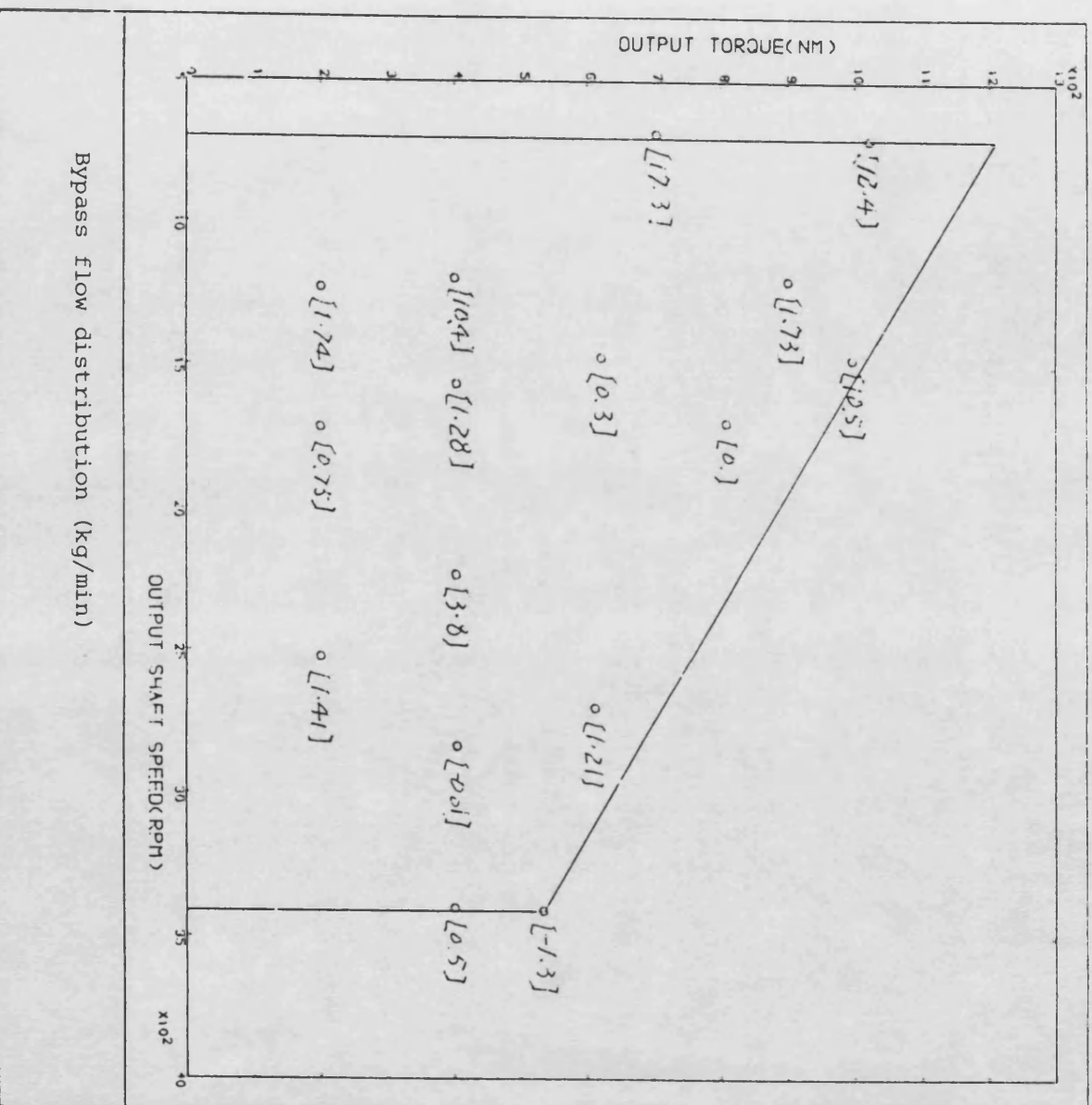


Fig-7.8

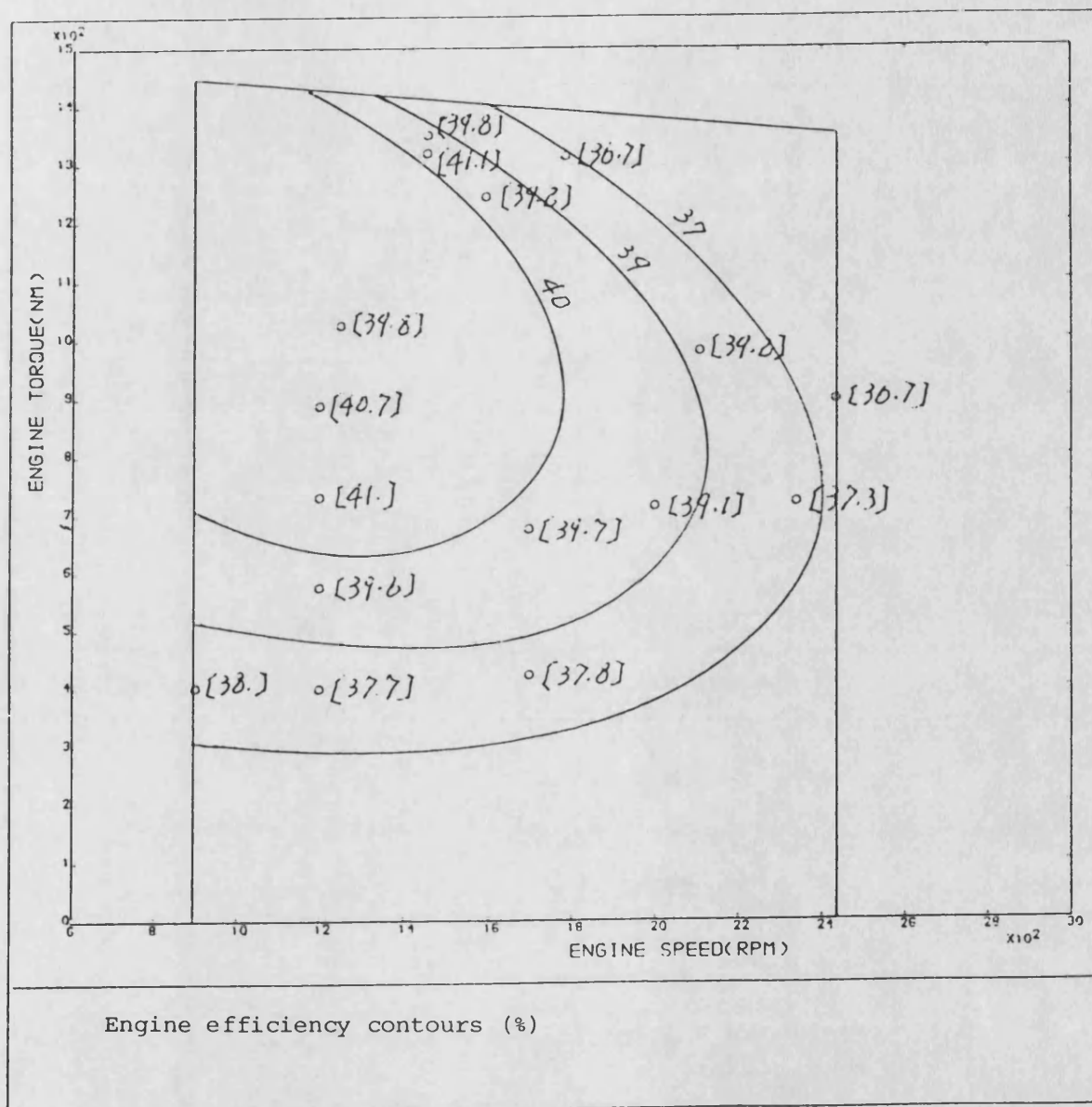


Fig-7.9

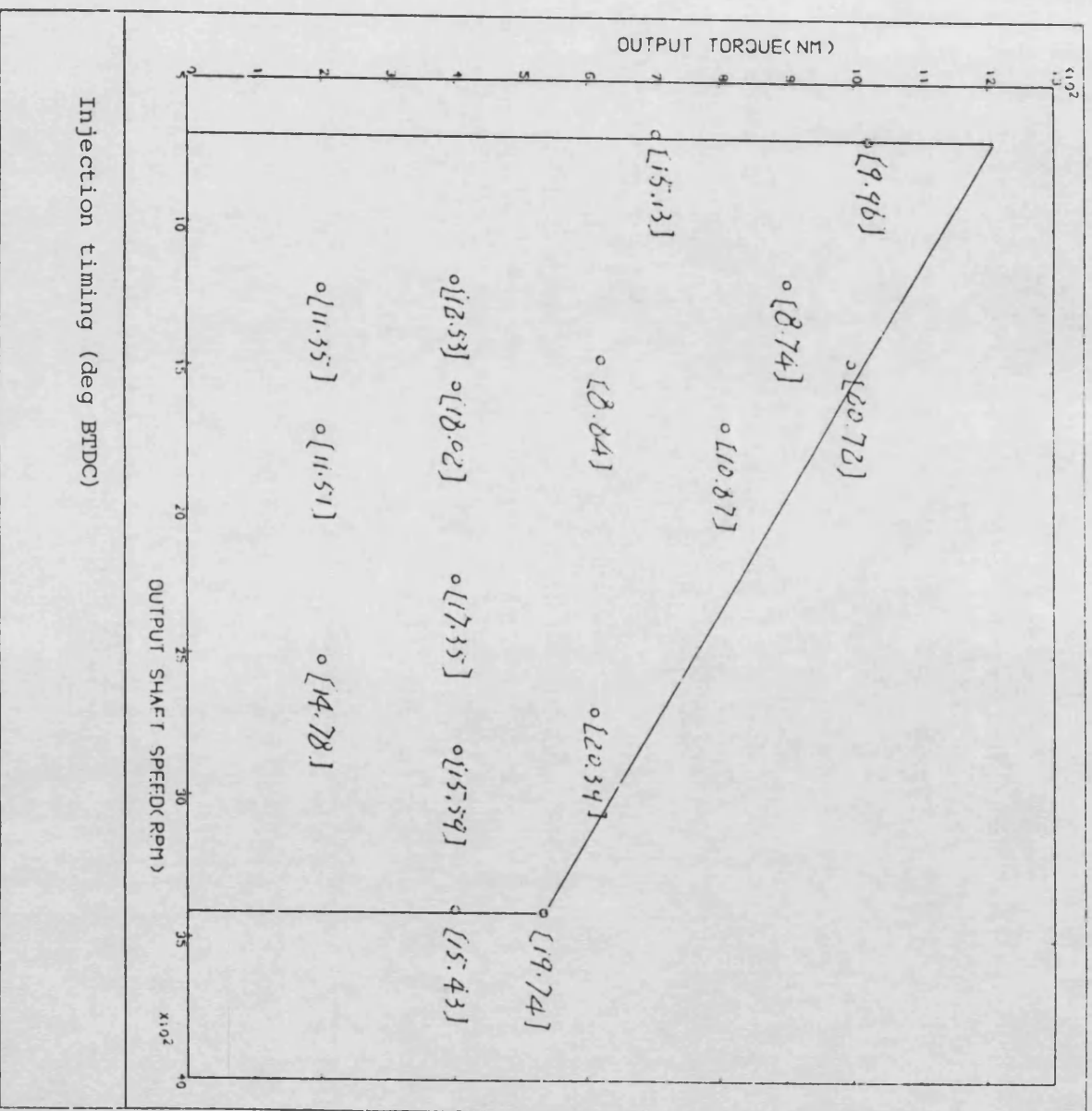


Fig-7.10

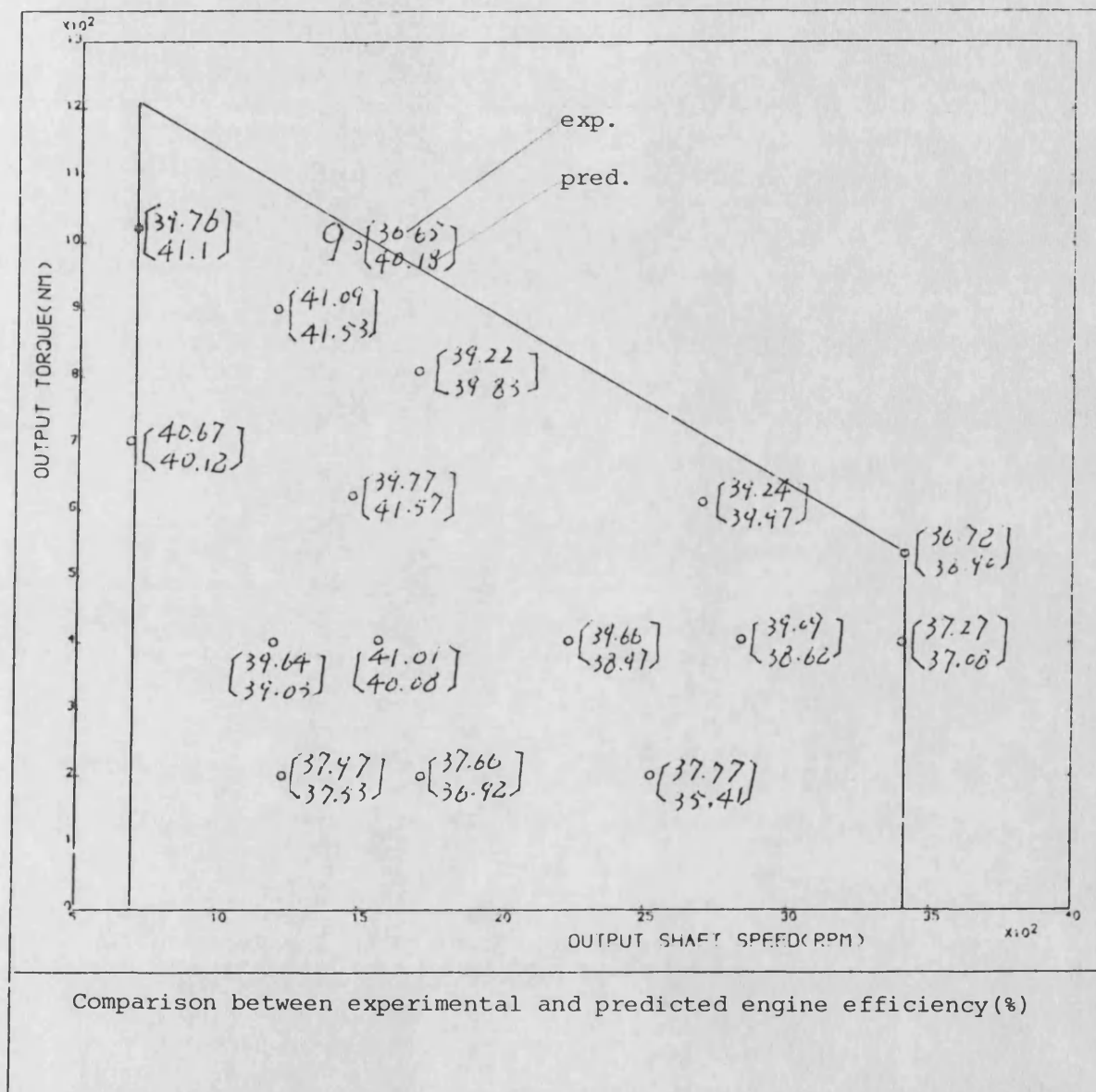


Fig-7.11

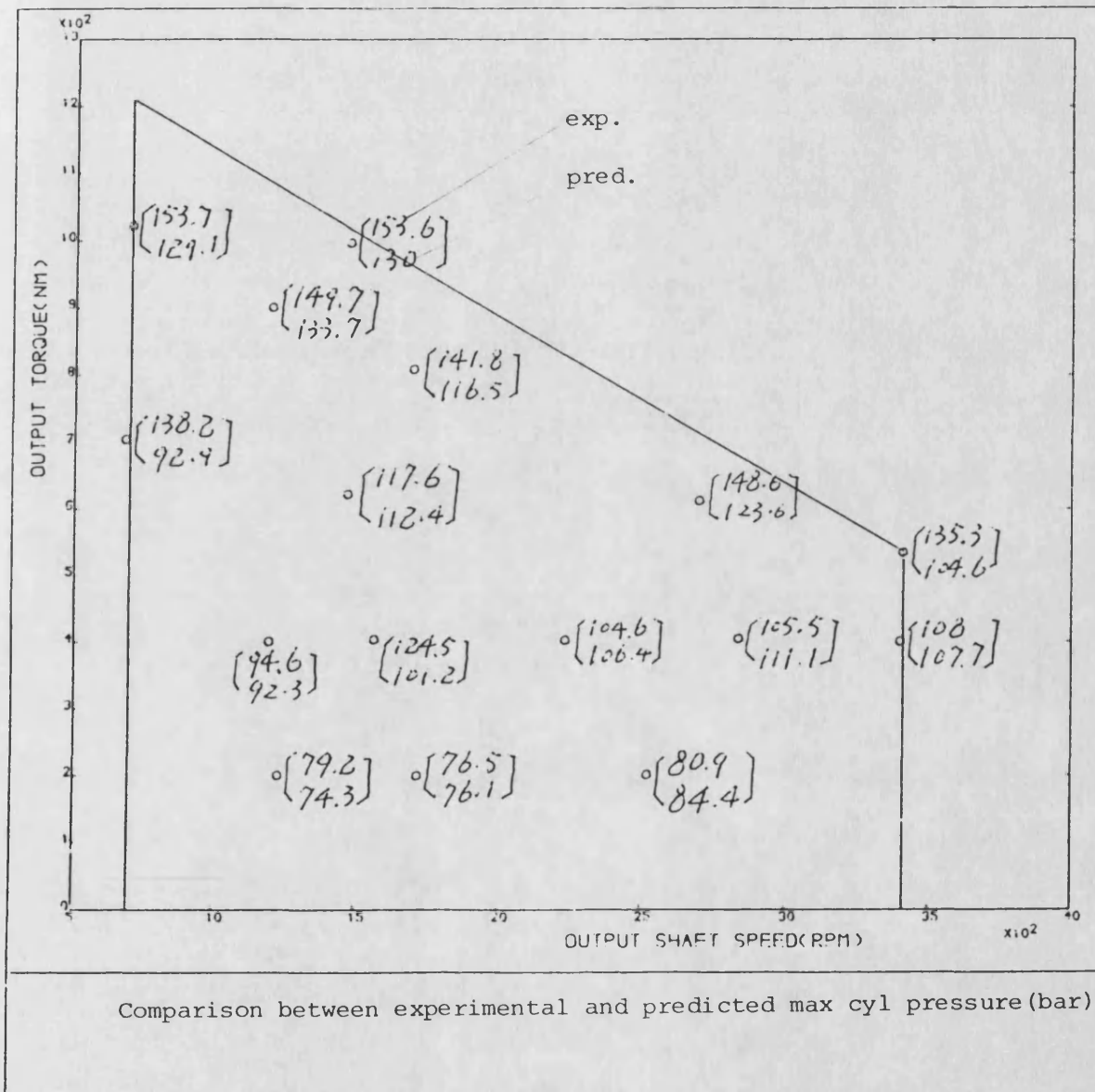


Fig-7.12

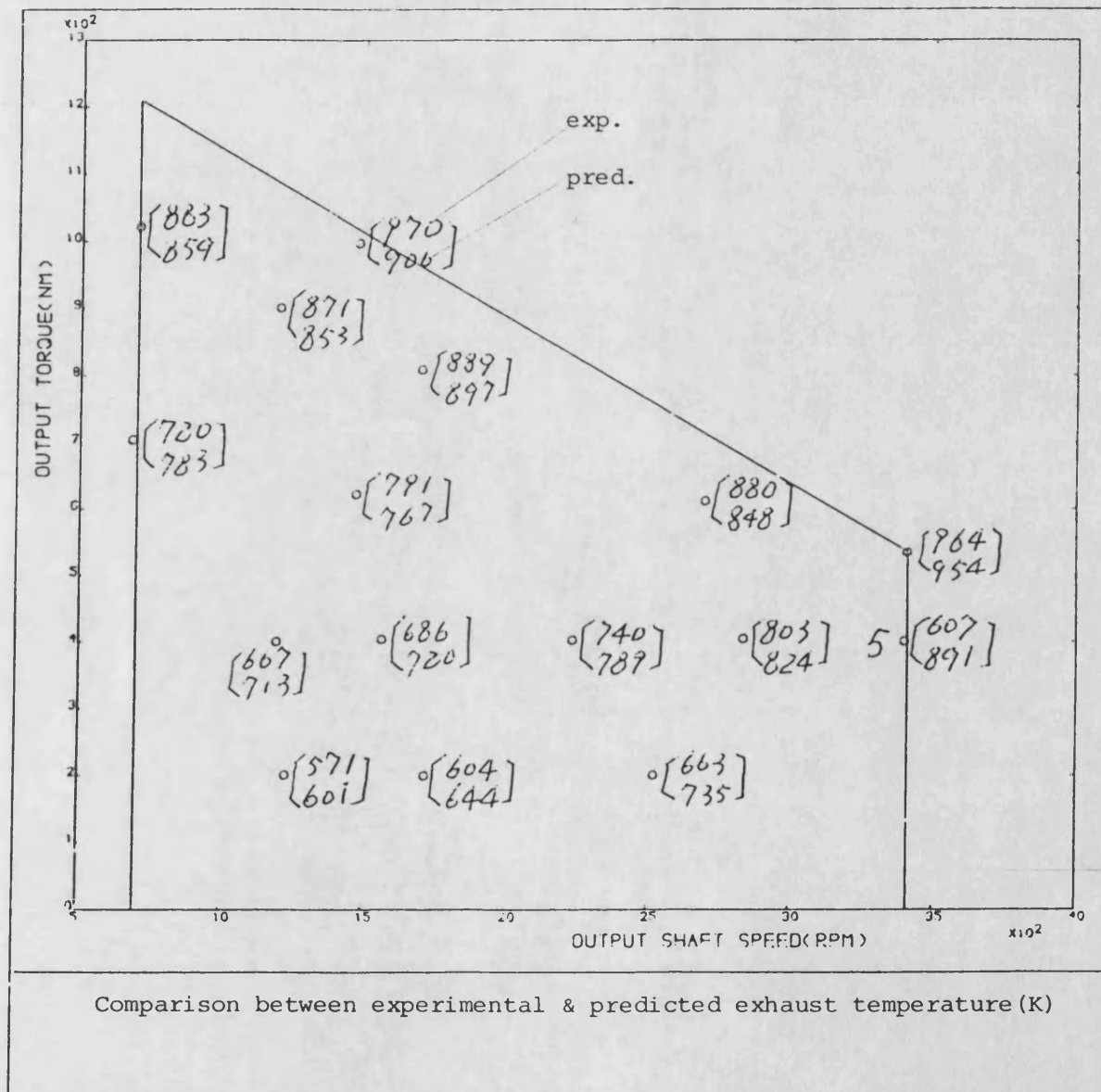


Fig-7.13

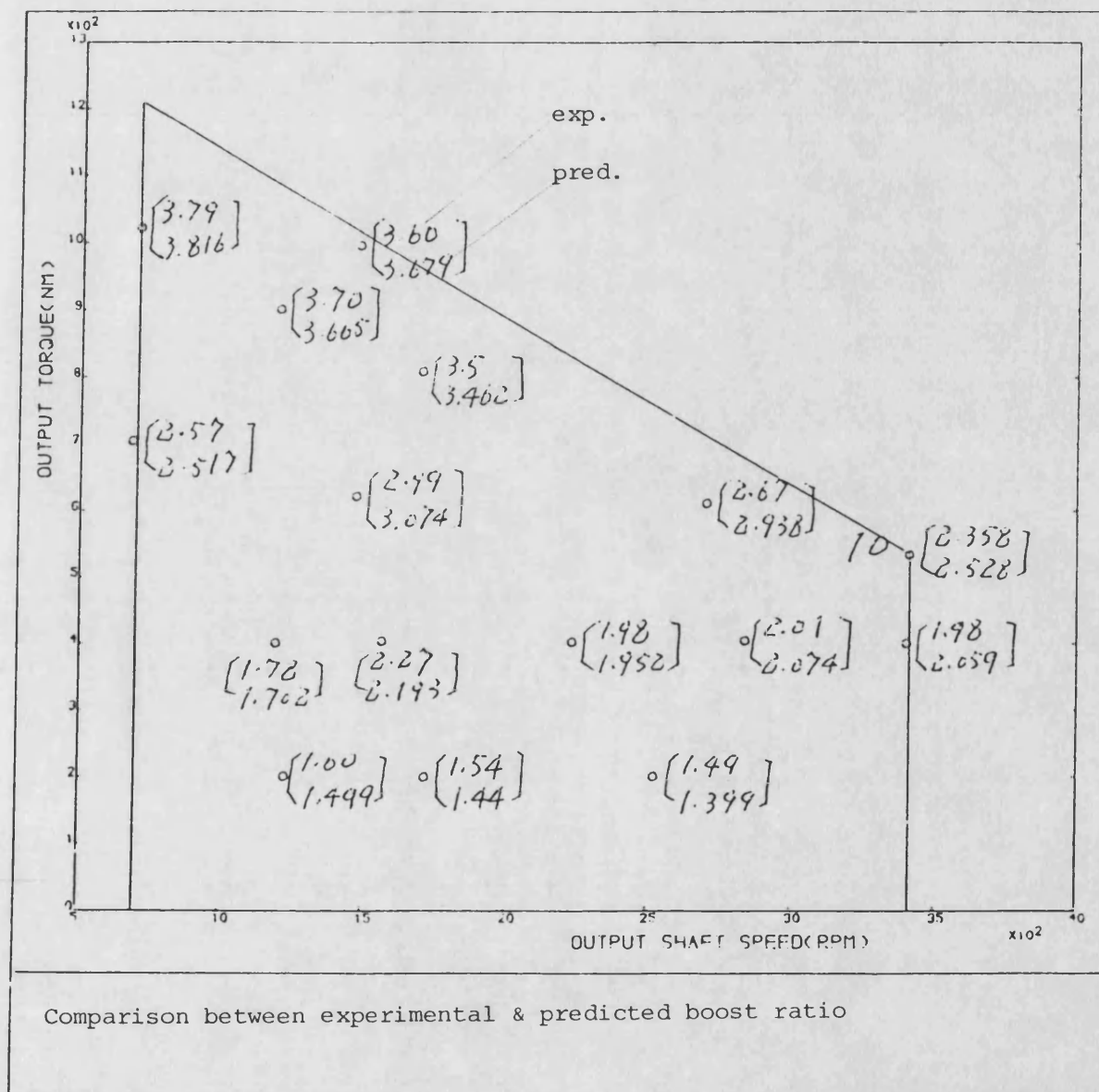


Fig-7.14

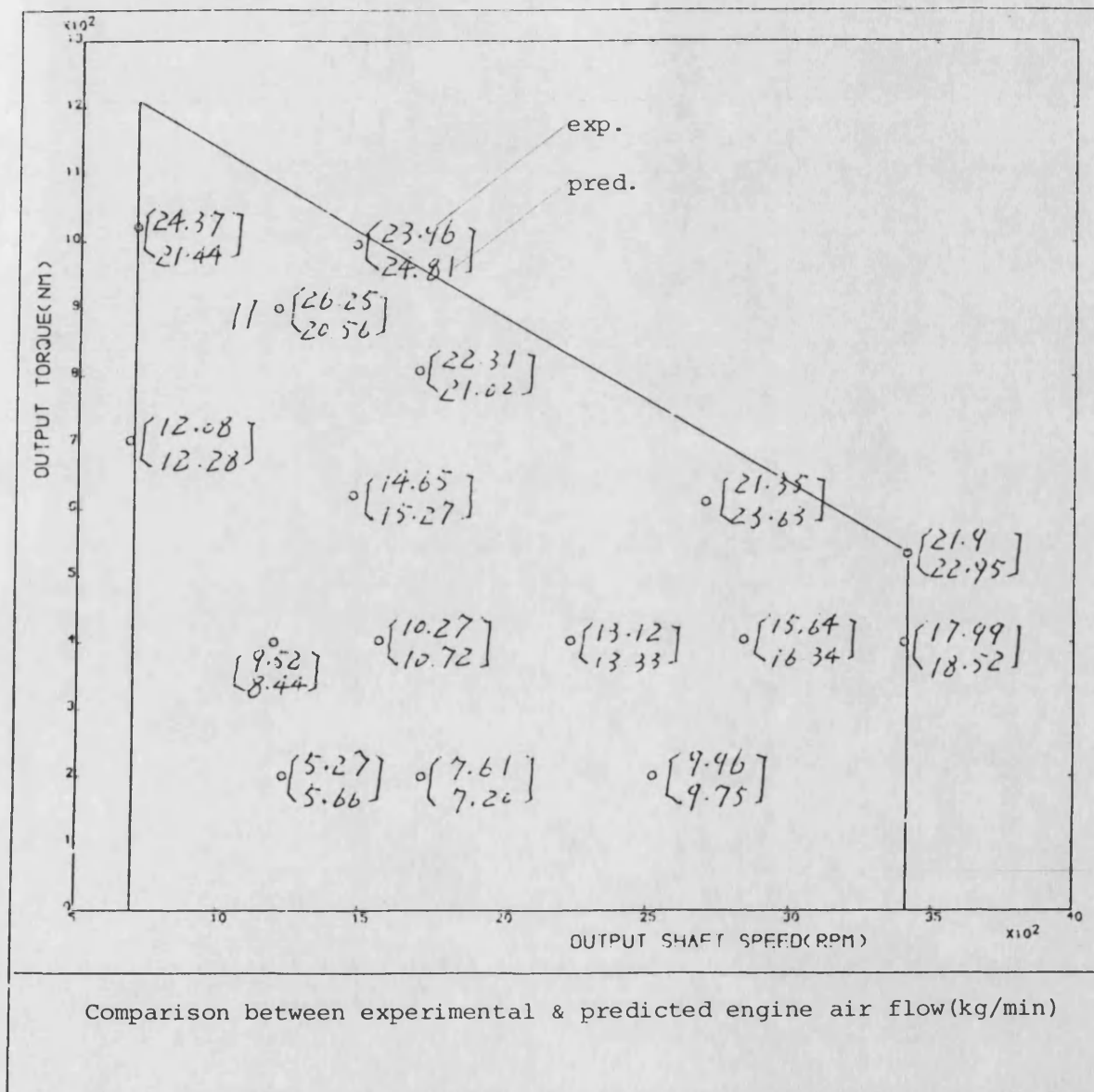


Fig-7.15

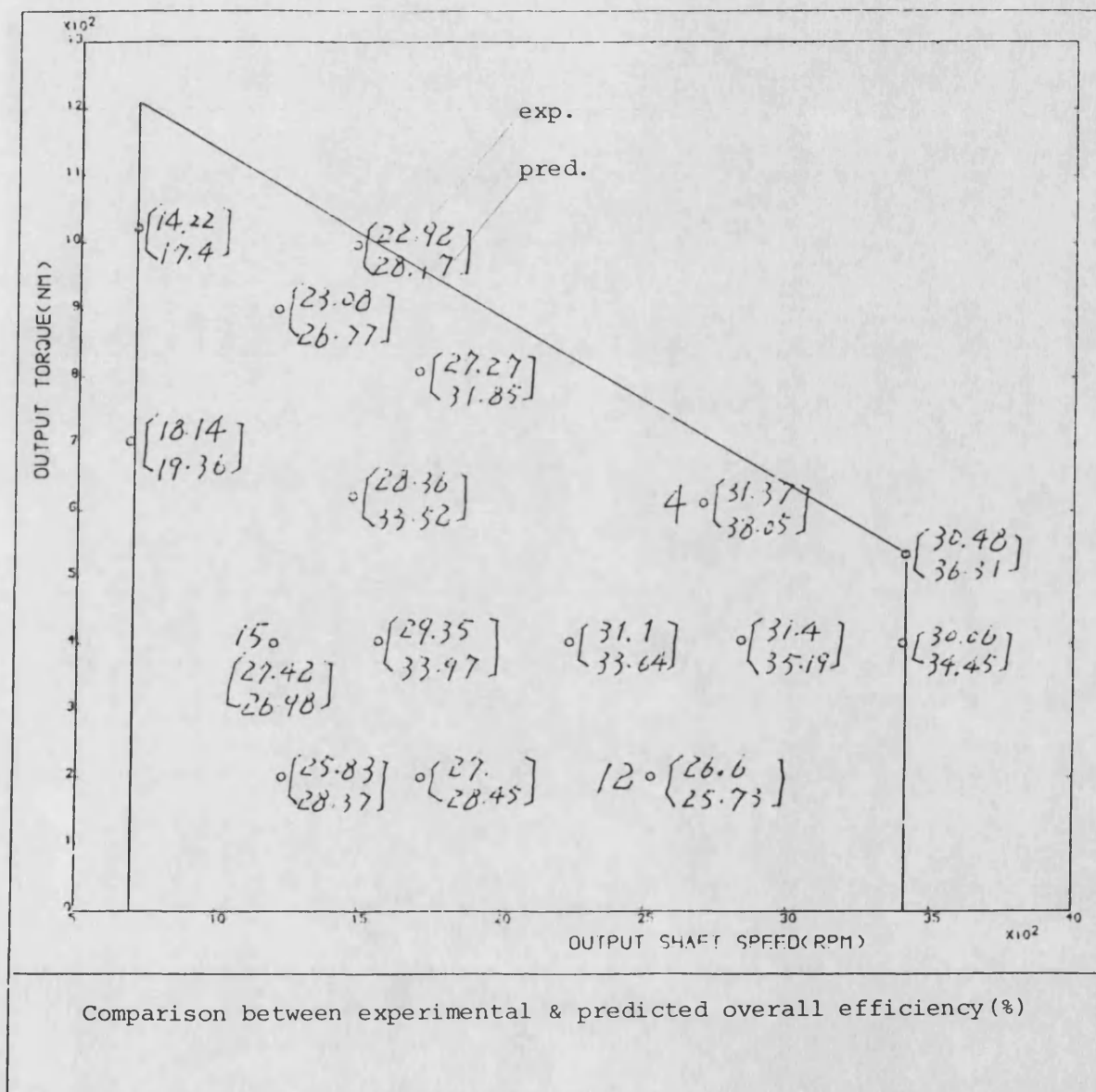


Fig-7.16

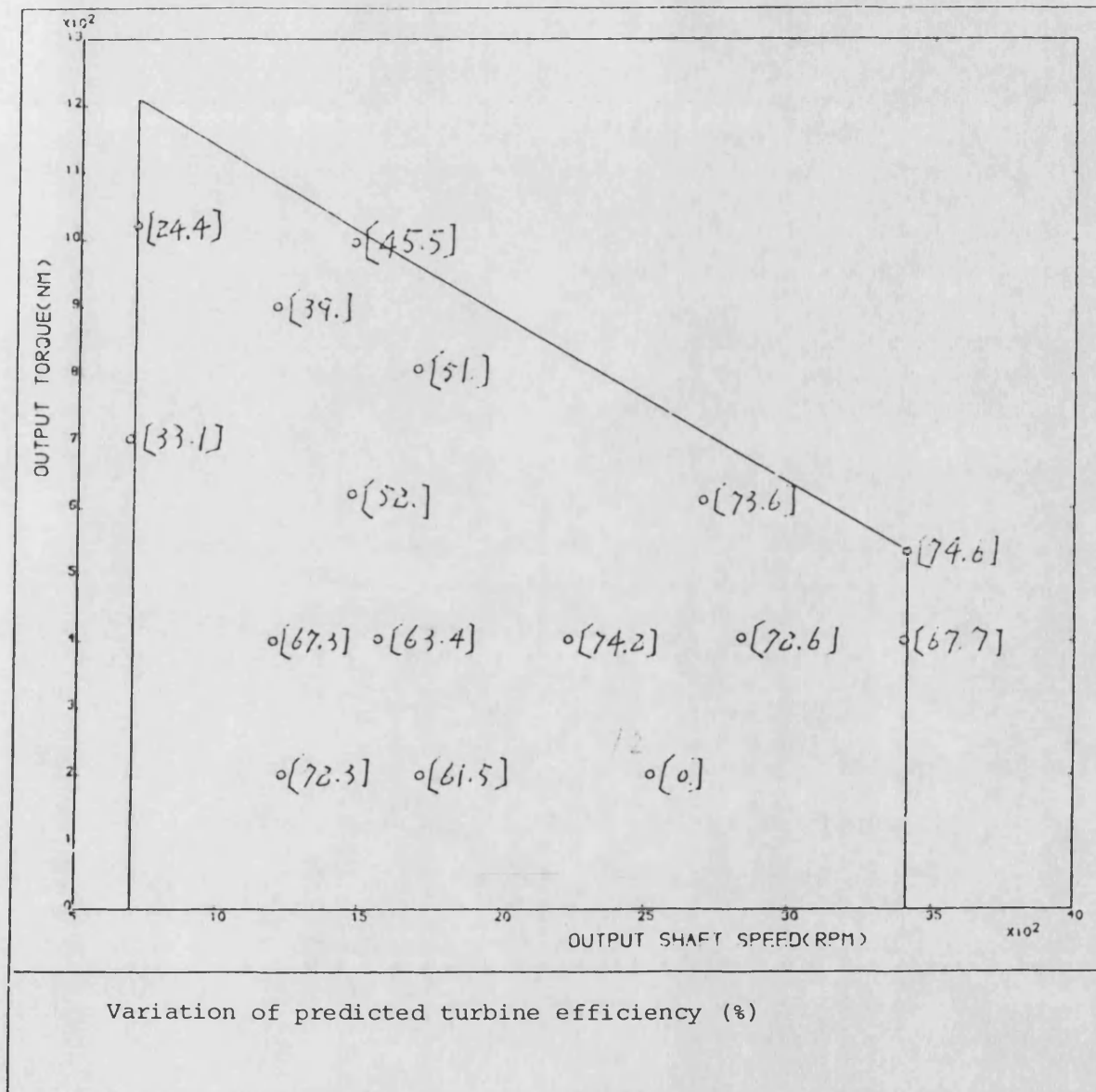


Fig-7.17

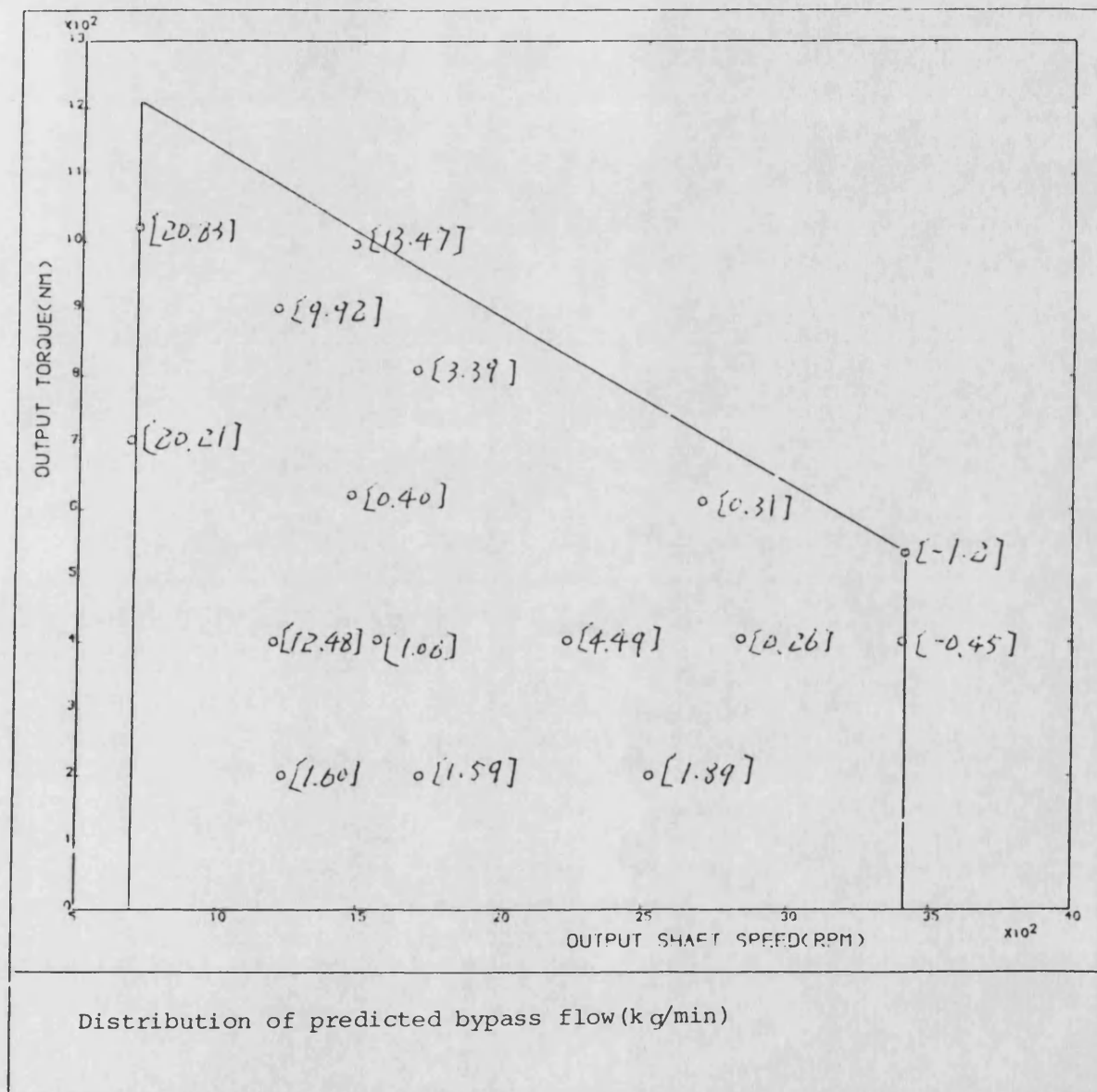


Fig-7.18

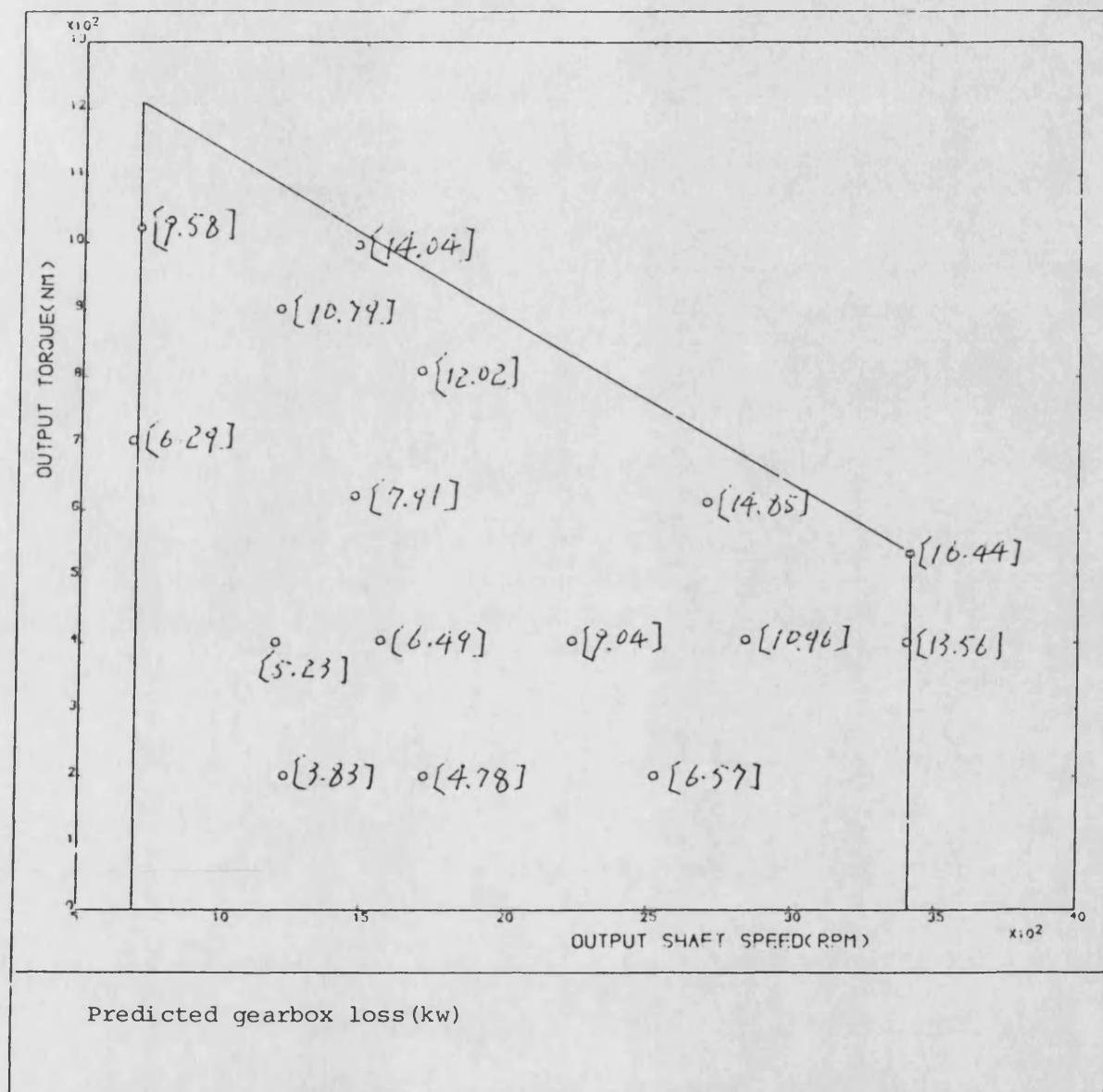


Fig-7.19

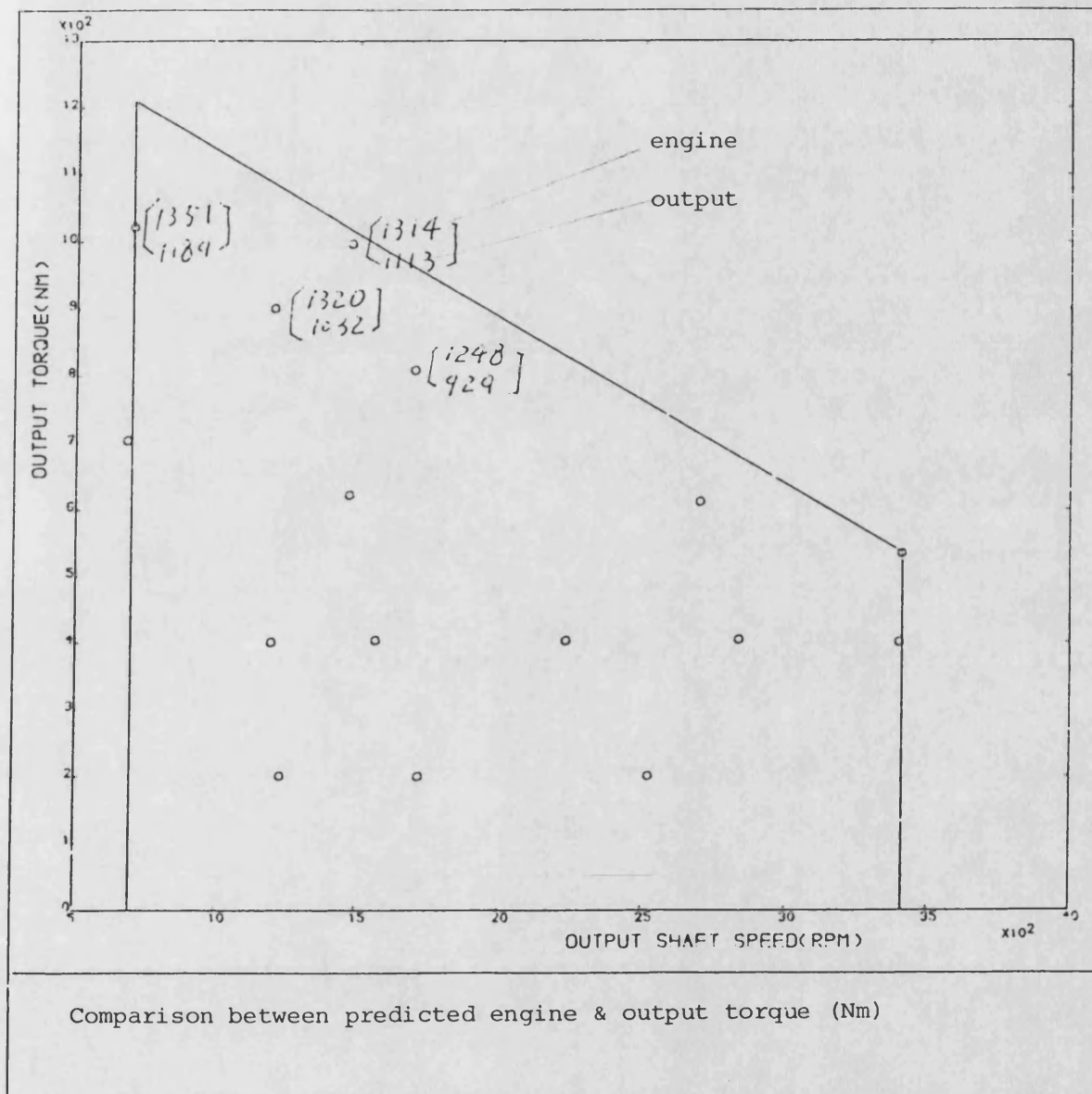


Fig-7.20

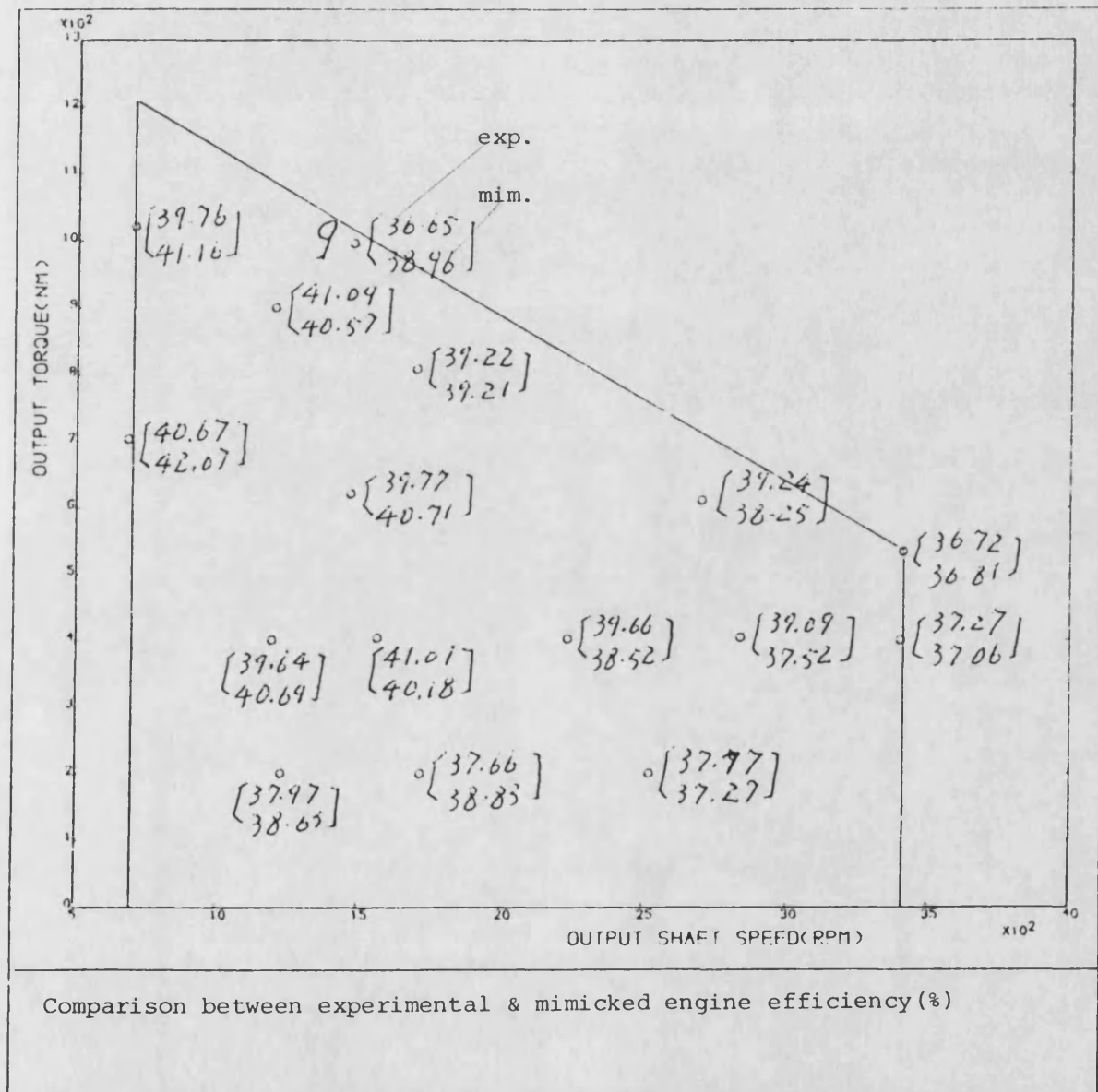


Fig-7.21

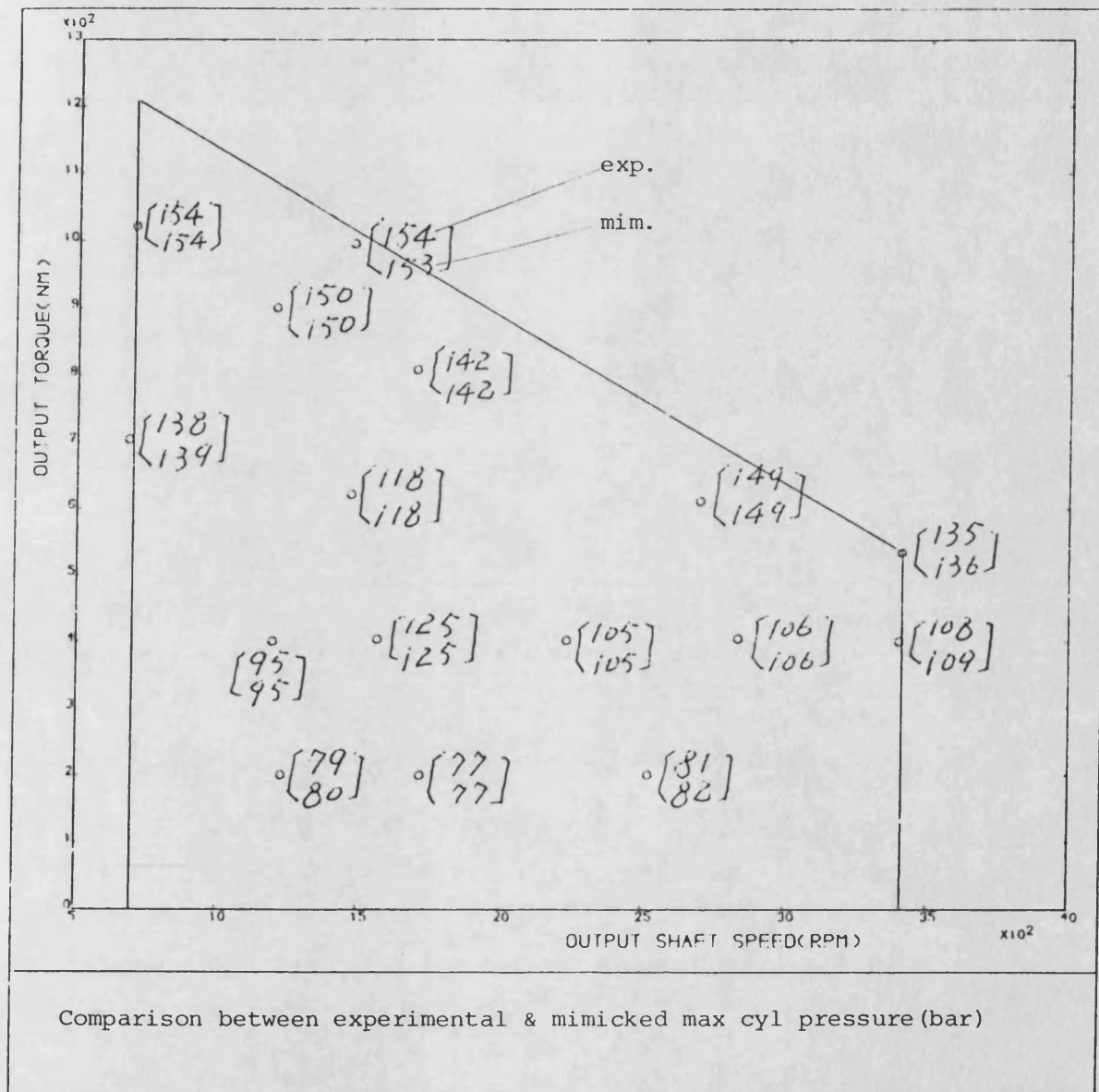


Fig-7.22

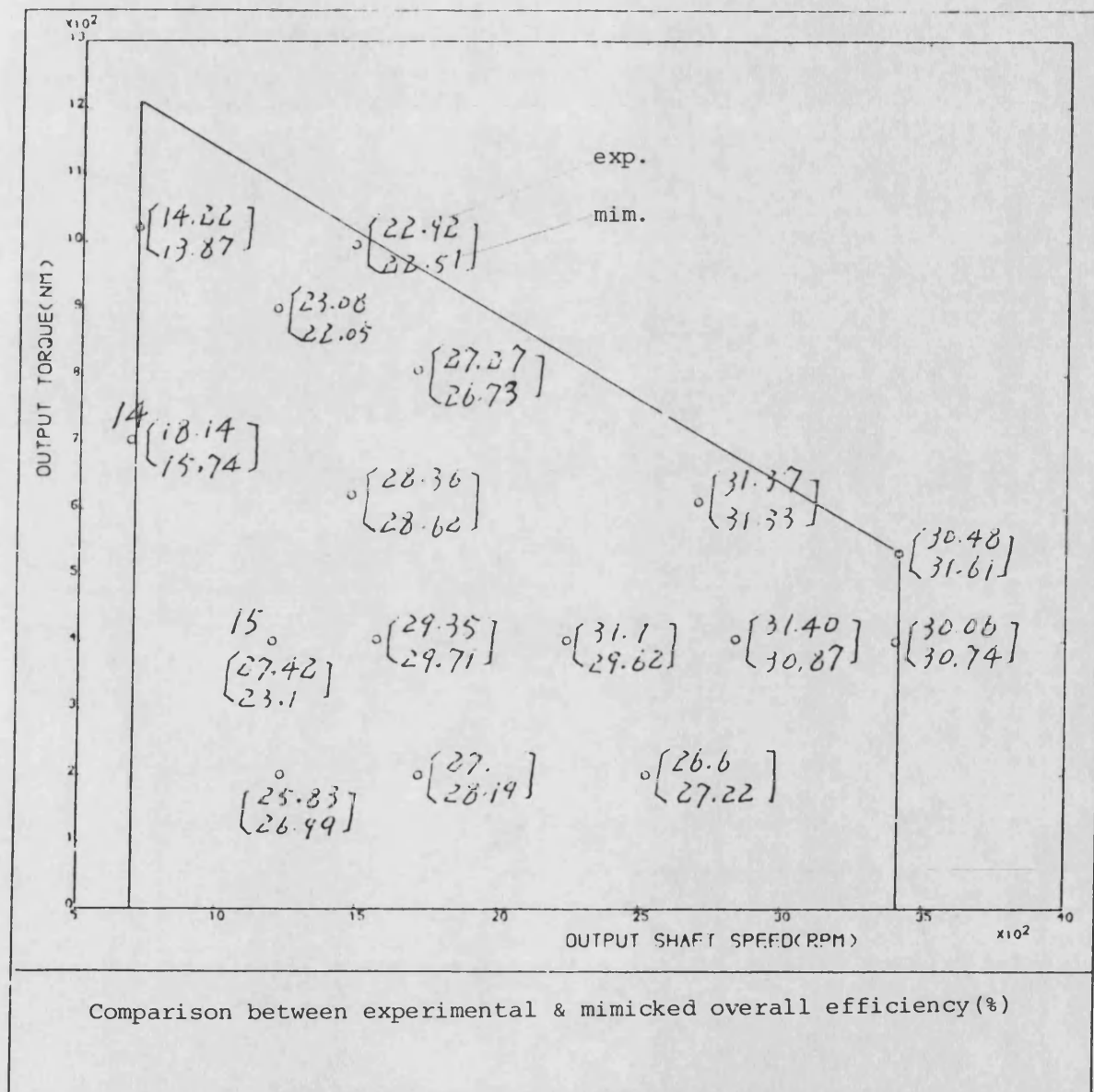


Fig-7.23

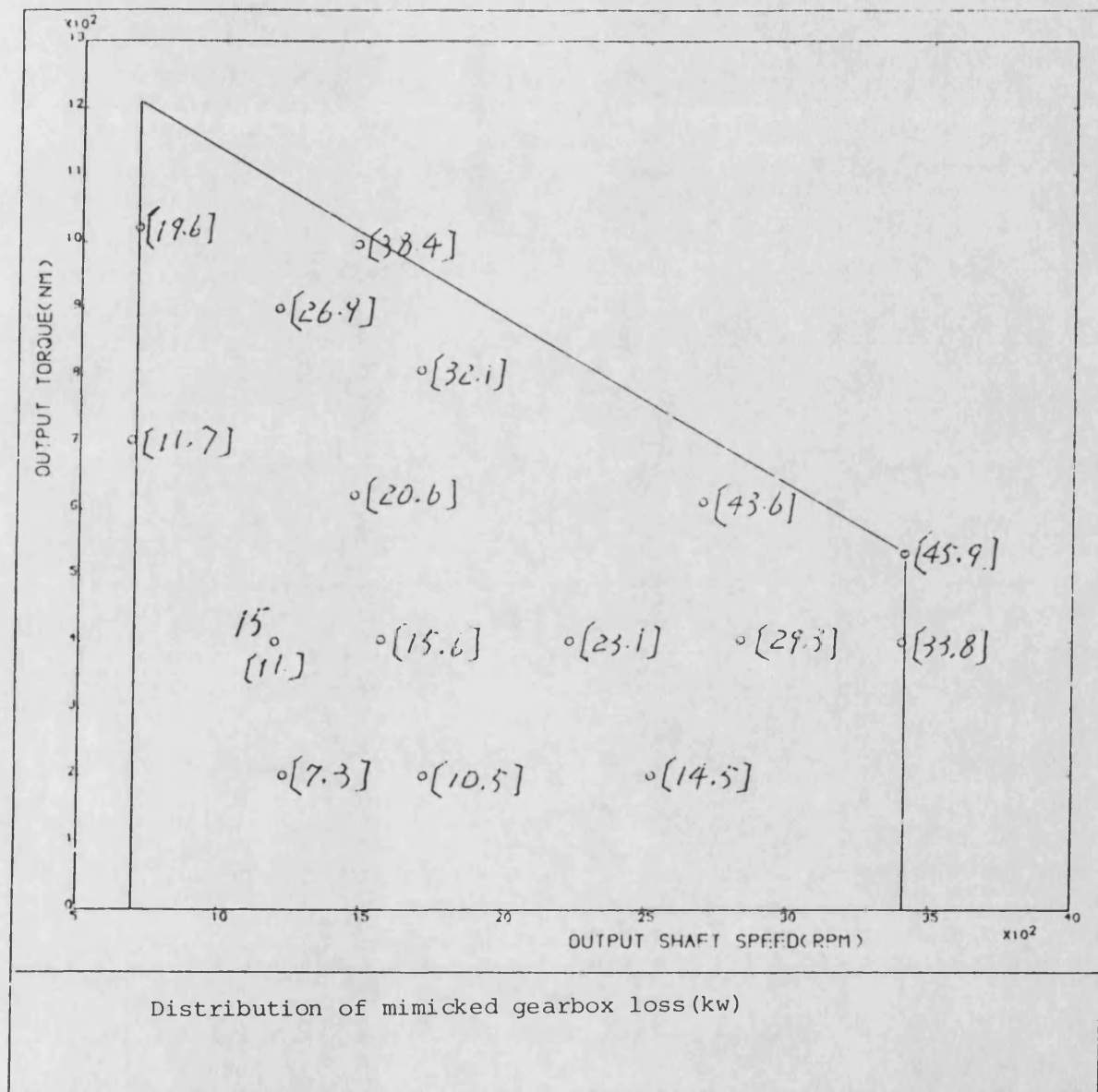


Fig-7.24

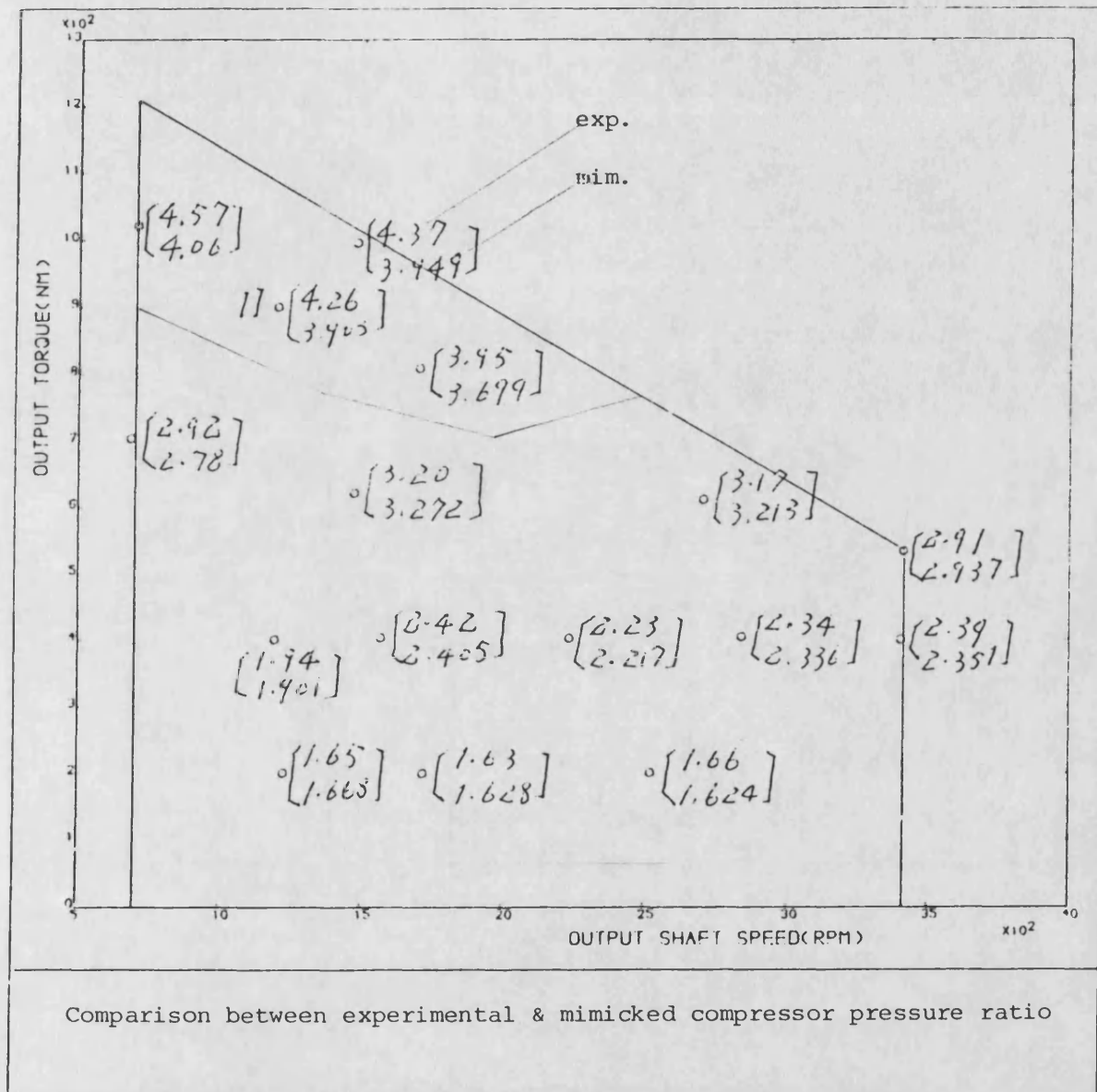


Fig-7.25

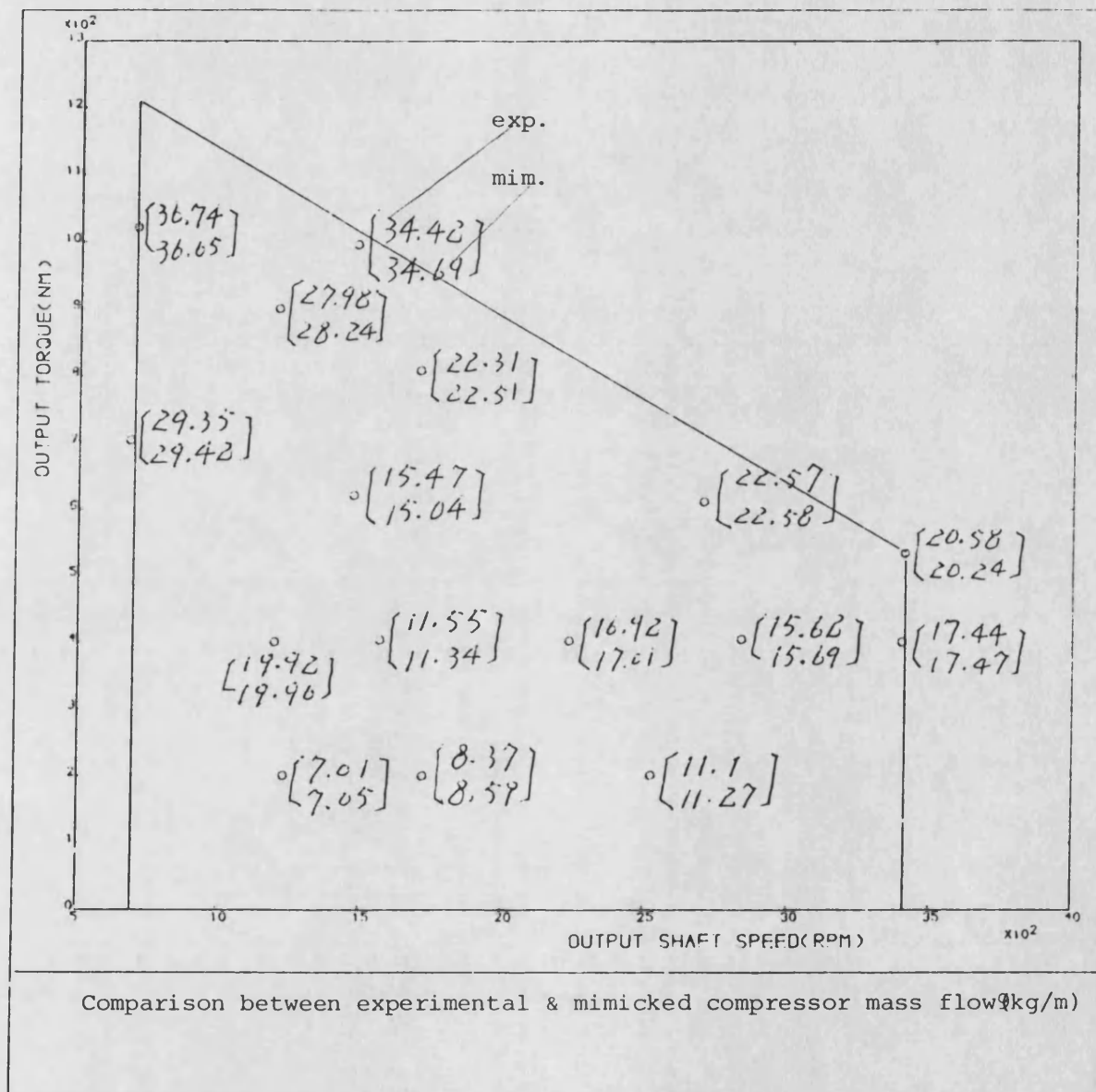


Fig-7.26

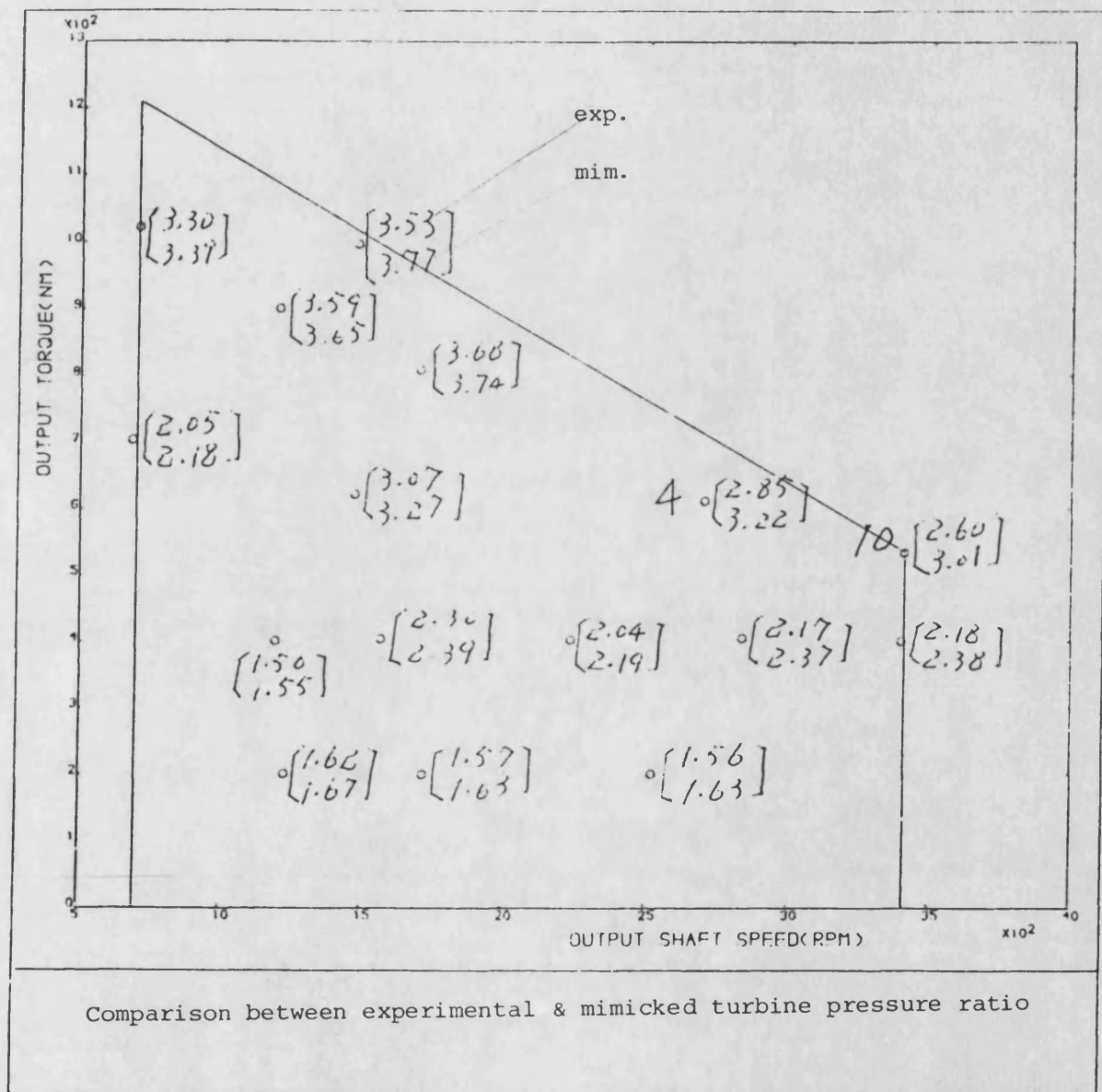


Fig-7.27

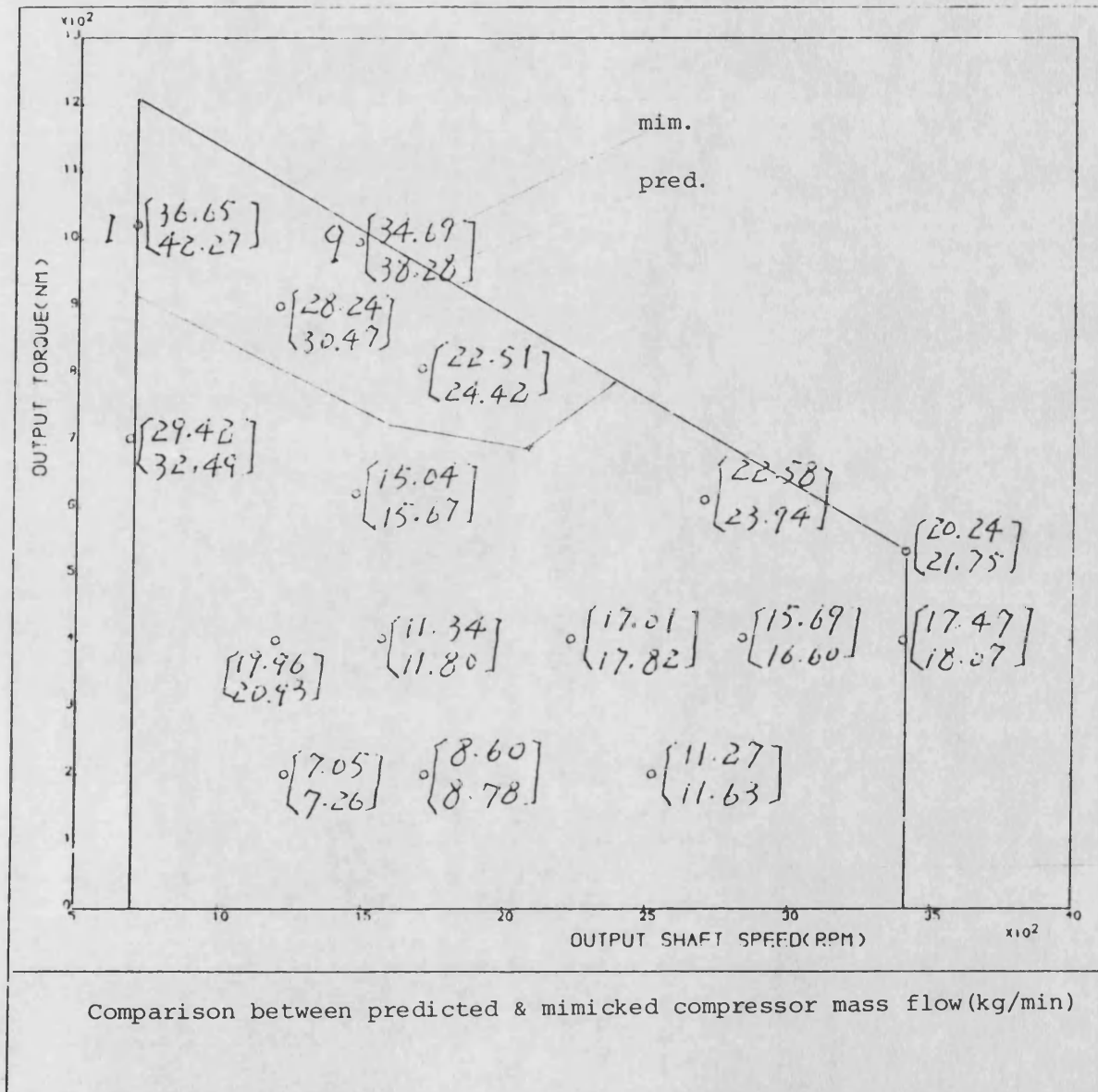


Fig-7.28

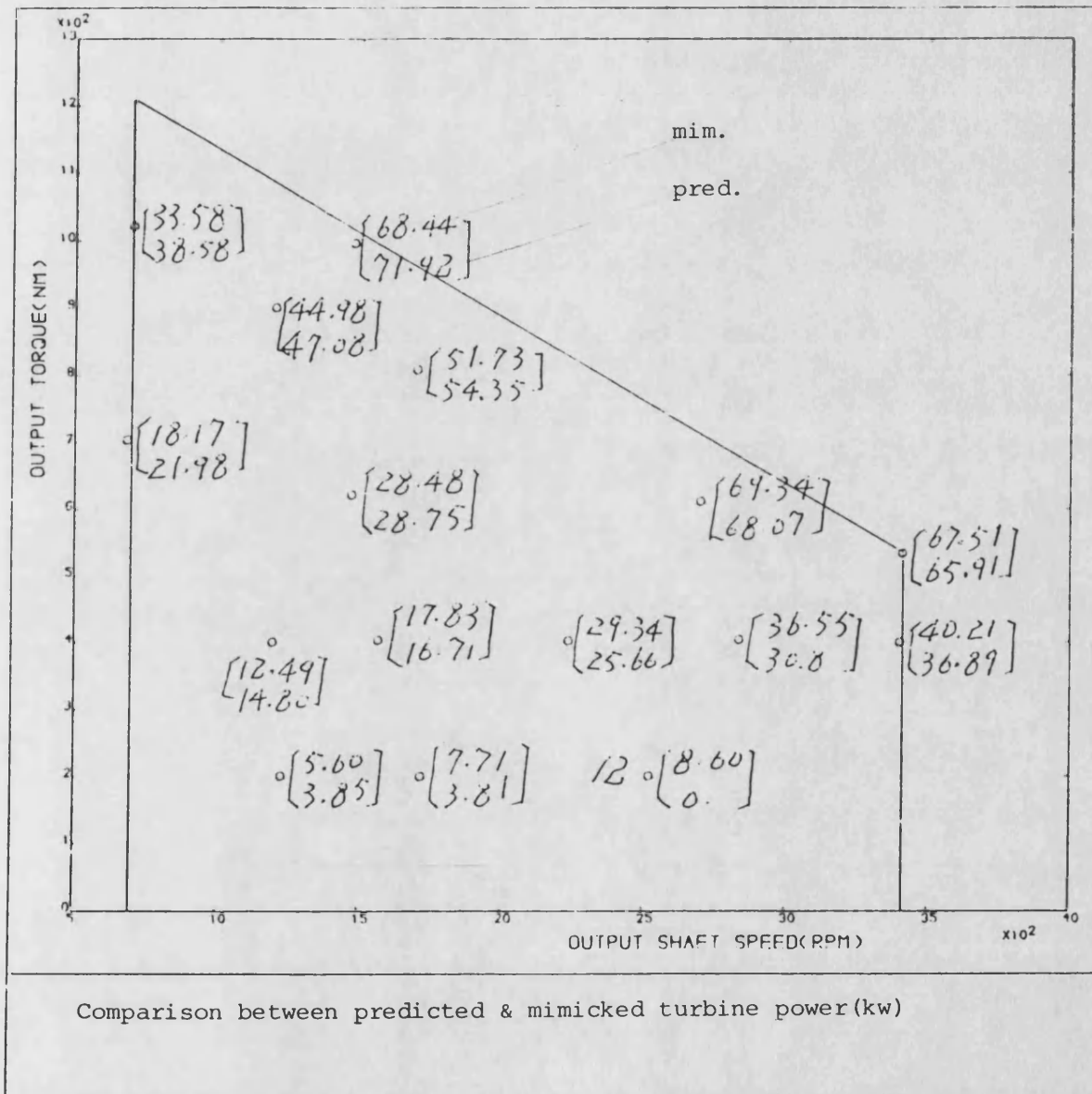


Fig-7.29

CHAPTER 8

CONCLUSIONS

8.1 Conclusions

From the previous investigations, the following conclusions can be drawn:

1) The DCE system has exceptionally high torque rise over its limiting torque curve, which is particularly suitable for vehicle applications, and which other system cannot achieve.

2) Compared with the conventional turbocharged engine, both the DCE and VG turbocharged engine can cope better with change in ambient conditions. This applies to almost the same extent to the FG DCE due to the ample air supply made possible by the epicyclic gear connection.

3) The programs used throughout are reasonably validated, and proved to be very effective and reliable for extensive theoretical investigation --- with great economy.

4) For the laboratory prototype, gearbox loss is very high due to its comparatively large gear set.

5) To take full advantage of the DCE concept, a turbine CVT is highly desirable.

8.2 Suggestions for Future Work

The theoretical investigations have shown that the DCE system has excellent characteristics. To realise these goals, the following aspects may be considered concerning the laboratory proto-type:

1) Implementation of a turbine CVT. This particularly applies to operating conditions at which both turbine and compressor power are very high, therefore the efficiency of the turbine can make a great difference to the overall system

performance.

2) Attention has to be paid to gearbox loss, particularly to the turbine gearbox loss. This means a more appropriately designed gearbox may be required.

3) To improve the reliability of the experimental data, direct torque measurements should be applied to both turbine and compressor.

REFERENCES

- [1] K. Zinner, Supercharging of Internal Combustion Engines.
- [2] N. Watson and S. Johnota, Turbocharging the Internal Combustion Engines.
- [3] L. C. R. Lilly, Diesel Engine Handbook.
- [4] N. Watson, Turbocharging developments on vehicle diesel engines, SAE 850315, 1985.
- [5] S. F. Burnnet et al., Developments in power train engineering, C20/77 IMechE, 1977.
- [6] J. D. Ledger et al., Improvement in transient performance of a turbocharged diesel engine by air injection into the compressor, SAE 770122, 1972.
- [7] S. G. Timoney, High pressure turbocharging of 2-stroke engines, SAE 690747, 1969.
- [8] M. L. Monaghan, Boosting for purpose, C55/78 I Mech E, Turbocharging and Turbochargers, 1978.
- [9] G. Cser, Some results of combined charging application, C64/78 IMechE, Turbocharging and Turbochargers, 1978.
- [10] N. Watson, Turbochargers for the 1980's -- current trends and future prospects, SAE 790063, 1979.
- [11] T. Suzuki et al., Developments of a higher boost turbocharged diesel engine for better fuel economy in heavy vehicles, SAE 830379, 1983.
- [12] F. J. Wallace et al., Variable geometry turbocharging for transport engines, C38/82 IMechE, Turbocharging and Turbochargers, 1982.
- [13] M. S. Ghadiri-Zare and F. J. Wallace, Variable geometry vs two stage turbocharging of high output diesel engines, C63/78, IMechE, Turbocharging and Turbochargers, 1982.

- [14] F. J. Wallace et al., Variable geometry turbocharging -- optimisation and control under steady state conditions, C97/86, IMechE, Turbocharging and Turbochargers, 1986.
- [15] F. J. Wallace and A. Whitfield, Experimental and theoretical performance of a radial flow turbocharger compressor with inlet prewhirl, Proc. IMechE, vol 189, 1975.
- [16] James L. Harp and Thomas P. Oatway, Centrifugal Compressor Development for a variable area turbocharging, SAE 790066, 1979.
- [17] S. G. berenyi and C. J. Raffa, Variable area turbocharging for high output diesel engine, SAE 790064, 1979.
- [18] G. E. Shwarzbauer, Turbocharging of tractor engines with exhaust gas turbochargers and the BBC-COMPRES, C69/78 IMechE, Turbocharging and Turbochargers, 1978.
- [19] I. Summerauer, F. Spinnler, A. Mayer and Hafner, A comparative study of the acceleration performance of a truck diesel engine with exhaust-gas turbocharger and with pressure-wave supercharger COMPRES, C70/78 IMechE, Turbocharging and Turbochargers, 1978.
- [20] E. Kellett, et al., Investigation of diesel engine and turbocharger interaction, proc. IMechE, 184, pt 1, No. 15(1967-68).
- [21] F. J. Wallace and G. Winkler, Very high output diesel engines -- a critical comparison of two stage turbocharged, hyperbar, and differential compound engines, SAE 770756, 1977.
- [22] J. melchior and T. Andre Thalamon, Hyperbar system of high supercharging, SAE 740723, 1974.
- [23] R. Kamo and W. Brysik, Adiabatic turbocompound engine performance, SAE 780068, 1978.
- [24] K. L. Hoag et al., Cummins/TACOM adiabatic engine program, SAE 850356, 1985.
- [25] R. Kamo, Cycles and performance of advanced diesel engines, Conference on ceramics for high performance applications, Newport, Rhode island, 1977.
- [26] F. J. Wallace, The differential compound engine, SAE 670110, 1967.

- [27] F. J. Wallace et al., The differential compound engine -- further development, SAE 710085, 1971.
- [28] F. J. Wallace, The differential compound engine as an advanced integrated engine-transmission system for trucks and off-high way applications, unpublished.
- [29] F. J. Wallace et al., Matching of high output diesel engines with associated turbomachinery, Proc. IMechE, vol 187, 1973.
- [30] F. J. Wallace et al, Design and performance characteristics of the laboratory differential compound engine at bath university, C196/86 IMechE, Turbocharging and Turbochargers, 1986.
- [31] P. B Spence and T. J. Willians, The influence of ambient temperature and pressure on compression-ignition engine performance, Proc. IMechE, vol 188, 1974.
- [32] I. Jebasvili and B. Kordzadze, Effect of atmospheric conditions on the performance of a turbo-supercharged diesel engine, CIMAC, 1981, D30.
- [33] K. Komiymama, et al., Heavy duty diesel engine performance under various ambient conditions, CIMAC, 1981, D41.
- [34] F. J. Wallace, Engine performance analysis, lecture notes, School of Engineering, University of Bath.
- [35] F. J. Wallace, Performance of two-stroke compression ignition engine in combination with compressors and turbines, Proc. IMechE, vol 177, 1963.
- [36] F. J. Wallace, Theoretical assessment of the performance characteristics of inward radial flow turbines, Proc. IMechE, vol. 182, 1967-68.
- [37] F. J. Wallace, J. Miles, Performance of inward radial flow turbines under steady flow conditions with special reference to high pressure ratios and partial admission, Proc. IMechE vol 184, 1969-70.
- [38] M. R. Ziarati, Mathematical modelling and experimental testing of variable geometry inward radial flow turbines, Ph.D. thesis, University of Bath, 1979.
- [39] R. J. B. Way, A simple theoretical model for the performance synthesis of radial or mixed flow turbines, unpublished report, University of Bath.

[40] T. Bevan, The theory of machines.

[41] D. Prince, Design, build and steady state test of a differential compound engine,
Ph.D thesis, University of Bath, 1987.

APPENDIX
BRIEF COMPARISON OF TRANSIENT RESPONSE
OF VG AND FG VERSIONS OF DCE
BASED ON SIMPLE FUEL STEP AND FIXED OUTPUT SHAFT SPEED

The characteristics of the DCE with fixed and variable geometry turbines have been studied (chapter-4 and 5). Under steady state operation, the performance of the two schemes is relatively comparable, with the VG scheme being marginally superior. In the following, a preliminary study is carried out, in an attempt to assess the operation of these two schemes under transient conditions. Again, comparison between the two will be made.

For simplicity, only a fuel step is applied (a step change of fuel per revolution). In all the cases, the output shaft speed is kept constant (infinite inertia) at 440rpm. As fuelling is increased, the engine will accelerate. As engine power increases, output torque will increase.

The DCE is a multi-variable system, therefore effort should be made to optimise its operation. This is particularly the case with turbine gear ratio and it is scheduled so that the turbine can work at reasonably high efficiency all the time.

With a sudden increase in fuelling, the air/fuel ratio will usually decrease, because sufficient air can only be available when the compressor is speeded up and boost pressure built up. Under this circumstance, fuel has to be input in a controlled manner, if necessary, to ensure that minimum air/fuel ratio do not exceed the allowed limit, in the present case not below 20.

With a fixed nozzle turbine, the computation is relatively straightforward. With a variable nozzle turbine, the system becomes more flexible. The scheduling of the nozzle angle becomes, therefore, significant. In the following, the performance of the FG scheme will be taken as the base line, and effects of nozzle angle schedule under transient condition are studied.

In all the cases, the system accelerates from a turbine nozzle angle of 8.886deg. which is the nozzle angle of the FG scheme (as used in the previous steady state simulations), for easy comparison, with an engine speed of 900rpm and engine power of 76kw (corresponding to f_{prev} of about 0.27mg). The system starts to accelerate with a sudden increase of fuel input (f_{prev} of 0.55mg).

A.1 Simulation Program

Again, the program is of a quasi-steady nature. In fact, all the subroutines used in the steady state simulation program are directly employed. The distinct feature of the transient program is the inclusion of the dynamic effects of the system. This has two aspects:

a) Mechanical Inertia

Under transient conditions, the various components, the engine, compressor and output shaft, will accelerate or decelerate under the action of unbalanced torques, according to the following relation:

$$J (ds/dt)=T$$

where J momentum of inertia

ds/dt acceleration

T net torque

A separate subroutine is incorporated to simulate the mechanism of the epicyclic gearbox. Another new subroutine is used to model the road conditions, therefore vehicle accelerations can be simulated. Further, the governor controlling the fuel pump, assumes a first order response.

b) Volume Effects in Gas Flow

This particularly refers to the inlet and exhaust manifold, in which increase of pressure entails accumulation of mass (and variation of gas properties).

The program is constructed such that a steady state initial point is obtained at first, various compatibilities being achieved by varying the parameter f_{prev} . Then, fuelling is increased and the system starts to accelerate, arriving at a new steady state operating point.

A.2 Effects of Nozzle Schedule

In this part, the computational results for both the FG and the VG schemes

are presented. For the VG schemes, the nozzle angle is scheduled such that it arrives at its initial value, i.e. the nozzle angle of the FG scheme, at the end of the transient. Two VG schemes are presented. The results are shown in Fig-1(a,b).

a)FG Scheme

As mentioned earlier, due to the air/fuel ratio limit imposed, at the start of the transient, fuelling has to be restricted. This is clearly shown in Fig-1a. With the FG scheme, the fuelling is controlled such that the lowest air/fuel ratio do not decrease to below 20. However, this only lasts for the first 0.2 second of the transient and then engine torque reaches its final value(from 810nm to 1724nm, Fig-1b). As the engine accelerates(from 900rpm to 1325rpm), the compressor speeds up(from 5687rpm to 9748rpm), which is particularly significant due to the mechanical link between the engine and compressor. As can be seen, boost ratio increases sharply, especially over the first 0.5 second, starting at 2 and reaching the final value of apprx. 4 after about 1.5 second. The initial air/fuel ratio is about 34, and after a sudden drop it increases quickly to a final value of about 31. It is worth noting that, due to the high mass flow rate of the DCE at low output shaft speed, the air fuel ratio is very high(34). This means that although fuelling has to be restricted at the beginning of the transient, the extent of this restriction can be substantially reduced because of the initial ample air. This is particularly reflected in the variations of engine torque and power, both increasing quickly (the engine gains its full power, from 76kw to 240kw, after about 1 second). Because of the fixed nozzle turbine, boost ratio, engine speed and output torque all vary smoothly. The system reaches its final steady state after about 1.5 second.

It can also be seen that better performance can be achieved if the engine mass flow at the start of the transient could be increased.

b)VG Schemes

With the VG turbine scheme, control of nozzle angle can produce this effect, i.e. increasing initial air flow through the engine. VG scheme 2 is an extreme case, in which, the nozzle angle is scheduled such that boost ratio is raised instantly to about its maximum value, hence the trapped air mass in the engine is increased. The air/fuel ratio varies similarly. As a result, the period over which the fuelling has to be restricted is substantially reduced, to about 0.07sec. This is also reflected in the variation of engine torque, which almost instantaneously reaches a very high level (maximum about 1800nm). Over the first 0.4 seconds, output torque has greatly

increased over the FG setting. However, this scheme has its own drawbacks. The turbine nozzle angle has a very strong influence on the system mass flow rate, therefore the compressor and engine speed. Because of severe nozzle restriction over a relatively long period of time, although higher boost ratio is obtained, the acceleration of the engine (compressor) is constrained, due to the higher torque demanded on it. As a consequence, the engine cannot develop its full power quickly, despite the relatively high engine torque. After higher initial values, the engine speed (compressor speed) and therefore engine power only rise very slowly, and their respective values are much lower than those for the FG scheme. This is also true for the output torque. In fact the final engine speed (compressor speed), and output torque are lower than those for the FG scheme while engine torque, boost ratio and air/fuel ratio higher.

In the VG scheme 1, the nozzle angle is scheduled such that the initial operation is improved and, at the same time, the negative effects are reduced as far as possible. As can be seen, with this scheme, boost ratio response is substantially improved over the FG setting, but not as much as for VG scheme 2. The period of fuelling restriction is reduced to almost the same level as in scheme 2. Although the acceleration of the engine is still inferior to that with the FG scheme, it is substantially improved compared with scheme 2. In fact, the engine speed reached the same final value, and at the same time, as in the FG scheme.

This is also reflected in the variation of various other parameters, such as engine power, output torque and compressor speed. Further examination of the variation of the output torque shows that the improvement (over the FG scheme) over the initial stage can well compensate for the drawback in the subsequent period. Further, a reasonable air/fuel ratio in the initial stage is critical. In this sense, the VG scheme could be considered somewhat superior to the FG scheme.

Clearly, under transient operation, the VG scheme has a certain advantage over the FG scheme, provided that the nozzle angle is properly scheduled. Otherwise, a deterioration can result.

A.3 Effects of System Rating

In the previous section, the nozzle angle at the end of the transient is set to the same value, i.e. its initial value (nozzle angle of the FG setting) for all cases. Obviously, this is not realistic. Usually, the nozzle angle in the FG and VG schemes will be different except, probably, at the design points. Further, under steady state

conditions, overall efficiency is the priority whereas, under transient conditions, fast response is the chief objective. As declared earlier, in the present investigation, the fuel per revolution is held constant (unless restriction is needed due to air/fuel ratio limitation). This implies that engine torque is relatively fixed and, therefore, the central task will be to achieve a fast acceleration of the engine, and as high an engine speed as possible (high power), provided all the limiting conditions are satisfied. Further, for the DCE, excessively high engine speed (relative to the steady state operation), if achievable, will result in high compressor mass flow. This will in turn result in a high turbine power, and more significantly, the output torque contributed by the turbine will be greatly increased due to the high gear ratio. In the following, this aspect of the matter is studied.

The results for the FG scheme are unchanged and, again, two VG schemes are presented, being somewhat similar to those in the previous section. The only change made is to increase the final nozzle angle to a value of 10.5deg. rather than 8.886deg. This allowed the engine to be accelerated to a higher speed, limited by the maximum compressor speed of about 11000rpm. The relevant results are presented in Fig-2(a,b).

The initial operation for the VG schemes is very similar to that in the previous section. However, because the maximum engine speed is increased (1450rpm cf. 1325rpm), the engine can work with a higher power over a substantial period (final value of 252kw cf 240kw), which is unobtainable for the FG scheme. Over the second half of the transient, the output torque is substantially increased (final value of 4070nm cf. 3784nm). Clearly, with the air/fuel ratio being controlled under reasonable level, the performance of the VG scheme 1 is improved over the entire period in terms of the response of boost ratio, engine speed (compressor speed) and power, and hence the output torque. For the VG scheme 2, although there is a certain deterioration over a short period after the initial stage, the improvement over the initial and final stages is much greater. Generally, for the VG schemes, the final engine torque, boost ratio and air/fuel ratio are somewhat lower than those for the FG scheme, but engine power and output torque are higher.

Further, in the present investigations, only the transient of the engine system over the first 3 seconds is studied. Vehicle acceleration takes longer time, the advantage of the VG scheme can be more significant.

A.4 Conclusion

This study shows that due to its greater flexibility over the FG scheme, the VG scheme can achieve a marginally better transient response. However, even the FG scheme shows excellent response characteristics compared with turbocharged engines.

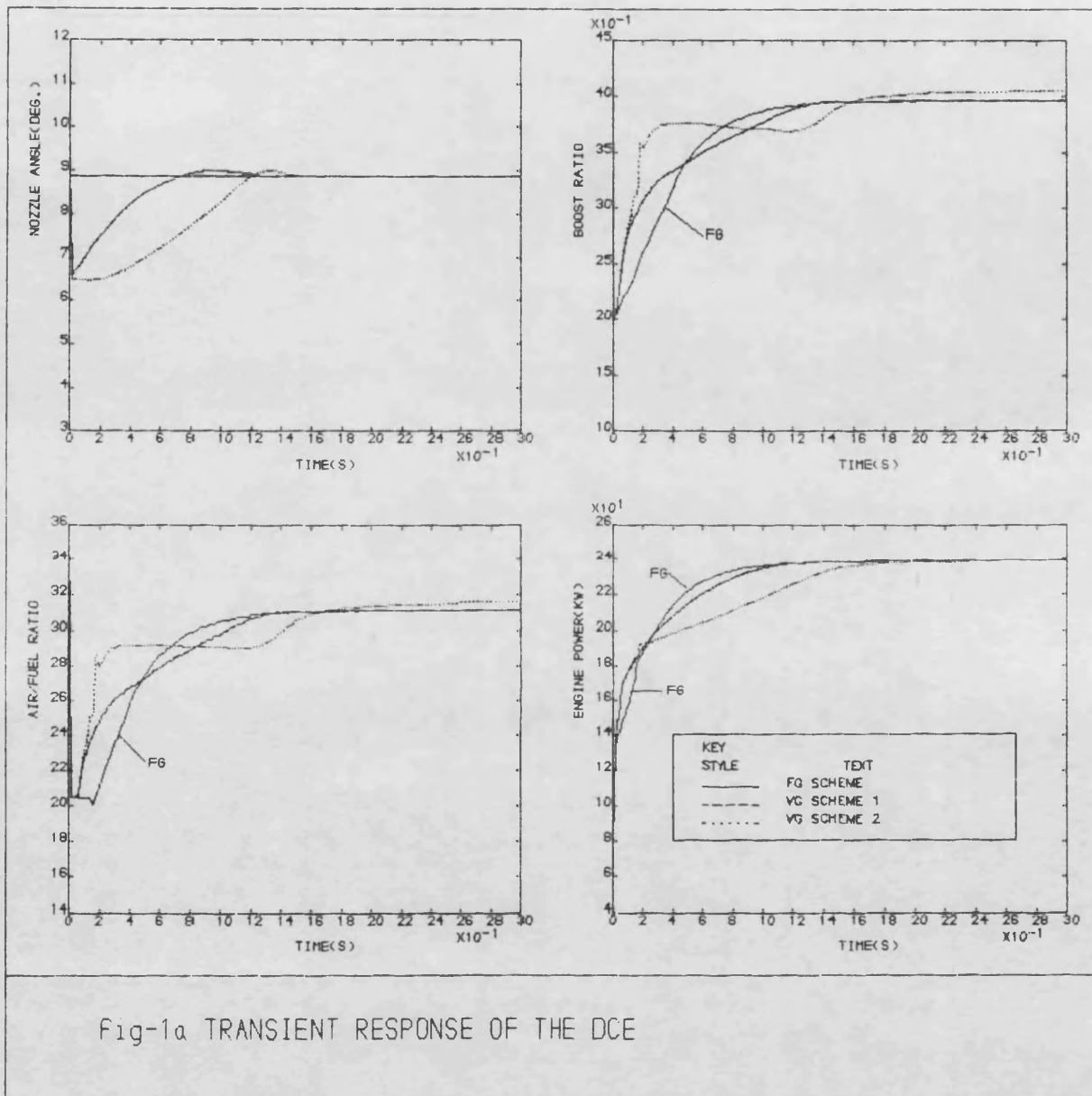


Fig-1a TRANSIENT RESPONSE OF THE DCE

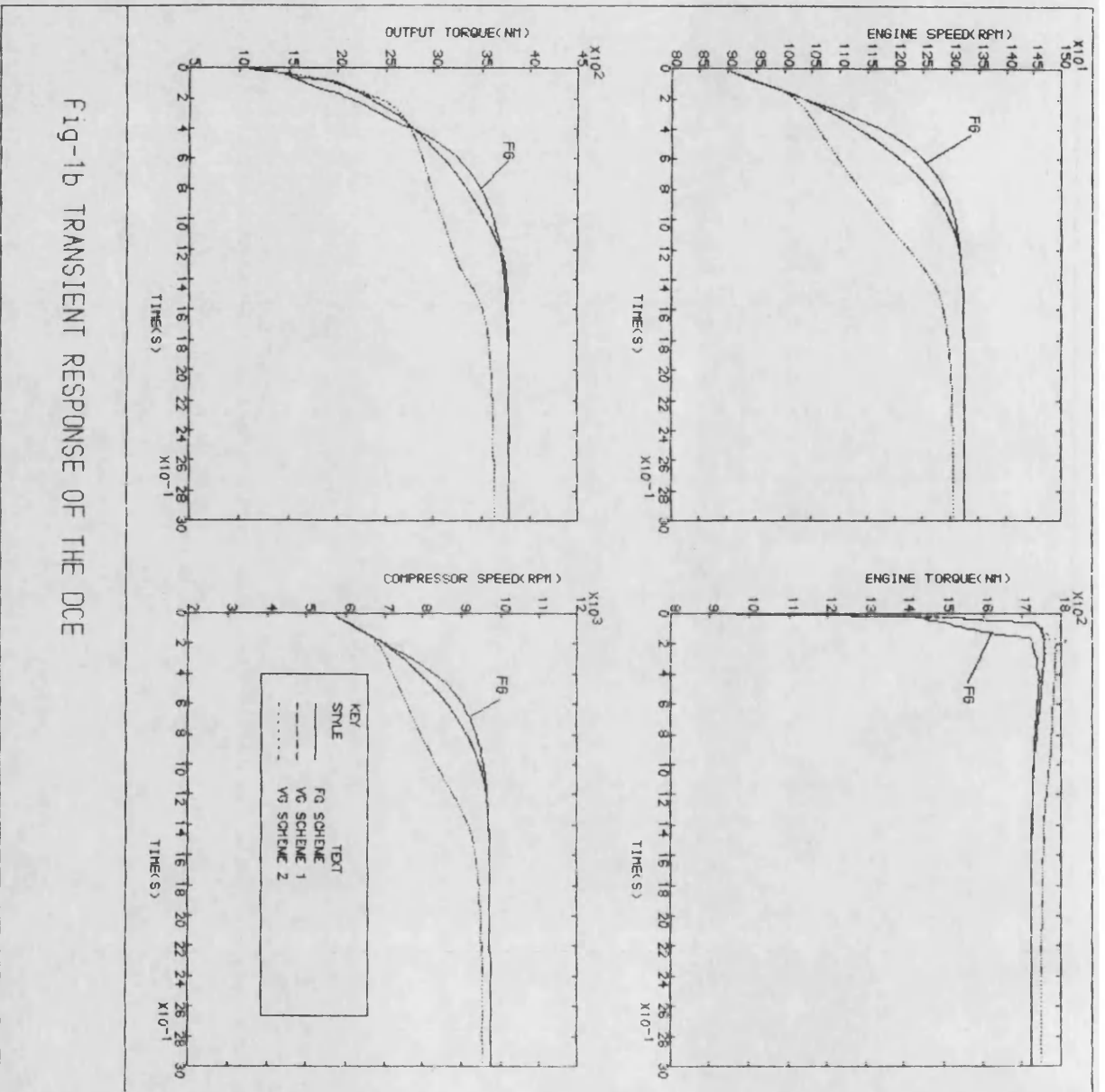


Fig-1b TRANSIENT RESPONSE OF THE DCE

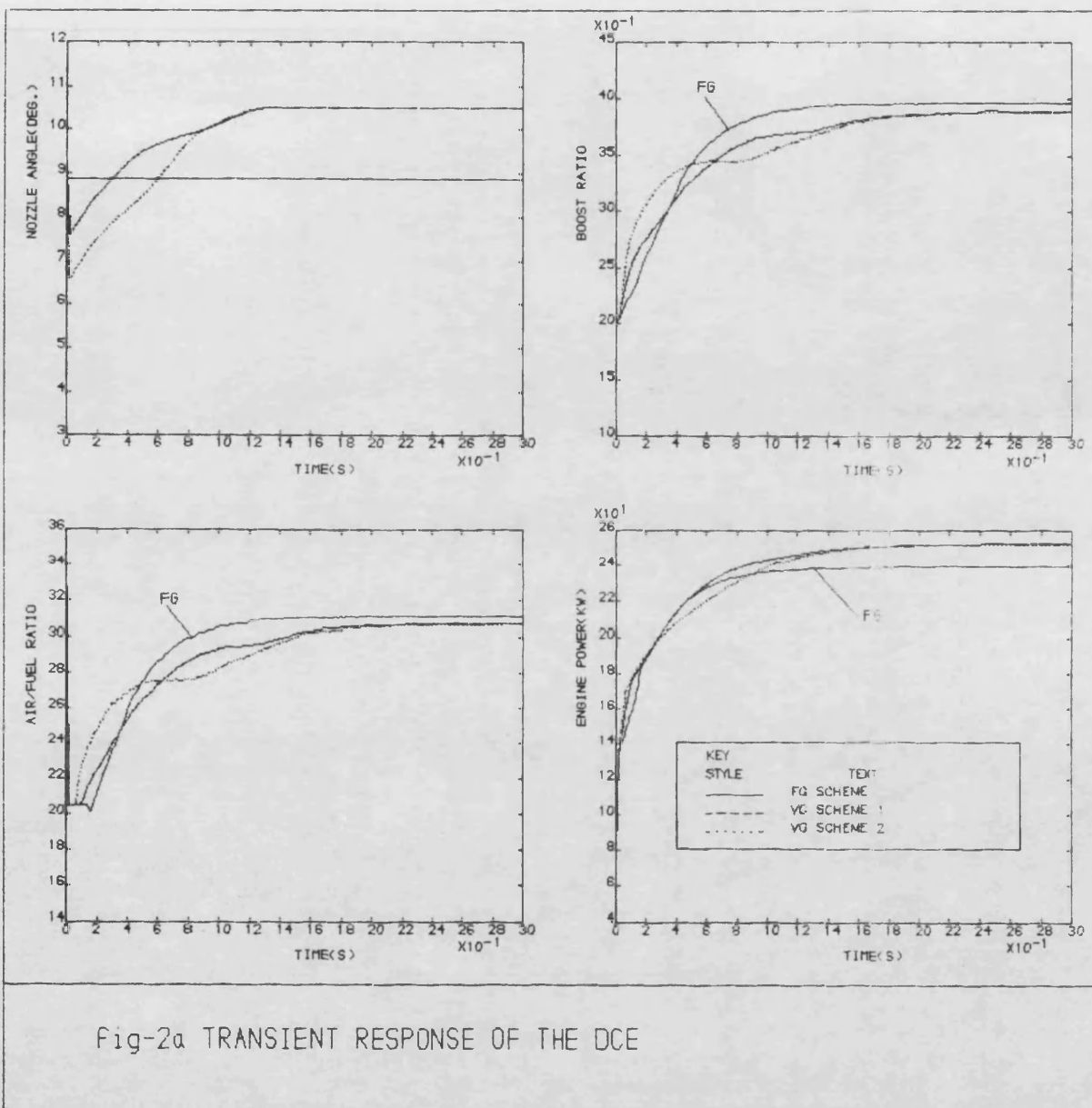


Fig-2a TRANSIENT RESPONSE OF THE DCE

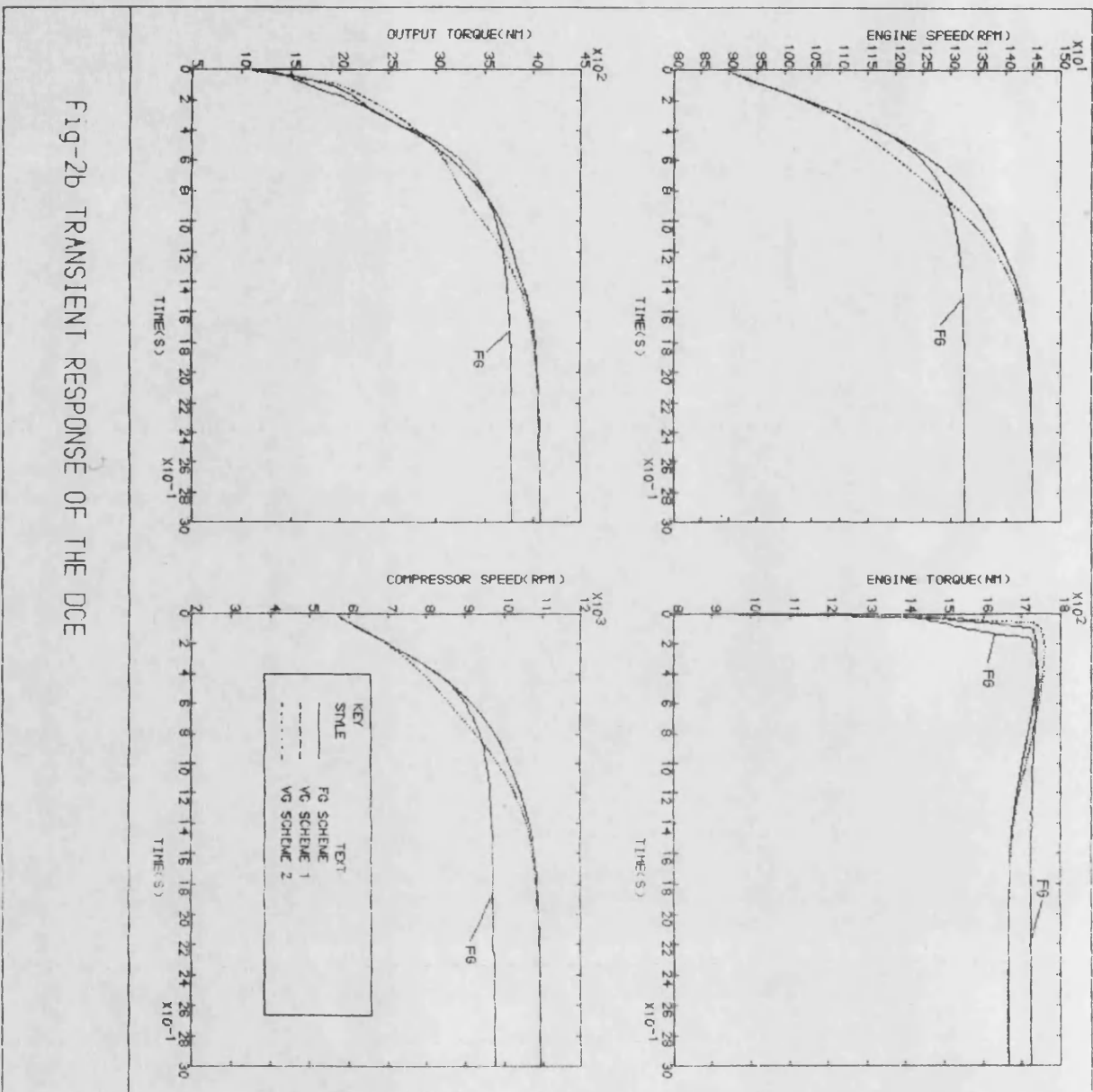


Fig-2b TRANSIENT RESPONSE OF THE DCE